

DIAGNOSTIC PERFORMANCE OF 64-SLICE CT CORONARY ANGIOGRAPHY

Willem Bob Meijboom

PROMOTIECOMMISSIE

Promotoren: Prof.dr. P.J. de Feyter
Prof.dr. G.P. Krestin

Overige leden: Prof.dr. D. Poldermans
Prof.dr. A.J.J.C. Bogers
Prof.dr. M.G.M. Hunink

Cover design : Dennis Bergsma
Layout : A.W. Everaers
Printed by : Ipskamp drukkers, Enschede, the Netherlands
ISBN : 978-90-9023958-3

Financial support by the Netherlands Heart Foundation for the publication of this thesis is gratefully acknowledged.

Copyright © 2009 Bob Meijboom, Rotterdam, the Netherlands
All rights reserved. No part of this thesis may be reproduced, stored in a retrieval system or transmitted in any form or by any means, without written permission of the author, or, when appropriate, of the scientific journal in which parts of this thesis may have been published.

For my family

The research described in this thesis was supported by a grant of the Netherlands government, the Zon/MW.

DIAGNOSTIC PERFORMANCE OF 64-SLICE CT CORONARY ANGIOGRAPHY

*Diagnostische Accuraatheid van
64-slice CT Coronair
Angiografie*

Proefschrift

Ter verkrijging van de graad van doctor aan de
Erasmus Universiteit Rotterdam
op gezag van Rector Magnificus

Prof.dr. S.W.J. Lamberts

en volgens besluit van het College voor Promoties.

De openbare verdediging zal plaatsvinden op
woensdag, 18 maart 2009 om 09.45 uur

door

Willem Bob Meijboom

Geboren te Amstelveen



TABLE OF CONTENT

Part 1: Preface

- Chapter 1** **General Introduction and Outline of the Thesis**
- Chapter 2** **Use of High Resolution Spiral CT for the
Diagnosis of Coronary Artery Disease**
Current treatment options in cardiovascular medicine. 2007 Feb; 9(1): 29-38
Meijboom WB, van Pelt N, De Feyter PJ
- Chapter 3** **Spiral Multislice Computed Tomography
Coronary Angiography: a current status report**
Clinical Cardiology. 2007 Sep 5;30(9):437-442
De Feyter PJ, Meijboom WB, Weustink AC, van Mieghem CA,
Mollet NR, Vourvouri E, Nieman K, Cademartiri F
- Addendum 1** **Post-processing using multislice CT coronary angiography
improves image interpretability in patients with fast
heart-rates and heart rate variations: a case report**
Journal of Cardiovascular Medicine. 2007 Dec;8(12):1088-90
Pugliese F, Alberghina F, Meijboom WB,
Malago R, Gopalan D, de Feyter PJ

Part 2: Detection of significant coronary artery disease

- Chapter 4** **Diagnostic Accuracy of 64-slice Computed
Tomography Coronary Angiography: A
Prospective Multicenter, Multivendor Study**
Journal of American College of Cardiology. 2008. Dec 16;52(25):2135-44
Meijboom WB, Meijs MFL, Schuijf JD, Cramer MJ, Mollet NR,
van Mieghem CAG, Nieman K, van Werkhoven JM, Pundziute G,
Weustink AC, de Vos AM, Pugliese F, Rensing B, Jukema JW, Bax JJ,
Prokop M, Doevendans PA, Hunink MGM, Krestin GP, de Feyter PJ

Chapter 5 **Comparison of Diagnostic Accuracy of 64-Slice Computed Tomography Coronary Angiography in Women-vs-Men with Angina Pectoris**
American Journal of Cardiology. 2007 Nov 15;100(10):1532-7.
Meijboom WB, Weustink AC, Pugliese F, van Mieghem CA, Mollet NR, van Pelt N, Cademartiri F, Nieman K, Vourvouri E, Regar E, Krestin GP, De Feyter PJ

Chapter 6 **Reliable High-speed Coronary Computed Tomography in Symptomatic Patients**
Journal of American College of Cardiology. 2007 Aug 21;50(8):786-94.
Weustink AC, Meijboom WB, Mollet NR, Otsuka M, Pugliese F, van Mieghem CAG, Malago R, van Pelt N, Dijkshoorn ML, Cademartiri F, Krestin GP, De Feyter PJ

Addendum 2 **Angina pectoris due to steal phenomenon created by a left anterior descending-right ventricle fistula originating from repeated myocardial biopsies**
Submitted.
Meijboom WB, van Mieghem CAG, Weustink AC

Part 3: Clinical application of CTCA

Chapter 7 **64-Slice Computed Tomography Coronary Angiography in Patients with High, Intermediate or Low Pre-test Probability of Significant Coronary Artery Disease**
Journal of American College of Cardiology. 2007 Oct 9;50(15):1469-75.
Meijboom WB, van Mieghem CAG, Mollet NR, Pugliese F, Weustink AC, van Pelt N, Cademartiri F, Nieman K, Boersma H, de Jaegere P, Krestin GP, de Feyter PJ

Chapter 8 **64-slice Computed Tomography Coronary Angiography in Patients with Non-ST Elevation Acute Coronary Syndrome**
Heart. 2007 Nov;93(11):1386-92.
Meijboom WB, Mollet NR, van Mieghem CA, Weustink AC, Pugliese F, van Pelt N, Cademartiri F, Vourvouri E, de Jaegere P, Krestin GP, de Feyter PJ

- Chapter 9** **Comprehensive assessment of coronary artery stenoses: CT coronary angiography versus conventional coronary angiography and correlation with FFR**
Journal of American College of Cardiology. 2008 Aug 19; 52(8):636-43.
Meijboom WB, Van Mieghem CAG, van Pelt N, Weustink AC, Pugliese F, Mollet NR, Boersma E, Regar E, van Geuns RJ, de Jaegere PJ, Serruys PW, Krestin GP, de Feyter PJ
- Chapter 10** **Value of combined use of Calcium Score and 64-slice CT coronary angiography in symptomatic patients referred for conventional coronary angiography**
Submitted
Meijs MFL, Meijboom WB, Schuijf JD, Prokop M, Mollet NR, van Mieghem CAG, van Werkhoven JM, Jukema JW, Doevendans PA, Bax JJ, de Feyter PJ, Cramer MJ
- Chapter 11** **MSCT lesion calcium to predict stenosis severity of calcified lesions**
Submitted.
Pugliese F, Hunink MGM, Meijboom WB, Gruszynska K, Rengo M, Mollet NR, Weustink AC, Neeffjes L, Dijkshoorn ML, Krestin GP, De Feyter PJ
- Chapter 12** **Computed Tomography Coronary Angiography in patients with suspected CAD: decision making from various perspectives in the face of uncertainty. A cost-effectiveness analysis**
Submitted.
Genders TSS, Meijboom WB, Meijs MFL, Schuijf JD, Mollet NR, Weustink AC, Pugliese F, Bax JJ, Cramer MJ, Krestin GP, de Feyter PJ, Hunink MG

Part 4: CTCA before and after cardiac surgery

- Chapter 13** **CT coronary angiography in Cardiothoracic Surgery**
Chapter in: Advances in MDCT Volume 3, Pt. 2:
CT Angiography. Clinical Publishing Ltd.
Meijboom WB, Mollet NR, van Pelt N

- Chapter 14** **Preoperative Computed Tomography Coronary Angiography to Detect Significant Coronary Artery Disease In Patients Referred for Cardiac Valve Surgery**
Journal of American College of Cardiology. 2006 Oct 17;48(8):1658-65.
Meijboom WB, Mollet NR, Van Mieghem CA, Kluin J, Weustink AC, Pugliese F, Vourvouri E, Cademartiri F, Bogers AJ, Krestin GP, de Feyter PJ
- Chapter 15** **64-Slice CT in Symptomatic Patients After Coronary Bypass Surgery Evaluation of Grafts and Coronary Arteries**
European Heart Journal. 2007 Aug 28(15)1879-85.
Malagutti P, Nieman K, Meijboom WB, van Mieghem CA, Pugliese F, Cademartiri F, Mollet NR, Boersma E, de Jaegere PP, de Feyter PJ
- Chapter 16** **Ultrasonographic and DSCT Scan Analysis of single LIMA versus Arterial T grafts 12 years after Surgery**
Submitted
Hartman JM, Meijboom WB, Galema TW, Takkenberg JJM, Schets AM, De Feyter PJ, Bogers AJJC
- Chapter 17** **Anatomical and functional assessment of single LIMA versus arterial composite T-grafts 12 years after bypass surgery**
Submitted.
Hartman JM, Meijboom WB, Galema TW, Takkenberg JJM, Schets AM, De Feyter PJ, Bogers AJJC
- Addendum 3** **Unusual cause of myocardial ischemia non-invasive assessed with ECG-gated computed tomography coronary angiography**
European Journal of Cardiothoracic Surgery. 2006 May;29(5):840.
Pugliese F, Meijboom WB, Cademartiri F, Krestin GP

Part 5 CTCA and bifurcations

Chapter 18 Detection and characterization of coronary bifurcation lesions with 64-slice computed tomography coronary angiography

European Heart Journal. 2007 Aug 28(16):1968-76.

Van Mieghem CAG, Thury A, Meijboom WB, Cademartiri F, Mollet NR, van der Giessen AG, Wentzel JJ, Kluin J, Sianos G, van der Ent M, van der Giessen WJ, de Jaegere P, Krestin GP, Serruys PW, de Feyter PJ

Chapter 19 Plaque distribution relates to shear stress in human coronary bifurcations: A multi-slice computed tomography study

Euro Intervention, 2008;4

van der Giessen A, Wentzel J, Meijboom WB, Mollet NR, van der Steen T van de Vosse F, de Feyter, PJ, Gijzen F

Addendum 4 Reliable angiographic evaluation by 64-slice computed tomography after trifurcation stenting of the left main coronary artery

Euro Intervention, 2006;1:482-483.

Van Mieghem CAG, Sianos G, Meijboom WB, Vourvouri E, Serruys PW, de Feyter PJ

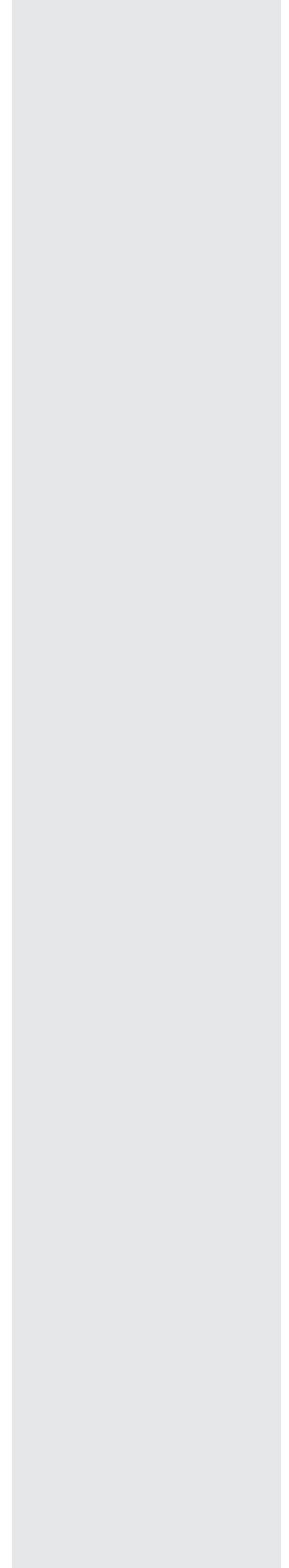
Part 6: Summary and conclusion

Chapter 20 Summary and conclusions

- Samenvattingen en conclusies**
- Acknowledgements**
- List of publications**
- Curriculum vitae**
- Color section**

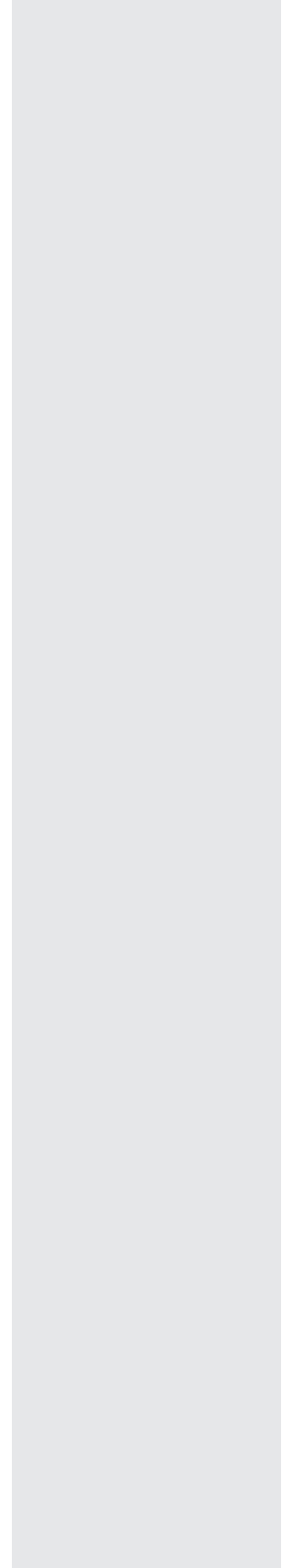
Part 1

Preface



1

General Introduction



INTRODUCTION

Conventional, invasive X-ray coronary angiography (CCA) has been the standard of reference for the assessment of coronary artery disease (CAD). In patients with angina pectoris coronary angiography is the key diagnostic procedure to identify who would benefit from medical therapy, percutaneous coronary intervention or coronary artery bypass surgery. However, coronary angiography is an invasive procedure, potentially harmful with a small risk of serious adverse events (approx 0.1%) (ventricular fibrillation, stroke, coronary artery dissection, myocardial infarction, death) and discomfort to the patient. Furthermore, the catheterization-procedure is rather expensive, because of its invasive nature it involves admission to a hospital or day-care facility.

Non-invasive coronary angiography using computed tomography is a relatively recent development. In 1998 the first multi-slice spiral CT scanners were introduced, which could acquire 4 slices simultaneously during the scan (1,2). However, the temporal resolution and spatial resolution of these scanners was limited and a breath hold of 40 seconds for most of the patients too long. The early results with these scanners were promising but lacked sufficient robustness to be useful in clinical practice. Technological advances, with improvement of temporal and spatial resolution and shortening of patients breath holds to less than 10 seconds, have rendered the newest multi-slice CT scanners more clinically useful. The introduction of a 64-slice CT-scanner and dual source scanners, have dramatically improved the clinical reliability of the CT technique and now permit evaluation of the entire coronary tree in patients with stable and unstable angina pectoris (3-7) (Table 1,2). These technical developments have further increased the diagnostic performance of CT resulting in a high sensitivity and specificity and negative predictive value of more than 90% without excluding coronary segments due to poor image quality.

Multiple reports have been published on the excellent diagnostic performance of CT coronary angiography (CTCA) (8-18). However, the presented data and the interpretation of these results is sometimes confusing. A short explanation of the different ways of analyzing CTCA is mandatory.

Table 1 Results of published meta-analyses, per patient analysis

	N, studies	Sensitivity, %	Specificity, %	PPV %	NPV, %
Vanhoenacker	6	93	96	-	-
Abdulla	13	97	91	93	96
Hamon	9	87	96	93	96
Stein	23	98	88	93	96
Mowatt	18	99	89	93	100

Table 2 Results of published meta-analyses, per segment analysis

	N, studies	% non evaluable	Sensitivity, %	Specificity, %	PPV %	NPV %
Vanhoenacker	6	-	93	96	-	-
Abdulla	19	4	86	96	83	96
Stein	21	8	90	96	73	99
Mowatt	17	-	90	97	76	99

THE PER-PATIENT ANALYSIS

CTCA can be seen as a binary, diagnostic test, which may be presented as a per-patient analysis. The test provide answers to various questions. Is their presence of any significant obstruction? Should we send these patients for coronary angiography for further evaluation? The test is either positive or negative (or inconclusive). The test merely provides information whether a $\geq 50\%$ stenosis is present on CCA, independent from the location of this coronary stenosis in the coronary tree. The results often show an excellent sensitivity and a lower specificity. In other words, a coronary lesion is not often missed, but the severity of the lesion is sometimes overestimated. These diagnostic capabilities make CTCA useful especially in patients with an intermediate or low pre-test likelihood for obstructive CAD, since a negative CTCA will reliably exclude significant CAD and a positive CTCA will increase the post-test probability for CAD to a high probability (19). The benefit of patients using CTCA as a binary test in patients with a high pre-test probability for obstructive CAD would be less since these patients will anyhow be referred for CCA because a negative test will not reliably exclude significant CAD and a positive test does not significantly increase the post-test probability.

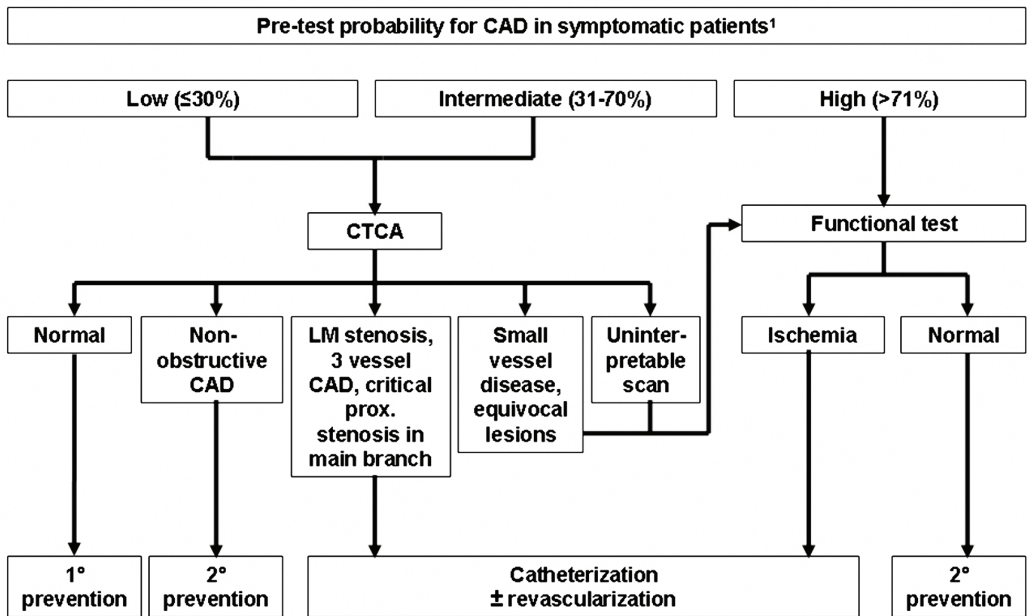
THE PER-VESSEL ANALYSIS

CTCA offers more information than just the presence or absence of CAD. CTCA visualization of the entire coronary tree provides anatomical evidence of the extent and location of significant CAD, all of which play an important role in clinical decision making and provide important prognostic information. Using the per-vessel analysis we can get an impression on the severity and extent of disease. Patients with single vessel disease don't necessarily have to be sent for CCA, since survival of these patients will not decrease by revascularization, and aggressive medical therapy will result in the similar outcome. Patients with significant three vessel disease and significant left main disease have been shown to benefit from revascularization. A recent study showed that conservative management of a patient with a negative CT scan is safe and associated with an excellent 1-year outcome (20). The presence and extent of both non-obstructive and obstructive CAD as

seen on CTCA predicted adverse cardiovascular events in particular in patients with left main and three-vessel disease (21). Long-term follow up of patients who underwent CTCA with Electron Beam Tomography showed that the burden of angiographic disease detected by CTCA provided both independent and incremental value in predicting all-cause mortality independent of age gender, conventional risk factors and coronary calcium score (22).

A recent study reported on the use of CTCA in 1000 asymptomatic middle-aged patients of whom 22% had atherosclerotic plaques and 5% had significant CAD. Longer follow-up will reveal if CTCA can risk stratify these patients in different cardiac risk groups (23). Studies evaluating the effectiveness and cost-effectiveness of various diagnostic workup algorithms using CTCA and functional tests prior to referral to angiography need to be performed to determine the clinical role of CTCA. A proposed diagnostic work-up using CTCA is shown in Figure 1.

Figure 1



¹ Estimated using Duke clinical Score (including Diamond-Forrester criteria and prognostic clinical variables).

THE PER-SEGMENT ANALYSIS

The final step of clinical implementation would be the replacement of CCA by CTCA. This would require an extremely robust CT-technique because on the basis of the CT-outcome patients may be referred to or deferred from medical treatment, percutaneous coronary intervention or coronary artery bypass surgery. To evaluate whether CTCA can replace CCA a site-by-site analysis of coronary lesions is required. This is presented as the per-segment analysis. Although sensitivities and specificities in published papers are generally quite good, a substantial overestimation of the severity of stenosis is observed resulting in lower positive predictive values. Furthermore, in attempting to reliably replace CCA, reproducible quantitative grading of coronary stenosis severity should be possible. In our and other experience the quantification of stenosis severity is moderate, even after exclusion of segments with massive calcifications or coronary motion artifacts (11,16,24). For instance, we analyzed 50 patients who had 150 coronary stenoses with a diameter stenosis on QCA between 20% and 100% and used a quantification tool to measure the diameter stenosis on CT. Correlation statistics revealed that the Pearson r is 0.74 with 95% CI from 0.65 to 0.80, with an r square of 0.54 (Figure 2). The Bland-Altman analysis revealed a bias of 2.43 with standard deviation of the bias of 10.9. 95% limits of agreement are -18.93 to 23.80 (Figure 3). Given this current limitation, CTCA technology may need to evolve further before it can accurately guide future management of symptomatic coronary patients.

Figure 2

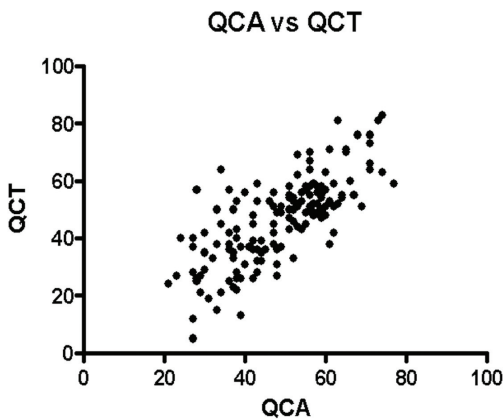
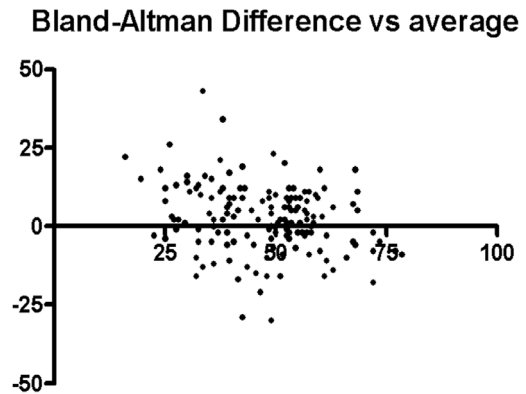


Figure 3



64-SLICE CT CORONARY ANGIOGRAPHY MULTICENTER STUDIES

Recently, three 64-slice CT coronary angiography multicenter studies have been published (25,26,27). The results of the studies vary in diagnostic performance with a sensitivity ranging from 85% to 99% and a specificity from 64% to 90% (Table 3-5).

LIMITATIONS

Despite spectacular technological progress, there are still challenges for CTCA in the near future. The heart rate of patients still has to be lowered with beta blockers to improve image quality, although Dual Source scanners are able to provide sufficient quality at higher heart rates (28). Atrial fibrillation remains a contra indication for CTCA. Coronary calcification, creating blooming artefacts, still hamper the precise evaluation of coronary stenosis. Similarly, artefacts limit the evaluation of patients who have previously undergone stent placement. The increased radiation dose during CTCA remains an issue. In the near future different scan protocols and CT techniques will lower the radiation dose considerably. CTCA merely provides anatomical information. The haemodynamic significance of intermediate coronary stenosis is therefore difficult to assess.

OUTLINE OF THESESES

Two reviews on CTCA are provided in Part 1 which describe potential implementations of CTCA in different clinical situations. Furthermore, it provides advice on how to perform CTCA, patient selection and potential drawbacks of CTCA (Chapters 2-3). The diagnostic performance of 64-slice CTCA (Chapter 4-5) and Dual-source CTCA (Chapter 6) to detect significant coronary stenosis compared to conventional coronary angiography in selected patients is discussed in Part 2. Potential clinical applications with CTCA are discussed in Part 3 in patients presenting with various symptoms (Chapter 7-8) and stenosis severity is compared to hemodynamic significance as measured by fractional flow reserve (Chapter 9). The value of a combined use of a calcium score and CTCA in a per-patient analysis are given (Chapter 10) and the usage of the segmental calcium score and clinical factors to predict the probability of stenosis in calcified lesions (Chapter 11). The following chapter provides a cost-effectiveness analysis regarding the use of CTCA (Chapter 12). Part 4 emphasizes on CTCA in the field of pre- and post revascularization with either percutaneous coronary interventions or coronary artery bypass grafting (Chapter 13-17). The potential of CTCA in the in-vivo detection and evaluation of the presence, location and extent anatomical distribution of bifurcations lesions is described in Part 5 (Chapter 18-19).

Table 3 Diagnostic Performance and Predictive Value of 64-Slice CT Coronary Angiography for the Detection of $\geq 50\%$ Stenosis on QCA in a per Patient Analysis.

	Prevalence of disease, %	N	TP	TN	FP	FN	Sensitivity, %	Specificity, %	PPV, %	NPV, %
Budoff *	23	227	52	142	30	3	95	83	64	99
Miller †	56	291	139	115	13	24	85	90	91	83
Meijboom ‡	68	360	244	73	41	2	99	64	86	97

* Patients without known CAD, intermediate pre-test probability for CAD. † Patients with calcium scores > 600 excluded, 10% prior percutaneous coronary intervention, 20% previous myocardial infarction. ‡ Patients between 50-70 years old, both acute and stable anginal syndromes, 15% previous myocardial infarction.

Table 4 Diagnostic Performance and Predictive Value of 64-Slice CT Coronary Angiography for the Detection of $\geq 50\%$ Stenosis on QCA in a per Vessel Analysis.

	Prevalence of disease, %	N	TP	TN	FP	FN	Sensitivity, %	Specificity, %	PPV, %	NPV, %
Budoff	10	910	73	744	79	14	84	90	51	99
Miller	31	866	203	553	44	66	75	93	82	89
Meijboom	26	1440	354	821	245	20	95	77	59	98

Table 5 Diagnostic Performance and Predictive Value of 64-Slice CT Coronary Angiography for the Detection of $\geq 50\%$ Stenosis on QCA in a per Segment Analysis.

	Prevalence of disease, %	N	TP	TN	FP	FN	Sensitivity, %	Specificity, %	PPV, %	NPV, %
Meijboom	9	5297	422	4345	471	59	88	90	47	99

REFERENCES

1. Nieman K, Oudkerk M, Rensing BJ, et al. Coronary angiography with multi-slice computed tomography. *Lancet* 2001;357:599-603.
2. Achenbach S, Giesler T, Ropers D, et al. Detection of coronary artery stenoses by contrast-enhanced, retrospectively electrocardiographically-gated, multislice spiral computed tomography. *Circulation* 2001;103:2535-8.
3. Vanhoenacker PK, Heijenbrok-Kal MH, Van Heste R, et al. Diagnostic performance of multidetector CT angiography for assessment of coronary artery disease: meta-analysis. *Radiology* 2007;244:419-28.
4. Abdulla J, Abildstrom SZ, Gotzsche O, Christensen E, Kober L, Torp-Pedersen C. 64-multislice detector computed tomography coronary angiography as potential alternative to conventional coronary angiography: a systematic review and meta-analysis. *Eur Heart J* 2007;28:3042-50.

5. Mowatt G, Cook JA, Hillis GS, et al. 64-Slice computed tomography angiography in the diagnosis and assessment of coronary artery disease: systematic review and meta-analysis. *Heart* 2008;94:1386-93.
6. Stein PD, Yaekoub AY, Matta F, Sostman HD. 64-slice CT for diagnosis of coronary artery disease: a systematic review. *Am J Med* 2008;121:715-25.
7. Vanhoenacker PK, Decramer I, Bladt O, Sarno G, Bevernage C, Wijns W. Detection of non-ST-elevation myocardial infarction and unstable angina in the acute setting: meta-analysis of diagnostic performance of multi-detector computed tomographic angiography. *BMC Cardiovasc Disord* 2007;7:39.
8. Ehara M, Surmely JF, Kawai M, et al. Diagnostic accuracy of 64-slice computed tomography for detecting angiographically significant coronary artery stenosis in an unselected consecutive patient population: comparison with conventional invasive angiography. *Circ J* 2006;70:564-71.
9. Fine JJ, Hopkins CB, Ruff N, Newton FC. Comparison of accuracy of 64-slice cardiovascular computed tomography with coronary angiography in patients with suspected coronary artery disease. *Am J Cardiol* 2006;97:173-4.
10. Herzog C, Zwerner PL, Doll JR, et al. Significant coronary artery stenosis: comparison on per-patient and per-vessel or per-segment basis at 64-section CT angiography. *Radiology* 2007;244:112-20.
11. Leber AW, Knez A, von Ziegler F, et al. Quantification of obstructive and nonobstructive coronary lesions by 64-slice computed tomography: a comparative study with quantitative coronary angiography and intravascular ultrasound. *J Am Coll Cardiol* 2005;46:147-54.
12. Leschka S, Alkadhi H, Plass A, et al. Accuracy of MSCT coronary angiography with 64-slice technology: first experience. *Eur Heart J* 2005;26:1482-7.
13. Mollet NR, Cademartiri F, van Mieghem CA, et al. High-resolution spiral computed tomography coronary angiography in patients referred for diagnostic conventional coronary angiography. *Circulation* 2005;112:2318-23.
14. Nikolaou K, Knez A, Rist C, et al. Accuracy of 64-MDCT in the diagnosis of ischemic heart disease. *AJR Am J Roentgenol* 2006;187:111-7.
15. Pugliese F, Mollet NR, Runza G, et al. Diagnostic accuracy of non-invasive 64-slice CT coronary angiography in patients with stable angina pectoris. *Eur Radiol* 2006;16:575-82.
16. Raff GL, Gallagher MJ, O'Neill WW, Goldstein JA. Diagnostic accuracy of noninvasive coronary angiography using 64-slice spiral computed tomography. *J Am Coll Cardiol* 2005;46:552-7.
17. Ropers D, Rixe J, Anders K, et al. Usefulness of multidetector row spiral computed tomography with 64- x 0.6-mm collimation and 330-ms rotation for the noninvasive detection of significant coronary artery stenoses. *Am J Cardiol* 2006;97:343-8.
18. Schuijf JD, Pundziute G, Jukema JW, et al. Diagnostic accuracy of 64-slice multislice computed tomography in the noninvasive evaluation of significant coronary artery disease. *Am J Cardiol* 2006;98:145-8.

19. Meijboom WB, van Mieghem CA, Mollet NR, et al. 64-slice computed tomography coronary angiography in patients with high, intermediate, or low pretest probability of significant coronary artery disease. *J Am Coll Cardiol* 2007;50:1469-75.
20. Min JK, Shaw LJ, Devereux RB, et al. Prognostic value of multidetector coronary computed tomographic angiography for prediction of all-cause mortality. *J Am Coll Cardiol* 2007;50:1161-70.
21. Gilard M, Le Gal G, Cornily JC, et al. Midterm prognosis of patients with suspected coronary artery disease and normal multislice computed tomographic findings: a prospective management outcome study. *Arch Intern Med* 2007;167:1686-9.
22. Ostrom MP, Gopal A, Ahmadi N, et al. Mortality incidence and the severity of coronary atherosclerosis assessed by computed tomography angiography. *J Am Coll Cardiol* 2008;52:1335-43.
23. Choi EK, Choi SI, Rivera JJ, et al. Coronary computed tomography angiography as a screening tool for the detection of occult coronary artery disease in asymptomatic individuals. *J Am Coll Cardiol* 2008;52:357-65.
24. Hoffmann MH, Shi H, Schmitz BL, et al. Noninvasive coronary angiography with multislice computed tomography. *Jama* 2005;293:2471-8.
25. Budoff MJ, Dowe D, Jollis JG, et al. Diagnostic performance of 64-multidetector row coronary computed tomographic angiography for evaluation of coronary artery stenosis in individuals without known coronary artery disease: results from the prospective multicenter ACCURACY (Assessment by Coronary Computed Tomographic Angiography of Individuals Undergoing Invasive Coronary Angiography) trial. *J Am Coll Cardiol* 2008;52:1724-32.
26. Miller JM, Rochitte CE, Dewey M, et al. Diagnostic performance of coronary angiography by 64-row CT. *N Engl J Med* 2008;359:2324-36.
27. Meijboom WB, Meijs MFL, Schuijf JD, et al. Diagnostic accuracy of 64-slice Computed Tomography Coronary Angiography: a Prospective, Multicenter, Multivendor Study. *J Am Coll Cardiol* 2008;52:2135-44.
28. Weustink AC, Meijboom WB, Mollet NR, et al. Reliable high-speed coronary computed tomography in symptomatic patients. *J Am Coll Cardiol* 2007;50:786-94. *Coll*

2

Use of High Resolution Spiral CT for the Diagnosis of Coronary Artery Disease

Current treatment options in cardiovascular medicine.
2007 Feb; 9(1): 29-38

Willem B. Meijboom, MD^{1,2},
Niels van Pelt, MD^{1,2}, Pim de
Feyter, MD, PhD^{1,2}

¹ Department of Cardiology,
² Department of Radiology,
Erasmus Medical Center,
Rotterdam, the Netherlands

OPINION STATEMENT

Multislice computed tomography coronary angiography (CTCA) is a rapidly emerging technique for the non-invasive visualization of coronary arteries. Over the past 5 years several scanner generation have been introduced with a progressive improvement in the diagnostic accuracy in the detection of coronary artery stenosis in selected patient populations. The introduction of 64-slice technology, which allows high resolution and nearly motion-free coronary artery imaging, has resulted in further improvement in the diagnostic accuracy. This technique is at the verge of widespread clinical implementation and, even in the absence of large clinical trials, a high demand for CTCA is already observed all over the world.

INTRODUCTION

Conventional, invasive coronary angiography (CCA) has been the standard of reference for the assessment of obstructive coronary artery disease (CAD). In patients with angina pectoris CCA is the key diagnostic procedure to identify who may benefit from medical treatment, percutaneous coronary intervention or coronary artery bypass surgery (CABG). Although CCA is generally safe and well tolerated, there is a small risk of major complications (1). Given also the high cost of CCA and the need for an experienced team to perform the procedure, a search for a reliable non invasive alternative to visualize the entire coronary tree is ongoing. Due to the heart's motion, small size and tortuous trajectory of the coronary arteries, non-invasive imaging of the coronary tree is complicated. The introduction of the 4 - and 16 slice CT scanners revealed promising results and the currently widely available 64-slice CT scanners allows nearly motion free visualisation of the coronary tree with excellent diagnostic accuracy in detecting coronary stenosis.

TECHNICAL REQUIREMENTS FOR CARDIAC SCANNING

With the introduction of spiral scanning total scan time reduced significantly. Instead of moving the table position with every scan, known as the step-and-shoot principle, the patient moved continuously at a pre-defined speed through the gantry acquiring volumetric data from which cross-sectional images could be reconstructed. This configuration diminished total scan time, but was not fast enough for cardiac scanning. Multislice CT scanners (MSCT) were the next major development. The use of thinner, multiple detectors combined with faster gantry rotation allowed successful imaging of the coronary tree. For obtaining nearly motion-free images of the continuously moving coronaries of the heart, the following prerequisites have to be fulfilled.

Temporal resolution

To capture the rapid moving coronaries in a single frame, the scanner needs to rotate fast enough to “freeze the image”, minimising artefacts related to coronary motion. By reducing the rotation time of the x-ray tube and detector around the patient, temporal resolution decreases, which in the fastest current 64 slice MSCT is 330msec. The temporal resolution refers to the duration of the reconstruction window during the mid-to-end-diastolic - or end-systolic phase of each heart cycle. Using a half-scan reconstruction algorithm, data can be extrapolated during a 180 degree rotation resulting in a temporal resolution of 165 msec. Multi-segment reconstruction, a post-processing technique collecting and merging data from different consecutive cardiac cycles lowers the temporal resolution ever further, but is highly sensitive to heart rate irregularities and requires a lower pitch resulting in a longer scan duration and higher radiation dose.

Spatial resolution

In the transition from 4- to 16- en 16- to 64 slice MSCT scanners spatial resolution improved due to the increase in detectors and decrease in detector width. With the latest CT scanners a spatial resolution in the x/y/z axis provides a submillimeter near isotropic voxel of $0.4 \times 0.4 \times 0.4 \text{mm}^3$ (in comparison CCA has a spatial resolution of 0.2×0.2). This improved resolution allows CTCA to interrogate the entire coronary tree (including the smaller vessels). By reducing the blooming effect of stents and severe calcifications, the lumen inside stents and plaque can be better delineated.

Synchronization with the ECG

Contraction of the heart can cause extensive motion artefacts when visualising the coronary arteries. To overcome this problem the heart is continuously scanned while an ECG trace is registered. ECG retrospective gating generates reconstruction windows in the diastolic phase when cardiac motion is minimal, providing datasets for further analysis. If the quality of diastolic datasets is not satisfactory additional reconstruction windows can be made in end-systolic phases, contributing to image quality. The continuous data acquisition also gives the opportunity to edit the ECG signal when extrasystole's or premature beats occurs during scanning. Persistent irregular heart rhythm like atrial fibrillation still precludes the accurate use of CTCA.

Scan coverage

Especially with the release of the 16 slice CT scanners, a manageable breath hold of ± 18 seconds was possible for nearly all patients (4 slice MSCT scanner: 40 seconds). Total scan time of current 64-slice scanners is between 8 -13 seconds.

THE DIAGNOSTIC PERFORMANCE OF THE MSCT SCANNER

4 slice scanner

The initial results of stenosis detection with the 4 slice scanners showed promising results. However a considerable number of segments had to be excluded from analysis due to poor image quality, making this scanner not robust enough for clinical cardiac implementation.

16 slice scanner

The major improvement of the 16 slice scanner was the lowering of total scan time from approximately 40 sec to 18 sec making an appropriate breath hold more feasible. Furthermore, these scanners had improved temporal and spatial resolution. All 16-slice studies classified coronary lesions with a minimum lumen diameter reduction of 50% as determined by quantitative coronary angiography (QCA) as a significant coronary obstruction. Assessment of significant lesions yielded a sensitivity of 87% (range 67%-96%), a specificity of 96% (range 79-98%), a positive predictive value of 81% (range 64%-95%) and a negative predictive value of 97.5% (range 94-99%). But up to 8% of segments were excluded because of poor image quality, either due to motion artefacts or extensive calcifications.

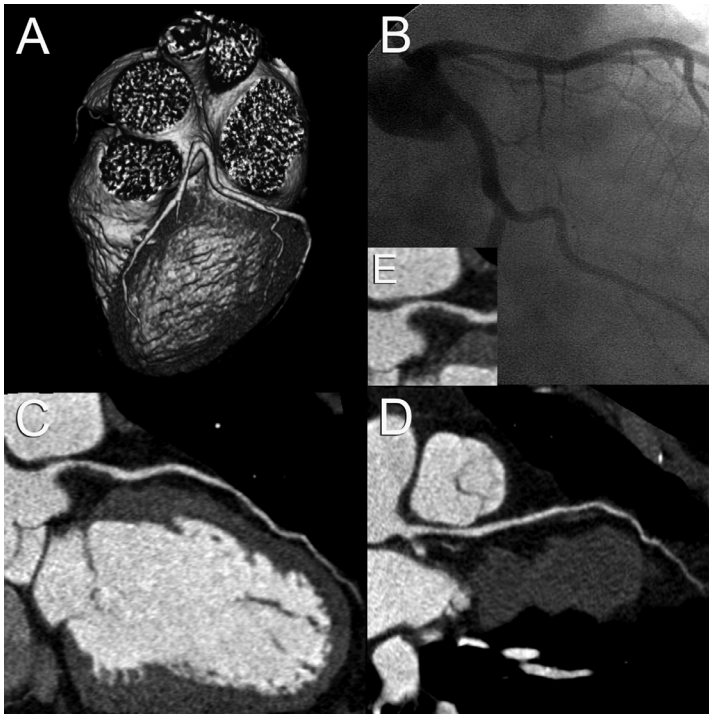


Figure 1 Volume-rendered CTCA image (A) reveals the anatomy of the left coronary artery of a 50 year-old patient who presented with unstable angina. His total calcium score was zero. Two curved multiplanar reconstructions (C,D) disclose a significant stenosis in the proximal left anterior descending coronary artery which was corroborated by CCA (B). In the inset the non-calcified significant plaque is displayed (E). (A full color version of this illustration can be found in the color section).

64 slice scanner

The 64-slice CT-scanner provides a major improvement in image quality and robustness of CT-coronary angiography. The assessability of the coronary tree is significantly increased and includes all major coronary segments as well as

Table 1 Diagnostic performance of 64-MSCT for detection of significant coronary stenosis (luminal diameter > 50%).

Author	Year	N	Segmental analysis				
			Excl.%	Sensitivity %	Specificity %	PPV %	NPV %
Leschka	2005	1005	0	94	97	87	99
Raff	2005	935	12	86	95	66	98
Leber	2005	732	0	76	97	75	97
Mollet	2005	725	0	99	95	76	100
Ropers	2006	1083	4	93	97	56	100
Schuijf	2006	842	1,2	85	98	82	99
TOTAL (weighted)		5322	2,9	90	97	76	99

larger side branches. The 64-slice MSCT scanner has a spatial resolution of 0.4 x 0.4 x 0.4 and a temporal resolution of 330 – 400 msec (tube rotation speed) which has reduced the scan acquisition time and hence the single breath hold time to 6 – 13 seconds.

The diagnostic performance of the 64-row (slice) MSCT scanner is presented in table 1. The number of inevaluable coronary segments is reduced (compared to 16-slice CT scanners) to ~ 3%, while 3 studies did not exclude any coronary segments from analysis. The sensitivity is 90% (range 76%-99%), specificity 97% (range 95%-98%), the predictive value 76% (range 56%-87%) and negative predictive value 99% (range 97%-100%) (2-7) (Figure1). These data show that current 64-slice MSCT scanners are close to becoming a reliable alternative to invasive diagnostic coronary angiography. However, before widespread clinical use multicenter studies of CTCA in a wide spectrum of populations, including lower risk patients should be performed.

POST REVASCULARIZATION IMAGING

Stents

Although the introduction of the drug eluting stents has reduced restenosis rate considerably, clinically driven target vessel revascularisation occurs in approximately ~8% of patients compared to ~15% of patients with bare metal stents (8). Chest discomfort after percutaneous coronary intervention is relatively common and a non invasive evaluation for stent restenosis would be highly desirable. However, coronary stents are difficult to assess with CTCA due to stent related high density artefacts. These artefacts tend to enlarge the apparent size of the stent struts, obscuring the visualization of the in-stent lumen. This “blooming artefact” caused by a combination of partial volume and beam hardening, is increased in smaller and stents of higher density.

Studies using 16 slice scanners for detecting in-stent restenosis reported sensitivity and specificity values of 54%-100% and 88%-100%, respectively (9-14). Improved spatial resolution of the 64 slice scanners should allow more accurate assessment in stent restenosis and further studies are awaited.

Patients undergoing left main stenting are generally recommended to have surveillance CCA at 3-6 months. Due to larger diameter stents used in the left main coronary artery CTCA may be particularly suitable for LM stent follow up. Gilard et al. and Van Mieghem et al. reported a good diagnostic accuracy in excluding in-stent restenosis in left main stents (15,16).

Some studies assessing stent patency used the presence of a distal run-off as an indicator of stent patency. However, this criterion should not be used as distal coronary vessels can be filled retrogradely by collateral filling. Newer generation 64 slice CTCA should allow more accurate assessment of the intra-stent coronary lumen throughout the coronary tree.

Coronary artery bypass grafting

Coronary artery bypass grafts are relatively easy to visualise with CTCA as motion is limited, the presence of calcifications in grafts is usually sparse and the size of grafts is large compared to native coronaries (17). However previous scanners were limited by a modest temporal resolution and a long scan time and breath hold. Faster rotating scanners and more and thinner detectors resulted in a better temporal and spatial resolution and shorter scan time diminishing the limitations of post-CABG patients evaluation (18-20). Two recent papers by Pache and Malagutti with 64 slice scanners yielded an excellent diagnostic accuracy to detect significant graft lesions or occlusions (21,22). Complex graft anatomy may also be clearly delineated by CTCA. However, complete angiographic evaluation of post-CABG patients includes assessment of the grafts and the native coronary arteries, which often remains challenging due to the presence of extensive calcifications, stents and surgical clips.

LIMITATIONS AND PITFALLS

MSCT-coronary angiography is feasible in patients with a stable heart rhythm. The breath hold of 8 to 13 seconds with 64 slice scanners is manageable for most patients. A rigorous explanation and practise of the breath hold manoeuvre as well as a description of the warm sensation they are going to perceive during contrast injection will minimize breathing artefacts.

Irregular heart rhythm creates artefacts due to the inconsistent length of the R-R interval and results in a deterioration of image quality. However, an occasional extrasystolic or premature beat can be overcome by editing the ECG signal obtained during scanning. Atrial fibrillation remains a contra-indication for performing the scan.

Other limitations of CT angiography in general are contra-indications to X-ray exposure (e.g. pregnancy) and contra-indications for iodinated contrast material (e.g. allergy, impaired renal function, hyperthyroidisms).

Reduction of heart rate during the CT angiography is mandatory for acquiring high-quality images and ideally the heart rate should be kept below 70 bpm. Oral or IV beta blockers and/or benzodiazepines can reduce the heart rate below this threshold. If the heart rate exceeds this upper limit the prevalence of motion artefacts increases. These motion artefacts occur most frequently in the mid right coronary artery, since this segment moves most rapidly. Adequate image quality in this segment is often a guarantee for good image quality in the rest of the coronary tree.

The presence of significant calcification is problematic for the correct interpretation of CTCA. Calcium creates blooming artefacts, which obscure the visualization of the underlying non-calcified plaque or lumen. Sensitivity and negative predictive value in studies detecting obstructive coronary artery disease remain high, but specificity and positive predictive value decreases, leading to an overall decrease in accuracy.

This raises the question whether CTCA should be avoided when the calcium score exceeds a certain threshold. A high calcium score is associated with increased risk of obstructive coronary stenosis with CCA. However the calcium score is influenced by age and gender and there is no clear cut-off value. The total calcium score may also be somewhat misleading, because calcium distributed along the entire coronary tree may not interfere with the interpretation of the CTCA examination, while a single heavily calcified plaque can make interpretation difficult.

Although a high calcium score may reduce accuracy of CTCA and also its usefulness as a gate-keeper for CCA, it provides additional information to calcium scoring such as direct visualisation of the coronary lesions and plaque burden and characteristics which may influence patient management.

A disadvantage of CTCA is a higher radiation dose compared to conventional invasive coronary angiography. The evolution of 4-slice to 64 slice MSCT scanners has seen an improvement in spatial and temporal resolution making the CT scanners more robust. The cost of having more and thinner detectors lies in a decrease of the contrast to noise ratio. To compensate for this loss the radiation dose has to be increased. Hausleiter et al. compared radiation doses of 16 and 64 slice CT coronary angiography. The estimated effective radiation exposure was 10.6 ± 1.2 mSv and 14.8 ± 1.8 mSv in 16 and 64 slice MSCT respectively (120kV, 870mAs). This study used ECG dependent tube modulation, which reduced the tube current by 80% in systole, resulting in a reduction in the radiation dose of approximately 40% (23).

An issue of concern with ECG dependent tube modulation is its dependence on a regular heart rhythm. Arrhythmia including premature ventricular beats may cause an inappropriate reduction in tube output during diastole leading to a decline in image quality. Alternative methods that effectively reduce the radiation dose without impacting on image quality should be further developed.

To allow differentiation of the tissue surrounding the coronaries an intravenous bolus injection of iodinated contrast material is administered into an antecubital vein. Depending of the entire scan length a bolus of 70- 100 ml contrast is given. The risk for contrast allergies therefore remains.

CLINICAL APPLICATION

The diagnostic performance of 64 slice CT-scanners to detect coronary stenoses is high in patients who have a high prevalence of coronary artery disease. The negative predictive value allows exclusion of significant obstructive coronary artery disease in this patient group. However similar data in lower risk populations are lacking. These studies are necessary as CTCA is likely to be most useful as a screening tool in lower risk populations. In addition, the role of CTCA in patients with unstable angina or non-ST-segment elevation myocardial infarction is largely unknown.

Other evolving clinical application include the follow-up of patients after coronary bypass surgery and left main stenting, exclusion of significant coronary artery disease in patients scheduled for valve surgery, evaluation of coronary anomalies and visualization of chronic total coronary occlusions prior to percutaneous coronary intervention.

FUTURE PERSPECTIVE

MSCT imaging is emerging as the most promising imaging modality for non-invasive coronary atherosclerotic disease detection. The possibility of identifying or excluding significant stenotic lesions, measurement of atherosclerotic plaque burden and characterization of plaque components makes this imaging modality very enticing.

The qualities of CCA with its high spatial resolution and its high temporal resolution providing information about coronary blood flow will probably not be met. Yet, MSCT coronary angiography may become an acceptable alternative to invasive diagnostic coronary angiography.

The main challenges for MSCT coronary imaging are the temporal and spatial resolution. Novel technical advances have been developed to address these issues by either increasing the number

of detector rows or by increasing the X-ray tube rotational speed. A 256 detector CT-scanner has been introduced which allows assessment of LV-function and the proximal coronary arteries but currently the performance is severely limited by the long-scan time and temporal resolution (24,25).

The next generation dual-source CT scanners, using 2 x-ray sources simultaneously, will allow scanning at higher heart rates due to the improved temporal resolution of 83 ms, thereby avoiding or diminishing the use of beta-blockers for heart rate reduction (26,27). The radiation exposure can be limited with the ultra fast dual-source CT scanner with its heart rate dependant pitch and use of x-ray tube modulation compared to 64 slice CT scanning. Preliminary results on the accuracy of dual source CT scanners and the feasibility of scanning at higher heart rates will be published shortly.

REFERENCES

1. Scanlon PJ, Faxon DP, Audet AM, et al. ACC/AHA guidelines for coronary angiography. A report of the American College of Cardiology/American Heart Association Task Force on practice guidelines (Committee on Coronary Angiography). Developed in collaboration with the Society for Cardiac Angiography and Interventions. *J Am Coll Cardiol* 1999;33:1756-824.
2. Leschka S, Alkadhi H, Plass A, et al. Accuracy of MSCT coronary angiography with 64-slice technology: first experience. *Eur Heart J* 2005;26:1482-7.
3. Raff GL, Gallagher MJ, O'Neill WW, Goldstein JA. Diagnostic accuracy of noninvasive coronary angiography using 64-slice spiral computed tomography. *J Am Coll Cardiol* 2005;46:552-7.
4. Leber AW, Knez A, von Ziegler F, et al. Quantification of obstructive and nonobstructive coronary lesions by 64-slice computed tomography: a comparative study with quantitative coronary angiography and intravascular ultrasound. *J Am Coll Cardiol* 2005;46:147-54.
5. Mollet NR, Cademartiri F, van Mieghem CA, et al. High-resolution spiral computed tomography coronary angiography in patients referred for diagnostic conventional coronary angiography. *Circulation* 2005;112:2318-23.
- * *One of the first papers which reported on the high diagnostic accuracy of 64 slice CT angiography in detecting coronary stenosis.*
6. Ropers D, Rixe J, Anders K, et al. Usefulness of multidetector row spiral computed tomography with 64- x 0.6-mm collimation and 330-ms rotation for the noninvasive detection of significant coronary artery stenoses. *Am J Cardiol* 2006;97:343-8.
7. Schuijf JD, Pundziute G, Jukema JW, et al. Diagnostic accuracy of 64-slice multislice computed tomography in the noninvasive evaluation of significant coronary artery disease. *Am J Cardiol* 2006;98:145-8.

8. Ong AT, van Domburg RT, Aoki J, Sonnenschein K, Lemos PA, Serruys PW. Sirolimus-eluting stents remain superior to bare-metal stents at two years: medium-term results from the Rapamycin-Eluting Stent Evaluated at Rotterdam Cardiology Hospital (RESEARCH) registry. *J Am Coll Cardiol* 2006;47:1356-60.
9. Schuijf JD, Bax JJ, Jukema JW, et al. Feasibility of assessment of coronary stent patency using 16-slice computed tomography. *Am J Cardiol* 2004;94:427-30.
10. Cademartiri F, Mollet N, Lemos PA, et al. Usefulness of multislice computed tomographic coronary angiography to assess in-stent restenosis. *Am J Cardiol* 2005;96:799-802.
11. Gilard M, Cornily JC, Pennec PY, et al. Assessment of coronary artery stents by 16 slice computed tomography. *Heart* 2006;92:58-61.
12. Kitagawa T, Fujii T, Tomohiro Y, et al. Noninvasive assessment of coronary stents in patients by 16-slice computed tomography. *Int J Cardiol* 2006;109:188-94.
13. Hong C, Chrysant GS, Woodard PK, Bae KT. Coronary artery stent patency assessed with in-stent contrast enhancement measured at multi-detector row CT angiography: initial experience. *Radiology* 2004;233:286-91.
14. Ohnuki K, Yoshida S, Ohta M, et al. New diagnostic technique in multi-slice computed tomography for in-stent restenosis: pixel count method. *Int J Cardiol* 2006;108:251-8.
15. Gilard M, Cornily JC, Rioufol G, et al. Noninvasive assessment of left main coronary stent patency with 16-slice computed tomography. *Am J Cardiol* 2005;95:110-2.
16. Van Mieghem CA, Cademartiri F, Mollet NR, et al. Multislice Spiral Computed Tomography for the Evaluation of Stent Patency After Left Main Coronary Artery Stenting. A Comparison With Conventional Coronary Angiography and Intravascular Ultrasound. *Circulation* 2006;114:878-881.
- * *This paper nicely illustrates the potential clinical use of CT coronary angiography in the follow-up of patients after left main coronary stenting.*
17. Nieman K, Pattynama PM, Rensing BJ, Van Geuns RJ, De Feyter PJ. Evaluation of patients after coronary artery bypass surgery: CT angiographic assessment of grafts and coronary arteries. *Radiology* 2003;229:749-56.
18. Martuscelli E, Romagnoli A, D'Eliseo A, et al. Evaluation of venous and arterial conduit patency by 16-slice spiral computed tomography. *Circulation* 2004;110:3234-8.
19. Schlosser T, Konorza T, Hunold P, Kuhl H, Schmermund A, Barkhausen J. Noninvasive visualization of coronary artery bypass grafts using 16-detector row computed tomography. *J Am Coll Cardiol* 2004;44:1224-9.
20. Anders K, Baum U, Schmid M, et al. Coronary artery bypass graft (CABG) patency: assessment with high-resolution submillimeter 16-slice multidetector-row computed tomography (MDCT) versus coronary angiography. *Eur J Radiol* 2006;57:336-44.
21. Pache G, Saueressig U, Frydrychowicz A, et al. Initial experience with 64-slice cardiac CT: non-invasive visualization of coronary artery bypass grafts. *Eur Heart J* 2006;27:976-80.

22. Malagutti P, Nieman K, Meijboom WB, et al. Use of 64-slice CT in symptomatic patients after coronary bypass surgery: evaluation of grafts and coronary arteries. *Eur Heart J* 2006.
 - ★ *This paper provides a thorough analysis of the use of 64 slice CT scanners in the diagnosis of obstructive coronary artery disease in coronary bypass grafts as in the native coronaries.*
23. Hausleiter J, Meyer T, Hadamitzky M, et al. Radiation dose estimates from cardiac multislice computed tomography in daily practice: impact of different scanning protocols on effective dose estimates. *Circulation* 2006;113:1305-10.
24. Funabashi N, Yoshida K, Tadokoro H, et al. Three dimensional segmented myocardial perfusion images by selective intracoronary injection of contrast using 256 slice cone beam computed tomography. *Heart* 2005;91:1349-51.
25. Mori S, Kondo C, Suzuki N, et al. Volumetric cine imaging for cardiovascular circulation using prototype 256-detector row computed tomography scanner (4-dimensional computed tomography): a preliminary study with a porcine model. *J Comput Assist Tomogr* 2005;29:26-30.
26. Achenbach S, Ropers D, Kuettner A, et al. Contrast-enhanced coronary artery visualization by dual-source computed tomography--initial experience. *Eur J Radiol* 2006;57:331-5.
27. Flohr TG, McCollough CH, Bruder H, et al. First performance evaluation of a dual-source CT (DSCT) system. *Eur Radiol* 2006;16:256-68.
 - ★ *This paper demonstrates the concept and potential of dual-source computed tomography.*

3

Spiral Multislice CT Coronary Angiography in 2006: A Current Status Report

Clinical Cardiology.
2007 Sep 5;30(9):437-442

P.J. de Feyter MD, PhD^{1,2}
W.B. Meijboom MD^{1,2}
A. Weustink MD^{1,2}
C. van Mieghem, MD^{1,2}
N.R.A. Mollet MD, PhD^{1,2}
E. Vourvouri MD, PhD²
K. Nieman, MD, PhD¹
F. Cademartiri MD, PhD²

¹Department of Cardiology

²Department of Radiology

ABSTRACT

Multislice Computed Tomography coronary angiography (MSCT-CA) has emerged as a powerful non-invasive diagnostic modality to visualize the coronary arteries and to detect significant coronary stenoses. The latest generation 64-slice CT scanners is a robust technique which allows high-resolution, isotropic, nearly motion-free coronary imaging. Coronary stenoses are detected with high sensitivity and a normal scan accurately rules out the presence of a coronary stenosis. With the introduction of further novel concepts in CT-technology one may expect that MSCT-CA will become a clinically used diagnostic tool.

INTRODUCTION

The development of computed tomography (CT) has significantly improved non-invasive imaging, initially of non-moving organs of the body, and recently also of the heart. Electron Beam Computed Tomography (EBCT), a technique especially designed to examine the heart, was introduced in the early 80ties. Nowadays these scanners are largely replaced by spiral Multislice CT scanners which can detect coronary stenoses and non-obstructive coronary plaques with high diagnostic accuracy (1,2). This report highlights the current status of MSCT-CA, discusses its limitations and speculates about the role and future of MSCT-CA in clinical practice.

HIGH-QUALITY, MOTION FREE CT IMAGES: SPATIAL AND TEMPORAL RESOLUTION

Coronary imaging requires the highest technical demands of any non-invasive diagnostic modality because of the small size of the coronary arteries, the continuous motion during cardiac contraction and the inevitable respiratory motion. The spatial resolution should be as high as possible and ideally isotropic voxel imaging should be achieved. Isotropic imaging means that a voxel has the same size in all dimensions and is mandatory to reconstruct high-quality images in all planes. The spatial resolution of current CT-scanners is 0.4 mm^3 . High temporal resolution is mandatory to obtain motion-free image quality. The temporal resolution is defined as the required time for data acquisition per slice, and for cardiac spiral CT it refers to the duration of the reconstruction window during the end-diastolic phase of each heart cycle (Figure 1). The temporal resolution depends on the X-ray tube rotation-time and is equal to half of the X-ray tube rotation-time. Current 64-slice spiral CT-scanners have a temporal resolution of 165 to 200 msec.

MSCT ACQUISITION MODES AND ECG - SYNCHRONIZATION

The CT-data necessary for the reconstruction of the CT-imaging are acquired either in sequential mode or spiral mode. In the sequential mode the scanner acquires the data of one slice, after which the table (and thus the patient) is advanced to the next plane position to acquire the next data of an adjacent slice (slice-by-slice acquisition or stop-and-shoot principle). In the spiral mode, the CT-data are acquired continuously while the table (and thus the patient) moves at a constant speed.

The CT-data used for image reconstruction are preferentially obtained in the relatively motion-free mid-to-end diastolic phase of the cardiac cycle. This requires simultaneous recording of the ECG signal during the CT-scan. Prospective ECG-triggering is used in the sequential model

to prospectively acquire the CT-data in a certain predefined cardiac phase (in general the mid-to-end diastolic phase)(Figure 1). A retrospectively ECG-gated technique is used in the spiral mode which allows to select retrospective reconstruction of CT-data in any, but preferentially the mid-to-end diastolic phase of the cardiac cycle (Figure 1). Using this technique, data is acquired throughout the entire cardiac cycle, but only data of a small part of the cardiac cycle is used for image reconstruction after the scan has been performed. The sequential mode with prospective ECG-triggering is used for CT calcium scoring, and the spiral mode with retrospective ECG-gating is used for contrast-enhanced CT coronary angiography.

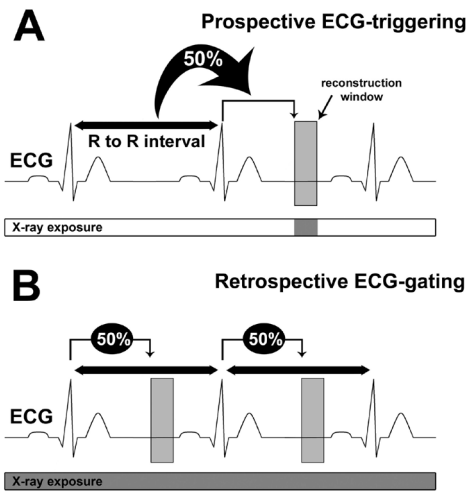


Figure 1. ECG-synchronized image reconstruction.

- A: Sequential scan protocols use prospective ECG-triggering to synchronize the data acquisition to the motion of the heart. Based on the measured duration of the previous heart cycles, the scan of one or more slices is initiated at a pre-specified moment after the R-wave, for instance at 50% of the previous R-to-R intervals.
- B: Spiral CT scanners acquire data continuously and record the patients ECG during the scan. Isocardiophasic images are reconstructed using retrospective ECG-gating. The reconstruction window can be positioned anywhere within the R-to-R interval, and images can be created during any phase, for instance at 50%. The duration of the reconstruction window determines the temporal resolution.

SCAN TIME

On average the cranio-caudal size of the heart measures 10 to 12 cm, but can be larger with ischemic heart disease. MSCT should cover the entire heart. The scan time is inversely related to the X-ray tube rotation speed and number of detector-rows (or reconstructed slices). Current CT-scanners have an X-ray tube rotation time of 330 to 400 msec and number of detectors rows (slices) of 64, which results in a scan time of less than 10 seconds.

TISSUE CONTRAST AND IMAGE QUALITY

The differences in X-ray attenuation between non-enhanced coronary blood, the vessel wall and epicardial fat are small and therefore hardly visible by MSCT imaging. An intravenous bolus injection of 80 to 100 ml of high iodinated X-ray contrast is administered to allow differentiation

of the contrast-enhanced coronary lumen from the coronary wall and coronary atherosclerotic plaques, which then permits detection of coronary lumen obstructions and non-obstructive coronary plaques (3).

HEART-RATE RELATED IMAGE QUALITY

CT-data used for reconstruction of coronary images are usually obtained from the relative motion-free mid-to-end diastolic phase of the cardiac cycle to reduce motion-artifacts. The duration of the motion-sparse diastolic phase is directly related to the heart rate, since faster heart rates have a shorter diastolic period. Therefore heart rates more than 70 b.p.m. are reduced to prolong the relative motion-free mid diastolic phase, by administration of an oral or intravenous β -blocker prior to the CT-investigation. It has been shown that the use of β -blockers results in better quality of the CT-coronary images (3).

RADIATION EXPOSURE AND IMAGE QUALITY

The radiation exposure (i.e. the effective dose) of diagnostic invasive coronary angiography is approximately 6.0 mSv. The radiation exposure during Multislice CT scanning using a gated retrospective reconstruction protocol is considerably higher. The radiation exposure of the 64-slice CT scanner using a continuous scan mode is estimated as an effective dose of 15.2 mSv for males and 21.4 mSv for females (4). Reduction of the X-ray radiation exposure can be achieved by the use of an ECG controlled X-ray tube current modulation. This feature reduces the tube current during the systolic phase and gives a full X-ray tube current only during the diastolic phase of the cardiac cycles, when the coronary image is reconstructed. This feature can reduce the effective dose by approximately 40% in slow heart rates.

64-SLICE SPIRAL CT SCANNER

The 64-slice CT-scanner boosted a major improvement in image quality and robustness of CT-coronary angiography. The assessability of the coronary tree was significantly increased and now included almost all major coronary segments and the larger side branches. The 64-slice MS-CT scanner has a spatial resolution of $0.4 \times 0.4 \times 0.4$ and a temporal resolution of 330 – 400 msec (tube rotation speed) which has reduced the total scan time and hence the single breath hold time to 6 – 12 seconds.

The diagnostic performance of the 64-slice spiral CT scanner to detect a significant stenosis is presented in Table 1 (5-11). The analysis was done per coronary segment according to the 17 coronary segment model of the AHA. The number of inevaluable coronary segments is reduced to an average of 4.7% while 3 studies did not exclude any coronary segment from analysis. The sensitivity was 89% (range 76%-99%), specificity 96% (range 95%-97%), the predictive value 78% (range 56%-88%) and negative predictive value 98.5% (range 96%-100%). The patient-based analysis (any disease per patient) is presented in Table 2.

Table 1. Diagnostic performance of 16-MSCT for detection of significant coronary stenosis (luminal diameter > 50%)

Author	NP	Excl. Segm. %	Sensitivity %	Specificity %	PPV %	NPV %
Nieman	58	0	95	86	80	97
Mollet ('04)	127	7	92	95	79	98
Martuscelli	72	16	89	98	90	98
Kuettner ('04)	58	21	72	97	72	97
Leta	31	12	75	91	65	94
Hoffmann** (2004)	33	17	67	95	64	96
Mollet ('05)	51	0	95	98	87	99
Kuettner	72	7	82	98	86	97
Cademartiri	40	0	96	96	86	99
Schuijf	45	6	98	97	89	99
Kefer	52	0	82	79	46	95
Hoffmann	103	7	95	98	95	99
Kuettner	120	7	85	98	93	95
Achenbach	50	4	94	96	68	99
(weighted)	912	7.8	87	96	81	97.5

** stenosis > 70%

PPV = positive predictive value

NPV = negative predictive value

CURRENT ROLE OF MSCT-CA IN CLINICAL PRACTICE

The presence of coronary anomalies can be adequately assessed by MSCT-CA (Figure 2). It has been shown that the diagnostic performance of 64 slice CT-scanners to detect coronary stenoses is high in patients who have a high prevalence of coronary artery disease (Figure 3). In these patients the negative predictive value of 64 CT-scanners, as was shown in all published reports, is very high allowing to exclude the presence of significant coronary artery disease with a very high accuracy. However, there is no or only little information about the diagnostic performance of CT coronary angiography in patients with a low to intermediate likelihood of coronary artery disease.

Table 2. Diagnostic performance of 64-MSCT for detection of significant coronary stenosis (luminal diameter > 50%)

Author	Year	NP	Patient-based analysis			
			Sensitivity %	Specificity %	PPV %	NPV %
Leschka	2005	67	100	100	100	100
Leber	2005	45	88	85	88	85
Raff	2005	70	95	90	93	93
Mollet	2005	51	100	92	97	100
Ropers	2006	81	96	91	83	98
Schuijf	2006	60	94	97	97	93
TOTAL (weighted)		374	96	92	94	95

* 4 patients were excluded

In addition the role of MSCT-CA in patients with unstable angina or non-ST-segment elevation myocardial infarction is beginning to evolve (Figure 4).

Spiral CT coronary angiographic techniques are constantly improving and should result in more reliable coronary imaging which will further affect (evolving) indications.

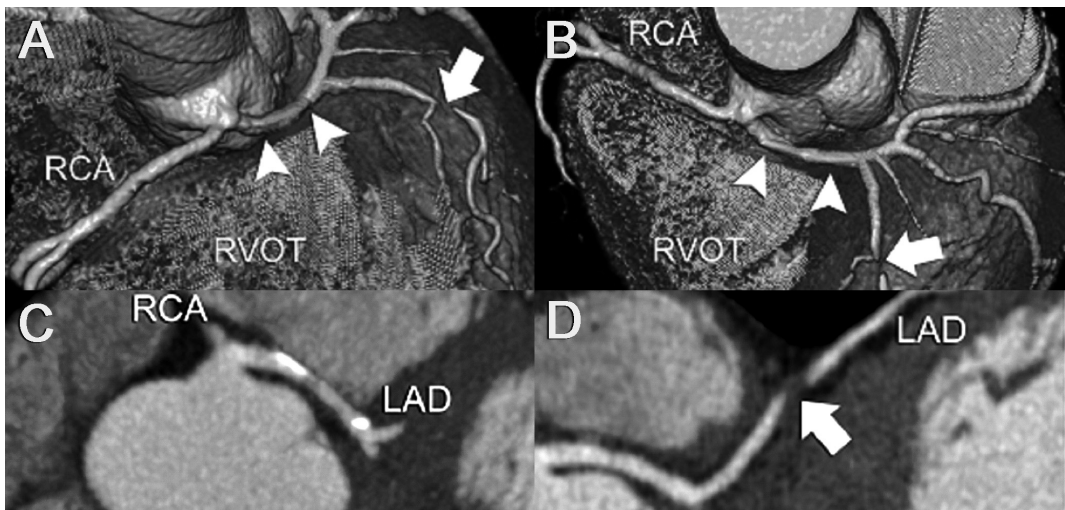


Figure 2: The left main and right coronary artery (RCA) arise from the right aortic sinus A-D. The anomalous left main coronary artery runs between the aorta and pulmonary trunk (arrowheads). Note also the severe stenosis (arrow) of the left anterior descending artery (LAD). RVOT: right ventricular outflow tract. (A full color version of this illustration can be found in the color section).

SPIRAL CT FOR STENT EVALUATION

Coronary stents are difficult to assess with spiral CT stent related high density artifacts. Due to the “blooming” artifact the apparent size of the stent struts is enlarged thereby obscuring the visualization of the in-stent lumen. Sixteen spiral CT is reliable to detect stent occlusion but non-occlusive in-stent restenosis or the more subtle in-stent neo-intimal hyperplasia remains largely unidentified. Improved spatial resolution of 64-slice scanners should allow more accurate assessment of in-stent restenosis, but published reports in humans are still lacking.

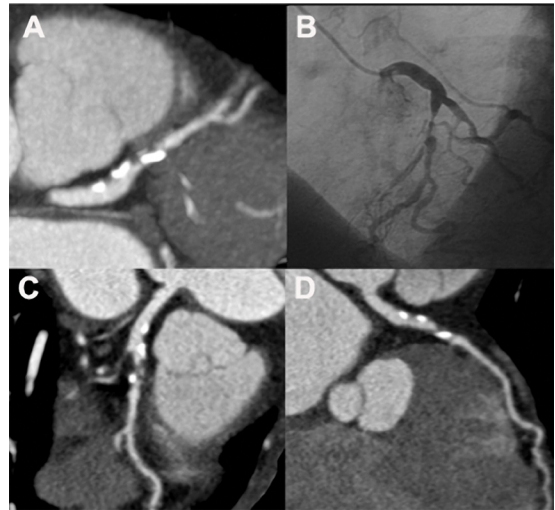


Figure 3: Curved multiplanar reconstructed images demonstrate the presence of a significant lesion in the LAD (A,C,D). The corresponding diagnostic invasive coronary angiogram (B) confirms the presence of a significant coronary stenosis in the proximal LAD. The bright dots represents coronary calcium deposits

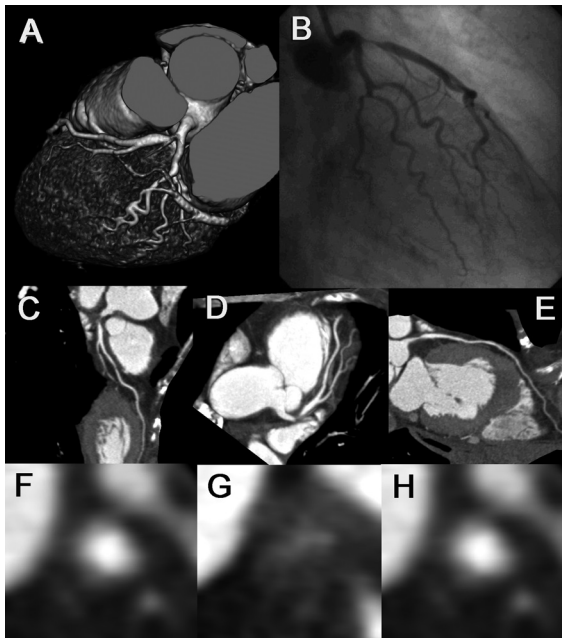


Figure 4: CT coronary angiogram and corresponding conventional angiogram of the left coronary artery in a patient presenting with unstable angina. Note that the volume-rendered images (A) provide an excellent anatomic overview of the coronary arteries but should not be used to score the presence and degree of coronary stenoses. Two detailed curved multiplanar reconstructed (cMPR) CT image (C, E) and a maximum-intensity projection reveal the presence of a significant stenosis located at the proximal LAD, which was confirmed on the conventional angiogram (B). Cross-sectional CT images show a large noncalcific plaque (G) and a normal coronary lumen of the left main (F) en distal LAD (H). (A full color version of this illustration can be found in the color section).

MSCT: POST-CABG EVALUATION

Since the motion of coronary bypasses is limited and the size is relatively large it is relatively easy for MSCT to visualize these grafts. The sensitivity and specificity for graft patency of 16-slice spiral CT

was 98% for both vein and arterial grafts with a PPV of 92% and NPV of 99% after exclusion of 6% non-evaluable segments Table 3 (12-17). Stenosis assessment in grafts was less accurate and the sensitivity, specificity, PPV and NPV was 91%, 98%, 83% and 99% respectively. Initial experi-

Table 3. 16 slice spiral CT for assessment of vessel occlusion in bypass grafts

Author	NP	Excluded segm.	Sensitivity %	Specificity %	PPV %	NPV %
Martuscelli	96	12	100	100	100	100
Chiurlia	52	1	100	100	100	100
Schlosser	48	4	95	95	81	99
Yamamoto	42	4	93	100	33	100
Anders	32	0	100	98	96	100
Salm	25	8	100	93	100	99
TOTAL (weighted)	295	6	98	98	92	99

ence with the 64 spiral CT-scanner showed somewhat better results. The sensitivity, specificity, positive and negative predictive value was 96%, 100%, 100%, 98% respectively in a study of 64 patients (18).

LIMITATIONS OF SPIRAL CT CORONARY ANGIOGRAPHY

Persistent irregular heart rhythm such as atrial fibrillation and frequent extra systoles precludes the use of MSCT-CA. However, an occasional extra systole can be corrected by post-processing ECG-editing.

High-density material, such as calcified plaques or stents cause several image artifacts (e.g. blooming, partial voluming and beam hardening), which may hamper accurate assessment of the integrity of the coronary lumen. In particular, severe coronary calcifications do not allow inspection of the underlying coronary lumen, and cause misinterpretation. Moreover, coronary calcifications adjacent to a luminal obstruction may overestimate the severity of the obstruction.

FUTURE OF MSCT CORONARY ANGIOGRAPHY

The quality of current MSCT coronary imaging is still hampered by the limited temporal and spatial resolution. Novel technical advances have been developed to address these issues by either increasing the number of detector rows (slices) or by increasing the X-ray tube rotational speed. A 256 detector CT-scanner has been introduced which allows assessment of LV-function and the proximal coronary arteries but currently the performance is severely limited by the long-scan time

and poor temporal resolution(19).

A significant step forward has been the very recent introduction of the Dual-source 64 slice CT-scanner which has decreased the temporal resolution (to 83 msec) by use of two X-ray sources and two detectors, while the shorter scan time, in combination with a shorter ECG-gated maximal X-ray tube output should significantly lower the radiation dose (20,21). The improved temporal resolution allows “motion-free” imaging also at higher heart rates thus obviating the need for pre-investigational β -blockade. Clinical evaluation of this new CT-technology in a wide spectrum of patients should reveal whether this degree of expected image-improvement will suffice for clinical decision making in an individual presenting with chest pain.

Further novel technical approaches requiring many years will be needed to resolve the problems associated with coronary calcification (subtraction techniques using dual-X-ray sources?) and arrhythmia's (volumetric imaging during one heart beat).

REFERENCES

1. Ohnesorge B, Flohr T, Becker C, Kopp AF, Schoepf UJ, Baum U, Knez A, Klingenberg-Regn K, Reiser MF. Cardiac imaging by means of electrocardiographically gated multisection spiral CT: initial experience. *Radiology* 2000;217:564-71.
2. Becker CR, Knez A, Leber A, Hong C, Treede H, Wildhirt S, Ohnesorge B, Flohr T, Schoepf UJ, Reiser MF. [Initial experiences with multi-slice detector spiral CT in diagnosis of arteriosclerosis of coronary vessels]. *Radiologe* 2000;40:118-22.
3. Nieman K, Rensing BJ, van Geuns RJ, Vos J, Pattynama PM, Krestin GP, Serruys PW, de Feyter PJ. Non-invasive coronary angiography with multislice spiral computed tomography: impact of heart rate. *Heart* 2002;88:470-4.
4. Jakobs TF, Becker CR, Ohnesorge B, Flohr T, Suess C, Schoepf UJ, Reiser MF. Multislice helical CT of the heart with retrospective ECG gating: reduction of radiation exposure by ECG-controlled tube current modulation. *Eur Radiol* 2002;12:1081-6.
5. Leschka S, Alkadhi H, Plass A, Desbiolles L, Grunenfelder J, Marincek B, Wildermuth S. Accuracy of MSCT coronary angiography with 64-slice technology: first experience. *Eur Heart J* 2005;26:1482-7.
6. Leber AW, Knez A, von Ziegler F, Becker A, Nikolaou K, Paul S, Wintersperger B, Reiser M, Becker CR, Steinbeck G, Boekstegers P. Quantification of obstructive and nonobstructive coronary lesions by 64-slice computed tomography: a comparative study with quantitative coronary angiography and intravascular ultrasound. *J Am Coll Cardiol* 2005;46:147-54.
7. Raff GL, Gallagher MJ, O'Neill WW, Goldstein JA. Diagnostic accuracy of noninvasive coronary angiography using 64-slice spiral computed tomography. *J Am Coll Cardiol* 2005;46:552-7.

8. Mollet NR, Cademartiri F, van Mieghem CA, Runza G, McFadden EP, Baks T, Serruys PW, Krestin GP, de Feyter PJ. High-resolution spiral computed tomography coronary angiography in patients referred for diagnostic conventional coronary angiography. *Circulation* 2005;112:2318-23.
9. Ropers D, Rixe J, Anders K, Kuttner A, Baum U, Bautz W, Daniel WG, Achenbach S. Usefulness of multidetector row spiral computed tomography with 64- x 0.6-mm collimation and 330-ms rotation for the noninvasive detection of significant coronary artery stenoses. *Am J Cardiol.* 2006 Feb 1;97(3):343-8. Epub 2005 Dec 1.
10. Schuijf JD, Pundziute G, Jukema JW, Lamb HJ, van der Hoeven BL, de Roos A, van der Wall EE, Bax JJ. Diagnostic accuracy of 64-slice multislice computed tomography in the noninvasive evaluation of significant coronary artery disease. *Am J Cardiol.* 2006 Jul 15;98(2):145-8.
11. Ong AT, Serruys PW, Mohr FW, Morice MC, Kappetein AP, Holmes DR Jr, Mack MJ, van den Brand M, Morel MA, van Es GA, Kleijne J, Koglin J, Russell ME. The SYNergy between percutaneous coronary intervention with TAXus and cardiac surgery (SYNTAX) study: design, rationale, and run-in phase. *Am Heart J.* 2006 Jun;151(6):1194-204.
12. Martuscelli E, Romagnoli A, D'Eliseo A, Tomassini M, Razzini C, Sperandio M, Simonetti G, Romeo F, Mehta JL. Evaluation of venous and arterial conduit patency by 16-slice spiral computed tomography. *Circulation.* 2004 Nov 16;110(20):3234-8.
13. Chiurlia E, Menozzi M, Ratti C, Romagnoli R, Modena MG. Follow-up of coronary artery bypass graft patency by multislice computed tomography. *Am J Cardiol.* 2005 May 1;95(9):1094-7.
14. Schlosser T, Konorza T, Hunold P, Kuhl H, Schmermund A, Barkhausen J. Noninvasive visualization of coronary artery bypass grafts using 16-detector row computed tomography. *J Am Coll Cardiol.* 2004 Sep 15;44(6):1224-9.
15. Yamamoto M, Kimura F, Niinami H, Suda Y, Ueno E, Takeuchi Y. Noninvasive assessment of off-pump coronary artery bypass surgery by 16-channel multidetector-row computed tomography.
16. Anders K, Baum U, Schmid M, Ropers D, Schmid A, Pohle K, Daniel WG, Bautz W, Achenbach S. Coronary artery bypass graft (CABG) patency: assessment with high-resolution submillimeter 16-slice multidetector-row computed tomography (MDCT) versus coronary angiography. *Eur J Radiol.* 2006 Mar;57(3):336-44.
17. Salm LP, Bax JJ, Jukema JW, Schuijf JD, Vliegen HW, Lamb HJ, van der Wall EE, de Roos A. Comprehensive assessment of patients after coronary artery bypass grafting by 16-detector-row computed tomography. *Am Heart J.* 2005 Oct;150(4):775-81.
18. Pache G, Saueressig U, Frydrychowicz A, Foell D, Ghanem N, Kotter E, Geibel-Zehender A, Bode C, Langer M, Bley T. Initial experience with 64-slice cardiac CT: non-invasive visualization of coronary artery bypass grafts. *Eur Heart J.* 2006 Apr;27(8):976-80. Epub 2006 Mar 9

19. Mori S, Kondo C, Suzuki N, Yamashita H, Hattori A, Kusakabe M, Endo M. Volumetric cine imaging for cardiovascular circulation using prototype 256-detector row computed tomography scanner (4-dimensional computed tomography): a preliminary study with a porcine model. *J Comput Assist Tomogr* 2005;29:26-30.
20. Flohr TG, McCollough CH, Bruder H, Petersilka M, Gruber K, Suss C, Grasruck M, Stierstorfer K, Krauss B, Raupach R, Primak AN, Kuttner A, Achenbach S, Becker C, Kopp A, Ohnesorge BM. First performance evaluation of a dual-source CT (DSCT) system. *Eur Radiol* 2006;16:256-268.
21. Achenbach S, Ropers D, Kuettner A, Flohr T, Ohnesorge B, Bruder H, Theessen H, Karakaya M, Daniel WG, Bautz W, Kalender WA, Anders K. Contrast-enhanced coronary artery visualization by dual-source computed tomography-Initial experience. *Eur J Radiol* 2006;57:331-5.

Addendum 1

Post-processing using multislice CT coronary angiography improves image interpretability in patients with fast heart-rates and heart-rate variations: a case-report

Journal of Cardiovascular Medicine.
2007 Dec;8(12):1088-90

Francesca Pugliese, MD^{1,2}
Filippo Albergiina, MD^{1,2}
Willem Bob Meijboom, MD^{1,2}
Roberto Malago', MD^{1,2}
Deepa Gopalan, MBBS²
Pim J. de Feyter, MD PhD^{1,2}

Departments of Cardiology/
Thoraxcenter¹ and Radiology²
Erasmus MC University
Medical Center Rotterdam
Rotterdam
the Netherlands

ABSTRACT

Image quality in coronary CT angiography is inversely related to heart rate. Heart rate variations are another cause of impaired image quality. We adapted the acquisition protocol to individual patient's heart rate. We reconstructed and post-processed images in a customized fashion to obtain diagnostic image quality of the right coronary artery in a patient with heart rate changes between 81 and 111 bpm during the scan. Flexibility of acquisition protocols and expert post-processing are helpful to improve the clinical reliability of coronary CT angiography.

INTRODUCTION

Coronary CT angiography is becoming a practical alternative to coronary catheterization in selected patient groups (1). However, the literature reports that image quality is inversely related to heart rate (2); diagnostic accuracy is higher at lower heart rates and deteriorates at higher heart rates (3). Likewise, heart rate variation during the scan may impair image quality heavily.

We show how we obtained diagnostic image quality of the right coronary artery with 64-slice CT angiography in a patient whose heart rate ranged from 81 to 111 beats per minute during the scan. The average heart rate was of 99 beats per minute.

HISTORY

A 42-year-old obese woman with Kawasaki disease diagnosed at 2 years of age and mental retardation presented with exertional palpitations. Rest ECG and stress testing were inconclusive for recent ischaemia. Noninvasive study of coronary arteries was performed with CT angiography. The patient had sinus heart rhythm and average heart rate was 88 beats per minute (bpm) before preparation. One hour before the CT study, the patient received 100 mg metoprolol orally and medication to reduce anxiety. Five mg of atenolol were injected i.v. just before the scan. Nevertheless, average heart rate during scan was 99 bpm, ranging from 81 to 111 bpm (Fig. 1).

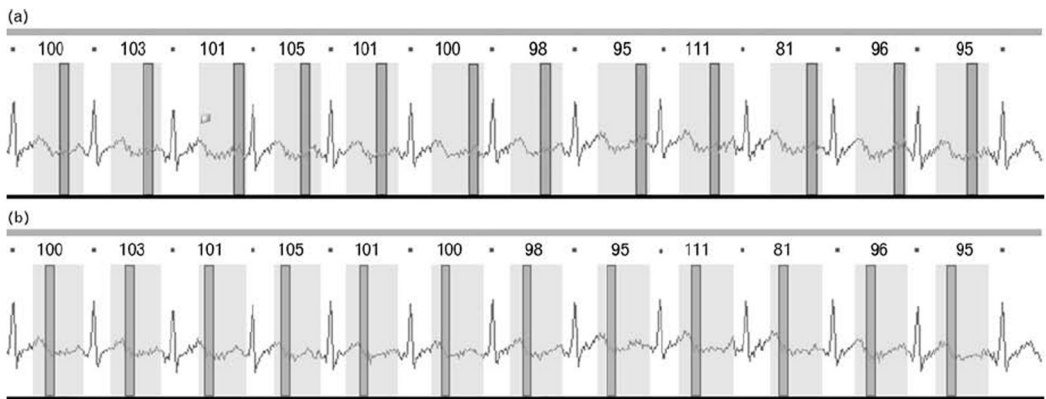


Figure 1. Electocardiogram registered during the CT scan. Maximal X-ray tube output is given from 25% to 70% of cardiac cycle (light boxes) so that data acquired during diastole (1A) and systole (1B) can be used for image reconstruction.

When the patient received instructions before the scan and the breath hold was rehearsed, we noted that the heart rate was subject to changes in frequency. Thereby we increased the interval during which maximum tube output was given from routinary 55-70% of the cardiac cycle to 25-70%.

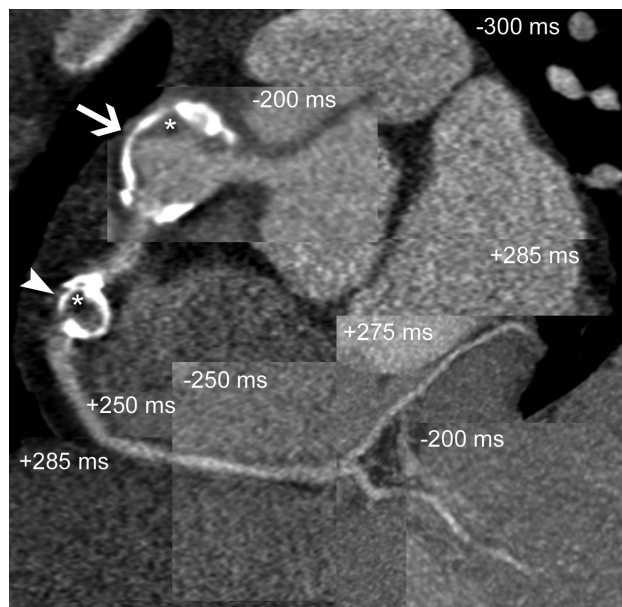


Figure 2. 'Panoramic' multiplanar CT view of the RCA obtained by combination of datasets from different phases of the cardiac cycle. A giant calcified aneurysm is seen proximally (arrow). A second calcified aneurysm is localized in the mid-tract of the RCA (arrowhead). Hypodense material consistent with thrombus is visible in both aneurysms (asterisks). The lumen is, however, patent.

Coronary CT angiography was performed with a 64-slice scanner (Siemens Sensation 64, Erlangen, Germany). Gantry rotation time was 330 ms, detector size was 2x32x0.6 mm (z-flying focal spot technology). These parameters translated into a temporal resolution of 165 ms and a spatial resolution of isotropic 0.4 mm³. Contrast agent (Iomeron[®]

400 mg/ml, Bracco, Italy) was injected into the antecubital vein at a flow rate of 5.0 ml/s.

Firstly, we reconstructed two datasets 300 ms before the R wave with monosegmental and bi-segmental reconstruction algorithms, respectively. Since the latter did not result into better image quality, we proceeded by reconstructing multiple datasets using the monosegmental algorithm. Both diastolic (Fig. 1 A) and systolic (Fig. 1 B) reconstruction windows were used.

Reconstructed slice thickness was 0.75 mm with an increment of 0.4 mm.

Tracts of the right coronary artery (RCA) could be visualized with diagnostic image quality in different datasets. By combining multiplanar views on an offline computer, the RCA could be visualized in its entirety (Fig. 2). The left coronary artery was less affected by motion artifacts and was unremarkable. Despite high patient's heart-rate, diagnostic image quality was obtained due to the enhanced temporal resolution of 64-slice CT compared to previous generation CT scanners.



Figure 3. Conventional angiogram of the RCA confirms CT findings.

Two partially calcified coronary aneurysms were seen in the RCA. The proximal, larger aneurysm (Fig. 2, arrow) was patent with a small amount of thrombus (Fig. 2, asterisk) layered on its walls. The aneurysm localized in the mid-RCA (Fig. 2, arrowhead) was partially filled with thrombus (asterisk). At this level, 2 experienced readers (F.P, W.B.M) scored in consensus the severity of luminal narrowing as <50%. The total time needed for preparation of the datasets and their evaluation was 20 minutes.

The patient eventually underwent conventional angiography (Fig. 3). Fractional flow reserve (FFR) measurement in the mid-RCA yielded a value >0.75 confirming the CT findings.

DISCUSSION

Coronary CT angiography is a fast, noninvasive diagnostic modality where data for image formation can be acquired over the entire cardiac cycle or over a portion of the R-R interval. The latter acquisition technique is called ECG-controlled dose modulation. ECG-controlled dose modulation involves maximal X-ray tube output during diastole accompanied by a decrease in tube output during systole. The result is a total dose reduction of 30% to 50%, depending on patient's heart rate (4). Therefore, the use of dose modulation is always recommendable.

When patient's heart rate is high and refractory to beta-blockers, however, reconstructions in the systolic phase are often necessary, especially for the visualization of the middle RCA. By widening the maximal tube output interval to 25-70%, we used data acquired in both systole and diastole for image formation. A wider pulsing interval also allows to manually edit the position of reconstruction windows along the cardiac cycle in order to compensate for heart rate changes during the scan.

After analysing the RCA segment by segment in different datasets, we selected the best images from each dataset and provided an interpretable view of the entire RCA, as shown in Figure 2.

It can be argued that increasing the interval of maximal tube output increases X-ray exposure. However, a percent increase of the modulation interval does not imply an absolute increase in patient X-ray exposure when patient's heart rate is very high. Moreover, it has been reported that at heart-rates less than 85 bpm best image quality occurs in diastole, whereas with higher heart-rates the best reconstruction phase shifts to end-diastole (5). Setting the maximal tube output to the end-systole might therefore reduce the radiation exposure without decreasing image quality in patients with high heart-rates.

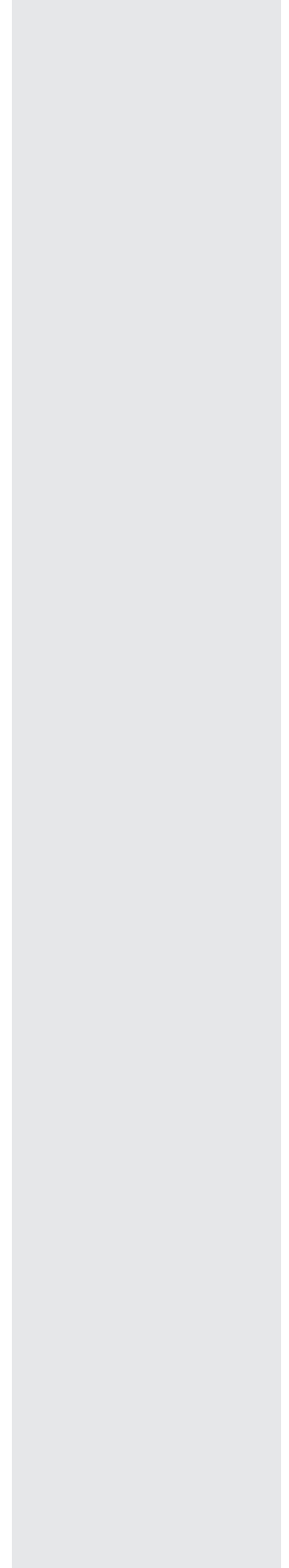
If the acquisition protocol is flexible and adapted to patient's heart-rate, coronary CT angiography has advantages over other noninvasive coronary imaging modalities, e.g. magnetic resonance imaging (MRI). In uncooperative patients, CT is easier than MRI because it is faster and one single breath-hold is required. The capability to intervene with customized image reconstruction and expert post-processing to minimize motion artifacts is an additional tool for improving the clinical reliability of coronary CT angiography.

REFERENCES

1. Pugliese F, Mollet NR, Runza G, et al. Diagnostic accuracy of non-invasive 64-slice CT coronary angiography in patients with stable angina pectoris. *Eur Radiol* 2006; 6: 575-582.
2. Hong C, Becker CR, Huber A. ECG-gated reconstructed multi-detector row CT coronary angiography: effect of varying trigger delay on image quality. *Radiology* 2001; 220:712-717.
3. Nieman K, Rensing BJ, van Geuns RJ, et al. Non-invasive coronary angiography with multislice spiral computed tomography: impact of heart rate. *Heart* 2002; 88:470-474.
4. Hausleiter J, Meyer T, Hadamitzky M, et al. Radiation dose estimates from cardiac multislice computed tomography in daily practice: impact of different scanning protocols on effective dose estimates. *Circulation* 2006; 113:1305-1310.
5. Leschka S, Wildermuth S, Boehm T, et al. Noninvasive coronary angiography with 64-section CT: effect of average heart rate and heart rate variability on image quality. *Radiology* 2006; 241:378-385.

PART 2

Detection of significant
coronary artery disease



4

Diagnostic Accuracy of 64-slice Computed Tomography Coronary Angiography: A Prospective Multicenter, Multivendor Study

Journal of American College of Cardiology.
2008. Dec 16;52(25):2135-44

W. Bob Meijboom, MD^{1,2*},
Matthijs F. L. Meijs, MD^{3,4*},
Joanne D. Schuijff MD,
PhD^{5,6}, Maarten J. Cramer,
MD, PhD³, Nico R. Mollet,
MD, PhD^{1,2}, Carlos A.G.
van Mieghem, MD^{1,2}, Koen
Nieman, MD, PhD^{1,2}, Jacob
M. van Werkhoven, MD^{5,6},
Gabija Pundziute, MD^{5,6},
Annick C. Weustink, MD^{1,2},
Alexander M. de Vos, MD^{3,4},
Francesca Pugliese, MD^{1,2},
Benno Rensing, MD, PhD⁷,
J. Wouter Jukema, MD, PhD⁵,
Jeroen J. Bax, MD, PhD⁵,
Mathias Prokop, MD, PhD⁴,
Pieter A. Doevendans, MD,
PhD³, Myriam G. Hunink,
MD, PhD^{2,8}, Gabriel P.
Krestin, MD, PhD², Pim J. de
Feyter, MD, PhD^{1,2}

¹Department of Cardiology,
Erasmus University Medical
Center, Rotterdam, the
Netherlands

²Department of Radiology,
Erasmus University Medical
Center, Rotterdam, the
Netherlands

³Department of Cardiology,
Utrecht University Medical
Center, Utrecht, the
Netherlands

⁴Department of Radiology,
Utrecht University Medical
Center, Utrecht, the
Netherlands

⁵Department of Cardiology,
Leiden University Medical
Center, Leiden, the Netherlands

⁶Department of Radiology,
Leiden University Medical
Center, Leiden, the Netherlands

⁷Department of Cardiology,
St. Antonius Ziekenhuis,
Nieuwegein, the Netherlands

⁸Department of Epidemiology,
Erasmus University Medical
Center, Rotterdam, the
Netherlands

ABSTRACT

Objectives

To determine the diagnostic accuracy of 64-slice CT coronary angiography (CTCA) to detect or rule out significant coronary artery disease (CAD).

Background

CTCA is emerging as a non-invasive technique to detect coronary atherosclerosis.

Methods

We conducted a prospective, multicenter, multivendor study involving 360 symptomatic patients with acute and stable anginal syndromes who were between 50 and 70 years of age, and referred for diagnostic conventional coronary angiography (CCA) from September 2004 through June 2006. All patients underwent a non-enhanced calcium scan and a CTCA which was compared to CCA. No patients or segments were excluded because of impaired image quality due to either coronary motion or calcifications. Patient-, vessel-, and segment based sensitivities and specificities were calculated to detect or rule out significant CAD, defined as $\geq 50\%$ lumen diameter reduction.

Results

The prevalence among patients of having at least one significant stenosis was 68%. In a patient-based analysis, the sensitivity for detecting patients with significant CAD was 99% (95%;CI:98-100); specificity 64% (95%;CI:55-73); positive predictive value 86% (95%;CI:82-90); and negative predictive value 97% (95%;CI:94-100). In a segment-based analysis, the sensitivity was 88% (95%;CI: 85-91); specificity 90% (95%;CI:89-92); positive predictive value 47% (95%;CI:44-51); negative predictive value 99% (95%;CI:98-99).

Conclusions

Among patients in whom a decision had already been made to obtain CCA, 64 slice CTCA was reliable for ruling out significant CAD in patients with stable and unstable anginal syndromes. A positive 64 CTCA scan often overestimates the severity of atherosclerotic obstructions and requires further testing to guide patients' management.

INTRODUCTION

Non-invasive coronary angiography using computed tomography is a recent development and multiple small single-center studies have been published with different generation scanners, but only one multicenter study using a 16-slice scanner has been published (1). CT coronary angiography (CTCA) using 4- and 16 slice scanners lacked sufficient robustness to be useful in clinical practice (2,3). The 64-slice CT-technology featuring increased spatial and temporal resolution has improved the clinical reliability and permits evaluation of all clinically relevant branches of the coronary tree (4-16).

We conducted a prospective, multi-center, multi-vendor study to investigate the diagnostic accuracy of 64-slice CT scanners to detect or rule out significant coronary artery disease (CAD) including all coronary segments, in a consecutive series of symptomatic patients with acute and stable anginal syndromes whom were scheduled for invasive conventional coronary angiography (CCA).

METHODS

Study design

The study was designed to prospectively include symptomatic patients who presented with stable anginal syndromes and unstable anginal syndromes who were referred for clinically indicated CCA. Patients were requested to undergo an additional CTCA for research purposes besides their CCA. The study protocol was approved by the institutional review board of the Erasmus University Medical Center.

Study group

From October 2004 until June 2006 433 symptomatic patients with stable or unstable anginal syndromes who were between the age of 50 and 70 years were enrolled in three university hospitals. In order to avoid radiation exposure in young patients, who have a higher lifetime attributable risk than older individuals receiving the same dose, patients enrolled in the study were 50 years or older (17). A maximum age limit was set to minimize the presence of severe coronary calcifications which especially occurs in the elderly and is known to hamper precise coronary stenosis evaluation. Sixty-two patients denied (written) informed consent and 11 patients were excluded because of CT-related criteria (5 scanner malfunction, 3 poor intravenous access, 2 contrast extravasation and 1 second degree AV block due to beta blockers). Thus, the remaining study population comprised 360 patients (Figure 1).

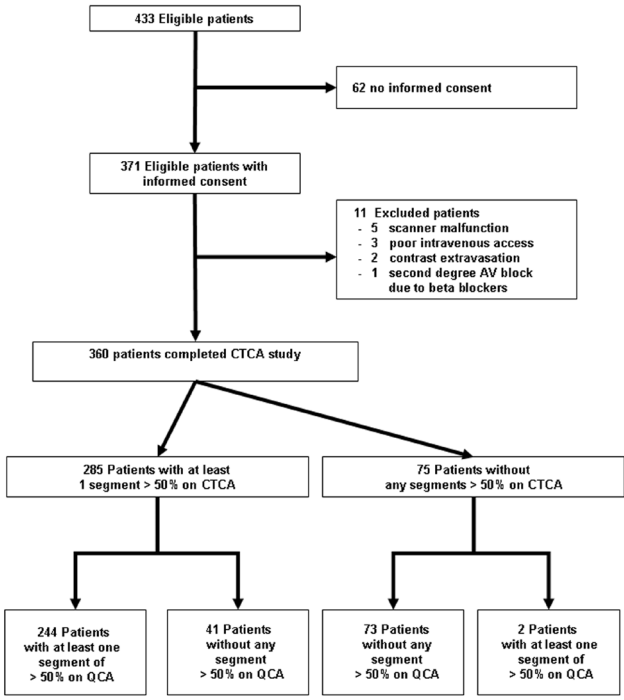


Figure 1: Flow of patients through the study. CTCA: Computed Tomography Coronary Angiography; QCA: Quantitative Coronary Angiography.

Patients with stable chest pain were categorized as having typical or atypical angina pectoris. Typical angina was defined when the following three characteristics were present: 1) sub-sternal discomfort 2) precipitated by physical exertion or emotion and 3) relieved with rest or nitroglycerine within 10 minutes. Atypical angina pectoris was defined when only one or two out of these three symptom characteristics were met. Patients presenting with an acute coronary syndrome were categorized as having unstable angina pectoris (in the absence of a troponin rise as measured at 2 separate time intervals) or as non ST-segment elevation

myocardial infarction whenever troponin levels were elevated. Only patients with an acute coronary syndrome that did not require an urgent invasive strategy were included.

Patients with a previous history of percutaneous coronary stent placement, coronary artery bypass surgery, impaired renal function (serum creatinine > 120 $\mu\text{mol/l}$), persistent arrhythmias, inability to perform a breath hold of 15 seconds, or known allergy to Iodinated contrast material, were excluded.

Scan protocol

Each center used a 64-slice CT scanner from a different vendor (Sensation 64, Siemens, Forchheim, Germany; Brilliance 64, Philips Medical Systems, Best, the Netherlands; Toshiba Multi-Slice Aquilion 64 system, Toshiba Medical Systems, Tokyo, Japan). Patients with a heart rate exceeding 65 bpm received either additional oral or intravenous beta-blockers

A non-enhanced scan to calculate the total calcium score was performed prior to the CTCA. The scan parameters of the scanners are shown in Table 1. A bolus-tracking technique was used to synchronize the start of image acquisition with the arrival of contrast agent in the coronary arteries. The effective dose of the non-enhanced scan and the CTCA was estimated from the product of

Table 1: Scan parameters of the different scanners

	Sensation 64, Siemens	Brilliance 64, Philips	Aquilion 64, Toshiba
CT coronary angiography			
Gantry rotation time	330 ms	420 ms	400ms
Slices per rotation	32×2	64×1	64×1
Individual detector width	0.6 mm	0.625 mm	0.5 mm
Table feed	3.8 mm/rotation	8 mm/rotation	5.76 mm/rotation
Tube voltage	120 kV	120 kV	120 kV
Tube current	850 - 960 mAs	900 mAs	670-710 mAs
Retrospective gating	Yes	Yes	Yes
ECG X-ray tube modulation	OFF	OFF	OFF
Contrast material	Iomeron 400	Ultravist 300-370	Iomeron 400
Volume	95 ml	100-140 ml	80-110 ml
Iodine flux	2.0 g/s	1.6 - 2.0 g/s	2.0 g/s
Estimated effective dose	15.5 ± 2.2 mSv	18.4 ± 3.2 mSv	16.0 ± 2.3 mSv
Calcium score			
Tube current	150 mAs	150 mAs	150 mAs
ECG-synchronization	Retrospective gating	Retrospective gating	Prospective triggering
ECG X-ray tube modulation	ON	ON	-
Estimated Radiation Exposure	1.7 ± 0.8 mSv	1.8 ± 0.9 mSv	1.2 ± 0.5 mSv

the dose-length product and a conversion coefficient ($k=0.017 \text{ mSv}/(\text{mGy} \times \text{cm})$) for the chest as the investigated anatomic region (18).

Image reconstruction

To acquire optimal motion-free images, datasets were reconstructed with retrospective ECG gating using an absolute reverse or percentage technique. Datasets were reconstructed immediately after the scan following a stepwise approach. Initially, a single dataset was reconstructed during the mid-to-end diastolic phase (350ms before the next R-wave or at 65-70 percent of the R-R interval). In case of insufficient image quality of one or more coronary segments, additional datasets were reconstructed in the diastolic phase (between 250ms and 450ms before the next R-wave or between 60% and 80% of the R-R interval). In case of persistent artifacts related to coronary motion, an alternative approach using an absolute forward or percentage technique (between 250msec and 400msec after the previous R-wave or between 20% and 40% of the R-R interval) was utilized to obtain datasets during the end-systolic phase. If necessary, multiple datasets of a single patient were used separately in order to obtain optimal image quality for all coronary segments. These best selected datasets were stored on CD or DVD and used for CTCA analysis.

Quantitative coronary angiography (QCA)

All were carried out within two weeks before or after CCA. Three experienced cardiologists (CAM, KN, JMW) unaware of the results of CTCA, received the CCA's on a CD, and identified and analyzed all coronary segments, using a modified 17-segment AHA classification (19) on a separate work station. Segments were visually classified as normal (smooth parallel or tapering borders; visually less than 20% narrowing) or as having non-significant or significant coronary obstruction (visually more than 20% narrowing). The stenoses in segments visually scored as having more than 20% narrowing, were quantified by a validated quantitative coronary angiography (QCA) algorithm (CAAS, Pie Medical, Maastricht, the Netherlands)(20).

Stenoses were evaluated in the worst angiographic view and classified as significant if the lumen diameter reduction exceeded $\geq 50\%$.

CT image evaluation

The total calcium scores of all patients were calculated using dedicated software. The CTCA scans of a certain study center were always graded by a team from another study center. Two observers graded each CTCA scan and in case of disagreement consensus was obtained by a third reader. Experienced observers (WBM, MFM, JDS, NRM, AMV, JWJ) unaware of the results of the CCA, evaluated the CTCA data sets on an offline workstation (Leonardo, Siemens, Forchheim, Germany).

Image quality was evaluated on a per-segment basis and classified as good (defined as absence of any image-degrading artefacts related to motion, calcification, or noise), moderate (presence of image-degrading artefacts, but evaluations possible with moderate confidence), or poor (presence of image-degrading artefacts and evaluation possible with low confidence). The influence of calcium on a per-segment basis was evaluated and graded as none (not calcified), moderate (calcium present and covering $< 50\%$ of lumen), and high (calcium covering $> 50\%$ of lumen in all planes including in cross section).

The axial source images, as well as multiplanar or curved reformatted reconstructions and maximum intensity projections were used to evaluate the CT dataset for the presence of significant segmental stenosis. Segments were scored as having significant CAD if there was $\geq 50\%$ diameter reduction of the lumen by visual assessment. Segments distal to a chronic total occlusion were excluded. An intention to diagnose design was used: thus all scanned patients including all vessels and segments were analyzed even if the image quality was poor due to extensive calcification, coronary motion, or breathing artifacts.

Power calculation

We assumed a 70% prevalence of significant CAD in this study population. Sample size calculations demonstrated that 320 patients were necessary to estimate the sensitivity and specificity of CTCA versus CCA as reference standard with a 95% confidence interval of 6% (ie. a standard error of approximately 3%) above and below the expected CTCA sensitivity and specificity of 90%. To allow for possible incomplete data we included 40 extra patients.

Statistical analysis

Descriptive statistics were performed for patients, coronary vessels, and segments. All 360 patients and all coronary segments were included in the analysis. Categorical patients' demographics and characteristics, expressed as numbers and percentages, were compared using chi-square tests. Continuous variables were expressed as mean (standard deviation) and compared with an unpaired two-sided student t test when normally distributed. Normality was determined using the software program SPSS which uses the Shapiro-Wilk test for sample sizes from 3 to 2000. Furthermore, graphical methods were used such as frequency distribution histograms to visualize a normal distribution. When not normally distributed, continuous variables were expressed as medians (25th to 75th percentile range) and compared using the nonparametric Mann-Whitney test. For the evaluation of patient demographics and characteristics, p-values <0.01 were considered statistically significant. Diagnostic performance of CTCA for the diagnosis significant CAD compared to the standard of reference QCA on CCA was determined with sensitivity, specificity, positive predictive value (PPV), and negative predictive value (NPV) and their corresponding 95% confidence intervals. Definitions of descriptive parameters used in the different diagnostic analyses are seen in Table 2.

Table 2: Definitions of descriptive parameters used in the different diagnostic analyses.

	True positive	True negative	False positive	False negative
Patient analysis	At least one significant stenosis in a patient detected by CTCA and CCA regardless of location of stenosis	No significant stenosis in a patient detected either by CTCA or CCA	Significant stenosis detected by CTCA and no significant stenosis detected by CCA.	No significant stenosis detected by CTCA and at least one significant stenosis detected by CCA.
Vessel analysis	At least one significant stenosis in a vessel detected by CTCA and CCA, regardless of location of stenosis	No significant stenosis in a vessel detected either by CTCA or CCA	Significant stenosis detected by CTCA and no significant stenosis detected by CCA.	No significant stenosis detected by CTCA and at least one significant stenosis detected by CCA.
Segment analysis	Significant stenosis in a segment detected by CTCA and CCA	No significant stenosis in a segment detected either by CTCA or CCA	Significant stenosis detected by CTCA and no significant stenosis detected by CCA.	No significant stenosis detected by CTCA and a significant stenosis detected by CCA.

CTCA: Significant stenosis is defined as a 50% lumen diameter reduction of the lumen by visual assessment.
 CCA: Significant stenosis is defined as a 50% lumen diameter reduction as quantified with QCA.

The data was clustered implying that potential correlation existed between the multiple (seventeen) segments analyzed per patient (21-23). To adjust for the clustered nature of the data, we used a bootstrap approach for the analyses with the patient as cluster, sampling with replacement, performing 1000 replications, and analyzing the bias-corrected 95% confidence intervals in both the vessel and segment analyses and their sub-analyses (23,24).

Three pair of observers for different centers conducted the analysis resulting in three intervariabilities presented as range of inter-variability. The data of the three inter-variabilities were averaged and presented as mean inter-observer variability. Intra-observer agreement of one observer in a set of 50 patients is presented using kappa-statistics. The statistical analyses were performed using SPSS (version 12.1. SPSS Inc., Chicago, Ill.) and STATA (SE 8.2, College Station, Texas).

RESULTS

Patient characteristics of those included and excluded from the study are shown in Table 3. There were no significant differences between the two groups. The prevalence of having at least one significant coronary stenosis was 68%. Patient demographics of patients presenting with stable or unstable symptoms were comparable, except for a higher prevalence of smokers ($p: <0.001$) and a higher prevalence and extent of significant CAD ($p: <0.01$) in patients presenting with unstable anginal syndromes (Chi-square test).

Additional beta-blockers prior to CTCA scanning were administered in 56% (200/360) of patients, decreasing the mean heart to 59 ± 9 bpm. The mean scan time was 10.7 ± 1.6 seconds. One patient needed a short period of observation on the coronary care unit because of a second-degree AV block after beta-blocker administration but recovered completely. In 2 patients contrast extravasation occurred which resolved without further complications and three patients had mild contrast allergy which was successfully treated with anti-histaminica.

Diagnostic performance of 64-slice CT coronary angiography: patient-based analysis

The diagnostic performance of CTCA for detecting significant stenoses on a patient-level is detailed in Table 4. Almost all patients with significant CAD on CCA were identified by CTCA (99%, 244/246) (Figure 2,3). Two patients with one vessel disease were missed. CTCA detected at least one significant coronary stenosis in all patients with left main or 3 vessel disease (100%, 27/27) which means that per patient-analysis all these patients were correctly identified. Forty-one patients with angiographic non-significant disease were incorrectly classified as having significant CAD by CTCA: 49% (20/41) of patients were scored as having single-vessel disease, 27% (11/41) of patients as having two-vessel disease, 17% (7/41) of patients as having three-vessel disease, and

Table 3: Patient demographics (N: 360)

Variable	Included patients (N:360, %)	Excluded patients (N:73, %)	p-value	Stable anginal syndromes (N: 233, %)	Unstable anginal syndromes (N: 127, %)	p-value
Typical angina pectoris	151 (42%)	34 (47%)		151 (65%)	-	-
Atypical angina pectoris	82 (23%)	13 (18%)		82 (35%)	-	-
Unstable angina pectoris	77 (21%)	15 (21%)	ns	-	77 (61%)	-
Non ST segment elevation myocardial infarction	50 (14%)	11 (15%)		-	50 (39%)	-
Men	245 (68%)	54 (76%)	ns	156 (67%)	89 (70%)	ns
Age (yrs)*	60 ± 6	60 ± 6	ns	60 ± 6	60 ± 6	ns
Body mass index (kg/m ²)*	27.3 ± 3.8	27.2 ± 4.2	ns	27.6 ± 3.9	26.8 ± 3.5	ns
Heart rate (bpm)*	59 ± 9	-	-	59 ± 10	59 ± 8	ns
Risk factors						
Hypertension ‡	219 (61%)	44 (60%)	ns	149 (64%)	70 (55%)	ns
Hypercholesterolemia §	228 (63%)	45 (63%)	ns	151 (65%)	77 (61%)	ns
Diabetes mellitus	63 (18%)	15 (21%)	ns	47 (20%)	16 (13%)	ns
Smoker	137 (38%)	27 (37%)	ns	74 (32%)	63 (50%)	< 0.001
Family history of coronary artery disease	183 (51%)	40 (55%)	ns	113 (48%)	70 (55%)	ns
Body mass index ≥ 30 kg/m ²	85 (24%)	18 (25%)	ns	59 (25%)	26 (20%)	ns
Previous myocardial infarction	53 (15%)	14 (19%)	ns	36 (15%)	17 (13%)	ns
Calcium score (Agatston score)†	213 (42-553)	-	-	211 (31-639)	216 (44-478)	ns
Conventional coronary angiography						
Prevalence of obstructive coronary artery disease	246 (68%)	58 (79%)	ns	146 (63%)	100 (79%)	< 0.01
Absence of significant coronary artery disease	114 (32%)	15 (21%)		87 (37%)	27 (21%)	
Single vessel disease	141 (39%)	26 (36%)		88 (38%)	53 (42%)	
Two vessel disease	78 (22%)	20 (27%)	ns	46 (20%)	32 (25%)	
Three vessel disease	21 (6%)	10 (14%)		10 (4%)	11 (9%)	< 0.01
Left main coronary artery disease	6 (2%)	2 (3%)		2 (1%)	4 (3%)	

* Mean and standard deviation. † Median and quartiles. Values are n (%) unless otherwise indicated. Categorical patients' demographics and characteristics were compared using chi-square tests. Continuous variables were tested with unpaired two sided student t test. If not normally distributed, continuous variables were compared with the Mann-Whitney test. P values are significant if values < 0.05. ‡ Blood pressure ≥ 140/90 mm Hg or treatment for hypertension. § Total cholesterol > 180 mg/dl or treatment for hypercholesterolemia. || Treatment with oral anti-diabetic medication or insulin.

Table 4: Diagnostic performance of 64-Slice CT Coronary Angiography for the detection of $\geq 50\%$ stenosis on QCA in the per-patient analysis (95% CI).

	Prevalence of disease, %	N	TP	TN	FP	FN	Sensitivity, %	Specificity, %	PPV, %	NPV, %
Patient based analysis	68	360	244	73	41	2	99 (98-100)	64 (55-73)	86 (82-90)	97 (94-100)
Stable angina pectoris	63	233	145	56	31	1	99 (98-100)	64 (53-74)	82 (76-88)	98 (95-100)
Non-ST elevation acute coronary syndrome	79	127	99	17	10	1	99 (97-100)	63 (45-81)	91 (85-96)	94 (84-100)
Men	76	245	185	38	20	2	99 (97-100)	66 (53-78)	90 (86-94)	95 (88-100)
Women	51	115	59	35	21	0	100 (100-100)	63 (50-75)	74 (64-83)	100 (100-100)
Typical angina pectoris	70	151	104	31	15	1	99 (97-100)	67 (54-81)	87 (81-93)	97 (91-100)
Atypical angina pectoris	50	82	41	25	16	0	100 (100-100)	61 (46-76)	72 (60-84)	100 (100-100)
Unstable angina pectoris	75	77	57	13	6	1	98 (95-100)	68 (48-89)	90 (83-98)	93 (79-100)
Non-ST elevated myocardial infarction	84	50	42	4	4	0	100 (100-100)	50 (15-85)	91 (83-99)	100 (100-100)

TP indicates true positive; TN, true negative; FP, false positive; FN, false negative; PPV, positive predictive value; NPV, negative predictive value.

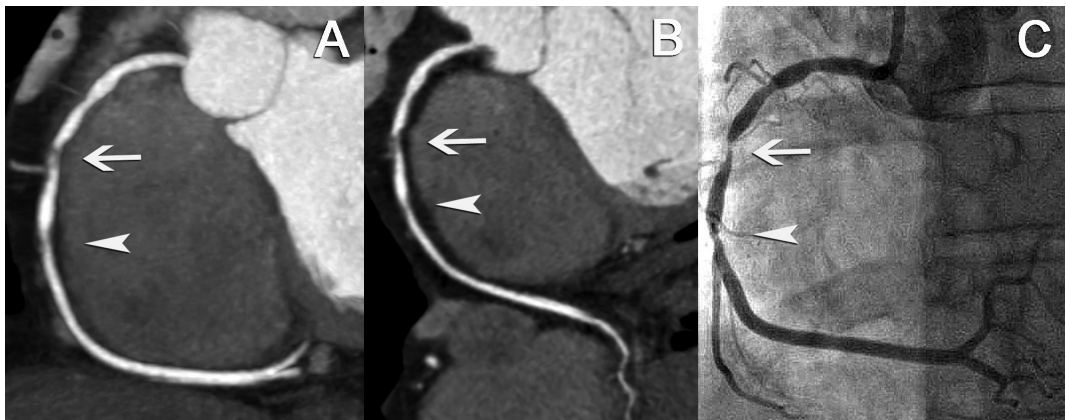


Figure 2: A thick maximum intensity projected CT coronary artery (CTCA) image (A) reveals the anatomy of the right coronary artery (RCA). A curved multiplanar reformatted image (B) discloses a significant coronary stenosis (arrow) in the mid right coronary artery and distally an intermediate coronary stenosis which both were corroborated by conventional coronary angiography (C).



Figure 3: Three curved multiplanar reconstructed images reveal the right coronary artery (A), the left anterior descending coronary artery (LAD) (B) and the circumflex coronary artery (C). In the left main coronary artery, proximal and mid LAD non-obstructive calcified plaques can be seen. The conventional coronary angiography confirms the absence of significant coronary artery disease.

7% (3/41) having significant left main CAD (Figure 4). Sensitivity and specificity between patients who presented with stable versus unstable symptoms were similar.

Diagnostic performance of 64-slice CT coronary angiography: vessel-based analysis

The diagnostic performance of CTCA for the detection of significant lesions on a vessel-based analysis is detailed in Table 5. Significant lesions in the right coronary artery and circumflex coronary artery were more often undetected than lesions in the left anterior descending coronary artery and left main coronary artery. The severity of a lesion was overestimated in 245 non-obstructive vessels (false positives).

Diagnostic performance of 64-slice CT coronary angiography to predict the extent of significant vessel disease.

CTCA correctly predicted the absence of significant vessel disease and presence of one, two and three vessel disease in 53% (192/360) of the patients. In 3% (11/360) CTCA underrated the extent of disease and in 44% (157/360) overestimated the extent of disease. The weighted kappa to



Figure 4: A volume-rendered CT coronary angiography (CTCA) image (A) reveals the anatomy of the right coronary artery (RCA). A maximum intensity projected image (B) and two curved multiplanar reconstructed images depict a non-calcified obstructive coronary stenosis in the mid RCA. However, conventional coronary angiography only reveals a non-significant stenosis. Quantitative coronary angiography showed a 40% diameter reduction of the coronary lumen. (A full color version of this illustration can be found in the color section).

predict the extent of vessel disease was moderate (0.47).

The prevalence of three vessel disease was 6%. The sensitivity for predicting the presence of significant three vessel disease was 90% (95%;CI:68-98); specificity 77% (95%;CI:72-81); positive predictive value 19% (95%;CI:12-29); and negative predictive value 99% (95%;CI:97-100) (Table 6).

Table 5: Diagnostic performance of 64-Slice CT Coronary Angiography for the Detection of $\geq 50\%$ Stenosis on QCA in the per-vessel analysis (95% CI)

	Prevalence of disease, %	N	TP	TN	FP	FN	Sensitivity, %	Specificity, %	PPV, %	NPV, %
Vessel based analysis	26	1440	354	821	245	20	95 (92-97)	77 (74-80)	59 (55-63)	98 (96-99)
Right coronary artery	39	360	132	170	50	8	94 (90-98)	77 (71-82)	73 (66-79)	96 (92-98)
Left main coronary artery	2	360	5	338	16	1	83 (50-100)	95 (93-97)	24 (8-44)	100 (99-100)
Left anterior descending coronary artery	37	360	133	126	100	1	99 (97-100)	56 (49-63)	57 (51-63)	99 (97-100)
Circumflex coronary artery	26	360	84	187	79	10	89 (83-95)	70 (65-76)	52 (45-60)	95 (92-98)

Bias-corrected 95% confidence intervals from a bootstrap analysis are reported for the vessel analyses and the individual vessel analyses. TP indicates true positive; TN, true negative; FP, false positive; FN, false negative; PPV, positive predictive value; NPV, negative predictive value.

Table 6: The performance of CT coronary angiography to predict the extent of CAD as seen on conventional coronary angiography.

Extent of CAD as seen on CT coronary angiography	Extent of CAD as seen on conventional coronary angiography			
	0	1	2	3
0	74	2	0	0
1	21	59	7	1
2	11	46	40	1
3	8	37	34	19

The weighted kappa = 0.47 and the strength of agreement is considered to be moderate. The left main coronary artery was left out of the analysis. CAD: Coronary artery disease.

Diagnostic performance of 64-slice CT coronary angiography: segment-based analysis

The diagnostic performance of CTCA for the detection of significant lesions on a segment-based analysis is detailed in Table 7. Overall 5297 (out of 6120 potentially available segments) were included for comparison with CCA. Unavailable segments included 628 anatomically absent segments on CCA and 195 segments distal to an occluded coronary segment. All coronary segments were evaluated, also including segments with severe calcifications or poor image quality.

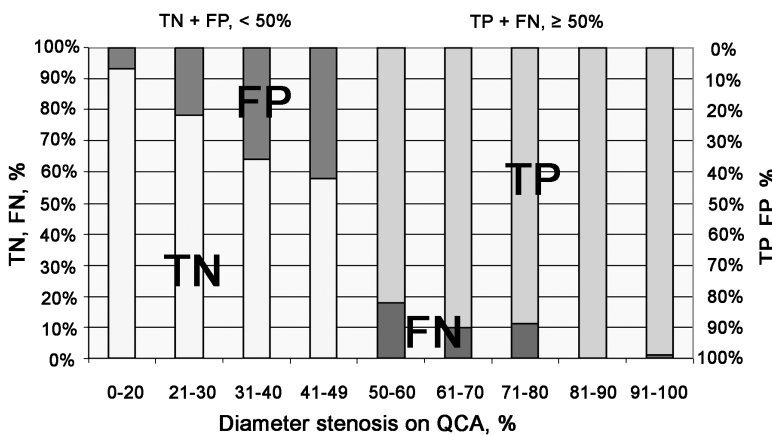


Figure 5: In the graph the diagnostic performance of CT coronary angiography (CTCA) is shown according to various diameter stenoses as measured by quantitative coronary angiography in a per-segment analysis. The absolute number of segments per stenosis category is presented in the table. The highest frequency of overestimated (FP) and underestimated (FN) coronary stenoses by CTCA was clustered around the cut-off value of 50% diameter reduction (= significant coronary stenosis). TP: true positive, TN: true negative, FP: false positive, FN: false negative.

FP	286	34	77	74	180	102	50	10	80	TP
TN	3993	116	137	99	41	11	7	0	1	FN

Table 7: Analysis of the influence of coronary diameter, image quality and coronary calcium of the diagnostic performance of 64-Slice CT Coronary Angiography for the Detection of $\geq 50\%$ Stenosis on QCA in the per-segment analysis (95% CI).

	Prevalence of disease, %	N	TP	TN	FP	FN	Sensitivity, %	Specificity, %	PPV, %	NPV, %
Segment based analysis	9	5297	422	4345	471	59	88 (85-91)	90 (89-92)	47 (44-51)	99 (98-99)
Diameter										
> 2 mm	10	4531	407	3655	419	50	89 (86-92)	90 (88-91)	49 (45-53)	99 (98-99)
1.5-2 mm	3	449	10	396	40	3	77 (54-100)	91 (88-94)	20 (10-32)	99 (98-100)
< 1.5 mm	3	317	5	294	12	6	45 (10-75)	96 (94-98)	29 (7-58)	98 (96-99)
Image quality										
Good	9	3710	282	3188	206	34	89 (85-93)	94 (93-95)	58 (53-62)	99 (98-99)
Moderate	11	851	78	641	117	15	84 (76-91)	85 (82-88)	40 (33-47)	98 (96-99)
Poor	10	736	62	516	148	10	86 (78-94)	78 (74-82)	30 (24-36)	98 (97-99)
Calcium										
None	5	3640	128	3367	108	37	78 (71-84)	97 (96-98)	54 (48-60)	99 (99-99)
Moderate	17	1235	192	829	197	17	92 (88-95)	81 (78-84)	49 (44-55)	98 (97-99)
High	25	422	102	149	166	5	95 (91-99)	47 (41-54)	38 (32-44)	97 (94-99)

Bias-corrected 95% confidence intervals from a bootstrap analysis are reported for the segment analyses and their sub-analyses. TP indicates true positive; TN, true negative; FP, false positive; FN, false negative; PPV, positive predictive value; NPV, negative predictive value.

Sensitivity decreased with vessel diameter and increased with the presence of calcifications. Specificity decreased with poor image quality and in the presence of severe calcifications.

The severity of 59 significant coronary stenoses was underestimated or missed and classified as non-significant by CTCA and the severity of 471 non-significant lesions was overestimated by CTCA. The highest percentage of overestimated and underestimated coronary stenoses was clustered around the cut-off value of 50% diameter reduction (Figure 5). The kappa-values for the mean interobserver variability and the intraobserver variability were 0.66 (range 65-67) and 0.69, respectively.

DISCUSSION

This prospective, multicenter, multivendor study showed that 64-slice CTCA in intermediate-to-high risk symptomatic patients accurately detects significant CAD and is reliable to rule out significant CAD. The sensitivity to detect CAD was 99% and the negative predictive value 97%.

Because of overestimation of severity of a stenosis the specificity was moderate, 64%, with a positive predictive value of 86%. All patients with three-vessel disease or left main CAD were detected. The study was performed in three independent centers, with different types of 64-slice CT scanners and using different dedicated scan protocols.

The high sensitivity of CTCA for CAD demonstrated in our study is in keeping with the sensitivity of 64-slice CTCA studies performed in single-center studies. The specificity of 64% is, however, lower than results published previously which ranged from 79% to 100% (4,5,7-15). The main reason for the lower specificity was the rather high rate of false positive outcomes, which was related to the difficulties to grade the severity of stenosis and the inclusion in the analysis of all available coronary segments regardless of image quality. We included in our analysis segments with poor image quality caused by blurring due to cardiac motion or step artifacts due to breathing or an irregular heart rate. The precise grading of the severity of a coronary stenosis is hampered in calcified obstructions, due to the blooming effect, which overestimates the severity of stenosis. In case of extensive focal calcifications the visualization of the underlying coronary lumen is obscured. However, we did not exclude these segments from the analysis but tended to grade these lesions as having a significant obstruction.

Our coronary stenosis grading policy, and inclusion of all coronary segments in an intention-to-diagnose approach, is based on the premises that patients with either positive CTA results or non-evaluable segments will undergo CCA. Since the clinical implication is the same, we graded non-evaluable segments as positive which means that the calculated sensitivity and specificity reflect clinically decision making. Our approach is different from many single-center reports about the diagnostic performance of 64-slice CTCA, in which approximately 6% of all segments were excluded from further analysis because they were considered non-evaluable (4,5,7-15).

The in- or exclusion of non-evaluable coronary segments from further analysis on the diagnostic performance of CTCA can have significant effects as shown in the multicenter CT-study reported by Garcia et al. They studied 187 symptomatic patients using 16-slice CT-scanners. After exclusion of non-evaluable segments (29% of all available segments) the sensitivity was 75% and specificity was 77%. Scoring all non-evaluable segments as a positive test result, sensitivity increased to 98% but at the expense of specificity which decreased to 54%.

The outcome of a negative CTCA scan is important. A recent study showed that conservative management of a patient with a negative CT scan is safe and associated with an excellent 1-year outcome (25). The presence and extent of both non-obstructive and obstructive CAD as seen on CTCA showed to predict adverse cardiovascular events in particular in patients with left main and three-vessel disease (26). In our study we demonstrated that CTCA reliably detected patients with left main or three-vessel disease, although CTCA overestimated the extent of disease compared

to CCA. For clinical decision making the high number of false positive CTCA outcomes necessitates further testing with either functional tests or CCA. Alternatively, a functional test could be performed prior to or in addition to CTCA.

The time is ready for clinical trials testing the effectiveness and cost-effectiveness of various workup algorithms in a randomized fashion to see which yields the best outcomes and lowest costs.

LIMITATIONS

Our study was performed in pre-selected middle-aged patients referred for CCA who presented with atypical and typical stable angina and unstable angina which have been shown to fall into categories of patients with intermediate to high pre-test probabilities of having CAD (27). Thus, our study population is neither representative of patients with a low-to-intermediate probability where CTCA is currently recommended (28) nor of unstable patients with ongoing ischemia, or with hemodynamic or electrical instability, who require an immediate intervention. A study comparing CTCA to CCA in patients at low-to-intermediate risk would be difficult to perform because CCA is not always indicated. However, the negative-predictive value for low-to-intermediate risk patients can be estimated using Bayesian revision adjusting the prior probability and is very high. Despite the high sensitivity and lower specificity, our study did not suffer from referral bias. A referral bias occurs when patients are selected for referral to the reference test based on the results of the index test. In our study all patients underwent the reference test, CCA, irrespective of the results of the index test, CTCA. Ideally, a consecutive series of patients who are referred for CTCA, and not CCA, needs to be considered where all patients should undergo CCA regardless of CTCA results.

The high radiation exposure, with an estimated effective dose of 15-18m mSv is of concern. In this study we did not use prospective ECG triggered X-ray tube modulation to reduce the radiation dose because the first generation 64-slice MDCT systems were equipped with non-flexible tube current modulation ability. We were concerned that the use of this mode would increase the number of coronary segments with poor image quality because the technique limits the ability to reconstruct images in all coronary phases and may cause motion artifacts.

CONCLUSION

Among patients in whom a decision had already been made to obtain CCA, we found that 64 slice CTCA was reliable for ruling out significant CAD in patients with stable and unstable anginal syndromes. A positive 64 CTCA scan often overestimates the severity of atherosclerotic obstructions and requires further testing to guide patients' management.

REFERENCES

1. Garcia MJ, Lessick J, Hoffmann MH. Accuracy of 16-row multidetector computed tomography for the assessment of coronary artery stenosis. *Jama* 2006;296:403-11.
2. Achenbach S, Giesler T, Ropers D, et al. Detection of coronary artery stenoses by contrast-enhanced, retrospectively electrocardiographically-gated, multislice spiral computed tomography. *Circulation* 2001;103:2535-8.
3. Nieman K, Oudkerk M, Rensing BJ, et al. Coronary angiography with multi-slice computed tomography. *Lancet* 2001;357:599-603.
4. Ehara M, Surmely JF, Kawai M, et al. Diagnostic accuracy of 64-slice computed tomography for detecting angiographically significant coronary artery stenosis in an unselected consecutive patient population: comparison with conventional invasive angiography. *Circ J* 2006;70:564-71.
5. Fine JJ, Hopkins CB, Ruff N, Newton FC. Comparison of accuracy of 64-slice cardiovascular computed tomography with coronary angiography in patients with suspected coronary artery disease. *Am J Cardiol* 2006;97:173-4.
6. Hamon M, Biondi-Zoccai GG, Malagutti P, et al. Diagnostic performance of multislice spiral computed tomography of coronary arteries as compared with conventional invasive coronary angiography: a meta-analysis. *J Am Coll Cardiol* 2006;48:1896-910.
7. Herzog C, Zwerner PL, Doll JR, et al. Significant coronary artery stenosis: comparison on per-patient and per-vessel or per-segment basis at 64-section CT angiography. *Radiology* 2007;244:112-20.
8. Leber AW, Knez A, von Ziegler F, et al. Quantification of obstructive and nonobstructive coronary lesions by 64-slice computed tomography: a comparative study with quantitative coronary angiography and intravascular ultrasound. *J Am Coll Cardiol* 2005;46:147-54.
9. Leschka S, Alkadhi H, Plass A, et al. Accuracy of MSCT coronary angiography with 64-slice technology: first experience. *Eur Heart J* 2005; 26(15):1482-7.
10. Mollet NR, Cademartiri F, van Mieghem CA, et al. High-resolution spiral computed tomography coronary angiography in patients referred for diagnostic conventional coronary angiography. *Circulation* 2005;112:2318-23.

11. Nikolaou K, Knez A, Rist C, et al. Accuracy of 64-MDCT in the diagnosis of ischemic heart disease. *AJR Am J Roentgenol* 2006;187:111-7.
12. Pugliese F, Mollet NR, Runza G, et al. Diagnostic accuracy of non-invasive 64-slice CT coronary angiography in patients with stable angina pectoris. *Eur Radiol* 2006;16:575-82.
13. Raff GL, Gallagher MJ, O'Neill WW, Goldstein JA. Diagnostic accuracy of noninvasive coronary angiography using 64-slice spiral computed tomography. *J Am Coll Cardiol* 2005;46:552-7.
14. Ropers D, Rixe J, Anders K, et al. Usefulness of multidetector row spiral computed tomography with 64- x 0.6-mm collimation and 330-ms rotation for the noninvasive detection of significant coronary artery stenoses. *Am J Cardiol* 2006;97:343-8.
15. Schuijf JD, Pundziute G, Jukema JW, et al. Diagnostic accuracy of 64-slice multislice computed tomography in the noninvasive evaluation of significant coronary artery disease. *Am J Cardiol* 2006;98:145-8.
16. Vanhoenacker PK, Heijenbrok-Kal MH, Van Heste R, et al. Diagnostic performance of multidetector CT angiography for assessment of coronary artery disease: meta-analysis. *Radiology* 2007;244:419-28.
17. Einstein AJ, Henzlova MJ, Rajagopalan S. Estimating risk of cancer associated with radiation exposure from 64-slice computed tomography coronary angiography. *Jama* 2007;298:317-23.
18. Menzel H, Schibila H, Teunen D eds. European guidelines on quality criteria for computed tomography. Luxembourg: European Commission Publication 2000. No. EUR 16262 EN.
19. Austen WG, Edwards JE, Frye RL, et al. A reporting system on patients evaluated for coronary artery disease. Report of the Ad Hoc Committee for Grading of Coronary Artery Disease, Council on Cardiovascular Surgery, American Heart Association. *Circulation* 1975;51:5-40.
20. Reiber JH, Serruys PW, Kooijman CJ, et al. Assessment of short-, medium-, and long-term variations in arterial dimensions from computer-assisted quantitation of coronary cineangiograms. *Circulation* 1985;71:280-8.
21. Fleiss JL, Levin B, Cho Paik M. *Statistical Methods for Rates and Proportions*. Third ed, 2003.
22. Scanlon PJ, Faxon DP, Audet AM, et al. ACC/AHA guidelines for coronary angiography. A report of the American College of Cardiology/American Heart Association Task Force on practice guidelines (Committee on Coronary Angiography). Developed in collaboration with the Society for Cardiac Angiography and Interventions. *J Am Coll Cardiol* 1999;33:1756-824.
23. Zhou XH, Obuchowski NA, McClish DK. *Statistical Methods in Diagnostic Medicine*, 2002.
24. Efron B, Tibshirani RJ. *An Introduction to the Bootstrap*, 1993.
25. Gilard M, Le Gal G, Cornily JC, et al. Midterm prognosis of patients with suspected coronary artery disease and normal multislice computed tomographic findings: a prospective management outcome study. *Arch Intern Med* 2007;167:1686-9.

26. Min JK, Shaw LJ, Devereux RB, et al. Prognostic value of multidetector coronary computed tomographic angiography for prediction of all-cause mortality. *J Am Coll Cardiol* 2007;50:1161-70.
27. Hendel RC, Patel MR, Kramer CM, et al. ACCF/ACR/SCCT/SCMR/ASNC/NASCI/SCAI/SIR 2006 appropriateness criteria for cardiac computed tomography and cardiac magnetic resonance imaging. *J Am Coll Cardiol* 2006;48:1475-97.
28. Budoff MJ, Achenbach S, Blumenthal RS, et al. Assessment of coronary artery disease by cardiac computed tomography: a scientific statement from the American Heart Association Committee on Cardiovascular Imaging and Intervention, Council on Cardiovascular Radiology and Intervention, and Committee on Cardiac Imaging, Council on Clinical Cardiology. *Circulation* 2006;114:1761-91.

5

Comparison of Diagnostic Accuracy of 64-Slice Computed Tomography Coronary Angiography in Women-vs-Men with Angina Pectoris

American Journal of Cardiology.
2007 Nov 15;100(10):1532-7.

W. Bob Meijboom, MD^{a,b},
Annick C. Weustink MD^{a,b},
Francesca Pugliese MD^{a,b},
Carlos A.G. van Mieghem,
MD^{a,b}, Nico R. Mollet, MD,
PhD^{a,b}, Niels van Pelt MD^{a,b},
Filippo Cademartiri MD,
PhD^b, Koen Nieman MD,
PhD^a, Eleni Vourvouri MD,
PhD^{a,b}, Eveline Regar MD,
PhD^a, Gabriel P. Krestin MD,
PhD^b, Pim J. de Feyter, MD,
PhD^{a,b}

Erasmus University Medical
Center, Rotterdam, the
Netherlands

^a Department of Cardiology,
Thoraxcenter

^b Department of Radiology

ABSTRACT

Objectives

We compared the diagnostic accuracy of 64-slice Computed Tomography coronary angiography (CTCA) to detect significant coronary artery disease (CAD) in female and male patients.

Methods

64-slice CT coronary angiography was performed in 402 symptomatic patients, 123 females and 279 males, with CAD prevalence of 51% and 68%, respectively. Significant CAD, defined as $\geq 50\%$ coronary stenosis on quantitative coronary angiography, was evaluated on a patient, vessel and segment level.

Results

The sensitivity and negative predictive value to detect significant CAD was very good, both for women and men (100% vs. 99%, p : ns; 100% vs. 98%, p : ns), whereas diagnostic accuracy (88% vs. 96%; p : <0.01), specificity (75% vs. 90%, p : <0.05) and positive predictive value (81% vs. 95%, p : <0.001) were lower in women. The per-segment analysis demonstrated lower sensitivity in women compared to men (82% vs. 93%; p : <0.001). The sensitivity in women did not show a difference in proximal and mid segments, but was significantly lower in distal segments (56% vs. 85%; p : <0.05) and side branches (54% vs. 89%; p : <0.001).

Conclusion

CTCA reliably rules out the presence of obstructive CAD in both men and women. Specificity and positive predictive value of CTCA were lower in women. The sensitivity to detect stenosis in small coronary branches was lower in women compared to men.

INTRODUCTION

CT coronary angiography (CTCA) is a rapidly evolving coronary imaging technique, and a potential alternative to established non-invasive tests for coronary artery disease (CAD). The diagnostic accuracy of CTCA in women per se has not been investigated, but is extrapolated from reports that were performed in populations largely consisting of men¹⁻⁹. Although earlier data suggested a discrepancy between men and women with regard to the diagnostic performance of ischemia-driven tests, recent reports using contemporary exercise ECG testing, stress echocardiography, and gated SPECT myocardial perfusion imaging refute these earlier conclusions, and state similar diagnostic results for both women and men¹⁰⁻¹⁶. Apart from varying age, disease prevalence and severity, additional anatomical and physiological differences, including body composition, heart rate, coronary calcium and coronary diameter size, between men and women may affect the diagnostic performance of CTCA. The purpose of this study was to ascertain the diagnostic accuracy of CTCA in women-vs-men with chest pain to detect or exclude the presence of obstructive CAD.

METHODS

During a 24-month period 402 patients with acute or stable chest pain symptoms that were referred for conventional coronary angiography (CCA) were included in the study. No patients with previous history of percutaneous coronary intervention or coronary artery bypass surgery, impaired renal function (serum creatinine > 120 $\mu\text{mol/l}$), persistent arrhythmias and known intolerance to Iodinated contrast material were included. CCA was performed before or after the CTCA and served as the standard of reference. The institutional review board of the Erasmus MC Rotterdam approved the study and all subjects gave informed consent.

Patients with a heart rate exceeding 65 bpm received additional beta-blockers (50/100mg Metoprolol) 1 hour before the CT examination. All scans were performed on a 64-slice CT scanner with a gantry rotation time of 330 msec, a temporal resolution of 165 msec and a spatial resolution of 0.4 mm³ (Sensation 64, Siemens, Forchheim, Germany). For the coronary calcium score a low-dose, non-enhanced scan was performed with the following, standardized parameters: 32×2 slices per rotation; individual detector width of 0.6 mm, 330 ms rotation time, 3.8 mm/rotation table feed, 120 kV tube voltage, 150 mAs tube current, with activated prospective x-ray tube modulation. The CTCA scan was performed with identical parameters except for a higher tube current between 850 and 960 mAs without prospective ECG x-ray tube modulation. The estimated radiation exposure was estimated using dedicated software (ImPACT[®], version 0.99x, St. George's Hospital, Tooting, London, UK). A 95-ml bolus of Iomeprol (IomeronTM, 400 mgI/mL; Bracco, Milan, Italy) was injected intravenously into an antecubital vein at 5 mL/s. A bolus-

tracking technique was used to monitor the arrival of contrast in the coronary arteries. The scan was started once the contrast material in the ascending aorta reached a predefined threshold of +100 Hounsfield units.

Datasets were reconstructed immediately after the scan following a stepwise outline. Images were obtained during a half x-ray tube rotation, resulting in an effective temporal resolution of 165 msec. To acquire optimal motion-free images were reconstructed by retrospective ECG-gating. Initially, a single dataset was reconstructed during the mid-to-end diastolic phase (350 ms before the next R-wave or at 65 percent of the R-R interval). In case of insufficient image quality of one or more coronary segments, additional datasets were reconstructed in the diastolic phase (between 250 ms and 450 ms before the next R-wave or between 60% and 70% of the R-R interval). In case of persistent artifacts related to coronary motion, a second reconstruction approach was carried out. Datasets were reconstructed during the end-systolic phase using an absolute forward or percentage technique (between 250 msec and 400 msec after the previous R-wave or between 25% and 35% of the R-R interval). In 34% (137/402) of the cases end-systolic reconstructions were used for image analysis. If necessary, multiple datasets of a single patient were used separately in order to obtain optimal image quality of all available coronary segments.

All scans were carried out within one week before or after CCA. One experienced cardiologist, who was unaware of the CTCA results, identified and analyzed all coronary segments according to the modified 17-segment American Heart Association classification¹⁷. Regardless of diameter size all segments were included for comparison with CTCA. Segments were classified as normal (smooth parallel or tapering borders), non-significantly stenosed (wall irregularities or <50% narrowed) or significantly stenosed ($\geq 50\%$ narrowed). Stenoses were evaluated in the worst view, and classified as significant if the lumen diameter reduction exceeded 50 % measured by validated quantitative coronary angiography (QCA) algorithm (CAAS, Pie Medical, Maastricht, the Netherlands)¹⁸.

For each patient the total calcium score was measured, and expressed using the Agatston score¹⁷. Two experienced, blinded observers evaluated the CTCA data on an offline workstation (Leonardo, Siemens, Forchheim, Germany). The axial source images, as well as multiplanar or curved reformatted reconstructions and maximum intensity projections were used to evaluate the CT angiograms and assess the presence of significant segmental stenosis. Segments were scored positive for significant CAD if there was $\geq 50\%$ diameter reduction of the lumen by visual assessment. Segments distal to an occluded segment were excluded. Inter-observer disagreement was resolved by a third reader.

Descriptive statistics were performed for coronary segments, vessels and patients. The diagnostic performance of CTCA for the detection of significant stenoses in the coronary arteries with QCA

as the standard of reference is presented as sensitivity, specificity, positive- and negative predictive values. Precision of the diagnostic parameters is presented using a 95% confidence interval (CI). Chi square tests were performed to show significant differences in diagnostic accuracy. Positive and negative likelihood ratios are given. The likelihood ratio incorporates both the sensitivity and specificity of a test and provides a direct estimate of how much a test result will change the odds of having a disease. Post-test odds can be calculated by multiplying the pre-test odds (pre-test probability/[1 - pre-test probability]) by the positive likelihood ratio (Sensitivity/[1-Specificity]) and negative likelihood ratio ((1-Sensitivity)/Specificity). Post-test probability can be re-calculated by using the following formula (post-test probability = post-test odds/[1 + post-test odds]).

A subanalysis was performed between the two sexes. Categorical characteristics are expressed as numbers and percentages, and compared between the two groups with the chi square test. Continuous variables are expressed as mean (standard deviation) and compared with an unpaired two-sided student t test when normally distributed. When not normally distributed, continuous variables are expressed as medians (25th to 75th percentile range) and compared using the non-parametric Mann-Whitney test. P-values <.05 were considered statistically significant.

An additional sensitivity analysis was done to investigate the effect of nesting, since repeated assessments within the same patient were made that were not independent observations. Inter-observer and intraobserver variability for the detection of significant coronary stenosis was determined by *k*-statistics.

RESULTS

The analysis comprised 123 females and 279 males (Table 1). On average women were older (62 ± 11 vs. 58 ± 11 ; $p < 0.01$). Hypertension and diabetes were more frequent in women, with no significant difference for BMI. There were more active smokers among men. Women had lower disease prevalence (51% vs 68%, $p < 0.01$), which was defined as having at least one significant stenosis. The severity and extent of obstructive CAD was significantly lower in women compared to men ($p < 0.05$), with fewer cases of multivessel disease (24% vs. 35%; $p < 0.05$), and more non-obstructive lesions on CCA (26% vs. 17%, $p < 0.05$). There was a nonsignificant trend towards fewer absence of CAD on CCA in women (23% vs. 15%, $p = 0.06$). Furthermore, the calcium score was lower in women (146 (0–373) vs. 207 (18–530); $p < 0.05$). During the CT scan women had a significantly higher heart rate than men: 61 ± 7 vs. 58 ± 8 ; $p < 0.001$). Additional beta-blockers prior to CT scanning were administered in 73% (90/123) and 70% (196/279) (p : ns) of female and male patients, decreasing the mean heart rate from 69 ± 10 to 61 ± 7 bpm and from 69 ± 11 to 58 ± 8 , respectively.

Table 1: Patient demographics (n=402)

Variable	Women (N:123)	Men (N:279)	p
Age (years)*	62 ± 11	58 ± 11	< 0.01
Calcium score (Agatston score)†	146 (0-373)	207 (18-530)	< 0.05
Body mass index (kg/m ²)*	26.7 ± 5.0	27.0 ± 3.6	ns
Heart rate (beats per minute)*	61 ± 7	58 ± 8	< 0.001
Prevalence of obstructive coronary artery disease	63 (51%)	190 (68%)	< 0.01
Atypical angina pectoris	47 (38%)	99 (35%)	
Typical angina pectoris	48 (39%)	107 (38%)	
Unstable angina pectoris	14 (11%)	36 (13%)	ns
Non ST segment elevation myocardial infarction	14 (11%)	37 (13%)	
Hypertension ‡	78 (63%)	138 (49%)	< 0.05
Hypercholesterolemia §	75 (61%)	161 (58%)	ns
Diabetes mellitus #	23 (19%)	28 (10%)	< 0.05
Active smoker	30 (24%)	99 (35%)	< 0.05
Previous smoker	9 (7%)	20 (7%)	ns
Body mass index ≥ 30 kg/m ²	34 (28%)	64 (23%)	ns
Previous myocardial infarction.	15 (12%)	27 (10%)	ns
Conventional coronary angiography			
Absence of coronary disease	28 (23%)	42 (15%)	
Non-significant disease	32 (26%)	47 (17%)	
Single-vessel disease	34 (28%)	91 (33%)	< 0.05
Multivessel disease	29 (24%)	99 (35%)	

* Mean and standard deviation. † Median and quartiles. Values are n (%) unless otherwise indicated. Categorical variables were tested with Chi square test. Continuous variables were tested with unpaired two sided student t test. If not normally distributed, continuous variables were compared with the Mann-Whitney test. P values are significant if values < 0.05. ‡ Blood pressure ≥ 140/90 mm Hg or treatment for hypertension. § Total cholesterol > 180 mg/dl or treatment for hypercholesterolemia.

Treatment with oral anti-diabetic medication or insulin.

The estimated radiation exposure using prospective x-ray tube modulation for the calcium score in women and men was 1.8 and 1.4 mSv and the estimated radiation exposure for the contrast-enhanced scan without prospective x-ray tube modulation was calculated as 17.0 and 13.4 mSv which is in line with previous reports¹⁹.

The diagnostic performance of CTCA for detecting significant stenoses on a patient-based analysis is detailed in Table 2. All female (63/63) and 99% of male (188/190) patients with significant CAD on CCA were correctly identified by CT (Figure 1,2). Fifteen women (25%, 15/60) and 9 men (10%, 9/89) with non-significant CAD were incorrectly classified as having significant coronary stenoses by CT.

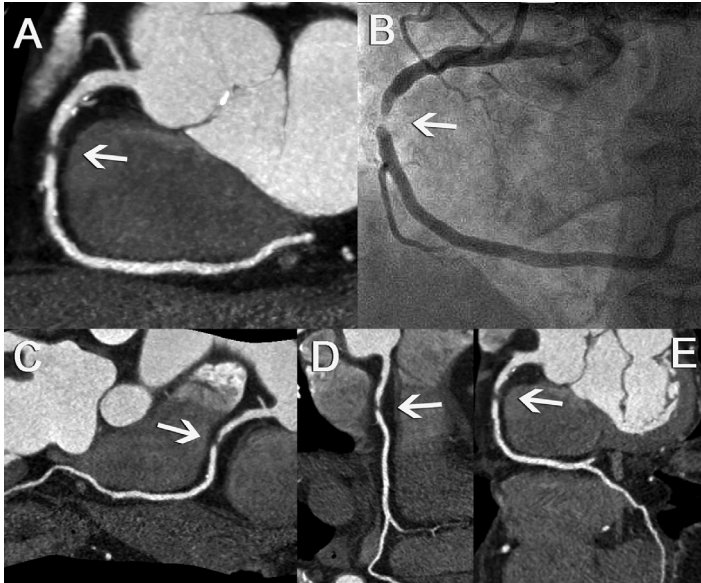
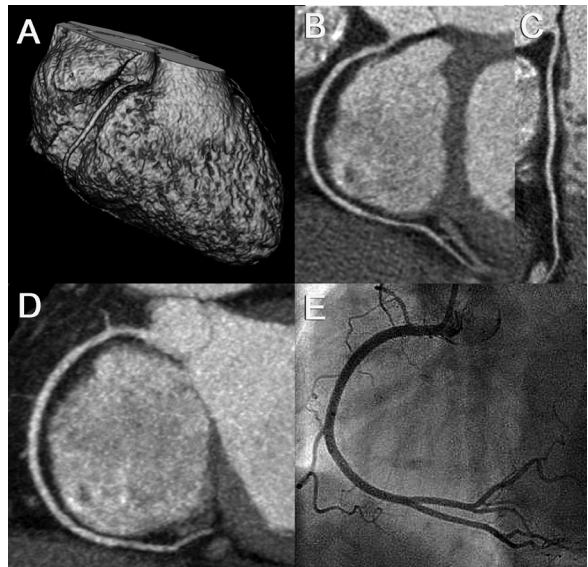


Figure 1: A maximum intensity projected (MIP) CTCA image (A) depicts the anatomy of the right coronary artery (RCA). In the mid RCA a non-calcified obstructive coronary stenosis is visualized with proximally and distally non-obstructive calcified plaques. Three curved multiplanar reconstructed images (cMPR) confirm the significant lesions from three orthogonal projections (C, D, E), which was confirmed by CCA (B).

significantly diseased right coronary arteries, one left anterior descending coronary artery and three diseased circumflex coronary arteries were incorrectly classified as non-significantly diseased. In men, significant coronary stenosis in 2 right coronary arteries, 2 left anterior descending coronary arteries and 4 circumflex coronary arteries were missed. Significant left main disease was identified in all cases. Fifty-one and 125 non-obstructive vessels were overestimated in female and male patients and scored as false positives. The diagnostic accuracy was equal in women and men. Agreement between CTCA and QCA on a per-vessel level was both good for women and men (k -value: 0.69; 0.74).

Figure 2: A volume-rendered CTCA image (A) reveals the anatomy of the RCA. Two orthogonal cMPR images (B, C) and a MIP image (D) disclose a normal coronary artery without obstructive or non-obstructive plaques which was confirmed by CCA (E). (A full color version of this illustration can be found in the color section).



In women specificity (75% vs. 90%; $p < 0.05$), positive predictive value (81% vs. 95%; $p < 0.001$), and overall accuracy (88% vs. 96%; $p < 0.01$) were significantly lower, compared to men. Agreement between CTCA and QCA on a per-patient (no or any disease) level for women and men was good (k -value: 0.75) and very good (k -value: 0.91).

The diagnostic performance of CTCA for the detection of significant coronary stenosis on a vessel-based analysis is detailed in Table 2. In the female population 2 significantly diseased right coronary arteries, one left anterior descending coronary artery and three diseased circumflex coronary arteries were incorrectly classified as non-significantly diseased.

Table 2: Overall diagnostic performance of 64 slice Computed Tomography coronary angiography

Variable	Women n% (95% CI), n/n	Men n% (95% CI), n/n	p
Patients level			
Sensitivity	100% (93-100) 63/63	99% (96-100) 188/190	ns
Specificity	75% (62-85) 45/60	90% (81-95) 80/89	< 0.05
Positive predictive value	81% (70-88) 63/78	95% (91-98) 188/197	< 0.001
Negative predictive value	100% (93-100) 45/45	98% (91-100) 80/82	ns
Diagnostic accuracy	88% (82-94) 108/123	96% (94-98) 268/279	< 0.01
+ Likelihood ratio	4.00 (2.58-6.20)	9.78 (4.70-14.25)	-
- Likelihood ratio	0.00 (0-/-)	0.01 (0.00-0.05)	-
Vessel level			
Sensitivity	94% (87-98) 93/99	97% (95-99) 307/315	ns
Specificity	87% (83-90) 342/393	84% (82-87) 676/801	ns
Positive predictive value	65% (56-72) 93/144	71% (66-75) 307/432	ns
Negative predictive value	98% (96-99) 342/348	99% (98-99) 676/684	ns
Diagnostic accuracy	88% (86-91) 435/492	88% (86-90) 983/1116	ns
+ Likelihood ratio	7.24 (5.58-9.40)	6.25 (5.31-7.34)	-
- Likelihood ratio	0.07 (0.03-0.15)	0.03 (0.02-0.06)	-
Segment level			
Sensitivity	82% (74-88) 111/136	93% (91-96) 400/428	< 0.001
Specificity	94% (93-95) 1551/1648	92% (91-93) 3249/3523	< 0.05
Positive predictive value	53% (46-60) 111/208	59% (56-63) 400/674	ns
Negative predictive value	98% (98-99) 1551/1576	99% (99-99) 3249/3277	< 0.05
Diagnostic accuracy	93% (92-94) 1662/1784	92% (92-93) 3523/3951	ns
+ Likelihood ratio	13.87 (11.25-17.09)	12.02 (10.70-13.50)	-
- Likelihood ratio	0.20 (0.14-0.28)	0.07 (0.05-0.10)	-

Diagnostic performance and predictive value with corresponding likelihood ratios of 64-Slice CT coronary angiography for the detection of $\geq 50\%$ stenosis on QCA in females and males. Chi square test was used for categorical variables. P values were significant if values < 0.05. Values in parentheses represent 95 CIs.

After exclusion of anatomically absent segments (833) and segments distal to an occlusion (266), 5735 out of 6834 potentially available segments (with a maximum of 17 segments per patient) could be included for comparison with QCA. No segments were excluded for reasons of calcifications or poor image quality. The overall sensitivity and specificity of CTCA for the detection of significantly stenosed coronary segments was 91% and 93%. Sensitivity was lower in women (82% vs. 93%; p: < 0.001). Also the specificity (94% vs 92%; p: < 0.05) and negative predictive value (98% vs. 99%; p: <0.05) showed a small, but significant difference between men and women (Table 2).

The performance of CTCA was similar between men and women in the proximal and middle segments (Table 3). However, in the distal segments (56% vs. 85%; $p < 0.05$) and side branches more lesions were not detected in women (sensitivity 54% vs. 89%; $p < 0.001$, negative predictive value 97% vs. 99%; $p < 0.05$). The specificity (96% vs. 93%; $p < 0.05$) was slightly higher in women. Inter- and intraobserver variability for detection of a significant stenosis per segment had a k -value of 0.70 and 0.72, respectively. Agreement between CTCA and QCA on a per-segment level was good both for women and men (k -value: 0.61; 0.68). To exclude the possible confounding effect of nesting, random selection of a single segment per patient was done and the diagnostic accuracy for detecting significant artery disease resulted in a sensitivity 92% (44/48; 95% CI, 79 to 97), specificity 93% (331/356; 95% CI, 90 to 95), positive predictive value 64% (44/69; 95% CI, 51 to 75), negative predictive value 99% (331/335; 95% CI, 97-100).

Table 3: Diagnostic performance of 64 slice Computed Tomography coronary angiography depending on segment location

	Women n% (95% CI), n/n	Men n% (95% CI), n/n	p
Analysis op proximal segments			
Sensitivity	96% (84-99) 44/46	98% (93-99) 130/133	ns
Specificity	92% (89-94) 411/446	91% (87-92) 891/983	ns
Positive predictive value	56% (44-67) 44/79	59% (52-65) 130/228	ns
Negative predictive value	100% (98-100) 411/413	100% (99-100) 891/894	ns
Analysis op mid segments			
Sensitivity	93% (81-98) 43/46	96% (90-98) 133/139	ns
Specificity	91% (87-94) 285/314	88% (86-91) 575/650	ns
Positive predictive value	60% (47-71) 43/72	64% (57-70) 133/208	ns
Negative predictive value	99% (97-100) 285/288	99% (98-100) 575/581	ns
Analysis op distal segments			
Sensitivity	56% (31-79) 9/16	85% (74-93) 53/62	< 0.05
Specificity	97% (94-98) 364/376	96% (94-97) 754/786	ns
Positive predictive value	43% (23-66) 9/21	62% (51-72) 53/85	ns
Negative predictive value	98% (96-99) 364/371	99% (98-99) 754/763	ns
Analysis op side branches			
Sensitivity	54% (34-72) 15/28	89% (81-95) 84/94	< 0.001
Specificity	96% (94-97) 491/512	93% (92-95) 1029/2104	< 0.05
Positive predictive value	42% (26-59) 15/36	53% (45-61) 84/59	ns
Negative predictive value	97% (96-99) 491/504	99% (98-100) 1029/1039	< 0.05

Chi square test was used for categorical variables. P values were significant if values < 0.05. Values in parentheses represent 95 CIs.

DISCUSSION

We demonstrated that the sensitivity of 64-slice CTCA to detect significant CAD was almost equally high in women and men (100% vs. 99%) due to the very low occurrence of false-negative outcomes. Therefore, the diagnostic accuracy of 64-slice CTCA to rule out the presence of significant obstructive CAD was equally high in women and men and a negative CT-scan reliably obviates the need for further downstream evaluation with invasive coronary angiography. The lower prevalence of CAD in women, with a trend towards more non-significant CAD ($p: 0.06$) likely contributed to the overestimation of coronary stenosis severity and resulted thus in lower specificity (75% vs. 90%).

The segment based diagnostic accuracy of CTCA performed on a site-by-site analysis (segmental analysis) compared to CCA revealed a more complex outcome. The sensitivity to detect a stenosis was lower in women than in men. The overall reduced sensitivity was mainly caused by the lower sensitivity of CTCA to detect coronary obstructions in distal coronary segments and side branches. This may be partly explained by the combination of a milder stenosis severity and smaller size of the coronary arteries in women than in men. However, this outcome does not affect the reliability to rule out the presence of significant CAD in case of a negative CT-scan, because on a segment based analysis the overwhelming majority of these segments have no significant CAD and the calculation of the negative predictive value is almost not affected by the higher occurrence of false negative outcomes.

The studied patients were not a prospective, consecutive group of patients. However, selection was not based on particular patient demographics, but rather on the availability of the 64 slice CT scanner for the examination of cardiac patients.

Fundamental limitations of cardiac CT include the use of radiation, potentially nephrotoxic contrast media and the need to use betablockers in patients with a fast heart rate. The substantial radiation exposure of 64-slice CTCA for women (17 mSv) and men (13.4 mSv) as compared to CCA (3-6 mSv) is of concern¹⁹. In this study prospective electrocardiographic X-ray tube modulation, which can significantly reduce radiation exposure, was not applied. This technique limits the possibility of reconstructing images in the end-systolic phase. In our study end-systolic data sets provided better image quality in 34% of patients. Furthermore, the use of prospective electrocardiographic X-ray tube modulation requires a regular heart rhythm throughout the scan. In case of an extra-systole the use of prospective electrocardiographic X-ray tube modulation can miss-trigger the X-ray pulsing, limiting the possibility to edit valuable reconstruction window datasets during high-dose scanning.

REFERENCES

1. Leschka S, Alkadhi H, Plass A, Desbiolles L, Grunenfelder J, Marincek B, Wildermuth S. Accuracy of MSCT coronary angiography with 64-slice technology: first experience. *Eur Heart J* 2005;26:1482-1487.
2. Raff GL, Gallagher MJ, O'Neill WW, Goldstein JA. Diagnostic accuracy of noninvasive coronary angiography using 64-slice spiral computed tomography. *J Am Coll Cardiol* 2005;46:552-557.
3. Leber AW, Knez A, von Ziegler F, Becker A, Nikolaou K, Paul S, Wintersperger B, Reiser M, Becker CR, Steinbeck G, Boekstegers P. Quantification of obstructive and nonobstructive coronary lesions by 64-slice computed tomography: a comparative study with quantitative coronary angiography and intravascular ultrasound. *J Am Coll Cardiol* 2005;46:147-154.
4. Mollet NR, Cademartiri F, van Mieghem CA, Runza G, McFadden EP, Baks T, Serruys PW, Krestin GP, de Feyter PJ. High-resolution spiral computed tomography coronary angiography in patients referred for diagnostic conventional coronary angiography. *Circulation* 2005;112:2318-2323.
5. Ropers D, Rixe J, Anders K, Kuttner A, Baum U, Bautz W, Daniel WG, Achenbach S. Usefulness of multidetector row spiral computed tomography with 64- x 0.6-mm collimation and 330-ms rotation for the noninvasive detection of significant coronary artery stenoses. *Am J Cardiol* 2006;97:343-348.
6. Schuijf JD, Pundziute G, Jukema JW, Lamb HJ, van der Hoeven BL, de Roos A, van der Wall EE, Bax JJ. Diagnostic accuracy of 64-slice multislice computed tomography in the noninvasive evaluation of significant coronary artery disease. *Am J Cardiol* 2006;98:145-148.
7. Nikolaou K, Knez A, Rist C, Wintersperger BJ, Leber A, Johnson T, Reiser MF, Becker CR. Accuracy of 64-MDCT in the diagnosis of ischemic heart disease. *AJR Am J Roentgenol* 2006;187:111-117.
8. Fine JJ, Hopkins CB, Ruff N, Newton FC. Comparison of accuracy of 64-slice cardiovascular computed tomography with coronary angiography in patients with suspected coronary artery disease. *Am J Cardiol* 2006;97:173-174.
9. Ehara M, Surmely JF, Kawai M, Katoh O, Matsubara T, Terashima M, Tsuchikane E, Kinoshita Y, Suzuki T, Ito T, Takeda Y, Nasu K, Tanaka N, Murata A, Suzuki Y, Sato K. Diagnostic accuracy of 64-slice computed tomography for detecting angiographically significant coronary artery stenosis in an unselected consecutive patient population: comparison with conventional invasive angiography. *Circ J* 2006;70:564-571.

10. Gibbons RJ, Balady GJ, Bricker JT, Chaitman BR, Fletcher GF, Froelicher VF, Mark DB, McCallister BD, Mooss AN, O'Reilly MG, Winters WL, Jr., Antman EM, Alpert JS, Faxon DP, Fuster V, Gregoratos G, Hiratzka LF, Jacobs AK, Russell RO, Smith SC, Jr. ACC/AHA 2002 guideline update for exercise testing: summary article: a report of the American College of Cardiology/American Heart Association Task Force on Practice Guidelines (Committee to Update the 1997 Exercise Testing Guidelines). *Circulation* 2002;106:1883-1892.
11. Kwok Y, Kim C, Grady D, Segal M, Redberg R. Meta-analysis of exercise testing to detect coronary artery disease in women. *Am J Cardiol* 1999;83:660-666.
12. Kim C, Kwok YS, Heagerty P, Redberg R. Pharmacologic stress testing for coronary disease diagnosis: A meta-analysis. *Am Heart J* 2001;142:934-944.
13. Mieres JH, Shaw LJ, Hendel RC, Miller DD, Bonow RO, Berman DS, Heller GV, Bairey-Merz CN, Cacciabauda JM, Kiess MC, Polk DM, Smanio PE, Walsh MN. American Society of Nuclear Cardiology consensus statement: Task Force on Women and Coronary Artery Disease--the role of myocardial perfusion imaging in the clinical evaluation of coronary artery disease in women [correction]. *J Nucl Cardiol* 2003;10:95-101.
14. Santana-Boado C, Candell-Riera J, Castell-Conesa J, Aguade-Bruix S, Garcia-Burillo A, Canela T, Gonzalez JM, Cortadellas J, Ortega D, Soler-Soler J. Diagnostic accuracy of technetium-99m-MIBI myocardial SPECT in women and men. *J Nucl Med* 1998;39:751-755.
15. Mieres JH, Shaw LJ, Arai A, Budoff MJ, Flamm SD, Hundley WG, Marwick TH, Mosca L, Patel AR, Quinones MA, Redberg RF, Taubert KA, Taylor AJ, Thomas GS, Wenger NK. Role of noninvasive testing in the clinical evaluation of women with suspected coronary artery disease: Consensus statement from the Cardiac Imaging Committee, Council on Clinical Cardiology, and the Cardiovascular Imaging and Intervention Committee, Council on Cardiovascular Radiology and Intervention, American Heart Association. *Circulation* 2005;111:682-696.
16. Klocke FJ, Baird MG, Lorell BH, Bateman TM, Messer JV, Berman DS, O'Gara PT, Carabello BA, Russell RO, Jr., Cerqueira MD, St John Sutton MG, DeMaria AN, Udelson JE, Kennedy JW, Verani MS, Williams KA, Antman EM, Smith SC, Jr., Alpert JS, Gregoratos G, Anderson JL, Hiratzka LF, Faxon DP, Hunt SA, Fuster V, Jacobs AK, Gibbons RJ, Russell RO. ACC/AHA/ASNC guidelines for the clinical use of cardiac radionuclide imaging--executive summary: a report of the American College of Cardiology/American Heart Association Task Force on Practice Guidelines (ACC/AHA/ASNC Committee to Revise the 1995 Guidelines for the Clinical Use of Cardiac Radionuclide Imaging). *J Am Coll Cardiol* 2003;42:1318-1333.
17. Agatston AS, Janowitz WR, Hildner FJ, Zusmer NR, Viamonte M, Jr., Detrano R. Quantification of coronary artery calcium using ultrafast computed tomography. *J Am Coll Cardiol* 1990;15:827-832.

18. Austen WG, Edwards JE, Frye RL, Gensini GG, Gott VL, Griffith LS, McGoon DC, Murphy ML, Roe BB. A reporting system on patients evaluated for coronary artery disease. Report of the Ad Hoc Committee for Grading of Coronary Artery Disease, Council on Cardiovascular Surgery, American Heart Association. *Circulation* 1975;51:5-40.
19. Hausleiter J, Meyer T, Hadamitzky M, Huber E, Zankl M, Martinoff S, Kastrati A, Schomig A. Radiation dose estimates from cardiac multislice computed tomography in daily practice: impact of different scanning protocols on effective dose estimates. *Circulation* 2006;113:1305-1310.
20. Thom T, Haase N, Rosamond W, Howard VJ, Rumsfeld J, Manolio T, Zheng ZJ, Flegal K, O'Donnell C, Kittner S, Lloyd-Jones D, Goff DC, Jr., Hong Y, Adams R, Friday G, Furie K, Gorelick P, Kissela B, Marler J, Meigs J, Roger V, Sidney S, Sorlie P, Steinberger J, Wasserthiel-Smoller S, Wilson M, Wolf P. Heart disease and stroke statistics--2006 update: a report from the American Heart Association Statistics Committee and Stroke Statistics Subcommittee. *Circulation* 2006;113:e85-151.
21. Vaccarino V, Parsons L, Every NR, Barron HV, Krumholz HM. Sex-based differences in early mortality after myocardial infarction. National Registry of Myocardial Infarction 2 Participants. *N Engl J Med* 1999;341:217-225.

6

Reliable High-speed Coronary Computed Tomography in Symptomatic Patients

Journal of American College of Cardiology.
2007 Aug 21;50(8):786-94.

Annick C. Weustink MD^{1,2},
Willem B. Meijboom MD^{1,2},
Nico R. Mollet MD, PhD^{1,2},
Masato Otsuka MD¹,
Francesca Pugliese MD^{1,2},
Carlos van Mieghem MD^{1,2},
Roberto Malago MD²,
Niels van Pelt MD^{1,2}, Marcel
L. Dijkshoorn BSc², Filippo
Cademartiri MD, PhD^{1,2},
Gabriel P. Krestin MD, PhD²,
Pim J. de Feyter, MD, PhD^{1,2}

¹ Department of Cardiology,
Thoraxcenter

² Department of Radiology
Erasmus MC, Rotterdam,
the Netherlands

ABSTRACT

Objectives

To prospectively evaluate the diagnostic performance of the high-speed Dual Source CT-scanner (DSCT), with an increased temporal resolution (83 ms), for the detection of significant coronary lesions ($\geq 50\%$ lumen diameter reduction) in a clinically wide range of patients.

Background

Cardiac motion artefacts may decrease coronary image quality with use of earlier computed tomography scanners.

Methods

We prospectively studied 100 symptomatic patients (79 men, 21 female, mean age 61 ± 11 years) with atypical (18%) or typical (55%) angina pectoris, or unstable coronary artery disease (27%) scheduled for conventional coronary angiography. Mean scan time was 8.58 ± 1.52 seconds. Mean heart rate was 68 ± 11 bpm. Quantitative coronary angiography (QCA) was used as the standard of reference. Irrespective of image quality or vessel size, all segments were included for analysis.

Results

Invasive coronary angiography demonstrated no significant disease in 23%, single-vessel disease in 31%, and multi-vessel disease in 46% of patients. 1489 coronary segments, containing two hundred-twenty significant (14.8%) stenoses, were available for analysis. Sensitivity, specificity, positive and negative predictive value of DSCT coronary angiography for the detection of significant lesions on a segment-by-segment analysis were 95% (95% CI: 90-97), 95% (95% CI: 93-96), 75% (95% CI: 69-80), 99% (95% CI: 98-99), respectively and on a patient based analysis: 99% (95% CI: 92-100), 87% (95% CI: 65-97), 96% (95% CI: 89-99) and 95% (95% CI: 74-100), respectively.

Conclusions

Non-invasive DSCT coronary angiography is highly sensitive to detect and to reliably rule out the presence of a significant coronary stenosis in patients presenting with atypical or typical angina pectoris, or unstable coronary artery disease.

INTRODUCTION

For almost 50 years, invasive coronary angiography has been the standard of reference for diagnosing coronary artery disease. However, non-invasive coronary imaging with computed tomography (CT) has rapidly emerged and initial experience with 4-, 16- and 64 slice CT coronary angiography has been reported (1-13). Despite technical advances in CT technology, a substantial number of coronary segments remain unevaluable due to presence of motion artefacts and a limited image resolution, which seriously hampered clinical implementation of CT coronary angiography (4,14).

A newly introduced Dual Source CT (DSCT) system, with an improved temporal resolution of 83 ms independent of patient's heart rate, allows for scanning of the coronaries without the use of prescan β -blockers. The pitch is adapted to the heart rate and scan times are reduced at higher heart rates. Shorter scan times allow for reduction of radiation exposure to the patient. We now report the diagnostic performance of DSCT coronary angiography to detect or rule out significant coronary stenoses in the clinically relevant coronary tree in 100 patients with a wide spectrum of symptomatic coronary artery disease.

METHODS

Study Population

After an initial 3-week test period during which scan protocols were optimized, we subsequently included during a 10-week period 111 symptomatic patients with atypical angina, typical angina and unstable coronary artery disease (unstable angina or Non-ST-segment elevation myocardial infarction) scheduled for conventional coronary angiography (CCA). All CT-examinations were performed before CCA. Only patients in sinus heart rhythm without previous history of percutaneous coronary intervention or bypass surgery were included. Excluded were 11 patients with known allergy to Iodinated contrast material (n=1), impaired renal function (serum creatinine > 120 $\mu\text{mol/l}$) (n=5), persistent arrhythmias (n=3) or logistic inability to perform a CT scan before CCA (n=2). Thus, the study population comprised 100 patients (79 male, 21 female, mean age 61 ± 10.9 ; range 28-87 years). The institutional review board approved the study and all patients gave informed consent.

Patient Preparation

No oral or intravenous pre-scan β -blockers were administered prior to the scan.

Scan Protocol and Image Reconstruction

All patients were scanned using a DSCT (Somatom Definition, Siemens Medical Solutions, Forchheim, Germany). The system combines two arrays each consisting of an X-ray tube plus detector (64 slices) mounted on a single gantry with an angular offset of 90° and a gantry rotation time of 330 ms. DSCT permits spiral CT scanning of the coronary arteries with an improved temporal resolution of 83 ms using single-segment reconstruction (15).

In DSCT, radiation exposure has been reduced by the application of an additional cardiac bowtie filter, a smaller FOV of the second detector and an increased pitch in higher heart rates. All patients underwent a non-enhanced CT scan for calcium scoring prior to DSCT coronary angiography. All patients received Nitroglycerin (0.4 mg/dose) sublingually just before scanning.

Calcium scoring scan parameters were: a tube current of 84 mAs/rot (maximum) and full X-ray tube current was given during 50-70% of the RR interval. A single dataset was reconstructed using ECG-gating with a slice thickness of 3 mm and increment of 1.5 mm using a medium convolution kernel (B35f) during 60% of the RR interval.

DSCT angiographic scan parameters were: number of slices/rotation 32 x 2 with z-flying focal spot for each detector, individual detector width 0.6mm, rotation time 330 ms, tube voltage 120 kV. Pitch values were adapted to heart rate after an estimation based on the last 10 heartbeats preceding the scan. Each tube provided 412 mAs/rot (maximum), and full X-ray tube current was given during 25-70% of the RR-interval.

The volume of Iodinated contrast material (Ultravist® 370 mg/ml, Schering AG, Germany) was adapted to the scan time. A contrast bolus (60-90 ml) was injected in an antecubital vein at a flow rate of 5.5 ml/s followed by a saline chaser of 40 ml at 5.5 ml/s. A bolus tracking technique was applied to synchronize the arrival of contrast in the coronary arteries and the start of the scan. All CT coronary angiography datasets were reconstructed with a slice thickness of 0.75 mm and increment of 0.4 mm using medium-to-smooth convolution kernel (B26f), resulting in a spatial resolution of 0.6-0.7 mm in-plane and 0.5 mm through-plane (15).

The reconstruction algorithm uses data from a single heart beat, obtained during a quarter X-ray tube rotation by two separate X ray tubes, resulting in a temporal resolution of 83 ms. Images were reconstructed following a stepwise pattern depending on patient's heart rate during scanning. Initially, a single dataset was reconstructed during the mid-to-end diastolic phase (350 ms before the next R-wave) in patients with low heart rates (<60 bpm), during both the mid-to-end diastolic phase and end-systolic phase (275 after the next R-wave) in patients with intermediate heart rates (60-80 bpm), and during the end-systolic phase in patients with high heart rates (>80 bpm). Image quality was assessed on a per-segment level. In case of persistent coronary motion artefacts in

patients with low and high heart rates, additional datasets were reconstructed in end-systolic and mid-to-end diastolic phase, respectively. If necessary, multiple datasets of a single patient were used separately in order to obtain optimal image quality of all available coronary segments.

The effective dose for DSCT coronary angiography was estimated based on Monte Carlo calculations (ImPACT[®], version 0.99x, St. George's Hospital, Tooting, London, UK).

Quantitative Coronary Angiography (QCA)

One experienced cardiologist, unaware of the results of DSCT coronary angiography, identified all available coronary segments using a 17-segment modified American Heart Association (AHA) classification (16). All segments, irrespective of size, were included for comparison with DSCT coronary angiography, except for segments distal to a total occlusion.

Segments were classified as normal (smooth parallel or tapering borders), as having non-significant disease (luminal irregularities or < 50% diameter stenosis), or as having significant stenoses (\geq 50% diameter stenosis). Stenoses were evaluated in two orthogonal views, and classified as significant if the mean lumen diameter reduction was \geq 50% using a validated quantitative coronary angiography algorithm (CAAS[®], Pie Medical, Maastricht, the Netherlands).

DSCT Image Evaluation

One experienced observer, unaware of the results of CCA, calculated total calcium scores as Agatston scores, using validated software (Syngo MMWP VE20A[®], Siemens, Forchheim Germany).

One observer evaluated image quality on a per segment level and classified as good image quality (defined as absence or presence of any image-degrading artefacts related to motion, calcification, or noise, but evaluations possible with good to moderate confidence), or poor (presence of image-degrading artefacts and evaluation only possible with low confidence). Irrespective of image quality, all available coronary segments (including poor image quality) were included for comparison of DSCT with CCA.

Two experienced observers, unaware of the results of CCA, scored all DSCT coronary angiography datasets. Axial views and maximum intensity projections were used to identify coronary lesions. In addition, (curved) multi-planar reconstructions were used to classify coronary lesions into significantly diseased or not. Inter-observer disagreements were resolved by consensus in a joint session.

Statistical analysis

The diagnostic performance of DSCT coronary angiography for the detection of significant lesions in coronary arteries with QCA as the standard of reference is presented as sensitivity, speci-

ficity, positive predictive value and negative predictive value and positive and negative likelihood ratios with the corresponding 95% confidence intervals (CIs). Comparison between DSCT coronary angiography and QCA was performed on three levels: segment-by-segment, vessel-by-vessel (no or any significant stenosis per vessel) and patient-by-patient (no or any significant stenosis per patient). An additional sensitivity analysis to detect significant stenoses was performed after random selection of a single segment per patient to explore the effect of nesting. Inter- and intra-observer variability for the detection of significant coronary artery stenosis was calculated using *k*-statistics. To determine the intra-observer variability, one observer evaluated 30 (33%, 30/100) CT datasets twice with a time interval of 3 weeks.

RESULTS

Patient demographics are shown in Table 1. The mean interval between conventional and DSCT coronary angiography was 4.0 ± 4.8 days (range: 0-17). All scans were performed without the use of oral or intravenous β -blockers.

Mean scan range was $11,9 \pm 1,1$ cm (range: 9.3-13.8 cm). Mean CT acquisition time was 8.6 ± 1.5 seconds (range: 5.7-12.7). Pitch varied between 0.20 and 0.53. Mean heart rate was 68 ± 11 bpm (range: 44-107). The overall radiation exposure for CT coronary angiography was estimated as 11.1-14.4 (male/female) mSv 71 (71%, 71/100) patients had long-term β -blocker medication. The estimated radiation exposure of DSCT coronary angiography was 13.5-16.9 (male/female) mSv in low heart rates (mean 56 bpm), 10.7-13.8 (male/female) mSv in moderate heart rates (mean 68 bpm) and 8.3-9.6 (male/female) mSv in high heart rates (mean 81 bpm). In 5% (5/100) of patients with a ventricular extra systole and in 3% (3/100) of patients with a premature atrial complex, ECG editing was successful.

Table 1. Patient demographics (N=100)

Age yrs		61 \pm 11 (28-87)
	Male %	79
	Female %	21
<hr/>		
Clinical presentation		
	Atypical angina %	18
	Typical Angina %	55
	Unstable CAD %	27
<hr/>		
Risk factors		
	Hypertension %	58
	Hypercholesterolemia %	55
	Smoker %	63
	Diabetic Mellitus %	19
	Family history of CAD %	38
	Obese (body mass index \geq 30 kg/m ²) %	65
<hr/>		
Invasive Coronary Angiography		
	Absence of CAD %	16
	Non-significant disease %	7
	Single-vessel disease %	31
	Multi-vessel disease %	46

Values in parentheses represent age range (yrs). N indicates number; CAD, coronary artery disease; Unstable CAD, patients with unstable angina or non ST-segment elevation myocardial infarction

Table 2. Diagnostic Performance and Predictive Value of Dual Source CT Coronary Angiography for the Detection of Significant ($\geq 50\%$) Stenoses

	Prevalence of disease, %	N	TP	TN	FP	FN	κ	Sensitivity (%)	Specificity (%)	PPV (%)	NPV (%)	ACC (%)	+LR	-LR
Patient based analysis														
All patients	77	100	76	20	3	1	0.88	99 (92-100)	87 (65-97)	96 (89-99)	95 (74-100)	96 (92-100)	7.6	0.01
Segment-based analysis														
All segments	15	1489	208	1200	69	12	0.81	95 (90-97)	95 (93-96)	75 (69-80)	99 (98-99)	95 (93-96)	17.4	0.06
Proximal segments	13	449	53	368	25	3	0.76	95 (84-97)	94 (91-96)	68 (56-78)	99 (97-100)	94 (92-96)	14.9	0.06
Mid segments	26	289	71	192	23	3	0.79	96 (88-99)	89 (84-93)	76 (65-84)	98 (95-100)	91 (88-94)	9	0.05
Distal segments	13	305	37	258	7	3	0.86	93 (79-93)	97 (94-99)	84 (69-93)	99 (96-100)	97 (95-99)	35.0	0.08
Side branches	11	446	47	382	14	3	0.83	94 (82-98)	97 (94-98)	77 (64-87)	99 (98-100)	96 (94-98)	26.6	0.06
Vessel-based analysis														
All vessels	38	400	148	223	26	3	0.85	98 (96-99)	90 (85-93)	85 (79-90)	99 (96-100)	93 (90-95)	9.4	0.02
LM	7	100	7	92	1	0	0.93	100 (100)	99 (93-100)	88 (47-99)	100 (95-100)	99 (97-100)	93	0
LAD	51	100	50	35	14	1	0.70	98 (95-100)	71 (57-83)	78 (66-87)	97 (84-100)	85 (78-91)	3.4	0.03
CX	47	100	47	46	7	0	0.86	100 (100)	87 (74-94)	87 (74-94)	100 (90-100)	93 (88-98)	7.6	0
RCA	46	100	44	50	4	2	0.88	96 (92-100)	93 (81-98)	92 (79-97)	96 (86-99)	94 (89-99)	12.9	0.05

N indicates number; TP, true positive; TN, true negative; FP, false positive; FN, false negative; κ kappa; PPI, positive predictive value; NPV, negative predictive value; ACC, accuracy; +LR, positive likelihood ratio; -LR, negative likelihood ratio; RCA, right coronary artery; LM, left main coronary artery; LAD, left anterior descending coronary artery; CX, circumflex coronary artery. According to the 17-segment modified AHA classification 1489 segments and 400 vessels visualized with conventional angiogram were included for segment and vessel analysis, respectively. For patient-based analysis 100 patients were included. Values in parentheses represent upper and lower bound for 95% confidence interval.

A single dataset for the assessment of significant stenoses was used in 81%, 2 datasets in 16% and 3 datasets in 3% of patients in order to obtain optimal image quality on a per-segment level.

Image quality was classified as good in 94% (1400/1489) and poor in 6% (89/1489) on a per-segment level. Reasons for poor image quality were breathing motion artefacts (33%, 29/89), cardiac motion artefacts (14%, 12/89), severe calcifications (46%, 41/89), or low contrast-to-noise (8%, 7/89).

Diagnostic performance of DSCT coronary angiography

The diagnostic accuracy of DSCT to detect significant stenoses on a patient-, segment-, and vessel-based analysis is detailed in Table 2. Typical examples are shown in Figures 1 and 2.

Patient-by-patient analysis

Sixteen patients with either an angiographically normal coronary angiogram (n=16) or with non-significant disease (n=4) were correctly identified with DSCT. Three patients were incorrectly classified as having single-vessel disease. One patient with significant disease was incorrectly classified as having non-significant disease with DSCT. Agreement between DSCT coronary angiography and QCA on a per-patient (no or any disease) level was good (*k*-value: 0.89). Agreement between both techniques for classifying patients as having no, single- or multi-vessel disease was very good (*k*-value: 0.85).

Vessel-by-vessel analysis

One significantly diseased left anterior descending artery and 2 significantly diseased right coronary arteries were incorrectly classified as non-significantly diseased on the CT-scan. Sensitivity for the detection of significantly diseased left anterior descending coronary arteries was 98%, for the right coronary arteries 96%, and for the left main and circumflex coronary arteries 100%. Agreement between CT coronary angiography and QCA on a per-vessel level was very good (*k*-value: 0.85).

Segment-by-segment analysis

A total of 1489 segments that were visualised with invasive coronary angiography were analysed with DSCT coronary angiography. There were 12 (5.5%, 12/220) segments, which were incorrectly classified as having non-significant stenosis by DSCT, of which 3 segments demonstrated poor image quality due to cardiac motion artefacts in 2 segments (mean heart rates; 65 and 78 bpm) and due to severe calcifications in one segment. There were 69 (5.4%, 69/1269) segments, which were incorrectly classified as having a significant stenosis by DSCT, of which 19 segments demonstrated poor image quality due to severe calcifications in 16 segments, a cardiac motion artefact in one segment (mean heart rate 68 bpm), a breathing artefact in one segment and low contrast-to-noise in one segment.

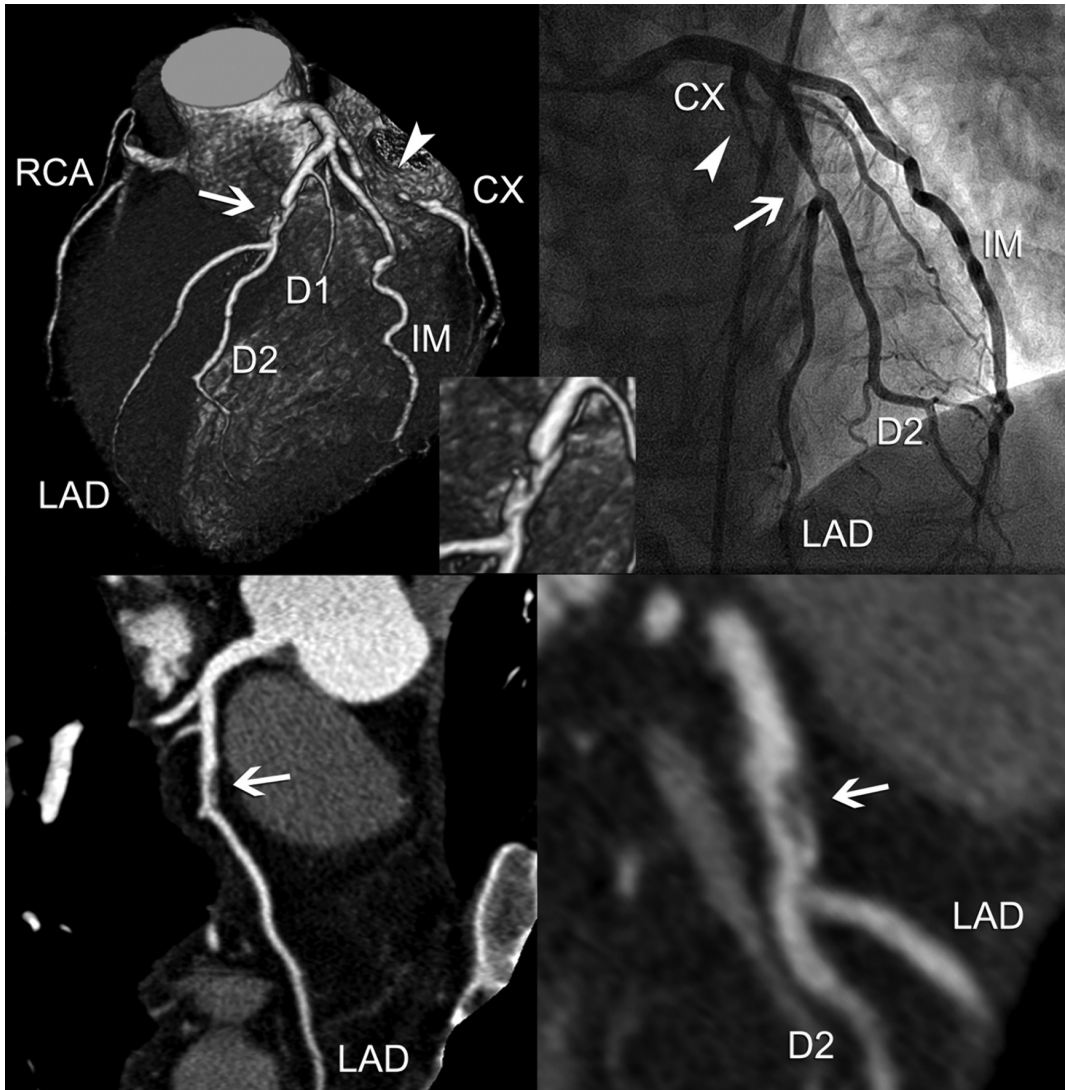


Figure 1. Volume rendered DSCT image (colored image) and corresponding conventional angiography image of the right coronary artery (RCA), left anterior descending artery (LAD), circumflex artery (CX) intermediate branch (IM), diagonal branches (D1, D2) in a 57-year-old man with stable angina and an equivocal bicycle test. Mean heart rate during scanning was 78 bpm. A significant lesion was found in the midpart of the LAD (arrow) with detailed color inlay, curved multiplanar reconstruction (bottom left) and maximum intensity projections (MIP) image (bottom right). The proximal part of the CX showed an occlusion (arrowhead). (A full color version of this illustration can be found in the color section).

Agreement between CT coronary angiography and QCA on a per-segment level was very good (k -value: 0.81).

The k -value of inter- and intra-observer variability for the detection of a significant stenosis per segment was 0.83 and 0.85, respectively.

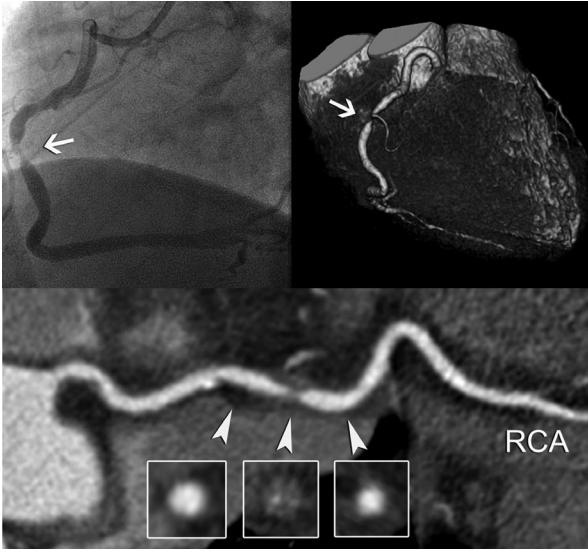


Figure 2. Conventional angiography image and corresponding volume rendered DSCT image (colored image) in a 68-year old man presenting with unstable coronary artery disease. Mean heart rate during scanning was 66 bpm. The arrow indicates a high-grade stenosis in the midpart of the right coronary artery. The arrowheads in the curved multiplanar reconstruction image (bottom) indicate cross-sections proximal, within and distal from the occlusion (arrowheads). (A full color version of this illustration can be found in the color section).

needed in 6% (2/33) of patients). In patients with intermediate heart rates (mean 67.9 bpm), optimal datasets reconstructed during the mid-to-end diastolic phase were selected in 74% (25/34) of patients and additional datasets in the end-systolic phase were needed in 26% (9/34) of patients). In patients with high heart rates (mean 80.7 bpm), optimal datasets reconstructed during the end-systolic phase were selected in 91% (30/33) of patients and additional datasets in the mid-to-end diastolic phase were needed in 9% (3/33) of patients.

Table 5 demonstrates the diagnostic accuracy of DSCT to detect significant coronary stenoses in patients with atypical and typical angina, and unstable coronary artery disease based on a segment based analysis.

A sensitivity analysis was performed after random selection of a single segment per patient. The sensitivity was calculated as 92% (12/13, 95% CI; 87 to 96), specificity was 94% (82/87, 95% CI; 90 to 99), positive predictive value was 71% (12/17, 95% CI; 62 to 80), and negative predictive value was 99% (82/83, 95% CI; 97 to 100).

Table 3 shows the diagnostic accuracy of DSCT to detect significant coronary stenoses in patients with low (17 ± 27), intermediate (198 ± 96), and high (927 ± 727) Agatston calcium scores based on per-segment based analysis.

Patients were divided into 3 groups based on the mean heart rate during DSCT. There was no significant difference in diagnostic accuracy on a segment-based analysis between these groups (Table 4).

In patients with low heart rates (mean 56.1 bpm), optimal datasets reconstructed during the mid-to-end diastolic phase were selected in 94% (31/33) of patients and additional datasets during the end-systolic phase were

Table 3. Influence of Agatston score on Diagnostic Accuracy of Dual Source CT Coronary Angiography (a segment-based analysis).

Group	Mean Agatston score	Prevalence of disease, (%)	N (segments)	TP	TN	FP	FN	κ	Sensitivity (%)	Specificity (%)	PPV (%)	NPV (%)	ACC (%)	+LR	-LR
1	17±27	8	520	39	471	6	4	0.88	91(77-97)	99 (97-99)	86 (73-94)	99 (98-100)	98 (97-99)	72.4	0.10
2	198±96	17	477	76	376	20	5	0.83	94 (86-98)	95 (92-97)	79 (69-87)	99 (97-100)	95 (93-97)	18.7	0.07
3	927±727	20	492	93	353	43	3	0.74	97 (90-99)	89 (86-92)	68 (60-76)	99 (97-100)	91 (88-93)	8.9	0.04

N indicates number; TP, true positive; TN, true negative; FP, false positive; FN, false negative; κ , kappa; PPI, positive predictive value; NPI, negative predictive value; ACC, accuracy; +LR, positive likelihood ratio; -LR, negative likelihood ratio. Values in parentheses represent upper and lower bound for 95% confidence interval.

DISCUSSION

Earlier studies using 4- and 16-slice CT scanners reported moderate to good diagnostic accuracy to detect significant lesions (1-8,14), but the technique was seriously limited by the presence of unevaluable segments which was on average 22% and 9% for the 4- and 16-slice CT, respectively (14). In a recent multi-center study using 16-slice CT scanners the percentage of unevaluable coronary segments was 29% (4).

The development of 64-slice CT scanners involved a significant improvement in image quality and robustness of CT coronary angiography, however, on average 5% and in one report even 12% of segments were reported to be unevaluable and diagnostic accuracy was reduced at higher heart rates (9,10,17,18).

The introduction of Dual Source CT is another step forward. This scanner is equipped with 2 X-ray tubes (dual source) thereby significantly reducing the temporal resolution to 83 milliseconds independent of heart rate, using single segment reconstruction. In non-DSCT systems, multi-segment algorithms are used to improve temporal resolution. However, this approach is very dependent on a regular heart rate. Minor variation in the time interval between consecutive heart beats can result in interpolation artifacts and image blurring. Furthermore, multi-segment reconstruction algorithms require a lower pitch thus longer scan times, more contrast material, and a higher radiation exposure. Multi-segment approaches can also be applied in DSCT, resulting in a mean temporal resolution of up to 40-60 ms at 0.33 s gantry rotation time. This approach is not recommended for coronary angiography examinations, but may be useful for advanced functional evaluation (15).

With the DSCT scanner, we were able to evaluate all coronary segments irrespective of heart rate and image quality. Despite the use of the high-speed DSCT scanner, poor image quality due to cardiac motion artefacts was observed in 14% of the coronary segments. However, the incidence of poor image quality oc-

Table 4. Influence of Heart Rate on the Diagnostic Accuracy of Dual Source CT Coronary Angiography (a segment-based analysis).

Mean Heart rate (sec.)	N (segments)	Prevalence of Disease (%)	TN	FP	FN	κ	Sensitivity (%)	Specificity (%)	PPV (%)	NPV (%)	ACC (%)	+LR	-LR	Eff. Dose (mSv)
56.1±4.2	480	20	358	26	3	0.83	97 (90-99)	93 (90-95)	78 (69-85)	99 (97-100)	94 (92-96)	14.3	0.07	13.5-16.9
67.9±3.8	490	12	54	418	15	3	95 (85-99)	97 (94-98)	79 (66-87)	99 (98-100)	96 (95-98)	27.4	0.05	10.7-13.8
80.7±8.5	519	13	61	424	28	6	91 (81-96)	94 (91-96)	68 (58-78)	99 (97-99)	93 (91-96)	14.7	0.10	8.3-9.6

N indicates number; TP, true positive; TN, true negative; FP, false positive; FN, false negative; κ , kappa; PPV, positive predictive value; NPV, negative predictive value; ACC, accuracy; Eff.Dose = effective dose (male-female). Values in parentheses represent upper and lower bound for 95% confidence interval.

Table 5. Diagnostic Performance and Predictive Value of Dual Source CT Coronary Angiography for the Detection of Significant ($\geq 50\%$) Stenoses in patients with Atypical Angina, Typical Angina, or Unstable CAD

	Prevalence of disease, (%)	N	TP	TN	FP	FN	κ	Sensitivity (%)	Specificity (%)	PPV (%)	NPV (%)	ACC (%)	+LR	-LR
Patient based analysis														
Atypical Angina	39	18	7	11	0	0	1.00	100 (56-100)	100 (68-100)	100 (56-100)	100 (68-100)	100	-	0
Typical Angina	89	55	49	4	2	0	0.78	100 (91-100)	67 (24-94)	96 (85-99)	100	100 (91-100)	3	0
Unstable CAD	78	27	20	5	1	1	0.79	95 (74-100)	100 (52-100)	100 (40-100)	86 (73-99)	96 (83-100)	-	0.05
Segment based analysis														
Atypical Angina	6	281	17	260	4	0	0.89	100 (77-100)	99 (96-100)	81 (57-94)	100 (98-100)	99 (97-100)	66.0	0
Typical Angina	17	809	125	633	42	9	0.79	93 (87-97)	94 (92-95)	75 (67-81)	99 (97-99)	94 (92-95)	15.0	0.07
Unstable CAD	17	399	66	307	23	3	0.80	96 (87-99)	93 (90-95)	74 (64-83)	99 (97-99)	93(91-96)	13.7	0.05

N indicates number; TP, true positive; TN, true negative; FP, false positive; FN, false negative; κ , kappa; PPV, positive predictive value; NPV, negative predictive value; ACC, accuracy; +LR, positive likelihood ratio; -LR, negative likelihood ratio; CAD, coronary artery disease; Unstable CAD, patients with unstable angina or non ST-segment elevation myocardial infarction

curred independent of heart rate and good image quality could also be obtained in high heart rates.

We demonstrated that DSCT coronary angiography had a high diagnostic accuracy to detect significant coronary lesions on a per-segment based level as compared to quantitative coronary angiography. We selected a $\geq 50\%$ diameter stenosis as the cut-off criterion for significant coronary artery disease to allow comparison with the majority of previous published reports (19). A segmental analysis is clinically useful in patients referred for coronary angiography to assess location (proximal, mid, distal, RCA, LAD, CX) severity (luminal narrowing $\geq 50\%$) and extent (1,2 or 3-vessel disease) of coronary artery disease, which determines the value of CT scanning as an alternative to invasive coronary angiography. The patient based diagnostic accuracy was high (96%) and a negative DSCT-scan reliably ruled out the presence of a significant coronary stenosis in patients with atypical and typical angina, and unstable coronary artery disease (Table 5). These findings indicate that DSCT-scanning is reliable as a gatekeeper of invasive coronary angiography.

In patients with a positive CT scan showing a severe ($>70\%$ diameter stenosis) lesion or a totally occluded vessel, no further evaluation is necessary. However, a positive CT scan with an estimated lesion severity of around 50% has limited value since it poorly discriminates functionally significant lesions from the ones that are not hemodynamically important (20). In this situation an additional functional imaging test such as myocardial perfusion scintigraphy or stress echocardiography would be a logical step before referring the patient for an invasive angiogram and possible revascularisation. In patients deemed necessary to undergo revascularisation direct referral to the cathlab may be more logical with invasive assessment of the functional relevance of a lesion using fractional flow reserve (FFR) and performance of percutaneous coronary intervention (PCI) in the same session.

Lastly, new developments in CT coronary angiography are desirable for further improvement in clinical performance. Increased gantry rotation speed can further improve temporal resolution but structural modifications will be required to account for a substantial increase in mechanical forces on the gantry. An alternative concept is the use of multiple (>2) X-ray sources and detectors within a single gantry, thereby obviating the need for an increased gantry rotation speed to improve temporal resolution. Further-improved spatial resolution of less than 0.6 mm can be achieved by the use of smaller detector rows. However, an equal contrast-to-noise ratio requires an exponential increase in X-ray power, which will result an excessive X-ray radiation exposure. Thus, new detector technology is needed to further improve spatial resolution.

LIMITATIONS

DSCT coronary angiography should not be performed in patients with significant renal dysfunction or contrast intolerance. This further restricts the use of CT coronary angiography to selected patients, which should be taken into account when the technique is going to be applied in general clinical practise.

One advantage of DSCT is that patients with higher heart rates do not require premedication with betablockers because necessary treatment with betablockers prior to CT-scanning hampers the CT-throughput. The majority of patients (73%) in our study population already received long-term beta-blocker treatment and therefore did not benefit from an increased workflow. However, the use of DSCT in a low or intermediate risk patient groups with expected lower use of chronic betablockers could be more efficient in terms of diagnostic throughput.

The rather high radiation exposure with CT coronary angiography is of concern. In our study the overall effective dose for DSCT coronary angiography was estimated as 11.1-14.4 mSv (male/female), which is lower than the reported effective dose in 64-slice CTA (15.2-21.4 mSv male/female) (21). The significant reduction of effective radiation dose (8.3-9.6 mSv male/female) in high (>80 bpm) heart rates as compared to low (<60 bpm) heart rates (13.5-16.9 mSv male/female) can mainly be ascribed to an increased pitch and therefore shorter scan times in patients with high heart rates. However, compared to the effective dose in diagnostic coronary angiography (3-10 mSv) (22), the effective dose in DSCT coronary angiography still remains relatively high.

In this initial experience with the DSCT scanner we selected a relatively wide pulsing window (25% to 70% of the RR-interval), which allows for reconstruction of datasets during both the mid-to-end diastolic phase and end-systolic phase to obtain optimal image quality. However there is a delicate balance between the width of the pulsing window and radiation exposure to the patient. Earlier technical feasibility studies demonstrated a significant reduction of the effective radiation dose by using a smaller width of the pulsing window (15). Further clinical studies should establish which pulsing window provides the optimal balance between radiation exposure and image quality, and the effect of a small pulsing window on diagnostic accuracy.

Persistent arrhythmias preclude accurate assessment with DSCT. For the purpose of this study, we excluded patients with persistent arrhythmias, which was also an exclusion criteria in studies using 64-slice scanners. However, our results demonstrate that DSCT technology enables us to scan patients with minor heart rate irregularities, such as a ventricular extra systole or a premature atrial complex by automatically switching off ECG pulsing during irregular heartbeats. This enables the operator to perform ECG-editing to correct for minor heart rate irregularities.

Severe calcifications remain problematic. Calcifications obscure the underlying lumen and preclude judgement of coronary lumen integrity resulting in overestimation of the severity of a coronary stenosis. This explains the observation that in 84% (16/19) of segments, which were incorrectly classified as having a significant stenosis by DSCT, severe calcifications resulted in poor image quality. In patients with high (mean 927 ± 727) Agatston scores diagnostic accuracy was lower (91%) as compared to patient with low (mean 17 ± 27) Agatston scores (98%) (Table 4).

Our study was performed in a selected population consisting of symptomatic patients who were referred for conventional coronary angiography. This was evidenced by the fact that our study population had a high prevalence of coronary disease (77%, 77/100), and that fairly a large population had multi-vessel disease (46%, 46/100). In this population DSCT coronary angiography performed well to excellent, but it remains to be demonstrated that such a high diagnostic accuracy will be achieved in a symptomatic patient population with a low to intermediate prevalence of disease or in a non-chest pain population.

CONCLUSION

Our study was performed in a high-risk population with a wide range of symptoms who were referred for conventional coronary angiography. DSCT coronary angiography demonstrated a high diagnostic accuracy for the detection or exclusion of significant stenoses in patients with various heart rates without exclusion of unevaluable segments. These results indicate that the technique may now be tested in a cohort with a low to intermediate pre-test probability of coronary artery disease or in patients with non-anginal chest pain to establish the role of DSCT coronary angiography in the management of patients with suspected coronary artery disease.

REFERENCES

1. Nieman K, Oudkerk M, Rensing BJ, et al. Coronary angiography with multi-slice computed tomography. *Lancet* 2001;357:599-603.
2. Knez A, Becker CR, Leber A, et al. Usefulness of multislice spiral computed tomography angiography for determination of coronary artery stenoses. *Am J Cardiol* 2001;88:1191-4.
3. Achenbach S, Ropers D, Pohle FK, et al. Detection of coronary artery stenoses using multi-detector CT with 16 x 0.75 collimation and 375 ms rotation. *Eur Heart J* 2005;26:1978-86.
4. Garcia MJ, Lessick J, Hoffmann MH. Accuracy of 16-row multidetector computed tomography for the assessment of coronary artery stenosis. *Jama* 2006;296:403-11.

5. Heuschmid M, Kuettner A, Schroeder S, et al. ECG-gated 16-MDCT of the coronary arteries: assessment of image quality and accuracy in detecting stenoses. *AJR Am J Roentgenol* 2005;184:1413-9.
6. Kuettner A, Beck T, Drosch T, et al. Diagnostic accuracy of noninvasive coronary imaging using 16-detector slice spiral computed tomography with 188 ms temporal resolution. *J Am Coll Cardiol* 2005;45:123-7.
7. Ropers D, Baum U, Pohle K, et al. Detection of coronary artery stenoses with thin-slice multi-detector row spiral computed tomography and multiplanar reconstruction. *Circulation* 2003;107:664-6.
8. Mollet NR, Cademartiri F, Nieman K, et al. Multislice spiral computed tomography coronary angiography in patients with stable angina pectoris. *J Am Coll Cardiol* 2004;43:2265-70.
9. Leschka S, Alkadhi H, Plass A, et al. Accuracy of MSCT coronary angiography with 64-slice technology: first experience. *Eur Heart J* 2005;26:1482-7.
10. Raff GL, Gallagher MJ, O'Neill WW, Goldstein JA. Diagnostic accuracy of noninvasive coronary angiography using 64-slice spiral computed tomography. *J Am Coll Cardiol* 2005;46:552-7.
11. Gallagher MJ, Ross MA, Raff GL, Goldstein JA, O'Neill W W, O'Neil B. The Diagnostic Accuracy of 64-Slice Computed Tomography Coronary Angiography Compared With Stress Nuclear Imaging in Emergency Department Low-Risk Chest Pain Patients. *Ann Emerg Med* 2006.
12. Stein PD, Hoffmann U, Beemath A, Moselewski F. Noninvasive imaging of the coronary arteries. *Minerva Cardioangiol* 2006;54:619-31.
13. Nikolaou K, Knez A, Rist C, et al. Accuracy of 64-MDCT in the diagnosis of ischemic heart disease. *AJR Am J Roentgenol* 2006;187:111-7.
14. Stein PD, Beemath A, Kayali F, Skaf E, Sanchez J, Olson RE. Multidetector computed tomography for the diagnosis of coronary artery disease: a systematic review. *Am J Med* 2006;119:203-16.
15. Flohr TG, McCollough CH, Bruder H, et al. First performance evaluation of a dual-source CT (DSCT) system. *Eur Radiol* 2006;16:256-68.
16. Austen WG, Edwards JE, Frye RL, et al. A reporting system on patients evaluated for coronary artery disease. Report of the Ad Hoc Committee for Grading of Coronary Artery Disease, Council on Cardiovascular Surgery, American Heart Association. *Circulation* 1975;51:5-40.
17. Leber AW, Knez A, von Ziegler F, et al. Quantification of obstructive and nonobstructive coronary lesions by 64-slice computed tomography: a comparative study with quantitative coronary angiography and intravascular ultrasound. *J Am Coll Cardiol* 2005;46:147-54.
18. Ropers D, Rixe J, Anders K, et al. Usefulness of multidetector row spiral computed tomography with 64- x 0.6-mm collimation and 330-ms rotation for the noninvasive detection of significant coronary artery stenoses. *Am J Cardiol* 2006;97:343-8.

19. Hamon M, Biondi-Zoccai GG, Malagutti P, Agostoni P, Morello R, Valgimigli M. Diagnostic performance of multislice spiral computed tomography of coronary arteries as compared with conventional invasive coronary angiography: a meta-analysis. *J Am Coll Cardiol* 2006;48:1896-910.
20. Schuijf JD, Wijns W, Jukema JW, et al. Relationship between noninvasive coronary angiography with multi-slice computed tomography and myocardial perfusion imaging. *J Am Coll Cardiol* 2006;48:2508-14.
21. Mollet NR, Cademartiri F, van Mieghem CA, et al. High-resolution spiral computed tomography coronary angiography in patients referred for diagnostic conventional coronary angiography. *Circulation* 2005;112:2318-23.
22. Morin RL, Gerber TC, McCollough CH. Radiation dose in computed tomography of the heart. *Circulation* 2003;107:917-22.

Addendum 2

Angina pectoris due to steal phenomenon created by a left anterior descending-right ventricle fistula originating from repeated myocardial biopsies

Submitted

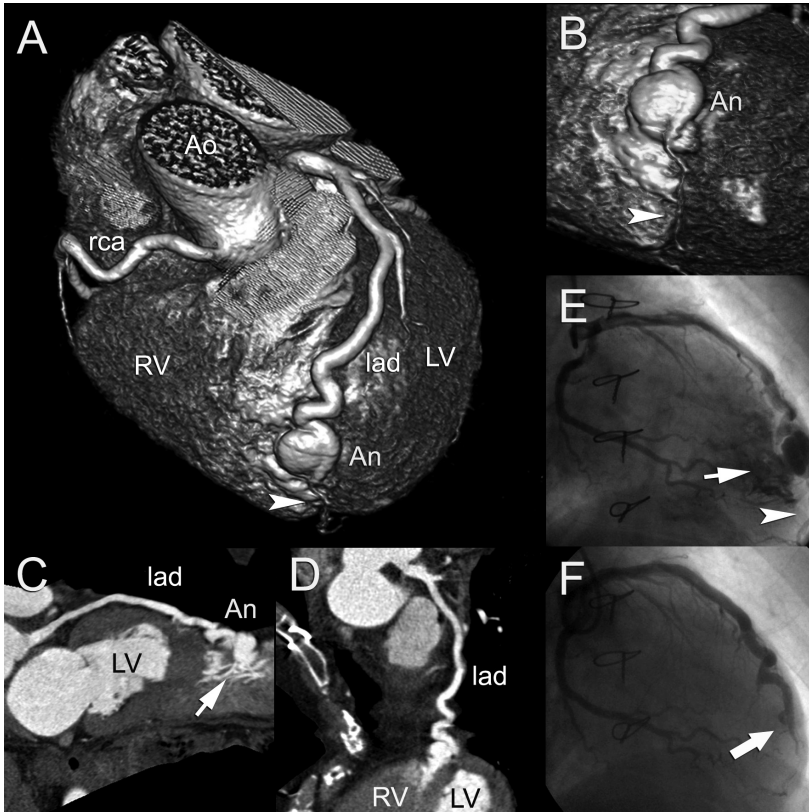
*W. Bob Meijboom, MD^{1,2},
Carlos A.G. van Mieghem,
MD^{1,2}, Annick C. Weustink,
MD^{1,2}*

*¹Department of Cardiology,
Thoraxcenter, Erasmus
Medical Center, Rotterdam, the
Netherlands*

*²Department of Radiology,
Erasmus Medical Center,
Rotterdam, the Netherlands*

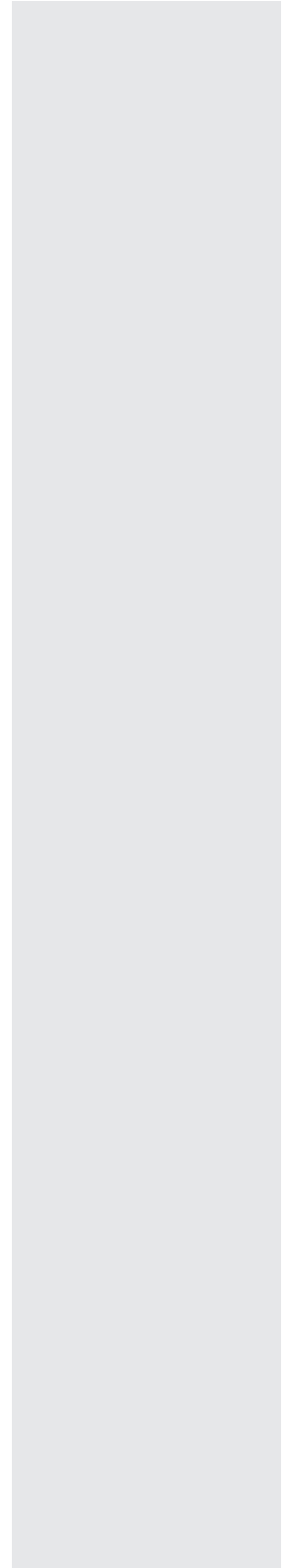
MANUSCRIPT:

A 54-year-old woman was admitted to our hospital because of angina pectoris. Four years before she had undergone orthotopic heart transplantation due to anthracyclin induced end-stage heart failure. Physical examination discovered a soft continuous murmur at the apex of the heart. Sixty-four slice CT coronary angiography was performed which showed an aneurysmatic part (An) of the left anterior descending artery (LAD) and a hypoplastic distal segment (arrowpoint) (A,B). Two curved multiplanar reconstructed CT images (C,D) displayed the LAD throughout its course, ruling out significant lesions and ending in the RV where increased contrast enhancement could be seen (arrow). Nuclear dobutamine-stress testing revealed apical ischemia. Conventional coronary angiography confirmed the aneurysmatic part in the LAD with a hypoplastic distal segment (arrowpoint) and its outflow in the right ventricle (RV) (arrow) which was probably caused by repeated myocardial biopsies taken into the RV. A pulmonary-to-systemic ratio shunt fraction of 1.5:1 was calculated, showing its hemodynamic importance. The fistula was percutaneously successfully sealed (F) using a covered stent revealing only a residual amount of contrast in the course of the former fistula (thick arrow).



PART 3

Clinical application of
CTCA



7

64-Slice Computed Tomography Coronary Angiography in Patients with High, Intermediate or Low Pre-test Probability of Significant Coronary Artery Disease

Journal of American College of Cardiology.
2007 Oct 9;50(15):1469-75.

W. Bob Meijboom, MD^{1,2},
Carlos A.G. van Mieghem,
MD^{1,2}, Nico R. Mollet, MD,
PhD^{1,2}, Francesca Pugliese
MD^{1,2}, Annick C. Weustink
MD^{1,2}, Niels van Pelt MD^{1,2},
Filippo Cademartiri MD,
PhD², Koen Nieman MD,
PhD¹, Eric Boersma, MSc,
PhD¹, Peter de Jaegere MD,
PhD¹, Gabriel P. Krestin MD,
PhD², Pim J. de Feyter, MD,
PhD, FACC^{1,2}

¹ Department of Cardiology,
Thoraxcenter,

² Department of Radiology,
Erasmus Medical Center,
Rotterdam, the Netherlands

ABSTRACT

Objectives

We assessed the usefulness of 64-slice CT coronary angiography (CTCA) to detect or rule out coronary artery disease (CAD) in patients with various estimated pre-test probabilities of CAD.

Background

The pre-test probability of the presence of CAD may impact on the diagnostic performance of CTCA.

Methods

64-slice CTCA (Siemens Sensation 64, Germany) was performed in 254 symptomatic patients. Patients with heart rates ≥ 65 bpm received beta-blockers before CTCA. The pre-test probability for significant CAD was estimated by type of chest discomfort, age, gender, traditional risk factors and defined as high ($\geq 71\%$), intermediate (31-70%) and low ($\leq 30\%$). Significant CAD was defined as the presence of at least one $\geq 50\%$ coronary stenosis on quantitative coronary angiography which was the standard of reference. No coronary segments were excluded from analysis.

Results

The estimated pre-test probability of CAD in the high (N:105), intermediate (N:83) and low (N:66) group was 87%, 53% and 13%, respectively. The diagnostic performance of the CT scan was different in the three subgroups. The estimated post-test probability of the presence of significant CAD after a negative CT scan was 17%, 0%, and 0%, and after a positive CT scan 96%, 88% and 68%.

Conclusions

CTCA is useful in symptomatic patients with a low or intermediate estimated pre-test probability of having significant CAD, and a negative CT-scan reliably rules out the presence of significant CAD. CTCA does not provide additional relevant diagnostic information in symptomatic patients with a high estimated pre-test probability of CAD.

INTRODUCTION

The estimated pre-test probability of having significant coronary artery disease (CAD) in a study population should be taken into account in the evaluation of the diagnostic accuracy of CT coronary angiography (CTCA) to detect or rule out the presence of coronary stenosis. The estimated pretest probability of having obstructive CAD in patients who present with chest pain is related to age, gender, type of chest discomfort and traditional risk factors. The estimated pre-test probability is lowest in younger female patients with non-anginal chest pain and highest in older male patients with typical angina (1).

The diagnostic performance of CTCA has mostly been tested in symptomatic patient populations with a high estimated pre-test probability of having significant CAD, and a few studies have reported on the impact of different estimated pre-test probabilities on the performance of CTCA (2).

The purpose of this study was to evaluate the diagnostic performance and clinical usefulness of 64-slice CTCA in 254 patients with high, intermediate or low estimated pre-test probability of having significant coronary stenosis.

METHODS

Study population

During a 24-month period 254 patients presenting with typical angina pectoris, atypical angina pectoris and non-anginal chest pain who were referred for conventional coronary angiography (CCA) were included into the study. Typical angina was defined as having three characteristics: 1) sub-sternal discomfort, 2) that is precipitated by physical exertion or emotion and 3) relieved with rest or nitroglycerine within 10 minutes. Atypical angina pectoris was defined as having two out of three of the definition characteristics. Non-anginal chest pain was characterized as one or absence of the described chest pain features. The estimated pre-test probability for obstructive CAD was estimated using the Duke Clinical Score, which includes type of chest discomfort, age, gender, and traditional risk factors (3,4). Patients were categorized into a low (1-30%), intermediate (31-70%), or high (71-99%) estimated pre-test probability group of having significant CAD. No patients with previous history of percutaneous coronary intervention, coronary artery bypass surgery, prior myocardial infarction, impaired renal function (serum creatinine > 120 $\mu\text{mol/l}$), persistent arrhythmias or known allergy to Iodinated contrast material, were included. CCA was performed before or after the CTCA and served as the standard of reference. The institutional review board of the Erasmus MC Rotterdam approved the study and all subjects gave informed consent.

Patient preparation

Patients with a heart rate exceeding 65 bpm received additional beta-blockers (50/100mg Metoprolol) 1 hour before the CT examination.

Scan protocol

All scans were performed with a 64-slice CT scanner that features a gantry rotation time of 330 msec, a temporal resolution of 165 ms and a spatial resolution of 0.4 mm³ (Sensation 64, Siemens, Forchheim, Germany). A calcium scoring scan was performed with following parameters; 64- × 0.6 mm collimation, 330 ms rotation time, 120 kV tube voltage, 150 mAs tube current, 3.8 mm/rotation table feed, prospective ECG X-ray tube modulation. Afterwards, the CTCA was performed using identical parameters aside from a higher tube current between 850 and 960 mAs and without the use of prospective ECG X-ray tube modulation. The radiation exposure was estimated using dedicated software (ImPACT®, version 0.99x, St. George's Hospital, Tooting, London, UK).

A bolus of 95 ml of contrast material (400 mgI/mL; Iomeron™, Bracco, Milan, Italy) was injected intravenously in an antecubital vein at 5 mL/s. and a bolus-tracking technique was used to synchronize the arrival of contrast in the coronary arteries and the initiation of the scan.

Image reconstruction

Datasets were reconstructed immediately after the scan following a stepwise approach as previously described (5,6). If necessary, multiple datasets of a single patient were used separately in order to obtain optimal image quality for all available coronary segments.

Quantitative coronary angiography (QCA)

All scans were carried out within one week before or after CCA. One experienced cardiologist, unaware of the results of CTCA, identified and analyzed all coronary segments, using a 17-segment modified AHA classification. All segments, regardless of size, were included for comparison with CTCA. Segments were classified as normal (smooth parallel or tapering borders), as having non-significant disease (wall irregularities or <50% stenosis) or having significant disease (stenosis ≥50%). Stenoses were evaluated in the worst view, and classified as significant if the lumen diameter reduction exceeded ≥50% measured by validated quantitative coronary angiography (QCA) algorithm (CAAS, Pie Medical, Maastricht, the Netherlands).

CT image evaluation

One observer analyzed total calcium scores of all patients using dedicated software. Two experienced observers, a radiologist and a cardiologist, unaware of the results of CCA, evaluated the CTCA data sets on an offline workstation (Leonardo, Siemens, Forchheim, Germany) using (curved) multiplanar reconstruction. Segments were scored positive for significant CAD if there

was $\geq 50\%$ diameter reduction of the lumen by visual assessment. Segments distally to a chronic total occlusion were excluded. Inter-observer disagreements were resolved by a third reader.

Statistical analysis

The diagnostic performance of CTCA for the detection of significant coronary artery stenoses as defined by QCA is presented as sensitivity, specificity, positive- and negative predictive values with the corresponding 95% CIs, and positive and negative likelihood ratios (LR) were calculated. Comparison between CTCA and QCA was performed on three levels: patient-by-patient, vessel-by-vessel and segment-by-segment analysis. A Mantel-Haenszel test was performed to evaluate the trend in sensitivity and specificity relative to the estimated pre-test probability for obstructive CAD.

Categorical characteristics are expressed as numbers and percentages, and compared between the 3 groups using the chi square test. Continuous variables are expressed as means (standard deviation) and compared with one-way analysis of variance followed by post hoc Bonferroni correction to adjust for multiple comparisons. If not normally distributed, continuous variables are expressed as medians (25th to 75th percentile range) and compared with Kruskal-Wallis test.

An additional analysis was done to investigate the effect of nesting since repeated assessments within the same patient were made that were not independent observations. A random selection of a single segment per patient was done and the diagnostic accuracy for detecting significant artery disease was calculated. Interobserver and intraobserver variability for the detection of significant coronary stenosis and agreement between techniques to classify patients as having no, single-, or multi-vessel disease was determined by *k*-statistics.

RESULTS

Patient demographics are shown in Table 1. Additional beta-blockers prior to CT scanning were administered in 74 % (188/254) of patients decreasing the mean heart rate from 71 ± 11 to 59 ± 8 bpm. The mean scan time was 12.7 ± 1.6 seconds. Initially all data-sets were reconstructed in the mid- to end diastolic phase. In 34% of the cases (86/254) additional higher quality reconstructions obtained during end-systole were used for evaluation.

The estimated radiation exposure using prospective x-ray tube modulation for the calcium score in women and men was 1.8 and 1.4 mSv respectively. The estimated radiation exposure for the contrast-enhanced scan without prospective x-ray tube modulation was 17.0 mSv in women and 13.4 mSv in men, which is in line with previous reports (7).

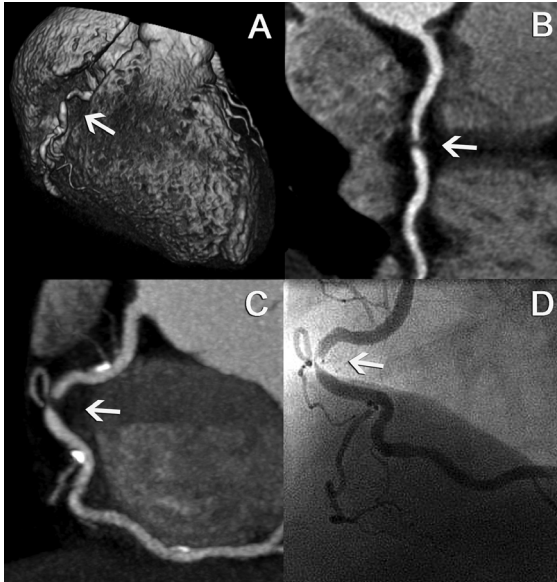


Figure 1. Volume-rendered CTCA image (A) of the right coronary artery. A curved MPR (B) and a thick MIP (C) disclose a significant coronary stenosis (arrow) in the mid right coronary artery which was corroborated by CCA (D). Proximally and distally of the significant obstructed lesion, non-significant calcified plaques can be seen (C). (A full color version of this illustration can be found in the color section).

the circumflex coronary artery (both 53% diameter reduction, one in the proximal and one in the mid segment). Forty patients with single-vessel disease were evaluated as having multi-vessel disease by CTCA due to overestimation of disease severity in other vessels. Agreement between CTCA and QCA on a per-patient (no or any disease) level was very good (k -value: 0.84), whereas agreement between techniques to classify patients as having no, single-, and multi-vessel disease was good (k -value: 0.61).

Diagnostic performance of 64-slice CT coronary angiography: patient-by-patient analysis

The analysis comprised 105 (43%) patients with a high estimated pre-test probability for CAD, 83 (33%) patients with an intermediate, and 66 (26%) patients with a low estimated pre-test probability for CAD. The mean age between patients with high estimated probability and intermediate estimated probability group was significantly different from the mean age in the low probability group, and the median calcium score was significantly different in all 3 groups. The mean heart rate was significantly lower in the high estimated probability group compared to the intermediate and low estimated probability group (Table 1).

Diagnostic performance of 64-slice CT coronary angiography: all patients with chest pain

The observed pre-test probability of significant CAD, defined as having at least one $\geq 50\%$ coronary stenosis per patient was 50%. The diagnostic performance of CTCA for detecting significant stenoses on a patient-level is detailed in Table 2. Eighteen patients with angiographic non-significant disease were incorrectly classified as having significant CAD by CT: 17 patients were scored as having single-vessel disease and one patient was misinterpreted as having multi-vessel disease. Ninety-eight percent (124/126) of patients with significant CAD on CCA were correctly identified by CTCA (Figure 1). The two patients in whom the severity of disease was underestimated both showed significant lumen narrowing in

Table 1. Patient demographics (n=254)

	Pre-test probability of significant CAD			p
	> 70% High (N: 105)	30-70% Intermediate (N: 83)	< 30% Low (N: 66)	
Typical angina	89 (85)	31 (37)	3 (4)	
Atypical angina	16 (15)	29 (35)	21 (32)	< 0.0001
Non-anginal chest pain	0 (0)	23 (28)	42 (64)	
Male	97 (92)	47 (57)	27 (41)	< 0.0001
Age (yrs)*	63 ± 9	61 ± 8	50 ± 12	< 0.0001
BMI (kg/m ²)*	27.5 ± 4.2	27.1 ± 4.8	26.7 ± 4.2	ns
Heart rate (bpm)*	57 ± 8	60 ± 7	61 ± 7	< 0.01
Risk factors				
Hypertension ‡	68 (65)	43 (52)	30 (45)	< 0.05
Hypercholesterolemia§	71 (68)	52 (63)	14 (21)	< 0.0001
Diabetes mellitus []	16 (15)	11 (13)	4 (6)	ns
Current smoker	32 (30)	16 (19)	16 (24)	ns
Previous smoker	14 (13)	6 (7)	4 (6)	ns
Family history of CAD #	57 (54)	39 (47)	29 (44)	ns
Obesity **	32 (30)	21 (25)	13 (20)	ns
Calcium score (Agatston score)†	354 (103-814)	134 (1-296)	0 (0-56)	< 0.0001
Conventional coronary angiography				
Prevalence of obstructive CAD	82 (78)	32 (39)	12 (18)	< 0.0001
Absence of CAD	6 (6)	21 (25)	36 (55)	
Nonsignificant disease	17 (16)	30 (36)	18 (27)	
Single-vessel disease	42 (40)	22 (27)	9 (14)	< 0.0001
Multivessel disease	40 (38)	10 (12)	3 (5)	

* Mean and standard deviation. † Median and quartiles. Values are n (%) unless otherwise indicated. Categorical variables were tested with Chi square test. Continuous variables were tested with one-way analysis of variance (ANOVA). If not normally distributed, continuous variables were compared with Kruskal-Wallis test. P-values < 0.05 were considered statistically significant. ‡ Blood pressure ≥ 140/90 mm Hg or treatment for hypertension. § Total cholesterol > 180 mg/dl or treatment for hypercholesterolemia. [] Treatment with oral anti-diabetic medication or insulin. # Family history of coronary artery disease (CAD), having first- or second-degree relatives with premature CAD (age < 55 years). ** Body mass index (BMI) ≥ 30 kg/m².

The diagnostic performance of CTCA was different in the patient groups with various estimated pre-test probabilities. The specificity showed a trend with a lower specificity in the high estimated pre-test probability (p: < 0.05, sensitivity, p: ns). The diagnostic impact of CTCA on the estimated pre-test probability of having significant CAD is shown in Figure 2 and 3.

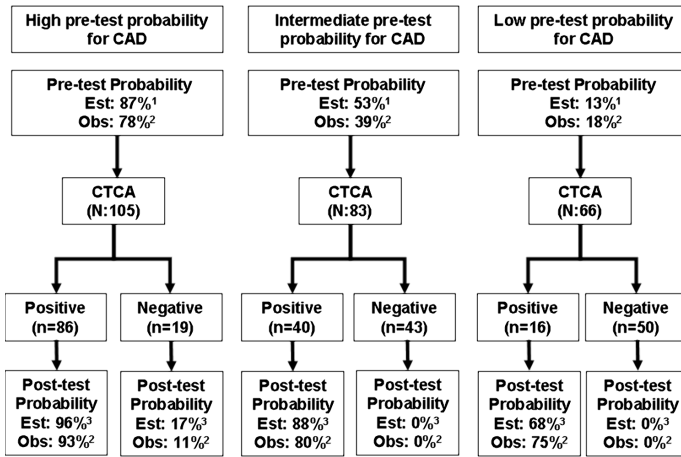


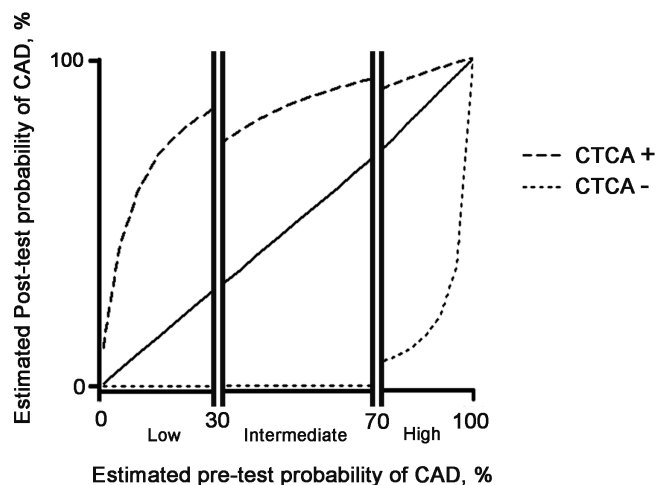
Figure 2. 1 Estimated using Duke Clinical Score (including Diamond-Forrester criteria and prognostic clinical variables). 2 Based on conventional coronary angiography (≥ 1 significant coronary stenosis as determined by QCA). 3 Calculated using Bayesian statistics (post-test odds = pre-test odds \times likelihood ratio). Est: Estimated, Obs.: Observed.

Of a total of 1016 vessels, the severity of a lesion was overestimated in 97 non-obstructive vessels (false positives). The diagnostic performance of the CT-scan was different in the three subgroups. The specificity showed a trend towards lower specificity in the high estimated pre-test probability ($p < 0.0001$, sensitivity, p : ns). Agreement between CTCA and QCA on a per-vessel level was good (k -value: 0.71).

Diagnostic performance of 64-slice CT coronary angiography: segment-by-segment analysis

Overall 3647 (out of 4318 potentially available segments) were included for comparison with QCA. Unavailable segments included 547 anatomically absent segments on CCA and 124 segments distal to an occluded coronary segment. Segments were not excluded for reasons such as severe calcifications or poor image quality. The kappa-value for

Figure 3. Using the positive and negative likelihood ratios obtained from Table 2, we calculated the estimated post-test probabilities of CAD after positive and negative findings on CT coronary angiography from various estimated pre-test probabilities of CAD.



Diagnostic performance of 64-slice CT coronary angiography: vessel-by-vessel analysis

The diagnostic performance of CTCA for the detection of significant lesions on a vessel-based analysis is detailed in Table 2. Two significantly diseased right coronary arteries, 1 left anterior descending artery and 5 diseased circumflex coronary arteries were incorrectly classified as non-significantly diseased by CTCA.

Table 2. Diagnostic Performance and Predictive Value of 64-Slice CT Coronary Angiography for the Detection of $\geq 50\%$ Stenosis on QCA; analysis for high, intermediate and low pre-test likelihood for obstructive CAD.

	Observed * pre-test probability %	Estimated † pre-test probability %	n	TP	TN	FP	FN	Kappa	Sensitivity ‡ %	Specificity § %	PPV %	NPV %	+LR	-LR
Patient based analysis: All	50	-	254	124	110	18	2	0.84	98 (94-100)	86 (78-91)	87 (80-92)	98 (93-100)	7.00	0.02
High	78	87	105	80	17	6	2	0.76	98 (91-100)	74 (51-89)	93 (85-97)	89 (65-98)	3.74	0.03
Intermediate	39	53	83	32	43	8	0	0.81	100 (87-100)	84 (71-93)	80 (64-90)	100 (90-100)	6.38	0.00
Low	18	13	66	12	50	4	0	0.82	100 (70-100)	93 (81-98)	75 (47-92)	100 (91-100)	13.50	0.00
Vessel based analysis : All	19	-	1016	181	730	97	8	0.71	96 (92-98)	88 (86-90)	65 (59-71)	99 (98-99)	8.16	0.05
High	31	-	420	126	229	60	5	0.68	96 (91-99)	79 (74-84)	68 (60-74)	98 (95-99)	4.63	0.05
Intermediate	13	-	332	40	261	28	3	0.67	93 (80-98)	90 (86-93)	59 (46-70)	99 (96-100)	9.60	0.08
Low	6	-	264	15	240	9	0	0.75	100 (75-100)	96 (93-98)	63 (41-80)	100 (98-100)	27.67	0.00
Segment based analysis: All	7	-	3647	228	3194	193	32	0.64	88 (83-91)	94 (93-95)	54 (49-59)	99 (99-99)	15.39	0.13
High	12	-	1468	163	1161	126	18	0.64	90 (85-94)	90 (88-92)	56 (50-62)	98 (98-99)	9.20	0.11
Intermediate	4	-	1219	46	1112	54	7	0.58	87 (74-94)	95 (94-96)	46 (36-56)	99 (99-100)	18.74	0.14
Low	3	-	960	19	921	13	7	0.65	73 (52-88)	99 (98-99)	59 (41-76)	99 (98-100)	52.50	0.27

* Observed pre-test probability; based on conventional coronary angiography (≥ 1 significant coronary stenosis as determined by QCA). † Estimated pre-test probability; estimated using Duke Clinical Score. ‡ The sensitivity showed a trend with a lower sensitivity in the low estimated pre-test probability in the per-segment analysis ($p < 0.05$). § The specificity showed a trend with a lower specificity in the high estimated pre-test probability in the per-patient, per-vessel and per-segment analysis. ($p < 0.05$, $p < 0.0001$, $p < 0.0001$, respectively). TP indicates true positive; TN, true negative; FP, false positive; FN, false negative; PPIV, positive predictive value; NPIV, negative predictive value, +LR, positive predictive value, -LR, negative predictive value. Values in parentheses represent 95 CIs.

inter- and intraobserver variability was 0.70 and 0.72, respectively. The diagnostic performance of CTCA for detecting significant stenoses is detailed in Table 2. Agreement between CTCA and QCA on a per-segment level was good (k -value, 0.64).

The severity of 32 significant coronary stenoses was underestimated or missed and classified as non-significant by CTCA. Most of these significant lesions (24/32) were located in distal segments or in side branches. The severity of 193 non-significant lesions was overestimated by CTCA. The diagnostic performance of the CT-scan was different in the three subgroups with a lower sensitivity ($p < 0.05$) and a higher specificity ($p < 0.0001$) in the low pre-test probability group.

Analysis on the randomly selected segments resulted in a sensitivity 92% (24/26; 95% CI, 73 to 99), specificity 93% (212/228; 95% CI, 89 to 96), positive predictive value 60% (16/40; 95% CI, 43 to 75), negative predictive value 99% (212/214; 95% CI, 96-100). The effect of nesting is probably minimal as the result of this analysis is very similar to the results shown in the per-segment analysis (Table 2).

DISCUSSION

The diagnostic performance of 64-slice CTCA to detect or rule out the presence of significant coronary stenosis has mainly been reported for patients with stable angina pectoris scheduled for invasive CCA and these studies have shown that CTCA can reliably rule out significant CAD (5,8-10). The majority of these patients presented with a high estimated pre-test probability of having significant CAD and only scant information is available on the diagnostic performance of 64-slice CTCA in patients with a low or intermediate estimated pre-test probability of having significant CAD.

In this study, we used the Duke Clinical Score that incorporates clinical presentation of chest pain, age, gender and traditional risk factors, to estimate the pre-test probability of having significant CAD. Using the likelihood ratio's of the tests, which were obtained in this study, post-test probabilities were calculated.

The pre-test probability of CAD may impact of the diagnostic performance of the CT scan. Indeed, the diagnostic performance of CTCA in the three groups was different. The specificity was lower in the high pre-test probability group compared to the low pre-test probability group, whereas sensitivity was lower in the per-segment analysis in the low pre-test probability group. This observation can probably be explained by the higher calcium scores in the higher probability groups, which tend to overestimate the severity of stenosis.

A negative CT-scan was present in 75% of the patients with a low estimated pre-test probability and in approximately 50% of the patients with an intermediate estimated pre-test probability. The negative predictive value of CTCA to exclude significant CAD was excellent in these patients, reducing the estimated post-test probability to zero. Thus, these patients would not need further downstream diagnostic tests. They may be candidates for secondary prevention measures, such as statin therapy in the presence of non-obstructive plaques or could be discharged from further cardiac follow-up in the absence of any visible plaque.

A positive CT-scan occurred in approximately 25% and 50% of the patients with a low or intermediate estimated pre-test probability, respectively. The number of false positive outcomes was rather high in these patients which renders a positive CT scan rather unreliable for clinical decision making. In these patients it may be reasonable to proceed to invasive CCA in the case of left main disease, 3 vessel disease and in the presence of a critical stenosis in the proximal part of a major coronary artery. In case of vessel disease in distal vessels or side branches, equivocal lesions or uninterpretable scans one may consider a non-invasive stress test to determine the functional significance of a doubtful coronary stenosis. A negative functional test may overrule the clinical significance of a (false) positive CT-scan and reduce the need for invasive coronary angiography. A positive functional test may further increase the probability of having significant CAD and should be followed by invasive coronary angiography and coronary revascularisation if symptoms are not alleviated by the anti-anginal medication. However, further studies are necessary to evaluate the diagnostic value of the combination of functional data from a stress test with the anatomical data provided by CTCA.

In the high estimated pre-test probability group a negative CTCA reduced the estimated post-test probability to 17%, whereas a positive CTCA increased the estimated post-test probability to as high as 96%. Given the high estimated pre-test probability of significant CAD in this group, the majority of these symptomatic patients are likely to proceed to invasive CCA even if CTCA is negative, since the post-test probability of significant CAD was still greater than 10%. CTCA therefore appears to be of limited clinical value in the evaluation of the high estimated pre-test probability group. Assessment for the presence of myocardial ischemia with a functional test may be more appropriate in this situation.

LIMITATIONS OF THE STUDY

The studied patients were not a prospective, consecutive group of patients. However, selection was not based on particular patient demographics, but rather on the availability of the 64 slice CT scanner for the examination of cardiac patients. The rather high estimated radiation exposure of 64-slice CTCA (17–13.4 mSv) as compared to CCA (3–6 mSv) is concerning (7). In this study

we did not use prospective ECG X-ray tube modulation which can significantly reduce radiation exposure, but requires a regular heart rhythm and limits the possibility of reconstructing images in the end-systolic phase. In our study end-systolic data sets provided optimal image quality in 34% of patients

Currently, there is no validated software available able to quantify the degree of stenoses. So far, the severity of coronary stenosis as assessed by CT is rather crudely visually estimated as more or less than 50% luminal diameter stenosis.

REFERENCES

1. Diamond GA, Forrester JS. Analysis of probability as an aid in the clinical diagnosis of coronary-artery disease. *N Engl J Med* 1979;300:1350-8.
2. Hendel RC, Patel MR, Kramer CM, et al. ACCF/ACR/SCCT/SCMR/ASNC/NASCI/SCAI/SIR 2006 appropriateness criteria for cardiac computed tomography and cardiac magnetic resonance imaging. *J Am Coll Cardiol* 2006;48:1475-97.
3. Gibbons RJ, Balady GJ, Bricker JT, et al. ACC/AHA 2002 guideline update for exercise testing: summary article. A report of the American College of Cardiology/American Heart Association Task Force on Practice Guidelines (Committee to Update the 1997 Exercise Testing Guidelines). *J Am Coll Cardiol* 2002;40:1531-40.
4. Pryor DB, Shaw L, McCants CB, et al. Value of the history and physical in identifying patients at increased risk for coronary artery disease. *Ann Intern Med* 1993;118:81-90.
5. Mollet NR, Cademartiri F, van Mieghem CA, et al. High-resolution spiral computed tomography coronary angiography in patients referred for diagnostic conventional coronary angiography. *Circulation* 2005;112:2318-23.
6. Meijboom WB, Mollet NR, Van Mieghem CA, et al. Pre-operative computed tomography coronary angiography to detect significant coronary artery disease in patients referred for cardiac valve surgery. *J Am Coll Cardiol* 2006;48:1658-65.
7. Hausleiter J, Meyer T, Hadamitzky M, et al. Radiation dose estimates from cardiac multislice computed tomography in daily practice: impact of different scanning protocols on effective dose estimates. *Circulation* 2006;113:1305-10.
8. Leschka S, Alkadhi H, Plass A, et al. Accuracy of MSCT coronary angiography with 64-slice technology: first experience. *Eur Heart J* 2005.
9. Raff GL, Gallagher MJ, O'Neill WW, Goldstein JA. Diagnostic accuracy of noninvasive coronary angiography using 64-slice spiral computed tomography. *J Am Coll Cardiol* 2005;46:552-7.
10. Leber AW, Knez A, von Ziegler F, et al. Quantification of obstructive and nonobstructive coronary lesions by 64-slice computed tomography: a comparative study with quantitative coronary angiography and intravascular ultrasound. *J Am Coll Cardiol* 2005;46:147-54.

8

64-slice Computed Tomography Coronary Angiography in Patients with Non-ST Elevation Acute Coronary Syndrome

Heart.

2007 Nov;93(11):1386-92.

*Willem B. Meijboom, MD^{1,2},
Nico R. Mollet, MD, PhD^{1,2},
Carlos A. Van Mieghem,
MD^{1,2}, Annick C. Weustink,
MD^{1,2}, Francesca Pugliese,
MD^{1,2}, Niels van Pelt, MD^{1,2},
Filippo Cademartiri, MD,
PhD², Eleni Vourvouri, MD,
PhD^{1,2}, Peter de Jaegere, MD,
PhD¹, Gabriel P. Krestin,
MD, PhD², Pim J. de Feyter,
MD, PhD^{1,2}*

¹ Department of Cardiology,
Thoraxcenter

² Department of Radiology
Erasmus Medical Center
Rotterdam, the Netherlands

ABSTRACT

Objectives

We studied the diagnostic performance of 64-slice CT coronary angiography in patients with non-ST elevation acute coronary syndrome.

Background

A high diagnostic accuracy of 64-slice CT coronary angiography in selected patients with stable angina pectoris has been reported, but only scant information is available in patients with non-ST elevation acute coronary syndrome.

Methods

64-slice CT coronary angiography was performed in 104 patients (mean age 59 ± 9 years) with non ST elevation acute coronary syndrome. Two independent, blinded observers assessed all coronary arteries for stenosis, using conventional quantitative angiography as a reference. Coronary lesions with ≥ 50 percent luminal narrowing were classified as significant.

Results

Conventional coronary angiography demonstrated the absence of significant disease in 15% (16/104), and the presence of single-vessel disease in 40% (42/104), and multivessel disease in 44% (46/104) of patients. Sensitivity for detecting significant coronary stenoses on a patient-by-patients analysis was 100% (88/88; 95% CI, 95-100), specificity 75% (12/16; 95% CI, 47-92) and positive and negative predictive values were 96% (88/92; 95% CI, 89-99) and 100% (12/12; 95% CI, 70-100).

Conclusion

64-slice CT coronary angiography has a high sensitivity to detect significant coronary stenoses and is reliable to exclude the presence of significant coronary artery disease in patients who present with a non-ST elevation acute coronary syndrome.

INTRODUCTION

Patients with a non-ST elevation acute coronary syndrome (ACS) are usually stratified into high and low risk for progression to myocardial infarction or death based on clinical presentation, ECG changes, biomarkers, electrical or hemodynamical instability, and presence of diabetes mellitus (1). An invasive management strategy including conventional coronary angiography (CCA) and revascularization is recommended in high-risk patients while a conservative strategy with ischemia-guided revascularization is recommended in low risk patients (1-3). We investigated the feasibility and diagnostic accuracy of 64-slice CT coronary angiography (CTCA) in 104 patients with non-ST elevation ACS as a first step to evaluate the potential decision-making role of CT in this patient cohort.

METHODS

Study population

Over a 12-month period we included 104 patients presenting with unstable angina pectoris or non-ST-segment elevation myocardial infarction. They were stratified as either high or low risk group according to current European guidelines on the basis of baseline characteristics, troponin rise, or ECG changes (1). High risk patients and low risk patients with a positive or inconclusive exercise ECG test or high suspicion for obstructive CAD underwent both CTCA and CCA. Furthermore, patients presenting with a ST-segment elevation myocardial infarction were not included, but immediately referred for direct percutaneous coronary intervention (PCI). No patients with previous history of PCI or coronary artery bypass surgery (CABG), impaired renal function (serum creatinine > 120 $\mu\text{mol/l}$), known intolerance to Iodinated contrast material, and atrial fibrillation were included. All patients underwent CCA which was the standard of reference. The institutional review board of Erasmus MC Rotterdam approved the study and all subjects gave informed consent.

Patient preparation

Patients with a heart rate exceeding 65 bpm before the examination received additional beta-blockers (50/100mg Metoprolol) and all were given thorough breath hold instructions.

Scan protocol

All scans were made with a 64-slice CT scanner which has a gantry rotation time of 330 msec, a temporal resolution of 165 msec, and a spatial resolution of 0.4 mm^3 (Sensation 64, Siemens, Forchheim, Germany). First a calcium scan was performed using standardized scan parameters; 64- \times 0.6 mm collimation, 330 ms rotation time, 3.8 mm/rotation table feed, 120 kV tube voltage, 150 mAs tube current and prospective X-ray tube modulation. Then, the CTCA was completed

which had similar parameters unless a higher tube current of 900 mAs and without X-ray tube modulation. The radiation exposure for CTCA using this scan-protocol was calculated as 15.2-21.4 (male/female) mSv using dedicated software (WinDose®, Institute of Medical Physics, Erlangen, Germany). The radiation exposure of calcium scoring using a comparable scan-protocol (including prospective X-ray tube modulation) on a 16-slice scanner was calculated as 1.3-1.7 (male/female) mSv (4).

A bolus of 80-100 ml of contrast material (400 mgI/mL; Iomeron™, Bracco, Milan, Italy) was injected intravenously in an antecubital vein at a flow rate of 5 mL/s. A bolus-tracking technique was used to synchronize the arrival of contrast in the coronary arteries, and the scan was started once the contrast attenuation in a pre-selected region of interest in the ascending aorta had reached a predefined threshold of +100 Hounsfield Units.

Image reconstruction

Images were obtained during a half x-ray tube rotation, resulting in an effective temporal resolution of 165 msec. Data sets were reconstructed immediately after the scan. To obtain optimal image quality, datasets were reconstructed in the mid-to-end diastolic phase using retrospective ECG gating with an absolute reverse or percentage technique as previously described by Mollet (5). In case of impaired image quality due to motions artifacts or breathing artifacts additional reconstructions were made in the end-systolic phase.

Quantitative coronary angiography (QCA)

All CT scans were carried out within 1 to 2 days of the performance of the CCA. One experienced cardiologist, unaware of the results of CTCA, identified and analyzed all coronary segments, using a 17-segment modified AHA classification (6).

All segments, regardless of size, were included for comparison with CTCA. Segments were classified as normal (smooth parallel or tapering borders), as having non-significant disease (wall irregularities or <50% stenosis) or having significant disease (stenosis ≥50%). Stenoses were evaluated in the worst view, and classified as significant if the reduction in lumen diameter exceeded 50 % measured by validated quantitative coronary angiographic (QCA) algorithm (CAAS, Pie Medical, Maastricht, the Netherlands).

CT image evaluation

One observer analyzed total calcium scores of all patients with dedicated software, expressing results as an Agatston score (7). Two experienced observers, a radiologist and a cardiologist, all unaware of the results of CCA, evaluated the CTCA data sets on an offline workstation (Leonardo, Siemens, Forchheim, Germany). The axial slices were initially evaluated for the presence of significant segmental disease and additionally multiplanar and curved multiplanar reconstructed

images were used. Segments located distally to a chronic total occlusion were excluded, because of poor distal filling by collaterals. Inter-observer disagreements were resolved by a third reader.

Statistical analysis

The diagnostic performance of CTCA for detecting significant stenoses in the coronary arteries using QCA as the standard of reference is presented as sensitivity, specificity, positive predictive value and negative predictive values with the corresponding 95% CIs. Positive (Sensitivity/[1-Specificity]) and negative ($[1-\text{Sensitivity}]/\text{Specificity}$) likelihood ratios are given. The likelihood ratio incorporates both the sensitivity and specificity of a test and provides a direct estimate of how much a test result will change the odds of having a disease. Post-test odds can be calculated by multiplying the pre-test odds by the likelihood ratios. Comparison between CTCA and QCA was performed on three levels of analysis: patient-by-patient, vessel-by-vessel and segment-by-segment. To investigate the effect of nesting an additional sensitivity analysis was done; repeated assessments (segment by segment and vessel by vessel) within the same patient were made that were not independent observations. Interobserver and intraobserver variability for the detection of significant coronary stenosis and agreement between techniques to classify patients as having no, single-, or multi-vessel disease was determined by *k*-statistics.

RESULTS

Patient demographics are shown in Table 1. Eighty-six (89/104) percent of patients received oral beta blockers as treatment for their ACS. Additional beta-blockers were administered in 63% (65/104) of patients and the mean heart rate dropped within 60 minutes from 66 ± 9 to 60 ± 8 bpm in these patients. The mean scan time was 12.3 ± 1.2 seconds. As a first step all datasets were reconstructed in the mid-to-end diastolic phase. In 34% of the cases (35/104) additional higher quality end-systolic reconstructions were used.

Diagnostic performance of 64-slice CT coronary angiography: patient-by-patient analysis

The prevalence of significant coronary artery disease (CAD), defined as having at least one $\geq 50\%$ stenosis per patient was 85%. The diagnostic performance of CTCA for detecting significant stenoses on a patient-based analysis is detailed in Table 2. The diagnostic accuracy of patients in the low and high risk group was similar.

Twelve patients with either an angiographically normal CCA (4) or with non-significant disease (8) were correctly identified with CT. However, two patients with only wall irregularities on the CCA were incorrectly classified as having single-vessel disease on the CT scan and two patients as having multi-vessel disease. All 88 patients with significant CAD on CCA were correctly iden-

Table 1. Patient demographics (N=104)

	Low risk	High risk
N	33	71
Age (yrs) §	58 ± 7 (38-75)	59 ± 10 (30-84)
Males	23 (70)	52 (73)
Calcium score, mean*	473.9 ± 738.2	440.0 ± 513.6
BMI, mean †	25.8 ± 3.6	26.5 ± 3.7
Recurrent ischemia ‡	-	49 (71)
Early post infarct unstable angina	-	9 (13)
Elevated troponin levels	-	55 (78)
Diabetes Mellitus	-	9 (13)
Normal ECG	21 (64)	-
ECG with negative or flat T-waves	12 (36)	-
Positive exercise ECG test	23 (70)	-
Inconclusive exercise ECG test	3 (9)	-
Highly suspicious for obstructive CAD	7 (21)	-
Traditional risk factors		
Hypertension	17 (52)	37 (52)
Hypercholesterolemia	22 (67)	40 (56)
Diabetes mellitus	0 (0)	9 (13)
Smoker	14 (42)	35 (49)
Ex-smoker	2 (6)	2 (3)
Family history of CAD	24 (73)	32 (45)
Obese †	8 (24)	15 (21)
Previous myocardial infarction	1 (3)	17 (24)
Conventional angiography		
Absence of coronary disease	2 (6)	2 (3)
Nonsignificant disease	3 (9)	9 (13)
Single-vessel disease	15 (45)	27 (38)
Two-vessel disease	10 (30)	26 (37)
Three-vessel disease	3 (9)	7 (10)

According to ESC guidelines: Two groups were stratified into a high and a low risk group which give a risk estimate for progression to myocardial infarction or death.

§ Ranges age

* Agatston score

† Body mass index ≥ 30 kg/m²

‡ Recurrent ischemia defined as either recurrent chest pain or dynamic ST-segment changes (in particular ST-segment depression, or transient ST-segment elevation)

Values are n (%) unless otherwise indicated

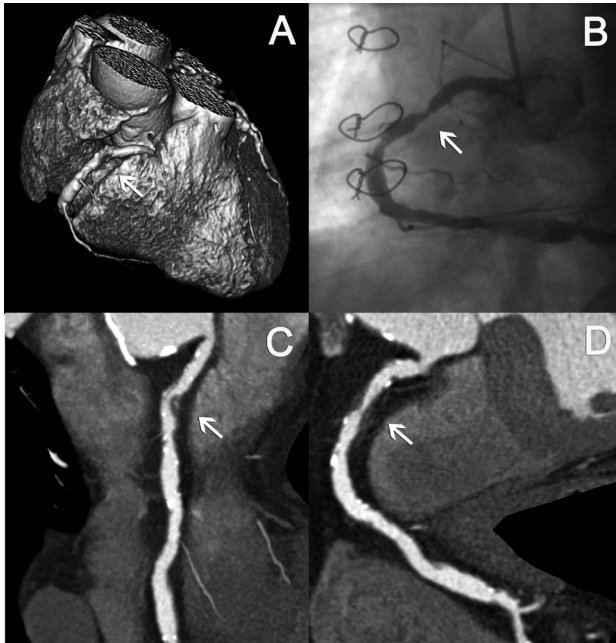


Figure 1. This patient with prior history of a mitral valve plasty for endocarditis was admitted with a non-ST segment elevation myocardial infarction. A volume-rendered CTCA image (A) reveals the anatomy of the right coronary artery. Two curved multiplanar reconstructed images (cMPR) (C, D) disclose a significant stenosis (arrow) in the proximal right coronary artery which was corroborated by CCA (B). (A full color version of this illustration can be found in the color section).

tified on the CT-scan (Figure 1,2). However, in 23 patients with single-vessel disease on CCA, CTCA overestimated the severity of additional lesions which resulted in incorrect classification as having multi-vessel disease on CTCA. Twenty-seven patients in the low risk group underwent PCI, one CABG and five were treated medically. In the high risk group 55 received PCI, five CABG

and eleven were treated medically. Agreement between CTCA and QCA on a per-patient (no or any disease) level was very good (k -value: 0.84), whereas agreement between techniques to classify patients as having no, single-, and multi-vessel disease was moderate (k -value: 0.55).

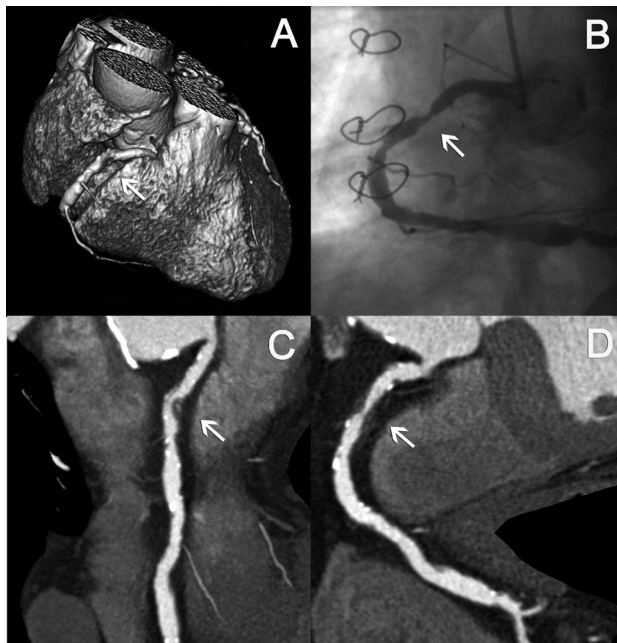
Diagnostic performance of 64-slice CT coronary angiography: vessel-by-vessel analysis

The diagnostic performance of CTCA for the detection of significant lesions on a vessel-based analysis is detailed in Table 2. Two significantly diseased right coronary arteries and one diseased circumflex coronary artery were incorrectly classified as non-significantly diseased on the CT-scan. Of a total of 416 vessels, 59 non-obstructive vessels were overestimated and scored as false positives. Agreement between CTCA and QCA on a per-vessel level was good (k -value: 0.70).

Diagnostic performance of 64-slice CT coronary angiography: segment-by-segment analysis

A total of 1525 segments were included for comparison with QCA. Potentially, 17 segments per patient can be present for analysis. A total of 243 segments were not visualized on the CCA. Hundred-eighty-one segments were excluded due to variations in coronary anatomy and 62 segments due to the presence of a proximal occlusion and poorly filled distal segments by collaterals. All segments were included despite the presence of calcifications or poor image quality. Interobserver and intraobserver variability for detection of a significant stenosis per segment had a k -value of 0.69 and 0.73, respectively. The diagnostic performance of CTCA for detecting significant

Figure 2. A maximum intensity projected CTCA image shows a large non-calcified plaque in the proximal segment of the right coronary artery (A). Two cMPR (C, D) disclose the high grade stenosis which is confirmed by CCA (B).



stenoses is detailed in Table 2. Agreement between CTCA and QCA on a per-segment level was good (k -value, 0.68).

Fifteen significant coronary stenoses were underestimated or missed and classified as non-significant. Most of these significant lesions (11/15) were located in distal segments or in side branches. Hundred-twenty-three non-significant lesions were detected with CTCA but the severity of these stenoses was overestimated. This overestimation, in 67% (83/123) due to heavy calcification, resulted in incorrect classification as significant stenoses on the CT-scan. Patients were divided into tertiles based on the mean calcium score. The presence of calcium decreased the diagnostic accuracy (low calcium score: 0.95, mid: 0.89, high: 0.88) (Table 3).

To exclude the possible confounding effect of nesting random selection of a single segment per patient was done and the diagnostic accuracy for detecting significant coronary artery disease resulted in a sensitivity 93% (13/14; 95% CI, 64 to 100), specificity 93% (84/90; 95% CI, 93 to 97), positive predictive value 68% (13/19; 95% CI, 43 to 86), negative predictive value 99% (84/85; 95% CI, 93 to 100).

DISCUSSION

Several recent reports about the diagnostic performance of 64-slice CTCA have shown a high sensitivity and negative predictive value to detect or exclude the presence of significant coronary stenosis in patients scheduled for CCA (5, 8-14). However, only scant information is available about the diagnostic performance of CTCA in a limited number of patients with acute coronary syndromes (5, 8, 15, 16).

Table 2. Diagnostic Performance and Predictive Value of 64-Slice CT Coronary Angiography for the Detection of $\geq 50\%$ Stenosis on QCA

	Prevalence of disease, %	n	TP	TN	FP	FN	Kappa	Sensitivity, % (95% CI)	Specificity, % (95% CI)	PPV, % (95% CI)	NPV, % (95% CI)	+LR	-LR
All patients	85	104	88	12	4	0	0.84	100 (95-100)	75 (47-92)	96 (89-99)	100 (70-100)	4.00	0.00
High risk	85	71	60	8	3	0	0.82	100 (93-100)	73 (39-93)	95 (86-99)	100 (60-100)	3.67	0.00
Low risk	85	33	28	4	1	0	0.87	100 (85-100)	80 (30-99)	93 (80-100)	100 (40-100)	5.00	0.00
Vessel based analysis													
All vessels	35	416	141	214	58	3	0.70	98 (94-99)	79 (73-83)	71 (64-77)	99 (96-100)	4.59	0.03
RCA	48	104	48	39	15	2	0.68	96 (85-99)	72 (58-83)	76 (64-86)	95 (82-99)	3.46	0.06
LM	3	104	3	98	3	0	0.65	100 (31-100)	97 (91-99)	50 (14-86)	100 (95-100)	33.67	0.00
LAD	47	104	49	32	23	0	0.57	100 (91-100)	58 (44-71)	68 (56-78)	100 (87-100)	2.39	0.00
CX	39	104	40	46	17	1	0.66	98 (86-100)	73 (60-83)	70 (56-81)	98 (87-100)	3.62	0.03
Segment based analysis													
All segments	13	1525	183	1205	122	15	0.68	92 (88-96)	91 (89-92)	60 (54-65)	99 (98-99)	10.05	0.08
Proximal	14	416	58	312	44	2	0.65	97 (87-99)	88 (84-91)	57 (47-67)	99 (97-100)	7.82	0.04
Mid	23	302	67	199	34	2	0.71	97 (89-99)	85 (80-90)	66 (56-75)	99 (96-100)	6.65	0.03
Distal	9	327	24	286	11	6	0.71	80 (61-92)	96 (93-98)	69 (51-83)	98 (95-99)	21.60	0.21
Side branch	8	480	34	408	33	5	0.60	87 (72-95)	92 (90-95)	51 (38-63)	99 (97-100)	11.65	0.14

TP indicates true positive; TN, true negative; FP, false positive; FN, false negative; PPV, positive predictive value; NPV, negative predictive value; +LR, positive likelihood ratio; -LR, negative likelihood ratio; RCA, right coronary artery; LM, left main coronary artery; LAD, left anterior descending coronary artery; LCx, circumflex coronary artery.
According to the 17-segment modified AHA classification 1525 segments and 416 vessels visualized with conventional coronary angiography were included for segment and vessel analysis. For patient-based analysis 104 patients were included. Values in parenthesis represent 95% CIs.

Table 3. Influence of Coronary Calcifications on Diagnostic Accuracy of 64-slice CT Coronary Angiography on a Segment-based Analysis

Calcium score	N, pat	N, segm	Mean \pm SD, (ranges) Agatston Score	TP	TN	FP	FN	Kappa	Sensitivity, % (95% CI)	Specificity, % (95% CI)	PPV, % (95% CI)	NPV, % (95% CI)	+ LR	-LR
1st tertile	35	530	30 \pm 34 (0-105)	42	465	20	3	0.76	93 (81-98)	96 (94-97)	68 (55-79)	99 (98-100)	22.63	0.07
2nd tertile	35	505	266 \pm 81 (107-375)	57	394	47	7	0.62	89 (79-95)	89 (86-92)	55 (45-64)	98 (96-99)	8.36	0.12
3rd tertile	34	490	1073 \pm 665 (400-2870)	84	346	55	5	0.66	94 (87-98)	86 (82-89)	60 (52-69)	99 (97-99)	6.88	0.07

TP indicates true positive; TN, true negative; FP, false positive; FN, false negative; PPV, positive predictive value; NPV, negative predictive value; +LR, positive likelihood ratio; -LR, negative likelihood ratio; Values in parentheses represent 95% CI's.

In our study the prevalence of obstructive CAD was 85% which was in keeping with previous reports evaluating acute coronary syndromes angina syndromes (2, 3, 17-19). In this high pre-test risk population we demonstrated a high diagnostic accuracy in patients with non-ST elevation ACS. In segments where interpretation was difficult due heavy calcification there was a tendency for observers to score these as positive for significant stenosis in order to reduce the chance of missing an important lesion. This "defensive scoring" approach is also likely to be used in clinical practice when evaluating symptomatic patients. The high negative predictive value of the CT-scan despite significant coronary calcification and high prevalence of CAD demonstrates that significant CAD can be ruled out in this patients group.

Patients with non-segment elevation ACS classified as high risk on the basis of baseline characteristics, troponin or ECG changes are best managed with an invasive strategy (1-3). These patients should generally have a CCA followed by revascularisation, if appropriate in the first few days after admission to hospital. The role of CTCA in these patients is not just the detection of significant disease but the detailed delineation of coronary anatomy may be useful to guide subsequent management. In this study, the agreement between CTCA and QCA in the classification of patients as having no, single or multivessel disease was moderate. This is due to the relatively high number of false positive segments scored due predominantly to calcification. In 41 out of the 104 patients, at least 1 vessel was overestimated as having a significant stenosis. Given this current limitation, CTCA may need to evolve further before it can more accurately guide future management, in particular either percutaneous or surgical revascularisation in these high risk patients. At the moment, even though the results are promising, a clinical role of CTCA in these high risk patients is not defined.

Currently CTCA may be more suited in the low risk non-segment-elevation ACS group. These patients, without recurrent chest pain or evidence of myocardial necrosis are recommended to undergo a stress test after an observation period. CCA is only recommended in these patients if significant ischemia is demonstrated during stress testing (1). However, stress testing, particularly treadmill or

bicycle stress testing may be inconclusive. The role of CTCA may be to replace the stress test as the first investigation in this population group. Given the excellent negative predictive value as demonstrated in this study, a negative CTCA would allow patients to be discharged and other non cardiac causes of the presenting chest pain to be considered. Patients with non obstructive CAD on CTCA would be continued to be managed medically, including appropriate secondary prevention and the need for future stress testing or CCA would depend on further symptoms.

Patients with significant disease on CTCA in this patient group could be referred directly for CCA, particularly if there was left main disease, 3 vessel or proximal segment disease of a main coronary artery. Patients with small vessel disease (i.e. distal disease < 2mm), equivocal lesions or uninterpretable scans could undergo a stress test to further guide the need for CCA. However, the use of sequential testing is controversial as no data is available showing better test results than a stress test alone.

LIMITATIONS OF THE STUDY

We did not include patients with severe ongoing ischemia, or hemodynamic or electrical instability, to prevent further delays of revascularization treatment. Furthermore, inclusion comprised a non-consecutive group of patients. Due to logistic reasons it was not feasible to scan and include every patient presenting with a non-ST elevation ACS. Moreover, patients in the low risk group with a negative exercise ECG test were not included, since these patients did not receive a CCA. Heart rate reduction with beta-blockers is standard practise in patients presenting with a non-ST elevation ACS. Additional beta-blockers were given to reduce the heart rate even more to achieve optimal heart rate control. With the next generation dual-source CT scanners scanning at higher heart rates will be possible due to the improved temporal resolution of 83 ms (20, 21).

The rather high radiation exposure of CTCA as compared to CCA is of concern (22, 23). The radiation exposure can be reduced by 40% with use of prospective X-ray tube current modulation. However, this limits the possibility to reconstruct valuable datasets during the end-systolic phase.

The presence of atrial fibrillation precludes the use of CTCA and was one of the exclusion criteria.

CONCLUSIONS

64-slice CT angiography has a high sensitivity to detect significant coronary stenoses and is reliable to exclude the presence of significant coronary artery disease in patients who present with a non-ST elevation acute coronary syndrome. The role of CT coronary angiography in these patients, particular in the lower risk group, needs to be further evaluated.

REFERENCES

1. Bertrand ME, Simoons ML, Fox KA, et al. Management of acute coronary syndromes in patients presenting without persistent ST-segment elevation. *Eur Heart J* 2002;23:1809-40.
2. Invasive compared with non-invasive treatment in unstable coronary-artery disease: FRISC II prospective randomised multicentre study. FRagmin and Fast Revascularisation during InStability in Coronary artery disease Investigators. *Lancet* 1999;354:708-15.
3. Cannon CP, Weintraub WS, Demopoulos LA, et al. Comparison of early invasive and conservative strategies in patients with unstable coronary syndromes treated with the glycoprotein IIb/IIIa inhibitor tirofiban. *N Engl J Med* 2001;344:1879-87.
4. Trabold T, Buchgeister M, Kuttner A, et al. Estimation of radiation exposure in 16-detector row computed tomography of the heart with retrospective ECG-gating. *Rofo* 2003;175:1051-5.
5. Mollet NR, Cademartiri F, van Mieghem CA, et al. High-resolution spiral computed tomography coronary angiography in patients referred for diagnostic conventional coronary angiography. *Circulation* 2005;112:2318-23.
6. Austen WG, Edwards JE, Frye RL, et al. A reporting system on patients evaluated for coronary artery disease. Report of the Ad Hoc Committee for Grading of Coronary Artery Disease, Council on Cardiovascular Surgery, American Heart Association. *Circulation* 1975;51:5-40.
7. Agatston AS, Janowitz WR, Hildner FJ, et al. Quantification of coronary artery calcium using ultrafast computed tomography. *J Am Coll Cardiol* 1990;15:827-32.
8. Leschka S, Alkadhi H, Plass A, et al. Accuracy of MSCT coronary angiography with 64-slice technology: first experience. *Eur Heart J* 2005;26:1482-7
9. Raff GL, Gallagher MJ, O'Neill WW, et al. Diagnostic accuracy of noninvasive coronary angiography using 64-slice spiral computed tomography. *J Am Coll Cardiol* 2005;46:552-7.
10. Leber AW, Knez A, von Ziegler F, et al. Quantification of obstructive and nonobstructive coronary lesions by 64-slice computed tomography: a comparative study with quantitative coronary angiography and intravascular ultrasound. *J Am Coll Cardiol* 2005;46:147-54.
11. Ropers D, Rixe J, Anders K, et al. Usefulness of multidetector row spiral computed tomography with 64- x 0.6-mm collimation and 330-ms rotation for the noninvasive detection of significant coronary artery stenoses. *Am J Cardiol* 2006;97:343-8.

12. Schuijf JD, Pundziute G, Jukema JW, et al. Diagnostic accuracy of 64-slice multislice computed tomography in the noninvasive evaluation of significant coronary artery disease. *Am J Cardiol* 2006;98:145-8.
13. Ehara M, Surmely JF, Kawai M, et al. Diagnostic accuracy of 64-slice computed tomography for detecting angiographically significant coronary artery stenosis in an unselected consecutive patient population: comparison with conventional invasive angiography. *Circ J* 2006;70:564-71.
14. Nikolaou K, Knez A, Rist C, et al. Accuracy of 64-MDCT in the diagnosis of ischemic heart disease. *AJR Am J Roentgenol* 2006;187:111-7.
15. Dirksen MS, Jukema JW, Bax JJ, et al. Cardiac multidetector-row computed tomography in patients with unstable angina. *Am J Cardiol* 2005;95:457-61.
16. Dorgelo J, Willems TP, Geluk CA, et al. Multidetector computed tomography-guided treatment strategy in patients with non-ST elevation acute coronary syndromes: a pilot study. *Eur Radiol* 2005;15:708-13.
17. Diver DJ, Bier JD, Ferreira PE, et al. Clinical and arteriographic characterization of patients with unstable angina without critical coronary arterial narrowing (from the TIMI-IIIa Trial). *Am J Cardiol* 1994;74:531-7.
18. Roe MT, Harrington RA, Prosper DM, et al. Clinical and therapeutic profile of patients presenting with acute coronary syndromes who do not have significant coronary artery disease. The Platelet Glycoprotein IIb/IIIa in Unstable Angina: Receptor Suppression Using Integrilin Therapy (PURSUIT) Trial Investigators. *Circulation* 2000;102:1101-6.
19. Glaser R, Herrmann HC, Murphy SA, et al. Benefit of an early invasive management strategy in women with acute coronary syndromes. *Jama* 2002;288:3124-9.
20. Flohr TG, McCollough CH, Bruder H, et al. First performance evaluation of a dual-source CT (DSCT) system. *Eur Radiol* 2006;16:256-68.
21. Achenbach S, Ropers D, Kuettner A, et al. Contrast-enhanced coronary artery visualization by dual-source computed tomography--initial experience. *Eur J Radiol* 2006;57:331-5.
22. Hausleiter J, Meyer T, Hadamitzky M, et al. Radiation dose estimates from cardiac multislice computed tomography in daily practice: impact of different scanning protocols on effective dose estimates. *Circulation* 2006;113:1305-10.
23. Coles DR, Smail MA, Negus IS, et al. Comparison of radiation doses from multislice computed tomography coronary angiography and conventional diagnostic angiography. *J Am Coll Cardiol* 2006;47:1840-5.

9

Comprehensive assessment of coronary artery stenoses: CT coronary angiography versus conventional coronary angiography and correlation with FFR in patients with stable angina

Journal of American College of Cardiology.
2008 Aug 19; 52(8):636-43.

Willem B. Meijboom, MD^{1,2},
Nico R. Mollet, MD, PhD^{1,2},
Carlos A. Van Mieghem,
MD^{1,2}, Annick C. Weustink,
MD^{1,2}, Francesca Pugliese,
MD^{1,2}, Niels van Pelt, MD^{1,2},
Filippo Cademartiri, MD,
PhD², Eleni Vourvouri, MD,
PhD^{1,2}, Peter de Jaegere, MD,
PhD¹, Gabriel P. Krestin,
MD, PhD², Pim J. de Feyter,
MD, PhD^{1,2}

¹ Department of Cardiology,
Thoraxcenter

² Department of Radiology
Erasmus Medical Center
Rotterdam, the Netherlands

ABSTRACT

Objectives

We sought to determine the diagnostic accuracy of non-invasive visual (CTCA) and quantitative CT coronary angiography (QCT) to predict the hemodynamic significance of a coronary stenosis, using intracoronary fractional flow reserve (FFR) as the reference standard.

Background

It has been demonstrated that CTCA provides excellent diagnostic sensitivity for identifying coronary stenoses, but may lack accurate delineation of the hemodynamic significance.

Methods

We investigated 79 patients with stable angina pectoris who underwent both 64 slice - or dual source CTCA and FFR measurement of discrete coronary stenoses. CTCA and CCA, and QCT and QCA, were performed to determine the severity of a stenosis which was compared with FFR measurements. A significant anatomical or functional stenosis was defined as $\geq 50\%$ diameter stenosis or $\text{FFR} < 0.75$. Stented segments and bypass grafts were not included in the analysis.

Results

A total of 89 stenoses were evaluated of which 18% (16/89) had an $\text{FFR} < 0.75$. The diagnostic accuracy of CTCA, QCT, CCA and QCA to detect a hemodynamic significant coronary lesion was 49%, 71%, 61% and 67%, respectively. Correlation between QCT and QCA with FFR measurement was weak (R-value of respectively -0.32 and -0.30). Correlation between QCT and QCA was significant, but only moderate ($R = 0.53$; $p < 0.0001$).

Conclusions

The anatomical assessment of the hemodynamic significance of coronary stenoses determined either by visual CTCA, CCA or quantitative QCT or QCA does not correlate well with the functional assessment of FFR. Determining the hemodynamic significance of an angiographic intermediate stenosis remains relevant before referral for revascularization treatment.

INTRODUCTION

Currently available 64 slice cardiac CT scanners and recently introduced dual-source scanners have the ability to completely assess the entire coronary tree and have been demonstrated to have good diagnostic accuracy for the identification of anatomically important coronary artery disease (CAD), generally defined as coronary artery stenoses with a lumen diameter reduction of at least 50 % (1-11). However, the anatomical significant appearance of a coronary stenosis does not always equate with functional significance and this is particularly so for intermediate type coronary lesions (12-16). According to the guidelines (ESC, ACC/AHA), the decision to perform angioplasty or bypass surgery should integrate anatomical information with a test that provides objective proof of ischemia (17,18).

Only few reports have studied the relationship between the significance of a stenosis in a coronary vessel as defined by CTCA, and the functional importance of this stenosis in that particular coronary vessel territory (19-22). This study evaluates the relationship between anatomy and functional significance of a coronary stenosis in patients who both underwent CTCA and CCA using the lesion-specific intracoronary fractional flow reserve (FFR) measurement.

METHODS

Study population

We retrospectively analyzed all patients who in the period between July 2004 and March 2007 underwent both a cardiac CT scan and invasive CCA and a subsequent measurement of the FFR. The decision to measure FFR was based entirely on the appearance of a coronary narrowing on CCA and was performed at the interventional cardiologist's discretion. All patients were assessed by either a 64-slice CT scanner (period July 2004 to March 2006) or dual-source CT scanner (period April 2006 to March 2007). Contra-indications for a CT scan included impaired renal function (creatinin clearance < 60 ml/min as defined with the Cockcroft formula), irregular heart rhythm and known contrast allergy. Patients with previous percutaneous coronary intervention (PCI) using stents or coronary artery bypass surgery (CABG) were excluded from further analysis. Due to the hemodynamic interaction between 2 or more stenoses in series (23,24), we only included patients in whom FFR of a single discrete lesion had been performed. In total 89 segments in 79 patients were included in the study. Sixteen segments were excluded due to CTCA related artefacts and one because of inability to obtain a good angiographic view to perform QCA.

For this retrospective analysis, all patients gave their informed consent to undergo CTCA as part of research protocols approved by the institutional review board. FFR was carried out as part of routine clinical management.

Conventional coronary angiography

All patients underwent CCA through the femoral approach, using a 6 or 7 french guiding catheter. After intracoronary injection of 2 mg isosorbide dinitrate, an angiogram of the right and left coronary artery was performed in multiple projections using standard techniques. All angiograms were analyzed off-line by 2 cardiologists who were not involved in the patient's medical care. They independently analyzed the selected coronary artery stenosis where FFR had been informed using visual estimation and quantitative assessment, the latter using an automated edge contour detection system (Cardiovascular Angiographic Analysis System, Pie Medical Equipment, Maastricht, the Netherlands)(25). Qualitative and quantitative analysis was based on the angiographic projection showing the most severe narrowing. A coronary stenosis was defined as significant based on visual inspection or when the degree of stenosis as measured with quantitative coronary angiography (QCA) was $\geq 50\%$.

FFR measurement

FFR was measured with a sensor-tipped 0.014 inch guide wire (Pressure WireTM, Radi Medical Systems, Uppsala, Sweden). After positioning of the pressure sensor just distal to the stenosis, maximal myocardial hyperemia was induced by a continuous intravenous infusion of adenosine in a femoral vein at an infusion rate of 140 $\mu\text{g}/\text{kg}$ body-weight per minute for minimum of 2 minutes. During maximum hyperemia, FFR was calculated as the ratio of mean distal pressure measured by the pressure wire divided by the mean proximal pressure measured by the guiding catheter (26). A coronary stenosis with an FFR value < 0.75 was considered functionally significant (27-29).

CT coronary angiography

Patient preparation

Patients scanned with the 64-slice scanner who had a heart rate exceeding 65 bpm received additional oral and/or IV beta-blockers (metoprolol) before the CT-scan in order to obtain a heart rate below 65 bpm. Patients scanned with dual-source CT did not receive pre-medication irrespective of the heart rate.

Scan protocol

Thirty-eight patients were scanned with a 64-slice CT scanner (Sensation 64, Siemens, Forchheim, Germany). Angiographic scan parameters were: 32 x 2 x 0.6 mm collimation with z-flying focal spot, 330 ms rotation time, temporal resolution 165ms, 120 kV tube voltage, 900 mAs tube current, 3.8 mm/rotation table feed. Prospective x-ray tube modulation was not applied.

Forty patients were scanned using a dual-source CT scanner (Somatom Definition, Siemens, Forchheim, Germany). DSCT angiographic scan parameters were: 120 kV, 330 ms rotation time, temporal resolution 83ms and 32x 2 X 0.6 mm collimation with z-flying focal spot for both detectors. Pitch values were adapted to heart rate based on the average of the last 10 heartbeats preced-

ing the scan. Each tube provided 412 mAs/rot. Prospective tube modulation was applied with full dose radiation only given during 25-70% of the RR-interval.

With the 64-slice scanner a bolus of 100 ml of contrast material (400 mgI/mL; IomeronTM, Bracco, Milan, Italy) was injected intravenously in an antecubital vein at 5 ml/s. With dual-source CT the volume of iodinated contrast material (Ultravist[®] 370 mgI/ml, Schering AG, Germany) was adapted to the scan time, which varied between 5 and 13 seconds. A bolus of contrast material (60-90 ml) was injected in an antecubital vein at a flow rate of 5 ml/s followed by a saline chaser of 40 ml at 5 ml/s. In both scanners a bolus-tracking technique was used to synchronize the arrival of contrast in the coronary arteries and the scan was started once the contrast material in the ascending aorta reached a predefined threshold of +100 Hounsfield units.

Image reconstruction

Images were reconstructed with ECG gating to obtain near motion-free image quality. Optimal data sets were reconstructed in the mid- to end-diastolic phase and in the end systolic phase.

Qualitative evaluation of the CT coronary angiogram

Two experienced observers unaware of the results of CCA evaluated the CTCA data sets on an offline workstation (Leonardo, Siemens, Forchheim, Germany). Initially the specific lesion was evaluated with axial slices for the presence of significant disease and additionally (curved) multiplanar reformatted reconstructions were used.

Quantitative evaluation of the CT coronary angiogram

Two experienced observers performed the quantification manually. After positioning the planes orthogonal to the course of the coronaries cross-sectional images were obtained in the most severe narrowing and in the proximal and distal reference site. In these three images the minimal lumen diameter was measured. The reference diameter was calculated by averaging the proximal and distal minimal lumen diameters. The percent diameter stenosis was calculated by subtracting the reference diameter by the minimal lumen diameter which was divided by the reference diameter. The average of both measurements by the two observers was reported. A 50 percent diameter stenosis measured with QCT was described as significant.

Statistical analysis

The diagnostic performance of qualitative and quantitative CCA and CTCA for the detection of significant stenoses in the coronary arteries with FFR as the standard of reference is presented as sensitivity, specificity and diagnostic accuracy (true positives + true negatives / true positives + true negatives + false positives + false negatives), with the corresponding 95% CIs. The relation between anatomical (QCA and QCT) and functional parameters (FFR) were analyzed with correlation statistics. Pearson correlation-coefficient was used since QCA, QCT and FFR were nor-

mally distributed. Bland-Altman analysis was performed by plotting the difference of QCA and QCT versus QCA (30). Interobserver variability for the detection of significant coronary stenosis and agreement between techniques to classify segments as having a functional significant lesion was determined by *k*-statistics.

RESULTS

Patient's characteristics and angiographic data are shown in Table 1. A total of 17 segments were excluded due to the presence of heavy calcifications (11 segments), motion artifacts (2 segments), breathing artifacts (2 segments), low contrast opacification (1 segment) and absence of a good angiographic view to perform QCA (1). Average heart rate during CT data acquisition was 60 ± 9 bpm for 64-slice CT and 68 ± 11 bpm for DSCT.

Table 1. Patient and lesion characteristics.

Patients (n=79)	
Segments, n	89
Sex (male, female)	64/15
Mean age, y	60 ± 9
Body Mass Index, mean (kg/m ²)	26.6 ± 3.9
Prior myocardial infarction	10
Angiographic data	
Affected artery	
Left main coronary artery	5
Left anterior descending coronary artery	41
Circumflex coronary artery	19
Right coronary artery	24
Reference diameter (mm)	2.82 ± 0.67
Percent diameter stenosis (%)	44 ± 11
Minimal luminal diameter (mm)	1.57 ± 0.50

Overall, 89 discrete stenoses in 79 patients were included for comparison with FFR. Seventy-one percent (63/89) of these stenoses were of angiographic intermediate severity (between 40 and 70% diameter stenosis as determined by QCA), twenty-nine stenoses were less than 40% and 1 stenosis was measured as more than 70%. Of these 89 coronary stenoses, 35 had a diameter stenosis of more than 50% by QCA, but only 16 lesions were hemodynamically significant (FFR < 0.75). Patient management is shown in Table 2.

Diagnostic performance of CT coronary angiography and conventional coronary angiography versus fractional flow reserve: visual assessment

The diagnostic performance of CTCA and CCA for the assessment of a functionally important coronary stenosis (FFR < 0.75) is detailed in Table 3 and Figure 1. Agreement between visual CT and FFR assessment was present in 49% (44/89) of the evaluated segments: 15 of the 16 hemodynamically significant stenoses were identified correctly. One functionally important lesion in the mid left anterior descending coronary artery was underestimated and classified as non-

significant by CTCA (44% diameter stenosis by QCA) (Figure 2). Overestimation of hemodynamic severity occurred in 44 cases (Figure 3). Corresponding sensitivity and specificity were respectively 94% and 40%. Interobserver variability for detection of a functionally important coronary stenosis was good (k -value of 0.76). Agreement between CTCA and FFR was poor (kappa value of 0.16).

By comparison, visual lesion assessment by CCA showed an agreement with FFR in 61% (54/89) of the segments. Visual scoring identified 10 of the 16 functionally important lesions and 44 of the 73 functionally insignificant lesions. Six functionally important lesions were underestimated (Figure 2). In 29 lesions the hemodynamic severity was overestimated (Figure 3). Consequently, the sensitivity was 63% and the specificity 60% for CCA to detect a functionally significant lesion. Interobserver variability for the detection of a functionally important coronary stenosis was moderate (k -value of 0.61). Agreement between CCA and FFR was poor (kappa value of 0.15). Furthermore, the diagnostic performance of CTCA and CCA for the assessment of a functionally important coronary stenosis, defined as a $FFR < 0.80$, is detailed in Table 3 and Figure 1.

Diagnostic performance of quantitative CT coronary angiography (QCT) and quantitative coronary angiography (QCA) versus fractional flow reserve: quantitative assessment

The diagnostic accuracy of QCT and QCA for detecting functionally relevant coronary stenoses is described in Table 3 and Figure 1. Overall the diagnostic accuracy for both quantitative measures was slightly better than when performed with visual estimation.

Table 2. Patient management

Therapeutic decision	
Medical therapy, n	57
Percutaneous coronary intervention, n	29
Coronary artery bypass grafting, n	3
Revascularized segments	
FFR < 0.75, n	16
0.75 < FFR < 0.80, n	11
FFR > 0.80, IVUS obstructive plaque, n	5

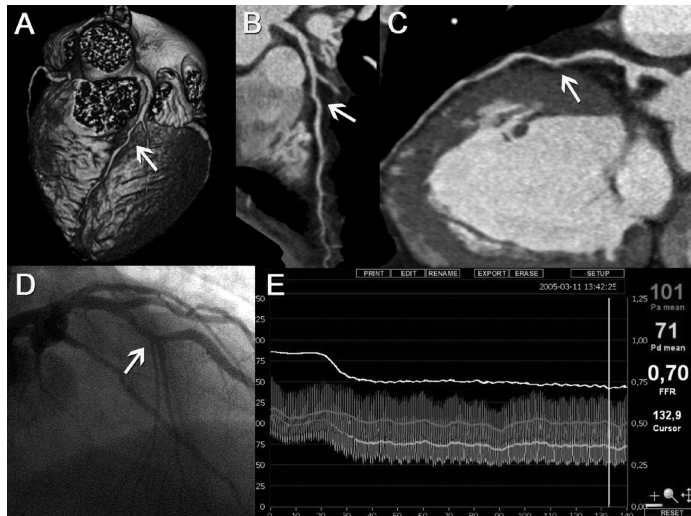


Figure 1. Quantitative coronary angiography (QCA), Quantitative CT coronary angiography (QCT), conventional coronary angiography and CT coronary angiography are plotted versus fractional flow reserve (FFR). There was a weak, but significant negative correlation between QCA and FFR ($r: -0.30$) and between QCT and FFR ($r: -0.32$). Coronary arteries smaller than 3.5 mm are depicted as solid dots, coronary arteries larger than 3.5 mm as open circles. (A full color version of this illustration can be found in the color section).

Table 3. Diagnostic performance of CCA and CTCA to detect a functional significant coronary stenosis (FFR < 0.75, FFR < 0.80).

FFR <0,75 (N=16)	TP	TN	FP	FN	kappa	Sensitivity, %	Specificity, %	Diagnostic accuracy, %
CT coronary angiography, visual score	15	29	44	1	0.16	94 (82-100)	40 (29-51)	49 (39-60)
Quantitative CT coronary angiography	8	55	18	8	0.20	50 (26-75)	75 (65-85)	71 (61-80)
Conventional coronary angiography, visual score	10	44	29	6	0.15	63 (39-86)	60 (49-72)	61 (51-71)
Quantitative coronary angiography	11	49	24	5	0.25	69 (46-91)	67 (56-78)	67 (58-77)
FFR <0,80 (N=31)	TP	TN	FP	FN	kappa	Sensitivity, %	Specificity, %	Diagnostic accuracy, %
CT coronary angiography, visual score	29	28	30	2	0.35	94 (58-100)	48 (35-61)	64 (54-74)
Quantitative CT coronary angiography	14	46	12	17	0.25	45 (28-63)	79 (69-90)	67 (58-77)
Conventional coronary angiography, visual score	17	36	22	14	0.16	55 (37-72)	62 (50-75)	60 (49-70)
Quantitative coronary angiography	17	41	18	13	0.25	57 (39-74)	69 (58-81)	65 (55-75)

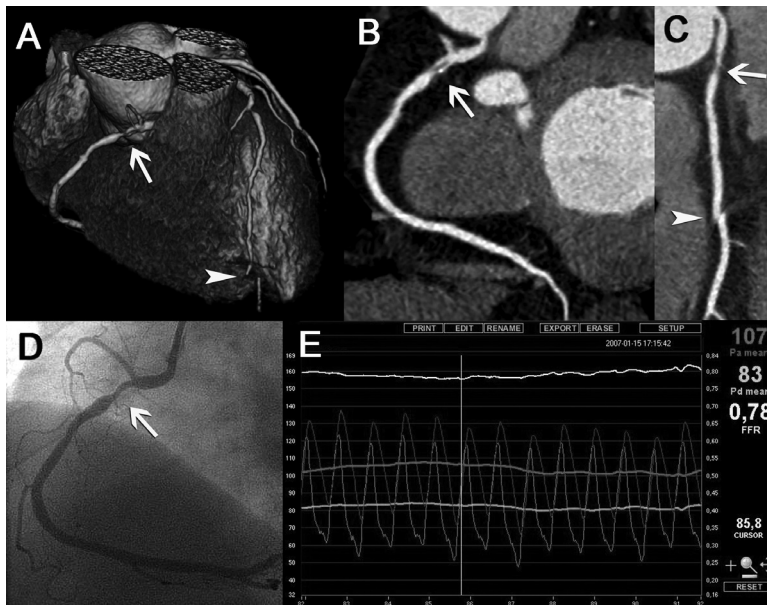


Figure 2. Patient showing a coronary artery stenosis (arrow) in the left anterior descending coronary artery, as visualized with CT coronary angiography (CTCA) (panel A, volume-rendered image; panels B and C, two orthogonal curved multiplanar reconstructions) and conventional coronary angiography (CCA) (panel D). By visual assessment, the coronary lesion was estimated as less than 50% diameter stenosis, both by CTCA and CCA. By quantitative analysis, the diameter stenosis was measured as 44% by quantitative coronary angiography and 40% by quantitative CT coronary angiography. The fractional flow reserve was 0.71. Based on the functional assessment, the patient underwent a successful percutaneous coronary intervention for this anatomically intermediate stenosis. (A full color version of this illustration can be found in the color section).

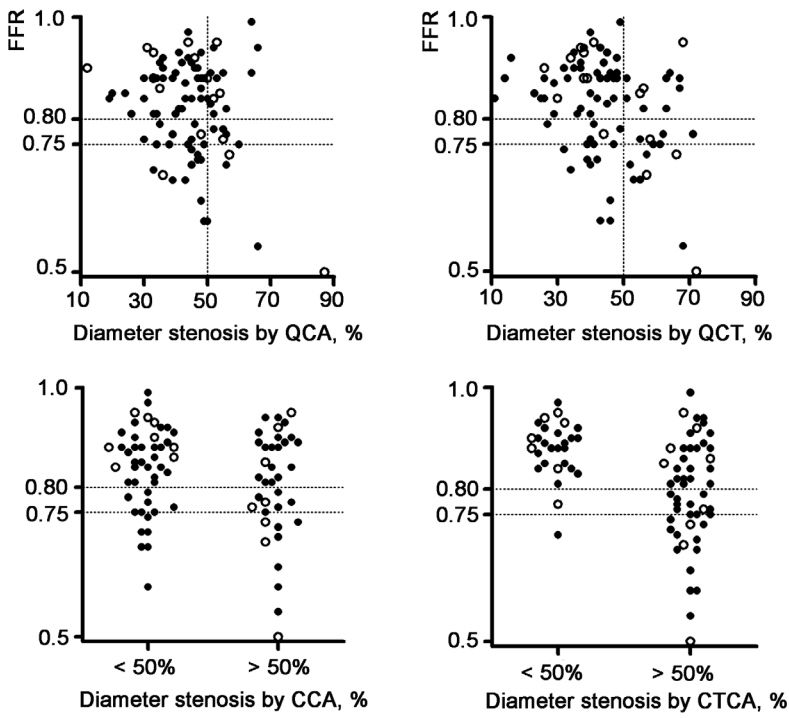


Figure 3. Patient with a coronary artery stenosis (arrow) in the proximal part of the right coronary artery, as visualized with CT coronary angiography (panel A, volume-rendered image; panels B and C, two orthogonal curved multiplanar reconstructions) and conventional coronary angiography (CCA) (panel D). Visually, the diameter stenosis was estimated as more than 50%, both by CTCA and CCA. Also after quantification (56% diameter stenosis by quantitative coronary angiography, 70% diameter stenosis by quantitative CT coronary angiography), the lesion appeared to be anatomically significant. The fractional flow reserve was 0.78. In the distal segments, a step artefact can be seen (panels A and C, arrowhead).

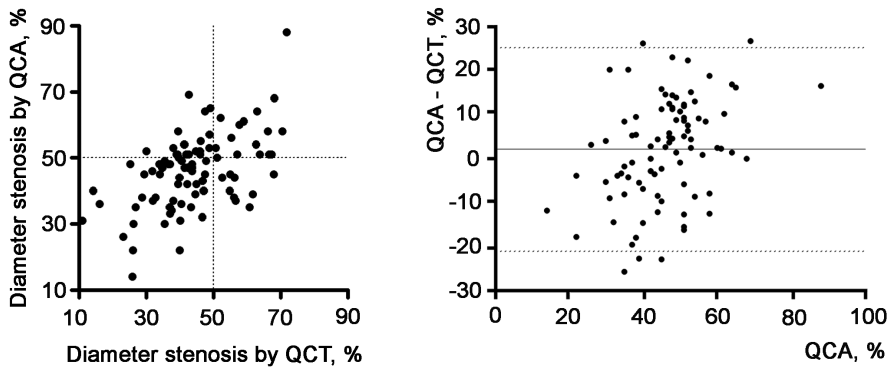


Figure 4. In the left panel quantitative CT coronary angiography is plotted versus quantitative coronary angiography. A significant correlation is seen between both anatomical techniques ($r: 0.53$). In the right panel Bland-Altman analysis showed a bias of +2% with 95% limit of agreement ranging from -21% to 25%.

Agreement between QCA and FFR as well as between QCT and FFR (Table 3) was only fair (kappa value of respectively 0.25 and 0.20). The interobserver variability for QCA (k -value of 0.58) and QCT (k -value of 0.69) was moderate. The correlation between QCT and FFR was $R = -0.32$ and between QCA and FFR $R = -0.30$.

Correlation of the percent diameter stenosis as determined by QCT and QCA was significant, but only moderate ($R = 0.53$; $p < 0.0001$) (Figure 4). The Bland-Altman analysis plot revealed important variability: the mean difference between QCA and QCT was +2% with 95% limits of agreement ranging between -21% to +25% (Figure 4).

DISCUSSION

FFR is a lesion specific technique to determine the functional importance of a coronary stenosis and is correlated with non-invasive tests that demonstrate ischemia (27,31-34). It has been shown to be a useful guide for decision making regarding the revascularisation of a specific lesion. In lesions where the FFR is ≥ 0.75 , revascularization can be safely deferred (35-37).

Limitations of anatomical imaging. Previous reports have demonstrated that the anatomical assessment of a coronary stenosis as determined by CCA correlates poorly with the hemodynamic significance of the stenosis in particular in intermediate severity lesions (12-16). Although QCA is accurate and reproducible, it does not reflect the hemodynamic impairment of coronary flow. QCA does not account for the effects of factors such as collateral circulation, mass of viable myocardium, shape and length of stenosis, inflow and outflow configuration and transient vasoconstriction with resulting dynamic changes in the diameter of a stenosis (38). The diffuseness of the atherosclerotic process often results in disease in the reference segments proximal and distal to the site of maximal diameter reduction and as a result leads to underestimation of extent and severity of coronary atherosclerosis (39).

Integrating anatomy with functional information. These findings were also demonstrated in this study, not only for CTCA, but also when assessing the severity of a coronary artery stenosis with CCA. Using visual assessment, CTCA had high sensitivity to detect lesions with functional significance ($FFR < 0.75$). However, it had poor specificity due to frequent false positives; CTCA overestimated the functional severity of a coronary stenosis, even when excluding segments with extensive calcifications or coronary motion. Quantification of stenosis severity by QCT and QCA improved the prediction of a functional relevant coronary stenosis slightly.

Previous studies have compared the anatomical findings of CTCA with functional imaging using nuclear stress testing (19,20,22). These studies also showed a poor correlation between anatomy

and function with only ~ 50% of patients with significant coronary stenosis as demonstrated by CTCA having ischemia demonstrated by nuclear stress testing. Besides methodological limitations, these noninvasive tests measure the effect of impaired coronary perfusion at the level of the myocardium and thus do not discriminate between epicardial flow impairment and microvascular perfusion abnormalities. Intracoronary measurement of the FFR has the disadvantage of being invasive, but has the benefit of determining the ischemic potential of a specific epicardial coronary stenosis.

Clinical implementation. Given the above findings, and the consistently high negative predictive value of CTCA in different population groups, CTCA appears best suited as an effective rule out test for significant CAD. Those patients with suspected CAD and no or minimal coronary atherosclerosis on CTCA would not need further investigation (40,41). However patients with obstructive CAD on CTCA may best be investigated using a combined approach with a subsequent functional test such as nuclear stress testing, stress echocardiography or magnetic resonance perfusion imaging.

Anatomical evaluation of CAD has limitations and makes functional assessment necessary. Comprehensive non invasive anatomical and functional imaging may best identify patients who are likely to benefit most from secondary preventive measures and medical therapy (coronary atherosclerosis without ischemia) or who may be candidates for coronary revascularization (coronary atherosclerosis with ischemia). All-in-one approaches such as SPECT-CTCA or PET-CTCA, which provide integrated evaluation of anatomy and physiology in a non-invasive way, might theoretically solve these diagnostic problems.

Now that we are able to non-invasively access coronary anatomy one should be reminded of the limitations of non-invasive functional tests, especially in patients with multivessel disease or significant left main stenosis on CTCA, without evidence of ischemia of a non-invasive functional test (42,43). In case of doubt it seems prudent to refer such a patient to the cathlab for further invasive assessment and definitive exclusion of the functional severity of a specific epicardial stenosis, using FFR.

LIMITATIONS OF THE STUDY

Patient inclusion was not performed in a prospectively designed study, but as a retrospective analysis. Consecutive patients were enrolled based on the access to the 64-slice or dual-source CT scanner.

Seventeen segments in 15 patients had to be excluded due to the presence of heavy calcifications, motion artifacts, breathing artifacts, low contrast opacification and absence of a good angiographic view which made it, both visually as well as quantitatively, impossible to reliably estimate stenoses severity.

Quantification of coronary artery stenoses with CTCA continues to be a challenge due to the difficulty in ascertaining the normal reference segment of the coronary artery because of atherosclerotic involvement of the vessel wall proximal and distal to the stenosis (2,3,44). Especially in the presence of extensive calcifications of the artery it becomes impossible to accurately define the reference vessel diameters. Further improvement in spatial resolution will enhance the ability to accurately grade stenosis severity. However, particularly in coronary stenoses of intermediate severity, this may not improve the ability to predict functional significance, as is also observed with invasive CCA.

CONCLUSION

The correlation between stenosis severity as determined by CTCA or CCA and ischemia measured by FFR in coronary lesions of intermediate severity is poor. Functional information, whether provided by FFR or a noninvasive stress test, is essential in these circumstances for appropriate clinical decision making.

REFERENCES:

1. Leschka S, Alkadhi H, Plass A, et al. Accuracy of MSCT coronary angiography with 64-slice technology: first experience. *Eur Heart J* 2005; 26(15):1482-7.
2. Raff GL, Gallagher MJ, O'Neill WW, Goldstein JA. Diagnostic accuracy of noninvasive coronary angiography using 64-slice spiral computed tomography. *J Am Coll Cardiol* 2005;46:552-7.
3. Leber AW, Knez A, von Ziegler F, et al. Quantification of obstructive and nonobstructive coronary lesions by 64-slice computed tomography: a comparative study with quantitative coronary angiography and intravascular ultrasound. *J Am Coll Cardiol* 2005;46:147-54.
4. Mollet NR, Cademartiri F, van Mieghem CA, et al. High-resolution spiral computed tomography coronary angiography in patients referred for diagnostic conventional coronary angiography. *Circulation* 2005;112:2318-23.
5. Ropers D, Rixe J, Anders K, et al. Usefulness of multidetector row spiral computed tomography with 64- x 0.6-mm collimation and 330-ms rotation for the noninvasive detection of significant coronary artery stenoses. *Am J Cardiol* 2006;97:343-8.

6. Schuijf JD, Pundziute G, Jukema JW, et al. Diagnostic accuracy of 64-slice multislice computed tomography in the noninvasive evaluation of significant coronary artery disease. *Am J Cardiol* 2006;98:145-8.
7. Nikolaou K, Knez A, Rist C, et al. Accuracy of 64-MDCT in the diagnosis of ischemic heart disease. *AJR Am J Roentgenol* 2006;187:111-7.
8. Fine JJ, Hopkins CB, Ruff N, Newton FC. Comparison of accuracy of 64-slice cardiovascular computed tomography with coronary angiography in patients with suspected coronary artery disease. *Am J Cardiol* 2006;97:173-4.
9. Ehara M, Surmely JF, Kawai M, et al. Diagnostic accuracy of 64-slice computed tomography for detecting angiographically significant coronary artery stenosis in an unselected consecutive patient population: comparison with conventional invasive angiography. *Circ J* 2006;70:564-71.
10. Leber AW, Johnson T, Becker A, et al. Diagnostic accuracy of dual-source multi-slice CT-coronary angiography in patients with an intermediate pretest likelihood for coronary artery disease. *Eur Heart J* 2007;28:2354-2360.
11. Weustink AC, Meijboom WB, Mollet NR, et al. Reliable high-speed coronary computed tomography in symptomatic patients. *J Am Coll Cardiol* 2007;50:786-94.
12. White CW, Wright CB, Doty DB, et al. Does visual interpretation of the coronary arteriogram predict the physiologic importance of a coronary stenosis? *N Engl J Med* 1984;310:819-24.
13. Kern MJ, Lerman A, Bech JW, et al. Physiological assessment of coronary artery disease in the cardiac catheterization laboratory: a scientific statement from the American Heart Association Committee on Diagnostic and Interventional Cardiac Catheterization, Council on Clinical Cardiology. *Circulation* 2006;114:1321-41.
14. Tobis J, Azarbal B, Slavin L. Assessment of intermediate severity coronary lesions in the catheterization laboratory. *J Am Coll Cardiol* 2007;49:839-48.
15. Christou MA, Siontis GC, Katritsis DG, Ioannidis JP. Meta-analysis of fractional flow reserve versus quantitative coronary angiography and noninvasive imaging for evaluation of myocardial ischemia. *Am J Cardiol* 2007;99:450-6.
16. Uren NG, Melin JA, De Bruyne B, Wijns W, Baudhuin T, Camici PG. Relation between myocardial blood flow and the severity of coronary-artery stenosis. *N Engl J Med* 1994;330:1782-8.
17. Silber S, Albertsson P, Aviles FF, et al. Guidelines for percutaneous coronary interventions. The Task Force for Percutaneous Coronary Interventions of the European Society of Cardiology. *Eur Heart J* 2005;26:804-47.
18. Smith SC, Jr., Feldman TE, Hirshfeld JW, Jr., et al. ACC/AHA/SCAI 2005 guideline update for percutaneous coronary intervention: a report of the American College of Cardiology/American Heart Association Task Force on Practice Guidelines (ACC/AHA/SCAI Writing Committee to Update 2001 Guidelines for Percutaneous Coronary Intervention). *Circulation* 2006;113:e166-286.

19. Schuijf JD, Wijns W, Jukema JW, et al. Relationship between noninvasive coronary angiography with multi-slice computed tomography and myocardial perfusion imaging. *J Am Coll Cardiol* 2006;48:2508-14.
20. Hacker M, Jakobs T, Hack N, et al. Sixty-four slice spiral CT angiography does not predict the functional relevance of coronary artery stenoses in patients with stable angina. *Eur J Nucl Med Mol Imaging* 2007;34:4-10.
21. Rispler S, Keidar Z, Ghersin E, et al. Integrated single-photon emission computed tomography and computed tomography coronary angiography for the assessment of hemodynamically significant coronary artery lesions. *J Am Coll Cardiol* 2007;49:1059-67.
22. Hacker M, Jakobs T, Matthiesen F, et al. Comparison of spiral multidetector CT angiography and myocardial perfusion imaging in the noninvasive detection of functionally relevant coronary artery lesions: first clinical experiences. *J Nucl Med* 2005;46:1294-300.
23. De Bruyne B, Pijls NH, Heyndrickx GR, Hodeige D, Kirkeeide R, Gould KL. Pressure-derived fractional flow reserve to assess serial epicardial stenoses: theoretical basis and animal validation. *Circulation* 2000;101:1840-7.
24. Pijls NH, De Bruyne B, Bech GJ, et al. Coronary pressure measurement to assess the hemodynamic significance of serial stenoses within one coronary artery: validation in humans. *Circulation* 2000;102:2371-7.
25. Reiber JH, Serruys PW, Kooijman CJ, et al. Assessment of short-, medium-, and long-term variations in arterial dimensions from computer-assisted quantitation of coronary cineangiograms. *Circulation* 1985;71:280-8.
26. Pijls NH, Van Gelder B, Van der Voort P, et al. Fractional flow reserve. A useful index to evaluate the influence of an epicardial coronary stenosis on myocardial blood flow. *Circulation* 1995;92:3183-93.
27. De Bruyne B, Bartunek J, Sys SU, Heyndrickx GR. Relation between myocardial fractional flow reserve calculated from coronary pressure measurements and exercise-induced myocardial ischemia. *Circulation* 1995;92:39-46.
28. Pijls NH, De Bruyne B, Peels K, et al. Measurement of fractional flow reserve to assess the functional severity of coronary-artery stenoses. *N Engl J Med* 1996;334:1703-8.
29. Kern MJ. Coronary physiology revisited : practical insights from the cardiac catheterization laboratory. *Circulation* 2000;101:1344-51.
30. Bland JM, Altman DG. Statistical methods for assessing agreement between two methods of clinical measurement. *Lancet* 1986;1:307-10.
31. De Bruyne B, Baudhuin T, Melin JA, et al. Coronary flow reserve calculated from pressure measurements in humans. Validation with positron emission tomography. *Circulation* 1994;89:1013-22.
32. Bartunek J, Marwick TH, Rodrigues AC, et al. Dobutamine-induced wall motion abnormalities: correlations with myocardial fractional flow reserve and quantitative coronary angiography. *J Am Coll Cardiol* 1996;27:1429-36.

33. Costa MA, Shoemaker S, Futamatsu H, et al. Quantitative magnetic resonance perfusion imaging detects anatomic and physiologic coronary artery disease as measured by coronary angiography and fractional flow reserve. *J Am Coll Cardiol* 2007;50:514-22.
34. Rieber J, Huber A, Erhard I, et al. Cardiac magnetic resonance perfusion imaging for the functional assessment of coronary artery disease: a comparison with coronary angiography and fractional flow reserve. *Eur Heart J* 2006;27:1465-71.
35. Pijls NH, van Schaardenburgh P, Manoharan G, et al. Percutaneous coronary intervention of functionally nonsignificant stenosis: 5-year follow-up of the DEFER Study. *J Am Coll Cardiol* 2007;49:2105-11.
36. Legalery P, Schiele F, Seronde MF, et al. One-year outcome of patients submitted to routine fractional flow reserve assessment to determine the need for angioplasty. *Eur Heart J* 2005;26:2623-9.
37. Wongpraparut N, Yalamanchili V, Pasnoori V, et al. Thirty-month outcome after fractional flow reserve-guided versus conventional multivessel percutaneous coronary intervention. *Am J Cardiol* 2005;96:877-84.
38. Gould KL, Kelley KO, Bolson EL. Experimental validation of quantitative coronary arteriography for determining pressure-flow characteristics of coronary stenosis. *Circulation* 1982;66:930-7.
39. de Feyter PJ, Serruys PW, Davies MJ, Richardson P, Lubsen J, Oliver MF. Quantitative coronary angiography to measure progression and regression of coronary atherosclerosis. Value, limitations, and implications for clinical trials. *Circulation* 1991;84:412-23.
40. Gilard M, Le Gal G, Cornily JC, et al. Midterm prognosis of patients with suspected coronary artery disease and normal multislice computed tomographic findings: a prospective management outcome study. *Arch Intern Med* 2007;167:1686-9.
41. Min JK, Shaw LJ, Devereux RB, et al. Prognostic value of multidetector coronary computed tomographic angiography for prediction of all-cause mortality. *J Am Coll Cardiol* 2007;50:1161-70.
42. Ragosta M, Bishop AH, Lipson LC, et al. Comparison between angiography and fractional flow reserve versus single-photon emission computed tomographic myocardial perfusion imaging for determining lesion significance in patients with multivessel coronary disease. *Am J Cardiol* 2007;99:896-902.
43. Lima RS, Watson DD, Goode AR, et al. Incremental value of combined perfusion and function over perfusion alone by gated SPECT myocardial perfusion imaging for detection of severe three-vessel coronary artery disease. *J Am Coll Cardiol* 2003;42:64-70.
44. Hoffmann MH, Shi H, Schmitz BL, et al. Noninvasive coronary angiography with multislice computed tomography. *Jama* 2005;293:2471-8.

10

Value of Combined Use of Calcium Score and 64-slice CT Coronary Angiography in Symptomatic Patients Referred for Conventional Coronary Angiography

Submitted

Matthijs F.L. Meijs, MD*†,
W. Bob Meijboom, MD‡,§,
Joanne D. Schuijf PhD||, #,
Mathias Prokop, MD, PhD‡,
Nico R. Mollet MD, PhD‡,§,
Carlos A.G. van Mieghem
MD, PhD‡,§, Jacob M. van
Werkhoven MD||, J. Wouter
Jukema MD, PhD||, Pieter
A. Doevendans, MD, PhD,*
Jeroen J. Bax, MD, PhD||,
Pim J. de Feyter, MD, PhD,
‡,§, Maarten J. Cramer, MD,
PhD*

*Department of Cardiology,
Utrecht University Medical
Center, Utrecht, the
Netherlands

†Department of Radiology,
Utrecht University Medical
Center, Utrecht, the
Netherlands

‡Department of Cardiology,
Erasmus University Medical
Center, Rotterdam, the
Netherlands

§Department of Radiology,
Erasmus University Medical
Center, Rotterdam, the
Netherlands

||Department of Cardiology,
Leiden University Medical
Center, Leiden, the Netherlands

#Department of Radiology,
Leiden University Medical
Center, Leiden, the Netherlands

ABSTRACT

Objectives:

A low calcium score (CS) may overlook patients with significant coronary artery disease (CAD), while a high CS may decrease the diagnostic performance of 64-slice CT coronary angiography (CTCA). CTCA uses contrast medium and more radiation than CS.

Methods:

We studied the combination of CS and CTCA in the work-up of angina patients referred for conventional coronary angiography (CCA) in 360 patients between 50 and 70 years old with stable and unstable angina from a multicenter multivendor study clinically referred for CCA.

Results:

The prevalence of significant CAD was 24% in patients with CS <10, and 87% in those with CS > 400. In the 62 patients with CS <10, CTCA detected all 15 patients with significant CAD. Specificity and positive likelihood ratio were 89% (95%CI: 76-96%) and 9.4 (95%CI: 4.1-22), respectively, for patients with CS <10, and 20% (95%CI: 32-68%) and 1,3 (95%CI: 1.0-1.6), respectively, for those with CS >400.

Conclusions:

A negative CTCA ruled out significant CAD whereas a low CS did not. However, in angina patients with CS >400 the value of 64-slice CTCA was limited. In angina patients with CS <400 CS should be combined with CTCA, whereas angina patients with CS >400 should be referred to CCA directly.

INTRODUCTION:

CT coronary angiography (CTCA) has been postulated as a gatekeeper to conventional coronary angiography (CCA) [1]. In addition, the coronary calcium score (CS) has been suggested as a risk-estimate of significant CAD [2]. CS may stratify patients according to the risk of significant coronary artery disease (CAD), but cannot actually detect a coronary artery stenosis. CTCA can detect or rule out coronary artery stenosis. However, CTCA is associated with additional health risks compared to CS due to the use of iodine contrast and a higher radiation dose [1;3].

Therefore, it is necessary to determine the combination of CS and CTCA which in patients referred for CCA results in a work-up with optimal diagnostic performance but minimal health risk. For this aim, several important issues need to be addressed. The prevalence of CAD increases with CS [4]. Previous studies suggested that a low CS reliably rules out significant CAD in asymptomatic individuals [4-6]. However, in a recent study in patients with acute and non-acute chest pain syndromes with a CS of 0 or <10 a prevalence of significant CAD on CCA of 7% and 9%, respectively, was found [7]. Also, in a recent study 16% of patients who were clinically referred to positron emission tomography (PET) and had no coronary calcification had evidence of myocardial ischemia on PET [8]. Thus, CTCA may be able to detect patients with significant CAD who would be overlooked if only the CS would be considered. At the other end of the spectrum, blooming artifacts caused by coronary calcification resulting in over-estimation of lesion severity may result in false positive findings [9;10]. As the prevalence of CAD and false positive findings increase with CS, a high CS may decrease the additional diagnostic value of CTCA. Previous studies on the influence of CS on the diagnostic performance of CTCA have provided contradictory evidence. While some have reported a high number of false positive findings in patients with a high CS [9;10], others have reported no significant or only a limited impact of coronary calcification on the diagnostic accuracy of CTCA [11;12]. The present study was undertaken to study the value of the combination of CS and CTCA.

METHODS

Study design

The study was designed to prospectively include symptomatic patients who presented with stable and unstable anginal syndromes who were referred for clinically indicated CCA (manuscript accepted for publication). Patients were requested to undergo an additional CTCA for research purposes besides their CCA. The study protocol was approved by the institutional review board of the Erasmus University Medical Center.

Study population

As described previously, for this multi-center multi-vendor study conducted from October 2004 until June 2006 360 patients between 50 and 70 years of age with stable angina pectoris or non-ST segment elevation acute coronary syndrome underwent a non-enhanced CT scan to determine the CS followed by a CTCA scan in addition to CCA. No patients, vessels or segments were excluded from the analysis, even if image quality was poor due to extensive calcification, coronary motion or breathing artifacts. No patients with previous history of percutaneous transluminal coronary angioplasty, coronary artery bypass surgery, impaired renal function (serum creatinine $> 120 \mu\text{mol/l}$), persistent arrhythmias, inability to perform a breath hold of 15 seconds or known allergy to iodinated contrast material, were included. The study was conducted in three university hospitals.

Patient preparation

Patients with a heart rate exceeding 65 beats per minute (bpm) received additional beta-blockers (up to 100 mg metoprolol p.o. or up to 20 mg metoprolol i.v.). All patients received thorough breath hold instructions

Scan protocol, Image reconstruction, and evaluation

All scans were performed with 64-slice CT scanners in Center A (Sensation 64, Siemens, Forchheim, Germany), Center B (Brilliance 64, Philips Medical Systems, Best, the Netherlands) and Center C (Toshiba Multi-Slice Aquilion 64 system, Toshiba Medical Systems, Tokyo, Japan). The scan protocol has been described in more detail elsewhere (manuscript accepted for publication). In brief, a non-enhanced scan to calculate the total CS was performed prior to CTCA. For CS tube settings were 120 kV and 150 mAs. For CTCA, the scanners had a collimation of $64 \times 0.5\text{-}0.67 \text{ mm}$, a rotation time of 330-420 ms, tube settings were 120 kV and 700-950 mAs, and a spatial resolution of 0.6 mm^3 . A bolus-tracking technique was used to synchronize the start of image acquisition with the arrival of contrast agent in the coronary arteries. A bolus of 80 to 140 ml iodine contrast was used.

Multiple datasets were reconstructed separately with retrospective ECG-gating in order to obtain optimal image quality for all coronary segments. The Agatston CS was calculated using dedicated software (Heartbeat-CS, Extended Brilliance Workspace, Philips Medical System, Best, the Netherlands) [13].

CTCA scans were evaluated by 2 experienced readers, blinded for the CCA results. In case of disagreement, a third reader was consulted. The kappa-value for inter- and intraobserver variability was 0.70 and 0.72, respectively.

Quantitative coronary angiography (QCA)

All coronary angiograms were evaluated by a core lab of experienced cardiologists, who were unaware of the results of the CTCA. Stenoses were evaluated in the worst view, and classified as significant if the lumen diameter reduction exceeded 50% as measured by QCA.

Statistical analysis

Descriptive statistics were used to evaluate the diagnostic performance of CS and CTCA to detect patients with significant CAD, including sensitivity, specificity, positive and negative predictive values, and positive and negative likelihood ratios. These diagnostic parameters were expressed with a 95% confidence interval (CI) calculated with binomial expansion. The diagnostic performance of CTCA was calculated for all patients combined, and for subgroups of patients with an Agatston CS <10, between 10 and 100, between 100 and 400 and >400 [14].

A Chi-square test was performed to test for statistical significance ($p < 0.05$). All analyses were repeated separately for patients with stable and unstable anginal syndromes

Prevalence of significant CAD was based on the presence of at least one significant stenosis as determined by QCA, which was considered the standard of reference.

RESULTS

Patient characteristics

Patient characteristics are listed in table 1. Two-hundred and forty-five (68%) of 360 study participants were male, and 233 (65%) presented with stable chest pain syndromes. The mean age was 60 ± 6 years, the mean body mass index was 27.3 ± 3.8 kg/m² and the median Agatston CS was 213 (inter-quartile range 42-553). The prevalence of having at least one significant coronary stenosis was 68%. No significant differences in patient demographics were seen in patients presenting with stable angina syndromes or unstable anginal syndromes, except for a higher incidence of smokers and a higher prevalence and extent of significant CAD in the unstable angina patients.

Diagnostic performance of CTCA. As shown in table 2, for all patients combined the sensitivity of CTCA to detect significant CAD was 99% (95%CI 97-100%), the specificity was 64% (95%CI 55-73%), positive and negative predictive value were 86% (95%CI 81%-89%) and 97% (95%CI 90-100%), respectively. Positive and negative likelihood ratios (LR+ and LR-) to detect or exclude significant CAD were 2.8 (95%CI 2.2-3.5) and 0.013 (95%CI 0.00-0.05) for CTCA. Six of 37 (16%) subjects with a CS of 0, and 15 of 62 (24%) subjects with a CS <10 had significant CAD on CCA. Detection of significant CAD by CTCA was successful in all these subjects.

The estimated average effective radiation exposure was 1.2 ± 0.5 to 1.8 ± 0.9 mSv for CS and 15.5 ± 2.2 mSv to 18.4 ± 3.2 mSv for CTCA.

Table 1. Patient characteristics

Variable	All patients (N:360, 100%)	Stable anginal syndromes (N: 233, 65%)	Unstable anginal syndrome (N: 127, 35%)	p
Typical angina pectoris	151 (42%)	151 (65%)	-	-
Atypical angina pectoris	82 (23%)	82 (35%)	-	
Unstable angina pectoris	127 (35%)	-	127 (100%)	
Men	245 (68%)	156 (67%)	89 (70%)	0.56
Age (yrs)*	60±6	60±6	60±6	0.72
Body mass index (kg/m ²)*	27.3±3.8	27.6±3.9	26.8±3.5	0.06
Heart rate (bpm)*	59±9	59±10	59±8	0.99
Risk factors				
Hypertension ‡	219 (61%)	149 (64%)	70 (55%)	0.11
Hypercholesterolemia §	228 (63%)	151 (65%)	77 (61%)	0.49
Diabetes mellitus	63 (18%)	47 (20%)	16 (13%)	0.08
Smoker	137 (38%)	74 (32%)	63 (50%)	0.001
Family history of CAD #	183 (51%)	113 (48%)	70 (55%)	0.27
Body mass index ≥ 30 kg/m ²	85 (24%)	59 (25%)	26 (20%)	0.36
Previous myocardial infarction.	53 (15%)	36 (15%)	17 (13%)	0.64
Calcium score (Agatston score)†	213 (42-553)	211 (31-639)	216 (44-478)	0.59
Conventional coronary angiography				
Prevalence of obstructive CAD	246 (68%)	146 (63%)	100 (79%)	0.002
Absence of significant CAD	114 (32%)	87 (37%)	27 (21%)	
Single vessel disease	141 (39%)	88 (38%)	53 (42%)	
Two vessel disease	78 (22%)	46 (20%)	32 (25%)	0.009
Three vessel disease	21 (6%)	10 (4%)	11 (9%)	
Left main coronary artery disease	6 (2%)	2 (1%)	4 (3%)	

*Mean and standard deviation. †Median and quartiles. Values are n (%) unless otherwise indicated. Categorical variables were tested with Fisher exact and chi square test. Continuous variables were tested with unpaired two sided student t test. If not normally distributed, continuous variables were compared with the Mann-Whitney test. P-values are significant if values <0.05. ‡Blood pressure ≥ 140/90 mm Hg or treatment for hypertension. §Total cholesterol >180 mg/dl or treatment for hypercholesterolemia.

|| Treatment with oral anti-diabetic medication or insulin.

Table 2 Diagnostic performance in all patients

	Prevalence of disease (%)	N	TP	TN	FP	FN	Sensitivity (%)	Specificity (%)	PPV (%)	NPV (%)	LR+	LR-	Diagnostic accuracy (%)
All patients	68	360	244	73	41	2	99 (97-100)	64 (55-73)	86 (81-89)	97 (90-100)	2.8 (2.2-3.5)	0.13 (0.00-0.05)	88 (85-91)
A: CS <10	24	62	15	42	5	0	100 (75-100)	89 (76-96)	75 (51-90)	100 (90-100)	9.4 (4.1-22)	0.00 (0.00-n/an)	92 (85-99)
B: CS 10-100	65	63	41	13	9	0	100 (89-100)	59 (37-79)	82 (68-91)	100 (72-100)	2.4 (1.5-4.0)	0.00 (0.00-n/an)	86 (77-94)
C: CS 100-400	75	118	86	15	15	2	98 (91-100)	50 (32-68)	85 (76-91)	88 (62-98)	2.0 (1.4-2.8)	0.12 (0.02-0.38)	86 (79-92)
D: CS >400	87	114	99	3	12	0	100 (95-100)	20 (5-49)	89 (82-94)	100 (31-100)	1.3 (1.0-1.6)	0.00 (0.00-n/an)	89 (84-95)
A vs D							NS	P = 0.017	NS	NS	P < 0.0001	n/an	NS

Diagnostic performance of CTCA in all patients combined, and in subgroups per Agatston CS (A: CS less than 10, B: CS between 10 and 100, C: CS between 100 and 400, and D: CS greater than 400). Specificity and positive likelihood ratio decreased with increasing CS (p-value for the comparison by Chi-squared test across groups A and D)

Abbreviations: N = number of patients; TP: true positive; at least one significant stenosis in a patient detected by CTCA and CCA regardless of location of stenosis; TN: true negative; no significant stenosis in a patient detected either by CTCA or CCA; FP: false positive; significant stenosis detected by CTCA and no significant stenosis detected by CCA; FN: false negative; no significant stenosis detected by CTCA and at least one significant stenosis detected by CCA; LR+ = positive likelihood ratio; LR- = negative likelihood ratio, n/an = not analyzed (division by zero).

Table 3a. Diagnostic performance in patients with stable angina

	Prevalence of disease (%)	N	TP	TN	FP	FN	Sensitivity (%)	Specificity (%)	PPV (%)	NPV (%)	LR+	LR-	Diagnostic accuracy (%)
Stable Angina	63	233	145	56	31	1	99 (96-100)	64 (53-74)	83 (76-88)	98 (89-100)	2.8 (2.1-3.7)	0.01 (0.00-0.08)	86 (82-91)
A: CS <10	16	43	7	32	4	0	100 (56-100)	89 (73-96)	64 (32-88)	100 (87-100)	9.0 (3.6-22.7)	0.00 (0.00-n/an)	91 (82-99)
B: CS 10-100	54	35	19	9	7	0	100 (79-100)	56 (31-79)	73 (52-88)	100 (63-100)	2.3 (1.3-4.0)	0.00 (0.00-n/an)	80 (67-93)
C: CS 100-400	70	76	52	13	10	1	98 (89-100)	57 (35-76)	84 (72-92)	93 (64-100)	2.3 (1.4-3.6)	0.03 (0.00-0.25)	86 (78-93)
D: CS >400	84	77	65	2	10	0	100 (93-100)	17 (3-49)	86 (76-93)	100 (20-100)	1.2 (0.9-1.5)	0.00 (0.00-n/an)	97 (80-95)
A vs D							NS	P = 0.023	NS	NS	P < 0.0001	n/an	NS

Table 3b. Diagnostic performance in patients with unstable angina

	Prevalence of disease (%)	N	TP	TN	FP	FN	Sensitivity (%)	Specificity (%)	PPV (%)	NPV (%)	LR+	LR-	Diagnostic accuracy (%)
Unstable Angina	79	127	99	17	10	1	99 (94-100)	63 (42-80)	91 (83-95)	94 (71-100)	2.7 (1.6-4.4)	0.02 (0.00-0.12)	91 (86-96)
A: CS <10	42	19	8	10	1	0	100 (60-100)	91 (57-100)	89 (51-100)	100 (66-100)	11.0 (1.7-71.3)	0.00 (0.00-n/an)	95 (85-100)
B: CS 10-100	79	28	22	4	2	0	100 (82-100)	67 (24-94)	92 (72-99)	100 (40-100)	3.0 (1.0-9.3)	0.00 (0.00-n/an)	93 (83-100)
C: CS 100-400	83	42	34	2	5	1	97 (93-100)	29 (5-70)	87 (72-95)	67 (13-98)	1.4 (0.9-2.2)	0.10 (0.01-1.39)	86 (75-96)
D: CS >400	92	37	34	1	2	0	100 (87-100)	33 (2-87)	94 (80-99)	100 (5-100)	1.5 (0.7-3.3)	0.00 (0.00-n/an)	95 (87-100)
A vs D							NS	NS	NS	NS	P < 0.0001	n/an	NS

Diagnostic performance of CTCA in all patients with stable angina combined, and in subgroups per Agatston CS. Specificity and positive likelihood ratio decreased with increasing CS (p-value for the comparison by Chi-squared test across groups A and D). Abbreviations as for table 2.

Diagnostic performance of CTCA in various CS categories

With increasing CS the prevalence of significant CAD increased steeply, and the specificity and LR+ of CTCA diminished significantly (table 2). Whereas for patients with a CS <10 the prevalence of significant CAD was 24%, in those with a CS >400 it was 87%. In patients with a CS <10 specificity and positive likelihood ratio were 89% (95%CI 76-96%) and 9.4 (95%CI 4.1-22), respectively, and the corresponding values were 20% (95%CI 5-49%) and 1.3 (95%CI 1.0-1.6) for patients with a CS >400. Only 3 of 15 patients with a CS >400 and no significant CAD on CCA were evaluated as negative by CTCA. As shown in table 3, the diagnostic impact of CS on the diagnostic performance of CTCA is similar for patients with stable and unstable anginal syndromes. In patients with stable angina the specificity decreased significantly from 89% (95%CI 73-96%) in those with a CS <10 to 17% (95%CI 3-49%) in those with a CS >400, and the LR+ decreased from 9 (95%CI 3.6-22.7) in those with a CS <10 to 1.2 (95%CI 0.9-1.5) in those with a CS >400. In patients with unstable angina the specificity decreased from 91% (95%CI 57-100%) in those with a CS <10 to 33% (95%CI 2-87%) in those with a CS >400, and the LR+ decreased significantly from 11.0 (95%CI 1.7-71.3) in those with a CS <10 to 1.5 (95%CI 0.7-3.3) in those with a CS >400.

DISCUSSION

In this study we set out to determine which combination of CS and CTCA would yield the best diagnostic performance for the detection of significant CAD with a minimum of health risk in stable and unstable angina patients referred for CCA. Our main findings are two-fold. Firstly, we report that in our population a negative CTCA reliably ruled out significant CAD, whereas a low CS did not. Secondly, we found that in patients with stable and unstable angina referred for CCA the prevalence of significant CAD increased with increasing CS, while the specificity and LR+ of CTCA decreased sharply.

Most studies, mostly performed in asymptomatic patients, have reported that in the absence of coronary calcium the likelihood of significant coronary artery disease is very small [4-6]. However, in a recent study in patients with acute and non-acute chest pain syndromes and a CS of 0 or <10 7% and 9%, respectively, had significant CAD [7]. Also, the absence of coronary calcification did not rule out myocardial ischemia on PET in patients clinically referred for PET [8]. The latter study did not provide CTCA or CCA data. In our population of symptomatic patients with stable and unstable angina the prevalence of significant CAD on CCA was high. Thus, the prevalence of 16% and 24% significant CAD on CCA in stable and unstable angina patients with a CS of 0 and with a CS <10, respectively, is in line with these previous studies. In the 62 patients in our study with a CS <10 CTCA correctly detected all 15 patients with significant CAD on CCA. These patients would have been overlooked if only the CS would have been considered. While CS can

be used to estimate the chance that significant CAD is present in a patient, CS cannot visualize the stenosis itself, especially if a non-calcified stenosis is present. Therefore, we recommend to combine CS with CTCA in stable and unstable angina patients with a CS <400.

In contrast, in patients with a CS >400 CTCA was of limited additional value to CS in our study as demonstrated by a specificity of only 20% (95%CI 5–49%) and a LR+ of only 1.3 (95%CI 1.0–1.6). Ninety-nine of 114 (87%) patients with a CS >400 had significant CAD on CTCA. Of the remaining 15 patients, i.e. those with a CS >400 and no significant CAD on CCA, only 3 were evaluated as negative by CTCA. Two factors may account for the latter findings. The 87% prevalence of significant CAD in patients with a CS >400 is probably the most important factor. In addition, calcium related blooming artifacts due to the limited spatial resolution of CTCA may have caused overestimation of lesion size, and thus false positive results [10]. These findings are well in line with a previous study in which CTCA was of limited additional value in symptomatic patients with a high prevalence of significant CAD [15]

Previous studies on the impact of CS on the diagnostic impact of CTCA are contradictory. While two previous studies found that coronary calcification was one of the main factors leading to false positive results [9;10], Pundziute et al. reported no significant impact of a CS greater than 400 on the diagnostic performance of CTCA in 110 patients clinically referred for CCA [12]. Also, Cademartiri et al. divided 120 patients clinically referred for CCA in groups with a CS below and above the median Agatston CS of 55 [11]. He reported that the diagnostic performance of CTCA was affected only to a small extent by the CS. The prevalence of significant CAD and the CS of our population are similar to the previous studies mentioned, yet our study has included substantially more subjects.

Interestingly, in a recent study in 664 asymptomatic individuals the prevalence of at least one significant stenosis on CTCA increased from 7.9% for patients with a CS between 1 and 100 to 14.5% for patients with a CS between 400 and 1000 [16]. Unfortunately, no CCA data were available for this study. Thus, due to the absence of a standard of reference the diagnostic performance of CTCA for the detection of significant CAD could not be determined. The prevalence of significant CAD in the highest CS categories was significantly lower than in our study. This could be explained by the fact that the former study included asymptomatic subjects whereas we studied symptomatic angina patients.

CTCA is associated with the use of iodine contrast medium, whereas CS is not. In addition, for CTCA a substantially higher radiation dose is required than for CS [3].

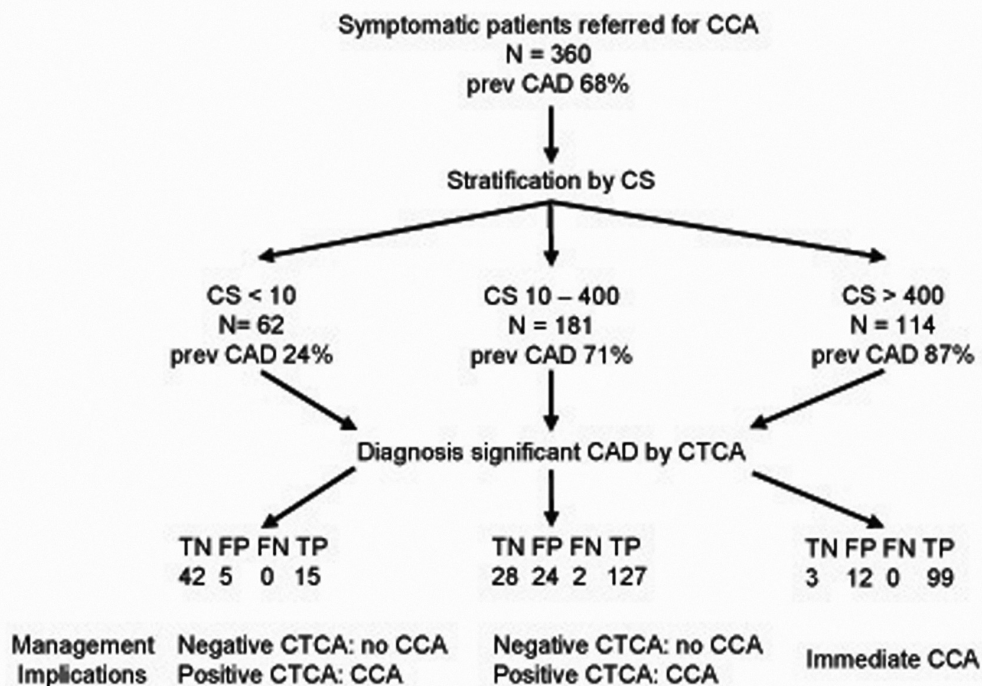


Figure 1. With CS the studied patients, who had a 68% prevalence of significant CAD, could be stratified into groups with a low, intermediate and high prevalence of significant CAD as indicated by the prevalence (prev) of significant CAD on CCA. CTCA reliably ruled out CAD in patients with CS <10 and with a CS between 10 and 400. In patients with a CS >400 CTCA was of limited additional value. Therefore we suggest to combine CS with CTCA in patients with a CS <400. If CTCA is negative, CCA is not indicated in these patients. If CTCA is positive, CCA should be performed. Patients with a CS >400 should be referred for immediate CCA.

Based on our findings we propose the following algorithm (Figure 1). In stable and unstable angina patients with a CS <400, a CS scan should be followed by CTCA. If this CTCA is negative, CCA is not indicated. If this CTCA is positive, CCA should be performed. However, given the reported limited additional value of CTCA for the detection of significant CAD in stable and unstable patients with a CS >400 we suggest not to perform a CTCA in patients with a CS >400, but to refer them to CCA directly. Such an algorithm would provide optimal diagnostic performance, as only 2 patients with significant CAD would have been overlooked by CTCA. Only 246 of 360 (68%) patients would have undergone both CS and CTCA. Furthermore, if CTCA would only have been performed in subjects with a CS <400, 72 of 243 (30%) subjects would not have undergone CCA. This algorithm could easily be implemented in routine clinical practice, since it takes a minimal amount of time to calculate the CS. Automated methods to calculate the CS may prove helpful [17].

Importantly however, CCA merely provides information on vessel lumen while CTCA also gives information on stenosis location and size, plaque burden, and plaque composition [18]. Future

research is needed to determine the clinical value of this information, and specifically so in stable and unstable patients with a high CS in whom CTCA seems to have limited additional value if only the detection of significant CAD is taken into consideration.

When compared to previous studies, the present study has included a larger number of subjects in a multicenter multivendor setting, allowing for a more reliable subgroup analysis. However, we acknowledge limitations of our study. Most importantly, in line with most previous studies, our subjects were derived from a selected population of symptomatic patients who were referred for CCA for clinical reasons. Thus our findings only apply to stable and unstable angina patients. Future studies will need to address the additive value of CTCA in asymptomatic patients with a high CS. Secondly, in the present study 64-slice CTCA scanners were used. Future research will need to determine whether improvements in spatial and temporal resolution with new generation scanners such as Dual Source or 256-slice scanners may improve the diagnostic performance of CTCA in patients with a high CS. Thirdly, we only studied patients between 50 and 70 years of age. The median CS for patients under 50 years of age is likely to be lower, and that of patients over 70 years of age is likely to be higher than the median CS of our population [19;20]. As the association between CS and significant CAD varies with age [19;20], our findings may not fully apply to subjects outside this age range. Fourthly, in line with previous studies, we excluded patients who were not in stable sinus rhythm, or did have renal insufficiency. In addition, a limited number of patients was not included for logistic reasons. Finally, the present study only focused on anatomical data. Additional research should focus on the value of the combination of CS, CTCA and functional tests such as PET and Single Photon Emission Computed Tomography (SPECT) in the diagnostic work-up of angina patients referred for CCA.

CONCLUSION

In conclusion, we suggest that in angina patients clinically referred for CCA with a CS <400, the CS scan is combined with CTCA. However, we recommend that these patients are referred for CCA directly in case of a CS >400.

REFERENCES:

1. Meijs MF, Meijboom WB, Cramer MJ et al (2007): Computed tomography of the coronary arteries: An alternative? *Scand Cardiovasc J* 41:277-286.
2. Greenland P, Bonow RO, Brundage BH et al (2007): ACCF/AHA 2007 clinical expert consensus document on coronary artery calcium scoring by computed tomography in global cardiovascular risk assessment and in evaluation of patients with chest pain: a report of the American College of Cardiology Foundation Clinical Expert Consensus Task Force (ACCF/AHA Writing Committee to Update the 2000 Expert Consensus Document on Electron Beam Computed Tomography). *Circulation* 115:402-426.
3. Hunold P, Vogt FM, Schmermund A et al (2003): Radiation exposure during cardiac CT: effective doses at multi-detector row CT and electron-beam CT. *Radiology* 226:145-152.
4. Budoff MJ, Diamond GA, Raggi P et al (2002): Continuous probabilistic prediction of angiographically significant coronary artery disease using electron beam tomography. *Circulation* 105:1791-1796.
5. Schmermund A, Baumgart D, Gorge G et al (1998): Measuring the effect of risk factors on coronary atherosclerosis: coronary calcium score versus angiographic disease severity. *J Am Coll Cardiol* 31:1267-1273.
6. Georgiou D, Budoff MJ, Kaufer E, Kennedy JM, Lu B, Brundage BH (2001): Screening patients with chest pain in the emergency department using electron beam tomography: a follow-up study. *J Am Coll Cardiol* 38:105-110.
7. Rubinshtein R, Gaspar T, Halon DA, Goldstein J, Peled N, Lewis BS (2007): Prevalence and extent of obstructive coronary artery disease in patients with zero or low calcium score undergoing 64-slice cardiac multidetector computed tomography for evaluation of a chest pain syndrome. *Am J Cardiol* 99:472-475.
8. Schenker MP, Dorbala S, Hong EC et al (2008): Interrelation of coronary calcification, myocardial ischemia, and outcomes in patients with intermediate likelihood of coronary artery disease: a combined positron emission tomography/computed tomography study. *Circulation* 117:1693-1700.
9. Kuettner A, Burgstahler C, Beck T et al (2005): Coronary vessel visualization using true 16-row multi-slice computed tomography technology. *Int J Cardiovasc Imaging* 21:331-337.
10. Hoffmann U, Moselewski F, Cury RC et al (2004): Predictive value of 16-slice multidetector spiral computed tomography to detect significant obstructive coronary artery disease in patients at high risk for coronary artery disease: patient-versus segment-based analysis. *Circulation* 110:2638-2643.
11. Cademartiri F, Mollet NR, Lemos PA et al (2005): Impact of coronary calcium score on diagnostic accuracy for the detection of significant coronary stenosis with multislice computed tomography angiography. *Am J Cardiol* 95:1225-1227.

12. Pundziute G, Schuijf JD, Jukema JW et al (2007): Impact of coronary calcium score on diagnostic accuracy of multislice computed tomography coronary angiography for detection of coronary artery disease. *J Nucl Cardiol* 14:36-43.
13. Agatston AS, Janowitz WR, Hildner FJ, Zusmer NR, Viamonte M, Jr., Detrano R (1990): Quantification of coronary artery calcium using ultrafast computed tomography. *J Am Coll Cardiol* 15:827-832.
14. Rumberger JA, Brundage BH, Rader DJ, Kondos G (1999): Electron beam computed tomographic coronary calcium scanning: a review and guidelines for use in asymptomatic persons. *Mayo Clin Proc* 74:243-252.
15. Meijboom WB, van Mieghem CA, Mollet NR et al (2007): 64-slice computed tomography coronary angiography in patients with high, intermediate, or low pretest probability of significant coronary artery disease. *J Am Coll Cardiol* 50:1469-1475.
16. Ho JS, Fitzgerald SJ, Stolfus LL et al (2008): Relation of a coronary artery calcium score higher than 400 to coronary stenoses detected using multidetector computed tomography and to traditional cardiovascular risk factors. *Am J Cardiol* 101:1444-1447.
17. Isgum I, Rutten A, Prokop M, van Ginneken B (2007): Detection of coronary calcifications from computed tomography scans for automated risk assessment of coronary artery disease. *Med Phys* 34:1450-1461.
18. Leber AW, Becker A, Knez A et al (2006): Accuracy of 64-slice computed tomography to classify and quantify plaque volumes in the proximal coronary system: a comparative study using intravascular ultrasound. *J Am Coll Cardiol* 47:672-677.
19. Bellasi A, Lacey C, Taylor AJ et al (2007): Comparison of prognostic usefulness of coronary artery calcium in men versus women (results from a meta- and pooled analysis estimating all-cause mortality and coronary heart disease death or myocardial infarction). *Am J Cardiol* 100:409-414.
20. Hoff JA, Chomka EV, Krainik AJ, Daviglius M, Rich S, Kondos GT (2001): Age and gender distributions of coronary artery calcium detected by electron beam tomography in 35,246 adults. *Am J Cardiol* 87:1335-1339.

11

MSCT lesion calcium score to predict stenosis severity of calcified lesions.

Submitted

*Pugliese F, Humink MGM,
Meijboom WB, Gruszczynska
K, Rengo M, Mollet NR,
Weustink AC, Neeffes L,
Dijkshoorn ML, Krestin GP,
de Feyter PJ.*

*Department of Radiology
Department of Cardiology
Erasmus MC, Rotterdam, the
Netherlands*

SUMMARY

Purpose

To develop an algorithm for predicting $\geq 50\%$ coronary stenoses based on segmental multislice computed tomography calcium score (MSCT CS) and clinical factors.

Materials and Methods

402 patients underwent MSCT CS and conventional coronary angiography. CS and calcification morphology were assessed in individual coronary segments. In a derivation dataset, we explored the predictive value of segmental CS, morphology, patient's symptoms and risk factors.

Results

Spotty calcifications had an OR for stenosis 2.3-fold ($p < 0.001$) greater than the absence of calcifications, wide calcifications 2.7-fold ($p < 0.001$) greater, diffuse calcifications 4.6-fold ($p < 0.001$) greater. In middle segments, each unit of CS had an OR 1.2-fold ($p < 0.001$) greater than in distal segments; in proximal segments the OR was 1.1-fold greater ($p = 0.021$). The OR was 1.8-fold greater ($p = 0.006$) in patients with typical chest pain, 2-fold ($p = 0.014$) greater in patients with acute coronary syndromes, 2-fold greater ($p < 0.001$) in patients with prior myocardial infarction. The ROC curve area of the prediction rule was 0.795 (0.95 confidence interval: 0.602-0.843). Validation in a validation dataset yielded similar results.

Conclusion

In conjunction with calcification morphology, anatomical location, patient's symptoms and risk factors, MSCT segmental CS can predict coronary stenosis.

INTRODUCTION

The quantification of the total amount of coronary calcification (calcium score) by electron beam tomography (EBT) or multislice computed tomography (MSCT) is useful for predicting the presence of angiographically significant ($\geq 50\%$ diameter reduction) coronary artery stenoses at the patient level (1-4). A calcium score ≥ 200 provides strong evidence of obstructive coronary artery disease in patients ≥ 50 years old, and a calcium score of 0 provides strong evidence about the absence of obstructive coronary artery disease (3). However, intermediate calcium scores are less useful in clinical practice. Moreover, the total calcium score does not provide information regarding the probability of stenosis at the level of a specific coronary segment or lesion. In these cases, contrast-enhanced MSCT coronary angiography (MSCT-CA) may be a beneficial next step. Unfortunately, coronary calcifications hinder the visualization of the coronary lumen at MSCT-CA ("blooming effect"), thus the evaluation of stenosis severity in calcified vessels is often impossible using MSCT-CA.

The purpose of this study was to assess the relationship between coronary calcification and the degree of luminal narrowing at the same site. We constructed an algorithm to facilitate the prediction of angiographically significant stenosis in symptomatic patients undergoing MSCT calcium score. The algorithm consists of a multivariable prediction rule which includes the MSCT calcium score measured in a given coronary segment, the patient's symptoms and risk factors in order to calculate the probability of significant coronary artery stenosis in the same coronary segment.

MATERIAL AND METHODS

Patients

During a 24-month period, 402 patients with stable or acute chest pain were recruited to an ongoing study at our institution comparing 64-MSCT-CA with conventional coronary angiography (CCA). Patients in sinus heart rhythm, able to hold their breath for 15 seconds, and without previous percutaneous coronary intervention or coronary bypass surgery were included. Impaired renal function (serum creatinine $> 120 \mu\text{mol/L}$) and known intolerance to iodinated contrast were exclusion criteria. The study protocol was approved by the Institutional Review Board and was in accordance with the declaration of Helsinki. Particular attention was paid to the additional radiation dose. All patients consented to undergo MSCT before CCA after being informed of the additional radiation dose. They also consented on the use of their data for future retrospective research.

Preparation and coronary artery calcium scans

Patients with heart rates >65 beats per minute (bpm) received 100 mg metoprolol (Seloken, Astra Zeneca, London, United Kingdom) orally 1 hour before the scan. Scans were performed with a 64-slice CT scanner with a gantry rotation time of 330 ms, a temporal resolution of 165 ms and a minimal spatial resolution of 0.4 mm³ (Sensation 64; Siemens, Forchheim, Erlangen, Germany). The non-enhanced coronary calcium scans were acquired with a standard spiral low-dose protocol using ECG-gating. Scan parameters were as follows: 32*2 slices per rotation; individual detector width of 0.6 mm, 330 ms rotation time, 3.8 mm/rotation table feed, 120 kV tube voltage, 150 mAs tube current, with activated prospective x-ray tube modulation. Overlapping slices were reconstructed at 65% of the R-R interval (retrospective ECG-gating) using B35f convolution kernel. Reconstructed slice thickness was 3.0 mm with an increment of 1.5 mm. The radiation exposure, estimated using dedicated software (ImPACT, version 0.99x, St. George's Hospital, Tooting, London, United Kingdom), was 1.4 mSv in men and 1.8 mSv in women.

MSCT-CA scans

For the MSCT-CA studies, 95 ml of contrast agent (iomeprol; Iomeron, 400 mg/ml; Bracco, Milan, Italy) were injected intravenously into an antecubital vein. The injection rate was 5 ml/s. A bolus-tracking technique was used to monitor the arrival of contrast in the coronary arteries (5, 6). Scan parameters were identical to those used for coronary calcium scanning except for a tube current of 900 mAs. Datasets were reconstructed using retrospective ECG gating and a mono-segmental reconstruction algorithm, as previously described (5, 6).

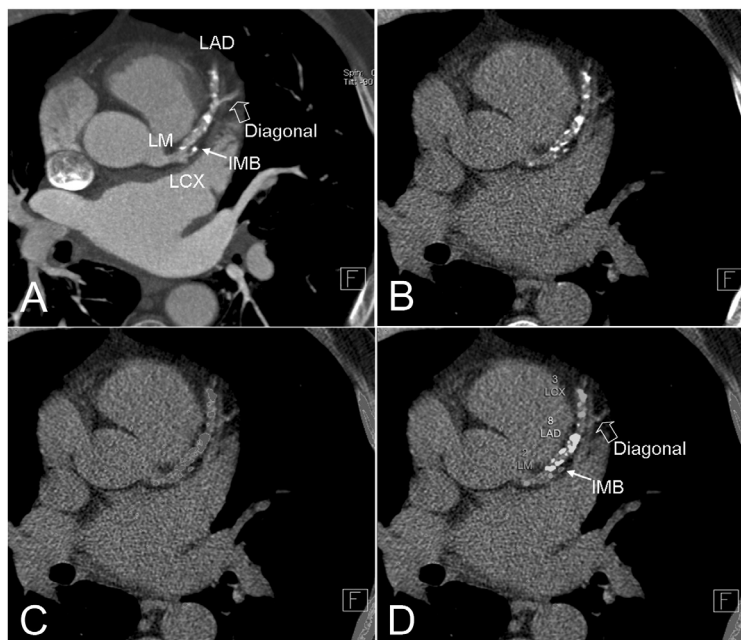


Figure 1. Measurement of calcium score at the segment level To classify coronary segments consistently, contrast-enhanced MSCT-CA axial images (A) were available to the observer. Side branches, especially if non-calcified, could have been difficult to detect on non-enhanced images (B, C). Because the quantification software did not allow labelling of the 17 coronary segments individually, the 4 available labels (named as the 4 major coronary vessels) were used interchangeably and applied to coronary segments (D). LM = left main artery; LAD = left anterior descending artery; LCx = left circumflex; IMB = intermediate branch. (A full color version of this illustration can be found in the color section).

Conventional coronary angiography (CCA)

MSCT and CCA were carried out within a time interval of 1 week. A single observer (>10-year experience) identified coronary segments on CCA following a 17-segment modified American Heart Association (AHA) classification model (7). Stenoses were classified as significant if the mean luminal narrowing was $\geq 50\%$ using validated quantitative coronary angiography (QCA) software (CAAS II[®], Pie Medical, Maastricht, the Netherlands).

Segmental calcium score (CS) and morphology

MSCT datasets were analyzed using an off-line workstation (syngo MultiModality Workplace VE25A, Siemens, Erlangen, Germany). Dedicated software (syngo Calcium Scoring VE31H, Siemens, Germany) was used for measuring calcium score (CS) in non-enhanced scans (8). One experienced observer, unaware of the CCA results, measured CS in individual coronary segments using a standard technique based on seed points and a region growing algorithm. Results were expressed using the Agatston (9), volume (10) and mass (11) scores.

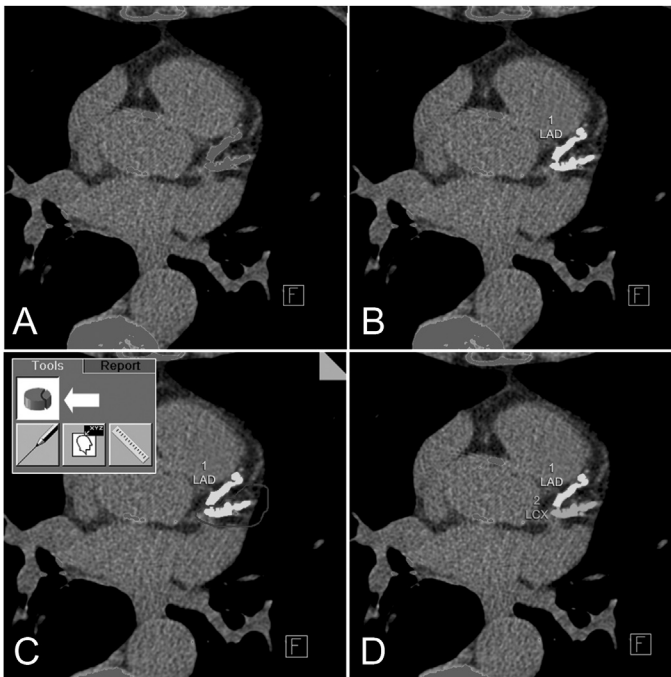


Figure 2. Method for separation of connected calcifications in a slice To assign calcifications to the corresponding individual coronary artery segment, there needed to be separation of connected lesions in a slice (A, B). To achieve this, calcifications were edited manually (C) and split (D) using the '3D Edit' function (C, insert and arrow) of the software (syngo Calcium Scoring). LAD = left anterior descending artery; LCx = left circumflex. (A full color version of this illustration can be found in the color section).

In order to obtain a consistent classification of the coronary tree into segments, contrast-enhanced MSCT-CA axial images were available to the observer (Figure 1). The MSCT-CA images were scrolled using a viewing application (syngo Viewing, Siemens, Erlangen, Germany).

Availability of MSCT-CA ensured the visualization of the origin of smaller side branches, especially when they were not calcified. These side branches might have remained undetected on the non-enhanced images. The visualization of the diagonal branches allowed the classification into segments of the left anterior descending coronary artery (LAD); the origin of marginal obtuse branches allowed the classification into segments of the left circumflex artery (LCx), and the ori-

gin of acute marginal branches allowed the classification into segments of the right coronary artery (RCA). MSCT-CA was used only for anatomical classification and not for CS measurement. CS was measured on non-enhanced images in accordance to clinical practice (8). To assign calcifications to the corresponding coronary segment, there needed to be separation of connected lesions in a slice (12). To achieve this, calcifications were edited manually slice-by-slice and split using the '3D Edit' function of the software (Figure 2).

In each segment, calcification morphology was classified as spotty, wide or diffuse (Figure 3) based on the width and length of the calcification in relation to the coronary segment diameter, following the classification model described in Table 1 (12). In the event of multiple calcifications with different morphology within the same segment, the segment was classified as the calcification with the largest size.

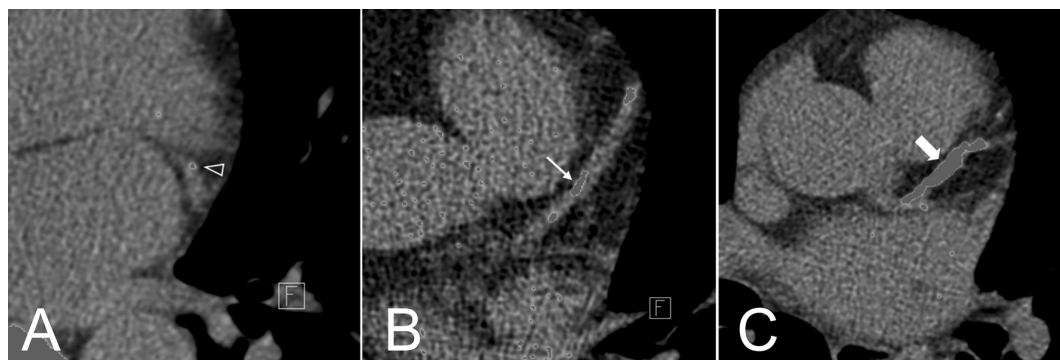


Figure 3. Calcification morphology

Calcification morphology was classified as spotty (A, arrowhead), wide (B, arrow) and diffuse (C, gross arrow) based on the width and length of the calcification in relation to the coronary segment diameter. (A full color version of this illustration can be found in the color section).

Statistical analysis

Statistical analysis was performed using commercially available software (SPSS, version 12.1. SPSS Inc., Chicago, IL., and STATA/SE 10.0, College Station, TX). Quantitative variables were expressed as means (standard deviations) and categorical variables were expressed as frequencies or percentages. The level of significance was chosen at a p-value <0.05.

The dataset was split into two equal datasets. Data from the first 201 patients were used to identify highly correlated variables, to explore the predictive value of the variables and to derive a multi-variable prediction rule. There was a high correlation between the Agatston and the volume score (Pearson $r = 0.990$; $p < 0.001$), the Agatston and the mass score ($r = 0.995$; $p < 0.001$) and the volume and the mass score ($r = 0.989$; $p < 0.001$). We used the Agatston score for further analyses because it has been extensively validated in clinical practice (1-4, 9). Using the derivation dataset, we determined the frequency of significant stenoses at the segment level, according to ranges of

Table 1. Classification of calcification morphology on non-enhanced MSCT images - modified from (12)

Calcification morphology	Lesion width ^a	Lesion length ^b
Diffuse	≥2/3 of coronary diameter	≥3/2 of coronary diameter
Wide	≥2/3 of coronary diameter	<3/2 of coronary diameter
	or	
Spotty	<2/3 of coronary diameter	≥3/2 of coronary diameter
	<2/3 of coronary diameter	<3/2 of coronary diameter
None	Undetectable	Undetectable

a Extent of calcification perpendicular to the longitudinal direction of the vessel

b Extent of lesion in the longitudinal direction of the vessel

segmental CS and calcification morphology. The natural log transforms of (CS + 1) were used because CS showed a skewed distribution. Categorical variables were compared with the chi-squared statistic. We also obtained receiver-operating characteristic (ROC) curves with luminal narrowing ≥50% at CCA as the reference standard to define positive cases. The prediction rule was then validated in the second set of 201 patients. The outcome of interest was the prediction of angiographically verified significant (≥50% diameter reduction) stenoses at the segment level.

The data was clustered implying that potential correlation existed between the multiple (seventeen) segments analyzed per patient. To adjust for the clustered nature of the data, we used generalized estimating equations (binomial family, logit link function, exchangeable correlation matrix, and robust –sandwich– standard errors adjusted for clustering on patient identification). We performed univariable analyses to evaluate the significance of the Agatston CS in each segment, calcification morphology, segment location (proximal, middle, and distal/side branches, as previously described (13)), major coronary vessel (RCA, LAD, LCx, LM), age, gender, patient’s symptoms (typical chest pain/atypical chest pain/acute coronary syndrome) and risk factors (obesity, hypertension, smoking, diabetes mellitus, hypercholesterolemia, prior myocardial infarction, family history). Variables with a p-value <0.10 in the univariable analyses were entered in the multivariable model. Interaction terms were explored between morphology and CS, location and CS, location and morphology, vessel and CS, and vessel and morphology. The final multivariable model included all variables with a p-value <0.05 and variables with a p-value <0.10 that were considered to be important based on clinical judgment and internal consistency of the model. Odds ratios (OR) and robust 95% confidence intervals (CI) are reported.

A prediction score was calculated based on the coefficients of the final multivariable model, and was subsequently validated in the second dataset. For both the derivation and validation dataset we report the area under the curve (AUC) with its 95% confidence interval (CI) as summary measure of the performance. To adjust for the clustered nature of the data, the 95% CI of the AUC was obtained with 1000 bootstrap samples using patient identification as clustering variable.

RESULTS

Baseline characteristics and angiographic findings (Table 2)

In the derivation dataset, 126/201 (62.7%) patients had at least one $\geq 50\%$ stenosis (Table 2). The mean (standard deviation) calcium score was 450.37 (661.23). Thirty/201 (14.9%) patients did not show any detectable calcification. Of these, 4/30 (13.3%) had at least one significant stenosis. A total of 3001 coronary segments were visualized angiographically. Of these, 136/3001 (4.5%) were localized distally to occluded coronary segments and supplied by collateral pathways. These segments were excluded from the analysis. There remained 2865 coronary segments, of which 282/2865 (9.8%) harboured $\geq 50\%$ stenoses. Among the lesions associated with significant stenosis, 89/282 (31.6%) were in the RCA, 110/282 (39%) in the LAD, 79/282 (29%) in the LCx, and 4/282 (1.4%) in the LM ($p < 0.001$).

Table 2. Baseline characteristics

Characteristic	Development sample	Validation sample	p-value ^e
No. of patients	201	201	-
Age			
Mean age (sd) ^a (years)	59 (12)	60 (10)	0.52 ^f
Age range	21-87	35-80	-
Age groups: no. (%)	-	-	0.81
≤ 50	38/201 (19%)	33/201 (17%)	-
51-60	79/201 (39%)	80/201 (40%)	-
61-70	50/201 (25%)	57/201 (28%)	-
> 70	34/201 (17%)	31/201 (15%)	-
Men / Women: no. (%)	142 (71%) / 59 (29%)	137 (68%) / 64 (32%)	0.59
Patient clinical presentation: no. (%)			
Typical chest pain ^b	97/201 (48%)	57/201 (28%)	< 0.001
Atypical chest pain ^c	71/201 (35%)	76/201 (38%)	0.61
Acute coronary syndrome ^d	33/201 (17%)	68/201 (34%)	< 0.001
Cardiovascular risk factors: no. (%)			
Obesity (Body Mass Index ≥ 30 Kg/m ²)	48/201 (24%)	50/201 (25%)	0.84
Smoking	63/201 (31%)	66/201 (33%)	0.75
Hypertension	106/201 (53%)	110/201 (55%)	0.69
Dyslipidemia (serum cholesterol > 200 mg/dL or 5.18 mmol/L)	136/201 (68%)	100/201 (50%)	< 0.001
Diabetes mellitus (plasma glucose ≥ 126 mg/dL or 7.0 mmol/L)	25/201 (12%)	26/201 (13%)	0.88
Family history	90/201 (45%)	106/201 (53%)	0.11
Prior myocardial infarction	43/201 (21%)	21/201 (11%)	0.003

Medication before MSCT and heart rate

Beta-blockers: no. (%)	142/201 (71%)	135/201 (67%)	0.11
Mean heart rate during scan (sd) ^a (beats/min.)	58 (11)	60 (8)	0.77

Total calcium score (Agatston; patient level)

Range	0-3839	0-3394	-
Mean (sd) ^a	450.37 (661.23)	346.60 (492.02)	0.70 ^f
Median	198.10	214.70	-
Calcium score groups: no. (%)	-	-	0.79
0-10	50/201 (25%)	47/201 (23%)	-
11-100	32/201 (16%)	32/201 (16%)	-
101-400	59/201 (29%)	68/201 (34%)	-
>400	60/201 (30%)	54/201 (27%)	-

a standard deviation

b retrosternal pain occurring with exercise, relieved by rest and administration of nitrates

c any 2 or 1 features of typical chest pain

d unstable angina or non-ST elevation myocardial infarction

e Chi squared test unless otherwise specified

f Mann-Whitney U test

Segmental CS

In the derivation dataset, the range in segmental CS was 0-1370. The mean (standard deviation) was 29.80 (88.40). The median was 0. There were 1735/2865 (60.6%) segments which did not show any detectable calcification (segmental CS = 0). Of these, 68/1735 (3.9%) harboured a significant stenosis.

Calcification morphology

In the derivation dataset, there were 431/2865 (15%) spotty calcifications, 325/2865 (11.3%) wide calcifications, and 374/2875 (13.1%) diffuse calcifications.

Frequency of significant stenoses

The frequency of coronary stenosis increased proportionally with increasing CS (Figure 4, left column), and from spotty, to wide, to diffuse morphology (all p-values <0.01). The frequency of significant stenoses associated with CS and morphology in men and women according to age is given in Table 3.

The AUCs for the detection of $\geq 50\%$ coronary stenosis were 0.74 (CI: 0.71-0.77) for CS, and 0.74 (CI: 0.71-0.77) for calcification morphology (Figure 4, right column).

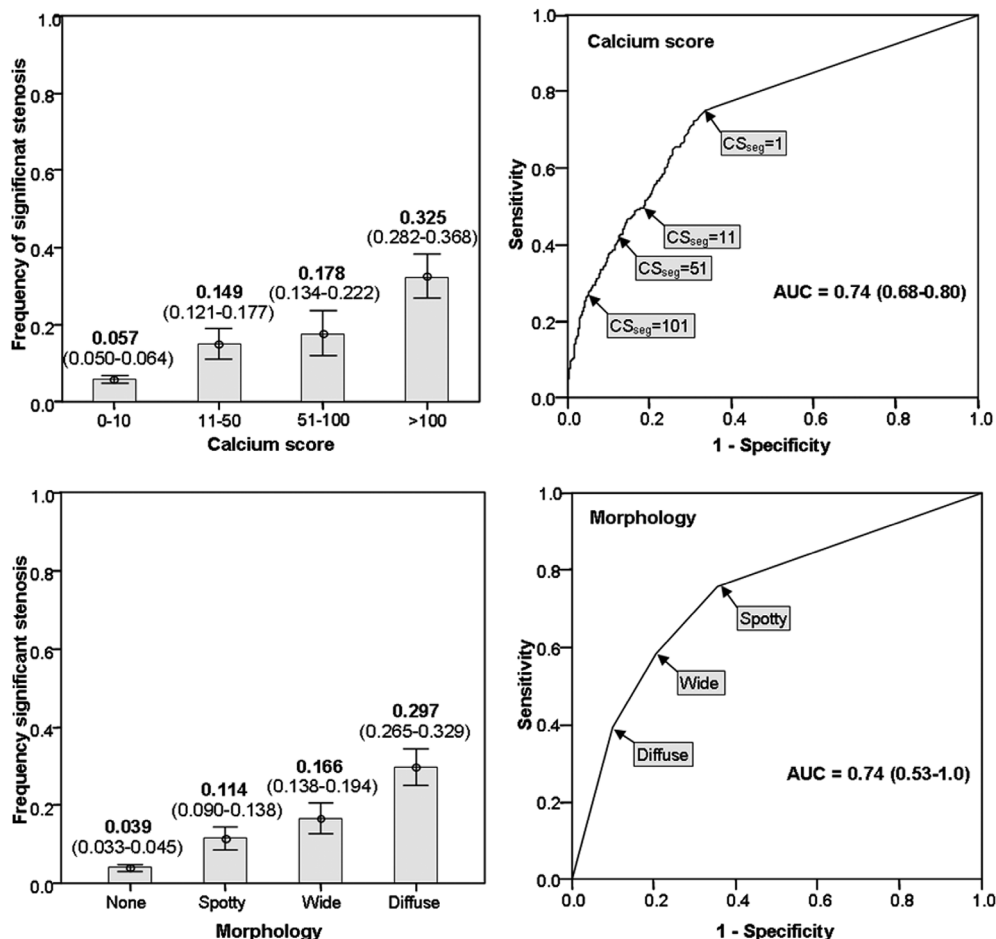


Figure 4. Segmental CS and morphology: frequency of associated significant stenoses (left column) and ROC curves (right column)
 The frequency of coronary stenosis (left column) increased proportionally with increasing CS. The frequency of stenosis also increased from spotty, to wide, to diffuse morphology. The diagnostic performances of CS and morphology in the detection of significant stenosis (right column) were similar (both AUC's = 0.74). Arrows and labels indicate different thresholds for significant coronary artery stenosis.

Univariable analysis (Table 4)

The odds ratio (OR) for significant stenosis was approximately 1.7-fold ($p = 0.005$) greater for patients with typical chest pain, and 1.6-fold ($p = 0.023$) greater for patients with unstable angina or non-ST elevation myocardial infarction (acute coronary syndrome). For patients with dyslipidemia, the OR was increased 2.6-fold ($p < 0.001$), and for patients with a prior myocardial infarction the OR was increased 2.5-fold ($p < 0.001$). With distal segments as comparator, the OR for significant stenosis was approximately 1.6-fold ($p < 0.001$) greater for middle segments, and 1.8-fold ($p = 0.001$) greater for proximal segments. With the RCA as comparator, the OR was approximately 0.7-fold ($p = 0.039$) smaller for the LCx, and 0.2-fold ($p < 0.001$) smaller for the LM; the OR for the LAD was similar. For each unit of natural log of segmental CS, the OR of

Table 3. Frequency of significant stenoses in relation to segmental CS ranges and morphology (in men and women according to age)

	CS				p-value*	Calcification morphology				p-value*
	0-10	11-50	51-100	>100		none	spotty	wide	diffuse	
Men										
≤50	16/384 (4.2%)	2/17 (11.8%)	0/2 (0%)	1/4 (25%)	0.114	11/328 (3.4%)	5/58 (8.6%)	1/13 (7.7%)	2/8 (25%)	0.012
51-60	43/623 (6.9%)	20/11 (18%)	12/63 (19%)	25/71 (35.2%)	<0.001	20/495 (4%)	20/140 (14.3%)	20/113 (17.7%)	40/120 (33.3%)	<0.001
61-70	13/260 (5%)	6/59 (10.2%)	9/35 (25.7%)	26/89 (29.2%)	<0.001	7/198 (3.5%)	5/63 (7.9%)	14/70 (20%)	28/112 (25%)	<0.001
>70	20/162 (12.3%)	8/39 (20.5%)	4/36 (11.1%)	15/49 (30.6%)	0.016	12/117 (10.3%)	7/48 (14.6%)	8/57 (14%)	20/64 (31.3%)	0.003
Women										
≤50	4/139 (2.9%)	0/6 (0%)	0/2 (0%)	value not observed	0.888	3/130 (2.3%)	1/13 (7.7%)	0/3 (0%)	0/1 (0%)	0.703
51-60	3/234 (1.3%)	0/10 (0%)	2/99 (22.2%)	3/4 (75%)	<0.001	3/211 (1.4%)	0/24 (0%)	2/11 (18.2%)	3/11 (27.3%)	<0.001
61-70	16/209 (7.7%)	7/39 (17.9%)	1/14 (7.1%)	5/14 (35.7%)	0.003	8/170 (4.7%)	6/48 (12.5%)	5/31 (16.1%)	10/27 (37%)	<0.001
>70	7/114 (6.1%)	4/35 (11.4%)	2/8 (25%)	8/24 (33.3%)	0.001	4/86 (4.7%)	5/37 (13.5%)	4/27 (14.8%)	8/31 (25.8%)	0.014

* Chi squared test. Significant p-values are **bolded**

Table 4. Univariable logistic regression models for the prediction of angiographically proven significant coronary stenosis

Characteristic	Odds Ratio (95% CI)	p-value*
Age	1.032 (1.015-1.0494)	<0.001
Gender (male)	1.629 (1.086-2.445)	0.018
Typical chest pain	1.694 (1.178-2.438)	0.005
Atypical chest pain	0.340 (0.214-0.538)	<0.001
Acute coronary syndrome	1.625 (1.068-2.472)	0.023
Obesity	0.986 (0.679-1.432)	0.941
Smoking	1.069 (0.755-1.513)	0.708
Hypertension	1.098 (0.763-1.579)	0.615
Dyslipidemia	2.606 (1.523-4.459)	<0.001
Diabetes	0.819 (0.513-1.307)	0.402
Family history of CAD	0.781 (0.550-1.108)	0.166
Prior myocardial infarction	2.537 (1.776-3.623)	<0.001
Segment location**		
Distal and side branches	odds ratio comparator	
Middle	2.545 (1.913-3.386)	<0.001
Proximal	1.777 (1.272-2.483)	0.001
Vessel		
RCA	odds ratio comparator	
LAD	0.995 (0.718-1.379)	0.976
LCx	0.722 (0.529-0.984)	0.039
LM	0.150 (0.054-0.416)	<0.001
CS (ln)	1.500 (1.399-1.604)	<0.001
Calcification morphology		
Spotty	2.732 (1.898-3.934)	<0.001
Wide	4.269 (2.836-6.427)	<0.001
Diffuse	9.144 (6.297-13.277)	<0.001

*Significant p-values are bolded

** Proximal segments included segments 1, 5, 6, and 11. Middle segments included segments 2, 3, 7, and 13. Distal and side branches included segments 4a, 4b, 8, 9, 10, 12, 14, 15, and 16 (7, 13).

significant stenosis was 1.5-fold ($p < 0.001$) greater. The presence of spotty calcifications had an OR for stenosis approximately 2.7-fold ($p < 0.001$) greater than the absence of calcification, wide calcifications approximately 4.3-fold ($p < 0.001$) greater, and diffuse calcifications approximately 9.1-fold ($p < 0.001$) greater than the absence of calcification.

Table 5. Multivariable logistic regression (final) model for the prediction of angiographically proven significant coronary stenosis

Model*	Odds Ratio (95% CI)	p-value**	Coefficient
Clinical presentation			
Typical chest pain	1.755 (1.175-2.622)	0.006	0.562
Acute coronary syndrome	1.989 (1.151-3.439)	0.014	0.688
Risk factors			
Prior myocardial infarction	1.982 (1.397-2.812)	<0.001	0.684
Vessel			
LM	0.169 (0.059-0.482)	0.001	-1.776
Calcification morphology			
Spotty	2.303 (1.567-3.384)	<0.001	0.834
Wide	2.690 (1.698-4.260)	<0.001	0.989
Diffuse	4.614 (2.842-7.491)	<0.001	1.529
CS (ln)			
If middle segment	1.189 (1.084-1.304)	<0.001	0.173
If proximal segment	1.125 (1.018-1.242)	0.021	0.117

*The model Wald chi-square was 226.32 ($p < 0.001$)

**Significant p-values are bolded

Multivariable analysis (Table 5)

In a multivariable model, the OR for coronary stenosis was approximately 1.8-fold greater ($p = 0.006$) in patients with typical chest pain, 2-fold ($p = 0.014$) greater in patients with acute coronary syndrome, and 2-fold greater ($p < 0.001$) in patients with prior myocardial infarction. The presence of spotty calcifications had an OR for stenosis approximately 2.3-fold ($p < 0.001$) greater than the absence of calcification, wide calcifications approximately 2.7-fold ($p < 0.001$) greater, and diffuse calcifications approximately 4.6-fold ($p < 0.001$) greater than the absence of calcification. With distal segments as comparator, each unit of natural log of CS in middle segments corresponded to an OR approximately 1.2-fold ($p < 0.001$) greater; in proximal segments this corresponded to an OR 1.1-fold greater ($p = 0.021$). The LM coronary artery had an OR for stenosis approximately 0.2-fold ($p = 0.001$) smaller than the RCA, whereas the remaining coronary vessels were similar.

Prediction score

Based on the coefficients (multiplied by 100) of the final multivariable model (Table 5), a score for the prediction of significant stenosis in a given segment (SCORE) was calculated as follows:

$$\text{SCORE} = 12 \cdot \ln(\text{CS}) \text{ (if proximal)} + 17 \cdot \ln(\text{CS}) \text{ (if middle)} + 83 \text{ (if spotty)} + 99 \text{ (if wide)} + 153 \text{ (if diffuse)} + 56 \text{ (if typical chest pain)} + 69 \text{ (if acute coronary syndrome)} + 68 \text{ (if prior myocardial infarction)} - 178 \text{ (if LM)} - 362$$

The probability of significant coronary stenosis increased with the extent (i.e., CS, morphology) of coronary calcification. This probability is related to the SCORE through the following equation:

$$\text{Probability (significant stenosis)} = 1 / [1 + \exp (- \text{SCORE})] \text{ (Figure 5)}$$

Derivation and validation datasets

Derivation and validation datasets revealed similar results. The AUC for the derivation set was 0.795 (CI: 0.602-0.843); the AUC for the validation set was 0.783 (CI: 0.598-0.827).

DISCUSSION

Calcification overrepresentation is a major limitation to MSCT-CA, which is mainly due to the limited spatial resolution. Calcification overrepresentation is generally referred to as ‘blooming effect’, and is frequently associated with beam hardening and partial volume artefacts. Calcification overrepresentation limits the visualization of adjacent structures and often yields overestimation of the severity of stenosis (false positive diagnoses). Sharp convolution kernels for image reconstruction partially compensate for the blooming effect, however this comes at the expense of increased image noise. Also several deconvolution filters have been developed with the goal of reducing the blooming effect without increasing image noise (14). These filters are based on iterative measurements, require long computational processing times and have not been validated in clinical practice. The introduction of dual source MSCT scanners and the ‘dual energy’ scan technique allow the acquisition of separate low- and high-energy images which are then synthesized in order to cancel high-density structures such as calcifications (15). However, the applicability of this technique to coronary imaging has not been evaluated yet. Therefore, MSCT-CA in calcified coronary arteries remains a diagnostic challenge. This study describes a practical approach to overcome such limitation of

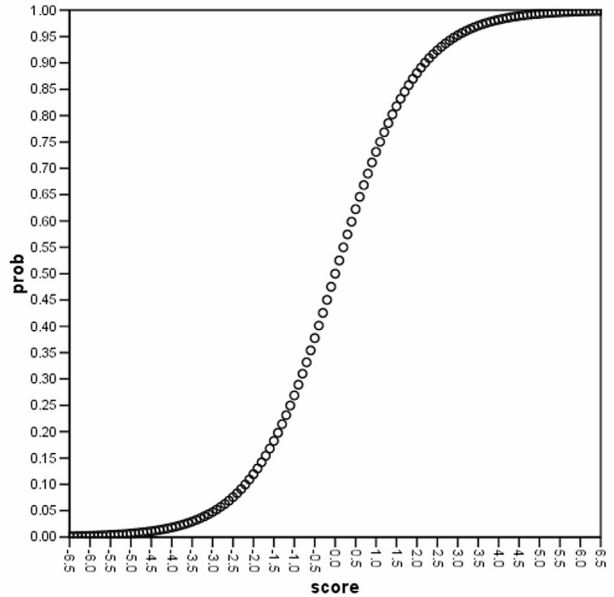


Figure 5. Continuous probabilistic prediction of significant coronary artery stenosis.

By entering the SCORE on the x axis, the associated probability of significant stenosis in the same coronary segment can be read on the y axis (see excel spreadsheet – supplemental file, Figure 6). SCORES < (-6.5) (not plotted) are associated with a negligible probability of significant stenosis; SCORES > 6.5 (not plotted) are associated with near certainty of significant stenosis.

MSCT-CA, facilitate diagnostic decision making and potentially reduce the number of false positive diagnoses.

We found that the probability of significant coronary stenosis associated to a given coronary calcification increased proportionally with the lesion CS, and from the spotty, to the wide, to the diffuse morphological patterns (Figure 4, left column). This is consistent with the findings of Lau et al. (16) and Kajinami et al.(12). However, our results revealed that for both CS and morphology the use of a high-specificity threshold was associated with a much lower sensitivity for the detection of significant coronary artery stenosis, and a high-sensitivity threshold was associated with a much lower specificity (Figure 4, right column). This implies that the amount and pattern of calcification of a given lesion, when considered per se, are probably rather crude parameters for the presence of an underlying significant stenosis. The most likely mechanism to explain this finding is the compensatory enlargement of atherosclerotic coronary arteries (positive remodeling) (17).

Nevertheless, by combining patient's symptoms, clinical history and lesion location within the coronary tree, the predictive value of CS and calcification morphology observed in a given segment could be improved. The CS is influenced by lesion location because the coronary artery diameter shows a wide variation depending on location. This also suggests the potential merit of morphologic evaluation additional to CS. Characteristics such as the type of chest pain and the history of prior myocardial infarction are important because the way we interpret MSCT-CA studies in daily practice is heavily influenced by the clinical context.

It can be argued that a diagnostic benefit from a complementary use of segmental CS to MSCT-CA cannot be expected in all lesions. Firstly, not all coronary lesions associated with significant stenosis are calcified. Secondly, there will be situations in which segmental CS will yield intermediate probability values. In a hypothetical patient with typical chest pain, prior myocardial infarction, a calcified lesion with diffuse pattern in the middle LAD, and a CS measured in that lesion of 148, the SCORE for the middle-LAD lesion will be:

$$\text{SCORE} = [17 \cdot \ln(148)] + 153 + 56 + 68 - 362 = 0.07 \approx 0$$

A SCORE ≈ 0 corresponds to a probability of significant stenosis of $\approx 50\%$ (Figure 5), which may not be very helpful for clinical decision making (presence and absence of significant stenosis are equally likely). However, because the SCORE proposed in this study was calculated as a function of the natural log transform of lesion CS (skewed distribution), the interval of CS associated to intermediate probabilities of coronary artery stenosis is quite narrow. Indeed, in the same patient, if the lesion had a CS of 158, the probability of significant stenosis would be $\approx 75\%$ (significant stenosis is likely present). If the same lesion had a CS of 118 the probability of stenosis would be

<5% (significant stenosis is unlikely present). These probabilities may be more helpful to support decision making.

Limitations of our study include the fact that the Agatston CS is not a physical measurement of calcification (9). However, as opposed to the other scores, the Agatston CS is commonly used in clinical practice. Moreover, we found a very high correlation between the Agatston and the volume/mass scores. Also, CS underestimates coronary plaque burden because it does not include non-calcified plaque. The measurement of coronary plaque burden by MSCT was beyond the purpose of our study. Although early studies (18, 19) have shown that measuring the plaque burden by MSCT is feasible, the robustness and the clinical implications of these methods are to be evaluated.

CONCLUSION

We developed a practical method which uses a major limitation to MSCT-CA (i.e., coronary calcification) to improve the ability of this technique to predict the presence of significant coronary stenosis and reduce the number of false positives. Further research is warranted to define in which patient population the analysis of segmental CS additional to MSCT-CA may be beneficial for improving the diagnostic performance.

REFERENCES

1. Budoff MJ, Diamond GA, Raggi P, Arad Y, Guerci AD, Callister TQ, Berman D. Continuous probabilistic prediction of angiographically significant coronary artery disease using electron beam tomography. *Circulation* 2002; 105(15):1791-1796.
2. Haberl R, Becker A, Leber A, Knez A, Becker C, Lang C, Bruning R, Reiser M, Steinbeck G. Correlation of coronary calcification and angiographically documented stenoses in patients with suspected coronary artery disease: results of 1,764 patients. *J Am Coll Cardiol* 2001; 37(2):451-457.
3. Bielak LF, Rumberger JA, Sheedy PF, 2nd, Schwartz RS, Peyser PA. Probabilistic model for prediction of angiographically defined obstructive coronary artery disease using electron beam computed tomography calcium score strata. *Circulation* 2000; 102(4):380-385.
4. Breen JF, Sheedy PF, 2nd, Schwartz RS, Stanson AW, Kaufmann RB, Moll PP, Rumberger JA. Coronary artery calcification detected with ultrafast CT as an indication of coronary artery disease. *Radiology* 1992; 185(2):435-439.

5. Meijboom WB, Weustink AC, Pugliese F, van Mieghem CA, Mollet NR, van Pelt N, Cademartiri F, Nieman K, Vourvouri E, Regar E, Krestin GP, de Feyter PJ. Comparison of diagnostic accuracy of 64-slice computed tomography coronary angiography in women versus men with angina pectoris. *Am J Cardiol* 2007; 100(10):1532-1537.
6. Mollet NR, Cademartiri F, van Mieghem CA, Runza G, McFadden EP, Baks T, Serruys PW, Krestin GP, de Feyter PJ. High-resolution spiral computed tomography coronary angiography in patients referred for diagnostic conventional coronary angiography. *Circulation* 2005; 112(15):2318-2323.
7. Austen WG, Edwards JE, Frye RL, Gensini GG, Gott VL, Griffith LS, McGoon DC, Murphy ML, Roe BB. A reporting system on patients evaluated for coronary artery disease. Report of the Ad Hoc Committee for Grading of Coronary Artery Disease, Council on Cardiovascular Surgery, American Heart Association. *Circulation* 1975; 51(4 Suppl):5-40.
8. Budoff MJ, Achenbach S, Blumenthal RS, Carr JJ, Goldin JG, Greenland P, Guerci AD, Lima JA, Rader DJ, Rubin GD, Shaw LJ, Wiegers SE. Assessment of coronary artery disease by cardiac computed tomography: a scientific statement from the American Heart Association Committee on Cardiovascular Imaging and Intervention, Council on Cardiovascular Radiology and Intervention, and Committee on Cardiac Imaging, Council on Clinical Cardiology. *Circulation* 2006; 114(16):1761-1791.
9. Agatston AS, Janowitz WR, Hildner FJ, Zusmer NR, Viamonte M, Jr., Detrano R. Quantification of coronary artery calcium using ultrafast computed tomography. *J Am Coll Cardiol* 1990; 15(4):827-832.
10. Callister TQ, Cooil B, Raya SP, Lippolis NJ, Russo DJ, Raggi P. Coronary artery disease: improved reproducibility of calcium scoring with an electron-beam CT volumetric method. *Radiology* 1998; 208(3):807-814.
11. McCollough CH, Ulzheimer S, Halliburton SS, Shanneik K, White RD, Kalender WA. Coronary artery calcium: a multi-institutional, multimanufacturer international standard for quantification at cardiac CT. *Radiology* 2007; 243(2):527-538.
12. Kajinami K, Seki H, Takekoshi N, Mabuchi H. Coronary calcification and coronary atherosclerosis: site by site comparative morphologic study of electron beam computed tomography and coronary angiography. *J Am Coll Cardiol* 1997; 29(7):1549-1556.
13. Pugliese F, Mollet NR, Hunink MG, Cademartiri F, Nieman K, van Domburg RT, Meijboom WB, Van Mieghem C, Weustink AC, Dijkshoorn ML, de Feyter PJ, Krestin GP. Diagnostic performance of coronary CT angiography by using different generations of multisection scanners: single-center experience. *Radiology* 2008; 246(2):384-393.
14. Rollano-Hijarrubia E, Niessen W, Weinans H, van der Lugt A, Stokking R. Histogram-based selective deblurring to improve computed tomography imaging of calcifications. *Invest Radiol* 2007; 42(1):8-22.

15. Johnson TR, Krauss B, Sedlmair M, Grasruck M, Bruder H, Morhard D, Fink C, Weckbach S, Lenhard M, Schmidt B, Flohr T, Reiser MF, Becker CR. Material differentiation by dual energy CT: initial experience. *Eur Radiol* 2007; 17(6):1510-1517.
16. Lau GT, Ridley LJ, Schieb MC, Brieger DB, Freedman SB, Wong LA, Lo SK, Kritharides L. Coronary artery stenoses: detection with calcium scoring, CT angiography, and both methods combined. *Radiology* 2005; 235(2):415-422.
17. Glagov S, Weisenberg E, Zarins CK, Stankunavicius R, Kolettis GJ. Compensatory enlargement of human atherosclerotic coronary arteries. *N Engl J Med* 1987; 316(22):1371-1375.
18. Leber AW, Becker A, Knez A, von Ziegler F, Sirol M, Nikolaou K, Ohnesorge B, Fayad ZA, Becker CR, Reiser M, Steinbeck G, Boekstegers P. Accuracy of 64-slice computed tomography to classify and quantify plaque volumes in the proximal coronary system: a comparative study using intravascular ultrasound. *J Am Coll Cardiol* 2006; 47(3):672-677.
19. Sun J, Zhang Z, Lu B, Yu W, Yang Y, Zhou Y, Wang Y, Fan Z. Identification and quantification of coronary atherosclerotic plaques: a comparison of 64-MDCT and intravascular ultrasound. *AJR Am J Roentgenol* 2008; 190(3):748-754.

12

Computed Tomography Coronary Angiography in Patients with Suspected Coronary Artery Disease: decision making from various perspectives in the face of uncertainty A cost-effectiveness analysis

Submitted

Tessa S.S. Genders^{2,7}, W. Bob Meijboom, MD^{1,2}, Matthijs F. L. Meijs, MD^{3,4}, Joanne D. Schuijf, PhD^{5,6}, Nico R. Mollet, MD, PhD^{1,2}, Annick C. Weustink, MD^{1,2}, Francesca Pugliese MD^{1,2}, Jeroen J. Bax, MD, PhD⁵, Maarten J. Cramer, MD, PhD³, Gabriel P. Krestin, MD, PhD², Pim J. de Feyter, MD, PhD^{1,2}, M.G. Myriam Hunink, MD, PhD^{2,7,8}

¹Department of Cardiology, Erasmus University Medical Center, Rotterdam, the Netherlands

²Department of Radiology, Erasmus University Medical Center, Rotterdam, the Netherlands

³Department of Cardiology, Utrecht University Medical Center, Utrecht, the Netherlands

⁴Department of Radiology, Utrecht University Medical Center, Utrecht, the Netherlands

⁵Department of Cardiology, Leiden University Medical Center, Leiden, the Netherlands

⁶Department of Radiology, Leiden University Medical Center, Leiden, the Netherlands

⁷Department of Epidemiology, Erasmus University Medical Center, Rotterdam, the Netherlands

⁸Department of Health Policy and Management, Harvard School of Public Health, Harvard University, Boston

ABSTRACT

Objectives:

Patients with stable chest pain suspected of having coronary artery disease (CAD) may be imaged with computed tomography coronary angiography (CTCA) to diagnose CAD, avoiding conventional coronary angiography (CCA). Our purpose was to determine the indication of CTCA as triage test prior to CCA.

Methods:

This study was approved by the Institutional review board. Using a Markov-model, we analyzed the decision from the perspective of the patient, physician, hospital, health-care system, and society using recommendations from the UK, US, and Netherlands (NL) for cost-effectiveness analyses. Outcome measures were revised post-test probability of CAD, life-years (LYs), quality-adjusted life-years (QALYs), costs, and incremental cost-effectiveness ratios (ICER). Extensive sensitivity analysis was performed.

Results:

For a prior probability below 40%, the post-negative-CTCA probability was <1%. CTCA maximizes LYs in 60-year-old men (and women) at a prior probability below 68% (71%) and maximizes QALYs at a prior probability below 39% (40%). CTCA minimizes health-care and direct non health-care costs (UK/US recommendations) below 92-96%, and all costs including production losses (NL recommendations) below 85-88%. Using a willingness-to-pay threshold of €50000/QALY, CTCA was cost-effective below a prior probability of 68-70%, which was the case in patients with atypical angina. Sensitivity analyses showed that results changed across the reported range of sensitivity of CTCA.

Conclusions:

The indication for CTCA as triage test prior to CCA depends on the optimization criterion, prior probability of CAD and sensitivity of CTCA. In patients with atypical angina, CTCA increases life expectancy but not QALY's, is cost-saving and is cost-effective.

INTRODUCTION

Patients with chest pain suspected of having coronary artery disease(CAD) usually undergo conventional coronary angiography(CCA) to diagnose CAD. These patients may be imaged non-invasively with computed tomography coronary angiography(CTCA) avoiding invasive CCA. Recent systematic reviews and meta-analyses have shown that CTCA is accurate in diagnosing CAD with a sensitivity analyzed at the patient level of 96%-99% and specificity of 74%-94%(1-3). Although CTCA is rapidly being introduced into clinical practice as a triage test prior to CCA, its effect on patient outcome and cost-effectiveness have not yet been determined.

Every year, approximately 4.5 per 1000 people visit a doctor with chest pain(4). Over 2 million CCA procedures are performed annually in Europe(5) and approximately 1.7 million in the USA(6). The use of CTCA as an initial triage test could save costs and minimize discomfort to patients. However, a trade-off must be made between the benefits and harms of CTCA.

Current guidelines recommend the use of CTCA in patients with a low to intermediate prior probability of CAD who are unable to exercise or have inconclusive functional test results(7). What constitutes a low to intermediate prior probability, however, remains to be elucidated. The purpose of this study was to determine the indication of CTCA as triage test prior to CCA in patients with suspected CAD.

MATERIALS AND METHODS

Study population

The study population were 233 stable patients presenting with chest pain suggestive of angina suspected of having CAD as observed in the prospective, multicenter, multi-vendor cohort study that evaluated 64-detector CTCA(8). In this study, all patients were referred for CCA based on a history or functional testing that suggested the presence of cardiac ischemia and all patients underwent CTCA prior to CCA. This study was approved by the institutional review board and all patients signed informed consent.

Decision model

We developed a decision model (in DATA Pro 2008 Suite, TreeAge Software Inc, Williamstown, MA, USA) to evaluate the use of CTCA as initial imaging test, if positive followed by CCA (new strategy) compared to direct CCA (current practice)(Figure 1). Short-term outcomes related to the diagnostic imaging tests were modeled with a decision tree and a Markov model was used to model long-term outcomes. The Markov model, with a cycle length of 1 year, modeled whether a

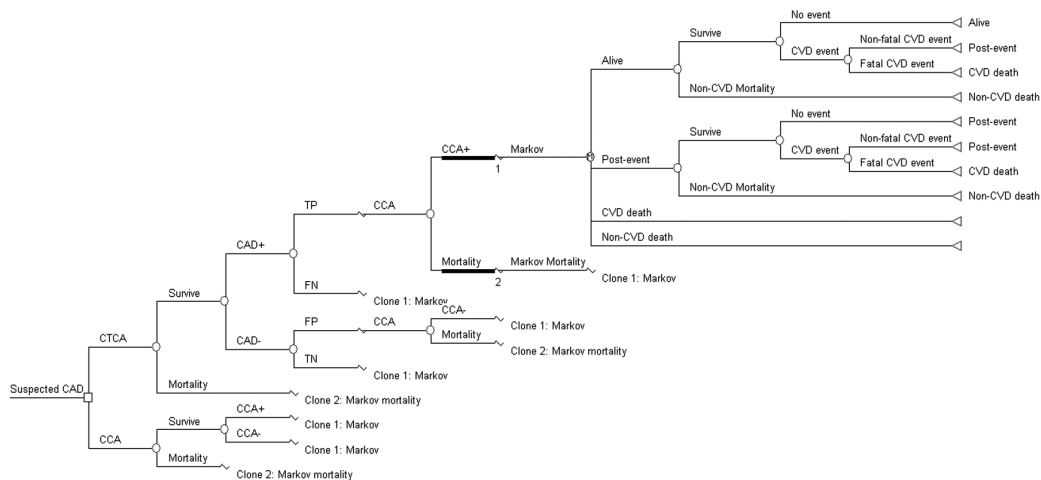


Figure 1. Schematic representation of the decision tree. The square indicates a decision node, circles indicate chance nodes, (M) indicates a Markov node. Following a positive CTCA result a CCA is performed. "Clone" indicates that the structure of the tree at that point is identical to another subtree, which is marked with a black line and a corresponding number. TP = True positive, FN = False Negative, FP = False positive, TN = True negative.

patient was alive or dead and whether a cardiovascular (CVD) event occurred. Quality of life was modeled depending on the chance of successful relief of angina through treatment. Costs were estimated for diagnostic tests, treatment (PCI, CABG, medication), and events during follow-up. The decision was analyzed from the perspective of the physician, patient, hospital, health-care system, and society using various optimization criteria(9) and taking into account the uncertainty involved.

Data sources and assumptions

The input data was based, where possible, on the cohort study. We searched the English language literature for data not available from the cohort study and for data to be used in sensitivity analyses (Table 1). All variables were entered in the model as distributions. To stay close to the cohort study data, sensitivity and specificity of CTCA were derived from the study (Table 1)(8) and were assumed to be independent of age, sex, risk factors, and presentation. Significant CAD was defined as $\geq 50\%$ lumen diameter reduction. The CTCA mortality rate was assumed to be equivalent to the mortality rate of using IV contrast materials(10). CCA was used as the reference test, assuming 100% sensitivity and specificity. Sex-specific probabilities of having CAD for 60-year old patients from the cohort study were used. Because age, sex and type of chest pain have been proven to be the major determinants of the prior probability of CAD(11), we used upper and lower limits from Diamond & Forrester for different types of chest pain (Table 1)(12). CVD event rates in patients without known CAD (patients with a true negative or false positive test result) were assumed to be equivalent to first CVD event rates in the general population and were therefore calculated with the Framingham-Heart-Score(13) and modeled specific for the average risk factor profiles

Table 1. Parameter estimates, their reported ranges and distributions, and data sources.

Parameter	Point estimate	95% CI / Range	Distribution	Source
Prevalence of CAD				
Overall				
Men	0.63			
Women	0.72	0.59 – 0.94	Triangular	(8),(12)
	0.43	0.32 – 0.91	Triangular	(8),(12)
CTCA				
Sensitivity	0.99	0.97 – 1.00	Beta	(8)
Specificity	0.63	0.53 – 0.73	Beta	(8)
Mortality	0.0000006	0 – 0.000016 149 – 248	(10)	
Costs in Euro's	198	Triangular 68 – 113	Cost-analysis	
Time cost for patients (min)	90	Triangular	Cost-analysis	
CCA				
Sensitivity	1	-	-	Assumption
Specificity	1	-	-	Assumption
Risk of MI	0.0005	0.0003 – 0.0007	Beta	(43)
Mortality	0.0011	0.0009 – 0.0014	Beta	(44)
Costs in Euro's	1360	1020 – 1700	Triangular	Cost-analysis
Time cost for patients (min)	362	272 – 453	Triangular	Cost-analysis
Event rates and hazard rate ratios				
Annual non-CVD mortality * †	-	-	-	Dutch Lifetables (23)
CVD event rate (no CAD)				
Men	0.024	0.014 – 0.077 0.008 – 0.053	Uniform	(13)
Women	0.014		Uniform	(13)
HRR CVD events,CAD vs. no CAD	1.50	1.32 – 1.70	Log-normal	(14)
HRR CVD events, Medication vs. no Medication	0.63	0.44 – 0.88	Log-normal	(15, 16)
HRR CVD events, prior MI vs. no prior MI	1.45	1.09 – 1.89	Log-normal	(14)
Proportion Fatal Event	0.17	0.10 – 0.25	Triangular	(19) (16)
Risk of cancer due to radiation exposure (1) (2)				
LAR in men	0.00067	0.00052–0.00081	Uniform	(21)
% fatal	0.65	-	-	(22)
LAR in women	0.0018	0.0014 – 0.0022	Uniform	(21)
% fatal	0.70	-	-	(22)
Quality of life weights				

no CAD	0.87	0.85 – 0.89	Beta	(25)
Treated CAD (TP) ‡	0.85	0.82 – 0.87	Beta	(25)
Untreated CAD (FN)	0.74	0.71 – 0.77	Beta	(25)
Disutility CVD event	0.04	0.02 – 0.07	Beta	(26)
Costs §				
Treatment †	7512	0 - 24866	Triangular	Standard Rates
Medication (per year)	364	99 - 738	Triangular	(28)
Myocardial infarction	13000	8000 - 18000 4 – 6	Uniform	Estimation
Travel cost (per visit)	5	13 – 22	Triangular	(35)
Time cost (per hour)	18	702 - 1085	Triangular	(35)
Reintervention	754		Triangular	(35)
Friction period (weeks)	22	-	-	(35)
Friction cost (per hour)				
Men	51	38-63	Triangular	(35)
Women	39	29-48	Triangular	(35)

CI = Confidence interval, CTCA = Computed tomography coronary angiography, CCA = Conventional coronary angiography, CAD = Coronary artery disease, CVD = Cardiovascular disease, RR = relative risk, HRR = Hazard rate ratio, MI = Myocardial infarction, LAR = Life-time attributable risk, TP = True positive, FN = False negative

* Age-specific

† Sex-specific

‡ Assuming 51% PCI, 25% CABG, 24% medication

§ All costs were converted to 2007 euro

|| Assuming 70% PCI, 30% CABG, average yearly costs

of such patients in the cohort study. CVD events included coronary death, myocardial infarction, coronary insufficiency, angina, stroke, cardiac arrest, peripheral arterial disease, and heart failure. We estimated that symptomatic patients diagnosed with CAD who are subsequently treated (true positives) will have a 1.5-fold (95%CI 1.3-1.7) CVD event rate compared to patients without symptomatic CAD based on a multivariable Cox model reported from the EUROPA study(14). Following a first CVD event, the CVD re-event rate will be 1.44 (95% CI 1.25 –1.66) times the risk compared to that in a patient with CAD and no previous CVD event(14). We assumed that the CVD event rate is reduced by treatment (HRR 0.63, range 0.44 – 0.88)(15, 16) modeled with a combined average effectiveness of CABG, PCI, and medical treatment(17, 18). Missed CAD patients (false negatives) forego the benefit of treatment implying reduced quality of life and a 2.4-fold (range 1.5-3.2) CVD event rate compared to a patient without CAD (Table 1)(15, 16). Following a CVD event during follow-up in patients with an initial negative test result, CAD will be diagnosed and treated. CVD-related 1-year mortality (including in-hospital mortality) following a CVD event was assumed to be 17% (range 10-25%)(16, 19, 20). Age- and sex- specific risks of radiation-induced fatal cancer associated with performing CTCA or CCA were based on reported estimates of lifetime attributable cancer incidence(21) and adjusted to reflect mortality based on the BEIR VII report(22). Age- and sex- specific non-CVD mortality rates were obtained

from the Dutch Central Bureau for Statistics(23). Technical details and assumptions are clarified in the Technical Appendix.

Quality of life

Quality of life weights following treatment were a pooled weighted average taking into account that 51% of patients with diagnosed symptomatic CAD undergo PCI, 25% undergo CABG and 24% will be on medication only(24), 5-years after CABG 15% and after PCI 16% of patients still have angina(25), and the quality-of-life weight for angina is 0.74 (0.71-0.77) and without angina 0.87 (0.86-0.88)(25). Patients in whom the diagnosis was missed (false negatives) were assumed to all have angina during follow-up until a CVD event occurred after which they would be diagnosed and treated(25). A temporary disutility of 0.04 (0.02-0.07) QALY's was modeled for a CVD event (MI) during follow-up(26).

Costs

Costs for CTCA and CCA were determined with a cost-analysis and included direct healthcare costs (personnel, materials, equipment), indirect health-care costs (housing, overhead), direct non-healthcare costs (patient travel and time costs), and indirect non-healthcare costs (production losses)(Table 1). Costs for CABG and PCI were based on estimates from the National Health Care Authority (Table 1)(27). Annual costs for medical therapy for diagnosed CAD patients was based on treatment with aspirin, nitrates, statins, and ACE-inhibitors and included 1 follow-up visit per year (Table 1)(28). Costs for CVD events were estimated to range from €8000 to €18000, which is consistent with previously published data(29). Costs for re-interventions were taken into account using weighted averages of re-intervention rates for the different treatment options. Non-CVD health-care costs arising from increased longevity (including costs associated with increased life expectancy) were not taken into account to avoid a financial advantage of reduced longevity(30-32). All costs were converted to the year 2007 based on Dutch consumer price indices and reported in euros(23).

Data analysis

To reflect the physician and patient's perspective, we determined the revised (post-test) probability depending on the prior (pre-test) probability for positive and negative CTCA results based on sensitivity and specificity from our cohort study and a meta-analysis(3). For the remaining analyses we used the sensitivity and specificity from the cohort study. Next, we determined the strategy that maximized life years (LYs) and quality-adjusted life years (QALYs) and calculated the threshold prior probability below which CTCA would be preferred. In an analysis from the hospital perspective we calculated the diagnostic costs and determined the threshold prior probability below which CTCA would be cost-saving. The analysis from the health-care perspective considered QALYs and health-care costs and was performed according to UK recommendations discounting both future costs and effectiveness at 3.5%(33, 34). Subsequently, we performed

the cost-effectiveness analysis from the societal perspective according to US recommendations, which considered QALYs, health-care costs, and direct non-health-care costs (patient time and travel costs) and discounted both future costs and effectiveness at 3%(30-32). Finally, an analysis from the societal perspective was performed according to Dutch recommendations, which, in addition to the above, also took productivity losses (friction costs) into account and discounted future costs and effectiveness at 4% and 1.5% respectively(35). A threshold willingness-to-pay of €50000/QALY (range 40000-80000) was used.

Using 1- and 2-way sensitivity analyses we assessed the impact of varying each parameter across its distribution. Probabilistic sensitivity analysis was performed drawing from all variable distributions (Table 1) using Monte Carlo simulation of 100,000 samples. We calculated the probability that performing CTCA as initial test was cost-effective compared to direct CCA for varying willingness-to-pay thresholds and present acceptability curves. Expected value of perfect information (EVPI; simulation with 100,000 samples) was calculated to assess the value of performing further research and partial EVPI calculations (2-level simulation with 1000x1000 samples) identified the parameters that were the major sources of uncertainty(36-38).

RESULTS

Study population

Data from 156 male and 77 female patients with stable angina in our cohort study were analyzed of whom 113 (72.4%) and 33 (42.9%), respectively, had significant CAD on CCA. Patients were on average 60 years old (ranging from 49-74), 151 (64.8%) presented with typical chest pain, 75 (31.8%) smoked, 149 (63.9%) had hypertension, 47 (20.2%) had diabetes mellitus, and 36 (15.5%) had a prior myocardial infarction. Based on these risk factors the average annual hazard rate for

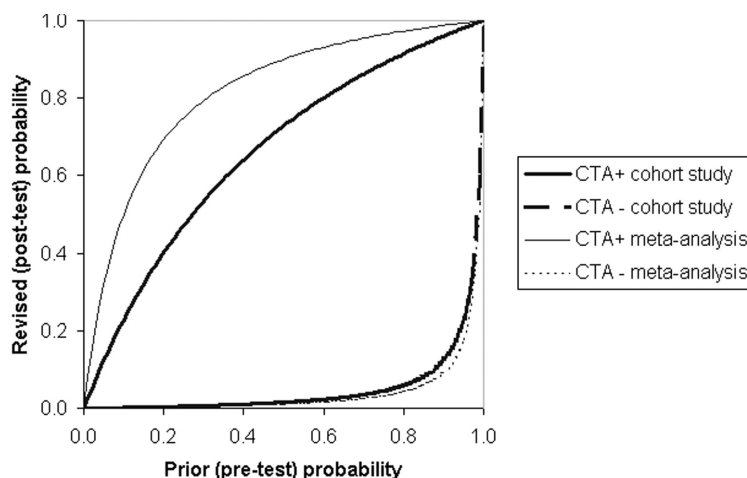


Figure 2. Revised (post-test) probability of CAD. Post-test probability is plotted as a function of the prior (pre-test) probability of CAD for positive and negative CTCA results using the test characteristics found in the cohort study and those found in the meta-analysis published by Mowatt et al(3). Notice that in the setting of a low to moderate prior probability of disease (prior below 40%) a negative CTCA result virtually excludes CAD (revised probability <1%). This applies irrespective of whether the cohort study results or the meta-analysis results are used.

a CVD event was 0.024 (range 0.014–0.077) for 60-year-old males and 0.014 (0.008–0.053) for 60-year-old females(13).

Baseline analysis

Patient and physician perspective

In the setting of a prior probability of disease below 40%, the revised post-negative CTCA probability is less than 1% (Figure 2), irrespective of whether the test characteristics of CTCA were based on the meta-analysis or the cohort study. In contrast, the post-positive CTCA probability varies over a wide range depending on the prior probability (Figure 2).

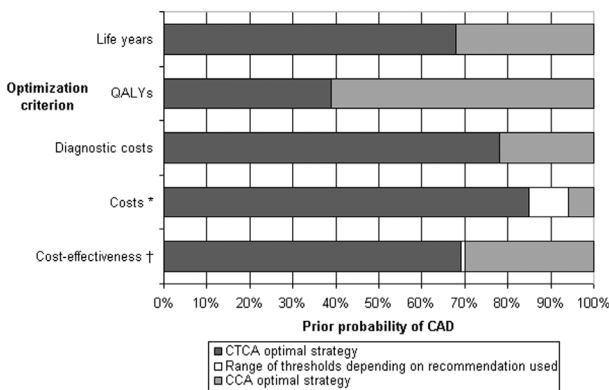


Figure 3a. Sensitivity analysis on prior probability of CAD in men. Threshold prior probability of CAD below which CTCA (if positive followed by CCA) is preferred to direct CCA from the perspective of the patient, physician, hospital, health-care system, and society. Above the threshold CCA optimizes the criterion used. The analysis was performed for 60-year-old men with a risk factor profile as observed in our cohort study. The cost-effectiveness analysis was performed using recommendations from the UK, US, and the Netherlands (NL) using a willingness-to-pay threshold of €50000/QALY.

* Depending on the recommendations used (US, UK, NL), the threshold below which CTCA is the optimal strategy (when optimizing costs) varies from 85–94%

† Depending on the recommendations used (US, UK, NL), the threshold below which CTCA is cost-effective varies from 69–70%

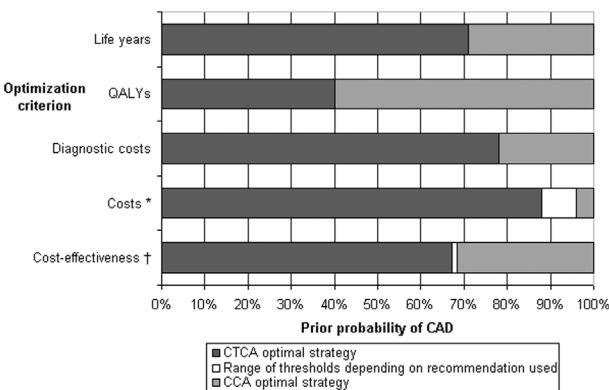


Figure 3b. Sensitivity analysis on prior probability of CAD in women. Threshold prior probability of CAD below which CTCA (if positive followed by CCA) is preferred to direct CCA from the perspective of the patient, physician, hospital, health-care system, and society. Above the threshold CCA optimizes the criterion used. The analysis was performed for 60-year-old women with a risk factor profile as observed in our cohort study. The cost-effectiveness analysis was performed using recommendations from the UK, US, and the Netherlands (NL) using a willingness-to-pay threshold of €50000/QALY.

* Depending on the recommendations used (US, UK, NL), the threshold below which CTCA is the optimal strategy (when optimizing costs) varies from 88–96%

† Depending on the recommendations used (US, UK, NL), the threshold below which CTCA is cost-effective varies from 68–69%

The analysis of LYs demonstrated that below a threshold prior probability of 68% in males and 71% in females, patients would on average benefit from CTCA as initial imaging test (Figure 3). CTCA maximizes QALYs at a prior below 39–40% (Figure 3).

Table 2. Cost-effectiveness of initial CTCA followed by CCA if positive and direct CCA performed according to recommendations in the UK, US, and Netherlands (NL) for 60-year-old men and women with a presentation and risk factor profile as observed in our cohort study. The results indicate that at a threshold willingness-to-pay of €50000/QALY, CCA is optimal in men and CTCA is optimal in women irrespective of the recommendation used.

Strategy	Cost (€)	Effectiveness (QALY)	ICER (€/QALY)	Incremental NHB of CCA vs CTCA
Men				
UK				
CTCA	34541	11.616		
CCA	34674	11.621	30911	0.0016
US				
CTCA	37209	12.215		
CCA	37340	12.219	28898	0.0019
NL				
CTCA	388569	14.409		
CCA	388687	14.415	22468	0.0029
Women				
UK				
CTCA	27044	13.330		
CCA	27326	13.331	237945	-0.0046
US				
CTCA	29198	14.124		
CCA	29490	14.125	230912	-0.0046
NL				
CTCA	252360	17.039		
CCA	252720	17.041	238748.8	-0.0057

CTCA = 64-detector computed tomography angiography of the coronary arteries. CCA = conventional catheterization coronary angiography. QALY = quality adjusted life year. ICER = incremental cost-effectiveness ratio. NHB = net health benefit. The ICER is calculated as the incremental difference in cost divided by the incremental difference in QALY compared to the next best strategy. A strategy is dominated if another strategy is equally effective or more effective and less costly. The incremental NHB is calculated as $NHB_{CCA} - NHB_{CTCA}$ with $NHB = QALY - (cost/50000)$ and expressed in units of QALY equivalents.

Hospital and Health care perspective

CTCA minimizes diagnostic costs below a prior of 78% in both men and women. Using the UK recommendations for cost-effectiveness analysis, health care costs were minimized below a prior of 94% in men (96% in women) (Figure 3). The incremental cost-effectiveness ratio of CCA compared to CTCA was €30911 per QALY gained in men (€237945 in women) (Table 2). In men, performing direct CCA increased net health benefit compared to initial CTCA by 0.0016 QALY equivalents whereas in women CTCA increased net health benefit by 0.0046 QALY equivalents compared to CCA (Table 2).

Societal perspective

Using the US recommendations for cost-effectiveness analysis, health care costs and direct non-health care costs were minimized below a prior of 92% in men (95% in women) (Figure 3). The incremental cost-effectiveness ratio of CCA compared to CTCA was €28898 per QALY gained in men (€230912 in women) (Table 2). In men, performing direct CCA increased net health benefit compared to initial CTCA by 0.0019 QALY equivalents whereas in women CTCA increased net health benefit by 0.0046 QALY equivalents compared to CCA (Table 2).

Using the Dutch recommendations for cost-effectiveness analysis, health care costs and direct non-health care costs including production losses were minimized below a prior of 85% in men (88% in women) (Figure 3). The incremental cost-effectiveness ratio of CCA compared to CTCA was €22468 per QALY gained in men (€238749 in women) (Table 2). In men, performing direct CCA increased net health benefit compared to initial CTCA by 0.0029 QALY equivalents whereas in women CTCA increased net health benefit by 0.0057 QALY equivalents compared to CCA (Table 2).

Sensitivity analyses

The prior probability thresholds were not sensitive to changes across plausible ranges of all parameter inputs, except for the sensitivity of CTCA. Varying the sensitivity of CTCA from 95% to 100%, the prior probability threshold below which CTCA maximizes QALYs ranged from 8% to

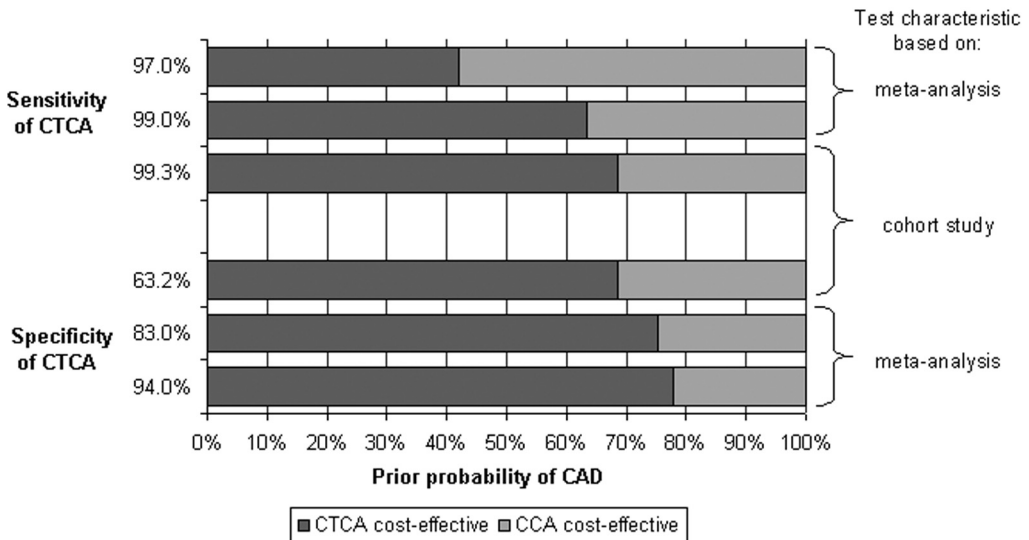


Figure 4. Two-way sensitivity analyses on test characteristics and prior probability of CAD. This graph shows the influence of the test characteristics on the threshold prior probability above which CCA would be more cost-effective. The upper and lower bars refer to the range in sensitivity and specificity as observed in the meta-analysis by Mowatt et al(3). The other bars refer to the sensitivity and specificity as observed in the cohort study (Table 1). Note that the range of sensitivities used in this analysis is rather narrow, but the effect on the threshold prior probability is substantial. Although the range of specificities used in this analysis is much wider, specificity does not alter the threshold prior probability as much as the sensitivity does. The analysis was performed for women, using the UK recommendations for cost-effectiveness analysis.

98%. Cost-effectiveness from the health care perspective using the UK recommendations was optimized at a threshold prior probability ranging from 42% to 69% for varying sensitivity of CTCA (Figure 4). Varying specificity of CTCA and test costs had little effect. Varying the disutility incurred by a CVD event and the fatality rate associated with a CVD event did not alter the results. The prior probabilities observed in our cohort study were consistent with Diamond & Forrester for all patients except for women with typical angina. Table 3 summarizes the implications for the optimal decision.

In probabilistic sensitivity analyses the probability that CTCA is cost-effective was 44% in men and 81% in women for a threshold willingness-to-pay of €50000/QALY (Figure 5). Value of information analysis showed an EVPI for further research of €50 per male patient and €47 per female patient, which for the entire European Union (EU) population (500 million, annual incidence 4.5 per 1000) over a period of 5 years (discounted at 3.5%) amounts to approximately €0.5 billion and for the USA population (300 million) over a period of 5 years (discounted at 3%) amounts to €0.3 billion. Partial EVPI calculations demonstrated that the expected value of information was mainly due to uncertainty in the sensitivity of CTCA (€29/patient in males and €16 in females) and the prior probability of CAD (€13 for males and €24 for females). The uncertainty in the parameters related to long-term outcome, quality of life, and costs had a negligible partial EVPI.

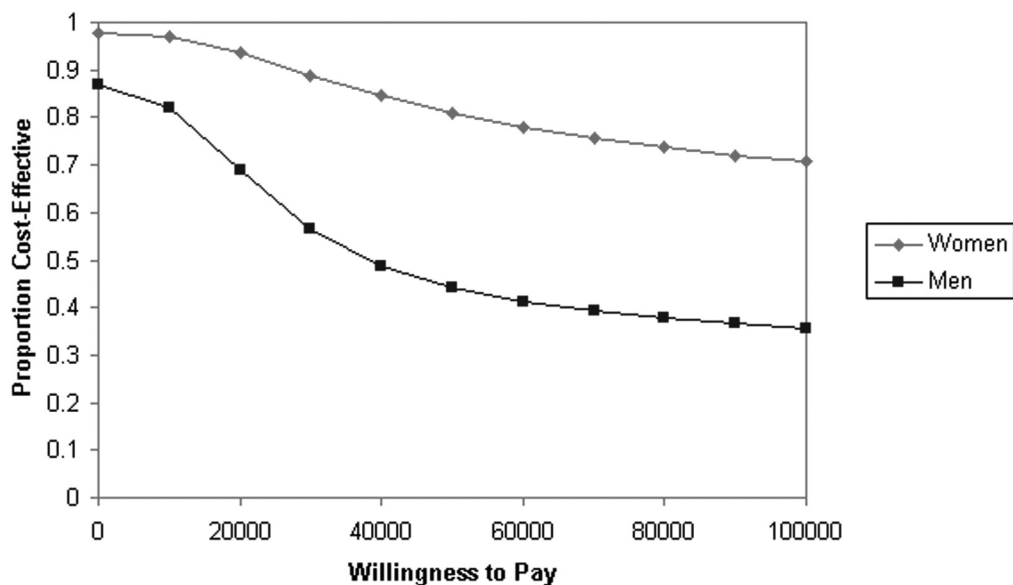


Figure 5. Acceptability curves for the CTCA strategy. The acceptability curve plots the probability that a strategy is cost-effective, given a particular willingness-to-pay threshold.

of patients. Considering harms, benefits and costs altogether, our results suggest that using CTCA as an initial test is cost-effective below a threshold prior probability of approximately 65%. Above this threshold, direct CCA remains the preferred strategy

The use of UK, US, and NL recommendations for cost-effectiveness analyses did not influence the results substantially. We demonstrate that apart from the perspective and optimization criterion, the decision to use CTCA is highly dependent on the prior probability of CAD and the sensitivity of CTCA. Furthermore, according to the observed probabilities in the cohort study and those reported by Diamond & Forrester, our results suggest that CTCA increases life expectancy

Table 3. Prior probabilities of CAD and optimal strategy for various optimization criteria according to sex and type of chest pain for a population with mean age of 60.

Type of chest pain	Males (n=156)		Females (n=77)	
	Typical (n=104)	Atypical (n=52)	Typical (n=47)	Atypical (n=30)
Prior probability according to:				
the cohort study (%)	82	54	43	43
Diamond & Forrester (%)†	93	63	85	43
Strategy optimizing				
LY's	CCA	CTCA	CTCA/CCA*	CTCA
QALY's	CCA	CCA	CCA	CCA
Costs	CTCA/CCA*	CTCA	CTCA/CCA*	CTCA
Cost-effectiveness	CCA	CTCA	CTCA/CCA*	CTCA

CTCA = 64-detector computed tomography angiography of the coronary arteries.

CCA = conventional catheterization coronary angiography

† Prior probabilities for 60-year-old patients were calculated by averaging the probabilities of age categories 50-59 and 60-69

* The estimate of prior probability as observed in our cohort study would favor using CTCA whereas the prior probability as reported by Diamond & Forrester would favor using CCA. Furthermore, to minimize costs the decision also depends on which recommendation (UK vs US vs NL) is used.

and is cost-saving and cost-effective compared to CCA in the workup of patients with atypical angina. A lower threshold exists (not addressed in the current study) below which the net gain of doing CTCA is too small and would therefore not be cost-effective compared to either not testing or performing another less invasive and less costly test.

Although our methods were different, our conclusions are consistent with those from previously published cost-effectiveness analyses. An analysis reported by Dewey and Hamm(39) used costs per correctly identified CAD patient as a measure of cost-effectiveness, did not consider costs of subsequent treatment, and ignored the benefit of correct exclusion of CAD. Nevertheless, they found a threshold of 60% prior probability of CAD below which CTCA is indicated. Kuntz and others(40) examined the cost-effectiveness of several non-invasive functional (imaging and non-

imaging) tests. Compared to exercise SPECT and exercise echocardiography, CCA had an incremental cost-effectiveness ratio of \$32600 and \$35200 respectively for 50-59 year old men with mild chest pain. This is similar to what we found for CCA compared to CTCA for men using the US recommendations.

In 2007, the Health Technology Assessment Program performed a review on the cost-effectiveness of different strategies for patients with stable chest pain(41). They reported cost-increases with exercise SPECT (€527, non-significant) and with exercise echocardiography (€1043 significant) compared to CCA. There was a non-significant increase in QALYs for both strategies (0.0362 and 0.0371) and the incremental cost effectiveness ratios were €14564/QALY and €28151/QALY, respectively.

Mowatt et al. (42) recently reported a review on effectiveness and cost-effectiveness of CTCA. However, they did not find any previously published cost-effectiveness analyses evaluating CTCA as triage test prior to CCA. Their own analysis considering long-term outcomes compared CTCA to stress ECG and myocardial perfusion scintigraphy only.

Our aim was to design a lucid decision model that would be easy to interpret that can guide decision making. Consequently, we had to make several assumptions. First, data related to CTCA, the prior probability, and costs were obtained from the cohort study whereas the best-available published evidence was used for parameters related to therapy and prognosis and in sensitivity analyses. For example, we used the test sensitivity and specificity as reported in the cohort study(8). However, a recent meta-analysis by Mowatt(3) reported a similar sensitivity but a much higher specificity. Varying specificity, however, did not affect the results in a major way. Second, for the purpose of estimating costs and disutility of a CVD event we assumed that CVD events were mainly myocardial infarctions and that costs and disutility of other CVD events were similar to that of myocardial infarctions. Third, the quality-of-life estimates were derived from Hlatky(25), which was a study on multivessel CAD. This may be an underestimate of the quality-of-life of patients with single vessel disease, which may therefore have overestimated the gain in effectiveness with treatment, which would have caused a small bias in favor of CCA. Fourth, work-up for chest pain following a negative CTCA was not modeled which may have caused a small bias in favor of CTCA. In our analysis, CTCA was assumed to be a dichotomous test identifying patients requiring some form of treatment for CAD. One could argue that physicians are primarily interested in diagnosing severe CAD, as these patients would be eligible for revascularization whereas others can be adequately treated medically. Next, we did not consider other non-invasive tests but rather considered only patients referred for CCA in whom either the history or functional testing will have suggested the presence of cardiac ischemia. Furthermore, the cost and cost-effectiveness analyses were based on European cost estimates because in this analyses we were interested in evaluating how the different perspectives (health care system vs societal) and the different recom-

mendations (UK vs US vs NL) would affect the results. Costs in the USA are generally higher as is the willingness-to-pay threshold, which could lead to different results and merits further study. Finally, it is important to note that the differences between the two strategies in terms of costs, QALYs, and net-health-benefits were very small which is why we performed extensive (probabilistic) sensitivity analysis and value of information analysis.

We used modern techniques to evaluate whether further research is necessary and to inform the choice of a future study. Value of information analysis showed a very high expected value of further research for both Europe and the USA and indicated that future research should focus on sensitivity of CTCA and developing clinical prediction rules for the diagnosis of CAD.

In conclusion, the indication for the use of CTCA depends on the optimization criterion, prior probability of CAD, and sensitivity of CTCA. The results of our cost-effectiveness analysis suggest that the use of CTCA as an initial test prior to conventional coronary angiography is cost-effective in patients with a prior probability of CAD below 69% which implies that CTCA is cost-effective in patients with atypical angina. Above this threshold, CCA remains the most cost-effective strategy. To maximize patient outcomes a lower threshold applies and to minimize costs a higher threshold should be used.

Role of the funding source

This study was funded by the Health Care Efficiency Research grant (number 945-04-263) from the Netherlands Organisation for Health Research and Development, a Dutch governmental organisation, and by internal funding through a Health Care Efficiency grant from the Erasmus University Medical Center, Rotterdam. The authors' work was independent of the funding organizations. The funding organizations had no involvement in the design or conduct of this study; data management and analysis; or manuscript preparation and review or authorization for submission.

REFERENCES

1. Vanhoenacker PK, Heijenbrok-Kal MH, Van Heste R, et al. Diagnostic performance of multidetector CT angiography for assessment of coronary artery disease: meta-analysis. *Radiology* 2007; 244:419-428.
2. Hamon M, Biondi-Zoccai GG, Malagutti P, et al. Diagnostic performance of multislice spiral computed tomography of coronary arteries as compared with conventional invasive coronary angiography: a meta-analysis. *J Am Coll Cardiol* 2006; 48:1896-1910.

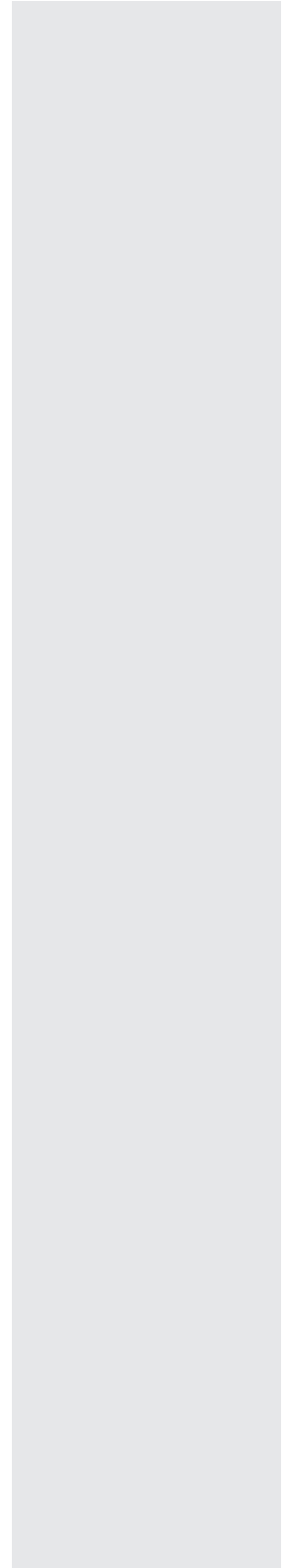
3. Mowatt G, Cook JA, Hillis GS, et al. 64-slice computed tomography angiography in the diagnosis and assessment of coronary artery disease: systematic review and meta-analysis. *Heart* 2008.
4. RIVM. Dutch National Institute for Public Health and the Environment. In, 2008.
5. Cook S, Walker A, Hugli O, Togni M, Meier B. Percutaneous coronary interventions in Europe: prevalence, numerical estimates, and projections based on data up to 2004. *Clin Res Cardiol* 2007; 96:375-382.
6. Merrill CE, A. Agency for Healthcare Research and Quality: Procedures in U.S. Hospitals. In, 2003.
7. Fox K, Garcia MA, Ardissino D, et al. Guidelines on the management of stable angina pectoris: executive summary: the Task Force on the Management of Stable Angina Pectoris of the European Society of Cardiology. *Eur Heart J* 2006; 27:1341-1381.
8. Meijboom WB. Diagnostic Accuracy of 64-slice Computed Tomography Coronary Angiography: A prospective, multicenter, multi-vendor cohort study. Accepted for publication by: *J Am Coll Cardiol* Expected year of publication: 2008.
9. Hunink MG. Cost-effectiveness Analysis: Some Clarifications. *Radiology* 2008; 249:753-755.
10. Katayama H, Yamaguchi K, Kozuka T, Takashima T, Seez P, Matsuura K. Adverse reactions to ionic and nonionic contrast media. A report from the Japanese Committee on the Safety of Contrast Media. *Radiology* 1990; 175:621-628.
11. Yamada H, Do D, Morise A, Atwood JE, Froelicher V. Review of studies using multivariable analysis of clinical and exercise test data to predict angiographic coronary artery disease. *Prog Cardiovasc Dis* 1997; 39:457-481.
12. Diamond GA, Forrester JS. Analysis of probability as an aid in the clinical diagnosis of coronary-artery disease. *N Engl J Med* 1979; 300:1350-1358.
13. D'Agostino RB, Sr., Vasan RS, Pencina MJ, et al. General cardiovascular risk profile for use in primary care: the Framingham Heart Study. *Circulation* 2008; 117:743-753.
14. Deckers JW, Goedhart DM, Boersma E, et al. Treatment benefit by perindopril in patients with stable coronary artery disease at different levels of risk. *Eur Heart J* 2006; 27:796-801.
15. Berger JS, Brown DL, Becker RC. Low-dose aspirin in patients with stable cardiovascular disease: a meta-analysis. *Am J Med* 2008; 121:43-49.
16. Dagenais GR, Pogue J, Fox K, Simoons ML, Yusuf S. Angiotensin-converting-enzyme inhibitors in stable vascular disease without left ventricular systolic dysfunction or heart failure: a combined analysis of three trials. *Lancet* 2006; 368:581-588.
17. Bravata DM, Gienger AL, McDonald KM, et al. Systematic review: the comparative effectiveness of percutaneous coronary interventions and coronary artery bypass graft surgery. *Ann Intern Med* 2007; 147:703-716.
18. Katritsis DG, Ioannidis JP. Percutaneous coronary intervention versus conservative therapy in nonacute coronary artery disease: a meta-analysis. *Circulation* 2005; 111:2906-2912.

19. Schulz H, Sinn R, Wolf R. [Cardiac risk in men with angiographically normal coronary arteries or minimal coronary arteriosclerosis]
Kardiales Risiko bei Männern mit angiographisch normalen oder minimal arteriosklerotisch veränderten Koronararterien. *Z Kardiologie* 2003; 92:245-253.
20. Adabag AS, Therneau TM, Gersh BJ, Weston SA, Roger VL. Sudden death after myocardial infarction. *Jama* 2008; 300:2022-2029.
21. Einstein AJ, Henzlova MJ, Rajagopalan S. Estimating risk of cancer associated with radiation exposure from 64-slice computed tomography coronary angiography. *Jama* 2007; 298:317-323.
22. BEIRVII. Board on Radiation Effects Research: Health Risks From Exposure To Low Levels of Ionizing Radiation. In:BEIR VII Phase 2, 2006.
23. CBS. Statline of Central Bureau of Statistics, the Netherlands. In, 2008.
24. Lenzen MJ, Boersma E, Bertrand ME, et al. Management and outcome of patients with established coronary artery disease: the Euro Heart Survey on coronary revascularization. *Eur Heart J* 2005; 26:1169-1179.
25. Hlatky MA, Boothroyd DB, Melsop KA, et al. Medical costs and quality of life 10 to 12 years after randomization to angioplasty or bypass surgery for multivessel coronary artery disease. *Circulation* 2004; 110:1960-1966.
26. Sullivan PW, Ghushchyan V. Preference-Based EQ-5D index scores for chronic conditions in the United States. *Med Decis Making* 2006; 26:410-420.
27. NZA. Dutch National Authority of Health Care. In, 2008.
28. Dutch Health Care Insurance Board: Farmacotherapeutic Compass. In.
29. Russell MW, Huse DM, Drowns S, Hamel EC, Hartz SC. Direct medical costs of coronary artery disease in the United States. *Am J Cardiol* 1998; 81:1110-1115.
30. Gold MR, et al. Cost-effectiveness in Health and Medicine. *Journal of Health Economics* 1996; 2:91-92.
31. Siegel JE, Weinstein MC, Russell LB, Gold MR. Recommendations for reporting cost-effectiveness analyses. Panel on Cost-Effectiveness in Health and Medicine. *Jama* 1996; 276:1339-1341.
32. Weinstein MC, Siegel JE, Gold MR, Kamlet MS, Russell LB. Recommendations of the Panel on Cost-effectiveness in Health and Medicine. *Jama* 1996; 276:1253-1258.
33. Brouwer WB, Niessen LW, Postma MJ, Rutten FF. Need for differential discounting of costs and health effects in cost effectiveness analyses. *Bmj* 2005; 331:446-448.
34. NICE. Guide to the methods of technology appraisal. In:NICE. London, 2004.
35. Oostenbrink J, et al. Dutch Manual for Cost-Analyses: Methods and Standard Values for Economical Evaluations in Health Care. In: Dutch Health Care Insurance Board, 2004.
36. Claxton K, Sculpher M, Drummond M. A rational framework for decision making by the National Institute For Clinical Excellence (NICE). *Lancet* 2002; 360:711-715.

37. Ades AE, Lu G, Claxton K. Expected value of sample information calculations in medical decision modeling. *Med Decis Making* 2004; 24:207-227.
38. Groot Koerkamp B, Hunink MG, Stijnen T, Hammitt JK, Kuntz KM, Weinstein MC. Limitations of acceptability curves for presenting uncertainty in cost-effectiveness analysis. *Med Decis Making* 2007; 27:101-111.
39. Dewey M, Hamm B. Cost effectiveness of coronary angiography and calcium scoring using CT and stress MRI for diagnosis of coronary artery disease. *Eur Radiol* 2007; 17:1301-1309.
40. Kuntz KM, Fleischmann KE, Hunink MG, Douglas PS. Cost-effectiveness of diagnostic strategies for patients with chest pain. *Ann Intern Med* 1999; 130:709-718.
41. Sharples L, Hughes V, Crean A, et al. Cost-effectiveness of functional cardiac testing in the diagnosis and management of coronary artery disease: a randomised controlled trial. The CECaT trial. *Health Technol Assess* 2007; 11:iii-iv, ix-115.
42. Mowatt G, Cummins E, Waugh N, et al. Systematic review of the clinical effectiveness and cost-effectiveness of 64-slice or higher computed tomography angiography as an alternative to invasive coronary angiography in the investigation of coronary artery disease. *Health Technol Assess* 2008; 12:iii-iv, ix-143.
43. Scanlon PJ, Faxon DP, Audet AM, et al. ACC/AHA guidelines for coronary angiography. A report of the American College of Cardiology/American Heart Association Task Force on practice guidelines (Committee on Coronary Angiography). Developed in collaboration with the Society for Cardiac Angiography and Interventions. *J Am Coll Cardiol* 1999; 33:1756-1824.
44. Noto TJ, Jr., Johnson LW, Krone R, et al. Cardiac catheterization 1990: a report of the Registry of the Society for Cardiac Angiography and Interventions (SCA&I). *Cathet Cardiovasc Diagn* 1991; 24:75-83.

PART 4

CTCA before and after
cardiac surgery



13

CT coronary angiography in Cardiothoracic Surgery

*Advances in MDCT Volume 3,
Pt. 2: CT Angiography.*

*Willem B. Meijboom,
Nico R. Mollet,
Niels van Pelt*

*Department of Radiology
Department of Cardiology
Erasmus MC, Rotterdam, the
Netherlands*

INTRODUCTION

With the introduction of multislice CT scanners and its brisk development in recent years, imaging of the small and rapidly moving coronaries has become feasible. With the last generations of 64-slice computed tomography and adequate patient preparation (which includes lowering of the heart rate) sensitivities and specificities above 90% have been reported for the detection of coronary artery stenoses in comparison with invasive coronary angiography (CCA) (1-8). Especially the high negative predictive value of $\pm 98\%$ found in these studies suggests that CT coronary angiography (CTCA) may be a useful diagnostic technique to rule out the presence of coronary stenoses in selected patients, especially those with a lower pretest likelihood of disease. An appropriate population, for example, may include patients undergoing cardiac valve surgery who have a prevalence of concomitant coronary artery disease of 25-35% (9-12). Imaging of coronary artery bypass grafts (CABG) is reliable, due to their larger diameter and lesser mobility. However, clinical applications can be hampered due to difficulties in assessing the native coronary arteries in patients with previous CABG, because of the presence of severe calcifications (13). In patients who undergo a redo CABG (14, 15) or totally endoscopic coronary artery bypass grafting (TECAB) (16) CTCA can add incremental information in planning these complicated procedures. CTCA provides three-dimension information of the intra-thoracic organs, an overview of the coronary tree and bypasses and information on location, severity and plaque characteristics of coronary artery disease. Furthermore, information on the cardiac valves and ventricle can be gathered. During CTCA a volume of data is obtained. By reconstruction of datasets with fixed intervals during the R-R interval, functional information can be acquired of the cardiac valves and ventricle(17).

PREOPERATIVE SCREENING FOR OBSTRUCTIVE CORONARY ARTERY DISEASE

Pre-operative computed tomography coronary angiography to detect significant coronary artery disease in patients referred for cardiac valve surgery

Meijboom WB, Mollet NR, van Mieghem CA, et al. JACC 2006, 48(8): 1658-1665

Background

Presence or absence of angina pectoris is a poor indicator of having obstructive coronary artery disease (CAD) in patients with valvular pathology and current non-invasive stress tests lack diagnostic accuracy. Therefore, current ACC/AHA guidelines advise to perform an invasive coronary angiogram prior to cardiac valve surgery in symptomatic patients and/or those who have an impaired left ventricular function in males over 35 years, post menopausal women, and pre-menopausal women over 35 years old with risk factors for coronary artery disease (18). The authors investigated the ability of non-invasive 64-slice CTCA to detect or rule out obstructive coronary artery disease in patients undergoing valve surgery.

Interpretation

Hundred forty-five patients were screened in a consecutive patient cohort. After exclusion of 35 patients due to CTCA criteria, 13 patients due to general criteria and 27 patients for not giving informed consent, 70 patients were enrolled in the analysis. Prevalence of having at least one significant lesion defined as ≥ 50 percent diameter reduction was 25,7 percent. In the per-patients analysis CTCA had a sensitivity of 100 percent (18/18), a specificity of 92% (48/52), positive predictive value (PPV) of 82% (18/22) and a negative predictive (NPV) value of 100% (48/48) for detecting or ruling out significant coronary stenosis.

Comment

Multiple studies using a 64-slice CT scanner have shown a good sensitivity and excellent negative predictive value in patient populations with a high risk for having obstructive CAD. However, the clinical benefit of CTCA lies in patient populations who have a low to intermediate risk for having obstructive CAD. In this study, a CCA could have been saved in 92 percent (48/52) of patients who did not have obstructive CAD. In 4 patients CTCA overestimated stenosis severity. Significant stenoses were reported, but only lumen irregularities were seen on CCA. All patients who did have obstructive CAD were detected. Limitations of this technique are the presence of coronary calcifications, which gradually increase with elderly age. These calcium deposits create blooming artefacts and comprise precise stenosis evaluation. Heart rate reduction with the use of beta-blockers and/or benzodiazepines remains necessary to retain optimal image quality. Further-

more, atrial fibrillation is often seen in this patient's population and remains a contraindication to perform a CTCA. This study shows promising results and demonstrates the expanding use of CTCA in the clinical field.

POST BYPASS IMAGING

Use of 64-slice CT in symptomatic patients after coronary bypass surgery: evaluation of grafts and coronary arteries

Malagutti P, Nieman K, Meijboom WB, et al. European Heart J. 2006, Jul. 17.

Background

The use of coronary bypass surgery to restore myocardial flow is widely used in patients with advanced CAD. During early and late post-operative follow-up patients can present with recurrent chest discomfort and dyspnea. These symptoms can either be caused by graft stenosis and occlusion or by the progression of coronary artery disease in the native coronary system. Currently, invasive catheter-based angiography is the reference method to evaluate both grafts and coronaries. Non-invasive tests such as exercise-ECG, stress echocardiography and nuclear imaging can detect myocardial ischemia, but are unable to determine the exact location of the culprit stenosis. In this study both graft patency, distal run-offs and non-grafted native coronaries were assessed.

Interpretation

After exclusion of 25 patients for various reasons, 52 patients were enrolled in the study. A total of 109 grafts were evaluated. Sensitivity and specificity for the detection of at least a 50% diameter stenosis on QCA were 100% and 98,3, respectively. Hundred twenty-three distal run-offs were seen. Sensitivity was 88.8% (8/9), specificity 93% (106/114), positive predictive value 50% (8/16) and negative predictive value 99% (106/107). Evaluation of the non-grafted vessels showed a sensitivity of 100%, a specificity of 68,4%, PPV of 63,6% and a NPV of 100%.

Comment

Previous studies with 4-slice and 16-slice scanners had already showed the possibility of imaging bypass grafts (19-21). Their diameter size, relative immobility in the thoracic cavity and the sparse presence of calcifications make them relatively easy to visualize. Image quality can be impaired due to the presence of metal orifice indicators, sternum wires and vascular clips. These high density structures cause blooming artefacts which obscure the underlying lumen or plaque. Visualizing the distal anastomosis is more difficult, which shows a slightly lower sensitivity and a positive predictive value of only 50%. The influence of cardiac motion is increased and the vessels are smaller

with more advanced disease. The analysis of non-grafted vessels has an excellent sensitivity and negative predictive value, but specificity and positive predictive value is lower. These results are less good in comparison with studies performed in patients without previous CABG surgery (1-8). Post-surgical patients are generally older and have more advanced atherosclerotic disease with more calcified plaques. The use of CTCA will increase in the assessment of patients with prior CABG. Although CCA remains the gold standard, it has its drawbacks. Besides the inherently invasive nature of the procedure with its known risks, it is sometimes difficult and time-consuming to find the origin of the graft and to selectively inject contrast. Especially when the exact procedure of the prior CABG is unknown, CTCA can clearly display its anatomy and patency. A limitation of CTCA remains that functional information is lacking. Finding the particular stenosis that causes symptoms is therefore difficult, especially with the knowledge that CTCA tends to overestimate severity of stenosis. In the near future combined systems, either SPECT-CT or PET-CT, will be introduced, which will display both the anatomical information and the functional information.

PREOPERATIVE CTCA BEFORE CABG

Multi-detector row CT versus coronary angiography: preoperative evaluation before totally endoscopic coronary artery bypass grafting

Herzog C, Dogan S, Diebold T, et al. Radiology 2003; 229:200-208

Background

The use of lesser invasive techniques like minimally invasive direct coronary artery bypass grafting or totally endoscopic coronary artery bypass grafting (TECAB) is becoming increasingly clinically important. However, one of the drawbacks in the latter technique is the lack of tactile perception during operation. For identification of the target vessel and site for the anastomosis the operator is solely dependent on visual information. The trajectory of the coronaries can follow an intramural course or can be buried deep inside the epicardial fatty tissue, making identification of the correct anastomosis site difficult. Although preoperative conventional coronary angiography is the golden standard to display the coronary tree, it lacks information of vessel wall characteristics. Furthermore, in case of chronic total occlusions without sufficient collateral filling the distal segments can not be properly displayed by CCA.

Interpretation

All patients underwent a CTCA with a 4-slice CT scanner before the TECAB. CTCA properly displayed relevant surgical coronary segments in 80% (154/194) versus 89% (172/194) in CCA. As expected all calcified plaques were correctly identified with CTCA. Sensitivity and specific-

ity were 76 % (42/55) and 99.6% (483/485), respectively. Bridging of coronary segments through either myocardium or epicardial fat was better seen with CTCA versus CCA. Final distal bypass touchdown segments were better identified with CTCA 76% (28/37) than with CCA 70% (26/37).

Comment

In this study the additive value of CTCA besides CCA is nicely evaluated.

Especially in this relatively new surgical technique that lacks tactile information, precise information on intrathoracic orientation and target vessel characteristics are valuable. 3D software can give a three-dimensional overview of the entire thorax, depict the presence of coronary anomalies and give an anatomical overview of the coronary tree. Vessel characteristics with information distally of chronic total occlusions with collateral filling, the presence of non-calcified or calcified plaques and pre-operative knowledge of target sites for placement of bypasses will facilitate surgery.

The development of newer CT-scanners, like the 16, 64 slice and dual source scanners will further improve image quality, due to better spatial and temporal resolution and faster scan acquisition which will increase the percentage of evaluable relevant coronary segments.

CTCA GUIDED PLANNING OF REDO CARDIAC SURGERY

Three dimensional computed tomography imaging in planning the surgical approach for redo cardiac surgery after coronary revascularization

Gasparovic H, Rybicki FJ, Millstine J, et al. Eur J Cardiothorac Surg 2005;28(2):244-9.

Background

Patients with a history of CABG, who undergo redo cardiac surgery, have a higher risk for complications than patients undergoing their first CABG (22). Re-entering the thorax has the risk of damaging patent coronary grafts or injuring other vital mediastinal structures like the aorta and right ventricle. Pre-operatively chest radiography (CXR) and CCA are normally performed to have insight into the mediastinal anatomy(23). However, both these techniques provide only limited and imprecise anatomic information. In this study the additive value of preoperative CTCA was quantified, when performed in conjunction with the standard of care.

Interpretation

All 33 patients were scanned with a 16-slice scanner. The correlation for distances measured by CXR and CCA from the LIMA-LAD graft, circumflex and right coronary artery graft, and the distance from the right ventricle and the aorta to the posterior sternum were all poor ($R < 0.6$). The combined evaluation of CXR and CCA offered incomplete insight into pertinent mediastinal topography in 85% of patients. In seven patients (21%) the surgical strategy was modified based on the location of patents grafts in the mediastinum.

Comment

In conclusion the authors state that both CXR and CCA only provide a rough estimate of the positions of grafts in relation to the midline and the posterior surface of the sternum.

CTCA, in comparison, provided an accurate assessment of the position of various vital mediastinal structures and delineated the relationship between bypass grafts, right ventricle aorta and the posterior sternum. CTCA can give additional information about the plaque burden of the ascending and descending thoracic aorta, pathology of the cardiac valves and left ventricular function. The authors advise implementation of routine preoperative CTCA evaluation of cardiac surgical patients with previous CABG to prevent potential catastrophically complications by revising surgical strategy (15).

ASSESSMENT OF VALVES WITH CT CORONARY ANGIOGRAPHY

Multislice Computed Tomography for detection of patients with aortic valve stenosis and quantification of severity.

Feuchtner GM, Dichtl W, Friedrich GJ, et al. JACC 2006, 47(7): 1410-1417

Background

Aortic valve replacement for degenerative aortic valve stenosis (AS) is nowadays a common operation for the cardiac surgeon. The presence and severity is routinely assessed by transthoracic echocardiography (TTE) using the Doppler continuity equation approach. Other approaches for diagnosis and quantification are transesophageal echocardiography (TEE), cardiac MRI and cardiac catheterization. During the last five years an exponential increase of the use of CTCA as a first non-invasive approach to visualize the coronaries is seen. During this acquisition the entire heart is scanned, which makes it possible, using dedicated reconstructions, to assess both the left ventricle as the valves and its pathology. In this study the diagnostic accuracy for the detection of

severe aortic valve stenosis was analyzed using a 16-slice CT scanner. The diagnostic cut-off for patients with AS was a peak transvalvular velocity $> 2\text{m/s}$ on TTE. Thirty patients had known AS en 16 patients suspected CAD. Furthermore, the severity of aortic stenosis was measured with TTE (aortic valve area, AVA).

Interpretation

The sensitivity of CTCA to detect degenerative aortic valve stenosis was 100% (30/30) and specificity was 93.7% (15/16), PPV was 97% (30/31), NPV was 100% (15/15). The linear regression revealed a good correlation between the AVA quantified by CTCA and TTE ($r: 0.89$; $p < 0.001$) in patients with aortic valve stenosis. The Bland-Altman plot demonstrated a good intermodality agreement between CTCA and TTE with a slight overestimation of the aortic valve area by CTCA. ($+0.04\text{cm}^2$).

Comment

TTE will remain the diagnostic tool of preference, as also stated by the authors. TTE is safe, relatively easy and fast to perform and widely available. Furthermore, other alternative as TEE and MRI are at hand. Although CTCA doesn't provide flow information it does give the possibility to visualize the valvular anatomy and to measure the AVA and the diameter of the annulus. Newer scanners have a temporal resolution of up to 83 msec with the dual-source scanners, and a higher spatial resolution of 0.4 mm. These characteristics may make the evaluation of valve more reliable. The use of CTCA will primarily be used for imaging of the coronaries. However, other cardiac pathology, like aortic valve stenosis, will be detected given the excellent spatial resolution. The prevalence of these pathologies will be lower than in the studied patient group (65%, 30/46). Other indications for CTCA of the valves and aortic annulus are pre-procedure placement of percutaneous valves. An exact measurement of the diameter of the annulus, the amount and localisation of calcifications and the origins of the right en left coronary arteries have to be acquired to guarantee successful placement of these percutaneous valves.

CONCLUSION

In conclusion, the last few years have seen continued exciting developments in CT angiographic imaging. Although many papers have been written on the diagnostic accuracy of CTCA for stenosis detection, relatively few papers discuss the use of CTCA for cardiothoracic surgical indications. However, the use of CTCA in clinical practice will probably increase gradually with the developing experience of cardiologist, radiologist and cardiothoracic surgeons. In particular, there is significant interest for CTCA to be used as gatekeeper for CCA in patients scheduled for cardiac valve surgery, as the need for an additional invasive procedure is avoided in the majority of cases. Furthermore, in patients who undergo redo cardiac surgery, imaging of the thorax helps the sur-

geon to reconstruct a 3D view of the intra-thoracic structures thereby reducing the risk for major complications.

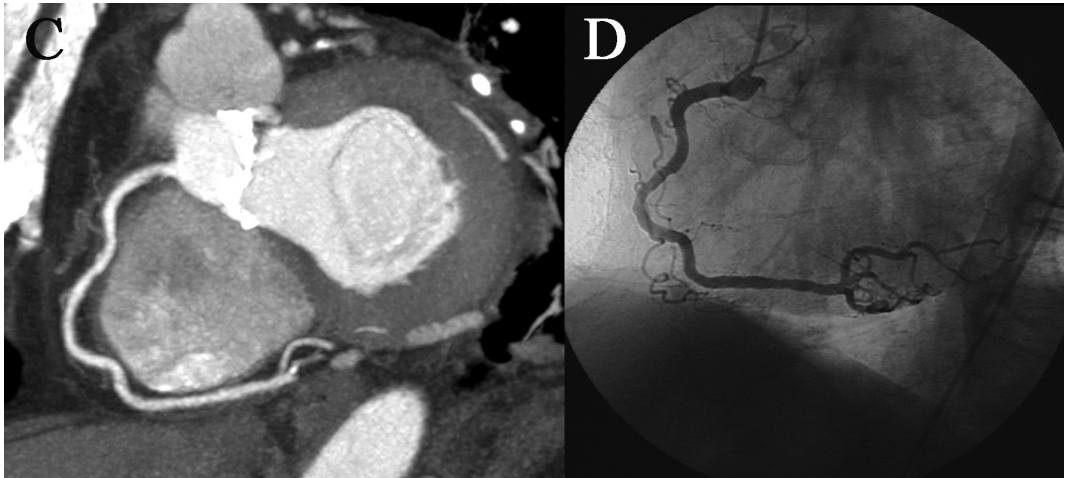


Figure 1. A CT image displays a patent right coronary artery without any signs of coronary artery disease (C). The bright white spots represent severe calcifications of the aortic valve. The CCA confirms the patency of the right coronary artery (D).

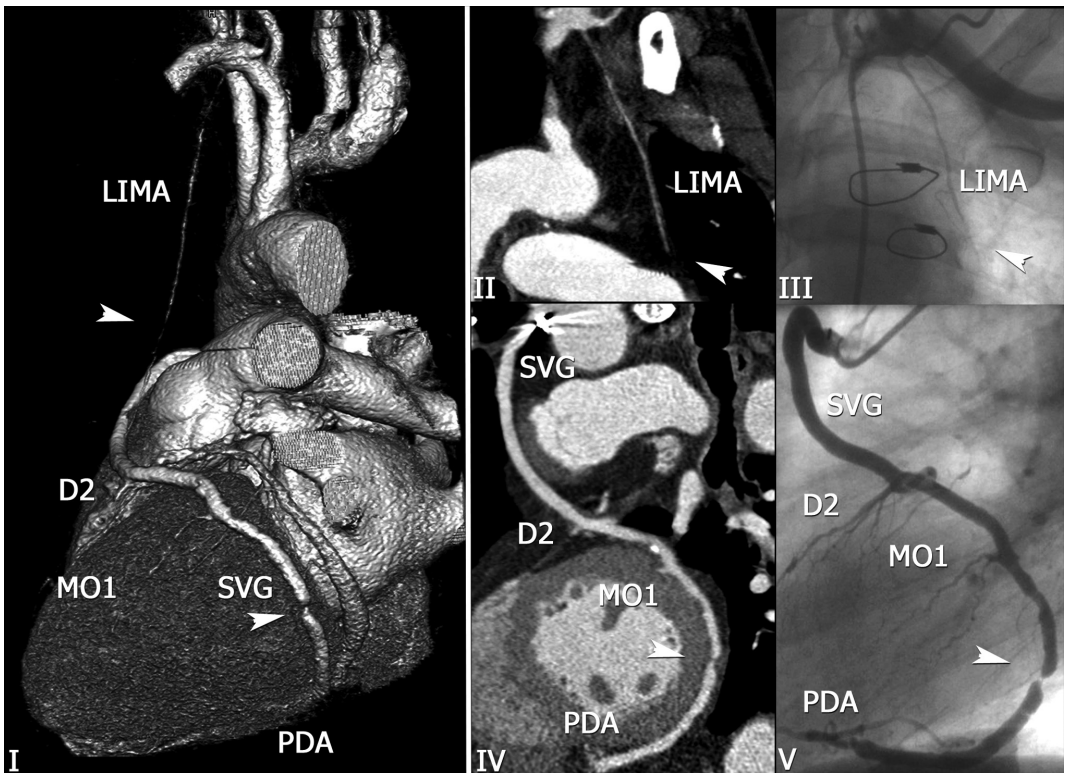


Figure 2. Volume-rendered reconstruction (I) and curved multiplanar reformations (II,IV) of a CT scan and corresponding conventional angiography (III, V), which show an occluded left internal mammary artery (LIMA, arrow in I,II,III) and obstructed vein graft (SVG). The venous graft has three coronary anastomoses: second diagonal branch (D2), first marginal branch (MO1), posterior descending artery (PDA), of which the terminal segment is significantly stenosed (arrow I, IV, V).

REFERENCES

1. Leschka S, Alkadhi H, Plass A, Desbiolles L, Grunenfelder J, Marincek B, Wildermuth S. Accuracy of MSCT coronary angiography with 64-slice technology: first experience. *Eur Heart J* 2005.
2. Raff GL, Gallagher MJ, O'Neill WW, Goldstein JA. Diagnostic accuracy of noninvasive coronary angiography using 64-slice spiral computed tomography. *J Am Coll Cardiol* 2005;46(3):552-7.
3. Leber AW, Knez A, von Ziegler F, Becker A, Nikolaou K, Paul S, Wintersperger B, Reiser M, Becker CR, Steinbeck G, Boekstegers P. Quantification of obstructive and nonobstructive coronary lesions by 64-slice computed tomography: a comparative study with quantitative coronary angiography and intravascular ultrasound. *J Am Coll Cardiol* 2005;46(1):147-54.
4. Mollet NR, Cademartiri F, van Mieghem CA, Runza G, McFadden EP, Baks T, Serruys PW, Krestin GP, de Feyter PJ. High-resolution spiral computed tomography coronary angiography in patients referred for diagnostic conventional coronary angiography. *Circulation* 2005;112(15):2318-23.
5. Ropers D, Rixe J, Anders K, Kuttner A, Baum U, Bautz W, Daniel WG, Achenbach S. Usefulness of multidetector row spiral computed tomography with 64- x 0.6-mm collimation and 330-ms rotation for the noninvasive detection of significant coronary artery stenoses. *Am J Cardiol* 2006;97(3):343-8.
6. Schuijf JD, Pundziute G, Jukema JW, Lamb HJ, van der Hoeven BL, de Roos A, van der Wall EE, Bax JJ. Diagnostic accuracy of 64-slice multislice computed tomography in the noninvasive evaluation of significant coronary artery disease. *Am J Cardiol* 2006;98(2):145-8.
7. Ehara M, Surmely JF, Kawai M, Katoh O, Matsubara T, Terashima M, Tsuchikane E, Kinoshita Y, Suzuki T, Ito T, Takeda Y, Nasu K, Tanaka N, Murata A, Suzuki Y, Sato K. Diagnostic accuracy of 64-slice computed tomography for detecting angiographically significant coronary artery stenosis in an unselected consecutive patient population: comparison with conventional invasive angiography. *Circ J* 2006;70(5):564-71.
8. Nikolaou K, Knez A, Rist C, Wintersperger BJ, Leber A, Johnson T, Reiser MF, Becker CR. Accuracy of 64-MDCT in the diagnosis of ischemic heart disease. *AJR Am J Roentgenol* 2006;187(1):111-7.
9. Gilard M, Cornily JC, Pennec PY, Joret C, Le Gal G, Mansourati J, Blanc JJ, Boschat J. Accuracy of multislice computed tomography in the preoperative assessment of coronary disease in patients with aortic valve stenosis. *J Am Coll Cardiol* 2006;47(10):2020-4.
10. Meijboom WB, Mollet NR, Van Mieghem CA, Kluin J, Weustink AC, Pugliese F, Vourvouri E, Cademartiri F, Bogers AJ, Krestin GP, de Feyter PJ. Pre-operative computed tomography coronary angiography to detect significant coronary artery disease in patients referred for cardiac valve surgery. *J Am Coll Cardiol* 2006;48(8):1658-65.

11. Reant P, Brunot S, Lafitte S, Serri K, Leroux L, Corneloup O, Iriart X, Coste P, Dos Santos P, Roudaut R, Laurent F. Predictive value of noninvasive coronary angiography with multidetector computed tomography to detect significant coronary stenosis before valve surgery. *Am J Cardiol* 2006;97(10):1506-10.
12. Russo V, Gostoli V, Lovato L, Montalti M, Marzocchi A, Gavelli G, Branzi A, Di Bartolomeo R, Fattori R. Clinical value of multidetector CT coronary angiography as a pre-operative screening test before noncoronary cardiac surgery. *Heart* 2006.
13. Malagutti P, Nieman K, Meijboom WB, van Mieghem CA, Pugliese F, Cademartiri F, Mollet NR, Boersma E, de Jaegere PP, de Feyter PJ. Use of 64-slice CT in symptomatic patients after coronary bypass surgery: evaluation of grafts and coronary arteries. *Eur Heart J* 2006.
14. Gasparovic H, Rybicki FJ, Millstine J, Unic D, Byrne JG, Yucel K, Mihaljevic T. Three dimensional computed tomographic imaging in planning the surgical approach for redo cardiac surgery after coronary revascularization. *Eur J Cardiothorac Surg* 2005;28(2):244-9.
15. Aviram G, Sharony R, Kramer A, Neshet N, Loberman D, Ben-Gal Y, Graif M, Uretzky G, Mohr R. Modification of surgical planning based on cardiac multidetector computed tomography in reoperative heart surgery. *Ann Thorac Surg* 2005;79(2):589-95.
16. Herzog C, Dogan S, Diebold T, Khan MF, Ackermann H, Schaller S, Flohr TG, Wimmer-Greinecker G, Moritz A, Vogl TJ. Multi-detector row CT versus coronary angiography: preoperative evaluation before totally endoscopic coronary artery bypass grafting. *Radiology* 2003;229(1):200-8.
17. Feuchtner GM, Dichtl W, Friedrich GJ, Frick M, Alber H, Schachner T, Bonatti J, Mallouhi A, Frede T, Pachinger O, zur Nedden D, Muller S. Multislice computed tomography for detection of patients with aortic valve stenosis and quantification of severity. *J Am Coll Cardiol* 2006;47(7):1410-7.
18. Bonow RO, Carabello B, de Leon AC, Jr., Edmunds LH, Jr., Fedderly BJ, Freed MD, Gaasch WH, McKay CR, Nishimura RA, O'Gara PT, O'Rourke RA, Rahimtoola SH, Ritchie JL, Cheitlin MD, Eagle KA, Gardner TJ, Garson A, Jr., Gibbons RJ, Russell RO, Ryan TJ, Smith SC, Jr. Guidelines for the management of patients with valvular heart disease: executive summary. A report of the American College of Cardiology/American Heart Association Task Force on Practice Guidelines (Committee on Management of Patients with Valvular Heart Disease). *Circulation* 1998;98(18):1949-84.
19. Nieman K, Pattynama PM, Rensing BJ, Van Geuns RJ, De Feyter PJ. Evaluation of patients after coronary artery bypass surgery: CT angiographic assessment of grafts and coronary arteries. *Radiology* 2003;229(3):749-56.
20. Martuscelli E, Romagnoli A, D'Eliseo A, Tomassini M, Razzini C, Sperandio M, Simonetti G, Romeo F, Mehta JL. Evaluation of venous and arterial conduit patency by 16-slice spiral computed tomography. *Circulation* 2004;110(20):3234-8.

21. Schlosser T, Konorza T, Hunold P, Kuhl H, Schmermund A, Barkhausen J. Noninvasive visualization of coronary artery bypass grafts using 16-detector row computed tomography. *J Am Coll Cardiol* 2004;44(6):1224-9.
22. Salomon NW, Page US, Bigelow JC, Krause AH, Okies JE, Metzdorff MT. Reoperative coronary surgery. Comparative analysis of 6591 patients undergoing primary bypass and 508 patients undergoing reoperative coronary artery bypass. *J Thorac Cardiovasc Surg* 1990;100(2):250-9; discussion 259-60.
23. Gilkeson RC, Markowitz AH, Ciancibello L. Multisection CT evaluation of the reoperative cardiac surgery patient. *Radiographics* 2003;23 Spec No:S3-17.

14

Preoperative Computed Tomography Coronary Angiography to Detect Significant Coronary Artery Disease in Patients Referred for Cardiac Valve Surgery

Journal of American College of Cardiology.
2006 Oct 17;48(8):1658-65.

Willem B. Meijboom, MD^{1,2},
Nico R. Mollet, MD, PhD^{1,2},
Carlos A.G. Van Mieghem,
MD^{1,2}, Jolanda Kluin, MD,
PhD³, Annick C. Weustink,
MD^{1,2}, Francesca Pugliese
MD^{1,2}, Eleni Vourvouri, MD,
PhD^{1,2}, Filippo Cademartiri,
MD, PhD^{1,2}, Ad J.J.C.
Bogers, MD, PhD³, Gabriel P.
Krestin, MD, PhD², Pim J. de
Feijter, MD, PhD, FACC^{1,2}

¹ Department of Cardiology,
Thoraxcenter,

² Department of Radiology,

³ Department of Cardiothoracic
Surgery, Thoraxcenter,
Erasmus Medical Center,
Rotterdam, the Netherlands

ABSTRACT

Objectives

We studied the diagnostic performance of 64-slice CT coronary angiography (CTCA) to rule out or detect significant coronary stenosis in patients referred for valve surgery.

Background

Invasive conventional coronary angiography (CCA) is recommended in most of patients scheduled for valve surgery.

Methods

During a 6-month period, 145 patients were prospectively identified from a consecutive patient population scheduled for valve surgery. Thirty-five patients were excluded because of CTCA criteria; irregular heart rhythm (n= 26), impaired renal function (n=5) and known contrast allergy (n= 4). General exclusion criteria were; hospitalization in community hospital (n=4), no need for CCA (n=4), previous coronary artery bypass surgery (n=1) or percutaneous coronary intervention (n=4). Of the remaining 97 patients, 27 denied written informed consent. Thus, the study population comprised 70 patients (49 male, 21 female; mean age 63 ± 11 years).

Results

Prevalence of significant coronary artery disease, defined as having at least one $\geq 50\%$ stenosis per patient was 25.7%. Beta-blockers were administered in 71% and 64% received lorazepam. The mean heart rate dropped from 72.5 ± 12.4 to 59.5 ± 7.5 bpm. The mean scan time was 12.8 ± 1.3 seconds. On a per-patient analysis the sensitivity, specificity, positive and negative predictive value were: 100% (18/18; 95% CI, 78-100), 92% (48/52; 95% CI, 81-98), 82% (18/22; 95% CI, 59-94), 100% (48/48; 95% CI, 91-100), respectively.

Conclusions

The diagnostic accuracy of 64 slice CTCA for ruling out the presence of significant coronary stenoses in patients undergoing valve surgery is excellent and allows CTCA implementation as a gatekeeper for invasive CCA in these patients.

INTRODUCTION

Pre-operative detection of obstructive coronary artery disease (CAD) with conventional coronary angiography (CCA) is recommended in most of patients scheduled for valve surgery (1).

Although CCA is considered a safe procedure it still carries a small, but relevant risk for major (death, stroke or vascular dissection) and minor (inguinal haematoma) complications (2). Furthermore, the catheterization-procedure is rather expensive, as its invasive nature involves admission to a hospital or day-care facility and requires surveillance of an experienced team. A non-invasive patient-friendly pre-operative work-up for these patients would be desirable.

The newest-generation 64 slice CT scanner with improved spatial and temporal resolution shows excellent diagnostic accuracy to detect significant coronary artery lesions (3-6). In this study we evaluated the clinical value of computed tomography coronary angiography (CTCA) in patients scheduled for elective surgical valve surgery.

METHODS

Study population

During a 6-month period we screened 145 consecutive patients scheduled for valve surgery. Patients were contacted before their final pre-operative appointment requesting them to conduct an additional CTCA. Thirty-five patients were excluded because of CTCA criteria and 13 patients because of general criteria (Table 1). Of the remaining 97 patients 27 denied written informed consent. Thus, the study population comprised 70 patients (49 male, 21 female; mean age 63 ±

11 years). The institutional review board of the Erasmus MC Rotterdam approved the study and all subjects gave written informed consent.

Patient preparation

Patients with an aortic stenosis and a good left ventricular function (LVF) with a heart rate exceeding 65 bpm were given 50 mg metoprolol and 1 mg lorazepam 60 minutes before the CT-scan. If the LVF

Table 1. Patient Inclusion

Screened patient population	145
Atrial fibrillation/ severe arrhythmia	26
Impaired renal function (serum creatinine > 120 mmol/L)	5
Known contrast allergy	4
Patient population after CTCA exclusion criteria	110
Hospitalisation in community hospital	4
Percutaneous coronary intervention	4
Coronary artery bypass graft	1
No conventional angiogram	4
Patient population after general exclusion criteria	97
Refusal informed consent	27
Final patient population	70

was impaired beta-blockers were withheld and only lorazepam was administered. Patients with other valve pathology and a heart rate above 65 and 70 bpm were given 1 mg of lorazepam and 50 and 100 mg metoprolol, respectively. If the LVF was impaired in these patients the doses of beta blockers were reduced or not given.

Scan protocol

All scans were performed with a 64-slice CT scanner having a temporal resolution of 330 msec and a spatial resolution of 0.4 mm³ (Sensation 64, Siemens, Forchheim, Germany). Angiographic scan parameters were: number of slices per rotation, 32×2; individual detector width, 0.6 mm; table feed, 3.8 mm per rotation, tube voltage, 120 kV; tube current, 900 mAs. Prospective x-ray tube modulation was not used. Calcium scoring parameters (similar unless indicated) were a tube current of 150 mAs and prospective x-ray tube modulation was used. The radiation exposure for CTCA with this scan protocol was calculated as 15.2 to 21.4 mSv (for men and women respectively) using dedicated software (WinDose, Institute of Medical Physics, Erlangen, Germany) which is in line with previously reported x-ray radiation exposure (7,8). The radiation exposure of calcium scoring (including prospective x-ray tube modulation) was calculated as 1.3 to 1.7 mSv (for men and women, respectively) (9).

A bolus of 100 ml of contrast material (400 mgI/mL; IomeronTM, Bracco, Milan, Italy) was injected intravenously in an antecubital vein at 5 mL/s. A bolus-tracking technique was used to synchronize the arrival of contrast in the coronary arteries and the scan was started once the contrast material in the ascending aorta reached a predefined threshold of +100 Hounsfield units.

Image reconstruction

The post-processing technique to acquire the best possible image quality is previously described by Mollet et al. (6). In short, images are obtained during a half x-ray tube rotation, resulting in an effective temporal resolution of 165 msec. Images were reconstructed with ECG gating to obtain near motion-free image quality. Optimal data sets were reconstructed in the mid- to end-diastolic phase. If non-diagnostic image quality was obtained, additional datasets were reconstructed in the end systolic phase.

Quantitative coronary angiography (QCA)

All scans were carried out within two months after CCA. One experienced cardiologist, unaware of the results of CTCA, identified and analyzed all coronary segments, using a 17-segment modified AHA classification (10).

All segments, regardless of size, were included for comparison with CTCA. Segments were classified as normal (smooth parallel or tapering borders), as having non-significant disease (wall irregularities or <50% stenosis) or having significant stenosis (stenosis ≥50%). Stenoses were

evaluated in two orthogonal views, and were classified as significant if the mean lumen diameter reduction exceeded 50 % measured by validated quantitative coronary angiography (QCA) algorithm (CAAS, Pie Medical, Maastricht, the Netherlands).

CT image evaluation

One observer analyzed total calcium scores of all patients with dedicated software and results were expressed as Agatston score (11). Two experienced observers, a radiologist and a cardiologist, unaware of the results of CCA, evaluated the CTCA data sets on an offline workstation (Leonardo, Siemens, Forchheim, Germany). The axial slices were initially evaluated for the presence of significant segmental disease and additionally (curved) multiplanar reformatted reconstructions were used. Segments distally to a chronic total occlusion were excluded because of poor distal filling by collaterals. Inter-observer disagreements were resolved by consensus in a joint session.

Statistical analysis

The diagnostic performance of CTCA for the detection of significant stenoses in the coronary arteries with QCA as the standard of reference is presented as sensitivity, specificity, positive- and negative predictive values with the corresponding 95% CIs. Positive (Sensitivity/ [1-Specificity]) and negative ([1-Sensitivity]/Specificity) likelihood ratios are given. The likelihood ratio incorporates both the sensitivity and specificity of a test and provides a direct estimate of how much a test result will change the odds of having a disease. Post-test odds can be calculated by multiplying the pre-test odds by the likelihood ratios.

Comparison between CTCA and QCA was performed on three levels: patient-by-patient, vessel-by-vessel and segment-by-segment analysis. Furthermore, the relation of angina pectoris to angiographically significant CAD was analyzed.

A subanalysis was performed for patients with aortic stenosis compared to other valve pathology and patients with or without angina pectoris. An unpaired two sided student t test was performed to reveal possible differences in age, calcium score and heart rate during the CTCA between both groups. P-values <.05 were considered statistically significant.

An additional sensitivity analysis was done to investigate the effect of nesting; repeated assessments (segment by segment and vessel by vessel) within the same patient were made that were not independent observations. Interobserver and intraobserver variability for the detection of significant coronary stenosis was determined by *k*-statistics.

Table 2. Patient demographics (n=70)

Age (yrs) §	63 ± 11 (35-80)
Aortic stenosis (yrs) §	68 ± 8 (44-80)
Other valve pathology (yrs) §	59 ± 11 (35-80)
Males	49/70 (70)
Symptoms	
Angina pectoris	21 (30)
No angina pectoris	49 (70)
Previous MI	5 (7)
Risk factors	
Hypertension	33 (47)
Hypercholesterolemia	29 (41)
Diabetes mellitus	2 (3)
Smoker	15 (21)
Ex-smoker	4 (6)
Family history of CAD	26 (37)
Obese (body mass index ≥ 30 kg/m ²)	11 (16)
Calcium score, median*	214.4
Aortic stenosis, median*	391.9
Other valve pathology, median*	116.6
Valve operation	
Aortic valve stenosis	31 (44)
Mitral valve insufficiency	24 (34)
Aortic valve insufficiency	9 (13)
Mitral valve stenosis	2 (3)
Pulmonary valve insufficiency	2 (3)
Congenital aortic stenosis	2 (3)
Tricuspid valve insufficiency	1 (1)
Tricuspid valve stenosis	1 (1)
Re-operation	6 (9)
Conventional angiography	
Absence of coronary disease	17 (24)
Nonsignificant disease	35 (50)
Single-vessel disease	11 (16)
Multivessel disease	7 (10)

Values are n (%) unless otherwise indicated

§ Ranges age

*Agatston score

RESULTS

Patient demographics are shown in Table 2. One patient had combined valve pathology: aortic stenosis and mitral regurgitation. Beta-blockers were administered in 71% of patients and 64% received lorazepam. The mean heart rate in these patients dropped within 60 minutes from 73±12 to 60±8 bpm. The mean scan time was 12.8±1.3 seconds. Initially all data-sets were reconstructed in the mid-to end diastolic phase. In 30% of the cases (21/70) additional higher quality reconstructions from data of the end-systolic phase were used.

Diagnostic performance of 64-slice CT coronary angiography: patient-by-patient analysis

The diagnostic performance of CTCA for detecting significant stenoses on a patient-based analysis is detailed in Table 3. CTCA documented absence of significant disease in 48 patients for an overall specificity per-patient of 92 % (Figure 1). The severity of a stenosis was overestimated in four patients who were misclassified as having significant CAD. CTCA correctly identified significant disease in all patients (18/70, prevalence 25.7%) with at least one significant stenosis, resulting in a sensitivity per-patient of 100% (Figure 2). An accurate determination of the presence or absence of significant coronary artery disease was made in 66 of 70 patients (94%). In 3 out of 11 patients with single-vessel disease, another stenosis was detected with CTCA. The sever-

ity of these stenoses was overestimated, which resulted in incorrect classification as multivessel disease. Agreement between CTCA and QCA on a per-patient level was very good (k -value, 0.86), agreement between both techniques for classifying patients as having no, single vessel or multivessel disease was good (k -value, 0.78).

Diagnostic performance of 64-slice CT coronary angiography: vessel-by-vessel analysis

The mean total per vessel calcium score for the LAD, RCA and CX was 96.72, 47.89 and 40.22, respectively. The diagnostic performance of CTCA for detecting significant stenoses is detailed in Table 3. All vessels with significant disease, as classified by QCA, were detected with CTCA. Of a total of 280 vessels, the severity of the stenoses in these eight vessels, six in the LAD and two in the RCA, were overestimated and scored as false positives. Agreement between CTCA and QCA on a per-vessel level was very good (k -value, 0.85).

Diagnostic performance of 64-slice CT coronary angiography: segment-by-segment analysis

A total of 1003 segments were included for comparison with QCA. Inter- and intraobserver variability for detection of a significant stenosis per segment had a k -value of 0.71 and 0.74, respectively. The diagnostic performance of CTCA for detecting significant stenoses is detailed in Table 3. Two significant stenoses were detected by CTCA but the severity of the stenosis was underestimated. Both lesions were adjacent to a correctly detected stenosis. Eighteen non-significant

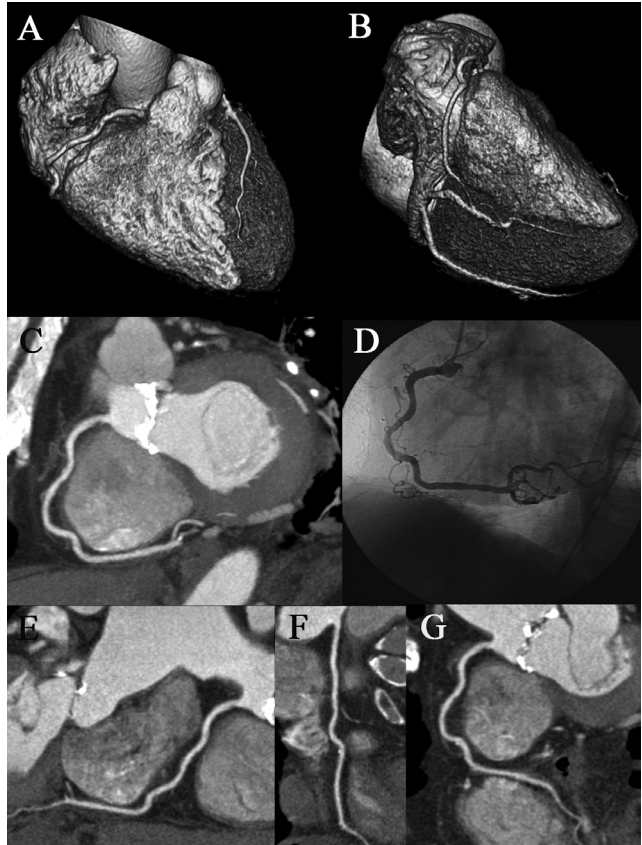


Figure 1. Three different types of post-processing techniques are shown: volume-rendered (VRT) CTCA images (A,B), a maximum intensity projected (MIP)- (C) and three curved multiplanar reconstructed images (cMPR, E,F,G) show a patent right coronary artery which is confirmed by CCA (D). The bright white spots (C, E, G) represent calcifications of the stenotic aortic valve. (A full color version of this illustration can be found in the color section).



Figure 2. Volume-rendered (VRT) CTCA image (A,B) reveal the anatomy of the left coronary artery. Two cMPR (E,F) disclose a significant stenosis in the left anterior descending coronary artery which was corroborated by CCA (C,D). Although the VRT images provide an excellent overview of the coronary anatomy they should not be used for the diagnostic assessment of presence of coronary stenoses. (A full color version of this illustration can be found in the color section).

stenoses were detected with CT and the severity of the stenoses was overestimated resulting in false positive scores. CCA revealed 5 wall irregularities and 13 nonsignificant stenoses, while the majority (83.3%, 15 of 18) of these segments was calcified.

The presence of coronary calcium induced overestimation of the severity of these stenoses with the CT scan (Table 4). Agreement between CTCA and QCA on a per-segment level was good (k -value, 0.76).

To exclude the possible confounding effect of nesting random selection of a single segment per patient was done and the diagnostic accuracy for detecting significant artery disease

resulted in a sensitivity 100 % (5 of 5; 95% CI, 46 to 100), specificity 98 % (63 of 64; 95% CI, 90 to 100), positive predictive value 83 % (5 of 6; 95% CI, 36 to 99), negative predictive value 100 % (63 of 63; 95% CI, 93 to 100).

Sub-analysis for patients with aortic stenosis vs. other valve pathology

The sub-analysis comprised 31 patients with aortic stenosis and 39 with other valve pathology. The diagnostic performance of CTCA for detecting significant stenoses on a patient-based analysis in patients with and without aortic stenosis is detailed in Table 3. The average age (68 vs. 59 yrs.; p : 0.0004) and calcium score (391.9 vs. 116.6; p : 0.02) of patients with aortic stenosis was significantly higher than in patients not having aortic stenosis (Table 2). The heart rate during CTCA for both groups was the same (both 60 bpm).

The relation of angina pectoris to significant coronary artery disease

The discordance between angina pectoris and the presence of significant CAD is displayed in Figure 3. Twenty-one patients had angina pectoris of which 8 had significant obstructive disease. Moreover, 10 patients out of 49 without angina pectoris did have significant stenoses. The diag-

Table 3. Diagnostic Performance and Predictive Value of 64-Slice CT Coronary Angiography for the Detection of $\geq 50\%$ Stenosis on QCA

	Prevalence of disease, %	n	TP	TN	FP	FN	Kappa	Sensitivity, %	Specificity, %	PPV, %	NPV, %	+LR	-LR
Patient based analysis	25.7	70	18	48	4	0	0.86	100 (78-100)	92 (81-98)	82 (59-94)	100 (91-100)	13,00	0,00
Vessel based analysis	9.3	280	26	246	8	0	0.85	100 (84-100)	97 (94-99)	76 (58-89)	100 (98-100)	31,75	0,00
RCA	14.3	70	10	58	2	0	0.89	100 (66-100)	97 (84-99)	83 (51-97)	100 (92-100)	30,00	0,00
LM	0.0	70	0	70	0	0	-	-	100 (94-100)	-	100 (94-100)	-	-
LAD	14.3	70	10	54	6	0	0.72	100 (66-100)	90 (79-96)	63 (36-84)	100 (92-100)	10,00	0,00
CX	8.6	70	6	64	0	0	1.00	100 (52-100)	100 (93-100)	100 (52-100)	100 (93-100)	∞	0,00
Segment based analysis	3.6	1003	34	949	18	2	0.76	94 (80-99)	98 (97-99)	65 (51-78)	100 (99-100)	50,74	0,06
Patient based sub-analysis													
AP	38.1	21	8	12	1	0	0.90	100 (60-100)	92 (62-100)	89 (51-99)	100 (70-100)	13,00	0,00
No AP	20.4	49	10	36	3	0	0.83	100 (66-100)	92 (78-98)	77 (46-98)	100 (88-100)	13,00	0,00
AS	29.0	31	9	19	3	0	0.79	100 (63-100)	86 (64-96)	75 (43-93)	100 (79-100)	7,33	0,00
No AS	23.1	39	9	29	1	0	0.93	100 (63-100)	97(81-100)	90 (54-99)	100 (85-100)	30,00	0,00

TP indicates true positive; TN, true negative; FP, false positive; FN, false negative; PPV, positive predictive value; NPV, negative predictive value; +LR, positive likelihood ratio; -LR, negative likelihood ratio; RCA, right coronary artery; LM, left main coronary artery; LAD, left anterior descending coronary artery; LCx, circumflex coronary artery; AP, angina pectoris; AS, aortic stenosis; MR, mitral regurgitation.

According to the 17-segment modified AHA classification 1003 segments and 280 vessels visualized with conventional angiogram were included for segment and vessel analysis, respectively. For patient-based analysis 70 patients were included, which were divided according to symptoms of angina pectoris. Sub-analysis for AS (n: 31) and other valve pathology is described. Values in parentheses represent 95% CIs.

Table 4. Influence of Coronary Calcifications on Diagnostic Accuracy of 64-slice CT Coronary Angiography on a Segment-based Analysis

Calcium score	n (pat.)	n (segm.)	Agatston Score, Mean (\pm SD)	TP	TN	FP	FN	Kappa	Sensitivity, %	Specificity, %	PPV, %	NPV, %
0-10	23	338	0.3 \pm 0,9	0	338	0	0	-	-	100 (99-100)	-	100 (99-100)
11-400	33	465	184 \pm 131	15	443	7	0	0.80	100 (75-100)	98 (97-99)	68 (45-85)	100 (99-100)
401-1000	10	146	675 \pm 23	16	124	5	1	0.82	94 (69-100)	96 (91-99)	76 (52-91)	99 (95-100)
> 1000	4	54	1394 \pm 273	3	44	6	1	0.40	75 (22-99)	88 (75-95)	33 (9-69)	98 (87-100)

TP indicates true positive; TN, true negative; FP, false positive; FN, false negative; PPV, positive predictive value; NPV, negative predictive value.

Values in parentheses represent 95% CIs.

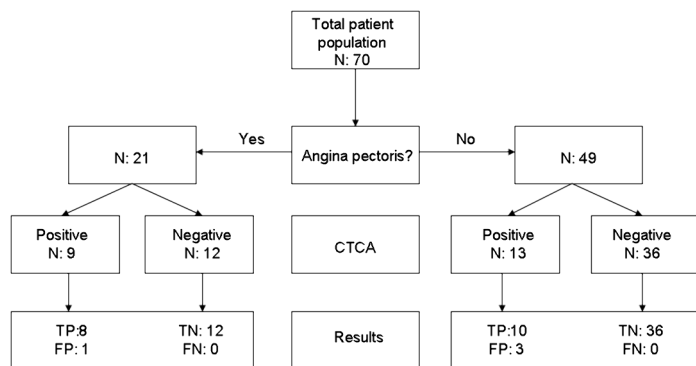


Figure 3. TP indicates true positive; TN, true negative; FP, false positive; FN, false negative.

nostic accuracy of angina pectoris was calculated and the sensitivity, specificity, positive and negative predictive value were 44% (8 of 18; 95% CI, 22 to 67), 75% (39 of 52; 95% CI, 61 to 86), 38% (8 of 21; 95% CI, 19 to 61) and 80%, (39 of 49; 95% CI, 65 to 89), respectively.

DISCUSSION

The presence of concomitant obstructive coronary artery disease in patients undergoing cardiac valvular surgery worsens prognosis (12-14). Various studies have shown that combined valve and bypass surgery of significant CAD, reduced early and late mortality (13,15). Because aortic stenosis and CAD share common risk factors and occur with advancing age and mitral regurgitation is often the consequence of CAD, concomitant significant CAD is found in approximately one third of these patients (16-19). Angina pectoris is present in 25%–to 35% of patients with valvular heart disease. Angina pectoris is a poor predictor of obstructive CAD in patients with valvular disease because angina pectoris can have multiple causes such as left ventricular enlargement, increased wall stress or wall thickening with subendocardial ischemia (17,20). This was also shown in our study and the low sensitivity of 44% and specificity of 75% is in keeping with the results observed in earlier reports. The value of non-invasive ECG-stress testing to detect concomitant CAD is limited due to the presence of left ventricular hypertrophy and left bundle branch block in patients with valvular disease. Resting or exercise induced wall motion abnormalities and myocardial perfusion abnormalities, as seen with stress echo and nuclear tests lack sufficient accuracy for reliable detection of concomitant CAD (21-24).

Due to the poor predictive value of angina pectoris and the lack of accuracy of non-invasive tests, the following guideline is recommended by the ACC/AHA committee; pre operative CCA is indicated in symptomatic patients and/or those with left ventricular dysfunction in men ≥ 35 years, pre-menopausal women ≥ 35 years with risk factors for CAD, and post-menopausal women (1). Non-invasive coronary angiography using 4 and 16 slice computed tomography is a relatively

recent development. The early results were promising but lacked sufficient robustness to be useful in clinical practice, but the diagnostic performance of 64 slice CT-scanners to detect coronary stenoses is very good in patients who have a high prevalence (more than 70%) of CAD. In these patients the negative predictive value of 64 CT-scanners is very high, allowing to exclude the presence of significant coronary artery disease (3-6). However, there is little information about the diagnostic performance of CT-coronary angiography in patients with a low or intermediate prevalence of coronary artery disease.

In our study the prevalence of concomitant CAD was 25.7%. We found that significant coronary stenoses were detected using a 64 slice CT scanner with a sensitivity of 100% and a specificity of 92% compared with CCA. A negative CT scan was correct in 92% (48 out of 52) patients in ruling out significant disease and all patients (18/18) with significant CAD were correctly diagnosed. The stenosis severity was overestimated in 4 patients using CTCA. Given the high reliability of CTCA, this would mean that CCA could have been avoided in 69% (48/70) of patients, in 26% (18/70) a CCA was performed to confirm the CTCA diagnosis and in 6% (4/70) an unnecessary CCA would have been performed on the basis of CTCA outcome.

Coronary calcium

The presence of calcium causes problems in the correct interpretation of the CTCA. Calcium creates blooming artefacts, which obscure the visualization of the underlying non-calcified plaque or lumen. Calcium tends to overestimate the severity of adjacent lesions either due to the blooming effect itself or in case of doubt or fear of “missing” a significant stenosis a “defensive” scoring is exercised. This has led to an ongoing debate whether a CTCA should be aborted when the calcium score exceeds a certain threshold. A generally accepted cut-off value is lacking and proposed thresholds are arbitrarily chosen. Usually a cut-off level is chosen derived from the total calcium score. The total calcium score is somewhat misleading, because calcium distributed along the entire coronary tree would make the interpretation of a CTCA examination relatively easy, while a single heavily calcified plaque would make interpretation doubtful.

Recently, Gilard et al. reported of a good accuracy of a 16 slice scanner in 55 patients referred for elective aortic valve surgery who had a mean calcium score of 609 ± 860 (25). They used the Agatston score of ≥ 1000 as a cut-off point by showing that patients with this score had a higher frequency of non-interpretable segments. In our subgroup of patients with aortic stenosis we found, not unexpectedly, also a higher calcium score. In this subgroup the diagnostic accuracy of CTCA was lower because the extensive calcifications negatively influenced grading of stenoses and resulted in overestimation of the stenosis severity.

What would be the role of CTCA in patients referred for CCA prior to cardiac valve surgery? We do recommend to first obtain a calcium score in all patients without atrial fibrillation, persistent

irregular heart rhythm or renal dysfunction. If the calcium score exceeds ≥ 1000 , we would advise not to proceed with CTCA. If lower, patients may be advised to undergo CTCA. Patients with a scan negative for significant CAD can directly be referred for cardiac valve surgery. In case of doubt, and in the presence of significant CAD, a confirmative CCA is required to either confirm or refute the presence of significant CAD.

Heart rate reduction in patients in patients with heart rates > 65 bpm is part of the protocol used with current 64 slice CT-scanners to increase image quality. Next generation dual-source CT scanners will allow scanning at higher heart rates due to the improved temporal resolution of 83 ms, thereby avoiding the use of heart rate reduction with beta-blockers (26,27). Especially, patients with severe aortic stenosis would benefit since the administration of beta-blockers is limited. The radiation exposure can be decreased with the ultrafast dual-source CT scanner during higher heart rates and use of x-ray tube modulation compared to 64 slice CT scanning.

LIMITATIONS OF THE STUDY

The presence of atrial fibrillation, which occurs frequently with mitral valve disease precludes the use of CTCA and was indeed a significant reason for exclusion in our study. Only patients scheduled for elective valve surgery were screened and patients in acute settings with hemodynamic compromise were not studied. Since most patients were referred from community hospitals for valve surgery, the pre-operative diagnostic work-up, including the CCA, was performed in many study patients which may have created a bias, although the CT scoring was done blinded to the coronary angiogram. The rather high radiation exposure of CTCA as compared to conventional coronary angiography is of concern (7,8). The radiation exposure can be reduced by 50% with use of prospective X-ray tube current modulation (28). However, this limits the possibility to reconstruct valuable datasets during the end-systolic phase (29). In our study we found that 30% of the patients end-systolic phase reconstructions were useful and were of higher image quality than the mid-to-end diastolic phase reconstructed images.

CONCLUSIONS

The diagnostic accuracy of 64 slice CTCA for ruling out the presence of significant coronary lesions in patients undergoing elective valve surgery is excellent and allows CTCA implementation as a gatekeeper in these patients.

REFERENCES

1. Bonow RO, Carabello B, de Leon AC, Jr., et al. Guidelines for the management of patients with valvular heart disease: executive summary. A report of the American College of Cardiology/American Heart Association Task Force on Practice Guidelines (Committee on Management of Patients with Valvular Heart Disease). *Circulation* 1998;98:1949-84.
2. Scanlon PJ, Faxon DP, Audet AM, et al. ACC/AHA guidelines for coronary angiography. A report of the American College of Cardiology/American Heart Association Task Force on practice guidelines (Committee on Coronary Angiography). Developed in collaboration with the Society for Cardiac Angiography and Interventions. *J Am Coll Cardiol* 1999;33:1756-824.
3. Leschka S, Alkadhi H, Plass A, et al. Accuracy of MSCT coronary angiography with 64-slice technology: first experience. *Eur Heart J* 2005.
4. Raff GL, Gallagher MJ, O'Neill WW, Goldstein JA. Diagnostic accuracy of noninvasive coronary angiography using 64-slice spiral computed tomography. *J Am Coll Cardiol* 2005;46:552-7.
5. Leber AW, Knez A, von Ziegler F, et al. Quantification of obstructive and nonobstructive coronary lesions by 64-slice computed tomography: a comparative study with quantitative coronary angiography and intravascular ultrasound. *J Am Coll Cardiol* 2005;46:147-54.
6. Mollet NR, Cademartiri F, van Mieghem CA, et al. High-resolution spiral computed tomography coronary angiography in patients referred for diagnostic conventional coronary angiography. *Circulation* 2005;112:2318-23.
7. Hausleiter J, Meyer T, Hadamitzky M, et al. Radiation dose estimates from cardiac multislice computed tomography in daily practice: impact of different scanning protocols on effective dose estimates. *Circulation* 2006;113:1305-10.
8. Coles DR, Smail MA, Negus IS, et al. Comparison of radiation doses from multislice computed tomography coronary angiography and conventional diagnostic angiography. *J Am Coll Cardiol* 2006;47:1840-5.
9. Trabold T, Buchgeister M, Kuttner A, et al. Estimation of radiation exposure in 16-detector row computed tomography of the heart with retrospective ECG-gating. *Rofo* 2003;175:1051-5.
10. Austen WG, Edwards JE, Frye RL, et al. A reporting system on patients evaluated for coronary artery disease. Report of the Ad Hoc Committee for Grading of Coronary Artery Disease, Council on Cardiovascular Surgery, American Heart Association. *Circulation* 1975;51:5-40.
11. Agatston AS, Janowitz WR, Hildner FJ, Zusmer NR, Viamonte M, Jr., Detrano R. Quantification of coronary artery calcium using ultrafast computed tomography. *J Am Coll Cardiol* 1990;15:827-32.
12. Lytle BW. Impact of coronary artery disease on valvular heart surgery. *Cardiol Clin* 1991;9:301-14.

13. Mullany CJ, Elveback LR, Frye RL, et al. Coronary artery disease and its management: influence on survival in patients undergoing aortic valve replacement. *J Am Coll Cardiol* 1987;10:66-72.
14. Jung B, Drissi MF, Michel PL, et al. Prognosis of valve replacement for aortic stenosis with or without coexisting coronary heart disease: a comparative study. *J Heart Valve Dis* 1993;2:430-9.
15. Lund O, Nielsen TT, Pilegaard HK, Magnussen K, Knudsen MA. The influence of coronary artery disease and bypass grafting on early and late survival after valve replacement for aortic stenosis. *J Thorac Cardiovasc Surg* 1990;100:327-37.
16. Vandeplas A, Willems JL, Piessens J, De Geest H. Frequency of angina pectoris and coronary artery disease in severe isolated valvular aortic stenosis. *Am J Cardiol* 1988;62:117-20.
17. Alexopoulos D, Kolovou G, Kyriakidis M, et al. Angina and coronary artery disease in patients with aortic valve disease. *Angiology* 1993;44:707-11.
18. Olofsson BO, Bjerle P, Aberg T, Osterman G, Jacobsson KA. Prevalence of coronary artery disease in patients with valvular heart disease. *Acta Med Scand* 1985;218:365-71.
19. Ramsdale DR, Bennett DH, Bray CL, Ward C, Beton DC, Faragher EB. Angina, coronary risk factors and coronary artery disease in patients with valvular disease. A prospective study. *Eur Heart J* 1984;5:716-26.
20. Green SJ, Pizzarello RA, Padmanabhan VT, Ong LY, Hall MH, Tortolani AJ. Relation of angina pectoris to coronary artery disease in aortic valve stenosis. *Am J Cardiol* 1985;55:1063-5.
21. Rask P, Karp K, Edlund B, Eriksson P, Mooe T, Wiklund U. Computer-assisted evaluation of dipyridamole thallium-201 SPECT in patients with aortic stenosis. *J Nucl Med* 1994;35:983-8.
22. Samuels B, Kiat H, Friedman JD, Berman DS. Adenosine pharmacologic stress myocardial perfusion tomographic imaging in patients with significant aortic stenosis. Diagnostic efficacy and comparison of clinical, hemodynamic and electrocardiographic variables with 100 age-matched control subjects. *J Am Coll Cardiol* 1995;25:99-106.
23. Kettunen R, Huikuri HV, Heikkila J, Takkunen JT. Preoperative diagnosis of coronary artery disease in patients with valvular heart disease using technetium-99m isonitrile tomographic imaging together with high-dose dipyridamole and handgrip exercise. *Am J Cardiol* 1992;69:1442-5.
24. Kupari M, Virtanen KS, Turto H, et al. Exclusion of coronary artery disease by exercise thallium-201 tomography in patients with aortic valve stenosis. *Am J Cardiol* 1992;70:635-40.
25. Gilard M, Cornily JC, Pennec PY, et al. Accuracy of multislice computed tomography in the preoperative assessment of coronary disease in patients with aortic valve stenosis. *J Am Coll Cardiol* 2006;47:2020-4.

26. Flohr TG, McCollough CH, Bruder H, et al. First performance evaluation of a dual-source CT (DSCT) system. *Eur Radiol* 2006;16:256-68.
27. Achenbach S, Ropers D, Kuettner A, et al. Contrast-enhanced coronary artery visualization by dual-source computed tomography--initial experience. *Eur J Radiol* 2006;57:331-5.
28. Jakobs TF, Becker CR, Ohnesorge B, et al. Multislice helical CT of the heart with retrospective ECG gating: reduction of radiation exposure by ECG-controlled tube current modulation. *Eur Radiol* 2002;12:1081-6.
29. Vogl TJ, Abolmaali ND, Diebold T, et al. Techniques for the detection of coronary atherosclerosis: multi-detector row CT coronary angiography. *Radiology* 2002;223:212-20.

15

64-Slice CT in Symptomatic Patients After Coronary Bypass Surgery – Evaluation of Grafts and Coronary Arteries

European Heart Journal.
2007 Aug 28(15)1879-85.

Patrizia Malagutti, MD^{a,b},
Koen Nieman, MD, PhD^{a,b},
Willem B Meijboom, MD^{a,b},
Carlos AG van Mieghem,
MD^{a,b}, Francesca Pugliese,
MD^{a,b}, Filippo Cademartiri,
MD, PhD^{a,b}, Nico R Mollet,
MD, PhD^{a,b}, Eric Boersma,
PhD^a, Peter P de Jaegere, MD,
PhD^a, Pim J de Feyter, MD,
PhD, FACC^{a,b}

Erasmus Medical Centre,
Rotterdam, the Netherlands
^aDepartment of Cardiology,
Thorax centre
^bDepartment of Radiology

ABSTRACT

Objectives

We explored the diagnostic performance of 64-slice CT in symptomatic patients after bypass surgery, for the assessment of both grafts and native coronary arteries.

Background

Although previous generations of multi-slice CT have demonstrated accurate detection of obstructive bypass graft disease, progression of coronary disease is a more frequent cause for ischemic symptoms late after bypass graft surgery.

Methods

64-slice CT angiography (Siemens Sensation 64, Germany) was performed in 52 symptomatic patients, 10 ± 5 years after bypass surgery. Two independent, blinded observers assessed all grafts and coronary arteries for stenosis, using conventional quantitative angiography as a reference.

Results

A total of 109 grafts (182 graft segments), 123 distal coronary run-offs and 116 non-bypassed coronary branches (288 segments) were analyzed. Per-segment detection of graft disease yielded a sensitivity of 99% (71/72) and specificity of 96% (106/110). Sensitivity and specificity to detect run-off disease were 89% (8/9) and 93% (106/114), positive predictive value was 50% (8/16). In non-grafted coronary segments, CT detected significant stenosis with a sensitivity and specificity of 97% (62/64) and 86% (192/224). Overestimation occurred more frequently in calcified segments ($P=0.002$).

Conclusion

64-slice CT allows angiographic evaluation of grafts and coronary arteries, although overestimation of coronary obstruction occurs, particularly in the presence of calcified disease.

INTRODUCTION

Restoration of myocardial flow by coronary artery bypass surgery (CABG) is performed in approximately 300,000 patients in the USA, annually. Often this is not a permanent solution, as up to 10% of grafts occlude during or shortly after surgery, and 59% of venous grafts and 17% of arterial grafts occlude within 10 years.¹ Although symptoms may be the result of graft failure, anginal complaints later after surgery (nearly 50% within 6 years^{2,3} are mostly caused by progression of obstructive disease in the native coronary arteries.⁴

Although catheter-based angiography is the reference method for detection of bypass graft disease, it is an invasive procedure that is costly and carries potential risk of harm. Non-invasive tests such as exercise-ECG, stress- echocardiography and nuclear imaging are useful for detection of myocardial ischemia, but are unable to exactly determine the site and extent of obstructive disease. Therefore, a number of non-invasive imaging techniques have been explored for non-invasive angiographic assessment of coronary artery bypass grafts. Magnetic resonance imaging^{5,6}, conventional CT⁷⁻⁹, electron-beam computed tomography¹⁰⁻¹² and (multi-slice) spiral computed tomography (CT)¹³⁻²² all allow accurate detection of graft occlusion, and more recently graft stenosis, although assessment of the coronary arteries has rarely been included in these studies. In patients without graft surgery the diagnostic performance of MSCT coronary angiography is good²³⁻³² Only few studies in post-CABG patients have included the assessment of the native coronary arteries, and have shown only modest accuracy (using 4- and 16- slice CT) for the detection of obstructive disease.^{16,20}

Improved technical performance of current CT technology^{30,32}, may overcome some of the imaging challenges after bypass surgery. Therefore, we evaluated the diagnostic accuracy of 64-slice multislice spiral CT (MSCT) angiography in symptomatic patients who previously underwent bypass surgery. In addition to assessment of bypass grafts, distal coronary run-offs and non-grafted coronary arteries were included in this study.

METHODS

Population

Patients with stable symptoms suggesting obstructive graft or coronary artery disease that required coronary angiography (CA) were approached for this study. Exclusion criteria were an irregular heart rate, allergy to iodine contrast media and renal failure (serum creatinine >100 mmol/l). Between November 2004 and September 2005 a total of 77 stable patients, scheduled for (elective) catheter angiography, were consecutively screened. Seventeen patients had contraindications, while another eight potential candidates declined. The remaining 52 patients were enrolled and

Table 1. Population characteristics.

Population characteristics (N=52)	
Male (n)	45 (87%)
Age (years)	65.0±8.1
Body-mass index (kg/m ²)	27.8±3.3
History	
Family history of coronary disease (%)	25 (48%)
Nicotine abuse (%)	7 (13%)
Hypertension (%)	39 (75%)
Dislipidemia (%)	48 (92%)
Diabetes (%)	19 (36%)
Transient ischemic attack/stroke (%)	4 (8%)
Myocardial infarction (%)	33 (63%)
Interventions with use of stents (%)	20 (38%)
Graft anatomy per patient	
Single graft (n)	10 (19%)
Two graft (n)	30 (58%)
Three grafts (n)	9 (17%)
More than three grafts (n)	3 (6%)
Venous and arterial grafts (n)	
Venous grafts, no arterial grafts (n)	14 (27%)
Arterial grafts, no venous grafts (n)	7 (14%)
CT examination	
Heart rate before CT scan (min-1)	68.1±8.5
Heart during CT scan (min-1)	60.0±7.4
β-blocker (%)	34 (65%)
Benzodiazepine (%)	27 (52%)

True positive (TP); true negative (TN); false positive (FP); false negative (FN); interobserver variability (k); positive predictive value (PPV); negative predictive value (NPV). Between brackets: 95% confidence interval

heart rates). Detector collimation was 32 x 0.6 mm, the pitch was 0.2 (3.8 mm table advancement per rotation). By rapidly alternation the longitudinal position of the focal spot (Z-Sharp® technology, Siemens), 64 slices could be acquired simultaneously. The tube voltage was 120 kV, and the tube current varied between 800-900 mAs. Depending on the presence of arterial grafts or only venous material, the scan range was cranially extended. With a table speed of 11.6 mm/s the scan time was 15.4±2.3 seconds (range 11.9-22.4 s). Patients with a heart rate over 65 min-1 were given a β-blocker (up to 100 mg of metoprolol) and/or anxiolytic medication (1 mg of lorazepam) 45 minutes before the scan. In 25 out of 35 patients that received medication the average heart rate

underwent CT angiography in addition to conventional catheter-based angiography (table 1). The local ethical committee approved the study and all participants gave written informed consent.

The mean interval between bypass surgery and CT angiography was 10.3±5.1 years (range 1-23 years). Forty-five patients had venous bypass grafts and 38 had arterial bypass grafts. Of the 64 venous grafts, 29 were anastomosed to a single coronary branch and 35 were jump grafts with at least two consecutive coronary anastomoses. Of the 45 arterial grafts, 34 were single grafts and 11 had more than one coronary anastomosis. In seven patients both the right and left internal mammary artery were used. Six patients underwent redo-CABG, as a result of which 12 coronary artery branches were grafted twice on separate occasions. Twenty patients underwent percutaneous coronary intervention with stent implantation, with a total of 57 coronary and 6 graft stents.

Msct data acquisition

All patients were examined with a 64-slice spiral CT scanner (Sensation 64®, Siemens, Forchheim, Germany). The roentgen tube rotation time was 330 ms, resulting in an effective temporal resolution of 165 ms (or less using a bisegmental reconstruction algorithm at higher

was below 65 min during the scan, average heart rate reduction $8.1 \pm 1.1 \text{ min}^{-1}$. Ten patients were scanned with a heart rate over 65 min^{-1} . A bolus of 100 ml of iomeprol 400 mgI/ml (Iomeron®, Bracco, Milan, Italy) was intravenously injected at a rate 3.5-5 ml/s, depending on the size of the patient. Bolus tracking, i.e. monitoring of contrast enhancement in the aortic root during contrast injection, was applied to synchronize the data acquisition with the contrast enhancement.

ECG-synchronized images were reconstructed at several time points within the diastolic cardiac phase. Occasionally, end-systolic reconstruction offered better image quality. A sharper kernel was applied in addition to the standard medium sharp kernel, in the presence of stents. Generally, the examination, including patient preparation and image reconstruction, required between 20-30 min. All examinations were performed without complications.

Msc vessel analysis

Two readers independently reviewed the CT data. Readers were informed about the previous surgical procedures, but blinded with respect to the invasive angiographic results. In cases of disagreement a final decision was made during a joint reading. The following vessels and conduits were assessed:

Arterial and venous grafts: in case of more coronary anastomoses per arterial or venous graft (jump grafts), all graft sections between the proximal anastomosis (aortic root or subclavian artery) and each coronary insertion (graft segment) was separately assessed and classified as occluded, significantly obstructed (50-99% luminal narrowing), or not (significantly) obstructed (figure 1).

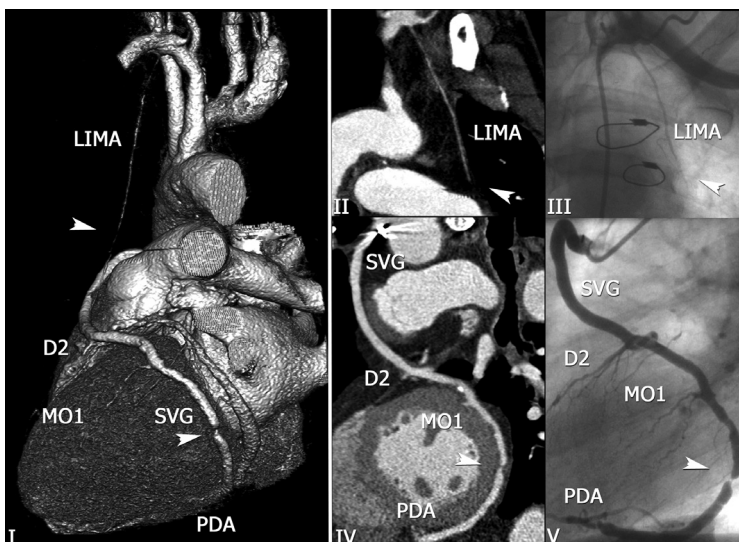


Figure 1. Arterial and venous graft disease.

Volume-rendered reconstruction (I) and curved multiplanar reformations (II,IV) of a CT scan and corresponding conventional angiography (III, V), which show an occluded left internal mammary artery (LIMA, arrow in I,II,III) and obstructed vein graft (SVG). The venous graft has three coronary anastomoses (and 3 graft segment): second diagonal branch (D2), first marginal branch (MO1), posterior descending artery (PDA), of which the terminal segment is significantly stenosed (arrow I,IV,V). (A full color version of this illustration can be found in the color section).

Distal coronary run-offs: all coronary branches that were supplied by a patent bypass graft were assessed for significant luminal narrowing ($>50\%$ lumen diameter reduction).

Native coronary arteries: coronary arteries that were not, or not completely revascularized at the time of surgery, were assessed per coronary segment, irrespective of the vessel diameter (17-segment ACC/AHA model)³³. The following coronary segments, unless anatomically absent, were assessed: proximal, middle and distal right coronary artery, posterior descending artery and (right) posterolateral branch, left main coronary artery, proximal, middle and distal left anterior descending coronary artery and (largest) first and second diagonal branch, the proximal and distal circumflex coronary artery with three obtuse marginal and/or posterolateral branches (and posterior descending branch in case of left dominance), and the intermediate branch, if present. Additionally, a per-vessel analysis (limited to segments without bypass graft anastomoses) was performed: right coronary artery, left main coronary artery, left anterior descending coronary artery and left circumflex branch (including intermediate branch).

Coronary arteries with occluded grafts: obstructive coronary disease proximal to the insertion of a patent graft was not included in the analysis. However, because of the therapeutic relevance in terms of amenability to percutaneous intervention, patency of coronary segments proximal and distal to occluded graft insertions was assessed.

Different post-processing tools were applied to locate lesions and classify luminal narrowing of the grafts and coronary branches. Double oblique, maximum-intensity projections were useful to locate suspect segments, particularly in the absence of severe calcifications or metal (stents, vascular clips). To assess stenosis severity axial slices and interactive (double-oblique) multiplanar reformation were used.

Stenosis severity was visually estimated by comparing the luminal diameter at the narrowing with (relatively) non-diseased locations immediately proximal and/or distal to the lesion. A stenosis was classified as significant if the minimal lumen diameter appeared $<50\%$ of the expected diameter, based on the proximal and distal reference site. Subjective confidence of assessment, which could be affected by calcification, stents, vascular clips, motion artifacts, etc, was evaluated per coronary/graft segment and classified as high (without doubt), moderate or low (insufficient image quality). Segmental coronary calcification was classified as absent, modest (isolated spots) or severe (extensive, dense and/or circumferential calcification). Coronary arteries or grafts with stents were not excluded from evaluation.

Conventional coronary angiography

The median interval between the CT examination and CA was 7 days (0.5-18.5). Selective X-ray angiography of the coronary arteries and bypass grafts was performed according to standard

techniques. An experienced cardiologist, who was unaware of the CT results, analyzed the angiographic findings. Using quantitative coronary angiography (QCA) evaluation (CAAS, Pie Medical Systems, Maastricht, the Netherlands), maximum diameter stenosis was determined out of at least two (orthogonal) projections. A quantitatively determined diameter stenosis of $\geq 50\%$ was considered significant.^{34,35} Classification criteria for segments and lesions were identical to those used for CT.

Statistical analysis

Descriptive statistics were performed for coronary segments and main coronary branches, graft segments and entire grafts, and patients. A coronary artery or graft was considered diseased if at least one segment was significantly obstructed. The diagnostic accuracy of CT for the detection of significant disease was expressed as sensitivity, specificity, positive predictive value, negative predictive value and accuracy. Precision of the diagnostic parameters was presented using a 95% confidence interval (CI). Continuous variables were reported as means and standard deviations (SDs) or median and interquartile ranges (IQR), as appropriate. Inter-observer variability for the assessment of significant coronary artery and graft obstruction was determined by *k* statistics. Comparison between different groups was calculated using Fisher's exact test. When appropriate, a Mantel-Haenszel Chi-square test was used in ordinal group comparisons. P values below 0.05 were considered significant. Because of potentially interdependent observations, i.e. multiple coronary segments in the same patient, descriptive statistic parameters were performed for a random selection of single observations per patient.

RESULTS

Bypass grafts

A total of 45 arterial grafts with 57 coronary anastomoses (representing 57 arterial graft segments) and 64 venous grafts with a total of 125 graft segments were analyzed. CT correctly assessed all arterial grafts and detected 14 occluded segments in 10 completely occluded grafts (figure 1,2). CT detected 41/43 occluded and 15/15 stenosed venous graft segments (figure 1,2,3). One missed segmental occlusion belonged to a stented graft, which contained additional occluded graft segments that were correctly detected by CT. CT incorrectly considered another completely occluded segment significantly stenosed but patent. Thus, sensitivity to detect obstructive graft disease (stenosis or occlusion) per-segment and per-graft was 99% and 100%, respectively (Table 2). Overestimation of disease occurred in 4 graft segments, of which 2 contained stents, and resulted in misclassification of one venous graft. There was complete agreement between observers for the detection of graft disease (table 2), and confidence of assessment for both arterial and venous grafts was high (89%) (table 3).

Table 2. Detection of significant graft and coronary artery disease.

	TP	TN	FP	FN	k	Sensitivity (%)	Specificity (%)	PPV (%)	NPV (%)
All grafts	109	49	59	1	0	0.96	100 (90.9-100)	98.3 (89.9-99.9)	100 (92.4-100)
Arterial grafts	45	10	35	0	1.0	100 (65.5-100)	100 (87.7-100)	100 (65.5-100)	100 (87.7-100)
Venous grafts	64	39	24	1	0	0.93	100 (88.8-100)	97.5 (85.3-99.9)	100 (82.8-100)
All graft segments	182	71	106	4	1	0.95	98.6 (91.5-99.9)	96.4 (90.4-98.8)	99.1 (94.2-99.9)
Arterial segments	57	14	43	0	1.0	100 (73.2-100)	100 (89.8-100)	100 (73.2-100)	100 (89.8-100)
Venous segments	125	57	63	4	1	0.93	98.3 (89.5-99.9)	94.0 (84.7-98.1)	98.4 (90.5-99.9)
Distal run-offs	123	8	106	8	1	0.92	88.8 (50.7-99.4)	93.0 (86.2-96.7)	99.0 (94.2-99.9)
Non-grafted native coronary arteries									
Coronary segments	288	62	192	32	2	0.86	96.9 (88.2-99.5)	85.7 (80.3-89.9)	99.0 (95.9-99.8)
Coronary vessels	116	42	50	24	0	0.83	100 (89.6-100)	68.4 (55.6-77.7)	100 (91.1-100)

Distal run-off

According to CA there were 125 patient graft segments, supplying 123 distal coronary run-offs. Ninety-two of these could be assessed with good or moderate confidence (75%). Small vessel size (diameter) contributed to reduced interpretability. CT detected nearly all lesions (8/9), although overestimation of stenosis frequently occurred (table 2, figure 3).

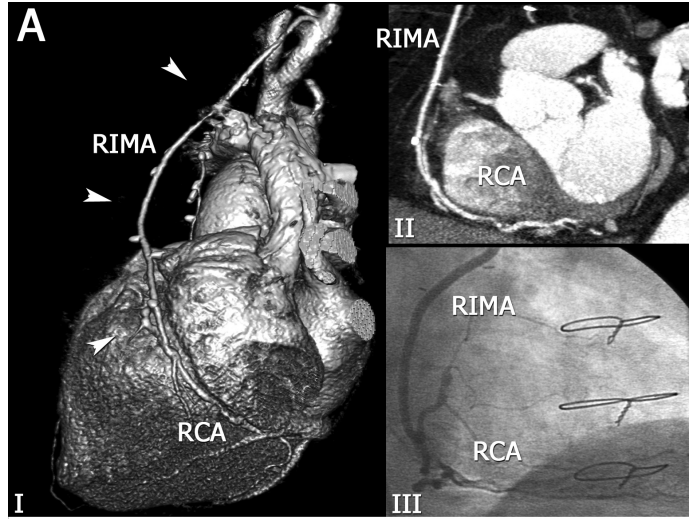
Coronary arteries

A total of 116 coronary arteries (including 288 segments) were not or incompletely revascularised by bypass surgery (figure 4). Significant stenosis was correctly detected in 62/64 coronary artery segments. Two undetected lesions by CT were located in vessels that contained additional lesions that were correctly detected by CT. Overestimation of stenosis severity frequently occurred resulting in a modest positive predictive value (66%).

Severe, modest and absent calcification was noted in 71 (25%), 100 (35%) and 117 (41%) of coronary segments. Of the 133 proximal and middle segments of the main branches (left main, right, left anterior descending and left circumflex branch) severe, moderate and absent calcification was detected in 46, 55 and 32 segments, respectively. Of the distal main and side branches (diagonal, marginal, posterolateral and posterior descending branches) severe, moderate and absent calcification was detected in

Figure 2. Patent right internal mammary artery graft.

Panel A. CT (Volume-rendered reconstruction (I), multiplanar reconstruction (II)) and conventional angiogram (III) of a patent right internal mammary artery (RIMA, arrows) connected to the RCA without obstructive disease. (A full color version of this illustration can be found in the color section).



25, 45 and 85 segments, respectively. Severe calcification was found in left main, right, left anterior descending and left circumflex coronary territory (including side branches) in 16/42 (38%), 17/81 (21%), 14/49 (29%) and 24/116 (21%)

segments, respectively. The accuracy of CT angiography for coronary segments with severe, moderate or absent calcification was 77.5%, 88%, 94.9%, respectively ($p=0.0004$). Accuracy was also

significantly lower in the presence of stents: 75.0% with and 90.1% without stents ($p=0.02$). For the detection of coronary stenosis, as well as run-off disease, accuracy was significantly lower in segments assessed with poor subjective confidence (table 3).

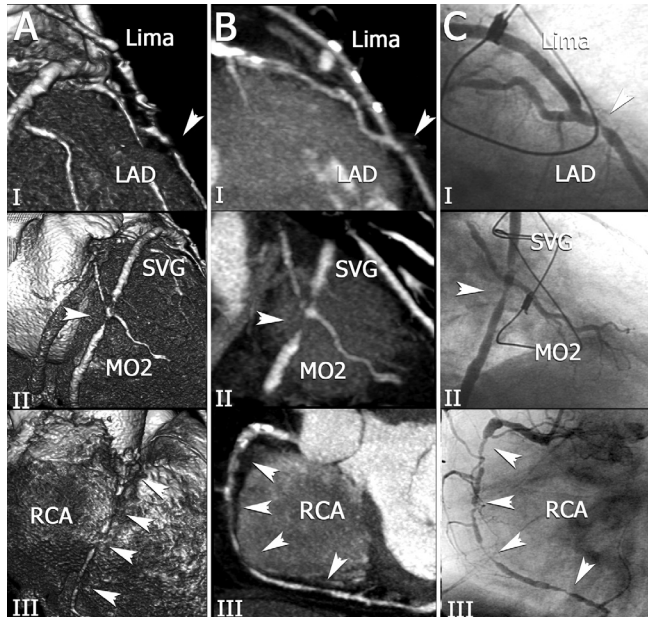


Figure 3. Bypass graft and coronary run-off disease.

CT (3D volume rendering (A); maximum intensity projection (B)) and conventional angiography (C), of a patent LIMA anastomosed to the LAD. Distal to the anastomosis is a significant lesion (arrow) in the run-off branch (I). A vein graft (SVG) is significantly obstructed (arrow) proximal and distal to the anastomosis with a marginal branch (MO2) (II). The (bypassed) RCA is diffusely diseased with extensive calcification and several sites of significant narrowing (III, arrows). (A full color version of this illustration can be found in the color section).

In cases of confirmed graft occlusion by CA, patency of dependent proximal and distal coronary artery segments was evaluated. Sensitivity, specificity, PPV and NPV for detection of occlusion per coronary segment were 83.3% (45/54), 92.2% (59/64), 90% and 86.8%, respectively.

Per-patient graft of coronary obstruction

In 16 patients CA showed no graft disease. Disease in one, two or three grafts was found in 25, 9 and 2 patients, respectively. The accuracy to detect or exclude any graft disease per patient was 98% (51/52) (table 4). While in 43 patients the coronary run-offs showed no significant stenosis, seven patients had disease in a single run-off, and one had double run-off disease. Accuracy per patient for the distal run-off disease was 86% (42/52). Although CT identified all 28 patients with significant stenosis in (partially) non-grafted coronary arteries, coronary obstruction was overestimated in 8/19 (42%) patients without significant disease.

Table 3. Diagnostic accuracy related to subjective confidence of assessment.

	Assessment confidence			P value
	High	Moderate	Low	
Graft Segments	161/162 (99.4%, 98.2-100%)	12/16 (75.0%, 53.8-96.2%)	4/4 (100%)	<0.001*
Arterial	46/46 (100%)	8/8 (100%)	3/3 (100%)	-
Venous	115/116 (99.1%, 97.4-100%)	4/8 (50.0%, 15.4-84.6%)	1/1 (100%)	<0.001*
Distal coronary run-off	30/30 (100%)	59/62 (95.2%, 89.9-100%)	25/31 (80.6%, 66.7-94.5%)	0.01*
Coronary segments	58/63 (92.1%, 85.4-98.8%)	117/126 (92.9%, 88.4-97.4%)	79/99 (79.8%, 71.9-87.7%)	<0.01

Accuracy in absolute numbers (percentage, 95%-confidence interval).

Mantel-Haenzel Chi-square test. *Fisher's exact test in case of insufficient group size.

DISCUSSION

Detection of graft disease

The diameter size, relative immobility and sparse presence of calcifications make grafts relatively approachable by noninvasive imaging techniques, such as computed tomography. Modest temporal resolution and long acquisition times restricted clinical use of earlier CT technology. Current technology with faster x-tube rotation and more, thinner detectors has resolved some of the practical limitations of CT imaging after bypass surgery. Using 16-slice CT technology (420-ms rotation time, 0.75-mm slice thickness), Schlosser et al, reported a sensitivity of 96% and specificity of 95% for the detection of obstructive graft disease.¹⁸ Martuscelli et al, compared 16-slice CT (rotation time 500 ms, 0.625-mm slice thickness) with conventional angiography in a large population (N=96), and reported a sensitivity of 97% and specificity of 100%, after exclusion of 9 examinations with insufficient image quality.¹⁷ Preliminary results with the latest generation 64-slice CT by Pache et al, yielded a sensitivity of 98% and specificity of 89% for the detection of obstructed graft disease.²²

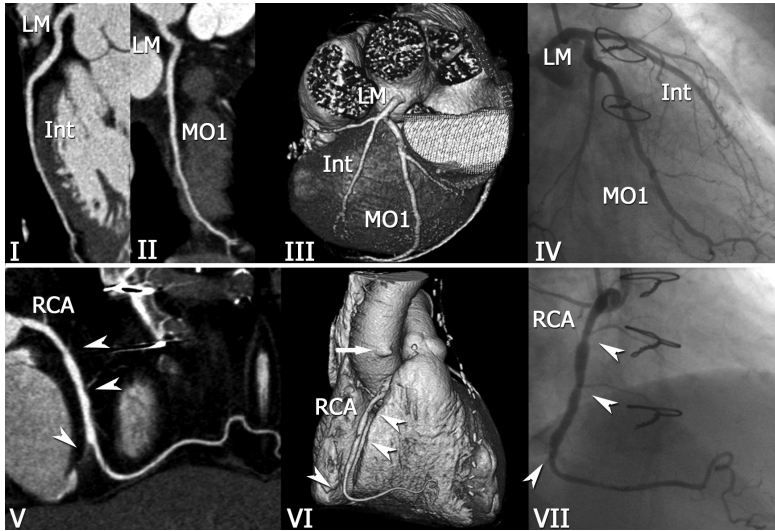


Figure 4. Non-grafted coronary arteries.
 Patient with an occluded vein graft to the distal RCA (arrow, panel VI), and occluded arterial graft to the left anterior descending coronary artery. The proximal and mid-segment of the RCA show plaque without significant narrowing (arrow heads), and the distal RCA is completely occluded. (V-VII). The left main coronary artery (LM), intermediate branch (Int) and first marginal branch (MO1) are all without significant disease (I-III). (A full color version of this illustration can be found in the color section).

In the present study, the latest 64-slice CT technology demonstrated comparable, accurate assessment of grafts, without exclusion of examinations due to image quality. Artifacts caused by metal within the vicinity of the graft (vascular clips, proximal anastomosis indicators, sternal wires) occurred, but likely because of the relatively large graft diameter and fewer motion artefacts these high-density artefacts did not affect assessment accuracy. In addition to graft occlusion, CT accurately detects stenosis. In case of jump grafts variable degrees of obstruction can be identified in consecutive graft segments, which has therapeutic consequences (figures 1-3).

Detection of coronary artery and run-off disease

For complete angiographic evaluation of symptomatic post-CABG patients, both coronary arteries and grafts need to be assessed. Assessment of non-grafted coronary artery segments yielded a sensitivity and specificity of 97% and 86%. CT detected most lesions in the distal coronary run-offs, although overestimation of stenosis severity frequently occurred in these small coronary branches. Most publications on the diagnostic accuracy of 64-slice CT angiography in patients without previ-

ous coronary bypass surgery reported superior sensitivity and specificity.²⁹⁻³² This discrepancy between the accuracy of CT in non- and post-CABG patients was previously described

Table 4. Diagnostic performance of CTA per patient

	TP	TN	FP	FN	Accuracy (95%CI)*
Any graft disease	36	15	1	0	98.1% (94.4-100%)
Any distal run-off disease	7	38	6	1	86.5% (77.2-95.8%)
Any non-grafted coronary disease	28	11	8	0	83.0% (72.3-93.7%)
Any obstructive coronary/graft disease	50	1	1	0	98.1% (94.4-100%)

True positive (TP); true negative (TN); false positive (FP); false negative (FN). Accuracy: $[TP+TN]/[TP+TN+FP+FN]$.

with 4- and 16-slice CT, and appears maintained with current state-of-the-art CT technology.^{16,20} Post-surgical patients are generally older and have more advanced atherosclerotic disease. Diffuse degeneration prevents distinction between non-obstructive vessel changes and significant coronary narrowing. Contrary to the assessment of bypass grafts, inaccurate assessment of coronary stenosis occurred significantly more frequently in vessels with stents or severe calcification.

Forty percent of patients underwent PCI before or after bypass surgery. Artifacts related to related blooming and beam hardening in the vicinity of stent struts significantly affected assessment of stented coronary arteries

In case of graft failure, the difference between stenosis or complete occlusion of the native coronary artery affects interventional options for treatment. We found that CT could exclude occlusion in the majority of previously surgically revascularised coronary arteries.

LIMITATIONS OF THE STUDY

Conventional coronary angiography is still the gold standard in the evaluation of both coronary artery and graft status, but its use is restricted by the invasive nature of the procedure. CT angiography lacks some of the practical disadvantages, such as the requirement for selective contrast injection. Particularly when the exact surgical history is incomplete, CT allows comprehensive graft visualization, including the site and identity of distal run-offs. Therefore CT graft imaging is increasingly used prior to planned invasive angiography, to assure optimal angiography of both coronary arteries and grafts. Despite advantages in terms of safety, comfort and cost, CT angiography is not without risk. It involves considerable exposure to roentgen radiation, recently reported to be 14.8 ± 1.8 mSv without and 9.4 ± 1.0 mSv with ECG-triggered tube output modulation, i.e. lowering tube output during the systole. Compared to an average coronary CT the scan range was extended by 37% (10-65% depending on whether venous and/or arterial grafts were investigated), which will result in a proportionally higher radiation dose. Currently CT angiography cannot be performed without use of potentially nephrotoxic contrast media. Finally, pharmacological heart rate modulation is still recommended to avoid motion artifacts, though may become obsolete with the development of faster scanner technology.

Because our population consisted of symptomatic patients long after surgery with a high incidence of graft and/or coronary artery disease, our results may not be applicable to a lower-risk (non-symptomatic) population. Graft occlusion may occur without ischemic consequences in case of competitive flow or in the presence of non-vital myocardial scar tissue. Particularly in these patients with chronic coronary insufficiency it may not be possible to determine the need for revascularization based on angiographic assessment alone.

Observations (segments) within the same patient are not statistically independent (nesting). We recalculated descriptive statistic parameters in randomly selected, single observations per patient. Accuracy (95%-confidence interval) for detection of significant stenosis was 100% for arterial grafts, 96% (90-100%) for venous grafts, 94% (88-100%) for run-offs and 87% (78-97%) for coronary artery segments. Fewer observations resulted in wider confidence intervals.

CONCLUSION

64-slice MSCT allows accurate detection and detailed imaging of obstructive graft disease, and may be of particular practical use when knowledge about previous surgery is incomplete. Complete angiographic evaluation of post-CABG patients includes assessment of the coronary arteries, which is challenging in the presence of calcium and stents. Nevertheless, the high negative predictive value, CT may be clinically useful for exclusion of significant stenosis in the distal run-offs and (non-grafted) coronary branches, in addition to the evaluation of the bypass grafts.

REFERENCES

1. Bryan AJ, Angelini GD. The biology of saphenous vein graft occlusion: etiology and strategies for prevention. *Curr Opin Cardiol* 1994;9:641-649.
2. Barner HB, Standeven JW, Reese J. Twelve-year experience with internal mammary artery for coronary artery bypass. *J Thorac Cardiovasc Surg* 1985;90:668-675.
3. Cameron AA, Davis KB, Rogers WJ. Recurrence of angina after coronary artery bypass surgery: predictors and prognosis (CASS Registry). *Coronary Artery Surgery Study. J Am Coll Cardiol* 1995;26:895-899.
4. Alderman EL, Kip KE, Whitlow PL, Bashore T, Fortin D, Bourassa MG, Lesperance J, Schwartz L, Stadius M. Native coronary disease progression exceeds failed revascularization as cause of angina after five years in the Bypass Angioplasty Revascularization Investigation (BARI). *J Am Coll Cardiol* 2004;44:766-774.
5. Bunce NH, Lorenz CH, John AS, Lesser JR, Mohiaddin RH, Pennell DJ. Coronary artery bypass graft patency: assessment with true fast imaging with steady-state precession versus gadolinium-enhanced MR angiography. *Radiology* 2003;227:440-446.
6. Langerak SE, Vliegen HW, de Roos A, Zwinderman AH, Jukema JW, Kunz P, Lamb HJ, van Der Wall EE. Detection of vein graft disease using high-resolution magnetic resonance angiography. *Circulation* 2002;105:328-33.
7. Brundage BH, Lipton MJ, Herfkens RJ, Berninger WH, Redington RW, Chatterjee K, Carlsson E. Detection of patent coronary bypass grafts by computed tomography. A preliminary report. *Circulation* 1980;61:826-831.

8. McKay CR, Brundage BH, Ulyot DJ, Turley K, Lipton MJ, Ebert PA. Evaluation of early postoperative coronary artery bypass graft patency by contrast-enhanced computed tomography. *J Am Coll Cardiol* 1983;2:312-317.
9. Moncada R, Salinas M, Churchill R, Love L, Reynes C, Demos TC, Hale D, Schreiber R. Patency of saphenous aortocoronary-bypass grafts demonstrated by computed tomography. *N Engl J Med* 1980;303:503-505.
10. Stanford W, Brundage BH, MacMillan R, Chomka EV, Bateman TM, Eldredge WJ, Lipton MJ, White CW, Wilson RF, Johnson MR. Sensitivity and specificity of assessing coronary bypass graft patency with ultrafast computed tomography: results of a multicenter study. *J Am Coll Cardiol* 1988;12:1-7.
11. Bateman TM, Gray RJ, Whiting JS, Matloff JM, Berman DS, Forrester JS. Cine computed tomographic evaluation of aortocoronary bypass graft patency. *J Am Coll Cardiol* 1986;8:693-698.
12. Achenbach S, Moshage W, Ropers D, Nossen J, Bachmann K. Noninvasive, three-dimensional visualization of coronary artery bypass grafts by electron beam tomography. *Am J Cardiol* 1997;79:856-861.
13. Engelmann MG, von Smekal A, Knez A, Kurzinger E, Huehns TY, Hofling B, Reiser M. Accuracy of spiral computed tomography for identifying arterial and venous coronary graft patency. *Am J Cardiol* 1997;80:569-574.
14. Ropers D, Ulzheimer S, Wenkel E, Baum U, Giesler T, Derlien H, Moshage W, Bautz WA, Daniel WG, Kalender WA, Achenbach S. Investigation of aortocoronary artery bypass grafts by multislice spiral computed tomography with electrocardiographic-gated image reconstruction. *Am J Cardiol* 2001;88:792-795.
15. Yoo KJ, Choi D, Choi BW, Lim SH, Chang BC. The comparison of the graft patency after coronary artery bypass grafting using coronary angiography and multi-slice computed tomography. *Eur J Cardiothorac Surg* 2003;24:86-91; discussion 91.
16. Nieman K, Pattynama PM, Rensing BJ, Van Geuns RJ, De Feyter PJ. Evaluation of patients after coronary artery bypass surgery: CT angiographic assessment of grafts and coronary arteries. *Radiology* 2003;229:749-756.
17. Martuscelli E, Romagnoli A, D'Eliseo A, Tomassini M, Razzini C, Sperandio M, Simonetti G, Romeo F, Mehta JL. Evaluation of venous and arterial conduit patency by 16-slice spiral computed tomography. *Circulation* 2004;110:3234-3238.
18. Schlosser T, Konorza T, Hunold P, Kuhl H, Schmermund A, Barkhausen J. Noninvasive visualization of coronary artery bypass grafts using 16-detector row computed tomography. *J Am Coll Cardiol* 2004;44:1224-1229.
19. Marano R, Storto ML, Maddestra N, Bonomo L. Non-invasive assessment of coronary artery bypass graft with retrospectively ECG-gated four-row multi-detector spiral computed tomography. *Eur Radiol* 2004;14:1353-1362.

20. Salm LP, Bax JJ, Jukema JW, Schuijf JD, Vliegen HW, Lamb HJ, van der Wall EE, de Roos A. Comprehensive assessment of patients after coronary artery bypass grafting by 16-detector-row computed tomography. *Am Heart J*. 2005;150:775-781.
21. Anders K, Baum U, Schmid M, Ropers D, Schmid A, Pohle K, Daniel WG, Bautz W, Achenbach S. Coronary artery bypass graft (CABG) patency: assessment with high-resolution submillimeter 16-slice multidetector-row computed tomography (MDCT) versus coronary angiography. *Eur J Radiol*. 2006;57:336-344.
22. Pache G, Saueressig U, Frydrychowicz A, Foell D, Ghanem N, Kotter E, Geibel-Zehender A, Bode C, Langer M, Bley T. Initial experience with 64-slice cardiac CT: non-invasive visualization of coronary artery bypass grafts. *Eur Heart J* 2006;27:976-980.
23. Nieman K, Cademartiri F, Lemos PA, Raaijmakers R, Pattynama PM, de Feyter PJ. Reliable noninvasive coronary angiography with fast submillimeter multislice spiral computed tomography. *Circulation* 2002;106:2051-2054.
24. Ropers D, Baum U, Pohle K, Anders K, Ulzheimer S, Ohnesorge B, Schlundt C, Bautz W, Daniel WG, Achenbach S. Detection of coronary artery stenoses with thin-slice multi-detector row spiral computed tomography and multiplanar reconstruction. *Circulation* 2003;107:664-666.
25. Kuettner A, Trabold T, Schroeder S, Feyer A, Beck T, Brueckner A, Heuschmid M, Burgstahler C, Kopp AF, Claussen CD. Noninvasive detection of coronary lesions using 16-detector multislice spiral computed tomography technology: initial clinical results. *J Am Coll Cardiol* 2004;44:1230-1237.
26. Martuscelli E, Romagnoli A, D'Eliseo A, Razzini C, Tomassini M, Sperandio M, Simonetti G, Romeo F. Accuracy of thin-slice computed tomography in the detection of coronary stenoses. *Eur Heart J* 2004;25:1043-1048.
27. Mollet NR, Cademartiri F, Nieman K, Saia F, Lemos PA, McFadden EP, Pattynama PM, Serruys PW, Krestin GP, de Feyter PJ. Multislice spiral computed tomography coronary angiography in patients with stable angina pectoris. *J Am Coll Cardiol* 2004;43:2265-2270.
28. Hoffmann MH, Shi H, Schmitz BL, Schmid FT, Lieberknecht M, Schulze R, Ludwig B, Kroschel U, Jahnke N, Haerer W, Brambs HJ, Aschoff AJ. Noninvasive coronary angiography with multislice computed tomography. *JAMA* 2005;293:2471-2478.
29. Leschka S, Alkadhi H, Plass A, Desbiolles L, Grunenfelder J, Marincek B, Wildermuth S. Accuracy of MSCT coronary angiography with 64-slice technology: first experience. *Eur Heart J* 2005;26:1482-1487.
30. Raff GL, Gallagher MJ, O'Neill WW, Goldstein JA. Diagnostic accuracy of noninvasive coronary angiography using 64-slice spiral computed tomography. *J Am Coll Cardiol* 2005;46:552-557.

31. Leber AW, Knez A, von Ziegler F, Becker A, Nikolaou K, Paul S, Wintersperger B, Reiser M, Becker CR, Steinbeck G, Boekstegers P. Quantification of obstructive and nonobstructive coronary lesions by 64-slice computed tomography: a comparative study with quantitative coronary angiography and intravascular ultrasound. *J Am Coll Cardiol* 2005;46:147-154.
32. Mollet NR, Cademartiri F, van Mieghem CA, Runza G, McFadden EP, Baks T, Serruys PW, Krestin GP, de Feyter PJ. High-resolution spiral computed tomography coronary angiography in patients referred for diagnostic conventional coronary angiography. *Circulation* 2005;112:2318-2323.
33. Austen WG, Edwards JE, Frye RL, Gensini GG, Gott VL, Griffith LS, McGoon DC, Murphy ML, Roe BB. A reporting system on patients evaluated for coronary artery disease. Report of the Ad Hoc Committee for Grading of Coronary Artery Disease, Council on Cardiovascular Surgery, American Heart Association. *Circulation* 1975;51:5-40.
34. Gottsauner-Wolf M, Sochor H, Moertl D, Gwechenberger M, Stockenhuber F, Probst P. Assessing coronary stenosis. Quantitative coronary angiography versus visual estimation from cine-film or pharmacological stress perfusion images. *Eur Heart J*. 1996;17:1167-74.
35. Arnese M, Salustri A, Fioretti PM, Cornel JH, Boersma E, Reijs AE, de Feyter PJ, Roelandt JR. Quantitative angiographic measurements of isolated left anterior descending coronary artery stenosis. Correlation with exercise echocardiography and technetium-99m 2-methoxy isobutyl isonitrile single-photon emission computed tomography. *J Am Coll Cardiol*. 1995;25:1486-91.36.
36. Hausleiter J, Meyer T, Hadamitzky M, Huber E, Zankl M, Martinoff S, Kastrati A, Schomig A. Radiation dose estimates from cardiac multislice computed tomography in daily practice: impact of different scanning protocols on effective dose estimates. *Circulation* 2006;113:1305-10.

16

Ultra Sonographic and DSCT Scan Analysis of Single Lima Versus Arterial T Grafts 12 Years After Surgery

Submitted

Hartman, J.M., M.D.¹,
Meijboom, W.B., M.D.²,
Galema, T.W., M.D.²,
Takkenberg J.J.M., M.D.,
Ph.D.¹, Schets, A.M.², De
Feyter, P.J. M.D., Ph.D.^{2,3},
Bogers, A.J.J.C. M.D Ph.D.¹

¹Department of Cardiothoracic
Surgery, Thoraxcentre

²Department of Cardiology,
Thoraxcentre

³Department of Radiology,
Erasmus Medical Centre
Rotterdam

ABSTRACT

Objective

To investigate the long term outcome in patients with left internal mammary artery to left anterior descending coronary artery (LIMA-LAD) and T-grafts by ultrasonography and dual source computed tomography (DSCT) and to analyse if ultrasonography can determine graft patency.

Methods

Thirty-two patients, 28 male, 50.8 ± 8.8 years at operation, were studied. Fifteen patients with single LIMA-LAD and additional vein grafts (group I) and seventeen patients with LIMA-free right internal mammary artery (FRIMA) T-grafts (group II) underwent DSCT, transthoracic ultrasonography of the LIMA and left ventricle, an electrocardiogram and a short questionnaire. Differences were tested with unpaired and paired t-tests.

Results

In group I, 4.1 ± 1.1 and in group II, 4.5 ± 1.1 anastomoses/pt were performed. DSCT showed three string sign LIMA (20 %) grafts and 6 occluded venous anastomoses (13 %) in group I and three (distal) string sign LIMA grafts (18 %), seven occluded LIMA anastomoses (23 %) and nine occluded FRIMA anastomoses (23 %) in group II. Ultrasonographic variables in the proximal part of the LIMA graft did not differ between the groups. No effect was found of left ventricular function, proximal string sign LIMA grafts and previous myocardial infarction on ultrasonographic graft performance. Four patients in group I and one patient in group II suffered angina within the last six months.

Conclusions

Ultrasonography can not distinguish between string sign and patent single LIMA or T-grafts nor demonstrate distal anastomosis patency in T-grafts twelve years after surgery. We do favour T-grafts because of the low incidence of recurrent angina.

INTRODUCTION

The use of the left internal mammary artery (LIMA) as a bypass graft has improved the durability of coronary artery bypass grafting (CABG)[1].

The free right internal mammary artery (FRIMA) can be anastomosed end-to-side to the LIMA, known as arterial composite T-graft with the proximal LIMA as the only source of inflow, to revascularize the anterior, lateral and/or inferior wall. Positron emission tomography as well as angiographic, intravascular and transthoracic ultrasonographic analyses have been reported for short and mid-term follow up of these T-graft configurations [2-4].

Invasive native coronary and bypass angiography is still the gold standard to determine patency of bypass grafts. However, invasive angiography also has disadvantages such as difficulties in finding the origin of the graft, inadequate contrast filling especially into distal coronary arterial parts and small side branches, catheter-induced spasm of the LIMA, underestimation of eccentric plaques and overprojection of coronary arteries.

To evaluate the long-term performance of the LIMA and the arterial T-graft accurate non-invasive tests would be useful. Non-invasive duplex (combination of 2D-mode ultrasonography and pulsed Doppler system) flow measurements of the LIMA have been performed in the past decade by several groups [5-6].

CT coronary angiography has become an accurate noninvasive method to detect or rule out coronary stenosis. Especially the analysis of stenosis and patency of arterial and venous bypass grafts are very promising [7-9].

We performed quantitative analyses of single LIMA-LAD versus arterial composite T-grafts by transthoracic ultrasonography compared to Dual Source computed tomography (DSCT) scans in order to investigate the long term outcome of these grafts and to analyse whether ultrasonographic findings can determine the patency of these grafts in patients long-term after CABG.

METHODS

Patients

Between September and December 2007, we screened seventy-three patients who were operated with single LIMA to the LAD and additional vein grafts or with composite arterial T-grafts in the period of 1994 until 1997. We scheduled these patients for inclusion in a protocol to compare transthoracic ultrasonographic LIMA variables with DSCT scans. Excluded were patients over 85

years of age, previous allergic reaction to contrast, serious co-morbidity, impaired renal function (creatinine $\geq 120 \mu\text{mol/l}$) and an irregular cardiac rhythm. Renal dysfunction (14 pts), deaths (8 pts), co-morbidity (8 pts), refusal to participate (5 pts), lost in follow-up (5 pts) and allergy to contrast (1 pt) were the drop-out reasons.

The Institutional Review Board of the Erasmus MC Rotterdam approved this study (NL 13011-078-06). Informed consent was obtained from all patients.

Thirty-two patients, 28 male and 4 female, mean age of 50.8 ± 8.8 years at the time of operation, were included in this transectional study. Group I consisted of 15 patients (12 male and 3 female, mean age at operation of 54.0 ± 10.4 years) with a single LIMA graft to the LAD and additional vein grafts. Group II consisted of 17 patients with LIMA-FRIMA-T-grafts (16 male and 1 female, mean age at operation of 48.0 ± 6.1 years).

All patients underwent DSCT, an electrocardiographically controlled duplex scanning of the proximal LIMA through the second or third intercostal space, transthoracic echocardiography (TTE) of the left ventricle, an electrocardiogram and a short questionnaire within one day in order to compare data without time interference. All patients were permitted to continue their cardiovascular medication including β -blockers. Diabetic patients were not allowed to take metformine medication during this day to prevent lactic acidosis induced by impaired renal function after iodinated contrast injection during the DSCT scan.

All patients were studied by DSCT scans in order to assess the patency of the grafts and were classified into (sub)groups:

Group I: single LIMA grafts to the LAD with additional vein grafts (n=15)

Subgroup I A: patent single LIMA grafts to the LAD with good contrast run off into the coronary system (n=12)

Subgroup I B: string sign single LIMA grafts to the LAD with contrast run off into the coronary system (n=3)

Group II: composite LIMA-FRIMA-T grafts (n=17)

Subgroup II A: patent LIMA-FRIMA-T-grafts (n=11)

Subgroup II B: distal string sign LIMA grafts (n=3)

Transthoracic ultrasonography protocol

We used the IE 33 208 ultrasound system (Philips, Best, the Netherlands) which combined 2-D imaging and pulsed Doppler ultrasound to evaluate blood velocity variables of the LIMA as well as

left ventricular function. TTE evaluation of the single LIMA and the main stem of the T graft were performed in all thirty-two patients with a 9 MHz linear array vascular probe (Philips, Bothell, WA, USA). The probe was placed at an angle of approximately 60 degrees in the second or third intercostal space with the patient in supine position. LIMA duplex recordings were electrocardiographically controlled during 3-5 cardiac cycles and data were quantified both online and offline and were interpreted by 2 physicians. The ultrasonographic LIMA variables analysed were: systolic and diastolic peak velocity (SPV and DPV), systolic, diastolic and total velocity integral (SVI, DVI and TVI), diastolic/systolic velocity integral ratio (DSVIR), diastolic/total (diastolic + systolic) velocity integral ratio (DTVIR) and peak diastolic/peak systolic velocity ratio (DSPVR).

The following echocardiographic standard views, using the S5-1 broadband phased array transducer (Philips, Bothell, WA, USA), were obtained in order to classify segmental wall motions and consecutively left ventricular function: parasternal long and short axis, apical four and two chamber and apical long axis.

The analyses of the LIMA ultrasonographic variables and the segmental wall motion score of the left ventricle were performed by two blinded observers.

Dual-Source Computed Tomography scan protocol

Patient preparation

No oral or intravenous beta-blockers nor nitroglycerin were administered prior to the scan.

DSCT Scan

All patients were scanned using a Somatom Definition DSCT scanner (Siemens Medical Solutions, Forchheim, Germany). The system is equipped with two X-ray tubes and two corresponding detectors mounted on a single gantry with an angular offset of 90° and a gantry rotation time of 330 ms. CT angiography scan parameters were: number of X-ray sources 2, detector collimation 32 x 0.6 mm with double sampling by rapid alteration of the focal spot in the longitudinal direction (z flying focal spot), rotation time 330 ms, tube voltage 120 kV.

Automatic tube current modulation in x,y,z-direction with Care Dose 4D® software, (Siemens Medical Solutions, Forchheim, Germany) was applied in all patients. The coronary arteries were scanned with 380 reference mAs/rot. In all patients, we used a relative wide ECG pulsing window (30-65% of the R-R-interval) during which full tube current was applied to include both the mid-diastolic and the end-systolic phases. A bolus of Ultravist® 370 mg I/ml iodinated contrast material (Schering AG, Berlin, Germany), which varied between 80-100 ml depending on the expected scan time, was injected (flow rate: 4.0-5.0 ml/s) in the right antecubital vein.

All CT coronary angiography datasets were reconstructed using a single-segmental reconstruction algorithm: slice thickness 0.75 mm; increment 0.4 mm; medium-to-smooth convolution kernel (B26); resulting in a spatial resolution of 0.6-0.7 mm in-plane and 0.5 mm through-plane.

DSCT Image Reconstruction

The reconstruction algorithm uses data from a single heart beat, obtained during a quarter X ray tube rotation by two separate X-ray tubes, resulting in a temporal resolution of 83 ms. Initially, a single dataset was reconstructed during the mid-diastolic phase (350 ms before the next R-wave). In case of impaired image quality datasets were reconstructed in the end-systolic phase (275 ms after the previous R-wave).

DSCT Image Evaluation

Axial views and multi-planar reconstructions (MPR) were used to identify patency of grafts and anastomoses of grafts to coronary run-offs. One experienced observer scored all DSCT coronary angiography datasets and quantified the lumen. Analyses were performed in the proximal part of the LIMA just distal from the subclavian artery, in the LIMA at the level of the second or third intercostal space and proximally and distally from each anastomosis of the graft with a coronary insertion. Visually the coronary branches (distal run-offs) supplied by a patent graft were separately evaluated.

Electrocardiogram

Additional electrocardiograms were taken from all patients and analysed by two blinded observers.

Statistical Analysis

Data entry and statistical analysis were performed with the use of Epi Info 6.04c (CDC, Atlanta, Georgia). Continuous variables are displayed as means \pm standard deviation and considered statistically significant when the P-value was 0.05 or less. Discrete variables are displayed as counts or proportions. Data within and between the groups were tested by paired and unpaired t-tests. Sample size calculation showed that at least 10-11 patients in each group are necessary to detect a significant difference in diastolic peak velocity between the 2 groups, assuming that diastolic peak velocity in single LIMA to LAD grafts is on average 22 cm/sec (range 15-30 cm/sec) [10] versus 35 cm/sec (range 25-45) [11] in T-grafts (assuming equal variances, SD = 10, α = 0.05, power = 0.80).

RESULTS

Patients characteristics are shown in Table 1. In group I, fifteen single LIMA to the LAD bypasses

Table 1. Characteristics of the patients in group I and II

Variable	Group I N = 15	Group II N = 17	p
Age at investigation (years)	65.9 ± 10.2	59.6 ± 6.2	0.04
Age at operation (years)	54.0 ± 10.4	48.0 ± 6.1	0.05
Time after CABG (years)	11.8 ± 0.7	11.6 ± 1.0	0.47
Male	12	16	
LIMA anastomoses/pt	1.0 ± 0.0	1.8 ± 0.7	
Total LIMA anastomoses	15	30	
FRIMA anastomoses/pt	0	2.4 ± 0.8	
Total FRIMA anastomoses	0	39	
Total venous anastomoses/pt	3.2 ± 1.1	0*	
Total GEA anastomoses/pt	0	0.4 ± 0.5	
RIMA (in situ)	0**	0	
Total anastomoses/pt	4.1 ± 1.1	4.5 ± 1.1	0.33
Intimectomic	1 (LAD)	1 (RCA)	
Preoperative anterior wall infarction	6	3	
Preoperative inferior infarction	2	3	
Preoperative inferoposterior infarction	1	2	
Preoperative lateral infarction	1	1	
Postoperative PCI (LAD)	1	0	
Mean systolic blood pressure (mmHg)	135 ± 15	142 ± 18	0.28
Mean diastolic blood pressure (mmHg)	77 ± 11	83 ± 14	0.20
Mean heart rate (beats/min)	72 ± 12	66 ± 11	0.14
Angina within last 6 months	4	1	
Diabetes	4	4	
Normal LVF	6	8	
Impaired LVF	6	5	
Abnormal relaxation LV	2	3	
Length (m)	1.76 ± 0.09	1.77 ± 0.06	0.56
Weight (kg)	85 ± 12	88 ± 11	0.40

Group I; Patients with a single LIMA graft to the left anterior descending artery LAD) and additional vein grafts, Group II; Patients with LIMA-free right internal mammary artery (FRIMA) -T graft, GEA; gastroepiploic artery, PCI; Percutaneous intervention. P = Unpaired p-values for differences between the groups, data are ± standard deviation. * in 1 patient a single venous bypass was additionally performed ** in 1 patient a single right internal mammary artery was additionally performed.

were constructed and one right internal mammary artery (RIMA) to the right coronary artery (RCA) and one single, one jump, six triples, five quadruple and one quintuple venous bypass grafts, a total of sixty-two anastomoses, 4.1 ± 1.1/patient, were performed. Two re-explorations due to excessive blood loss postoperatively and one percutaneous coronary intervention (PCI) of the LAD artery four years after surgery were performed.

In group II, six single, nine jump and two triple jump LIMA grafts to the LAD area with two single, eight jump and seven triple FRIMA bypass grafts were performed. In six patients, an additional single gastroepiploic artery (GEA) bypass graft to the posterior descending artery (PDA, n=4) or the RCA (n=2) and one additional vein graft to the RCA were performed, in total seventy-six anastomoses, 4.5 ± 1.1/patient. Re-exploration because of excessive blood loss postoperatively was done in one patient, one PCI of the

RCA was done three years after surgery and in the same patient PCI of the circumflex artery (CA) ten years after surgery was performed.

No patients had complaints of angina during the investigations.

DSCT scan follow-up

DSCT-scan findings are shown in Table 2. In group II, one FRIMA anastomosis (2.6 %) could not be judged. Also in group II, one patient with a distal string sign LIMA graft has severe left main stenosis but did not suffer angina.

Table 2. DSCT findings in patients from group I and II.

Variable	Group I N = 15	Group II N = 17
Patent LIMA graft	12	12
(distal) String sign LIMA graft	3 (20 %)	3 (17.6 %)
(distal) String sign FRIMA graft	-	0
Occluded LIMA grafts	0	2 (11.8 %)*
Occluded LIMA anastomoses	0	7 (23.3 %)
Occluded FRIMA anastomoses	-	9 (23.1 %)
Occluded venous anastomoses	6 (13 %)	-
Stenotic regions in venous jump grafts	7 (15.2 %)	-
String sign GEA graft	-	1 (16.7 %)
Occluded GEA anastomoses	-	1 (16.7 %)

*Group I, II, FRIMA and GEA as described in Table 1. * patent main stem with occluded distal LIMA grafts.*

I (Table 4) and versus all patent main stem LIMA grafts and patent LIMA grafts without myocardial infarction did also not reveal significant differences. Noticeably, proximal string sign LIMA grafts were only observed in group I.

Echocardiography

All patients underwent TTE in order to determine left ventricular function (Table 1). In two patients, no adequate window could be obtained.

Electrocardiogram

No ischemia could be detected in any patient electrocardiographically.

Ultrasonographic follow-up of the LIMA variables

In all thirty-two patients transthoracic ultrasonography of the LIMA was successful with adequate Doppler velocity profiles. No ischaemia could be detected electrocardiographically and all patients were in sinus rhythm. All LIMA variables of the LIMA to the LAD and the composite T-grafts are comparable (Table 3) without significant differences. Ultrasonographic differences between subgroups were also not observed: patent grafts between the groups (Table 3), preserved versus impaired LVEF, string sign versus patent LIMA grafts within group

Table 3. Transthoracic ultrasonographic proximal LIMA variables and only patent LIMA grafts in group I and II twelve years after CABG.

Variable	Group I	Group II	P	Group I *	Group II *	P
	N = 15	N = 17		N = 12	N = 11	
DPV (cm/s)	18 ± 7	21 ± 7	0.26	17.0 ± 7.0	22 ± 7.0	0.15
SPV (cm/s)	57 ± 19	62 ± 30	0.59	56.2 ± 15.9	67 ± 28	0.27
DVI (cm2)	7 ± 3	8 ± 4	0.34	6.6 ± 3.48	7.9 ± 3.2	0.38
SVI (cm2)	12 ± 5	12 ± 5	0.97	11.7 ± 4.0	12.4 ± 3.9	0.70
TVI (cm2)	17 ± 6	21 ± 9	0.17	16.2 ± 4.2	21.4 ± 6.6	0.04
DSVIR	0.6 ± 0.2	0.7 ± 0.2		0.56 ± 0.3	0.66 ± 0.2	
DTVIR	0.37 ± 0.1	0.39 ± 0.1		0.36 ± 0.1	0.38 ± 0.1	
DSPVR	0.33 ± 0.1	0.37 ± 0.1		0.31 ± 0.1	0.35 ± 0.1	

Group I, patients with single LIMA grafts to the LAD and additional vein grafts; Group II, patients with LIMA-free RIMA composite T grafts; * only patent grafts; DPV, diastolic peak velocity; SPV, systolic peak velocity; DVI, diastolic velocity integral; SVI, systolic velocity integral; TVI, total (diastolic + systolic) velocity integral; DSVIR, diastolic/systolic velocity integral ratio; DTVIR, diastolic/total (diastolic + systolic) velocity integral ratio; DSPVR, peak diastolic/peak systolic velocity ratio. P = unpaired p-values for differences between the groups, data are ± standard deviation.

Questionnaire

Sixteen patients are still controlled by their cardiologist. Eleven patients routinely and five patients because of recurrent complaints. Twenty-two patients do not suffer from any physical limitation. Four patients in group I and one patient in group II have suffered recurrent angina during exercise within the last six months. DSCT of these patients in group I showed one patient with a string sign LIMA graft with a patent quadruple venous graft, three patent LIMA grafts with two patent triple venous grafts and in one patient three occluded venous anastomoses in the quadruple venous graft. DSCT of the patient in group II showed a string sign LIMA graft and a partial occluded FRIMA graft. This patient underwent PCI of the CX but suffers from recurrent angina.

DISCUSSION

Follow up of bypass grafts is important for quantitative and qualitative analyses and coronary arteriography is the gold standard to perform this follow up. However, costs, the invasive nature and the risks in clinically stable patients of 0.7-4.0 % [12-13] limit the routine use of this method and for these reasons, non-invasive methods have been developed for graft follow-up purposes.

Postoperative ultrasonographic follow-up of the in situ LIMA graft has been extensively described in the last decade [4-6, 14] and it is well known that a shift from a predominantly systemic profile towards a coronary flow profile is present in these bypass grafts [14]. Until now, ultrasonographic LIMA analyses compared to DSCT scans have not been performed in a late follow-up setting (Fig. 1,2 and 3).

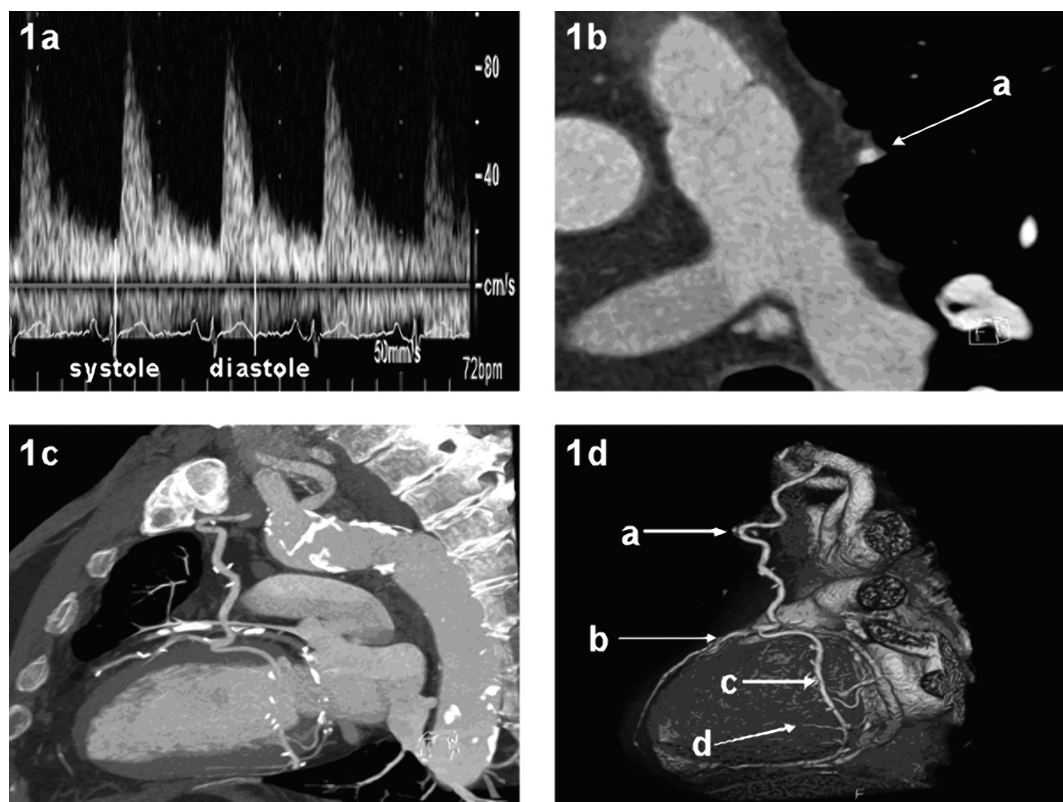


Figure 1. Late follow-up main stem transthoracic ultrasonography (1a) and DSCT coronary angiography of a patent composite arterial T graft from the transverse (1b), lateral (1c) and anterolateral view (1d). (a) main stem of the T graft; (b) LIMA branch of the T graft; (c) FRIMA branch of the T graft; (d) native obtuse margin branch. DSCT, Dual-source computed tomography; LIMA, left internal mammary artery; FRIMA, free right internal mammary artery. (A full color version of this illustration can be found in the color section).

LIMA (sequential) bypass grafting and arterial composite T-grafting are accepted methods for coronary revascularisation [15-16]. However, there are concerns surrounding composite arterial bypass grafting related to perioperative hypoperfusion, their ability to supply sufficient blood flow (especially in a composite T-graft and during hyperaemic response), and the unknown long-term effects on arterial conduit luminal size [2-4, 17].

Despite these concerns, arterial T-bypass grafting has been expanded in the last decade using the right GEA, the radial artery and the RIMA as (free) additional arterial conduits. Many strategies for arterial composite T-grafting have been described but we restrict to T-grafts with the FRIMA connected end-to-side to the attached LIMA graft.

It is remarkable that six anastomoses in venous grafts (13%) and not a single LIMA-LAD anastomosis were occluded in group I while seven LIMA anastomoses (23.3 %) and nine free RIMA anastomoses (23.1 %) were occluded in the T-grafts (group II). However, one of

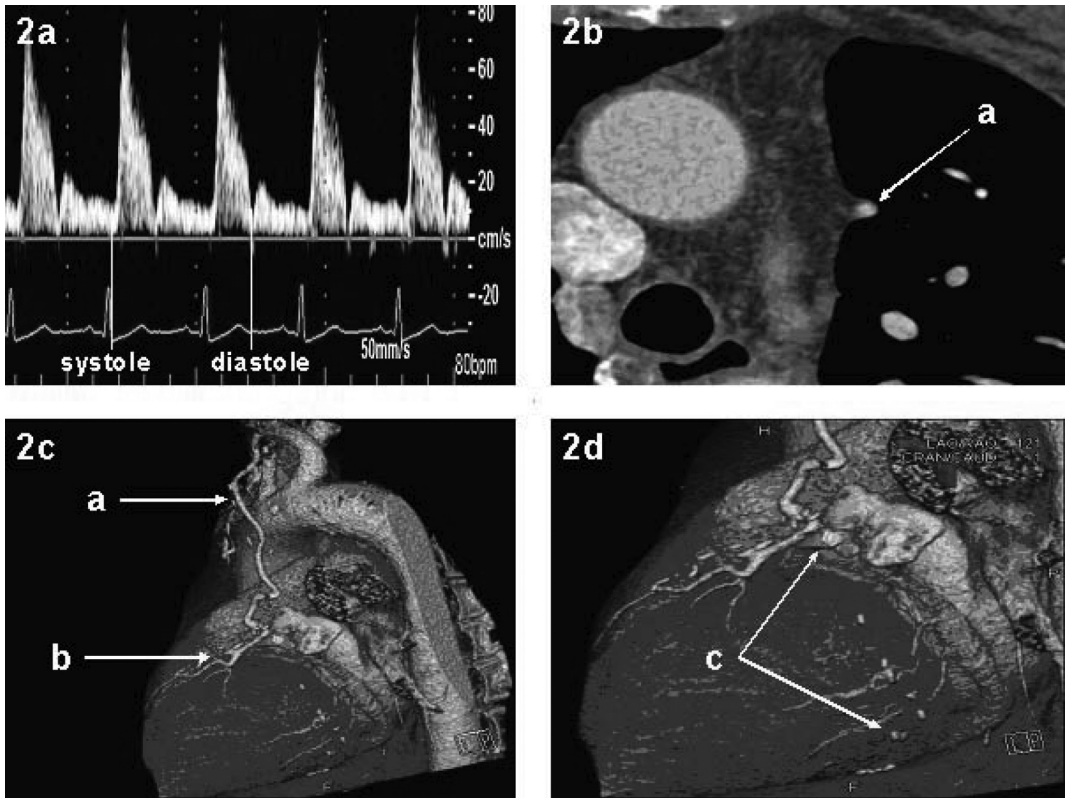


Figure 2. Late follow-up main stem transthoracic ultrasonography (2a) and DSCT coronary angiography of a composite arterial T graft from the transverse (2b), anterolateral (2c) and lateral view (2d). (a) main stem of the T graft; (b) LIMA branch of the T graft; (c) occluded FRIMA branch of the T graft. Abbreviations as in Figure 1. (A full color version of this illustration can be found in the color section).

the crucial questions concerning these findings is whether or not these findings affect the patients.

Five patients (15.6%) have suffered angina within the last six months but were free of complaints during the investigations: four patients in group I (26.7 %) and one patient in group II (5.9 %). These findings suggest that patients from our study population with T-grafts suffer less angina compared to patients with a conventional operation twelve years after CABG in spite of the much higher number of occluded anastomoses. We realise that this suggestion is based on a small population and without analysing the circumstances and causes of the occluded grafts.

The DSCT-scans showed that twelve LIMA single bypasses were patent and three LIMA grafts were string sign in group I. Many reports analysed the influence of competitive flow on the cause of string sign or occluded LIMA grafts but, so far, no consensus could be obtained concerning this association [18-21]. Previous reports describe that diastolic velocity measurements in string sign LIMA grafts are lower compared to patent LIMA grafts [5, 22] in a short - or mid - term follow

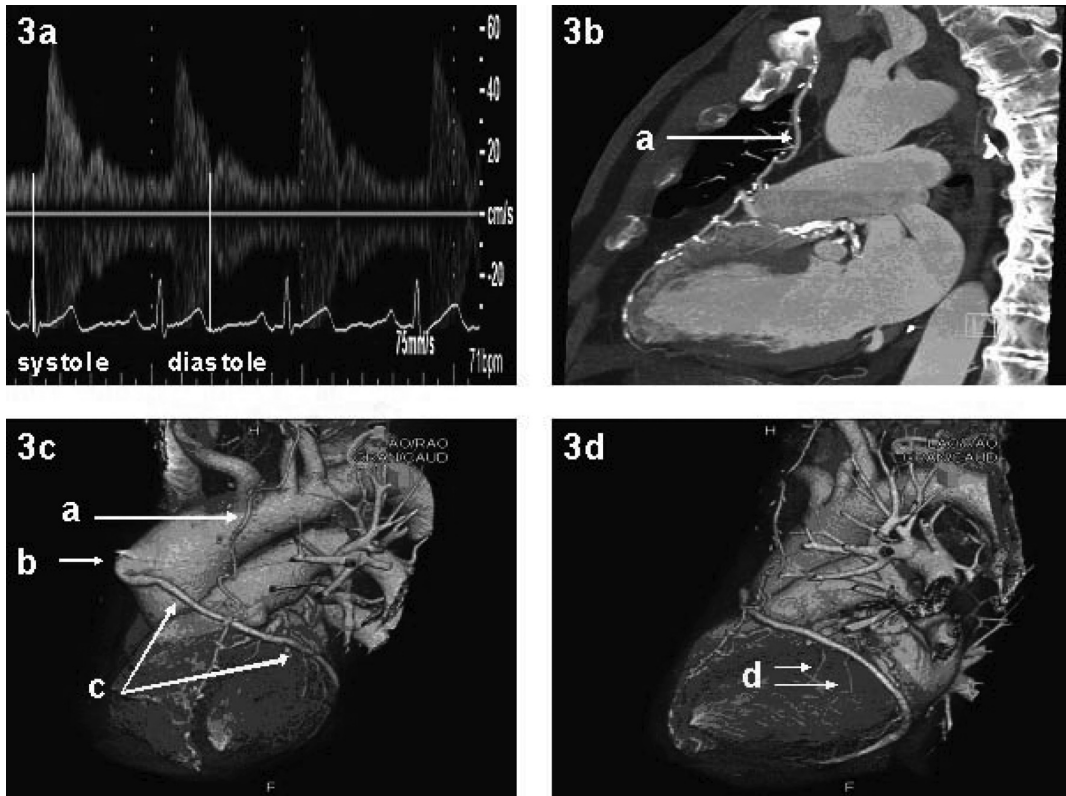


Figure 3. Late follow-up transthoracic ultrasonography (3a) and DSCT coronary angiography of a patent single LIMA graft to the LAD with an additional patent venous graft from the lateral (3b,3d) and anterolateral (3c) view. (a) LIMA graft; (b) proximal venous graft anastomoses to the aorta; (c) patent venous jump graft to the lateral and inferior wall; (d) native obtuse margin branches. LAD, left anterior descending artery. Abbreviations as in Figure 1. (A full color version of this illustration can be found in the color section).

up. In our data, all ultrasonographic measurements appeared to be more pronounced in string sign LIMA grafts (Table 4). Jones et al. [13] stated in a review that the diastolic fraction (DTVIR) of less than 0.5 is the best predictor of stenosis of the LIMA. Song et al. [23] stated that “occluded” LIMA grafts show diastolic fractions of less than 0.6. Our data differ from these findings: string sign LIMA grafts showed a DTVIR of 0.39 ± 0.04 versus patent LIMA grafts 0.36 ± 0.1 (Table 4).

Ultrasonographic analyses of the main stem of total patent T-grafts ($n=11$) also show this remarkable finding of a diastolic fraction of less than 0.5 namely 0.38 ± 0.1 (Table 3).

Early and mid term follow up reports describe that systolic and diastolic peak velocities at rest are significantly higher in patent LIMA grafts compared to string sign LIMA grafts [24–25]. These data do not correspond to our long term follow-up findings: diastolic and systolic peak velocities are comparable in both groups although SPV in both groups remains much higher compared to DPV as confirmed in other mid-term and long term follow-up reports (Table 3) [5, 10, 26].

Table 4. Proximal LIMA variables in patent and proximal string sign LIMA grafts in group I.

Variable	Patent LIMA	String sign LIMA	P
	N = 12	N = 3	
DPV (cm/s)	17.0 ± 7.0	22.1 ± 6.0	0.27
SPV (cm/s)	56.2 ± 15.9	60.0 ± 33.6	0.76
DVI (cm ²)	6.6 ± 3.48	8.1 ± 3.2	0.52
SVI (cm ²)	11.7 ± 4.0	13.3 ± 8.6	0.64
TVI (cm ²)	16.2 ± 4.2	21.5 ± 11	0.19
DSVIR	0.56 ± 0.3	0.67 ± 0.2	
DTVIR	0.36 ± 0.1	0.39 ± 0.04	
DSPVR	0.31 ± 0.1	0.41 ± 0.1	

Ultrasonographic variables and group I as described in Table 3. P = paired p-values for differences within the group. Data are ± standard deviation.

not even when only patent grafts are taken into account (Table 3). We found no effect of LVEF, proximal string sign LIMA grafts, and previous myocardial infarction on ultrasonographic graft performance.

The important questions remain why all proximal LIMA ultrasonographic variables do not differ between LIMA to LAD and composite T-grafts and also not differ between string sign LIMA and patent LIMA grafts and whether the extent of the LIMA perfusion area influences ultrasonographic variables at rest in the late postoperative period. The IMA graft patency is highest and most durable when performed as single bypass to the LAD. This finding is consistent with reports describing the patency of vein grafts to the LAD exceeding the patency to the CX and RCA [28-29]. These findings can be explained by the more direct course of the bypass to the target area as well as by the extent of the target area. The perfusion area supplied by the LAD is larger compared to other coronary arteries resulting in larger blood flow demands in LIMA grafts to the LAD compared to other coronary areas resulting in less tendency to fail or become string sign [18-21]. For this reason, diastolic blood flow in proximal LIMA grafts and also in T-grafts will be mainly relevant for the anterior and septal wall perfusion area. Consequently, the areas depending on the more distal anastomoses are probably less well perfused. When the distal LIMA branch in the T-graft shows string sign or is less functional, the flow competition in the proximal part of the LIMA graft will be minimal and the blood flow through the main stem can simply flow into the FRIMA branch.

In the long term follow-up, the ‘dynamic’ LIMA seems to create a ‘fixed’ or ‘steady’ state, at least at rest, expressed in equal values of the ultrasonographic variables from different perfusion areas in the proximal part of the LIMA. This consideration may also be an explanation for the equalisation

In our opinion, it is reasonable to assume that T-grafts have a larger myocardial perfusion area compared to single LIMA grafts. The myocardium is mainly perfused during the diastolic phase [27] and therefore we expect higher diastolic values in main stem of the T-grafts compared to the single LIMA grafts [11]. Remarkably, all variables in the proximal part of the single LIMA grafts are as high as in the main stem of the T-grafts without statistical significant differences (Table 3),

of the ultrasonographic variables between all subgroups and for our different findings in the late follow-up setting compared to reports which describe short- and midterm follow-up.

Limitations

First, the cross-sectional design of our study does not allow to draw further conclusions on patient cohort level. Ultrasonography was performed at rest and additional studies should include hyperemic response tests to analyse ultrasonographic behaviour of the LIMA grafts for different myocardial perfusion areas.

CONCLUSIONS

Noninvasive transthoracic ultrasonography allows detecting velocity patterns in the proximal part of a single or composite LIMA graft. However, these patterns can not determine differences between string sign and patent single LIMA or T-grafts and can not demonstrate patency of distal anastomoses in T grafts in patients twelve years after surgery.

LIMA grafts remodel into a 'fixed' or 'steady' state at rest in which all ultrasonographic variables equalize between (subdivided) groups twelve years after CABG in contrast to early and mid-term follow-up findings. Despite the increased number of occluded anastomoses in T grafts we do favour these composite grafts because of the low incidence of recurrent angina.

REFERENCES

- 1 Lytle B, Loop F, Cosgrove D, Ratliff N, Easley K, Taylor P. Long term (5 to 12 years) serial studies of internal mammary artery and saphenous vein coronary bypass grafts. *J Thorac Cardiovasc Surg.* 1985;89:248-58.
- 2 Sakaguchi G, Tadamura E, Ohnaka M, Tambara K, Nishimura K, Komeda M. Composite arterial Y graft has less coronary flow reserve than independent grafts. *Ann Thorac Surg.* 2002;74:493-6.
- 3 Ochi M, Hatori N, Bessho R, Fujii M, Saji Y, Tanaka S, et al. Adequacy of flow capacity of bilateral internal thoracic artery T graft. *Ann Thorac Surg.* 2001;72:2008-12.
- 4 Wendler O, Hennen B, Markwirth T, König J, Tscholl D, Huang Q, et al. T grafts with the right internal thoracic artery to the left internal thoracic artery versus the left internal thoracic artery and radial artery: flow dynamics in the internal thoracic artery main stem. *J Thorac Cardiovasc Surg.* 1999;118:841-8.

- 5 Hartman J, Kelder H, Ackerstaff R, van Swieten H, Vermeulen F, Bogers A. Preserved hyperaemic response in (distal) string sign left internal mammary artery grafts. *Eur J Cardiothorac Surg.* 2007;31:283-9.
- 6 Yoshitatsu M, Miyamoto Y, Mitsuno M, Toda K, Yoshikawa M, Fukui S, et al. Changes in left anterior descending coronary artery flow profiles after coronary artery bypass grafting examined by means of transthoracic Doppler echocardiography. *J Thorac Cardiovasc Surg.* 2003;126:1531-6.
- 7 Weustink AC, Meijboom WB, Mollet NR, Otsuka M, Pugliese F, van Mieghem C, et al. Reliable high-speed coronary computed tomography in symptomatic patients. *J Am Coll Cardiol.* 2007;50:786-94.
- 8 Malagutti P, Nieman K, Meijboom WB, van Mieghem CA, Pugliese F, Cademartiri F, et al. Use of 64-slice CT in symptomatic patients after coronary bypass surgery: evaluation of grafts and coronary arteries. *Eur Heart J.* 2007;28:1879-85.
- 9 Ropers D, Pohle FK, Kuettner A, Pflederer T, Anders K, Daniel WG, et al. Diagnostic accuracy of non-invasive coronary angiography in patients after bypass surgery using 64-slice spiral computed tomography with 330-ms gantry rotation. *Circulation* 2006;114:2334-41.
- 10 Ichikawa Y, Kajiwara H, Noishiki Y, Yamazaki I, Yamamoto K, Kosuge T, et al. Flow dynamics in internal thoracic artery grafts 10 years after coronary artery bypass grafting. *Ann Thorac Surg.* 2002;73:131-7.
- 11 Hartman JM, Kelder JC, Ackerstaff RG, Vermeulen FE, Bogers AJ. Differences in LIMA Doppler characteristics for different LAD perfusion areas. *Eur J Cardiothorac Surg.* 2001;20:1135-41.
- 12 Gobel F, Stewart W, Campeau L, Hickey A, Herd J, Forman S, et al. Safety of coronary arteriography in clinically stable patients following coronary bypass surgery. *Post CABG Clinical Trial Investigators. Cathet Cardiovasc Diagn.* 1998;45:376-81.
- 13 Jones C, Athanasiou T, Tekkis PP, Malinovski V, Purkayastha S, Haq A, et al. Does Doppler echography have a diagnostic role in patency assessment of internal thoracic artery grafts? *Eur J Cardiothorac Surg.* 2005;28:692-700.
- 14 de Bono DP, Samani NJ, Spyt TJ, Hartshorne T, Thrush AJ, Evans DH. Transcutaneous ultrasound measurement of blood-flow in internal mammary artery to coronary artery grafts. *Lancet* 1992;339:379-81.
- 15 Bonacchi M, Prifti E, Maiani M, Frati G, Giunti G, Di Eusanio M, et al. Perioperative and clinical-angiographic late outcome of total arterial myocardial revascularization according to different composite original graft techniques. *Heart vessels* 2006;21:69-77.
- 16 Dion R, Glineur D, Derouck D, Verhelst R, Noirhomme P, El Khoury G, et al. Long-term clinical and angiographic follow-up of sequential internal thoracic artery grafting. *Eur J Cardiothorac Surg.* 2000;17:407-14.
- 17 Raja SG. Composite arterial grafting. *Expert Rev Cardiovasc Ther.* 2006;4:523-33.

- 18 Shimizu T, Hirayama T, Suesada H, Ikeda K, Ito S, Ishimaru S. Effect of flow competition on internal thoracic artery graft: postoperative velocimetric and angiographic study. *J Thorac Cardiovasc Surg.* 2000;120:459-65.
- 19 Nasu M, Akasaka T, Okazaki T, Shinkai M, Fujiwara H, Sono J, et al. Postoperative flow characteristics of left internal thoracic artery grafts. *Ann Thorac Surg.* 1995;59:154-62.
- 20 Seki T, Kitamura S, Kawachi K, Morita R, Kawata T, Mizuguchi K, et al. A quantitative study of postoperative luminal narrowing of the internal thoracic artery graft in coronary artery bypass surgery. *J Thorac Cardiovasc Surg.* 1992;104:1532-8.
- 21 Sabik III JF, Lytle BW, Blackstone EH, Khan M, Houghtaling PL, Cosgrove DM. Does competitive flow reduce internal thoracic artery graft patency? *Ann Thorac Surg.* 2003;76:1490-7.
- 22 Gupta S, Murgatroyd F, Widenka K, Spyt TJ, de Bono DP. Role of transcutaneous ultrasound in evaluation of graft patency following minimally invasive coronary surgery. *Eur J Cardiothorac Surg.* 1998;14(suppl I):S88-S92.
- 23 Song M, Mamoru I, Sachie T, Keisuke T, Wataru K, Jinichi I, et al. Echocardiographic evaluation of internal mammary artery graft patency. *Asian Cardiovasc Thorac Surg.* 2004;12:130-2.
- 24 Akasaka T, Yoshida K, Hozumi T, Takagi T, Kaji S, Kawamoto T, et al. Flow dynamics of angiographically no-flow patent internal mammary artery grafts. *J Am Coll Cardiol.* 1998; 31: 1049-56.
- 25 Hartman JM, Kelder HC, Ackerstaff RGA, van Swieten HA, Vermeulen FEE, Bogers AJJC. Can late supraclavicular echo Doppler reliably predict angiographical string sign of LIMA to LAD area grafts? *Echocardiography* 2007;24:689-96.
- 26 Driever R, Fuchs S, Schmitz E, Vetter HO. Assessment of left mammary artery grafts (LIMA) to left anterior descending artery (LAD) after off-pump coronary artery bypass grafting by color Doppler. *Cardiovascular Surg.* 2002;10:49-51.
- 27 Bach RG, Kern MJ, Donohue TJ, Aguirre FV, Caracciolo EA. Comparison of phasic blood flow velocity characteristics of arterial and venous coronary artery bypass conduits. *Circulation* 1993;88(Suppl 2):133-40.
- 28 Frey RR, Brusckhe AV, Vermeulen FE. Serial angiographic evaluation 1 year and 9 years after aorta-coronary bypass. A study of 55 patients chosen at random. *J Thorac Cardiovasc Surg.* 1984;87:167-74.
- 29 Lytle BW, Loop FD. Elective coronary surgery. *Cardiovasc Clin.* 1981;12:31-47.

17

Anatomical and Functional Assessment of Single Lima Versus Arterial T-Grafts 12 Years After Surgery

Submitted

Joost M Hartman¹, MD, W.
Bob Meijboom^{2,3}, MD, Tjebbe
W Galema², MD, Johanna
JM Takkenberg¹, MD, PhD,
Anne-Maria Schets², Pim J de
Feyter^{2,3}, MD, PhD, Ad JJC
Bogers¹, MD, PhD

¹Department of Cardiothoracic
Surgery, Thoraxcentre

²Department of Cardiology,
Thoraxcentre

³Department of Radiology,
Erasmus Medical Centre
Rotterdam

ABSTRACT

Objectives

To determine whether functional ultrasonographic LIMA findings correspond with 64-MSCT in patients 12 years after CABG.

Methods

We entered thirty-four patients (63.2 ± 9.2 years), sixteen with conventional single LIMA (group I) and eighteen composite arterial T-grafts (group II), in a cross-sectional study. Patients underwent transthoracic proximal LIMA ultrasonography at rest and during the Azoulay maneuver, LV TTE and 64-MSCT, 11.5 ± 1.4 years postoperatively. Differences were tested with paired and unpaired T-tests.

Results

MSCT scans showed three string sign LIMA grafts (19 %) and six occluded venous anastomoses (12 %) in group I and three distal string sign LIMA grafts (17 %) and sixteen occluded T-graft anastomoses (22 %) in group II. LIMA diameters and areas are significantly larger in group II compared to group I in the origin, 3.5 ± 0.7 vs 2.5 ± 0.5 mm, $P = 0.00007$ and 0.09 ± 0.04 vs 0.05 ± 0.02 cm², $P = 0.00019$ and in the third intercostal space, 3.4 ± 0.7 vs 2.5 ± 0.5 mm, $P = 0.00009$ and 0.09 ± 0.03 vs 0.05 ± 0.02 cm², $P = 0.000047$ whereas most ultrasonographic LIMA findings do not differ between and within the groups, even not adjusted for differences in LVEF.

Conclusions

Proximal LIMA diameters and areas are significantly larger in T grafts compared to single LIMA grafts, probably due to larger myocardial perfusion areas, which can explain the equalization of ultrasonographic variables between and within both groups at rest and during the Azoulay maneuver 12 years after surgery.

INTRODUCTION

The in situ left internal mammary artery (LIMA) has become the first choice of conduit in coronary artery bypass grafting (CABG) to the left anterior descending artery (LAD) because of reduced cardiac events, superior graft patency, and enhanced short and long-term survival [1-2]. Due to these findings, composite arterial T-grafts (in situ LIMA grafts with another arterial conduit attached) are used in daily practice with good clinical results [3-5]. However, questions remain both on whether the main stem of the in situ LIMA of these T-grafts is able to supply sufficient blood flow at rest and during stress and as well as on the unknown long-term effects on arterial conduit luminal size [6-8]. In this regard, LIMA graft patency in patients with recurrent angina is usually assessed by angiography although other diagnostic techniques are additionally used nowadays and very promising, for example multislice computed tomography (MSCT) [9].

To investigate the long-term outcome of single LIMA to the LAD versus arterial T-grafts we assessed and compared anatomical and functional graft characteristics by 64-MSCT (DSCT) scan at rest and transthoracic ultrasonography at rest and during the Azoulay maneuver 12 years after bypass surgery.

MATERIALS

Patients

Between September 2007 and January 2008, we entered thirty-four patients in a cross-sectional study who were operated with single LIMA to the LAD and additional vein grafts and with T-grafts in the period of 1994 until 1997. Group I consisted of 16 patients (13 Male, 3 Female), mean age of 55.4 ± 11.5 years at the time of operation, with a single LIMA graft to the LAD and additional vein grafts. Group II consisted of 18 patients (17 Male and 1 Female), mean age of 48.5 ± 6.3 years at the time of operation, with LIMA-free right internal mammary artery (FRIMA)-T grafts. Excluded were patients over 85 years of age, previous allergic reaction to contrast, serious co-morbidity, impaired renal function (creatinine $\geq 120 \mu\text{mol/l}$) and an irregular cardiac rhythm.

The Institutional Review Board of the Erasmus MC Rotterdam approved this study (NL 13011-078-06). Written informed consent was obtained from all patients.

All patients underwent a DSCT scan, transthoracic duplex scanning of the proximal LIMA, transthoracic echocardiography (TTE) of the left ventricle, an electrocardiogram and a short questionnaire within one day.

The DSCT scans were performed to assess the anatomical function (patency) of the arterial grafts and were classified into patent or (distal) string sign grafts. Grafts larger or equal to 2 mm in diameter with good contrast run-off into the coronary system were classified as patent grafts. Small grafts with a diameter of less than 2 mm in diameter with contrast run-off into the coronary system were classified as string sign grafts.

Transthoracic ultrasonography protocol

The IE 33 208 ultrasound system (Philips, Best, the Netherlands) was used, which combined 2-D imaging and pulsed Doppler ultrasound to evaluate blood velocity variables of the LIMA as well as left ventricular function. TTE evaluation of the single LIMA and the main stem of the T graft were performed with a 9 MHz linear array vascular probe (Philips, Bothell, WA, USA). The probe was placed at an angle of 60 degrees in the second or third intercostal space with the patient in supine position. LIMA duplex recordings were electrocardiographically controlled during 3-5 cardiac cycles and data were quantified both online and off-line and were interpreted by 2 physicians. The ultrasonographic LIMA variables analysed were: systolic and diastolic peak velocity (SPV and DPV), systolic, diastolic and total velocity integral (SVI, DVI and TVI), diastolic/systolic velocity integral ratio (DSVIR), diastolic/total (diastolic + systolic) velocity integral ratio (DTVIR) and peak diastolic/peak systolic velocity ratio (DSPVR).

Echocardiographic standard views, parasternal long and short axis, apical four and two chamber and apical long axis, using the S5-1 broadband phased array transducer (Philips, Bothell, WA, USA), were obtained in order to classify left ventricular function and left ventricular ejection fraction (LVEF). Manual tracing of LV end-systolic and end-diastolic frames was performed offline according to Simpson's method [10] using commercially available Enconcert software (Philips, Best, the Netherlands).

We performed the Azoulay maneuver [11] at the end and measured the ultrasonographic LIMA variables afterwards at the same (marked) position as at rest.

We ultrasonographically analyzed and compared different (sub) groups: (a) distal string sign LIMA grafts versus patent LIMA grafts in Group II at rest and during the Azoulay maneuver. (b) LVEF smaller than 50 % (n = 6) versus LVEF greater or equal to 50 % (n = 25) at rest and during the Azoulay maneuver. (c) proximal string sign LIMA grafts (n = 3 in group I) versus all proximal patent grafts (n = 31) at rest and during the Azoulay maneuver. (d) All patients in group I versus group II.

The analyses were performed by two blinded observers.

Dual-Source Computed Tomography scan protocol

DSCT Scan

Neither β -blockers nor nitroglycerin were administered prior to the scan. All patients were scanned using a Somatom Definition DSCT scanner (Siemens Medical Solutions, Forchheim, Germany). The system is equipped with two X-ray tubes and two corresponding detectors mounted on a single gantry with an angular offset of 90° and a gantry rotation time of 330 ms. CT angiography scan parameters were: number of X-ray sources 2, detector collimation 32×0.6 mm with double sampling by rapid alteration of the focal spot in the longitudinal direction (z flying focal spot), rotation time 330 ms, tube voltage 120 kV.

The coronary arteries were scanned with 380 reference mAs/rot. We used a wide ECG pulsing window (30-65% of the R-R-interval) during which full tube current was applied to include both the mid-diastolic and the end-systolic phases. A bolus of Ultravist® 370 mg I/ml iodinated contrast material (Schering, Berlin, Germany), which varied between 80-100 ml depending on the expected scan time, was injected (flow rate: 4.0-5.0 ml/s) in the right antecubital vein.

All CT coronary angiography datasets were reconstructed using a single-segmental reconstruction algorithm: slice thickness 0.75 mm; increment 0.4 mm; medium-to-smooth convolution kernel (B26); resulting in a spatial resolution of 0.6-0.7 mm in-plane and 0.5 mm through-plane.

The reconstruction algorithm uses data from a single heart beat, obtained during a quarter X ray tube rotation by two separate X-ray tubes, resulting in a temporal resolution of 83 ms. Initially, a single dataset was reconstructed during the mid-diastolic phase (350 ms before the next R-wave).

Axial views and multi-planar reconstructions (MPR) were used to identify patency of grafts and anastomoses of grafts to coronary run-offs. Distal run-off supplied by a patent graft was separately evaluated.

Electrocardiogram

Additional 12-leads electrocardiograms were taken from all patients and analysed by two blinded observers.

Statistical Analysis

Data entry and statistical analysis were performed with the use of Epi Info 6.04c (CDC, Atlanta, Georgia). Continuous variables are displayed as means \pm standard deviation. Discrete variables are displayed as counts or proportions. Data within and between the groups were tested by paired and unpaired t-tests. A P-value of 0.05 or less was considered statistically significant. Sample size calculation showed that at least 10-11 patients in each group are necessary to detect a significant

difference in diastolic peak velocity between the 2 groups, assuming that diastolic peak velocity in single LIMA to LAD grafts is on average 22 cm/sec (range 15-30 cm/sec) [12] versus 35 cm/sec (range 25-45) [13] in T-grafts (assuming equal variances, $SD = 10$, $\alpha = 0.05$, power = 0.80).

RESULTS

In Group I, sixteen single LIMA to the LAD anastomoses were constructed with a total of sixty-six distal anastomoses, 4.1 ± 1.1 /patient. In group II, thirty-one LIMA anastomoses, forty-three FRIMA anastomoses, six gastro-epiploic artery anastomoses and one additional venous anastomoses were constructed, a total of eighty-one distal anastomoses, 4.5 ± 1.1 /patient, $P = 0.26$ between the groups.

The mean age of the 34 patients at the time of surgery differed significantly between the groups: $P = 0.034$. The time interval between operation and late follow-up is not significant: 11.5 ± 1.7 (Group I) versus 11.5 ± 1.1 years (Group II), $P = 0.91$.

Except for the heart rate, 74 ± 14 (Group I) versus 66 ± 11 b/min (Group II), $P = 0.046$, hemodynamic variables did not differ between both groups.

DSCT scan

In all thirty-four patients the DSCT scans were of diagnostic value. Examples are shown in Fig. 1, Fig. 2 and Fig. 3.

DSCT scans showed three string sign LIMA grafts (19 %) and six occluded venous anastomoses (12 %) in group I and three distal (downstream from the T anastomose) string sign LIMA grafts (17 %), two string sign FRIMA grafts (11 %), seven occluded LIMA anastomoses (23 %), nine occluded FRIMA anastomoses (21 %), one string sign GEA graft (17 %) and one occluded GEA anastomose (17 %) in group II.

Diameters and cross-sectional areas of the proximal LIMA grafts in group I are shown in Table 1. As expected, both variables differ significantly between the patent and string sign LIMA grafts. Diameters and cross-sectional area's of the proximal T-grafts in group II are shown in Table 2. As expected, both variables also differ significantly between both patent LIMA and FRIMA and distal string sign LIMA and distal string sign FRIMA grafts.

Finally, we selected only the patients with patent proximal LIMA grafts from group I and II to compare diameters and cross-sectional area's. Data are shown in Table 2.

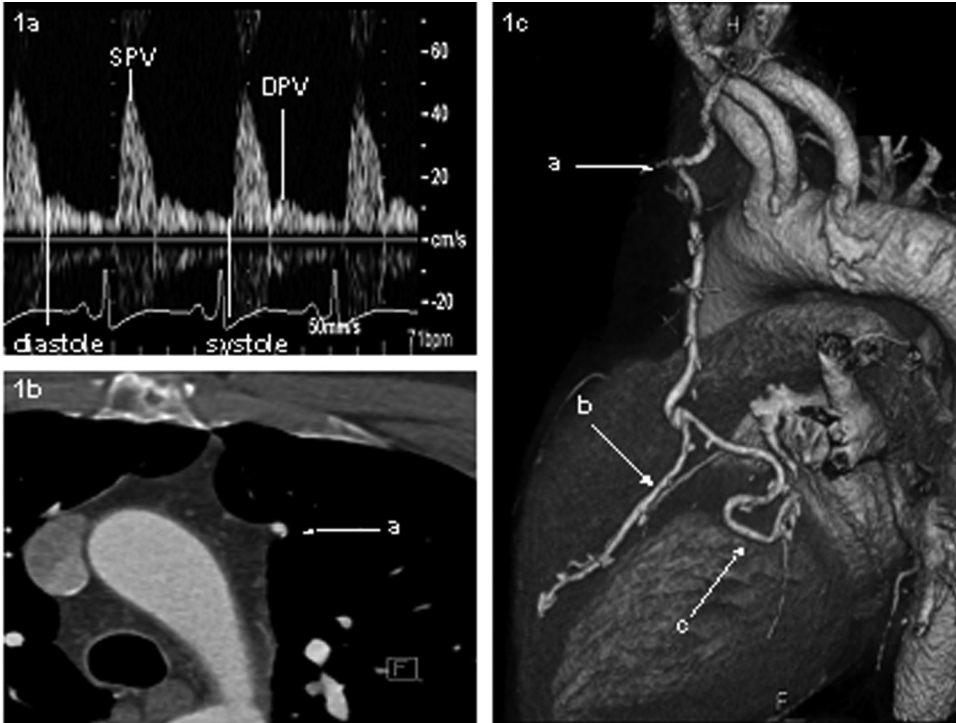


Figure 1. Late follow-up main stem transthoracic ultrasonography (1a) and DSCT coronary angiography of a patent composite arterial T-graft from the transverse (1b) and anterolateral view (1c). (a) main stem of the T-graft; (b) LIMA branch of the T-graft; (c) too large, not kinking, patent FRIMA branch of the T-graft. DSCT, Dual-source computed tomography; LIMA, left internal mammary artery; FRIMA, free right internal mammary artery; SPV, systolic peak velocity (cm/s); DPV, diastolic peak velocity (cm/s). (A full color version of this illustration can be found in the color section).

DSCT scans showed no proximal string sign LIMA grafts nor occluded LIMA grafts in the main stem of the T-grafts.

Table 1. Diameters and cross-sectional areas in proximal LIMA to LAD grafts

	LIMA-LAD N = 16	Patent LIMA graft N=13	String sign LIMA grafts N = 3	P
Diam origin (mm)	2.49 ± 0.5	2.7 ± 0.3	1.6 ± 0.44	0.00004
Area origin (cm ²)	0.05 ± 0.02	0.06 ± 0.01	0.02 ± 0.01	0.00024
Diam 2-3 ic (mm)	2.48 ± 0.47	2.66 ± 0.26	1.67 ± 0.25	0.00003
Area 2-3 ic (cm ²)	0.05 ± 0.02	0.06 ± 0.01	0.02 ± 0.01	0.00005

Diam = diameter, P = unpaired value for differences between patent en string sign LIMA grafts. Data are ± standard deviation.

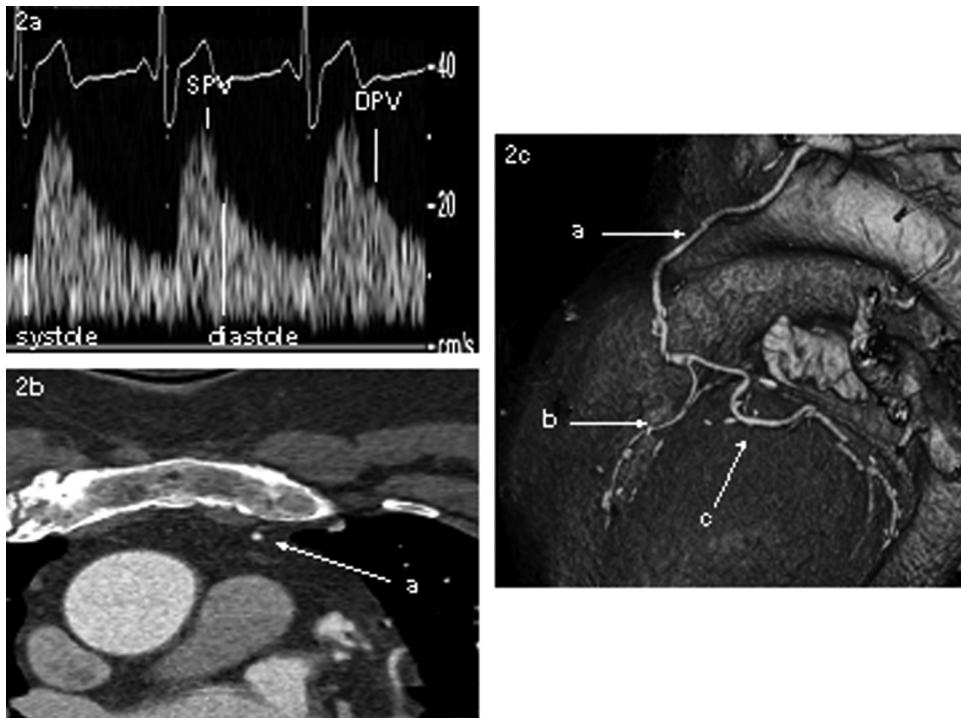


Figure 2. Late follow-up main stem transthoracic ultrasonography (2a) and DSCT coronary angiography of a composite arterial T-graft from the transverse (2b) and anterolateral view (2c). (a) main stem of the T-graft; (b) string sign LIMA branch of the T-graft; (c) patent FRIMA branch of the T-graft. Abbreviations as in Figure 1. (A full color version of this illustration can be found in the color section).

Ultrasonographic findings

Adequate Doppler profiles could be obtained from all 34 patients. Examples are shown in Fig. 1a, Fig. 2a and Fig. 3a. In 1 patient TTE and the Azoulay maneuver could not be performed due to time constraints.

No ultrasonographic differences could be obtained between the string sign LIMA grafts and the patent LIMA grafts within group I at rest nor during the Azoulay maneuver (Table 3). Even within these subgroups no differences appeared. Proximal string sign LIMA grafts were only observed in group I.

When only patent grafts in both groups were selected, only diastolic peak velocity at rest and total velocity integral values differs. Nevertheless, all variables are more pronounced in T-grafts at rest and during the Azoulay maneuver (Table 4).

Remarkably, ultrasonographic LIMA findings do not differ between and within the subgroups at rest and during the Azoulay maneuver and also hemodynamic observations do not differ between (sub) groups at rest and during the maneuver.

Table 2. Diameters and cross-sectional areas in proximal T-grafts and patent single LIMA grafts

	T-graft	LIMA-LAD	P
	N = 18	N = 13*	
Diam LIMA origin (mm)	3.47 ± 0.7	2.7 ± 0.3	0.001
Area LIMA origin (cm ²)	0.09 ± 0.04	0.06 ± 0.01	0.002
Diam LIMA 2-3rd i.c. (mm)	3.4 ± 0.7	2.7 ± 0.3	0.001
Area LIMA 2-3rd i.c. (cm ²)	0.09 ± 0.03	0.06 ± 0.01	0.001
Diam LIMA before T anastomose (mm)	3.4 ± 0.7		
Area LIMA before T anastomose (cm ²)	0.09 ± 0.04		
	T-graft	T-graft	
	Patent LIMA graft	Distal string sign LIMA graft	P*
	N = 13	N = 3	
Diam LIMA behind T anastomose (mm)**	3.0 ± 0.5	1.8 ± 0.1	0.003
Area LIMA behind T anastomose (cm ²)**	0.07 ± 0.02	0.04 ± 0.01	0.033
	Patent FRIMA graft	Distal string sign FRIMA graft	
	N = 14	N = 2	
Diam FRIMA behind T anastomose (mm)#	3.1 ± 0.5	1.8 ± 0.2	0.001
Area LIMA behind T anastomose (cm ²)#	0.08 ± 0.02	0.03 ± 0.01	0.009

LIMA, left internal mammary artery; FRIMA, free right internal mammary artery.

* proximal string sign LIMA grafts deleted. P = unpaired value for differences between proximal patent single LIMA and proximal patent T-grafts.

** 2 occluded distal LIMA grafts. # 2 occluded FRIMA grafts. P* = paired value for differences between patent and distal string sign T-grafts. Diam = diameter. Data are ± standard deviation.

Echocardiography

All but one patient underwent TTE to determine LVEF. In two patients, no adequate window could be obtained. In group I, the overall EF was 57 ± 16 versus 59 ± 9 % in group II, P = 0.71.

Electrocardiogram

All patients were in sinus rhythm and no ischemia could be detected in any patient.

Questionnaire

All but six patients (82 %) remained free of recurrent angina in the postoperative period until these late follow-up investigations. Four patients in group I and two patients in group II have suffered recurrent angina during exercise within the last six months but remained free of complaints during the investigations including during the Azoulay maneuver. Four patients already used β-blockers and 5 patients are controlled by their cardiologist. One patient in each group was already treated with stenting but still had complaints of angina. This patient in group II has three anastomoses on a string sign graft and 1 occluded FRIMA anastomose. The other patient in group II has four patent distal bypasses. Two patients from group I have string sign LIMA grafts with

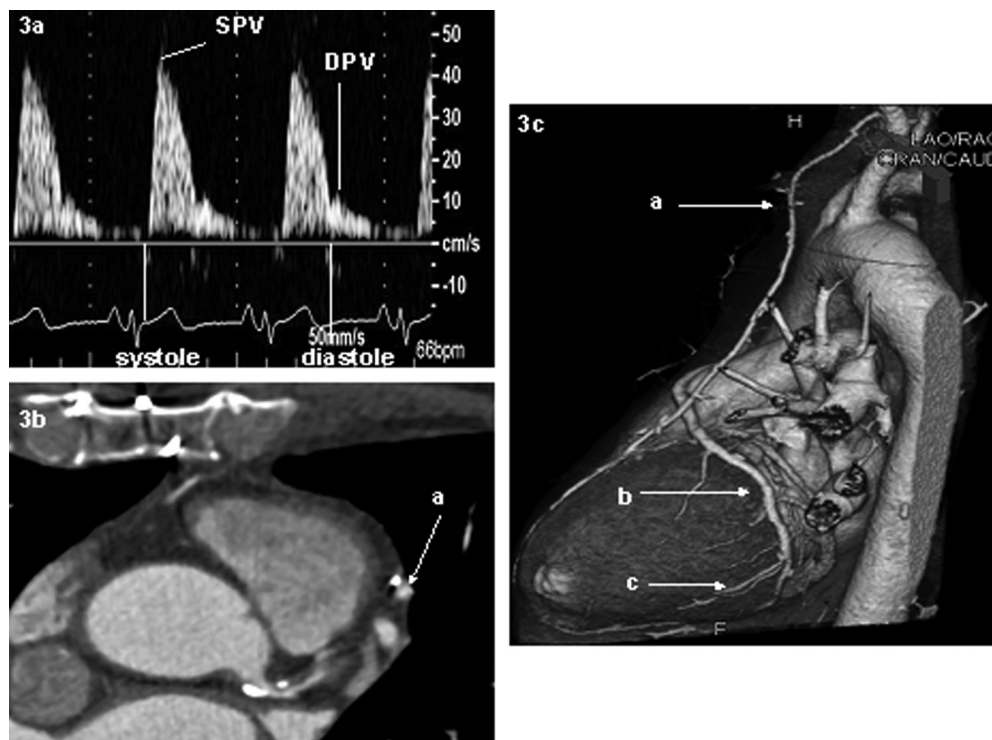


Figure 3. Late follow-up transthoracic ultrasonography (3a) and DSCT coronary angiography of a patent single LIMA graft to the LAD from the transverse view (3b) with an additional patent venous graft from the lateral view (3c). (a) patent LIMA graft. (b) patent venous jump graft to the lateral and inferior wall. (c) native obtuse margin branches. Abbreviations as in Figure 1. (A full color version of this illustration can be found in the color section).

Table 3. Ultrasonographic variables for string sign- and patent LIMA grafts in group I

Variable	Patent LIMA at rest	String sign LIMA at rest	P	Patent LIMA Azoulay	String sign LIMA Azoulay	P
	N = 13	N = 3		N = 13	N = 3	
DPV (cm/s)	16.5 ± 7.0	22.1 ± 6.0	0.22	17.2 ± 9.2	16.4 ± 5.1	0.89
SPV (cm/s)	56.2 ± 15.2	60.0 ± 33.6	0.76	57.6 ± 13.9	53.0 ± 31.3	0.68
DVI (cm ²)	6.3 ± 3.5	8.1 ± 3.2	0.44	6.3 ± 3.9	6.6 ± 4.3	0.90
SVI (cm ²)	11.7 ± 3.8	13.3 ± 8.6	0.61	12.0 ± 3.1	12.6 ± 8.7	0.85
TVI (cm ²)	16.1 ± 4.0	21.5 ± 11	0.16	17.7 ± 5.7	18.9 ± 12.6	0.80
DSVIR	0.54 ± 0.3	0.67 ± 0.2	0.43	0.53 ± 0.28	0.55 ± 0.15	0.90
DTVIR	0.35 ± 0.13	0.39 ± 0.04	0.60	0.34 ± 0.12	0.36 ± 0.07	0.81
DSPVR	0.3 ± 0.1	0.41 ± 0.1	0.09	0.3 ± 0.1	0.35 ± 0.14	0.49

DPV, diastolic peak velocity; SPV, systolic peak velocity; DVI, diastolic velocity integral; SVI, systolic velocity integral; TVI, total (diastolic + systolic) velocity integral; DSVIR, diastolic/systolic velocity integral ratio; DTVIR, diastolic/total (diastolic + systolic) velocity integral ratio; DSPVR, peak diastolic/peak systolic velocity ratio. P = paired values for differences within the groups. Data are ± standard deviation.

Table 4. Ultrasonographic variables in patent grafts in group I and II at rest and during the Azoulay maneuver

Variable	Group I at rest	Group II at rest	P	Group I Azoulay	Group II Azoulay	P
	N = 13	N = 13		N=13	N=13	
DPV (cm/s)	16.5 ± 7.0	23.5 ± 8.8	0.03	17.2 ± 9.2	25.4 ± 13.1	0.08
SPV (cm/s)	56.2 ± 15.2	76.8 ± 36.2	0.07	57.6 ± 13.9	97.7 ± 75.2	0.07
DVI (cm ²)	6.3 ± 3.5	9.0 ± 4.1	0.09	6.3 ± 3.9	9.3 ± 4.4	0.09
SVI (cm ²)	11.7 ± 3.8	14.2 ± 5.8	0.20	12.0 ± 3.1	18.7 ± 11.8	0.06
TVI (cm ²)	16.1 ± 4.0	24.8 ± 10.3	0.01	17.7 ± 5.7	25.9 ± 10.4	0.02
DSVIR	0.54 ± 0.3	0.66 ± 0.23	0.24	0.53 ± 0.28	0.56 ± 0.21	0.77
DTVIR	0.35 ± 0.13	0.37 ± 0.1	0.58	0.34 ± 0.12	0.34 ± 0.1	0.87
DSPVR	0.3 ± 0.1	0.34 ± 0.1	0.33	0.3 ± 0.1	0.3 ± 0.1	0.97

Group I, patients with single LIMA grafts to the LAD and additional vein grafts; Group II, patients with LIMA-free RIMA composite T-grafts. P = unpaired value for only patent grafts between the groups. Abbreviations as described in Table 3. Data are ± standard deviation.

four respectively three patent distal venous bypasses. The other two patients in this group have a patent LIMA graft, one with three patent distal venous bypasses and one with one patent venous bypass and three occluded venous bypasses.

DISCUSSION

The intrinsic properties of internal mammary arteries explain the long term survival of these bypass grafts [14-15] which results in the statement that arterial composite T-grafts also would have a good long-term graft patency. It can be employed in patients with a severe sclerotic aorta which favours complications due to aortic manipulations and complete revascularization can also be achieved in ventricular fibrillation with the use of extracorporeal circulation or in the beating heart reducing aortic manipulations [4].

Coronary arteriography (CA) is still the accepted method for quantitative evaluation of bypass grafts irrespectable whether the patient suffers angina. However, CA is an invasive procedure which in patients with T-grafts may result in serious events (hypoperfusion) due to induced spasm of the main stem. Therefore, we performed two different control methods in order to determine functional and anatomical patency of (T-) grafts.

With the introduction and development of cardiac CT scans in recent years, imaging of moving coronary arteries and bypass grafts has become feasible. Sensitivities and specificities above 90 % have been reported for coronary artery stenosis compared to coronary angiography [16-18]. However, cardiac CT scans are essentially a morphologic and not a functional diagnostic method

in coronary artery bypass control. So, we performed additionally ultrasonography at rest and during the Azoulay maneuver to assess the functionality of single LIMA grafts and the main stem of T-grafts. One of the aims of the study was to determine whether TTE can play a role in the assessment of different LIMA perfusion areas whereas TTE of T-grafts have not been described over a follow-up period over 10-years.

Adequate Doppler profiles of the single LIMA and the main stem of the T-grafts at rest and during the Azoulay maneuver were obtained in all patients which is extremely successful [19]. However, no overall ultrasonographically significant differences were obtained between the groups nor between subgroups at rest or during the Azoulay maneuver. With respect to the larger perfusion area of the T-grafts, one should expect higher ultrasonographic values in these grafts compared to single LIMA grafts. Even the number of occluded T-graft anastomoses does not influence Doppler profiles.

It is remarkable to notice that the Azoulay maneuver did not have any influence on the Doppler profiles. This finding strengthens the assumption that the 'dynamic' LIMA graft progresses into a 'fixed' or 'steady' (ultrasonographic) state. One of the explanations why the Azoulay maneuver does not affect patients from both groups may be related to the fact that physiological exercise does not appear to be as complete as pharmacological inducement [20].

Prifti et al. [21] stated in a short follow-up study that peak systolic and diastolic velocity ratios are good variables for demonstrating the functional T-graft status. Ratios of greater than 0.85 demonstrated good flow through both distal branches of the T-graft. This means that systolic and diastolic peak velocities equalize in contrast to preoperative values [22]. In spite of the in situ RIMA graft in their study, our findings in the in situ LIMA grafts are different. We found in patent T-grafts values of 0.3 ± 0.1 and we also measured these values in patent single LIMA grafts. So, these values are not discriminative in our long-term follow-up study. We did not extrapolate the values of main stems of patients with occluded FRIMA grafts because of the small number of these patients ($n = 2$).

Lemma et al. [23] described in a short term follow-up study their angiographic- and guide wire findings in the proximal and distal arterial composite T-grafts using radial arteries versus single LIMA to the LAD grafts. They found significant differences between the groups for proximal time-average peak velocities. We did not calculate this variable but in patent grafts DPV at rest appeared also significant with higher values in the T-grafts ($P = 0.03$) while SPV did not ($P = 0.07$). The ratio of these variables remains equal in our study, 0.3 ± 0.1 in both groups, while significant differences appear in their study: 0.9 ± 0.4 for single LIMA grafts versus 1.1 ± 0.2 for T-grafts, ($P = 0.03$), suggesting a higher diastolic part in the cardiac cycle in T-grafts. However, our data were derived from the transthoracic approach in a late follow-up setting. Neverthe-

less, angiography showed significantly greater proximal LIMA diameters in T-grafts than in single LIMA grafts (2.8 ± 0.4 versus 2.4 ± 0.5 mm, $P = 0.019$). Our DSCT findings are similar for the origin of the LIMA graft as well as for the third intercostal space. Diameters in the T-graft group in our study appeared higher compared to the study of Lemma et al. (3.5 ± 0.7 versus 2.8 ± 0.4 mm). An explanation for this finding can be the higher number of anastomoses with T-grafts per patient in our study although this should be interpreted carefully while we used another method to measure diameters and we performed the study in a different follow-up setting. However, Gurne et al. [24] already described the ability of the IMA graft to adapt its dimension to flow demand in the late postoperative period.

These findings probably explain the equalization of the Doppler profiles between the groups. We assume that the overall myocardial perfusion area of T-grafts is larger compared to single LIMA grafts. Therefore, we suppose that overall blood flow through the T-grafts is larger compared to the single LIMA grafts. This statement was enhanced by the DSCT findings. It would be interesting to perform also a DSCT scan during hyperemic response or the Azoulay maneuver. This was however not included in our protocol.

The number of occluded T-graft anastomoses in our study seems relatively high [25-26]. According to Pevni and Nakajima [25-25], besides technical problems, occluded bypass grafts can be the results of competitive flow, especially in patients with moderate stenoses in coronary arteries. This should be a subject for further detailed analysis in comparison with the findings of sequential LIMA grafts [25-27].

Study limitations

We were interested in absolute values of TTE variables in proximal LIMA grafts to discriminate between single LIMA and T-grafts. We did not consider the severity of coronary stenosis nor estimated competitive flow between these systems although we assume that these factors can influence absolute values. Cardioactive medication was continued during the study. This could affect ultrasonographic measurements during the Azoulay maneuver.

In conclusion, ultrasonography can detect adequate Doppler profiles in the proximal part of single LIMA bypass grafts as well as in T-grafts.

Proximal LIMA diameters and areas, assessed by DSCT, are significantly larger in T-grafts compared to single LIMA grafts, probably due to larger perfusion areas, which can explain the equalization of ultrasonographic variables with no significant differences between and within both groups at rest and during the Azoulay maneuver 12 years after surgery.

REFERENCES

1. Loop FD, Lytle BW, Cosgrove DM, et al. Influence of the internal mammary artery graft on 10-year survival and other cardiac events. *N Engl J Med* 1986;314:1-6.
2. Fiore AC, Naunheim KS, Dean P, et al. Results of internal thoracic artery grafting over 15 years: single versus double grafts. *Ann Thorac Surg* 1990;49:202-9.
3. Pevni D, Kramer A, Paz Y, et al. Composite arterial grafting with double skeletonized internal thoracic arteries. *Eur J Cardiothorac Surg* 2001;20:299-304.
4. Wendler O, Hennen B, Demertzis S, et al. Complete arterial revascularization in multivessel coronary artery disease with 2 conduits (skeletonized grafts and T grafts). *Circulation* 2000;102(Suppl 3):79-83.
5. Muneretto C, Bisleri G, Negri A, et al. Total artery myocardial revascularization with composite grafts improves results of coronary surgery in elderly: a prospective randomized comparison with conventional coronary artery bypass surgery. *Circulation* 2003;108(Suppl 2):29-33.
6. Wendler O, Hennen B, Markwirth T, et al. T grafts with the right internal thoracic artery to the left internal thoracic artery versus the left internal thoracic artery and radial artery: flow dynamics in the internal thoracic artery main stem. *J Thorac Cardiovasc Surg* 1999;118:841-8.
7. Raja SG. Composite arterial grafting. *Expert Rev Cardiovasc Ther* 2006;4:523-33.
8. Nakajima H, Kobayashi J, Funatsu T, et al. Predictive factors for the intermediate-term patency of arterial grafts in aorta no-touch off-pump coronary revascularization. *Eur J Cardiothorac Surg* 2007;32:711-7.
9. Ropers D, Pohle FK, Kuettner A, et al. Diagnostic accuracy of non-invasive coronary angiography in patients after bypass surgery using 64-slice spiral computed tomography with 330-ms gantry rotation. *Circulation* 2006;114:2334-41.
10. Schiller NB, Shah PM, Crawford M, et al. Recommendations for quantitation of the left ventricle by two-dimensional echocardiography. American society of echocardiography committee on standards, subcommittee on quantitation of two-dimensional echocardiograms. *J Am Soc Echocardiogr* 1989;2:358-67.
11. Calafiore AM, Teodori G, Di Giammarco G, et al. Minimally invasive coronary artery bypass grafting on a beating heart. *Ann Thorac Surg* 1997;63:S72-5.
12. Ichikawa Y, Kajiwara H, Noishiki Y, et al. Flow dynamics in internal thoracic artery grafts 10 years after coronary artery bypass grafting. *Ann Thorac Surg* 2002;73:131-7.
13. Hartman JM, Kelder JC, Ackerstaff RG, Vermeulen FE, Bogers AJ. Differences in LIMA Doppler characteristics for different LAD perfusion areas. *Eur J Cardiothorac Surg* 2001;20:1135-41.
14. Sons HJ, Godehardt E, Kunert J, Losse B, Bircks W. Internal thoracic artery: prevalence of atherosclerotic changes. *J Thoracic Cardiovasc Surg* 1993;106:1192-5.

15. Kobayashi H, Kitamura S, Kawachi K, Morita R, Konishi Y, Tsutsumi M. A pathohistological and biochemical study of atherosclerosis in the internal thoracic artery, a vessel commonly used as a grafts in coronary artery bypass surgery. *Surg Today* 1993;23:697-703.
16. Leber AW, Knez A, von Ziegler F, et al. Quantification of obstructive and nonobstructive coronary lesions by 64-slice computed tomography: a comparative study with quantitative coronary angiography and intravascular ultrasound. *J Am Coll Cardiol* 2005;46:147-54.
17. Mollet NR, Cademartiri F, van Mieghem CA, et al. High-resolution spiral computed tomography coronary angiography in patients referred for diagnostic conventional coronary angiography. *Circulation* 2005;112:2318-23.
18. Ropers D, Rixe J, Anders K, et al. Usefulness of multidetector row spiral computed tomography with 64-x0.6 mm collimation and 330-ms rotation for the non-invasive detection of significant coronary artery stenoses. *Am J Cardiol* 2006;97:343-8.
19. Gatti G, Bentini C, Maffei G, et al. Noninvasive dynamic assessment with transthoracic echocardiography of a composite arterial Y-graft achieving complete myocardial revascularization. *Ann Thorac Surg* 2005;79:1217-24.
20. Barnard RJ, Duncan HW, Livesay JJ, Bucberg GD. Coronary vasodilatory reserve and flow distribution during near maximal exercise in dogs. *J Appl Physiol* 1977;43:988-92.
21. Prifti E, Bonacchi M, Frati G, Proietti P, Giunti G, Leacche M. A graft with the radial artery or free left internal mammary artery anastomosed to the right internal mammary artery: flow dynamics. *Ann Thorac Surg* 2001;72:1275-81.
22. de Bono DP, Samani NJ, Spyt TJ, Hartshorne T, Thrush AJ, Evans DH. Transcutaneous ultrasound measurement of blood-flow in internal mammary artery to coronary artery grafts. *Lancet* 1992;339:379-81.
23. Lemma M, Innorta A, Pettinari M, et al. Flow dynamics and wall shear stress in the left internal thoracic artery: composite arterial graft versus single graft. *Eur J Cardiothorac Surg* 2006;29:473-8.
24. Gurte O, Chenu P, Polidori C, et al. Functional evaluation of internal mammary artery bypass grafts in the early and late postoperative periods. *J Am Coll Cardiol* 1995;25:1120-8.
25. Pevni D, Hertz I, Medalion B, et al. Angiographic evidence for reduced graft patency due to competitive flow in composite arterial T-grafts. *J Thorac Cardiovasc Surg* 2007;133:1220-5.
26. Nakajima H, Kobayashi J, Tagusari O, Bando K, Niwaya K, Kitamura S. Competitive flow in arterial composite grafts and effect of graft arrangement on off-pump coronary revascularization. *Ann Thorac Surg* 2004;78:481-6.
27. Dion R, Glineur D, Derouck D, et al. Long-term clinical and angiographic follow-up of sequential internal thoracic artery grafting. *Eur J Cardiothorac Surg* 2000;17:407-14.

Addendum 3

Unusual cause of myocardial ischemia non-invasively assessed with ECG-gated computed tomography coronary angiography

European Journal of Cardiothoracic Surgery.
2006; 29:840.

*Pugliese F, Meijboom WB,
Cademartiri F, Krestin GP.*

*Department of Radiology
Department of Cardiology
Erasmus MC, Rotterdam, the
Netherlands*

SUMMARY, METHODS AND RESULTS

A 71-year-old otherwise healthy woman presenting with atypical chest pain and inconclusive ECG-treadmill test was referred for ECG-gated, 64-detector row computed tomography to study coronary arteries noninvasively (Figures 1 and 2).

Non-ruptured Valsalva aneurysms do not usually cause cardiac dysfunction. However, coronary insufficiency may eventually develop with the expanding sinus.

Supplementary data

Supplementary data (Video 1) associated with this article can be found, in the online version, at doi:10.1016/j.cjcts.2006.02.028

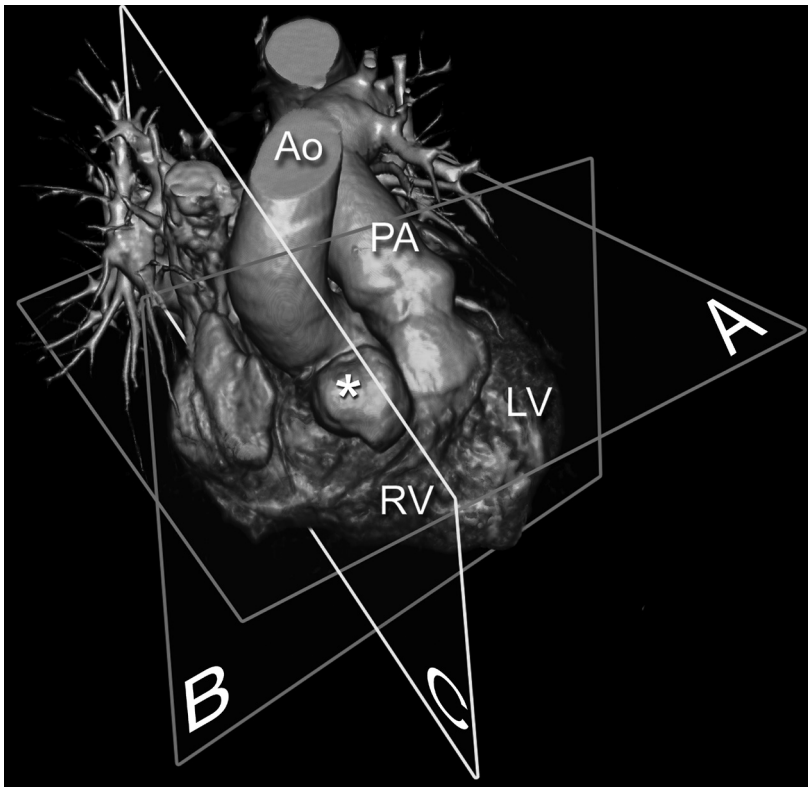


Figure 1. Volume-rendered ECG-gated CT image showing a right Valsalva sinus aneurysm (asterisk). Ao: aorta; PA: pulmonary artery; LV: left ventricle; RV: right ventricle.

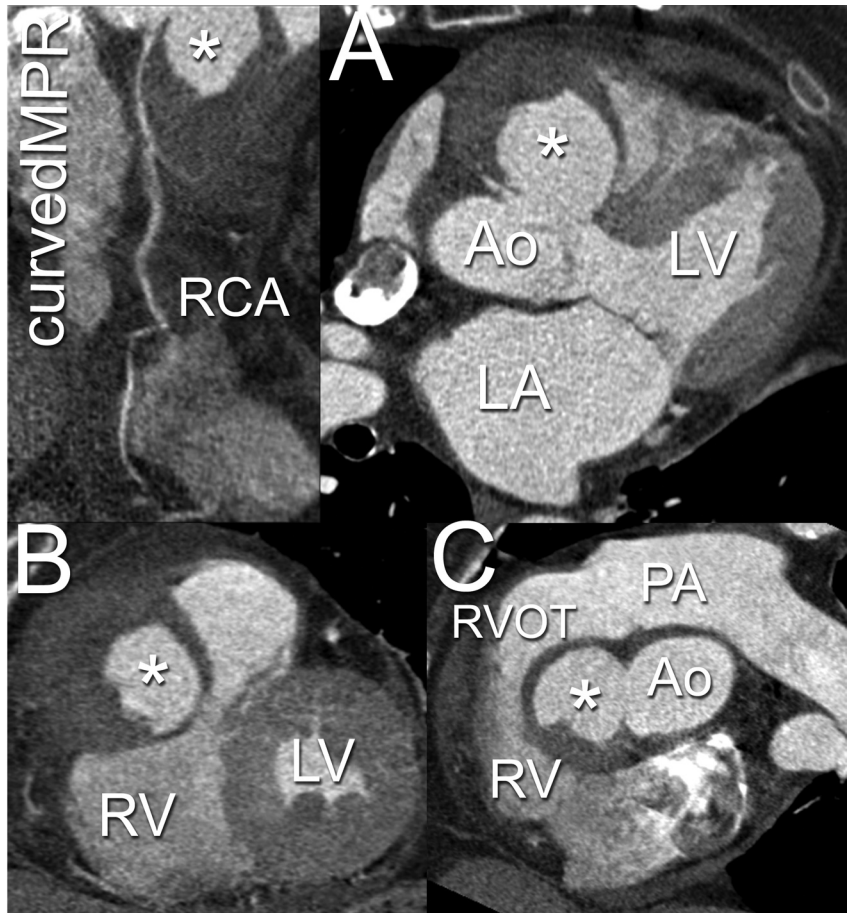
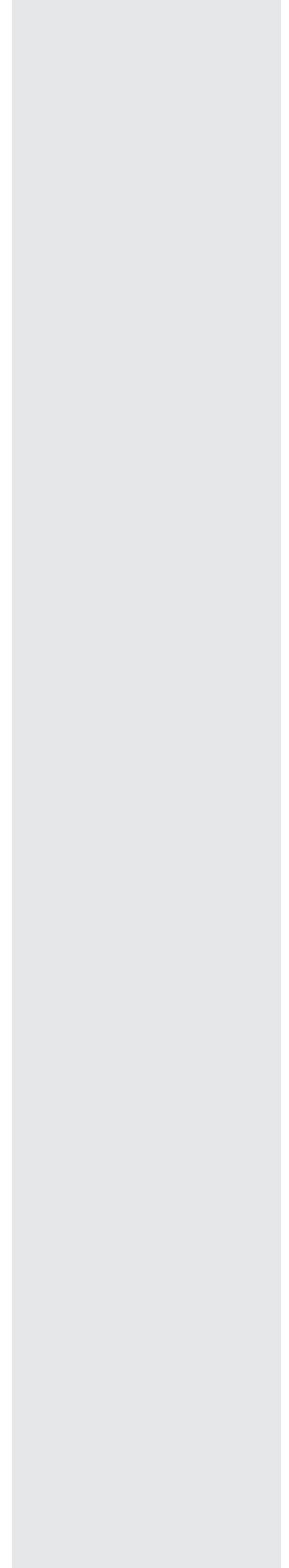


Figure 2. Curved multiplanar reconstruction (curved MPR) of the right coronary artery (RCA) and multiplanar reconstructions (A—C) obtained as indicated in Figure 1. On the curved MPR, the proximal RCA is critically narrowed due to the presence of the aneurysm (asterisk), which is seen bulging between the right ventricle (RV) and the aortic root (Ao) on multiplanar reconstructions (A—C). Thick eccentric thrombus is layered on the ectatic walls. As shown in (A), the ostium of the RCA opens at the level of the aneurysmal neck. No signs of rupture can be seen. The patient underwent uneventful surgery. The RCA was revascularized with a venous graft. Asterisk: aneurysm; Ao: aorta; LA: left atrium; LV: left ventricle; RV: right ventricle; RVOT: right ventricular outflow tract; PA: pulmonary artery.

PART 5

CTCA and bifurcations



18

Detection and characterization of coronary bifurcation lesions with 64-slice computed tomography coronary angiography

European Heart Journal.
2007 Aug 28(16):1968-76.

Carlos A.G. Van Mieghem^{1,2},
Attila Thury¹, Willem
B. Meijboom^{1,2}, Filippo
Cademartiri^{1,2}, Nico R.
Mollet^{1,2}, Annick C.
Weustink^{1,2}, Georgios Stanos¹,
Peter P.T. de Jaegere¹, Patrick
W. Serruys¹, Pim J. de Feyter^{1,2}

From the departments of
Cardiology ¹ and Radiology ²,
Erasmus MC, Rotterdam, the
Netherlands

ABSTRACT

Objectives

To compare the performance of 64-slice computed tomography coronary angiography (CTCA) and invasive coronary angiography (ICA) in the detection and classification (according to the Medina system) of bifurcation lesions (BL).

Methods

We studied 323 consecutive patients undergoing 64-slice CTCA prior to ICA. All coronary segments ≥ 2 mm in diameter were evaluated for the presence of a significant ($\geq 50\%$ diameter reduction on quantitative coronary angiography) BL. Evaluation of BL by CTCA included the assessment of significant lumen obstruction in both main and side branch vessels.

Results

Forty-one out of 43 patients (46/48 lesions) with significant BL were identified by CTCA. Excluding coronary segments with non-diagnostic image quality (5%), the sensitivity, specificity, positive and negative predictive values of CTCA for detecting significant BL was 96, 99, 85 and 99% respectively. In 39 of these 41 patients, CTCA assessment was concordant with the Medina lesion classification on ICA.

Conclusion

64-slice CTCA allows accurate assessment of complex BL.

INTRODUCTION

Invasive coronary angiography is regarded as the reference standard for the diagnosis of significant coronary artery disease and to plan and guide percutaneous coronary intervention (PCI). However, coronary angiography has major limitations. Factors such as vessel overlap and foreshortening may make it difficult to accurately assess the severity and extent of coronary artery lesions¹. Furthermore, as angiography only visualizes the lumen, it cannot identify plaque accumulation related to positive remodeling, a ubiquitous phenomenon at bifurcation sites².

The high diagnostic accuracy of computed tomography coronary angiography (CTCA) in the non-invasive detection of significant coronary artery disease (CAD) is well established^{3,4}. However, the potential role of CTCA in the detection and characterisation of coronary bifurcations is unclear. CTCA allows 3-dimensional evaluation of both the lumen and the wall of the vessel; thus, it has potential to provide a more comprehensive assessment of the complex geometry of bifurcation lesions (BLs). The purpose of the present study is to evaluate the diagnostic accuracy of CTCA in patients with bifurcation pathology. Furthermore, we provide a detailed comparison with conventional angiographic data by categorizing each BL according to a simplified classification system (Medina)⁵.

METHODS

Patient selection

The study population comprised 323 consecutive patients who underwent 64-slice CTCA, within a 2-week period prior to invasive coronary angiography (ICA) between March and December 2005. In patients with prior PCI or coronary artery bypass graft surgery (CABG), only the nonintervened coronary artery segments were included in the analysis. Contra-indications for CTCA were: an irregular heart rhythm, inability to breath hold for 15 seconds, renal dysfunction (creatinine clearance < 60 ml/min), and known contrast allergy. The institutional ethical review board approved the study protocol, which complied with the declaration of Helsinki. All patients gave written informed consent.

MSCT protocol, radiation dose calculation and image reconstruction

Patients with a resting heart rate above 65 beats per minute (bpm) received oral beta-blockers (metoprolol 50-100 mg) or a non-dihydropyridine calcium-antagonist (diltiazem 60-120 mg) together with 0.5-1 mg lorazepam 1 hour before the scan. An additional IV bolus of metoprolol (5-10 mg) was occasionally administered where the heart rate remained above 65 bpm. The examination was performed using previously reported methodology.⁴ In brief, CTCA data were acquired using a 64-slice CT scanner (Sensation 64, Siemens, Germany). A non-enhanced calcium-scoring

scan was only obtained in patients without previous PCI or CABG using the following parameters: collimation 64 x 0.6 mm, tube rotation time 330 ms, table feed 3.8 mm per rotation, tube current 150 mAs at 120 kV, and prospective x-ray tube modulation. Angiographic scan parameters were identical aside from a tube current that ranged between 850 and 960 mAs without the use of dose pulsing. The effective radiation dose was calculated separately for patients with and without previous CABG using dedicated software (ImPACT CT Patient Dosimetry Calculator, version 0.99x), as described in the European Guidelines on Quality Criteria for Computed Tomography (Available at: <http://www.dr.dk/guidelines/ct/quality/index.htm>).⁶

A bolus of 100 ml of contrast (iomeprol, 400 mg iodine/ml, Iomeron[®], Bracco, Milan, Italy) was administered in all patients. The standard injection rate was 5 ml/sec, but was decreased to 4 ml/sec in patients who had previous CABG. We did not use a saline chaser after contrast administration. A bolus tracking technique was used to monitor the appearance of contrast material in the aortic root cranial to the origin of the left coronary artery. Once the signal in the ascending aorta reached a predefined threshold of 100 Hounsfield units, CT data were acquired during an inspiratory breath-hold.

All scans were analyzed off-line using a Leonardo workstation (Siemens Medical Solutions) by 2 independent observers who were blinded to the results of ICA. Images were reconstructed using ECG-gating to obtain optimal, motion free image quality. Datasets were routinely obtained during the mid-to-end diastolic phase (-300, -350, -400, -450 ms before the next R-wave or at 60 to 70% of the R-R interval). Additional reconstruction windows in systole (in general at 25% to 35% of the R-R interval) were explored when image quality was suboptimal on the standard reconstructions. In 31% of the cases the end-systolic dataset was used for image analysis.

Image quality was evaluated on a per segment basis and classified as good (defined as absence of any image-degrading artefacts related to motion, calcification, or insufficient contrast enhancement), adequate (presence of image-degrading artefacts, but evaluations possible with moderate confidence), or poor (presence of image-degrading artefacts and evaluation only possible with low confidence). Coronary artery segments with poor image quality were judged to be "unevaluable".

CTCA analysis

All evaluable coronary segments were visually scored for the presence of significant BLs (diameter reduction of $\geq 50\%$) by careful axial scrolling and using (curved) multiplanar reconstructions. A bifurcation lesion was defined as a stenosis that involved the origin of a side branch, equal to or more than 2.0 mm in diameter.⁷ The presence or absence of side branch pathology was determined by evaluating the first 10 mm of the side branch for the presence of significant lumen

narrowing. Disagreement between observers was resolved by a third observer, and the consensus reading was subsequently compared with the ICA.

High-resolution thin slab multiplanar reconstructions (reconstructed slice thickness of 0.75 mm) were used for assessment of bifurcation angles. The 3 orthogonal planes as provided when opening a CT dataset were carefully orientated according to the geometrical orientation of the main vessel and side branch at the bifurcation point (Figure 1A). To determine the angle of bifurcation, we depicted 2 lines (in the centre of each vessel lumen) along the initial course of the distal part of the main branch (MBd) and side branch (SB) using the MPR view in which the angulation between the proximal parts of these 2 vessels was maximal (Figure 1B). We only used diastolic datasets to measure bifurcation angles. Subsequently, BL with significant lumen narrowing were categorized using a recently introduced classification scheme, known as the MEDINA bifurcation

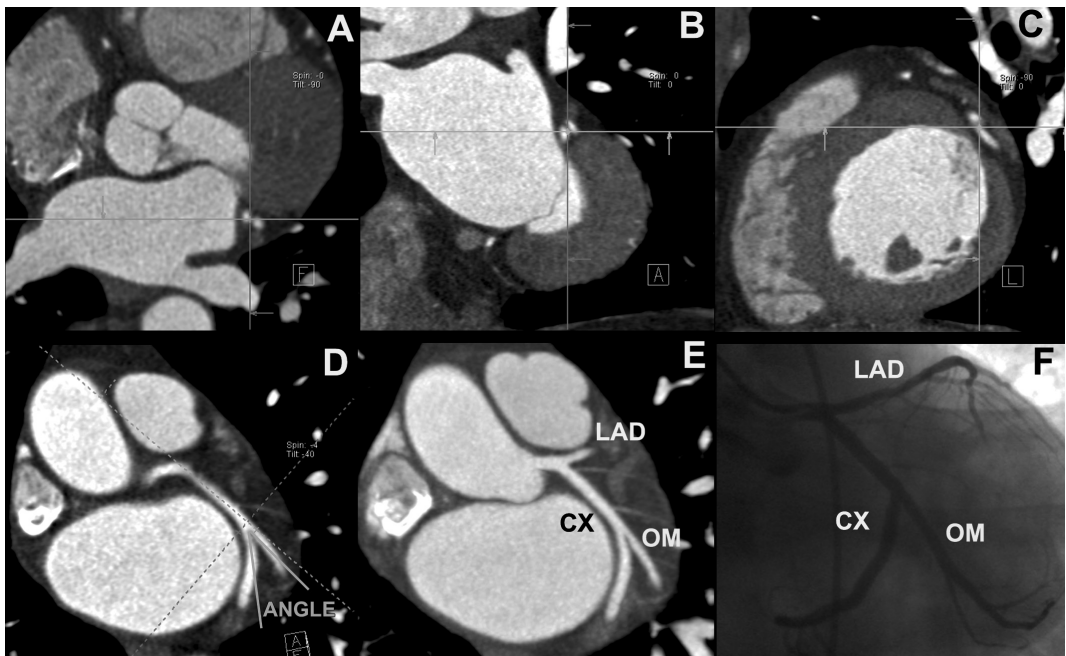


Figure 1a. Visualization of the circumflex obtuse marginal bifurcation by invasive coronary angiography (a) and volume-rendered computed tomography coronary angiography (b). The three-dimensional representation of the heart, as shown in (b), can be obtained by summation of the 'raw' axial computed tomography images that have a defined x-y-z dimension. The conventional planes that are used for visualization of this volume data set are the axial plane (axial), the coronal plane (coronal) and the sagittal plane (sagittal). CX, circumflex coronary artery; LAD, left anterior descending coronary artery; OM, obtuse marginal branch. (A full color version of this illustration can be found in the color section).

classification (Figure 2).⁵ The Medina classification is a simple binary system whereby significant lumen narrowing is classified as present (1) or absent (0) in the proximal MB, distal MB, and SB. Modification and scrolling of MPR images originating from the bifurcation site was used to confirm the exact spatial relation of the lumen obstruction in relation to the branching point.

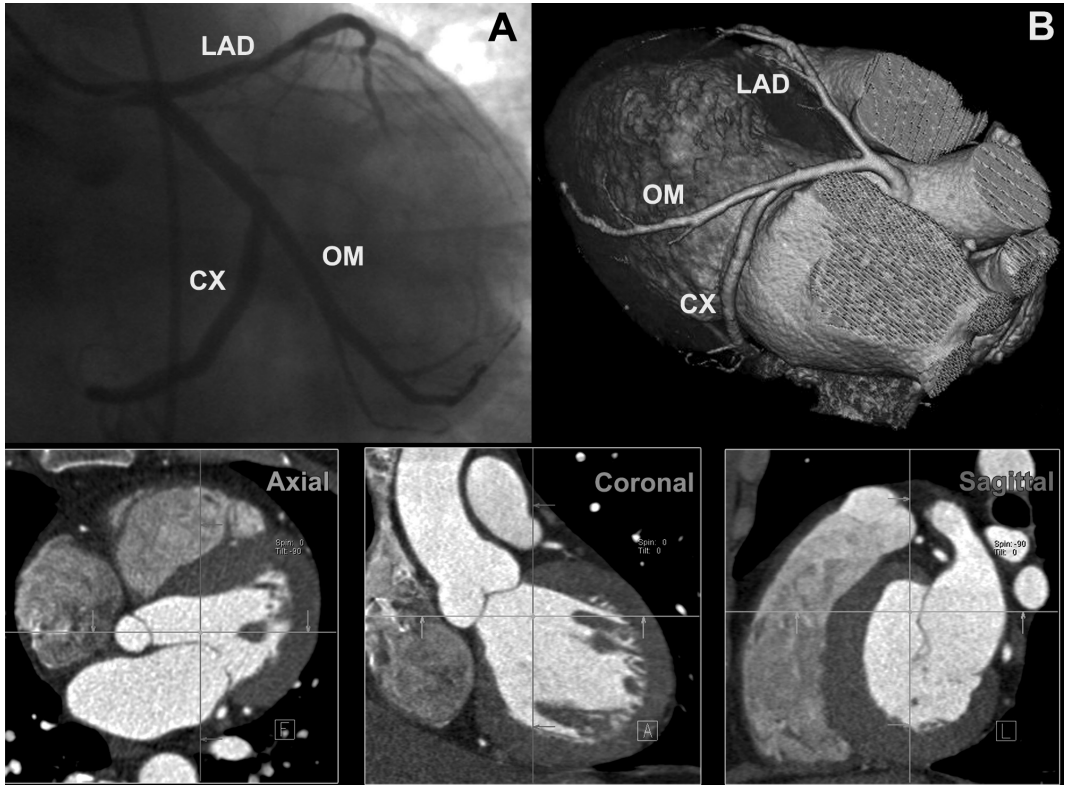


Figure 1b. Scrolling of axial images provides a quick view of the data set to assess crudely the main features of the coronary anatomy. To obtain a precise view of the structure of interest, in this example the circumflex-obtuse marginal bifurcation, the planes of visualization need to be orientated to the geometrical orientation of the coronary structures. As a first step, the three conventional image planes are centered at the level of the branching point (a-c). The three-dimensional nature of the CT data allows to subsequently tilt these image planes in any orientation. The resulting multiplanar reconstruction (d) precisely shows the relationship of the main vessel with the side branch and is used to assess the angle between the initial course of distal portion of the main vessel and side branch (in this example, 31°). Also shown is a maximum intensity projection computed tomography image (e) to demonstrate the anatomical correlation with the angiographic view. We did not use this maximum intensity projection reconstruction to determine bifurcation angles. CX, circumflex coronary artery; LAD, left anterior descending coronary artery; OM, obtuse marginal branch. (A full color version of this illustration can be found in the color section).

Quantitative coronary angiography

Coronary angiograms were obtained in multiple projections after intracoronary nitrate administration with standard techniques. Two experienced cardiologists blinded to CTCA results identified all available coronary segments using a 17-segment modified American Heart Association (AHA) classification and classified all coronary segments as < 2 and ≥ 2 mm in diameter using validated, automated, edgedetection software (CAAS II, Pie Medical, Maastricht, the Netherlands).⁸ Only segments classified as ≥ 2 mm in reference diameter were considered for comparison with CTCA. In the presence of an occluded coronary artery, we only assessed the segments that were located proximal to the occlusion. Standard measurements were made for the MB analysis; the proximal border of the SB was depicted manually by extending the reference point into the main vessel, as previously reported.⁹ Significant lumen narrowing was defined as a lumen diameter

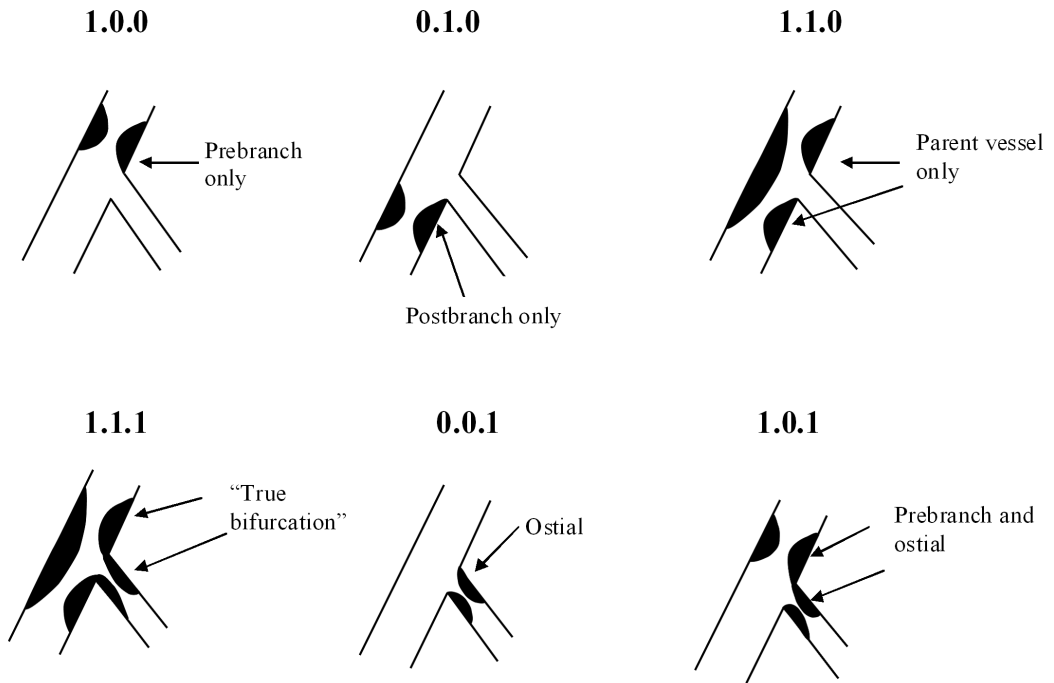


Figure 2. Medina binary classification of coronary bifurcation lesions.

reduction of $\geq 50\%$ in the MB and/ or SB. Identified BLs were subsequently classified according to the Medina classification system.⁵ All measurements, including bifurcation angles, were determined using end-diastolic frames.

Statistical analysis

Continuous variables are presented as mean \pm standard deviation and compared by Student's t-test. A two-sided p-value of <0.05 was considered to be significant. Categorical variables are presented as counts and percentages. The diagnostic performance of CTCA for the detection of significant BL, when compared with quantitative coronary angiography (QCA), is presented as sensitivity, specificity, positive and negative predictive value and reported with associated 95% confidence intervals based on binomial probabilities. Diagnostic performance indices are presented separately for all "evaluable" segments and for the overall population, including coronary segments with poor image quality. These "unevaluable" segments were classified as having a stenosis on CTCA. Because of potentially interdependent observations, i.e. multiple bifurcations in the same patient, an additional measurement of diagnostic accuracy was performed for a random selection of single observations per patient. Statistical analysis was performed with SPSS, version 11.5 (SPSS Inc., Chicago, USA).

Table 1. Patient characteristics (n= 323).

Characteristic	Value
Age	61.3 ± 10.4
Male (%)	72
Body mass index (kg/m ²)	27.2 ± 4.3
Clinical presentation	
Stable angina (%)	60
ACS (%)	14
Other (%)	26
Current smoker (%)	27
Hypertension (%)	53
Dyslipidemia (%)	81
Diabetes mellitus (%)	16
Creatinin (mg/dl)	0.97 ± 0.2
Prior MI (%)	33
Prior PCI (%)	32
Prior CABG (%)	10
Vessel disease (%)	
Non-significant disease	28
1-vessel disease	38
2-vessel disease	18
3-vessel disease	8
Left main disease	5
Graft disease	3
Basal heart rate	68.5 ± 10.2
Heart rate during CTCA	58 ± 7.2
CTDIvol no previous CABG (Gy)	70.5
CTDIvol previous CABG (Gy)	61
Dose estimate (no previous CABG) (mSv)a	19
Dose estimate (previous CABG) (mSv)a	22

Categorical data are presented as numbers (%) and continuous data as mean values ±SD.

ACS, acute coronary syndrome; CABG, coronary artery bypass graft surgery; CAD, coronary artery disease; CTCA, computed tomography coronary angiography; CTDIvol, volume computed tomography dose index; MI, myocardial infarction; PCI, percutaneous coronary intervention.

a The estimated radiation dose is higher in bypass patients because of the longer scan length.

RESULTS

All 323 patients tolerated the CTCA procedure well and no complications occurred. The average time required for the cardiac CT examination, including patient preparation for scanning, image acquisition and reconstruction of the appropriate datasets was 20 to 25 min. Evaluation of the CT coronary angiogram took on average about 5-10 min; the extra time needed to specifically assess the bifurcations was about 5 min.

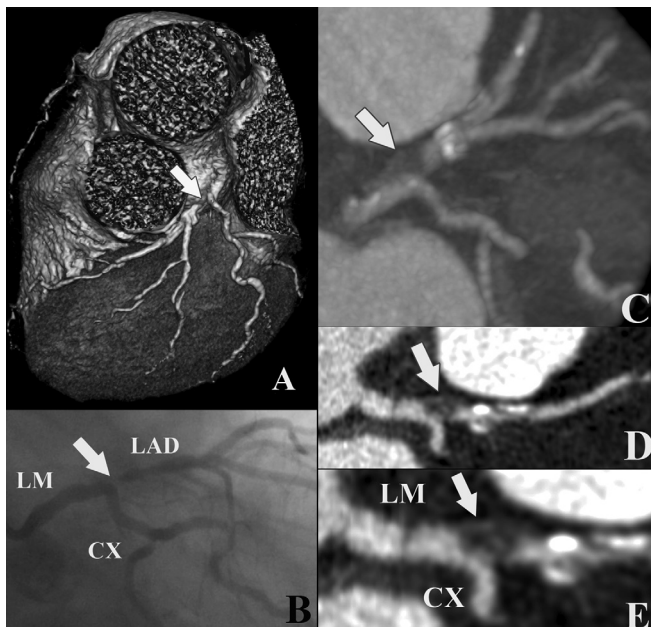
Patient characteristics are summarized in Table 1. Mean periscan heart rate was 58 ± 7.2 bpm. Of the theoretically available 5491 segments, 582 were excluded because the diameter was <2 mm and 161 because they were distal to an occluded segment. In addition, 470 segments were absent on CCA. After exclusion of 189 stented segments and 74 grafted vessels (267 segments), 3822 segments (1218 bifurcations) were available for further analysis. Poor image quality was present in 5% (211/ 3822; 88 bifurcations) of coronary segments and was related to a technically inadequate scan (breathing artifacts or fast or irregular heart rate, n=53), severe calcification (n=62), cardiac motion artifacts (n=58), or insufficient contrast enhancement (n=38). The effective radiation dose was calculated as 19 mSv (1.6 mSv for the calcium score scan and 17.4 mSv for the contrast-enhanced scan) in patients without previous CABG and 22 mSv in patients with previous CABG.

Table 2. Diagnostic accuracy of 64-slice CTCA for the detection of significant coronary bifurcation lesions ($\geq 50\%$ lumen diameter stenosis as defined by quantitative coronary angiography) in evaluable segments.

	Evaluable	Sensitivity	Specificity	PPV	NPV
Patients (n = 317)	317/323 98%	41/43 (95%, CI: 85-99)	266/274 (97%, CI: 94-98)	41/49 (84%, CI: 71-91)	266/268 (99%, CI: 97-100)
Bifurcations (n = 1149)	1149/1218 94%	46/48 (96%, CI: 86-99)	1074/1101 (97%, CI: 96-98)	46/73 (63%, CI: 52-73)	1074/1076 (99%, CI: 99-100)

Values are n (% with 95 percent confidence interval). CI, confidence interval; CTCA, computed tomography coronary angiography; NPV, negative predictive value; PPV, positive predictive value.

Table 2 summarizes the diagnostic accuracy of 64-slice CT compared with QCA for the evaluation of coronary bifurcations. A total of 1130 evaluable bifurcations were available for analysis. Fifty-four BL in 49 patients were identified on CTCA. QCA identified 48 BL in 43 patients. Thus, CTCA incorrectly classified the severity of BL in 10 patients. In 8 patients, a significant BL on CTCA was not confirmed on ICA; in 6 of these 8 patients this misclassification was related to the presence of calcification. In two patients the severity of the lesion was underestimated: one patient had a calcified lesion of the left main/ left anterior descending bifurcation; the second had a short lesion of the distal right coronary artery-posterolateral branch bifurcation. When the 88 bifurcations with poor image quality were arbitrarily scored as having significant lumen narrowing on CTCA, the sensitivity and specificity for detection of significant BL was 95% (41/43; 95% CI: 85-99) and 95% (266/280; 95% CI: 92-97) on a “patient-level” and 96% (46/48; 95% CI: 86-99) and 92% (1074/1170; 95% CI: 90-93) on a lesion level (1218 bifurcations).



The angiographic and CTCA characteristics of the patients with identified BL are shown in Table 3. Lesions were predominantly located in the left main or at the left anterior descending /

Figure 3. CT coronary angiogram and corresponding conventional angiogram in a patient presenting with unstable angina. The volume-rendered CT image (A) suggests the presence of a significant ostial narrowing (arrow) of the LAD. On ICA (B) the stenosis (arrow) was classified as Medina type 0.1.0. Maximal intensity projected (C) and multiplanar reconstructed (D and E) CT images however showed additional significant involvement of the distal LM (arrow) and thus reclassified the lesion as Medina type 1.1.0.

CX: circumflex coronary artery, LAD: left anterior descending coronary artery, LM: left main coronary artery. (A full color version of this illustration can be found in the color section).

Table 3. Angiographic and computed tomography characteristics of patients (n= 41) with bifurcation lesions (n= 46)

Variables	
Bifurcation lesions (n)	46
Location of bifurcation lesion	
Left main, n (%)	17 (37)
LAD/ diagonal, n (%)	22 (48)
CX/ OM, n (%)	6 (13)
RCA-PD/ RCA-PL, n (%)	1 (2)
Angiographic variables, main branch	
Lesion length (mm)	11.8 ± 6.6
Reference diameter (mm)	2.82 ± 0.53
MLD (mm)	1.14 ± 0.49
% diameter stenosis	59 ± 19
Angiographic variables, side branch	
Lesion length	6.54 ± 4.2
Reference diameter (mm)	2.34 ± 0.5
MLD (mm)	1.38 ± 0.64
% diameter stenosis	41 ± 24
Previous heart rate lowering medication (%)	82
Additional heart rate lowering drugs (%)	58
Angulation by CTCA (degrees)	60 ± 19
Angulation by ICA (degrees)	51 ± 18
Calcium score (mean ± SD)	704 ± 955

CABG, coronary artery bypass graft surgery; CTCA, computed tomography coronary angiography; CX, circumflex coronary artery; ICA, invasive coronary angiography; MLD, minimal lumen diameter; OM, obtuse marginal branch; PCI, percutaneous coronary intervention; PD, posterior descendens coronary artery; PL, posterolateral branch; RCA, right coronary artery; SB, side branch.
aAgatston-score.

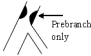

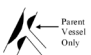




DISCUSSION

Bifurcation lesions provide a challenge in terms of both assessment and management. Vessel overlap, foreshortening, beam attenuation (particularly in obese patients), and underopacification may hinder accurate assessment of the anatomy, particularly with respect to the assessment of ostial side branch involvement. Errors in diagnosis may have significant consequences for patient management.¹⁰ When CABG is the treatment strategy, underestimation of a side branch lesion may inadvertently result in the side branch not being grafted. Where PCI is the preferred option, accurate anatomic information is crucial in planning the treatment strategy, to anticipate plaque shift

first or second diagonal bifurcation. The angle between MV and SB differed significantly when assessed by CTCA when compared with ICA (60 ± 19 versus $51 \pm 18^\circ$ respectively, $P < 0.0001$).

Table 4 describes in detail the lesion distribution in coronary bifurcations, as assessed by CTCA and ICA. In all but 2 patients, the bifurcation classification on CTCA was concordant with that on ICA (agreement between CTCA and ICA in 44/46 BLs). In one patient, ICA underestimated the severity of stenosis in the left main bifurcation and the patient was referred for CABG, based on the CTCA assessment (Figure 3). In the second patient, significant involvement of the ostium of the first diagonal branch was not detected on CTCA and the lesion was classified as Medina type 1.1.0 instead of type 1.1.1.

Table 4. Medina bifurcation classification: comparison of invasive coronary angiography with computed tomography coronary angiography.

Medina classification	Conventional angiography	CTCA
Medina: 1.0.0 	n=10	n=10
Medina: 0.1.0 	n=8	n=7 Medina 1.1.0: n=1
Medina: 1.1.0 	n=8	n=8
Medina: 1.1.1 	n=5	n=4 Medina 1.1.0: n=1
Medina: 0.0.1 	n=5	n=5
Medina: 1.0.1 	n=8	n=8
Medina: 0.1.1 	n=2	n=2

with resulting lumen compromise.^{11,12} In this study we demonstrated that in selected patients the use of 64 slice-CTCA accurately detected angiographically significant BL when compared to ICA, which is in keeping with the diagnostic accuracy of 64-CTCA to detect significant non-bifurcation coronary lesions with reported sensitivity values in the 90 to 95% range.^{4,13-16}

For the purpose of percutaneous treatment of BL, several BL classifications have been used, with the aim to better define treatment strategies.^{17,18} Such classifications may lead to initial treatment involving stenting of both the main and side branches (e.g.

crush or culotte technique) rather than main branch stenting first, followed by provisional balloon angioplasty with or without stenting of the side branch. We have demonstrated that 64-slice CTCA accurately classified BLs when compared to ICA. Furthermore, the 3-dimensional nature of the data provided by CTCA has the potential to allow for evaluation of lesion anatomy without vessel overlap or foreshortening and hence allows detailed evaluation of BLs. Calcified BLs remain problematic due to blooming artefacts that may lead to overestimation of stenosis severity and subsequent misclassification.

The general consensus with regard to the treatment of BLs is that, ideally, the MV only should be stented, with provisional stenting of the SB where the ostium is severely compromised.¹⁹ In situations where both branches need to be stented, the interventional approach (i.e. selection of stenting technique) is determined by the angle between the MV and SB. In our study, assessment of the bifurcation angle on CTCA was relatively straightforward. The angle determined by the

3-dimensional assessment on CTCA differed significantly from that measured on ICA. These findings are consistent with the results of a recent study demonstrating that bifurcation angles measured by CTCA were more accurate when compared with invasive angiography.¹⁶

Current 64-slice CT scanners are sufficiently reliable to exclude the presence of significant coronary artery stenoses. CTCA therefore seems most useful for the assessment of symptomatic patients who have a low-to-intermediate probability of significant coronary artery stenosis. A recent meta-analysis of all major published studies on 16- and 64-slice CT technology, showed that in patients with high prevalence of coronary artery disease the specificity of CT is still insufficient to allow its implementation as an alternative to ICA.²⁰ ICA should continue to be the preferred option in patients with typical angina and/or previously known CAD because it allows ad hoc PCI to be performed, where appropriate, and because the high prevalence of calcification in this population would hamper accurate assessment by CTCA. In the current study, the prevalence of pre-existing CAD was relatively high (50%) and severe calcifications were the main reason for uninterpretable coronary artery segments (39%, 62/158 segments) after exclusion of the 6 patients (53 segments) who had a technically inadequate CT scan. Our preliminary study provides proof of concept for the potential of CTCA to accurately detect coronary artery lesions, even in the presence of complex anatomy such as BLs.

LIMITATIONS

Although our report concerns a large consecutive series of patients who were scanned prior to ICA during a 9-month period, the retrospective nature of the study is a limitation. However, even with a prospectively conducted study it would be difficult to prove the clinical benefit of a 'pre-interventional' CT evaluation since the optimal approach to PCI for a BL is currently unknown. General limitations of CTCA are the additional contrast load and the considerably higher radiation exposure compared with ICA. However, these drawbacks should be balanced against the additional costs and risks of a prolonged angiographic procedure with, in general, the use of more contrast, catheters and additional invasive tools such as IVUS for assessment of difficult lesion subsets such as bifurcations.

In this study we demonstrated the feasibility of CTCA to accurately assess coronary bifurcations for the presence or absence of significant disease and we found CTCA to be more accurate than ICA for the measurement of bifurcation angles. Whether the information provided by a CT exam would influence the therapeutic strategy when attempting PCI for a BL remains unproven and needs further study.

The results of this study are only applicable to a selected patient population (patients in sinus rhythm, who are relatively young, with coronary arteries that do not contain severe calcifications) and were obtained in a center with experienced investigators.

Observations (bifurcations) within the same patient are not statistically independent. We recalculated the diagnostic accuracy parameters after random selection of a single bifurcation per patient. Sensitivity and specificity for detection of significant BLs was respectively 100% (10/10; 95% CI, 72 to 100) and 95% (296/313; 95% CI, 91 to 97). Fewer observations resulted in wider confidence intervals.

Finally, current studies reporting on the diagnostic accuracy of 64-slice CTCA in general included vessels with a reference size up to 1,5 mm. This is a reasonable threshold since smaller sized vessels usually do not constitute targets for revascularization. In this study, we limited the assessment of BL to branches with a reference diameter ≥ 2 mm for two reasons: (i) this cut-off value is a generally accepted criterion to define clinically relevant side branches, and (ii) current spatial resolution is not sufficient for accurate plaque imaging in vessels with a reference size < 2 mm. 17,21-24

CONCLUSIONS

Sixty four-slice CTCA provides an accurate and comprehensive assessment of coronary bifurcation pathology in a selected patient population. These preliminary data support the potential of CTCA to replace coronary angiography as the preferred diagnostic tool for coronary imaging in this setting.

Acknowledgements

We would like to thank Eugene Mc Fadden, MD, FRCPI and Niels van Pelt, MBChB, FRACP for careful revision of the manuscript. We wish to acknowledge the contributions of Alina G. van der Giessen, MSc, Jolanda J. Kluin, MD, PhD and Jolanda J Wentzel, MD, PhD to the study.

REFERENCES

1. Topol EJ, Nissen SE. Our preoccupation with coronary luminology. The dissociation between clinical and angiographic findings in ischemic heart disease. *Circulation*. 1995;92:2333-42.
2. Badak O, Schoenhagen P, Tsunoda T, Magyar WA, Coughlin J, Kapadia S, Nissen SE, Tuzcu EM. Characteristics of atherosclerotic plaque distribution in coronary artery bifurcations: an intravascular ultrasound analysis. *Coron Artery Dis*. 2003;14:309-16.

3. Nieman K, Cademartiri F, Lemos PA, Raaijmakers R, Pattynama PM, de Feyter PJ. Reliable noninvasive coronary angiography with fast submillimeter multislice spiral computed tomography. *Circulation*. 2002;106:2051-4.
4. Mollet NR, Cademartiri F, van Mieghem CA, Runza G, McFadden EP, Baks T, Serruys PW, Krestin GP, de Feyter PJ. High-resolution spiral computed tomography coronary angiography in patients referred for diagnostic conventional coronary angiography. *Circulation*. 2005;112:2318-23.
5. Medina A, Suarez de Lezo J, Pan M. A New Classification of Coronary Bifurcation Lesions. *Rev Esp Cardiol*. 2006;59:183.
6. Morin RL, Gerber TC, McCollough CH. Radiation dose in computed tomography of the heart. *Circulation*. 2003;107:917-22.
7. Ellis SG, Vandormael MG, Cowley MJ, DiSciascio G, Deligonul U, Topol EJ, Bulle TM. Coronary morphologic and clinical determinants of procedural outcome with angioplasty for multivessel coronary disease. Implications for patient selection. Multivessel Angioplasty Prognosis Study Group. *Circulation*. 1990;82:1193-202.
8. Austen WG, Edwards JE, Frye RL, Gensini GG, Gott VL, Griffith LS, McGoon DC, Murphy ML, Roe BB. A reporting system on patients evaluated for coronary artery disease. Report of the Ad Hoc Committee for Grading of Coronary Artery Disease, Council on Cardiovascular Surgery, American Heart Association. *Circulation*. 1975;51:5-40.
9. Costa RA, Mintz GS, Carlier SG, Lansky AJ, Moussa I, Fujii K, Takebayashi H, Yasuda T, Costa JR, Jr., Tsuchiya Y, Jensen LO, Cristea E, Mehran R, Dangas GD, Iyer S, Collins M, Kreps EM, Colombo A, Stone GW, Leon MB, Moses JW. Bifurcation coronary lesions treated with the "crush" technique: an intravascular ultrasound analysis. *J Am Coll Cardiol*. 2005;46:599-605.
10. Green NE, Chen SY, Hansgen AR, Messenger JC, Groves BM, Carroll JD. Angiographic views used for percutaneous coronary interventions: a three-dimensional analysis of physician-determined vs. computer-generated views. *Catheter Cardiovasc Interv*. 2005;64:451-9.
11. Meier B, Gruentzig AR, King SB, 3rd, Douglas JS, Jr., Hollman J, Ischinger T, Aueron F, Galan K. Risk of side branch occlusion during coronary angioplasty. *Am J Cardiol*. 1984;53:10-4.
12. Fischman DL, Savage MP, Leon MB, Schatz RA, Ellis S, Cleman MW, Hirshfeld JW, Teirstein P, Bailey S, Walker CM, et al. Fate of lesion-related side branches after coronary artery stenting. *J Am Coll Cardiol*. 1993;22:1641-6.
13. Leschka S, Alkadhi H, Plass A, Desbiolles L, Grunenfelder J, Marincek B, Wildermuth S. Accuracy of MSCT coronary angiography with 64-slice technology: first experience. *Eur Heart J*. 2005;26:1482-7.
14. Leber AW, Knez A, von Ziegler F, Becker A, Nikolaou K, Paul S, Wintersperger B, Reiser M, Becker CR, Steinbeck G, Boekstegers P. Quantification of obstructive and nonobstructive coronary lesions by 64-slice computed tomography: a comparative study with quantitative coronary angiography and intravascular ultrasound. *J Am Coll Cardiol*. 2005;46:147-54.

15. Raff GL, Gallagher MJ, O'Neill WW, Goldstein JA. Diagnostic accuracy of noninvasive coronary angiography using 64-slice spiral computed tomography. *J Am Coll Cardiol.* 2005;46:552-7.
16. Pflederer T, Ludwig J, Ropers D, Daniel WG, Achenbach S. Measurement of coronary artery bifurcation angles by multidetector computed tomography. *Invest Radiol.* 2006;41:793-8.
17. Lefevre T, Louvard Y, Morice MC, Dumas P, Loubeyre C, Benslimane A, Premchand RK, Guillard N, Piechaud JF. Stenting of bifurcation lesions: classification, treatments, and results. *Catheter Cardiovasc Interv.* 2000;49:274-83.
18. Popma J, Bashore T. Qualitative and quantitative angiography- Bifurcation lesions. In: Topol E, ed. *Textbook of interventional cardiology.* 1994;Philadelphia: W.B. Saunders; 1994.: p. 1055-8.
19. Steigen TK, Maeng M, Wiseth R, Erglis A, Kumsars I, Narbute I, Gunnes P, Mannsverk J, Meyerdierks O, Rotevatn S, Niemela M, Kervinen K, Jensen JS, Galloe A, Nikus K, Vikman S, Ravkilde J, James S, Aaroe J, Ylitalo A, Helqvist S, Sjogren I, Thayssen P, Virtanen K, Puhakka M, Airaksinen J, Lassen JF, Thuesen L. Randomized study on simple versus complex stenting of coronary artery bifurcation lesions: the Nordic bifurcation study. *Circulation.* 2006;114:1955-61.
20. Hamon M, Biondi-Zoccai GG, Malagutti P, Agostoni P, Morello R, Valgimigli M. Diagnostic performance of multislice spiral computed tomography of coronary arteries as compared with conventional invasive coronary angiography: a meta-analysis. *J Am Coll Cardiol.* 2006;48:1896-910.
21. Williams DO, Abbott JD. Bifurcation intervention: is it crush time yet? *J Am Coll Cardiol.* 2005;46:621-4.
22. Pan M, Suarez de Lezo J, Medina A, Romero M, Segura J, Ramirez A, Pavlovic D, Hernandez E, Ojeda S, Adamuz C. A stepwise strategy for the stent treatment of bifurcated coronary lesions. *Catheter Cardiovasc Interv.* 2002;55:50-7.
23. Al Suwaidi J, Berger PB, Rihal CS, Garratt KN, Bell MR, Ting HH, Bresnahan JF, Grill DE, Holmes DR, Jr. Immediate and long-term outcome of intracoronary stent implantation for true bifurcation lesions. *J Am Coll Cardiol.* 2000;35:929-36.
24. Iakovou I, Ge L, Colombo A. Contemporary stent treatment of coronary bifurcations. *J Am Coll Cardiol.* 2005;46:1446-55.

19

Plaque and shear stress distribution in human coronary bifurcations: A multi-slice computed tomography study

Euro Intervention, 2008;4

Authors: A.G. van der Giessen^a, J.J. Wentzel^a, W.B. Meijboom^a, N.R. Moller^b, A.F.W. van der Steen^{a,d}, F.N. van de Vosse^c, P.J. de Feyter^{a,b} and F.J.H. Gijsen^a

Department of ^aCardiology and ^bRadiology, Erasmus MC, Rotterdam, Department of ^cBiomedical Engineering, Eindhoven University of Technology, Eindhoven, ^dThe Interuniversity Cardiology Institute of the Netherlands, Utrecht, the Netherlands

ABSTRACT

Objectives

To study the presence of plaques at bifurcation regions we assessed the plaque distribution and morphology non-invasively with multi-slice computed tomography (MSCT) in relation to the wall shear stress (WSS) distribution.

Background

Early atherosclerosis is located in low shear-stress (SS) regions, however plaques are also found in the high SS sensing flowdivider walls of coronary bifurcations.

Methods

We inspected 65 cross-sections near coronary bifurcations for the presence of plaque. Cross-sections were divided into 4 equal parts. These parts were numbered according to expected levels of WSS, with part I the lowest WSS (outer wall) and increasing WSS's in part II (inner bend), III (outer bend) and IV (flowdivider).

Results

Of the cross-sections 88% had plaque. Of all parts I, 72% contained plaque. This was 62%, 38% and 31% in parts II, III and IV. Of the cross-sections with only 1 or 2 parts inflicted, plaque was found in part I and/or II in 94%. In 93% of the cross-sections with the flowdivider inflicted, parts I and/or II were also inflicted. Plaque was never found exclusively in the flowdivider part IV.

Conclusion

We assessed non-invasively with MSCT plaque distribution and morphology and demonstrated that plaque is mostly present in low WSS regions whereas plaque in high WSS regions is accompanied by plaque in adjacent low WSS regions. It is therefore plausible that plaque grows from the outer wall (low WSS) of the bifurcation towards the flowdivider (high WSS).

INTRODUCTION

The formation of atherosclerosis in coronary arteries is localized^{1,2}. A key player in localizing atherosclerosis is low wall shear stress (WSS)^{3,4}. In the presence of systemic risk factors, a vessel wall that is exposed to low WSS is more prone to develop atherosclerotic plaques^{5,6}.

The WSS to which a vessel wall is exposed to, is mainly determined by arterial geometry. In bifurcating arteries, the outer wall is exposed to low WSS compared to the flowdivider wall^{7,8}. In curved arteries, low and high WSS regions are present at the inner and outer bend, respectively⁹. Intravascular ultrasound studies show that plaques are predominantly found in low WSS regions¹⁰⁻¹³.

In clinical practice, however, it is common to observe plaques that cause lumen narrowing not only at low WSS regions but also at the high WSS sensing flowdivider of coronary bifurcations. Even in the classifications schemes used for typing bifurcation lesions on coronary angiography, most of the bifurcation types have luminal narrowing in the flowdivider region of the side-branches^{14,15}. Plaques incorporating the flowdivider are found more frequently in symptomatic patients, and thus may represent a more advanced stage of atherosclerosis. Apparently in this stage of the disease plaques are not limited to low WSS regions.

Angiography is only one of several imaging modalities to visualize the presence of atherosclerosis in the coronary arteries¹⁶. Recently several studies have shown the ability of multi-slice computed tomography (MSCT) angiography to detect coronary plaques non-invasively¹⁷. In contrast to conventional angiography, MSCT angiography gives 3D information about the coronary geometry and not only the lumen is visible, but also the vessel wall harboring the atherosclerotic plaque^{18,19}. This enables MSCT coronary angiography to detect atherosclerosis also in remodeled arteries without severe lumen narrowing^{20,21}.

In this study we imaged non-invasively with MSCT angiography the 3D geometry of the lumen and vessel wall of coronary artery bifurcations in patients. On the basis of geometry, we labeled regions in bifurcations according to the expected WSS in each region and related the WSS to the plaque frequency, distribution and morphology.

METHODS

Study Population

We retrospectively studied 28 (18 male, mean age 59.9 ± 6.6 years) consecutive symptomatic patients, suspected of coronary artery disease who underwent MSCT coronary angiography. Patient demographics are given in table 1. The patients had sinus heart rhythm, were able to hold breath for 15 s and had no contra-indications to iodinated contrast material. We only included patients who had not previously undergone percutaneous intervention or coronary bypass surgery, and had a heart rate lower than 65 beats per minute during scanning. Our institutional review board approved the study protocol, and all patients gave informed consent.

Scan Protocol and Image Reconstruction

The patient preparation, scan protocol, and image reconstruction procedure have been previously described²². Briefly, patients with heart rates above 70 beats per minute received heart-rate-lowering drugs before scanning. Scanning was performed on a 64-slice MSCT scanner (Sensation64®, Siemens, Germany) according to a standardized optimized contrast (Iomeron 400®, Bracco, Italy) enhanced scanning protocol. A bolus tracking technique was used to synchronize the arrival of contrast in the coronary arteries with the initiation of the scan. Images were reconstructed with ECG-gating, initially during the mid- to end-diastolic phase (350 ms before the next R wave) with a temporal window of

165 ms. If image quality was poor, more reconstructions at different phases of the cardiac cycle were generated to improve it. The dataset with the best image quality was chosen for further processing. The in-plane resolution was approximately 0.3 mm and the slice thickness was 0.4 mm.

Table 1: Patient characteristics

Male	18 (64%)
Age, year (\pm stdev)	59.9 (6.6)
Symptoms	
Atypical chest pain	1 (4%)
Stable angina pectoris	11 (39%)
Unstable angina pectoris	4 (14%)
Non-ST-segment elevation myocardial infarction	10 (36%)
Atypical chest pain	2(7%)
Risk factors	
Hypertension	21 (75%)
Hypercholesterolemia	21 (75%)
Smoking	8 (29%)
Family history of acute coronary syndrome	7 (25%)
Diabetes mellitus	6 (21%)
Obese (body mass index ≥ 30 kg/m ²)	5 (18%)

N=28. Values are n (%) unless otherwise indicated.

MSCT Image Processing

We investigated the plaque distribution in two bifurcations; 1) the LM-bifurcation, which is the branching of the left main (LM) coronary artery into the left anterior descending artery (LAD) and the left circumflex artery (LCX), and 2) the LAD-bifurcation, which is the bifurcation of the first diagonal artery (D1) from the distal LAD (LADdist). To study these bifurcations the reconstructed MSCT datasets were exported from the scanner to MeVisLab (MeVis, Bremen, Germany), a development environment for image processing and visualization.

The two bifurcations were analyzed separately. We defined a plane through each bifurcation, such that both the main branch and the side-branches were visible in this plane and that the angle between the side-branches was maximal (figure 1A and 1B). Perpendicular to this plane and the vessel axis, one cross-section of each of the side-branches was obtained 1 mm distal to the flow-divider (see figure 1C).

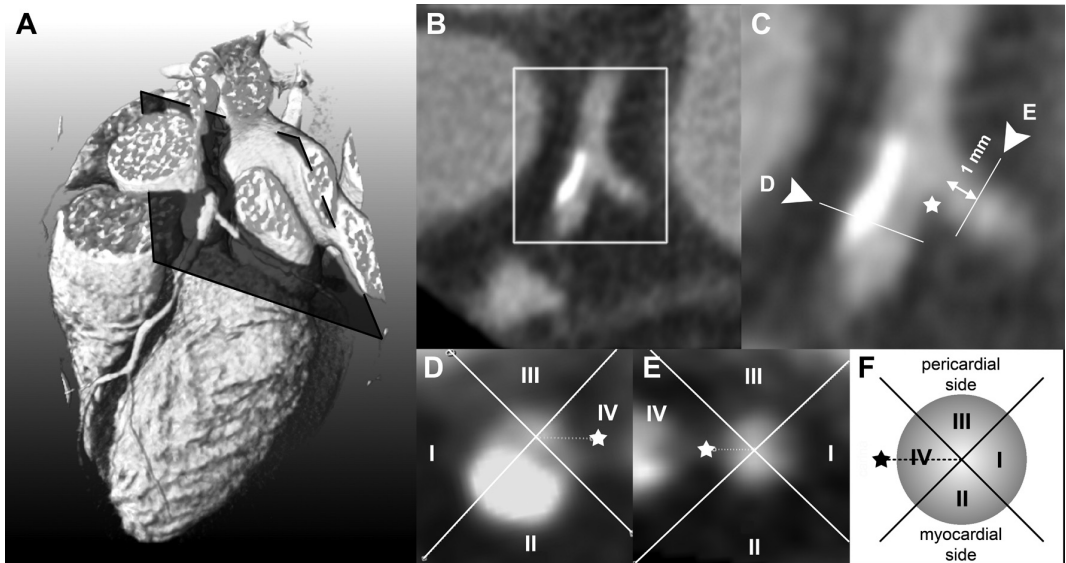


Figure 1: Selection of cross-sections from the bifurcation of interest

Panel A shows a volume rendered MSCTA dataset with a plane through the mother and side branches of the bifurcation of interest. The Hounsfield Unit distribution in this plane is shown in B and a magnification in C. In C, the * indicates the flowdivider and the arrows indicate the position of the cross-sections shown in D and E. The sketch in F illustrates the division into parts and also the numbering according to the expected shear stress levels, which is also applied in D and E.

We excluded trifurcations from the analysis (n=21). Cross-sections were excluded when the diameter of the artery was < 1mm (n=2), or when the plaque was too heavily calcified to clearly distinguish the lumen from the plaque (n=3), see also figure 2. In total we analyzed 65 cross-sections for this study.

Shear stress

To relate the plaque location to WSS, we divided the cross-sections into four parts from the center of the lumen. The cross-section was divided in such way that the flowdivider was in the middle of one of the parts. We labeled the part covering the outer wall of the bifurcation I, the part facing the myocardial side of the heart II, the part facing the pericardium III, and the part containing the flowdivider IV (figure 1D and 1E).

The bifurcation affects the WSS pattern primarily. High WSS is assumed in part IV due to the flow-division at the flowdivider, while in part I, the outer, non-flowdivider wall, low WSS is expected. Besides the effect of the bifurcation, the curvature of the artery over the myocardium also influences WSS²³. In comparison to part III, the WSS is assumed to be lower in part II, because the inner wall of a curved vessel is subjected to lower WSS than the outer wall. Thus, the numbering of the parts is according to the expected WSS: in part I the lowest and in part IV the highest WSS (figure 1F).

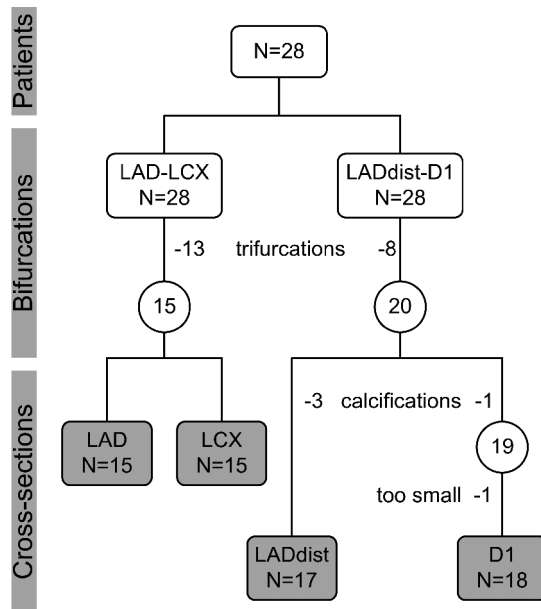


Figure 2: Exclusion of cross-sections

Exclusion numbers of bifurcations and cross-section because of trifurcations, calcifications and artery size. Abbreviations: LAD – Left anterior descending coronary artery, LCX – Left circumflex coronary artery, LADdist – distal left anterior descending coronary artery (distal to first diagonal), D1 – first diagonal coronary artery

Plaque Identification

In each cross-section, all parts were inspected for the presence of plaque. Plaque was defined as any discernable structure with 1) a lower attenuation than the contrast enhanced lumen and higher attenuation than the surrounding epicardial fat or 2) an attenuation ≥ 140 HU that could be separately visualized from the lumen (calcified part). The plaque had to be present at the cross-section of interest and at at least one cross-section adjacent (0.5 mm distance) to the cross-section of interest. When a cross-section had calcified parts, we also denoted the part that contained the densest structure, thus with the highest Hounsfield Unit.

The cross-sections with plaque present in only 1 part, we called minimally inflicted. When in 2, 3 or 4 parts plaques were observed we called these cross-sections respectively mildly, moderately and severely inflicted.

Statistical Analysis

To test whether plaque occurs in a preferential part of a cross-section, we used the numerical values assigned to each part. For each cross-section we computed the mean of the numbers of the parts that contain plaque. This mean value we call the mean shear stress index (MSSI). For instance, when plaque is present in the low WSS regions, thus in part I and II, than the MSSI of that cross-section is $(1+2)/2 = 1.5$. When plaques are randomly distributed over the numbered parts, and thus have no preferential location, the averaged MSSI is by definition 2.5. We denote this reference value as RMSSI. If the MSSI is lower than 2.5, plaque is located mainly in the low WSS part of cross-section, and if it is higher, plaque is mainly present in the high WSS part of the cross-section.

We calculated the average MSSI over all cross-sections, and separately over the minimally, mildly, moderately and severely inflicted cross-sections and reported the values as mean \pm std. With a student-t-test we tested whether the averaged MSSI was significantly different ($p < 0.05$) from the RMSSI of 2.5.

RESULTS

General

Most patients (96%) had plaque in one or more of the studied cross-sections. Of the 65 cross-sections 88% contained plaque. In the D1 branch, which is generally smaller than the other inspected branches, atherosclerosis was observed less often than in the other branches. Only 75% of the D1 cross-sections contained plaque versus 93%, 86% and 94% of the LAD, LCX and LADdist branches.

Calcified plaques were found in 62% of the patients, and in 29% of the cross-sections. Of the LADprox and LADdist 37% and 42% of the cross-sections were affected, whereas only 5% and 16% of the LCX and D1.

Plaque Distribution

Plaques were found in low WSS parts I and II in 72% and 62% of the cross-sections. The high WSS parts III, and IV were less often affected than parts I and II, only in 38% and 31% of the cross-sections (figure 3).

The distribution of the plaque configurations is in more detail given in figure 4. From the top to the bottom the rows show the possible plaque configurations for minimally, mildly, moderately and severely inflicted cross-sections. For each configuration the number of observations is given as well as the corresponding MSSI value.

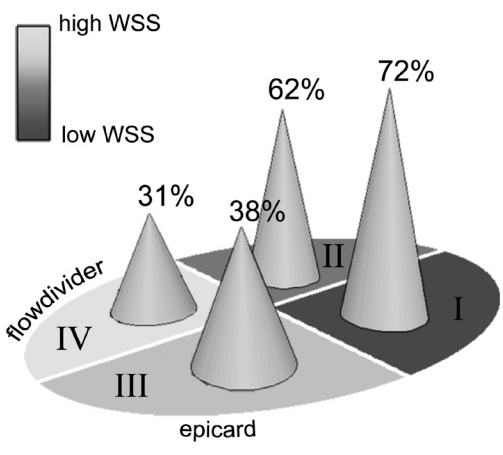


Figure 3: Plaque distribution
 The figure gives the percentage of occurrence of plaque in each part, i.e. 72% of all high WSS parts I were inflicted with plaque.

Plaque at the flowdivider was found in 20 out of the 65 analyzed cross-sections. The flowdivider was never affected in minimally inflicted cross-sections, while 6 out of 21 of the mildly inflicted cross-sections, 9 out of 20 of the moderately inflicted cross-sections, and 5 out of 5 of the severely inflicted cross-sections were affected in the flowdivider. In 19 out of the 20 cross-sections plaque in the flowdivider was accompanied by plaque in low WSS regions I or II.

Figure 3 also shows that the plaque configurations with the lowest MSSIs are the configurations that we observed most frequently. Figure 5 shows the averaged MSSIs for all, the minimally, mild, moderately and severely inflicted cross-sections. If the plaques are located preferentially at specific regions, the MSSIs will be significantly different from the reference

We found 8 cross-sections without plaque. In 10 of the 11 minimally inflicted cross-sections plaque was present in the low WSS parts I or II. The high WSS part IV was not affected once. In the 21 mildly inflicted cross-sections (2 parts inflicted per cross-section) we did not find configurations in which plaques are opposite to each other. Again, as in minimally inflicted cross-sections, the low WSS parts contained plaque most often. In the 20 moderately inflicted cross-sections (3 parts inflicted) plaque was always at least present in the lowest WSS part I. We found 5 severely inflicted cross-sections.

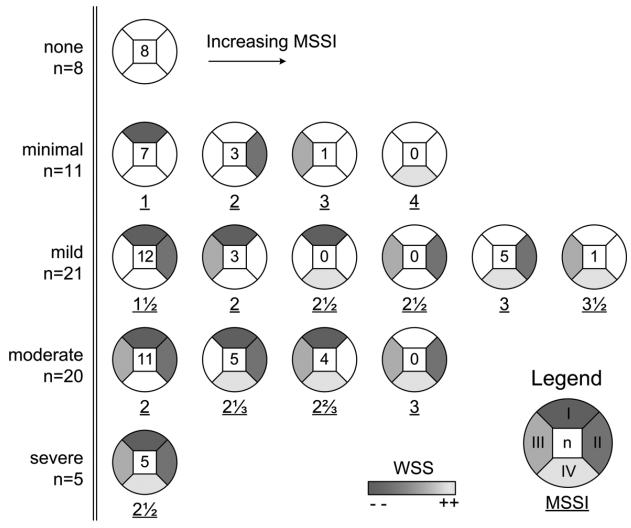


Figure 4: Plaque configurations
 All possible plaque configurations are shown, sorted from top to bottom on the basis of the number of affected parts and from left to right according to increasing mean shear stress index (MSSI). Each configuration depicts both the number of times (N) that it is observed and its MSSIs (underlined). The parts are colored according to the expected wall shear stress level (see legend).

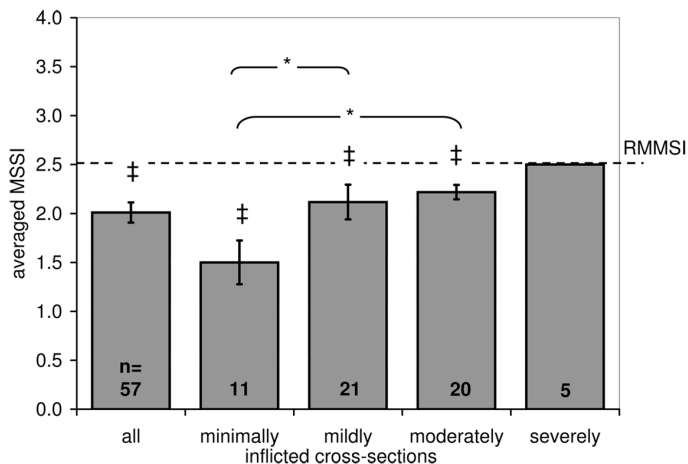


Figure 5: Mean shear stress values (MSSI) of plaques
 The averaged MSSI \pm variance is shown of the plaque parts over all, the minimally, mildly, moderately and severely inflicted cross-sections. The reference MSSI (RMSSI) is indicated at 2.5. The number of cross-sections is indicated with n. *, significant difference ($p < 0.05$) between the MSSIs. ‡, MSSIs lower ($p < 0.05$) than the RMSSI.

value, the RMSSI, which is 2.5. The averaged MSSI over all cross-sections was with 2.02 ± 0.62 lower than the RMSSI ($p < 0.05$). When we divided the cross-sections according to the severity of infliction, the averaged MSSIs are also lower than the RMSSI with the exception of the severely inflicted cross-sections, which by definition equals the RMSSI. The MSSI increases with the severity of infliction because high WSS parts get involved.

Calcium distribution

Similar to the plaque, the densest calcium spot was mostly found in the low WSS parts I and II. Both part I and part II were inflicted in 17% of the cross-sections while parts III and IV were only inflicted in 6% and 3% of the cross-sections.

Figure 6 shows all 19 cross-sections with calcium according to the severity of plaque inflictions from top to bottom. From left to right the configurations are ordered according to the part with the densest spot, which is indicated with a black dot in the cross-sections.

Of the 11 minimally inflicted cross-sections, only 1 (9%) was calcified. The percentage of cross-sections with calcium increased with the severity of infliction up to 60% for the severely inflicted cross-sections. The densest spot of

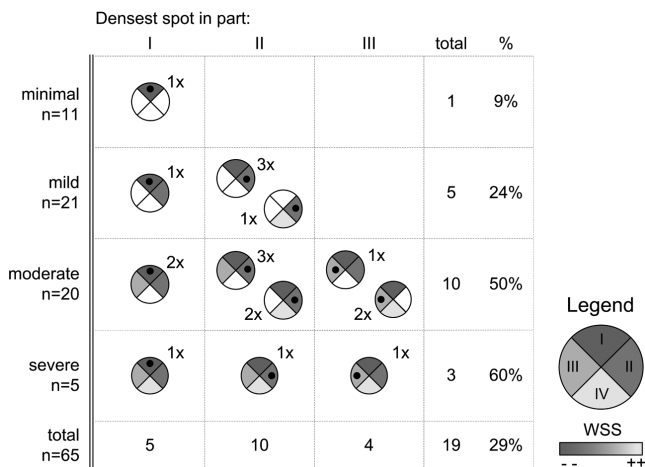


Figure 6: Plaque configurations with calcium
 Plaque configurations with calcium are shown and sorted from left to right according to part with the calcium spot. From top to bottom, the cross-sections are sorted by the severity of plaque infliction. The • indicates the position of the densest calcium spot.

the calcification was never found in high WSS part IV. Most of the calcified cross-sections ($n=10$) have the densest calcium spot in part II. Part I has the spot in 5 cross-sections and part III in 4 cross-sections. The plaques with the densest spot in part III always were in moderately or severely inflected cross-sections.

DISCUSSION

We reported on the plaque distribution in human coronary arteries assessed by MSCT in relation to expected shear stress patterns. We demonstrated that plaques in coronary artery bifurcations are most often located in the low WSS regions and that plaques at the flowdivider, which is exposed to high WSS, are always accompanied by plaques in a low WSS region, where plaques are supposed to originate from.

To compare our findings with histological reports in literature on the different phases of atherosclerosis we distinguish three phases in our study. A minimally inflected cross-section can be considered as early atherosclerosis, mildly and moderately inflected cross-sections as more advanced atherosclerosis, and severely inflected cross-sections as severe atherosclerosis. In early atherosclerosis we observed that plaque distal to a bifurcation was found mainly at the wall opposite the flowdivider. This is in agreement with histological findings of early atherosclerosis in the LM bifurcation of young adults²⁴. In an older population, Grøttum et al. studied the deposition of atherosclerosis also in the LM bifurcation²⁵. Most plaques distal to the bifurcation were observed opposite to the flowdivider and slightly directed to the myocardium. In our study we observe plaque in similar regions. These are the regions where we expect low WSS.

Our results are supported not only by histological findings, but also by intravascular ultrasound studies on plaque distribution near coronary bifurcations. These studies often include patient groups who have lumen narrowing on angiography and who may thus have advanced to severe atherosclerosis. Shimada et al. demonstrated that the plaque area was larger at the opposite wall of the flowdivider than at the flowdivider itself²⁶. The influence of the curvature of the arteries near bifurcations was investigated by Iwami et al¹³ using a combination of intravascular ultrasound and angiographic data. The percentage of plaque in the total cross-sectional plaque area was highest at the inner curve of the bifurcation and this was most pronounced in the most curved arteries. Badak et al. incorporated the position of the myocardium in their analysis. They found that when a side-branch was perpendicular to the artery the maximum plaque thickness was found at $190^\circ \pm 70^\circ$, thus opposite the side branch, slightly in direction of the myocardium²⁷. To compare our findings we calculated the average angle in a similar way in the mild and moderately diseased cross-sections and found that it was very close to that found by Badak, that is $205^\circ \pm 68^\circ$. Thus, on the basis of the plaque distribution observed in our study and in other studies, we show that not

only the bifurcation contributes to the low WSS region and initiates plaque formation, but also the curvature of the arteries over the myocardium.

Other studies lack detailed information on the distribution of calcifications with respect to the position of the bifurcation and myocardium. It is known that most calcium is found near bifurcations and that it initially occurs in the necrotic core of the plaque due partly to apoptosis of vascular smooth muscle cells or macrophages²⁸. In our data the calcium spot was found more often at the myocardial side (part II) of the coronary artery than at the outer wall of the flowdivider (part I), which is what one would expect on the basis of the plaque distribution. We observed calcium once in a cross-section that was mildly inflected and thus was by our definition, an early form of atherosclerosis. Due to expansive remodeling, it is possible that an advanced plaque only occupies one part of the cross-section instead of growing into the high WSS parts. This might explain the presence of calcium in a cross-section with only one inflected part.

Although we did not follow patients over time, several observations indicate that plaques grow circumferentially from a low WSS region into the high WSS flowdivider. The first is that the flowdivider was never diseased in early atherosclerosis. Secondly, low WSS regions were in all stages of the disease most often affected. Thirdly, if there is plaque at the flowdivider, the low WSS regions are also diseased. The fourth observation, that plaques are always found adjacently in low and high WSS regions indicate that growth is indeed circumferential. We already mentioned that low WSS regions are predilection sites of early atherosclerosis. As the plaque matures, fissuring at the shoulders of the plaque can cause the plaque to grow from the low WSS region along the circumference of the lumen²⁹.

Many studies on plaque distribution in human coronary arteries use IVUS as imaging modality. With its high resolution, it is the gold standard for determining lumen and plaque size. However, IVUS is invasive and as 3D information is lost, it is hard to identify the pericardial and myocardial side of a bifurcation. The influence of the curvature of the artery over the myocardium on plaque localization can therefore not be taken into account. Currently, MSCT angiography is the only non-invasive imaging modality that can provide both 3D lumen and plaque distribution. High sensitivities and specificities are achieved in scoring significant lesions on 64-slice MSCT angiography images³⁰ and the first comparisons with IVUS on plaque measurements are promising²⁰.

However, due to limitations of the MSCT angiography technique, measuring the exact size and position of the atherosclerotic plaque remains a challenge. In the first place, partial voluming effects caused by the high intensity calcium and contrast agent can obscure the vessel wall. Secondly, the resolution of MSCT angiography images cannot compete with those of IVUS: MSCT angiography cannot visualize small branches and intimal thickening. Because of these limitations we decided to exclude the heavily calcified bifurcations and very small arteries from our analysis. In

the analysis we chose to introduce a scoring system to assign the presence of plaque in predefined parts instead of measuring wall thickness. For calcified plaques, we determined only the densest part of the calcium.

A second limitation is that we included only two types of bifurcations in our study and only of the left coronary tree. We inspected two relatively large bifurcations, which could be easily identified in the MSCT datasets and which are often treated by catheterization. Although we excluded inspection of the complete right coronary artery tree, we do not expect WSS to influence plaque distribution here in a different way¹. Despite the limited resolution of MSCT, we observed a large number (more than one third) of bifurcations that appeared to be trifurcations in our dataset. We excluded these trifurcations because WSS is hard to predict in these geometries. This reduced the number of bifurcations inspected.

A third limitation is that we defined the WSS patterns on the basis of general geometrical features of coronary arteries, being the bifurcation and curvature. Local and patient specific varieties in geometry and/or flow may cause the actual WSS to deviate from the expected WSS distribution. This might explain the single observation of a plaque localized in an expected high WSS region.

We assessed plaque frequency, distribution and morphology near coronary bifurcations with MSCT. Our results are in good agreement with previous findings in IVUS and confirm that in early atherosclerosis, plaques are limited to the low WSS regions and that the plaque distribution is not only influenced by the bifurcation but also by the curvature of the arteries. A new observation is that we showed that the calcified spots in more advanced plaques are mostly located in the low WSS regions. Besides this we presented that circumferential growth of the plaque from the low WSS region into the high WSS regions is a plausible explanation for the presence of plaque in the high WSS sensing flowdivider.

REFERENCES

- 1 VanderLaan, P. A., Reardon, C. A. and Getz, G. S., Site specificity of atherosclerosis. Site-selective responses to atherosclerotic modulators, *Arteriosclerosis, Thrombosis and Vascular Biology*, 2004, 24: 1-11.
- 2 Slager, C. J., Wentzel, J. J., Gijzen, F. J. H., Schuurbiens, J. C. H., Wal, A. C. v. d., Steen, A. F. W. v. d. and Serruys, P. W., The role of shear stress in the generation of rupture-prone vulnerable plaques, *Nature Clinical Practice Cardiovascular Medicine*, 2005, 2: 401-407.
- 3 Cunningham, K. S. and Gotlieb, A. I., The role of shear stress in the pathogenesis of atherosclerosis, *Lab Invest*, 2005, 85: 9-23.

- 4 Malek, A. M. and Izumo, S., Control of endothelial cell gene expression by flow, *J Biomech*, 1995, 28: 1515-1528.
- 5 Giddens, D. P., Zarins, C. K. and Glagov, S., The role of fluid mechanics in the localization and detection of atherosclerosis, *J Biomech Eng*, 1993, 115: 588-594.
- 6 Malek, A. M., Alper, S. L. and Izumo, S., Hemodynamic shear stress and its role in atherosclerosis, *Journal of the American Medical Association*, 1999, 282: 2035-2042.
- 7 Asakura, T. and Karino, T., Flow patterns and spatial distribution of atherosclerotic lesions in human coronary arteries, *Circ Res*, 1990, 66: 1045-1066.
- 8 Tadjfar, M., Branch angle and flow into a symmetric bifurcation, *Journal of Biomechanics*, 2004, 126: 517-518.
- 9 Kirpalani, A., Park, H., Butany, J., Johnston, K. W. and Ojha, M., Velocity and wall shear stress patterns in the human right coronary artery, *J Biomech Eng*, 1999, 121: 370-375.
- 10 Jeremias, A., Huegel, H., Lee, D. P., Hassan, A., Wolf, A., Yeung, A. C., Yock, P. G. and Fitzgerald, P. J., Spatial orientation of atherosclerotic plaque in non-branching coronary artery segments, *Atherosclerosis*, 2000, 152: 209-215.
- 11 Krams, R., Wentzel, J. J., Oomen, J. A., Vinke, R., Schuurbiers, J. C., de Feyter, P. J., Serruys, P. W. and Slager, C. J., Evaluation of endothelial shear stress and 3D geometry as factors determining the development of atherosclerosis and remodeling in human coronary arteries in vivo. Combining 3D reconstruction from angiography and IVUS (ANGUS) with computational fluid dynamics, *Arterioscler Thromb Vasc Biol*, 1997, 17: 2061-2065.
- 12 Tsutsui, H., Yamagishi, M., Uematsu, M., Suyama, K., Nakatani, S., Yasumura, Y., Asanuma, T. and Miyatake, K., Intravascular ultrasound evaluation of plaque distribution at curved coronary segments, *Am J Cardiol*, 1998, 81: 977-981.
- 13 Iwami, T., Fujii, T., Miura, T., Otani, N., Iida, H., Kawamura, A., Yoshitake, S., Kohno, M., Hisamatsu, Y., Iwamoto, H. and Matsuzaki, M., Importance of left anterior descending coronary artery curvature in determining cross-sectional plaque distribution assessed by intravascular ultrasound, *Am J Cardiol*, 1998, 82: 381-384.
- 14 Sianos, G., Morel, M.-A., Kappetein, A. P., Morice, M.-C., Colombo, A., Dawkins, K., Brand, M. v. d., Dyck, N. V., Russel, M. E. and Serruys, P., The SYNTAX Score: an angiographic tool grading the complexity of coronary artery disease, *EuroIntervention*, 2005, 2: 219-227.
- 15 Lefèvre, T., Louvard, Y., Morice, M.-C., Pierre Dumas, Loubeyre, C., Benslimane, A., Premchand, R. K., Guillard, N. and Piéchaud, J.-F., Stenting of bifurcation lesions: Classification, treatments, and results, *Catheterization and Cardiovascular Interventions*, 2000, 49: 274-283.
- 16 Bhatia, V., Bhatia, R., Dhindsa, S. and Dhindsa, M., Imaging of the vulnerable plaque: new modalities, *South Med J*, 2003, 96: 1142-1147.
- 17 Mollet, N. R., Cademartiri, F. and de Feyter, P. J., Non-invasive multislice CT coronary imaging, *Heart*, 2005, 91: 401-407.

- 18 Leber, A. W., Knez, A., Becker, A., Becker, C., Ziegler, F. v., Nikolaou, K., Rist, C., Reiser, M., Carl White, M., Steinbeck, G. and Boekstegers, P., Accuracy of multidetector spiral computed tomography in identifying and differentiating the composition of coronary atherosclerotic plaques. A comparative study with intracoronary ultrasound, *Journal of the American College of Cardiology*, 2003, 43: 1241-1247.
- 19 Van Mieghem, C. A., McFadden, E. P., de Feyter, P. J., Bruining, N., Schaar, J. A., Mollet, N. R., Cademartiri, F., Goedhart, D., de Winter, S., Granillo, G. R., Valgimigli, M., Mastik, F., van der Steen, A. F., van der Giessen, W. J., Sianos, G., Backx, B., Morel, M. A., van Es, G. A., Zalewski, A. and Serruys, P. W., Noninvasive detection of subclinical coronary atherosclerosis coupled with assessment of changes in plaque characteristics using novel invasive imaging modalities: the Integrated Biomarker and Imaging Study (IBIS), *J Am Coll Cardiol*, 2006, 47: 1134-1142.
- 20 Leber, A. W., Knez, A., Ziegler, F. v., Becker, A., Nikolaou, K., Paul, S., Wintersperger, B., Reiser, M., Becker, C. R., Steinbeck, G. and Boekstegers, P., Quantification of obstructive and nonobstructive coronary lesions by 64-slice computed tomography - A comparative study with quantification coronary angiography and intravascular ultrasound, *Journal of the American College of Cardiology*, 2005, 26: 147-154.
- 21 Achenbach, S., Ropers, D., Hoffmann, U., MacNeill, B., Baum, U., Pohle, K., Brady, T. J., Pomerantsev, E., Ludwig, J., Flachskampf, F. A., Wicky, S., Jang, I.-k. and Daniel, W. G., Assessment of coronary remodeling in stenotic and nonstenotic coronary atherosclerotic lesions by multidetector spiral computed tomography, *Journal of the American College of Cardiology*, 2004, 43: 842-847.
- 22 Mollet, N. R., Cademartiri, F., van Mieghem, C. A., Runza, G., McFadden, E. P., Baks, T., Serruys, P. W., Krestin, G. P. and de Feyter, P. J., High-resolution spiral computed tomography coronary angiography in patients referred for diagnostic conventional coronary angiography, *Circulation*, 2005, 112: 2318-2323.
- 23 He, X. and Ku, D. N., Pulsatile flow in the human left coronary artery bifurcation: average conditions, *J Biomech Eng*, 1996, 118: 74-82.
- 24 Svindland, A., The localization of sudanophilic and fibrous plaques in the main left coronary bifurcation, *Atherosclerosis*, 1983, 48: 139-145.
- 25 Grottum, P., Svindland, A. and Walloe, L., Localization of atherosclerotic lesions in the bifurcation of the main left coronary artery, *Atherosclerosis*, 1983, 47: 55-62.
- 26 Shimada, Y., Courtney, B. K., Nakamura, M., Hongo, Y., Sonoda, S., Hassan, A. H., Yock, P. G., Honda, Y. and Fitzgerald, P. J., Intravascular ultrasonic analysis of atherosclerotic vessel remodeling and plaque distribution of stenotic left anterior descending coronary arterial bifurcation lesions upstream and downstream of the side branch, *Am J Cardiol*, 2006, 98: 193-196.

- 27 Badak, O., Schoenhagen, P., Tsunoda, T., Magyar, W. A., Coughlin, J., Kapadia, S., Nissen, S. E. and Tuzcu, E. M., Characteristics of atherosclerotic plaque distribution in coronary artery bifurcations: an intravascular ultrasound analysis, *Coron Artery Dis*, 2003, 14: 309-316.
- 28 Vattikuti, R. and Towler, D. A., Osteogenic regulation of vascular calcification: an early perspective, *Am J Physiol Endocrinol Metab*, 2004, 286: E686-696.
- 29 Burke, A. P., Kolodgie, F. D., Farb, A., Weber, D. K., Malcom, G. T., Smialek, J. and Virmani, R., Healed plaque ruptures and sudden coronary death: evidence that subclinical rupture has a role in plaque progression, *Circulation*, 2001, 103: 934-940.
- 30 Schmermund, A. and Erbel, R., Non-invasive computed tomographic coronary angiography: the end of the beginning, *Eur Heart J*, 2005, 26: 1451-1453.

Addendum 4

Reliable angiographic evaluation by 64-slice computed tomography after trifurcation stenting of the left main coronary artery

Euro Intervention 2006; 1: 482-483

*Carlos A.G. Van Mieghem^{1,2},
Georgios Sianos¹, Bob
Meijboom^{1,2}, Eleni Vourvouri^{1,2},
Patrick W. Serruys¹, Pim J. de
Feyter^{1,2}*

*From the departments of
Cardiology¹ and Radiology²,
Erasmus MC, Rotterdam, the
Netherlands*

A 39-year-old man underwent a complex percutaneous coronary intervention of the left main trifurcation due to unstable angina. Five paclitaxel-eluting stents were implanted successfully in the 3 major branches and left main trunk (Figure 1, panels A and B). Three months later follow-up 64-slice computed tomographic (MSCT) coronary angiography demonstrated excellent stent patency without signs of neointimal hyperplasia (Figure 2). Invasive coronary angiography and intravascular ultrasound (IVUS) confirmed these findings (Figure 1, panels C and D).

Current MSCT scanners provide a promising non-invasive alternative to conventional coronary angiography in the follow-up of patients after stenting of the left main coronary artery.

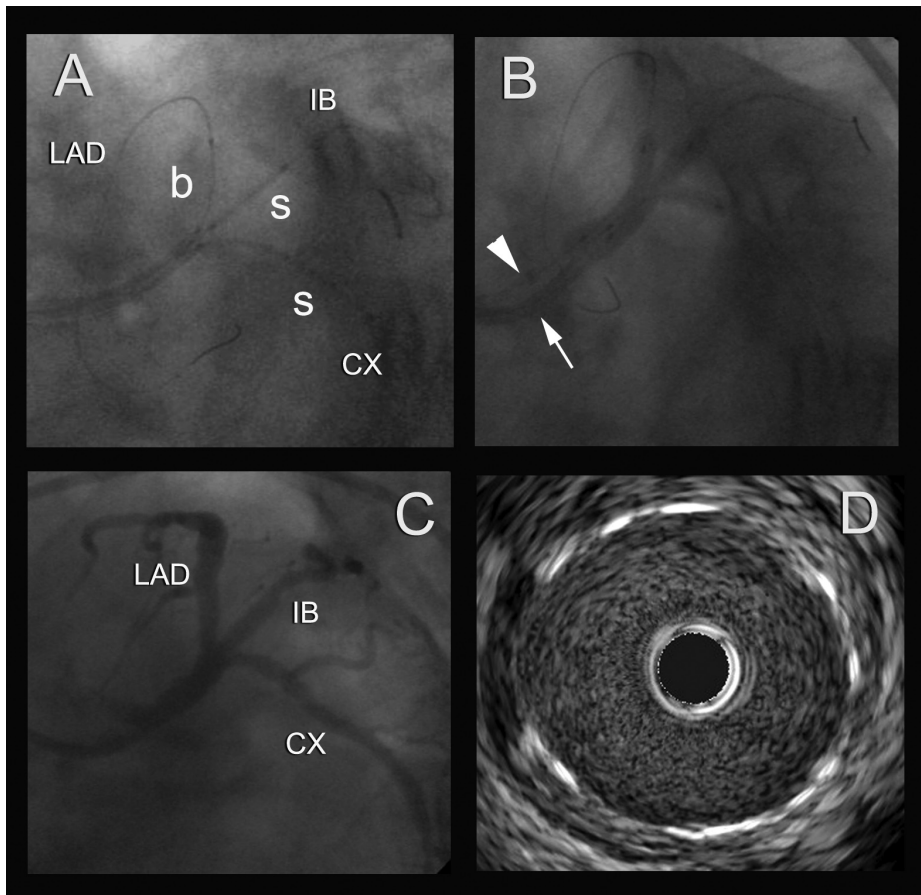


Figure 1. Two paclitaxel eluting stents (PES) were positioned simultaneously within the intermediate branch and circumflex artery (CX) together with balloon dilatation of the left anterior descending artery (LAD) to prevent plaque shift (panel A). The stent in the CX overlapped with a more distal stent in the same branch implanted at the start of the procedure. Due to dissection of the LAD ostium another PES was positioned in the proximal LAD and a fifth stent was deployed in the left main trunk (not shown). The procedure was completed with kissing balloon inflations of the 3 branches using 2 guiding catheters (one 5 and one 6 French guiding catheter), as indicated by the arrowhead and arrow (panel B). Invasive coronary angiography showed perfect patency of the 3 branches (panel C). Intravascular ultrasound confirmed the absence of neointimal hyperplasia, as shown by the IVUS cross-sectional image of the LMCA (panel D). *b* indicates balloon; CX, circumflex coronary artery; IB, intermediate branch; LAD, left anterior descending coronary artery; and *s*, stent.

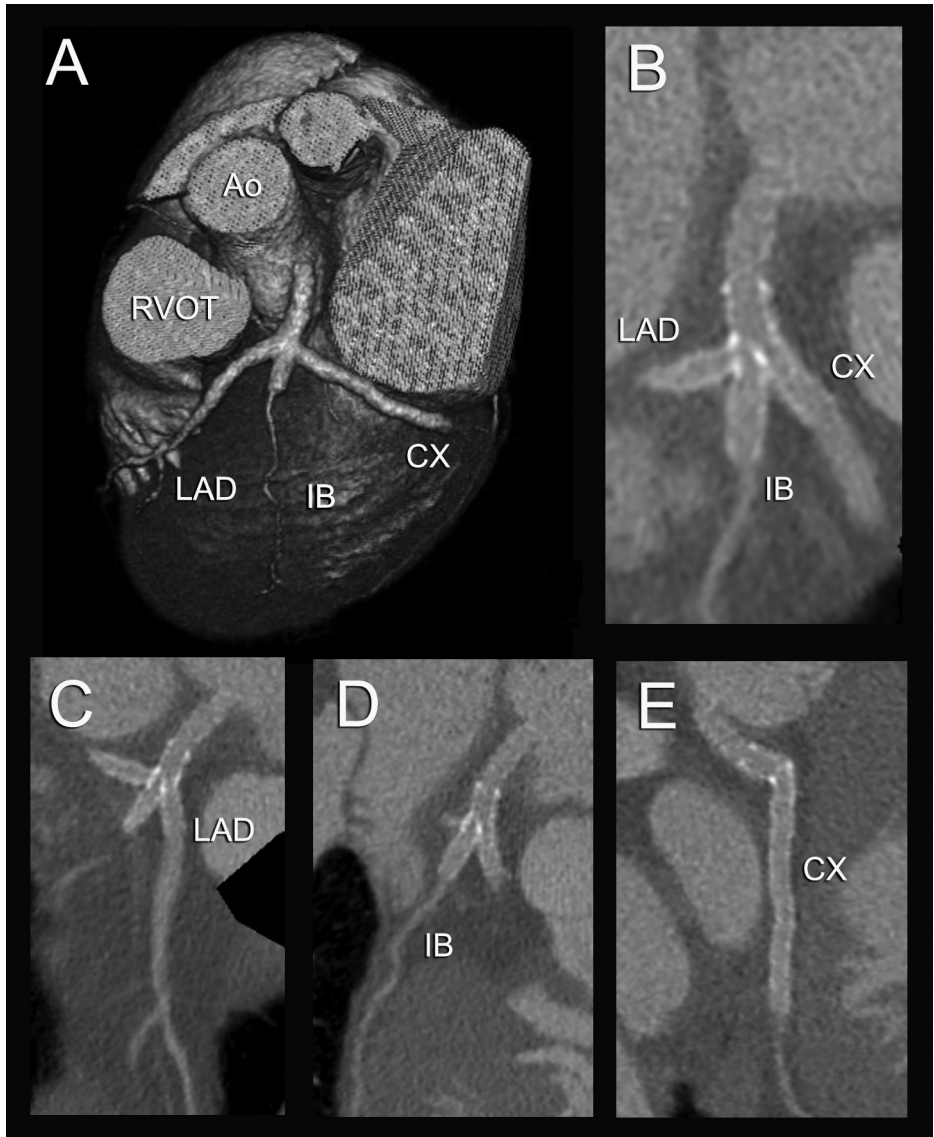
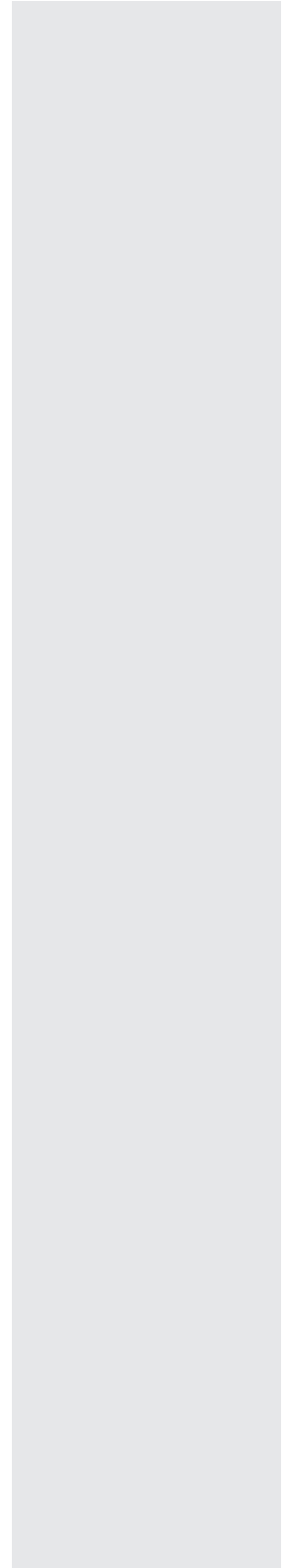


Figure 2. 64-slice CT coronary angiogram. Volume-rendered (panel A) and multiplanar reconstructed image (panel B) showing the stented left main trifurcation. The proximal stent edge in the left main trunk is well delineated (arrow). The lumen within the stents is clearly visible along the 3 branches of the trifurcation (panels C, D and E). It is obvious that the 4 stents, including the stent edges, are perfectly patent without signs of neointima hyperplasia.

Ao indicates ascending aorta; CX, circumflex coronary artery; IB, intermediate branch; LAD, left anterior descending coronary artery; RVOT, right ventricular outflow tract.

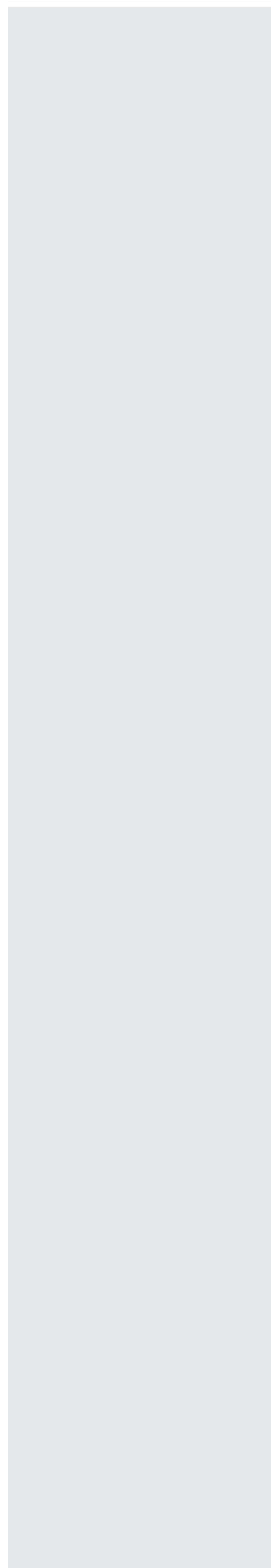
PART 6

Summary and conclusion



20

Summary and conclusion



SUMMARY AND CONCLUSIONS

Introduction

CT coronary angiography (CTCA) is a rapidly emerging technique able to non-invasively detect significant coronary stenosis as well as non-significant coronary plaques. Rapid developments in Multislice CT technology has resulted in a markedly improved image quality when imaging the small and rapidly moving coronary arteries. However, CTCA remains challenging, even using the latest generation Multislice CT scanners. In these chapters (**Chapter 1- 3**) an overview of the literature on CTCA, its potential clinical application and tips and tricks on data acquisition and image reconstruction are given. Furthermore, the limitations and pitfalls in cardiac CTCA are described.

Detection of significant coronary artery disease

In a prospective multicenter, multivendor study three participating centers prospectively approached 433 symptomatic patients with acute and stable anginal syndromes who were between 50 and 70 years of age, and referred for diagnostic conventional coronary angiography (CCA) (**Chapter 4**). Three hundred sixty patients underwent a non-enhanced calcium scan and a CTCA which was compared to CCA. No patients or segments were excluded because of impaired image quality due to either coronary motion or calcifications. The prevalence of having at least one significant stenosis was 68%. In a patient-based analysis, the sensitivity for detecting patients with at least 1 significant coronary stenosis was 99% and the specificity 64%. In conclusion, 64-slice CTCA was reliable to rule out significant coronary artery disease (CAD) in patients with stable and unstable anginal syndromes. However, a positive 64 CTCA scan often overestimated the severity of atherosclerotic obstructions and requires further testing to guide patients' management.

In a large mono-center study we assessed the diagnostic accuracy of 64-slice CTCA to detect significant CAD and compared the differences in diagnostic accuracy for women and men in 402 symptomatic patients (**Chapter 5**). The sensitivity and negative predictive value to detect significant CAD were very good, both for women and men; whereas diagnostic accuracy specificity and positive predictive value were lower in women. The per-segment analysis demonstrated lower sensitivity in women compared with men. The sensitivity in women did not show a difference in proximal and mid segments, but was significantly lower in distal segments and side branches.

A newly introduced multislice CT scanner, dual-source computed tomography, can obtain a higher temporal resolution during image acquisition than single tube scanners, making it able to obtain good image quality at higher patient's heart rates. We performed dual-source computed tomography (DSCT) coronary angiography in patients referred for CCA, but without premeditation of beta-blockers (**Chapter 6**). Sensitivity, specificity, and the negative predictive value of dual-source computed tomography were all >95%. Positive predictive value was lower, at 75%,

due to overgrading of segments with calcified plaque. In conclusion, non-invasive DSCT coronary angiography was highly sensitive to detect and to reliably rule out the presence of a significant coronary stenosis, even without the use of pre-scan beta blockers.

Clinical application of CT coronary angiography

The clinical utility of a test result requires knowledge of the sensitivity and specificity of the test as well as an assessment of the pretest probability. We calculated the pretest probability for significant CAD in 254 symptomatic patients based on the type of chest discomfort and their risk factors (**Chapter 7**). Patients were divided in three groups with a low, intermediate and high pre-test probability for significant CAD. All subjects had both undergone CTCA and traditional CCA. The post-test probability of significant CAD after a negative CT scan was 17% in the high-risk group versus 0% for the low- and intermediate-risk groups. After a positive CT test result, 96% of high-risk patients had significant CAD versus only 68% in the low-risk group. We concluded that CTCA is useful in symptomatic patients with a low or intermediate pretest probability of significant CAD, and a negative CT scan reliably rules out CAD in this group. However, there is limited utility of CTCA in patients with a high pretest probability of CAD.

A high diagnostic accuracy of 64-slice CTCA in selected patients with stable angina pectoris has been reported, but only scant information was available in patients with non-ST elevation acute coronary syndrome 64-slice. CTCA was performed in 104 patients with non ST elevation acute coronary syndrome (**Chapter 8**). The prevalence of significant CAD was 85%. Sensitivity for detecting significant coronary stenoses on a patient-by-patients analysis was 100% and specificity 75%. In conclusion, 64-slice CTCA has a high sensitivity to detect significant coronary stenoses and is reliable to exclude the presence of significant CAD in patients who present with a non-ST elevation acute coronary syndrome.

As mentioned in the above findings, it has been demonstrated that CTCA provides excellent diagnostic sensitivity for identifying coronary stenoses, but may lack accurate delineation of the hemodynamic significance. We sought to determine the diagnostic accuracy of visual and quantitative CTCA to predict the hemodynamic significance of a coronary stenosis, using intracoronary fractional flow reserve (FFR) as the reference standard. We investigated 79 patients with stable angina pectoris who underwent both 64 slice - or DSCT coronary angiography and FFR measurement of discrete coronary stenoses (**Chapter 9**). Both qualitative and quantitative CTCA and qualitative and quantitative CCA were performed to determine the severity of a stenosis which was compared with FFR measurements. A significant anatomical or functional stenosis was defined as $\geq 50\%$ diameter stenosis or $FFR < 0.75$. A total of 89 stenoses were evaluated of which 18% had a $FFR < 0.75$. The diagnostic accuracy of qualitative and quantitative CTCA and qualitative and quantitative CCA to detect a hemodynamic significant coronary lesion was 49%, 71%, 61% and 67%. Correlation between quantitative CTCA and quantitative CCA with fractional flow reserve

measurement was weak. Determining the hemodynamic significance of an angiographic intermediate stenosis remains relevant before referral for revascularization treatment.

Next, we performed a sub-analysis of the combination of the calcium score and CTCA in the work-up of patients with angina pectoris in 360 patients (**Chapter 10**). Firstly, we found that a negative CTCA reliably ruled out significant CAD, whereas a low calcium score did not. Secondly, we found that the prevalence of significant CAD increased with increasing calcium score, while the specificity and positive likelihood ratio of CTCA decreased sharply. The value of 64-slice CTCA in patients with a calcium score > 400 is limited when CTCA is used as a binary test and these patients with angina pectoris should be referred to CCA directly.

The presence of coronary calcification is a major limitation to detect or rule out significant CAD. Calcification overrepresentation is generally referred to as 'blooming effect', and is frequently associated with beam hardening and partial volume artefacts. Calcification overrepresentation limits the visualization of adjacent structures and often yields overestimation of the severity of stenosis (false positive diagnoses). An algorithm for predicting $\geq 50\%$ coronary stenoses based on segmental multislice computed tomography calcium score and clinical factors was developed (**Chapter 11**). 402 patients both underwent segmental multislice computed tomography calcium score, CTCA and CCA. The calcium score and calcification morphology were assessed in individual coronary segments. In a derivation dataset, we explored the predictive value of segmental calcium score, morphology, patient's symptoms and risk factors. In conjunction with calcification morphology, anatomical location, patient's symptoms and risk factors, segmental multislice computed tomography calcium score can predict coronary stenosis. Using this prediction model the amount of false positives results can be diminished.

Next, our purpose was to determine the indication of CTCA as triage test prior to CCA in a cost-effectiveness analysis (**Chapter 12**). Using a Markov-model, we analyzed the decision from the perspective of the patient, physician, hospital, health-care system, and society using recommendations from the UK, US, and the Netherlands for cost-effectiveness analyses. Outcome measures were revised post-test probability of CAD, life-years, quality-adjusted life-years, costs, and incremental cost-effectiveness ratios. In conclusion, the indication for CTCA as triage test prior to CCA depends on the optimization criterion, prior probability of CAD and sensitivity of CTCA. In patients with atypical angina, CTCA increases life expectancy but not quality-adjusted life-years, is cost-saving and is cost-effective.

CTCA before and after cardiac surgery

The next chapter provides a review of possible applications of CTCA in Cardiothoracic surgery (**Chapter 13**). The high negative predictive value of $\pm 98\%$ found in CTCA studies suggests that CTCA may be a useful as a diagnostic technique to rule out the presence of coronary stenoses

in selected patients, especially those with a lower pretest likelihood of disease. An appropriate population may be patients undergoing cardiac valve surgery who have a prevalence of concomitant CAD of 25-35%. We studied patients referred for elective valve surgery with both CTCA and CCA (**Chapter 14**). Using a 64-slice CT scanner, we were able to identify all patients with significant coronary stenosis. If this study had been set up as a protocol with CTCA as an initial screening, 69% of patients would avoid CCA, 26% would have CCA to confirm the findings from CTCA, and in only 6% would an “unnecessary” CCA be performed.

Imaging of coronary artery bypass grafts (CABG) is reliable, due to their larger diameter and lesser mobility. However, clinical applications can be hampered due to difficulties in assessing the native coronary arteries in patients with previous CABG, because of the presence of severe calcifications. We explored the diagnostic performance of 64-slice CT in symptomatic patients after bypass surgery, for the assessment of both grafts and native coronary arteries (**Chapter 15**).

Therefore 64-slice CTCA was performed in 52 symptomatic patients, 10 ± 5 years after bypass surgery. A total of 109 grafts, 123 distal coronary run-offs and 116 non-bypassed coronary branches were analyzed. Per-segment detection of graft disease yielded a sensitivity of 99% and specificity of 96%. Sensitivity and specificity to detect run-off disease were 89% and 93%, positive predictive value was 50%. In non-grafted coronary segments, CT detected significant stenosis with a sensitivity and specificity of 97% and 86%. Overestimation occurred more frequently in calcified segments.

In patients who undergo a redo CABG or totally endoscopic CABG CTCA can add incremental information in planning these complicated procedures. CTCA provides three-dimension information of the intra-thoracic organs, an overview of the coronary tree and bypasses and information on location, severity and plaque characteristics of CAD. Furthermore, information on the cardiac valves and ventricle can be gathered. During CTCA a volume of data is obtained. By reconstruction of datasets with fixed intervals during the R-R interval, functional information can be acquired of the cardiac valves and ventricle.

Thirty-two patients, 12 years after CABG, were studied to investigate the long term outcome in patients with left internal mammary artery to left anterior descending coronary artery (LIMA-LAD) and T-grafts. These patients were both studied by ultrasonography as by DSCT. Furthermore, we evaluated whether ultrasonography can determine graft patency (**Chapter 16**). Fifteen patients with single LIMA-LAD and additional vein grafts (group I) and seventeen patients with LIMA-free right internal mammary artery (FRIMA) T-grafts (group II) underwent DSCT and transthoracic ultrasonography of the LIMA and left ventricle. DSCT showed three string sign LIMA (20 %) grafts and 6 occluded venous anastomoses (13 %) in group I and three (distal) string sign LIMA grafts (18 %), seven occluded LIMA anastomoses (23 %) and nine occluded FRIMA

anastomoses (23 %) in group II. Ultrasonography could not distinguish between string sign and patent single LIMA or T-grafts nor demonstrate distal anastomosis patency in T-grafts twelve years after surgery.

To determine whether functional ultrasonographic LIMA findings correspond with DSCT in patients 12 years after CABG, we entered thirty-four patients, sixteen with conventional single LIMA (group I) and eighteen composite arterial T-grafts (group II), in a cross-sectional study (**Chapter 17**). Patients underwent transthoracic proximal LIMA ultrasonography at rest and during the Azoulay manoeuvre, left ventricle trans thoracic echocardiography and DSCT, 11.5 years postoperatively. Proximal LIMA diameters and areas were significantly larger in T grafts compared to single LIMA grafts, probably due to larger myocardial perfusion areas, which can explain the equalization of ultrasonographic variables between and within both groups at rest and during the Azoulay manoeuvre 12 years after surgery.

Bifurcation imaging

We compared the performance of 64-slice CTCA and in CCA in the detection and classification (according to the Medina system) of bifurcation lesions (**Chapter 18**). We studied 323 consecutive patients undergoing 64-slice CTCA prior to CCA. Evaluation of bifurcation lesions by CTCA included assessment of significant lumen obstruction in both main and side branch vessels. Forty-one out of 43 patients with significant bifurcation lesions were identified by CTCA. Excluding coronary segments with non-diagnostic image quality (5%), the sensitivity, specificity, positive and negative predictive values of CTCA for detecting significant bifurcation lesions was 96, 99, 85 and 99%. In 39 of these 41 patients, CTCA assessment was concordant with the Medina lesion classification on CCA.

Furthermore, we looked for an explanation for the presence of plaque in the high shear stress carina of coronary bifurcations. Early atherosclerosis is located in low shear-stress regions, however plaques are also found at the high shear stress sensing carinas of coronary bifurcations. We investigated the relationship between shear stress and the plaque distribution in bifurcations with CTCA (**Chapter 19**). In conclusion, we showed that plaque is mostly present in low shear stress regions whereas plaque in high shear stress regions is accompanied by plaque in adjacent low shear stress regions. It is therefore plausible that plaque grows from the outer wall (low shear stress) of the bifurcation towards the carina (high shear stress).

Samenvatting en conclusies

SAMENVATTING EN CONCLUSIES

Introductie

Computed Tomography coronair angiografie is een veelbelovende techniek die op een niet-invasieve manier vernauwingen in de kransslagvaten kan aantonen. De kransslagvaten van het hart zijn kleine en snel bewegende structuren die met voorgaande niet-invasieve apparatuur moeilijk visualiseerbaar waren. Door de snelle ontwikkelingen en verbeteringen in de technologie van de Multislice Computed is de beeldkwaliteit aanzienlijk gebeterd. Echter, het vervaardigen van een routine CT coronair angiogram blijft een uitdaging, zelfs met de laatste generatie multislice CT scanners. In de eerste drie hoofdstukken wordt een overzicht gegeven over de klinische mogelijkheden van CT coronair angiografie, een beschrijving van de literatuur en verschillende manieren van data-acquisitie (**Hoofdstuk 1-3**). Tevens worden limitaties en mogelijke valkuilen met bijgaande oplossingen besproken.

Detectie van significante vernauwingen in de kransslagvaten

In een prospectief opgezette multicenter studie waarin drie centra participeerden, werden 433 symptomatische patiënten met stabiele en onstabiele angina pectoris en patiënten met een myocardinfarct zonder ST-elevatie benaderd (**Hoofdstuk 4**). Patiënten hadden een leeftijd tussen de 50 en 70 jaar oud en waren doorgestuurd voor een diagnostische coronair angiografie. 360 patiënten ondergingen een calcium scan en een CT coronair angiogram welke werd vergeleken met de conventionele coronair angiografie. Er werden geen patiënten of segmenten van de kransslagvaten geexcludeerd omwille van verminderde beeldkwaliteit door bijvoorbeeld verkalkingen of snelle beweging van de kransslagvaten. De prevalentie van patiënten met tenminste 1 significante vernauwing was 68%. De sensitiviteit voor het detecteren van patiënten met tenminste 1 vernauwing was 99% en de specificiteit was 64%. 64 slice CT coronair angiografie kan op een betrouwbare manier uitsluiten of er significante vernauwingen aanwezig zijn in patiënten die zich op verschillende manieren presenteren met angina pectoris klachten. Echter CT coronair angiografie overschat vaak de ernst van de vernauwing waardoor het verdere beleid van patiënten met vervolgonderzoek bepaald moet worden.

In een grote mono-center populatie studie hebben we de diagnostische accuraatheid van 64 slice CT coronair angiografie om vernauwingen in de kransslagvaten te detecteren onderzocht en de verschillen geanalyseerd voor mannen en vrouwen in 402 symptomatische patiënten (**Hoofdstuk 5**). Zowel voor mannen en vrouwen was de sensitiviteit en negatieve predictieve waarde in de per-patient analyse zeer goed. De specificiteit en positieve predictieve waarde waren echter lager in vrouwen. In de segment analyse was de sensitiviteit echter ook lager voor vrouwen, niet in de proximale en mid segmenten, maar wel in de distale segmenten en de zijtakken van de kransslagvaten.

Een nieuw geïntroduceerde CT scanner, genaamd Dual Source CT, kan een hoger temporele resolutie verkrijgen gedurende data acquisitie dan een CT scanner met een enkele röntgenbuis. Door deze eigenschap kunnen patiënten met een hoger hartritme worden gescand met behoud van goede beeldkwaliteit. In de studie werden symptomatische patiënten vergeleken die zowel een Dualsource CT als een conventionele coronair angiografie ondergingen, waarbij patiënten voor de CT scan geen betablokkers kregen om het hartritme te verlagen (**Hoofdstuk 6**). De sensitiviteit, specificiteit en negatieve predictieve waarde waren allen > 95%. De positieve predictieve waarde was 75%, door het overschatten van vooral verkalkte segmenten. Concluderend was Dualsource CT zeer gevoelig in het detecteren en uitsluiten van vernauwingen in de kransslagvaten, zelfs zonder patiënten voor te bereiden met betablokkers.

Klinische applicatie van CT coronair angiografie

Kennis van de sensitiviteit en de specificiteit van een test en de waarschijnlijkheid van pathologie voor de test zijn noodzakelijk voor het goede klinisch gebruik van een uitslag van een test. In 254 patiënten werd de waarschijnlijkheid op vernauwingen in de kransslagvaten geschat met behulp van het type van klachten van de patient, leeftijd, geslacht en cardiale risicofactoren. Patiënten werden verdeeld in drie risicogroepen met een laag, intermediair of hoog risico op ziekte (**Hoofdstuk 7**). De waarschijnlijkheid na een negatieve CT coronair angiografie op significante vernauwingen was 17% in de hoog risico groep en 0% in de laag en intermediaire risico groep. Na een positieve CT coronair angiografie was de waarschijnlijkheid 96% in de hoog risico groep en 68% in de laag risicogroep. Concluderend is CT coronair angiografie nuttig in symptomatische patiënten met een laag en intermediaire risico op significante coronaire lesies en een negatieve CT sluit significante ziekte uit in deze groepen. In de hoog risico groep patiënten is beperkt nut voor CT coronair angiografie gezien meest van deze patiënten reeds vernauwingen hebben en zullen worden doorverwezen naar coronair angiografie.

Hoge diagnostische accuraatheid van 64 slice CT coronair angiografie is beschreven voor het detecteren van significante coronaire lesies in geselecteerde patiënten. Echter weinig informatie was bekend in patiënten met onstabiele angina pectoris of patiënten met non ST elevatie myocard infarct. Totaal werden 104 patiënten geïncludeerd met een non ST elevatie acuut coronair syndroom (**Hoofdstuk 8**). De prevalentie van ziekte was 85%. De sensitiviteit was 100 % en de specificiteit 75%. Ook in patiënten met een non ST elevatie acuut coronair syndroom is CT coronair angiografie accuraat in het detecteren en uitsluiten van significante vernauwingen.

Zoals al in bovenstaande tekst staat is het bekend dat CT coronair angiografie goed is in het detecteren van coronaire vernauwingen. Echter de accuraatheid van CT coronair angiografie om de hemodynamische impact van een coronaire lesie te voorspellen is onbekend.

In deze studie werd de diagnostische accuraatheid geanalyseerd van visuele en kwantitatieve CT coronair angiografie om de hemodynamische eigenschappen van een coronaire lesie te voorspellen, gebruikmakend van de fractional flow reserve als gouden standaard (**Hoofdstuk 9**). In totaal werden 79 patiënten geïncludeerd met stabiele angina pectoris die ofwel 64 slice of Dualsource CT coronair angiografie en een conventionele coronair angiografie met een fractional flow reserve hadden ondergaan. De mate van vernauwing werd zowel voor kwalitatieve en kwantitatieve CT coronair angiografie als voor kwalitatieve en kwantitatieve coronair angiografie bepaald. Een significante anatomische vernauwing werd gedefinieerd als $\geq 50\%$ diameter vernauwing en een functionele stenose als < 0.75 . In totaal werden 89 vernauwingen geanalyseerd waarvan 18% een fractionele flow reserve van < 0.75 hadden. De diagnostische accuraatheid van kwalitatieve en kwantitatieve CT coronair angiografie als voor kwalitatieve en kwantitatieve coronair angiografie was 49%, 71%, 61% and 67%. Correlatie tussen kwantitatieve CT coronair angiografie en kwantitatieve coronair angiografie met de fractional flow reserve metingen was zwak. De bepaling van de hemodynamische impact van een intermediaire stenose blijft relevant voor het uiteindelijke doorsturen voor coronaire revascularisatie.

Vervolgens hebben we een analyse gedaan naar de combinatie van de calciumscore en CT coronair angiografie in de diagnose van significant vernauwingen in 360 patiënten met angina pectoris (**Hoofdstuk 10**). Ten eerste, vonden we dat een negatieve CT coronair angiography significante ziekte uitsloot en dat een lage calcium score dit niet deed. Ten tweede, vonden we dat de prevalentie van significante vernauwingen toenam met een stijging van de calcium score en dat de specificiteit en positieve predictieve waarde met een stijgende calcium score fors daalde. De waarde van 64-slice CT coronair angiografie in patiënten met een calcium score > 400 is beperkt wanneer de CT coronair angiografie wordt gebruikt al een test die enkel het onderscheid maakt tussen wel of geen ziekte. Deze patiënten zouden best direct naar conventioneel coronair angiografie worden doorgestuurd.

De aanwezigheid van calcificaties in de kransslagaders maakt het bepalen of er significante vernauwingen aanwezig zijn moeilijk. Deze calcificaties resulteren in verscheidene artefacten die er vaak voor zorgen dat de stenose graad wordt overschat (vals positieve diagnose).

We hebben een algoritme ontwikkeld voor het schatten van $\geq 50\%$ coronary stenose met een segmentele calcium score en verscheidene klinische variabelen (**Hoofdstuk 11**). 402 patiënten ondergingen een segmentele multislice CT calcium score, een conventioneel en een CT coronair angiografie. De calciumscore en morfologie van de calcificaties werden bepaald per individueel coronair segment. De predictieve waarde van de segmentele calcium score, morfologie van de calcium, patiënten symptomen en risicofactoren werden geanalyseerd. Gebaseerd op de calciumscore, het morfologische patroon, de lokatie in de vaatboom, de symptomen van de patient en de aanwezigheid van risicofactoren, is deze predictie regel in staat om de diagnostische besluitvor-

ming te ondersteunen. Het aantal vals positieve diagnoses ten gevolge van de aanwezigheid van kalk kan op deze wijze verminderd worden.

Vervolgens werd in een kost effectiviteits analyse gekeken wanneer CT coronair angiografie geïndiceerd is als triage test voor verwijzing naar invasieve coronair angiografie (**Hoofdstuk 12**). Gebruikmakend van een Markov-model werd deze beslissing getoetst vanuit verschillende perspectieven: vanuit het perspectief van de patient, het ziekenhuis, ziekte-zorg en samenleving gebruikmakend van aanbevelingen vanuit de UK, US en Nederland. Concluderend hangt de indicatie om gebruik te maken van CT coronair angiografie als triage test naar coronair angiografie af van de optimalisatie criteria, de waarschijnlijkheid voor vernauwingen in de kransslagvaten en de sensitiviteit van CT coronair angiografie. In patienten met atypische angina pectoris vermeerderd CT coronair angiografie de levens verwachting, maar niet quality-adjusted life-years, is kosten besparend en kosten effectief.

CT coronair angiografie voor en na cardiale chirurgie

Het volgende hoofdstuk beschrijft de verschillende applicaties van CT coronair angiografie in cardiothoracale chirurgie (**Hoofdstuk 13**). De hoge negatief predictieve waarde van $\pm 98\%$ aangetoond in multiple CT coronair angiografie studies, geeft de mogelijkheid deze eigenschap te gebruiken om significante lesies uit te sluiten vooral in patienten met een lage waarschijnlijkheid op significante vernauwingen. Een mogelijk geschikte patientengroep zijn patienten die een hartklepoperatie ondergaan. Deze hebben gemiddeld een prevalentie van bijkomend significant coronaria lijden van 25-35%. We bestudeerden patienten gepland voor een klepoperatie die bijkomend een conventioneel coronair angiogram en een 64 slice CT coronair angiografie ondergingen (**Hoofdstuk 14**). Alle patienten met significante vernauwingen werden gedetecteerd. Indien deze studie was opgezet met CT coronair angiografie als een initiële screening had 69% een invasieve coronair angiogram bespaard kunnen blijven, 26% had een coronair angiogram ondergaan ter bevestiging van resultaten die gezien waren door CT coronair angiografie en enkel 6% had een onnodige coronair angiogram gekregen, ten gevolge van een vals positieve CT coronair angiografie.

Beeldvorming van coronaire bypassen is nauwkeurig door de relatief grote diameter van het vat en verminderde mobiliteit in de thorax. Echter klinische implementatie van CT coronair angiografie in deze patienten groep is gehinibeerd door de moeilijkheden die er zijn in de beeldvorming van de natieve coronairen welke vaak fors verkalkt zijn.

Wij analyseerde de diagnostische acuraatheid met een 64 slice CT coronair angiografie van zowel de bypassen als de natieve coronairen (**Hoofdstuk 15**). Daarvoor werden 52 symptomatische patienten, 10 ± 5 jaar na bypass chirurgie geïncludeerd. Een totaal van 109 grafts, 123 distale coronair run-offs en 116 niet gebypaste coronair takken werden geanalyseerd. De per-segment analyse van significante vernauwing in de grafts toonde een sensitiviteit van 99% en een specifi-

citeit van 96%. Sensitiviteit en specificiteit om distale run-off ziekte te detecteren was 89% and 93%, positive predictive value was 50%. In niet-gebypaste coronair segmenten detecteerde CT coronair angiografie significante vernauwingen met een sensitiviteit en specificiteit van 97% and 86%. Overschatting gebeurde meer frequent in verkalkte coronaire segmenten.

In patiënten die een redo CABG of totale endoscopische CABG ondergaan, kan CT coronair angiografie toegevoegde informatie verschaffen in de planning van deze ingewikkelde procedures. CTCA levert drie dimensionale informatie van de intrathoracale organen, een overzicht van de coronair boom en bypasses en informatie over de locatie, ernst en karakteristieken van de coronaire plaque. Gedurende de CTCA wordt een volume van data verkregen. Behalve informatie over de coronairen en de grafts kan ook informatie over de cardiale kleppen en de ventrikel worden verkregen. Door reconstructie van datasets met vaste intervallen in de R-R interval, kan functionele informatie verkregen worden van de kleppen en de ventrikel.

Om de lange termijn resultaten in patiënten met een linker arteria thoracica interna naar de linker anterior descending coronair arterie (LIMA-LAD) and T-grafts te onderzoeken werden 32 patiënten 12 jaar na CABG geanalyseerd middels Dual Source CT en transthoracale echografie. Verder werd gekeken of echografie kon evalueren of de bypasses nog open waren (**Hoofdstuk 16**). Vijftien patiënten met een enkele LIMA-LAD en bijkomende vene omleidingen (Groep 1) en 17 patiënten met een LIMA-vrije rechter arteria thoracica interna (FRIMA) T-grafts (groep II) ondergingen Dual Source CT en transthoracale echografie van de LIMA en de linker ventrikel. Dual Source CT toonde drie string signs bypasses (20%) en 6 geoccludeerde vene anastomoses (13%) in groep I and drie (distale) stringsign LIMA bypasses (18%), 7 dichte LIMA anastomoses (23%) and 9 dichte FRIMA anastomoses in groep II. Echografie kon geen onderscheid maken tussen een string sign en een patente singel LIMA of T-grafts. Tevens kon met echografie niet worden geevalueerd of de distale anastomose open was 12 jaar na CABG.

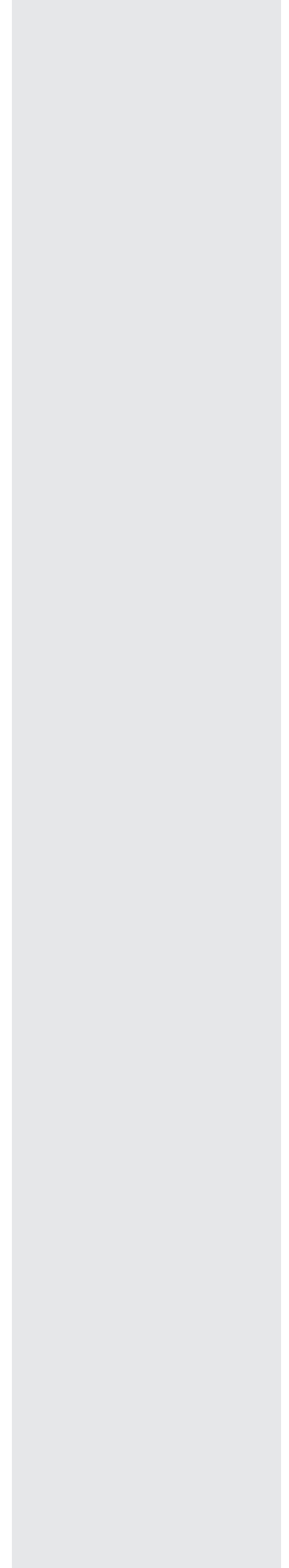
Om te analyseren of functionele data van de LIMA corresponderen met anatomische bevindingen van Dual Source CT werden 34 patiënten 12 jaar na CABG onderzocht (**Hoofdstuk 17**). Zestien patiënten bevonden zich in de enkele LIMA groep (Groep I) en 18 in de T-grafts groep (Groep II). Patiënten ondergingen zowel een transthoracale echografie van de proximale LIMA in rust en tijdens de Azoulay maneuver, van de linker ventrikel en een Dual Source CT, 11,5 jaar na CABG plaatsing. De proximale LIMA diameters waren significant groter in T grafts dan in enkele LIMA grafts, waarschijnlijk door een grotere perfusie gebied van het myocard. Dit kan de gelijkens in variabelen verkregen met echografie verklaren tussen beide groepen zowel in rust als tijdens de Azoulay maneuver.

Visualisatie van coronaire bifurcaties

Wij vergeleken de accuraatheid van 64-slice CT coronair angiografie en conventioneel coronary angiografie in de detectie en classificatie (volgens de Medina classificatie) van bifurcatie lesies (**Hoofdstuk 18**). We bestudeerden 323 consecutieve patienten die zowel 64 slice CT coronair angiografie als conventionele coronair angiografie ondergingen. Evaluatie van de bifurcatie lesie door CT coronair angiografie betrof analyse van significante stenose van het hoofdvat als de zijtak. CT coronair angiografie detecteerde 41 van de 43 patienten met een significante bifurcatie lesie. Na exclusie van coronaire segmenten met niet diagnostische beeld kwaliteit (5%), was de sensitiviteit, specificiteit, positieve - en negatieve predictieve waarde 96%, 99%, 85%, 99%. In 39 van de 41 patienten was de CT coronair angiografie analyse in concordantie met de Medina classificatie zoals gezien bij conventioneel coronair angiografie.

Vroege presentatie van atherosclerosis is gelocaliseerd in lage shear stress gebieden. Echter plaques worden ook aangetroffen in gebieden met hoge shear stress ter hoogte van de carina van coronaire bifurcaties. We zochten naar een verklaring voor de aanwezigheid van plaques in de carina van een bifurcatie, waar een hoge shear stress aanwezig is middels CT coronair angiografie (**Hoofdstuk 19**). We toonde aan dat coronaire plaques zich voornamelijk in gebieden van lage shear stress bevinden. Plaques in hoge shear stress gebieden zijn vaak gecompliceerd met plaques in aanliggende lage shear stress gebieden. Daardoor is het plausibel dat de coronaire plaque vanuit de buitenwand (in het gebied van lage shear stress) van de bifurcatie naar de carina groeit (hoge shear stress).

Acknowledgements



DANKWOORD

Dit proefschrift en mijn professionele ontwikkeling zijn mede tot stand gekomen met hulp van de afdelingen Cardiologie en Radiologie van het Erasmus Medisch Centrum Rotterdam. Ik ben een ieder veel dank verschuldigd.

Allereerst dank ik hartelijk mijn beide promotors, Professor De Feyter en Professor Krestin, voor hun bijdragen aan dit proefschrift.

Beste Pim, zonder jouw aanwezigheid was dit proefschrift niet tot stand gekomen in de huidige vorm. Jouw jarenlange ervaring in de wetenschappelijke wereld heeft mij telkens geïnspireerd. Jouw werkwijze, waarbij jij mij als promovendus initieel redelijk los liet en mij zelf mijn weg liet kiezen, beangstigde mij een beetje. Gelukkig heb jij mij altijd weer met subtiele opmerkingen en sturingen de juiste koers laten varen, heb jij mij gewaarschuwd om bepaalde zijwegen niet in te slaan, en heb jij ervoor gezorgd dat ik altijd gefocust bleef op het grote geheel. Deze visie heeft ons geen windeieren gelegd. Vaak op het einde van de dag discussieerde ik met jou en onze collega's over de actuele wetenschappelijke ontwikkelingen binnen en buiten ons gebied. Ook de zogeheten 'verhalen uit de oude doos' bleven dan niet achterwege.

Professor Krestin, ook u ben ik grote dank verschuldigd voor de promotieplek die u mij heeft gegeven binnen de cardiale imaging groep. Mede dankzij u heeft de gehele CT coronair angiografie groep met de meest geavanceerde apparatuur mogen werken. Hierdoor zijn prachtige onderzoeksresultaten tot stand gekomen. De rust en het vertrouwen welke u bleef uitstralen heb ik zeer gewaardeerd. Uiteraard keek u van een afstandje over mijn schouder mee.

De overige leden van de promotiecommissie, Professor Poldermans, Professor Bogers, Professor Hunink, Professor Simoons, Professor Mali, Professor Bax en Professor Niessen, dank ik hartelijk voor hun bereidwilligheid zitting te nemen in mijn promotiecommissie. Ik ben u zeer erkentelijk voor uw expertise bij de beoordeling van mijn proefschrift.

Beste Nico, slykes, oude vriend uit het Leuvense. Groot is mijn waardering voor het feit dat je me gewezen hebt op een vrijgekomen plek binnen de cardiale CT groep, en je aanmoedigen voor mijn sollicitatie in Rotterdam, die geresulteerd heeft in dit proefschrift. In de begintijd van mijn promotie heb je me alle kneepjes en technieken van de CT scanner en het onderzoek bijgebracht. Ook na de start van jouw Radiologie opleiding bleef jij actief binnen de research en heb jij een grote bijdrage geleverd aan het scoren van de CT datasets. Naast onze gezamenlijke wetenschappelijke interesse op het medische vlak, heb ik mooie herinneringen aan onze werkreizen tijdens de promotietijd, racend door Mumbai en Chicago, op de golfbaan in Victoria Island en skiënd in Zurs. Veel plezier en alle geluk met de recente aanwinst van jullie gezin.

Beste Carlos, onze samenwerking is altijd uitermate plezierig geweest. Door onze gezamenlijke studentenstad Leuven en voorliefde voor het Bourgondische leven vonden wij elkaar in de geneugten die België te bieden heeft. Met gemak was je altijd te overtuigen voor een “wetenschappelijke discussie”, uiteraard dan wel tijdens de lunch bij “de Italiaanse broodjes zaak”. Jij was de gouden spil van de interventie cardiologie en de cardiale CT. De discussies over mogelijke klinische implementatie van deze nieuwe techniek met jouw klinische input hebben een grote bijdrage geleverd aan mijn promotie. Dank voor de hulp met het includeren van stabiele en vooral onstabiele AP patiënten op het cathlab, en voor de vele QCA analyses die je hebt gedaan. Het ga je goed met jouw verdere carrière onder de rivier.

En dan natuurlijk mijn twee kamergenootjes Annick Weustink en Sharon Kirschbaum. We hadden allen een goede combinatie van hard werken en veel lol welke ons mooie promotiejaren heeft bezorgd. Deze haan had niet altijd veel in te brengen in ons onderzoekshok. Annick Weustink, mijn opvolgster binnen de cardiale CT groep. Sharon Kirschbaum, specialist van “the other” scanner (MRI). Ik heb groot respect voor de wijze waarop jullie werken. De combinatie van goed managen, doorzettingsvermogen, beetje delegeren en hard werken zullen zeker resulteren in mooie publicaties naast degene die jullie al hebben. Annick, nooit gedacht dat ik zo vaak op de verjaardag van een collega zou zijn!

Meerdere PhD studenten waarmee ik heb samen gewerkt, zijn mij voorgegaan in het afronden van hun promotie. Francesca Pugliese, I believe you always had the difficult papers to write using the most difficult statistics. Thanks for teaching me to stop drinking cappuccino after eleven since this is “not done” in Italy.

Filippo Cademartiri, unfortunately you left the cardiac group to start your own research group in Parma, Italy. Your output of producing papers on various subjects is unbelievably enormous. I am sure we will meet again during future congresses.

Koen Nieman, de tijd die we hebben samen gewerkt, heb ik het altijd prettig gevonden Je bent een goede schrijver en hebt een heldere geest. Jij was altijd goed gezelschap tijdens de cardiale congressen. Ik hoop op een voorspoedige toekomstige samenwerking.

Michael Hartman, in de nadagen van onze beider promotietijd hebben wij goed en vooral prettig samengewerkt. Ik heb vernomen dat je naar het hoge Noorden gaat. Veel succes aldaar.

Lisanne en Tirza, jullie zijn net begonnen met jullie PhD. Veel succes met jullie wetenschappelijke reis.

Matthijs Meijs, hardwerkende Utrechtse promovendus. Dank voor de intensieve samenwerking. Ik weet zeker dat we een mooi resultaat hebben geboekt en dat nog meer publicaties zullen volgen in de toekomst. Ik hoop dat ook jouw boekje niet al te lang meer op zich laat wachten.

Marcel Geleijnse, dank voor het helpen met inclusie van onze eerste projecten. Helaas hebben zij niet tot de gewenste grote aantallen geleid om tot echte publicaties te komen. Dank voor het introduceren van de golfwereld. Samen met Bob 2 hebben we een mooie tijd gehad met lange weekenden golfen, culinair barbecueën in de openhaard en uitgaan in de Buddha bar te Parijs. De GVB moeten we maar deze lente gaan halen. Robert-Jan van Geuns, ik heb het altijd erg interessant gevonden om de MRI discussies met één oor mee te luisteren. Dank voor onze introductie in een echt goede Jazz tent in New Orleans.

Multiple international fellows from all over the world have enforced the cardiac CT group. Giuseppe Runza (Don Peppe), Manual Belgrano, Patriacia Malagutti, thanks for teaching me “amarino, dami une bachino”, Ludovico La Grutta, Alessandro Palumbo, Eleni Vourvouri and Niels van Pelt, all the way from down under, I really enjoyed your presence in the group and our Dutch English discussions, Fillippo Alberghina, Roberto Malago, Dipa Gopalan, Masato Osuka, Marco Rengo. Thank you all for your enthusiasm and effort working in Rotterdam.

Mirjam Hunink en Erik Boersma, dank voor het meedenken en de implementatie van de statistiek en de hulp met statistische analyses. Zonder jullie hulp was deze promotie een hoop lastiger geworden.

Ton Everaerts, zonder jou had dit promotieboek niet in deze huidige vorm bestaan. Ik ben je veel dank verschuldigd voor de hulp die je de laatste maanden hebt geboden en voor het bundelen van al die losse artikelen in één mooi geheel. Linda Everse dank voor de wetenschappelijke ondersteuning en de laatste aansporingen naar een goed einde.

Marcel Dijkshoorn, Berend Koudstaal, Marieke Kreiter-de Jonge en Ronald Booij. Dank voor jullie flexibiliteit om weer eens een ongeplande patiënt toch nog even te scannen en jullie interesse in een nieuwe techniek. Ik realiseer me dat de onregelmatigheid jullie soms gek maakte, maar het kon niet anders.

Alle secretaresses van de interventie cardiologie, met name Laetitia Bautz en de secretaresses van de cardiochirurgie, dank voor het dogen van mijn aanwezigheid en excuses voor het af en toe verkeerd terug leggen van de patiëntengegevens. Denise Vrouwenraets, Marja Thijse en Janet Slob dank voor de altijd plezierige ontmoetingen en steun.

Joost Daemen, eigenlijk hadden we het nooit zo vaak over de cardiologie. Elkaars praatjes kunnen we nu ongeveer wel dromen. Naast onze wetenschappelijke bezigheden hebben wij fantastische tijden beleefd. Cruisend naar Key-West met onze Ford Mustang Cabrio, zonnend in ons appartement in Barcelona en een drankje drinkend op Bourbon Street. Hoewel we elkaar niet dagelijks tegen kwamen en we professioneel vrij weinig met elkaar te maken hadden, bezochten we altijd samen de "big three" van de cardiale congressen. Ik heb bewondering voor je harde werken tijdens jouw promotie. Dit heeft geresulteerd in een dik proefschrift, waarbij ik jou paranimf mocht zijn en maar liefst 5 stellingen voor mocht lezen. Het is een eer om je aan mijn zijde te hebben mogen staan.

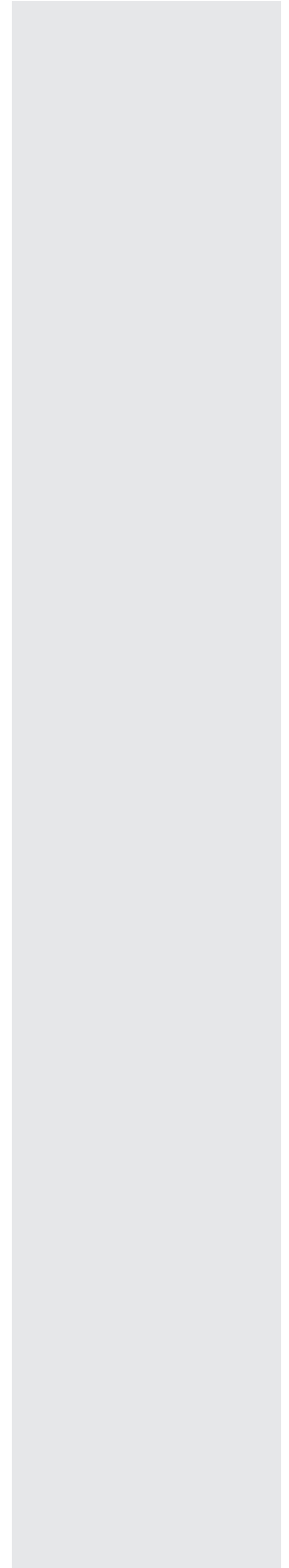
Alle Leuvense vrienden dank ik hartelijk voor de mooie avonden en de vele rib eye biefstukken die we hebben gegeten in Stobbe. Ik weet zeker dat we deze traditie in ere zullen houden. "Bokkerijders we love you".

Lilian, mijn kleine, maar toch ook grote zus. Jij hebt toch net iets meer "managing skills" geërfd van mama dan ik. Dit heeft geresulteerd in je promotie en je opleidingsplek Radiologie op je 27e. De manier waarop jij alles aanpakt, van kinds af aan al, en tot een succes brengt, wekt veel bewondering. Ik dank jou en Maarten voor al jullie nuttige adviezen zowel op wetenschappelijk als op persoonlijk vlak. Ik ben er erg trots op om oom te zijn geworden van Vera. Achter al het nieuwe leven, schuilt ook het einde van het leven. Oma, helaas kunt u de afronding van mijn promotie niet meemaken. Ik weet dat u er graag bij had willen zijn. Papa, ik weet dat je ergens mee kijkt.

Lieve mama, alles is toch goed gekomen. Er leiden meer wegen naar Rome en het is goed dat we één van de juiste wegen hebben gekozen, weliswaar met een klein omweggetje over de Zuidelijke grens. Dank voor mijn zorgeloze en plezierige jeugd en de steun die je altijd hebt gegeven. Ik realiseer me dat het niet altijd makkelijk is geweest om vader en moeder tegelijk te zijn, maar je mag trots op jezelf zijn.

Lieve Sabine, ik ben blij dat je op die bewuste vrijdagmiddagborrel de boot met je clubgenootjes hebt gemist, en ik jou hierdoor ontmoet heb. Je hebt altijd klaar voor me gestaan met veel liefde, humor en wijze raad en dat hoop ik jou ook terug te kunnen geven. Ik heb je lief.

List of publications



PUBLICATIONS

1. **Meijboom WB**, Vanderheyden M.
Biventricular pacing and persistent left superior vena cava.
Case report and review of the literature.
Acta Cardiol. 2002 Aug;57(4):287-90. Review.
2. **Meijboom WB**, Mollet NR.
Non-invasive computed tomography coronary angiography: a reliable gatekeeper for conventional angiography in patients referred for valve surgery?
Int J Cardiovasc Imaging. 2006 Oct;22(5):711-2.
3. **Meijboom WB**, Mollet NR, Van Mieghem CA, Kluin J, Weustink AC, Pugliese F, Vourvouri E, Cademartiri F, Bogers AJ, Krestin GP, de Feyter PJ.
Pre-operative computed tomography coronary angiography to detect significant coronary artery disease in patients referred for cardiac valve surgery.
J Am Coll Cardiol. 2006 Oct 17;48(8):1658-65.
4. **Meijboom WB**, Mollet NR, van Mieghem CAG, Weustink AC, Pugliese F, van Pelt N, Cademartiri F, Vourvouri E, de Jaegere P, Krestin GP, de Feyter PJ.
64-slice Computed Tomography Coronary Angiography in Patients with Non-ST Elevation Acute Coronary Syndrome.
Heart 2007 Nov;93(11):1386-92.
5. **Meijboom WB**, van Pelt N, de Feyter PJ.
Use of High Resolution Spiral CT for the Diagnosis of Coronary Artery Disease.
Current treatment options in cardiovascular medicine. 2007 Feb; 9(1): 29-36.
6. **Meijboom WB**, van Mieghem CAG, Mollet NR, Pugliese F, Weustink AC, van Pelt N, Cademartiri F, Nieman K, Boersma H, de Jaegere P, Krestin GP, de Feyter PJ.
64-Slice Computed Tomography Coronary Angiography in Patients with High, Intermediate or Low Pre-test Probability of Significant Coronary Artery Disease.
J Am Coll Cardiol. 2007 Oct 9;50(15):1469-75.
7. **Meijboom WB**, Weustink AC, Pugliese F, Mieghem CAG, Mollet NR, van Pelt N, Vourvouri V, Cademartiri F, Nieman K, Regar E, de Jaegere P, Krestin GP, de Feyter PJ.
Comparison of Diagnostic Accuracy of 64Slice Computed Tomography Coronary Angiography in Women-vs-Men with Angina Pectoris.
Am J Cardiol. 2007 Nov 15;100(10):1532-7.
8. **Meijboom WB**, Van Mieghem CAG, van Pelt N, Weustink AC, Pugliese F, Mollet NR, Boersma E, Regar E, van Geuns RJ, de Jaegere PJ, Serruys PW, Krestin GP, de Feyter PJ.
Comprehensive assessment of coronary artery stenoses: CT coronary angiography versus conventional coronary angiography and correlation with FFR.
J Am Coll Cardiol. 2008 Aug 19;52(8):636-43.

9. **Meijboom WB**, Meijs MFL, Schuijf JD, Mollet NR, van Mieghem CAG, Nieman K, van Werkhoven JM, Pundziute G, Weustink AC, Rensing B, Cramer MJ, Jukema JW, Bax JJ, Prokop M, Doevendans PA, Krestin GP, de Feyter PJ. Diagnostic Accuracy of 64-slice Computed Tomography Coronary Angiography: A Prospective Multicenter, Multivendor Study. *J Am Coll Cardiol.* 2008;52:2135-44
10. Cademartiri F, Malagutti P, Belgrano M, Runza G, Pugliese F, Mollet NR, **Meijboom WB**, Krestin GP, De Feyter PJ. Non-invasive coronary angiography with 64-slice computed tomography. *Minerva Cardioangiol.* 2005 Oct;53(5):465-72. Review.
11. Cademartiri F, Mollet NR, Runza G, Belgrano M, Malagutti P, **Meijboom WB**, Midiri M, de Feyter PJ, Krestin GP. Diagnostic accuracy of Multislice computed tomography coronary angiography is improved at low heart rates. *Int J Cardiovascular Imaging* 2006 Feb; 22(1): 101-5, discussion 107-9.
12. Pugliese F, Mollet NR, Runza G, van Mieghem C, **Meijboom WB**, Malagutti P, Baks T, Krestin GP, de Feyter PJ, Cademartiri F. Diagnostic accuracy of non-invasive 64-slice CT coronary angiography in patients with stable angina pectoris. *Eur Radiol.* 2006 Mar;16(3):575-82.
13. Mollet NR, Cademartiri F, Runza G, Belgrano M, Baks T, **Meijboom WB**, de Feyter PJ. Four-dimensional evaluation of a giant pseudo-aneurysm by multislice computed tomography. *Int J Cardiovasc Imaging.* 2005 Dec;21(6):667-8.
14. de Feyter PJ, **Meijboom WB**. Multislice computed tomography coronary angiography: prime time? *Rev Esp Cardiol.* 2005 Nov;58(11):1253-7. Review.
15. Pugliese F, **Meijboom WB**, Cademartiri F, Krestin GP. Unusual cause of myocardial ischemia noninvasively assessed with ECG-gated computed tomography coronary angiography. *Eur J Cardiothorac Surg.* 2006 May;29(5):840.
16. Pugliese F, Cademartiri F, van Mieghem C, **Meijboom WB**, Malagutti P, Mollet NR, Martinoli C, de Feyter PJ, Krestin GP. Multidetector CT for visualization of coronary stents. *Radiographics.* 2006 May-Jun;26(3):887-904. Review.
17. Malagutti P, Ligthart JM, Cademartiri F, **Meijboom WB**, Valgimigli M. Plaque sealing: are the benefits outweighing the risks? *Int J Cardiol.* 2007 Feb 7;115(2):265-6.

18. Malagutti P, Nieman K, **Meijboom WB**, van Mieghem CA, Pugliese F, Cademartiri F, Mollet NR, Boersma E, de Jaegere PP, de Feyter PJ. Use of 64-slice CT in symptomatic patients after coronary bypass surgery: evaluation of grafts and coronary arteries. *Eur Heart J*. 2007 Aug 28(15):1879-85.
19. Van Mieghem CA, Cademartiri F, Mollet NR, Malagutti P, Valgimigli M, **Meijboom WB**, Pugliese F, McFadden EP, Ligthart J, Runza G, Bruining N, Smits PC, Regar E, van der Giessen WJ, Sianos G, van Domburg R, de Jaegere P, Krestin GP, Serruys PW, de Feyter PJ. Multislice spiral computed tomography for the evaluation of stent patency after left main coronary artery stenting: a comparison with conventional coronary angiography and intravascular ultrasound. *Circulation*. 2006 Aug 15;114(7):645-53.
20. Cademartiri F, La Grutta L, Palumbo A, Malagutti F, **Meijboom WB**, Baks T, Mollet NR, Bruining N, Hamers R, de Feyter PJ. Non-invasive visualization of coronary atherosclerosis: state-of-art. *J Cardiovasc. Med*. 2007 Mar, 8(3):129-37.
21. Cademartiri F, Palumbo A, Maffei E, La Grutta L, Runga G, Pugliese F, Midiri M, Mollet NR, **Meijboom WB**, Menozzi A, Vignali L, Reverberi C, Ardissino D, Krestin GP. Diagnostic accuracy of 64-slice CT in the assessment of coronary stents. *Radiol Med (Torino)*. 2007 Jun 11.
22. Van Mieghem CAG, Thury A, **Meijboom WB**, Cademartiri F, Mollet NR, van der Giessen AG, Wentzel JJ, Kluyn J, Sianos G, van der Ent M, van der Giessen WJ, de Jaegere P, Krestin GP, Serruys PW, de Feyter PJ. Detection and characterization of coronary bifurcation lesions with 64-slice computed tomography coronary angiography. *European Heart J*. 2007 Aug 28(16):1968-76.
23. Weustink AC, **Meijboom WB**, Mollet NR, Otsuka M, Pugliese F, van Mieghem CAG, Malago R, van Pelt N, Dijkshoorn DL, Cademartiri F, Krestin GP, de Feyter PJ. Reliable High-speed Coronary Computed Tomography in Symptomatic Patients. *J Am Coll Cardiol*. 2007 Aug 21;50(8):786-94.
24. Van Mieghem CAG, Sianos G, **Meijboom WB**, Vourvouri E, Serruys PW, de Feyter PJ. Reliable angiographic evaluation by 64-slice computed tomography after trifurcation stenting of the left main coronary artery. *Eurointervention*. Volume 1, Issue 4. 2006.
25. Cademartiri F, Palumbo A, Maffei E, Casolo G, Mollet NR, **Meijboom WB**, Ligthart JM. Follow-up of internal mammary artery stent with 64-slice CT. *Int J Cardiovasc Imaging*. 2007 Aug;23(4):537-9.

26. Mollet NR, Cademartiri F, Van Mieghem CAG, **Meijboom WB**, Dikkeboer J, Freericks MP, Kerker JP, Zoet SK, Boersma E, Krestin GP, de Feyter PJ. Adjunctive Value of CT Coronary Angiography in the Diagnostic Work-up of Patients with Typical Angina Pectoris. *European Heart J.* 2007 Aug 28(15):1872-8.
27. De Feyter PJ, **Meijboom WB**, Weustink A, Van Mieghem C, Mollet NR, Vourvouri E, Nieman K, Cademartiri F. Spiral Multislice Computed Tomography Coronary Angiography: A Current Status Report. *Clin Cardiol.* 2007 Sep 5;30(9):437-442.
28. Meijs MFL, **Meijboom WB**, Cramer MJ, Prokop M, Doevendans PA, de Feyter PJ. Computed Tomography of the Coronary Arteries: An Alternative? Review. *Scand Cardiovasc J.* 2007 Jul 12; 1-10.
29. Pugliese F, Weustink AC, Van Mieghem C, Alberghina F, Otsuka M, **Meijboom WB**, Van Pelt N, Mollet NR, Cademartiri F, Krestin GP, Hunink MGM, de Feyter PJ. Dual-source coronary computed tomography angiography for detecting in-stent restenosis. *Heart.* 2008 Jul;94(7):848-54.
30. Cademartiri F, Aldrovandi A, Palumbo A, Maffei E, Fusaro M, Tresoldi S, Messalli G, Rossi A, Rengo M, Pugliese F, Salamousas BV, Reverberi C, **Meijboom WB**, Mollet NR, Ardissino D, De Feyter PJ. Multislice computed tomography coronary angiography: clinical applications. *Minerva Cardioangiol.* 2007 Oct;55(5):647-58.
31. Cademartiri F, Maffei E, Palumbo AA, Malago R, La Grutta L, **Meijboom WB**, Aldrovandi A, Fusaro M, Vignali L, Menozzi A, Brambilla V, Coruzzi P, Midiri M, Kirchin MA, Mollet NR, Krestin GP. Influence of intra-coronary enhancement on diagnostic accuracy with 64-slice CT coronary angiography. *Eur Radiol.* 2008 Mar;18(3):576-83
32. Pugliese F, Mollet NR, Hunink MG, Cademartiri F, Nieman K, van Domburg R, **Meijboom WB**, van Mieghem C, Weustink AC, Dijkhoorn M, de Feyter PJ, Krestin GP. Diagnostic accuracy of coronary CT angiography with different generation scanners. Single-centre experience. *Radiology.* 2008 Feb;246(2):384-93.
33. Pugliese F, Alberghina F, **Meijboom WB**, Malago R, Gopalan D, de Feyter PJ. Post-processing using multislice CT coronary angiography improves image interpretability in patients with fast heart-rates and heart-rate variations: a case-report. *J Cardiovasc Med (Hagerstown).* 2007 Dec;8(12):1088-90.

34. van der Giessen A, Wentzel J, **Meijboom WB**, Mollet NR, van der Steen T van de Vosse F, de Feyter, PJ, Gijssen F.
Plaque distribution relates to shear stress in human coronary bifurcations: A multi-slice computed tomography study.
Eurointervention 2008;4
35. Cademartiri F, La Grutta L, Malagò R, Alberghina F, **Meijboom WB**, Pugliese F, Maffèi E, Palumbo AA, Aldrovandi A, Fusaro M, Brambilla V, Coruzzi P, Midiri M, Mollet NR, Krestin GP.
Prevalence of anatomical variants and coronary anomalies in 543 consecutive patients studied with 64-slice CT coronary angiography.
Eur Radiol. 2008 Apr;18(4):781-91.
36. Weustink AC, Mollet NR, Pugliese F, **Meijboom WB**, Nieman K, Heijnenbroek-Kal MH, Flohr TG, Neefjes LA, Cademartiri F, de Feyter PJ, Krestin GP.
Optimal electrocardiographic pulsing windows and heart rate: effect on image quality and radiation exposure at dual-source coronary CT angiography.
Radiology. 2008 Sep;248(3):792-8.
37. Palazzuoli A, Cademartiri F, Geleijnse ML, **Meijboom WB**, Pugliese F, Soliman O, Calabrò A, Nuti R, de Feyter P.
Left ventricular remodelling and systolic function measurement with 64 multi-slice computed tomography versus second harmonic echocardiography in patients with coronary artery disease: A double blind study.
Eur J Radiol. 2008 Nov 12. [Epub ahead of print].
38. Pugliese F, Hunink MGM, Gruszczynska K, Alberghina F, Malago R, van Pelt N, Mollet NR, Cademartiri F, Weustink AC, **Meijboom WB**, Witteman C, de Feyter PJ, Krestin GP.
Learning curve for coronary CT angiography: what constitutes sufficient training?
Radiology, in press.
39. García-García HM, van Mieghem CAG, Gonzalo N, Meijboom WB, Weustink AC, Onuma Y, Mollet NR, Schultz CJ, Meliga E, van der Ent M, Sianos G, Goedhart D, den Boer A, de Feyter P, Serruys PW.
Computed Tomography in Total Coronary Occlusions (CTTO Registry): radiation exposure and predictors of successful percutaneous intervention
Accepted Eurointervention 2009
40. Meijjs MFL, **Meijboom WB**, Schuijf JD, Prokop M, Mollet NR, van Mieghem CAG, van Werkhoven JM, Jukema JW, Doevendans PA, Bax JJ, de Feyter PJ, Cramer MJ.
Value of Combined Use of Calcium Score and 64-slice CT Coronary Angiography in Symptomatic Patients Referred for Conventional Coronary Angiography
Submitted.

41. Pugliese F, Hunink MGM, **Meijboom WB**, Gruszynska K, Rengo M, Mollet NR, Weustink AC, Neeffjes L, Dijkshoorn ML, Krestin GP, De Feyter PJ. MSCT lesion calcium to predict stenosis severity of calcified lesions
Submitted.
42. Genders TSS, **Meijboom WB**, Meijs MFL, Schuijf JD, Mollet NR, Weustink AC, Pugliese F, Bax JJ, Cramer MJ, Krestin GP, de Feyter PJ, Hunink MG. Computed Tomography Coronary Angiography in patients with suspected CAD: decision making from various perspectives in the face of uncertainty. A cost-effectiveness analysis.
Submitted.
43. Hartman JM, **Meijboom WB**, Galema TW, Takkenberg JJM, Schets AM, De Feyter PJ, Bogers AJJC. Ultrasonographic and DSCT Scan Analysis of single LIMA versus Arterial T grafts 12 years after Surgery.
Submitted.
44. Hartman JM, **Meijboom WB**, Galema TW, Takkenberg JJM, Schets AM, De Feyter PJ, Bogers AJJC. Anatomical and functional assessment of single LIMA versus arterial composite T grafts 12 years after bypass surgery.
Submitted.
45. Meijs MFL, **Meijboom WB**, Cramer MJ, Kyzopoulos S, Eu RN, Prokop M, Doevendans PA, de Feyter PJ. Differentiation between stable and unstable coronary artery culprit plaques by 64-slice CT coronary angiography.
Submitted.
46. Weustink AC, Nieman K, Pugliese F, Mollet NR, **Meijboom WB**, van Mieghem CA, ten Kate GJ, Krestin GP, de Feyter PJ. Computed tomography coronary angiography and invasive coronary angiography are complementary to access symptomatic post CABG patients.
Submitted.

BOOKS (CO-EDITOR)

1. De Feyter PJ, Krestin GP, Cademartiri F, van Mieghem CA, **Meijboom WB**, Mollet NR, Nieman K. Computed tomography of the coronary arteries. Second Edition. Informa Healthcare. 2008.

BOOK CHAPTERS

1. **Meijboom WB**, Mollet NR, van Pelt N.
CT coronary angiography in Cardiothoracic Surgery.
Advances in MDCT. CT angiography. Volume 3, Number 2, 2007.
2. Mollet NR, Van Pelt N, **Meijboom WB**, Weustink AC,
Cademartiri F, Nieman K, Krestin GP, de Feyter PJ.
How to perform and interpret computed tomography coronary angiography.
In: Computer Tomography of the Cardiovascular System.
Informa Healthcare. 2007.

ABSTRACTS

American College of Cardiology, 2006

1. **Meijboom WB**, Van Mieghem CA, Kluin, Pugliese F, Mollet NR,
Cademartiri F, Malagutti P, Bogers AJ, Krestin GP, de Feyter PJ
Poster presentation: Comparison of computed topography coronary
angiography with conventional coronary angiograph for the detection of
significant coronary lesions in the preoperative valve surgery patient.

European Society of Cardiology, 2006

2. **Meijboom WB**, Van Mieghem CA, Pugliese F, Kluin J, Mollet
NR, Cademartiri F, Krestin GP, de Feyter PJ
Oral presentation: Pre-operative computed tomography coronary angiography to detect
significant coronary artery stenosis in patients referred for cardiac valve surgery.

Nederlandse Vereniging Van Cardiologie najaarscongres 2006

3. **Meijboom WB**, Van Mieghem CA, Pugliese F, Kluin J, Mollet
NR, Cademartiri F, Krestin GP, de Feyter PJ
Oral presentation: Pre-operative computed tomography coronary angiography to detect
significant coronary artery stenosis in patients referred for cardiac valve surgery.

Transcatheter Cardiovascular Therapeutics 2006

4. **Meijboom WB**, Van Mieghem CA, Pugliese F, Kluin J, Mollet NR, Cademartiri F, Krestin GP, de Feyter PJ
Oral presentation: Pre-operative computed tomography coronary angiography to detect significant coronary artery stenosis in patients referred for cardiac valve surgery.

American Heart Association 2006

5. **Meijboom WB**, Mollet NR, Van Mieghem CA, Weustink AC, Pugliese F, De Feyter PJ
Oral presentation: Diagnostic accuracy of 64-slice computed tomography versus Conventional coronary angiography: results of 180 consecutive patients.
6. **Meijboom WB**, Mollet NR, Van Mieghem CA, Kluin J, Pugliese F, Weustink AC, De Feyter PJ.
Oral presentation: Pre-operative computed tomography coronary angiography to detect significant coronary artery stenosis in patients referred for valve surgery.

Radiological Society of Northern America 2006

7. **Meijboom WB**, Mollet NR, Van Mieghem CA, Weustink AC, Pugliese F, Vourvouri E.
Oral presentation: Diagnostic accuracy of 64-slice computed tomography versus conventional coronary angiography: results of 180 consecutive patients.
8. **Meijboom WB**, Mollet NR, Van Mieghem CA, Pugliese F, Weustink AC, Vourvouri E.
Oral presentation: Pre-operative computed tomography coronary angiography to detect significant coronary artery stenosis in patients referred for cardiac valve surgery.

American College of Cardiology 2007

9. **Meijboom WB**, Mollet NR, Van Mieghem CA, Weustink AC, Pugliese F, De Feyter PJ. Poster presentation: Diagnostic accuracy of 64-slice computed tomography versus conventional coronary angiography: results of 300 consecutive patients.
10. **Meijboom WB**, Mollet NR, Van Mieghem CA, Weustink AC, Pugliese F, De Feyter PJ. Poster presentation: Diagnostic accuracy of 64-slice computed tomography coronary angiography in patients with unstable angina and non-ST-segment elevation myocardial infarction.

European Society of Cardiology 2007

11. **Meijboom WB**, Mollet NR, Van Mieghem CAG, Pugliese F, Weustink AC, Van Pelt N, Nieman K, Cademartiri F, Krestin GP, De Feyter PJ.
Oral presentation, State of the Art and featured research session: 64-slice computed tomography coronary angiography in patients with high, intermediate or low pre-test probability of significant coronary artery disease.
12. **Meijboom WB**, Weustink AC, Pugliese F, Van Mieghem CAG, Mollet NR, Van Pelt N, Nieman K, Cademartiri F, Krestin GP, De Feyter PJ.
Poster presentation: Diagnostic accuracy of 64-Slice Computed Tomography Coronary Angiography in women.
13. **Meijboom WB**, Van Pelt N, Van Mieghem CAG, Weustink AC, Pugliese F, Mollet NR, Krestin GP, De Feyter PJ.
Poster presentation: Can CT coronary angiography determine the significance of coronary artery stenosis- a comparison with invasive fractional flow measurements.

European Society of Cardiac Radiology 2007

14. **Meijboom WB**, Weustink AC, Pugliese F, Mollet NR, van Mieghem CA, van Pelt N, Cademartiri F, Krestin GP, De Feyter PJ
Oral presentation: Comparison of Diagnostic Accuracy of 64-Slice Computed Tomography Coronary Angiography in Women-vs-Men with Angina Pectoris.
15. **Meijboom WB**, van Mieghem CA, Mollet NR, Pugliese F, Weustink AC, van Pelt N, Cademartiri F, Krestin GP, De Feyter PJ.
Poster presentation: 64-Slice Computed Tomography Coronary Angiography in Patients with High, Intermediate or Low Pre-test Probability of Significant Coronary Artery Disease.

American Heart Association 2007

16. **Meijboom WB**, Mollet NR, Van Mieghem CAG, Pugliese F, Weustink AC, Van Pelt N, Nieman K, Cademartiri F, Krestin GP, De Feyter PJ.
Oral presentation: 64-slice computed tomography coronary angiography in patients with high, intermediate or low pre-test probability of significant coronary artery disease.

Radiological Society of Northern America 2007

17. **Meijboom WB**, Mollet NR, Van Mieghem CAG, Pugliese F, Weustink AC, Van Pelt N, Nieman K, Cademartiri F, Krestin GP, De Feyter PJ.
Oral presentation: 64-slice computed tomography coronary angiography in patients with high, intermediate or low pre-test probability of significant coronary artery disease.

American College of Cardiology 2008

18. **Meijboom WB**, Meijs MFL, Schuijf JD, Cramer MJ, Mollet NR, van Mieghem CA, Bax JJ, Doevendans PA, Krestin GP, De Feyter PJ.
Poster presentation: Diagnostic accuracy of 64-slice computed tomography coronary angiography: a prospective multicenter, multivendor study.

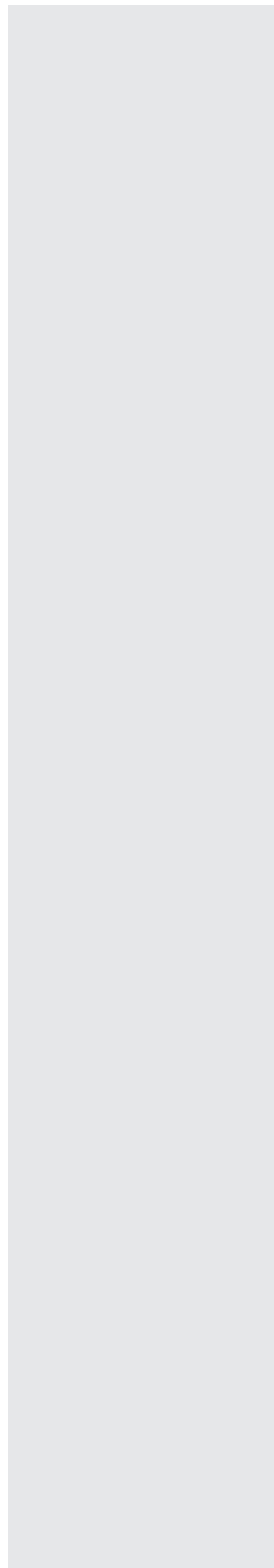
European Society of Cardiology 2008

19. **Meijboom WB**, Meijs MFL, Schuijf JD, Cramer MJ, Mollet NR, van Mieghem CA, Bax JJ, Doevendans PA, Krestin GP, De Feyter PJ.
Poster presentation: Diagnostic accuracy of 64-slice computed tomography coronary angiography: a prospective multicenter, multivendor study.

REVIEWER

Investigative Radiology
JACC Imaging

Curriculum vitae

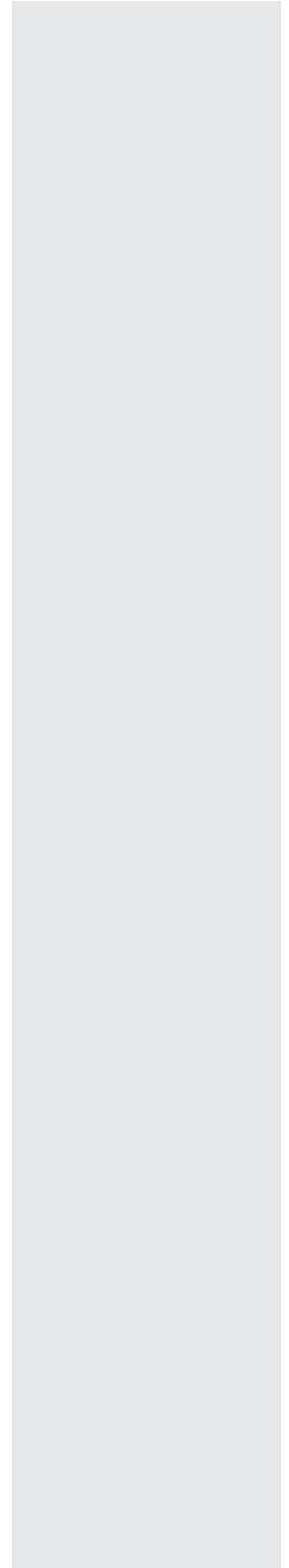


Bob Meijboom was born on the 27th of July 1976 in Amstelveen, the Netherlands. After finishing high school in 1994 at the Rijnlands Lyceum in Wassenaar, he studied Psychology at the University of Leiden for one year. Then he started to study Medicine at the Catholic University of Leuven (Belgium) of which he graduated in 2003. After a half year working as a cardiac resident at the department of Cardiology in the Leiden University Medical Center (the Netherlands) and a half year as a research fellow in the Gorlaeus Laboratory in Leiden, he started working in Rotterdam.

In October 2004, he was employed as a research fellow at the Erasmus Medical Center in Rotterdam (the Netherlands) under leadership of Professor Pim de Feyter (department of Cardiology) and Professor Gabriel Krestin (chairman of the department of Radiology). His achievements in the field of cardiac imaging with Multislice Computed Tomography resulted in this PhD thesis.

To date he is (co-)author of nearly 40 publications in peer-reviewed journals and 60 abstracts at international congresses, and co-editor of the textbook: "Computed Tomography of the coronary arteries, second edition". Currently, he is involved in his cardiology training, starting a 2 year residency at the department of Internal Medicine at the Sint Franciscus Gasthuis in Rotterdam, which will be followed by one year of cardiology training in a community hospital and three years of residency at the Thoraxcenter in Rotterdam.

PhD portfolio



SUMMARY OF PHD TRAINING AND TEACHING ACTIVITIES

Name PhD student: Willem Bob Meijboom
Erasmus MC Department: Cardiology / Radiology
 Research School: COEUR
PhD period: 2004-2008
Promotor(s): Prof Dr. de Feyter / Prof Dr. Krestin
Supervisor: Dr. Deckers

1. PHD TRAINING

	<i>Year</i>	<i>Workload (Hours/ECTS)</i>
<i>General academic skills</i>		
Biomedical English Writing and Communication	2006-2007	1.5
<i>Research skills</i>		
Statistics	2006	1.5
<i>In-depth courses (e.g. Research school, Medical Training)</i>		
COEUR (Cardiovascular Research School ErasmusMC Rotterdam).	2005-2007	
Molecular biology in atherosclerosis and cardiovascular research		1.5
Cardiovascular Medicine		1.5
Pathophysiology of ischemic heart disease		1.5
Cardiovascular imaging and diagnostics		1.5
Clinical cardiovascular epidemiology		1.5
Heart failure research		1.5
Congenital heart disease		1.5
Arrhythmia research methodology		1.5

Presentations

Pre-operative computed tomography coronary angiography to detect significant coronary artery stenosis in patients referred for cardiac valve surgery.

American College of Cardiology	2006	0.6
European Society of Cardiology	2006	0.6
Nederlandse Vereniging Van Cardiologie najaarscongres	2006	0.6
Transcatheter Cardiovascular Therapeutics	2006	0.6
American Heart Association	2006	0.6
Radiological Society of Northern America	2006	0.6

Diagnostic accuracy of 64-slice computed tomography versus Conventional coronary angiography: results of 180 consecutive patients.

American Heart Association	2006	0.6
Radiological Society of Northern America	2006	0.6

Diagnostic accuracy of 64-slice computed tomography versus conventional coronary angiography: results of 300 consecutive patients.

American College of Cardiology	2007	0.6
--------------------------------	------	-----

Diagnostic accuracy of 64-slice computed tomography coronary angiography in patients with unstable angina and non-ST-segment elevation myocardial infarction.

American College of Cardiology	2007	0.6
--------------------------------	------	-----

64-slice computed tomography coronary angiography in patients with high, intermediate or low pre-test probability of significant coronary artery disease.

European Society of Cardiology, State of the Art and featured research session.	2007	0.6
European Society of Cardiac Radiology	2007	0.6
American Heart Association	2007	0.6
Radiological Society of Northern America	2007	0.6

*Diagnostic accuracy of 64-Slice Computed Tomography
Coronary Angiography in women.*

European Society of Cardiology 2007 0.6

European Society of Cardiac Radiology 2007 0.6

*Can CT coronary angiography determine the significance
of coronary artery stenosis- a comparison with invasive
fractional flow measurements.*

European Society of Cardiology 2007 0.6

Read with the experts

Computed tomography in secondary prevention

European Society of Cardiology 2007 0.6

*Diagnostic accuracy of 64-slice computed tomography coronary
angiography: a prospective multicenter, multivendor study.*

American College of Cardiology 2008 0.6

European Society of Cardiology 2008 0.6

*Diagnostic accuracy of 64-slice CTA and its improvements
in Dual-Source CT*

Heerlen 2007 0.6

Multislice CT Coronary Angiography of CABG

Usermeeting, Mumbai, India 2006 0.6

Calcium scoring

Usermeeting, Mumbai, India 2006 0.6

<i>New Era of Coronary Imaging with Dual Source CT</i> <i>Experiences with cardiac imaging</i>		
Usermeeting, Hyderabad, India	2006	0.6
<i>Diagnostic accuracy of 64-slice CTA and its improvements</i> <i>in Dual-Source CT</i>		
Usermeeting, Hyderabad, India	2006	0.6
<i>Diagnostic Accuracy of CT Coronary Angiography</i>		
Juniorkamer, Utrecht	2007	0.6
<i>Non-invasive Multislice Computed Tomography Coronary</i> <i>Angiography</i>		
Thoraxcenter, Rotterdam	2007	0.6
Zwolle	2006	0.6
Venticare, Utrecht	2006	0.6
<i>64-slice CTCA and its improvements in Dual-Source CT</i>		
Mexico-City, Mexico	2007	0.6
<i>Innovations at the Cardiac CT Field with Dual-Source CT</i>		
Tel-aviv, Israël	2007	0.6
<i>International conferences</i>		
Radiological Society of Northern America	2005	1.0
American College of Cardiology	2006	1.0
European Society of Cardiology	2006	1.0
Nederlandse Vereniging Van Cardiologie	2006	1.0
American Heart Association	2006	1.0
Nederlandse Radiologen Dagen	2006	1.0
Radiological Society of Northern America	2006	1.0
American College of Cardiology	2007	1.0
European Society of Cardiology	2007	1.0

American Heart Association	2007	1.0
American College of Cardiology	2008	1.0
European Society of Cardiology	2008	1.0

Seminars and workshops

Cardiac CT&MRI Clinical Update, Cannes	2007	1.0
Cardiac CT training, Rotterdam	2005-2006	1.0

Didactic skills

-

Other

-

2. TEACHING ACTIVITIES

Year ***Workload***
(Hours/ECTS)

Lecturing

-

Supervising practicals and excursions

-

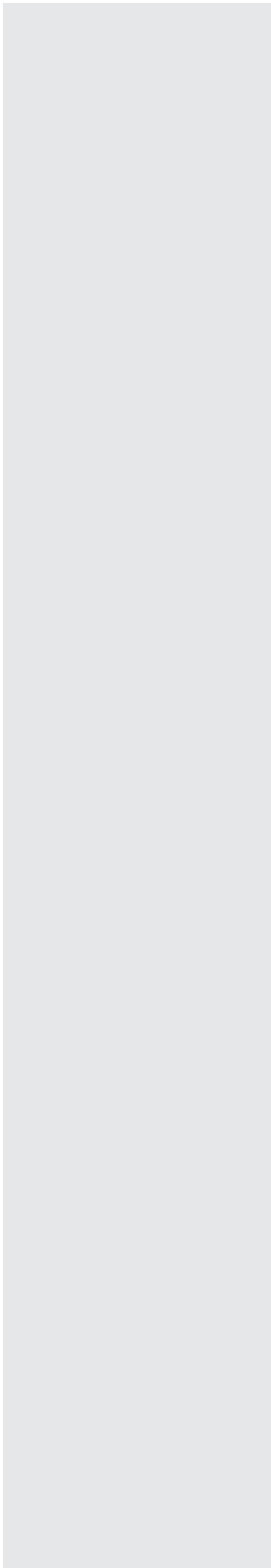
Supervising Master's theses

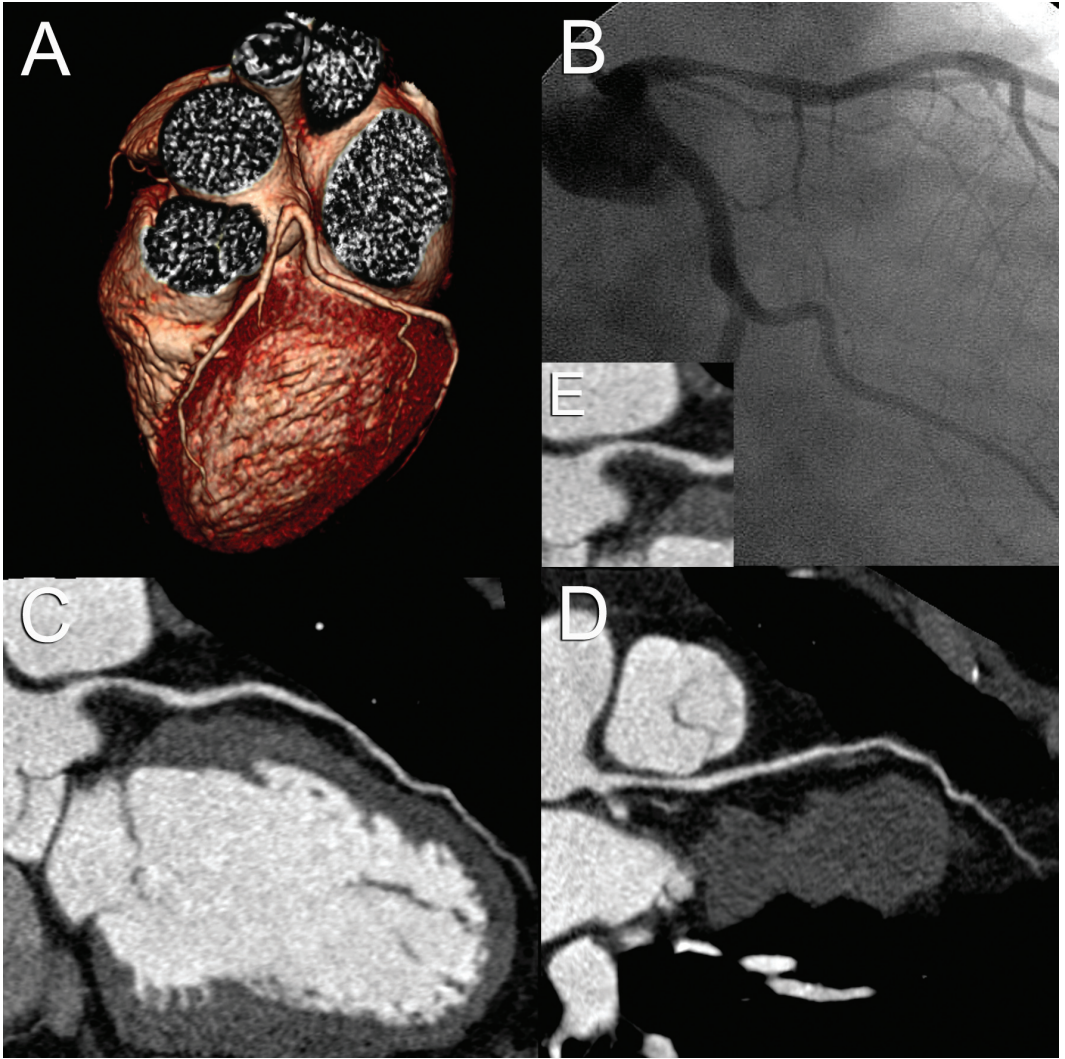
-

Other

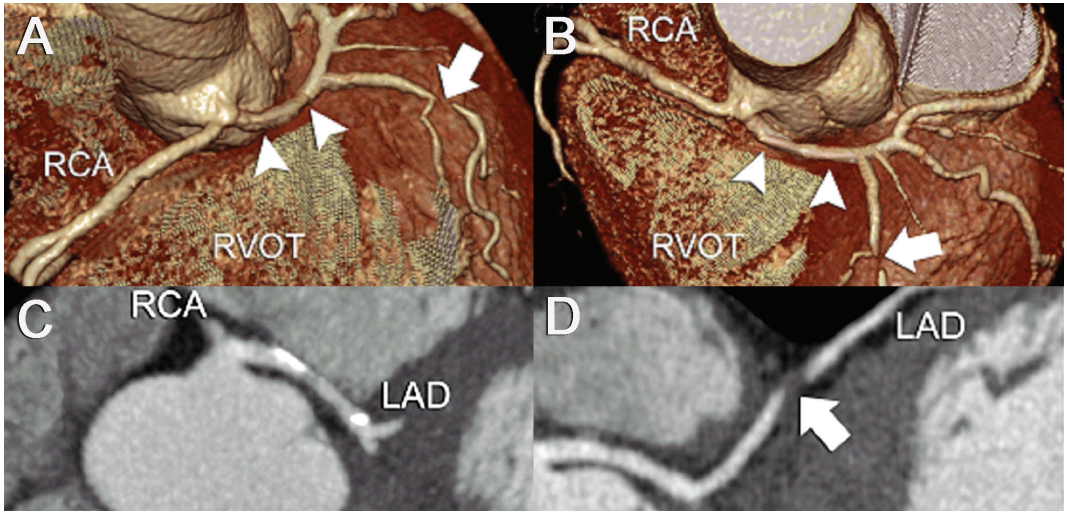
Reviewer "Investigative radiology"	2007-present	1.0
Reviewer "JACC imaging"	2007-present	0.3

Color section

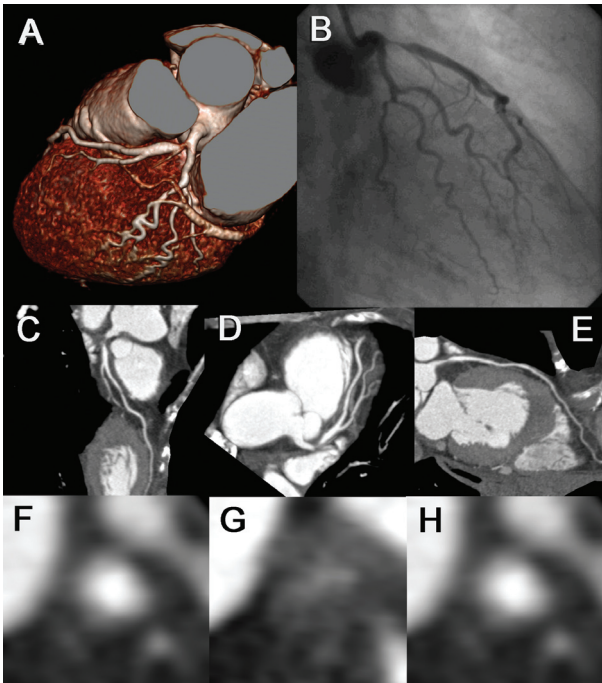




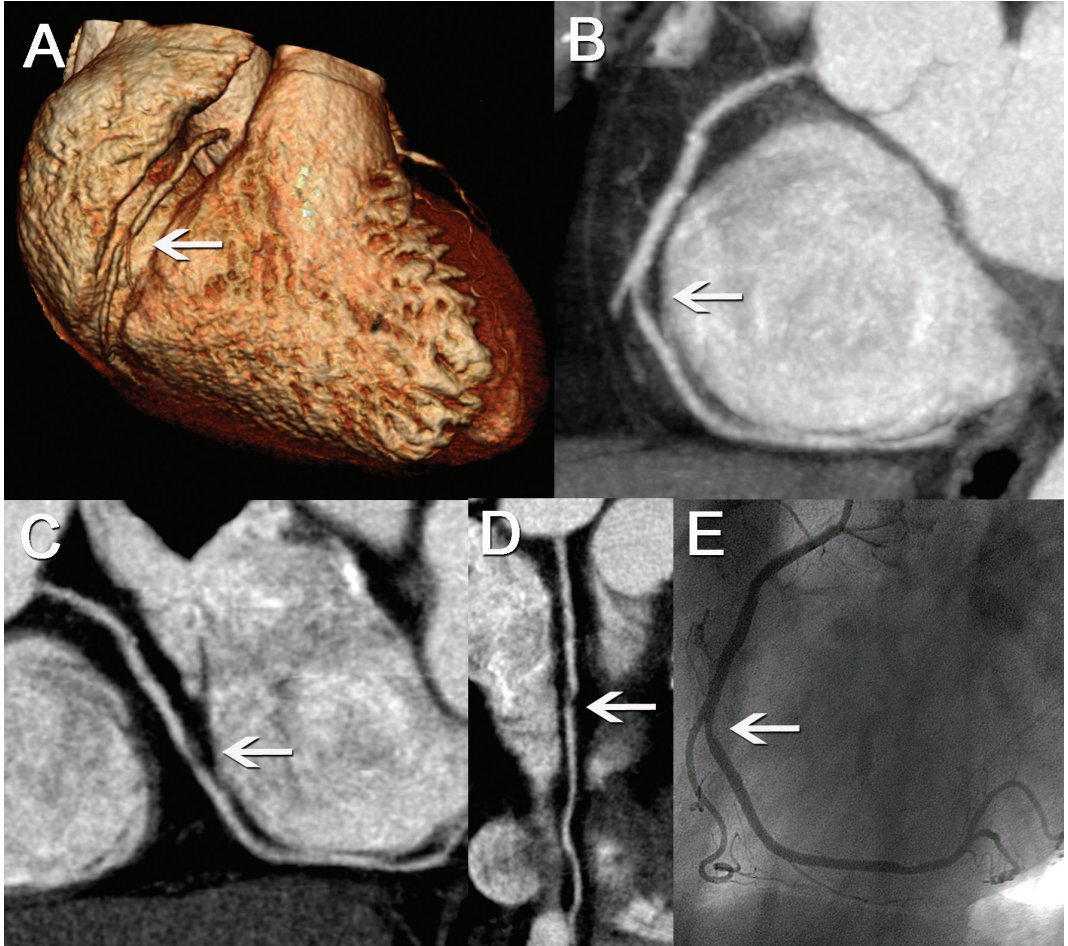
Chapter 2, Figure 1 Volume-rendered CTCA image (A) reveals the anatomy of the left coronary artery of a 50 year-old patient who presented with unstable angina. His total calcium score was zero. Two curved multiplanar reconstructions (C,D) disclose a significant stenosis in the proximal left anterior descending coronary artery which was corroborated by CCA (B). In the inset the non-calcified significant plaque is displayed (E).



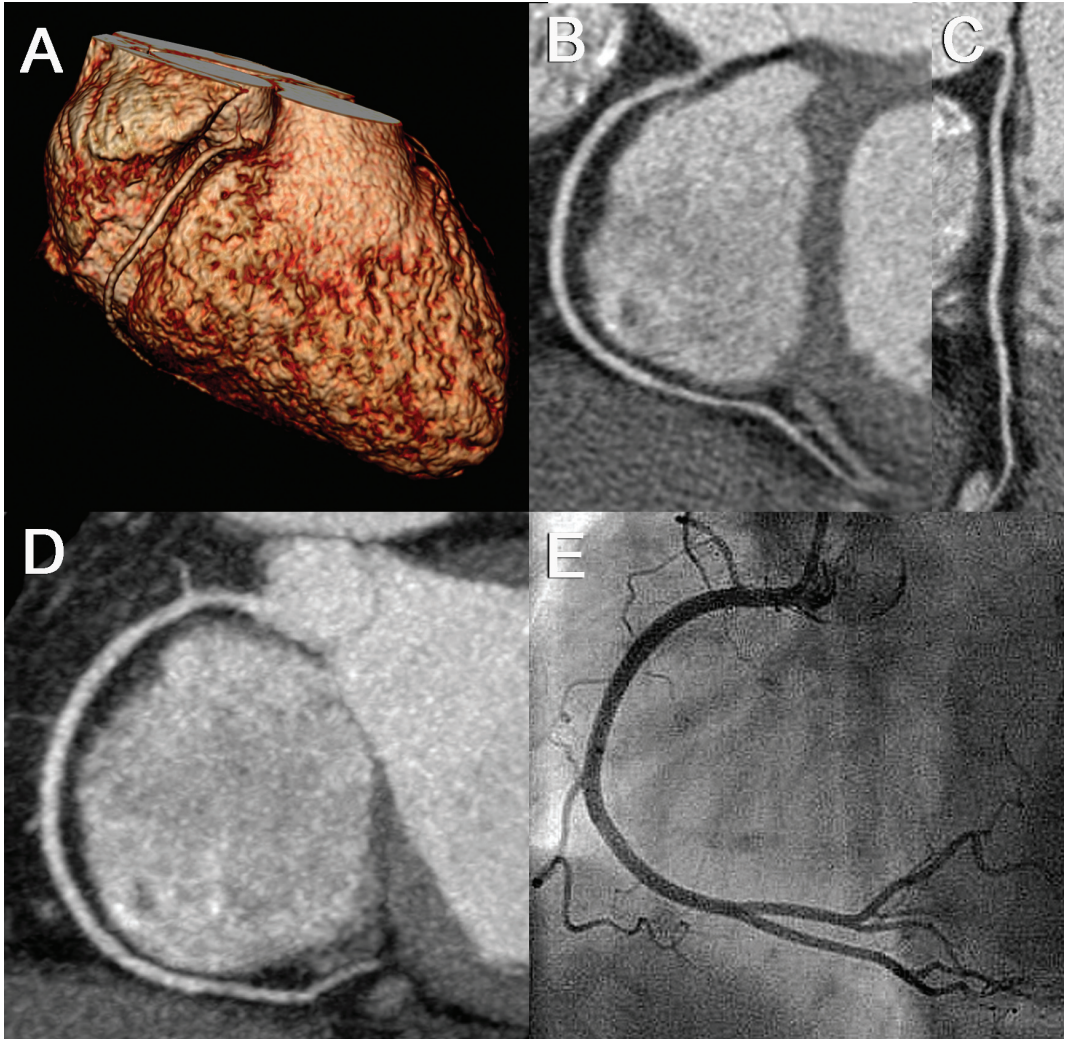
Chapter 3, Figure 2: The left main and right coronary artery (RCA) arise from the right aortic sinus A-D. The anomalous left main coronary artery runs between the aorta and pulmonary trunk (arrowheads). Note also the severe stenosis (arrow) of the left anterior descending artery (LAD). RVOT: right ventricular outflow tract.



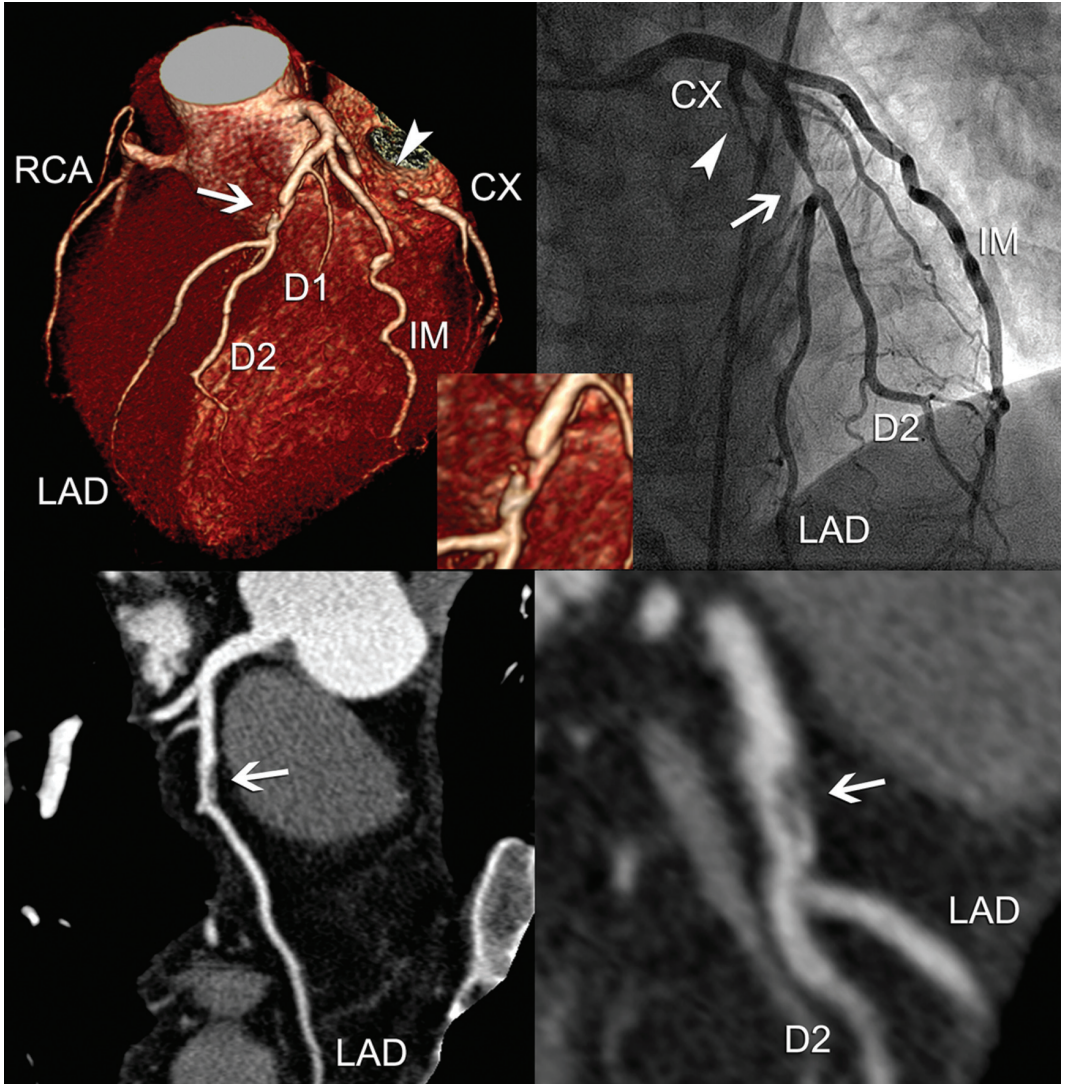
Chapter 3, Figure 4: CT coronary angiogram and corresponding conventional angiogram of the left coronary artery in a patient presenting with unstable angina. Note that the volume-rendered images (A) provide an excellent anatomic overview of the coronary arteries but should not be used to score the presence and degree of coronary stenoses. Two detailed curved multiplanar reconstructed (cMPR) CT image (C, E) and a maximum-intensity projection reveal the presence of a significant stenosis located at the proximal LAD, which was confirmed on the conventional angiogram (B). Cross-sectional CT images show a large noncalcific plaque (G) and a normal coronary lumen of the left main (F) en distal LAD (H).



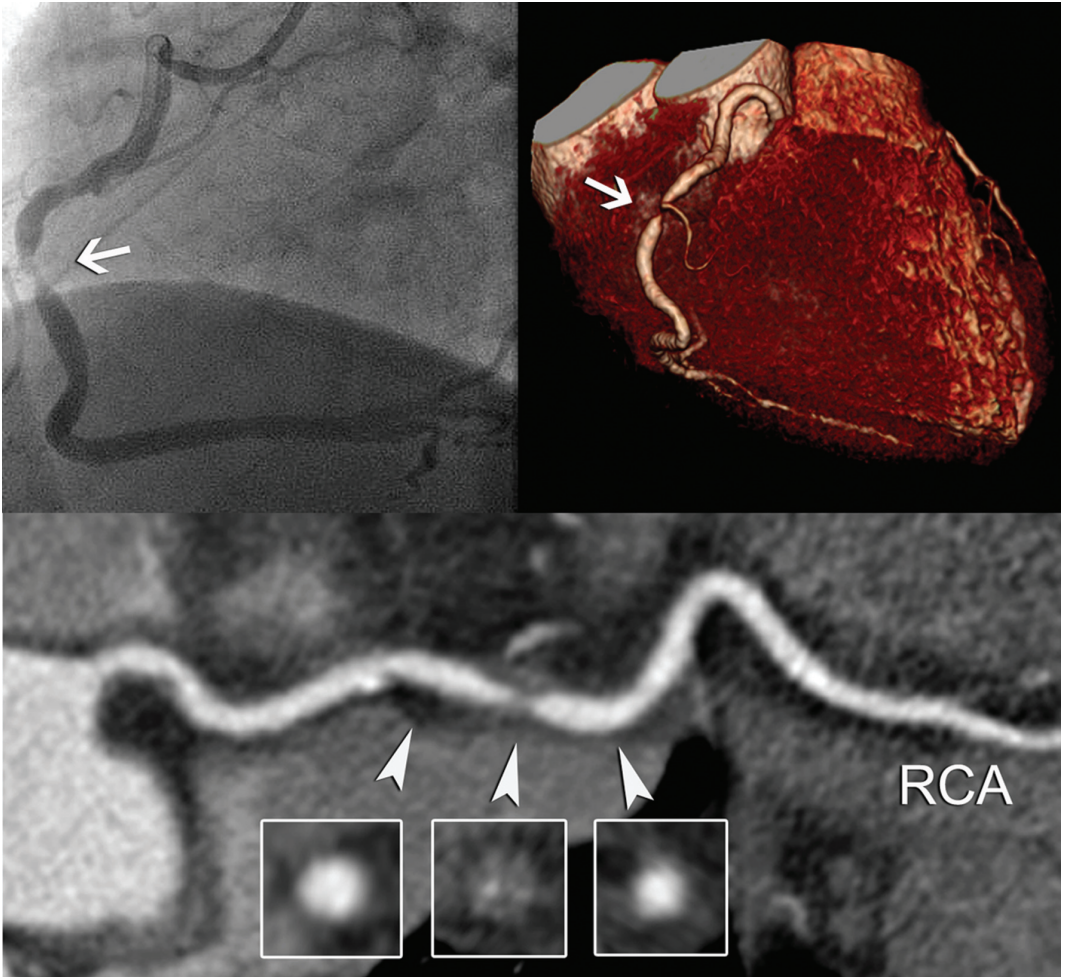
Chapter 4, Figure 4: A volume-rendered CT coronary angiography (CTCA) image (A) reveals the anatomy of the right coronary artery (RCA). A maximum intensity projected image (B) and two curved multiplanar reconstructed images depict a non-calcified obstructive coronary stenosis in the mid RCA. However, conventional coronary angiography only reveals a non-significant stenosis. Quantitative coronary angiography showed a 40% diameter reduction of the coronary lumen.



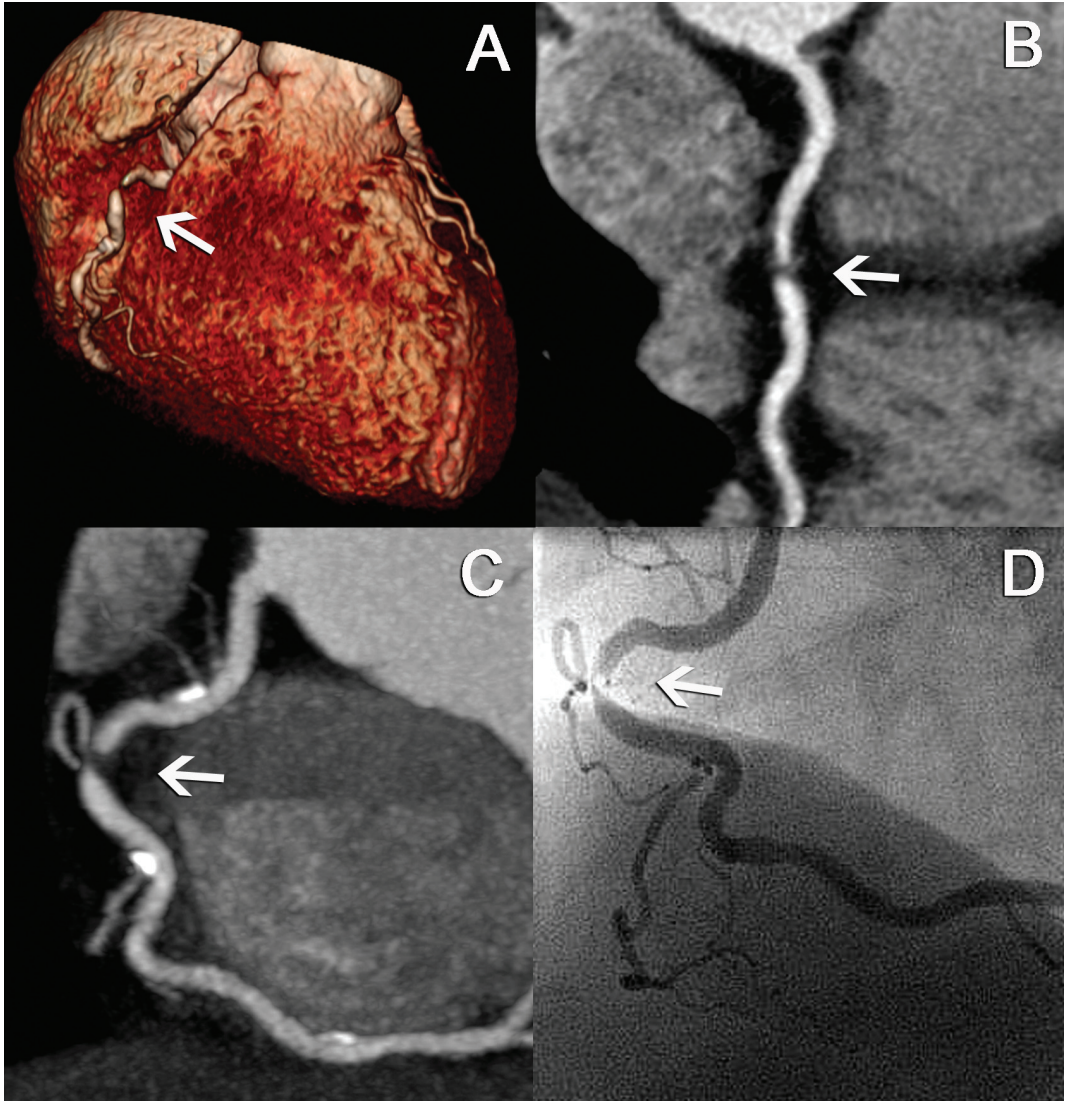
Chapter 5, Figure 2: A volume-rendered CTCA image (A) reveals the anatomy of the RCA. Two orthogonal cMPR images (B, C) and a MIP image (D) disclose a normal coronary artery without obstructive or non-obstructive plaques which was confirmed by CCA (E).



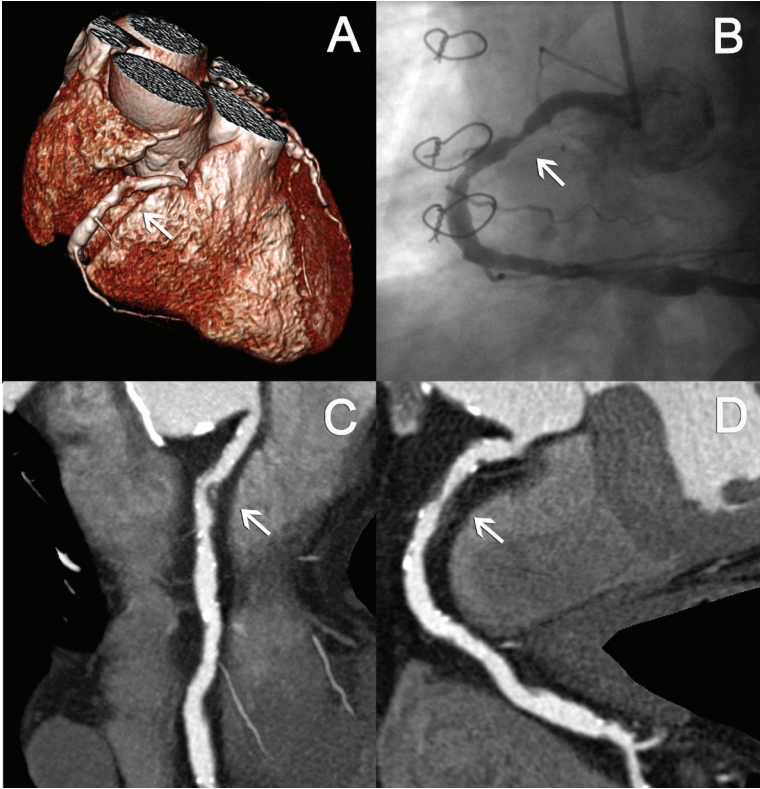
Chapter 6, Figure 1. Volume rendered DSCT image (colored image) and corresponding conventional angiography image of the right coronary artery (RCA), left anterior descending artery (LAD), circumflex artery (CX) intermediate branch (IM), diagonal branches (D1, D2) in a 57-year-old man with stable angina and an equivocal bicycle test. Mean heart rate during scanning was 78 bpm. A significant lesion was found in the midpart of the LAD (arrow) with detailed color inlay, curved multiplanar reconstruction (bottom left) and maximum intensity projections (MIP) image (bottom right). The proximal part of the CX showed an occlusion (arrowhead).



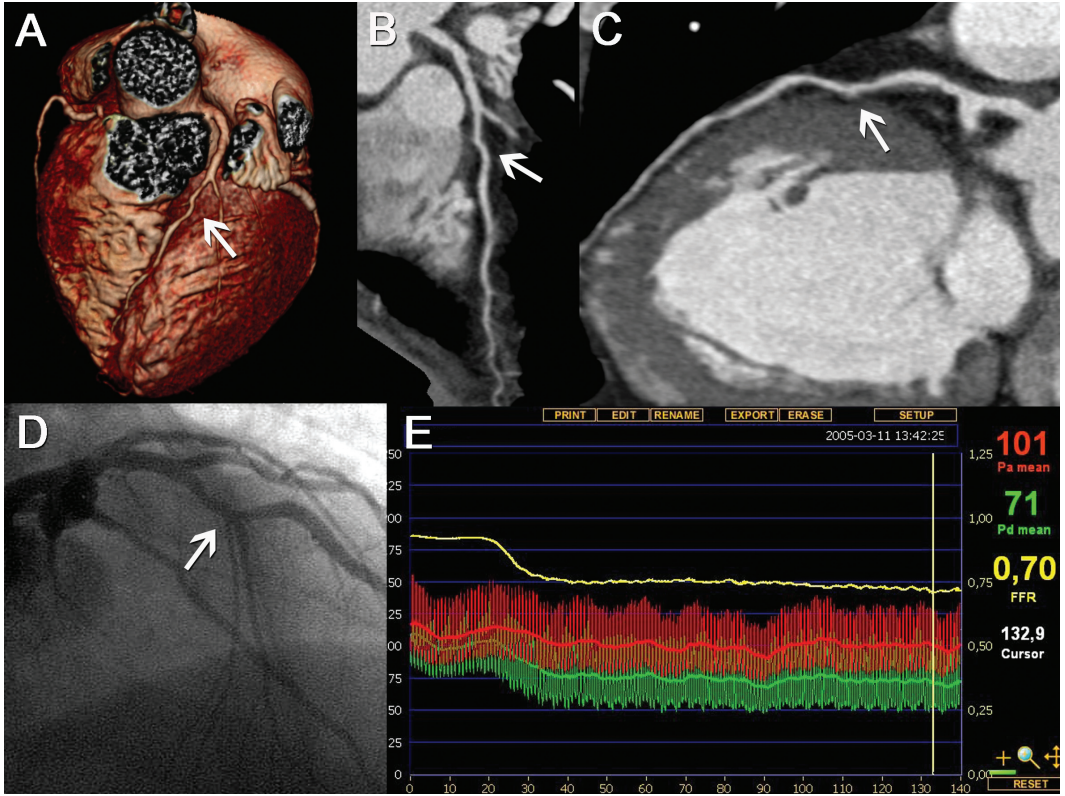
Chapter 6, Figure 2. Conventional angiography image and corresponding volume rendered DSCT image (colored image) in a 68-year old man presenting with unstable coronary artery disease. Mean heart rate during scanning was 66 bpm. The arrow indicates a high-grade stenosis in the midpart of the right coronary artery. The arrowheads in the curved multiplanar reconstruction image (bottom) indicate cross-sections proximal, within and distal from the occlusion (arrowheads).



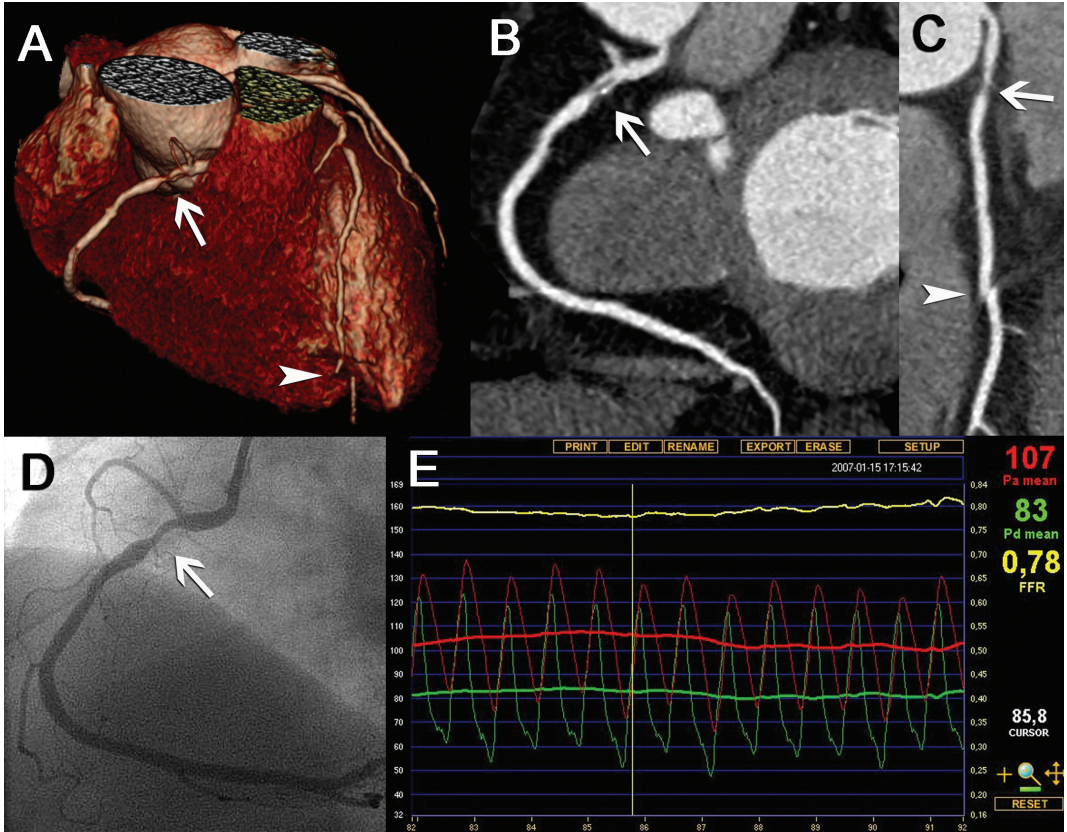
Chapter 7, Figure 1. Volume-rendered CTCA image (A) of the right coronary artery. A curved MPR (B) and a thick MIP (C) disclose a significant coronary stenosis (arrow) in the mid right coronary artery which was corroborated by CCA (D). Proximally and distally of the significant obstructed lesion, non-significant calcified plaques can be seen (C).



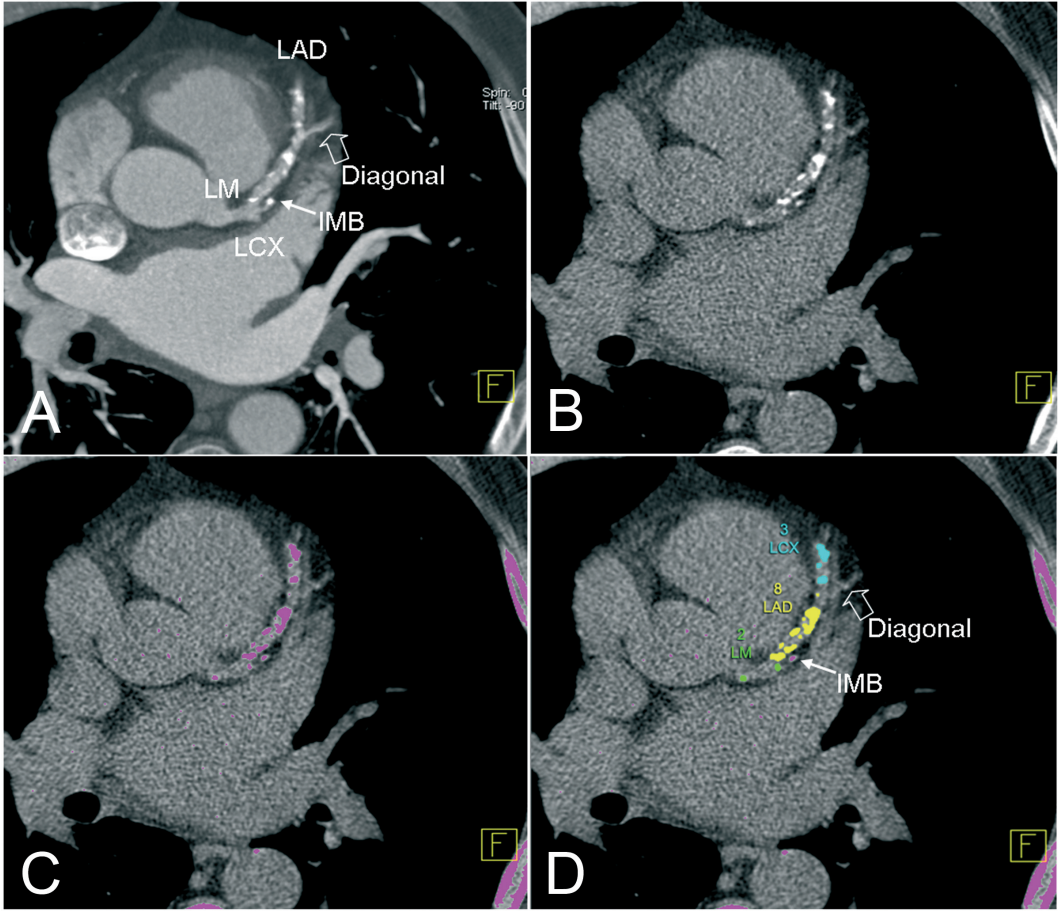
Chapter 8, Figure 1. This patient with prior history of a mitral valve plasty for endocarditis was admitted with a non-ST segment elevation myocardial infarction. A volume-rendered CTCA image (A) reveals the anatomy of the right coronary artery. Two curved multiplanar reconstructed images (eMPR) (C, D) disclose a significant stenosis (arrow) in the proximal right coronary artery which was corroborated by CCA (B).



Chapter 9, Figure 1. Quantitative coronary angiography (QCA), Quantitative CT coronary angiography (QCT), conventional coronary angiography and CT coronary angiography are plotted versus fractional flow reserve (FFR). There was a weak, but significant negative correlation between QCA and FFR ($r: -0.30$) and between QCT and FFR ($r: -0.32$). Coronary arteries smaller than 3.5 mm are depicted as solid dots, coronary arteries larger than 3.5 mm as open circles.

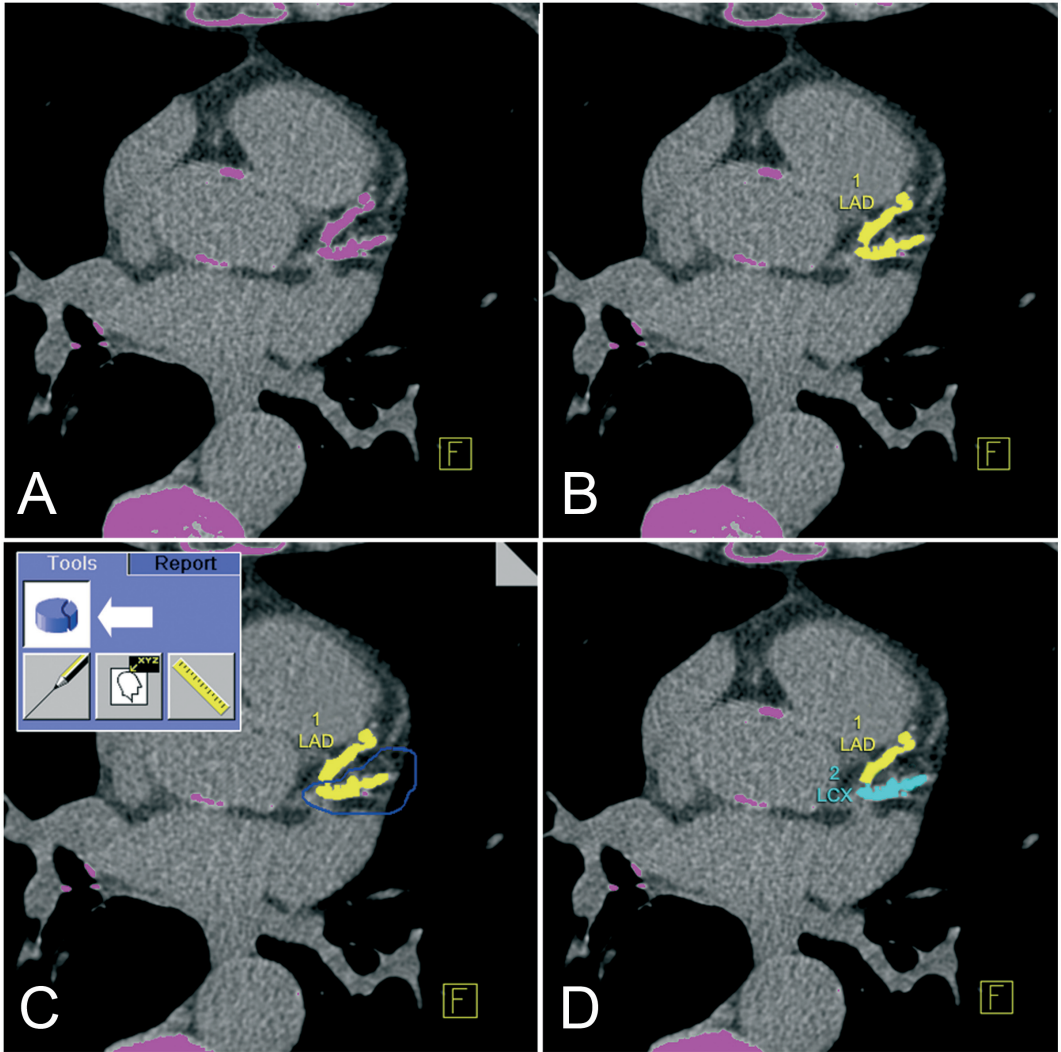


Chapter 9, Figure 2. Patient showing a coronary artery stenosis (arrow) in the left anterior descending coronary artery, as visualized with CT coronary angiography (CTCA) (panel A, volume-rendered image; panels B and C, two orthogonal curved multiplanar reconstructions) and conventional coronary angiography (CCA) (panel D). By visual assessment, the coronary lesion was estimated as less than 50% diameter stenosis, both by CTCA and CCA. By quantitative analysis, the diameter stenosis was measured as 44% by quantitative coronary angiography and 40% by quantitative CT coronary angiography. The fractional flow reserve was 0.71. Based on the functional assessment, the patient underwent a successful percutaneous coronary intervention for this anatomically intermediate stenosis.



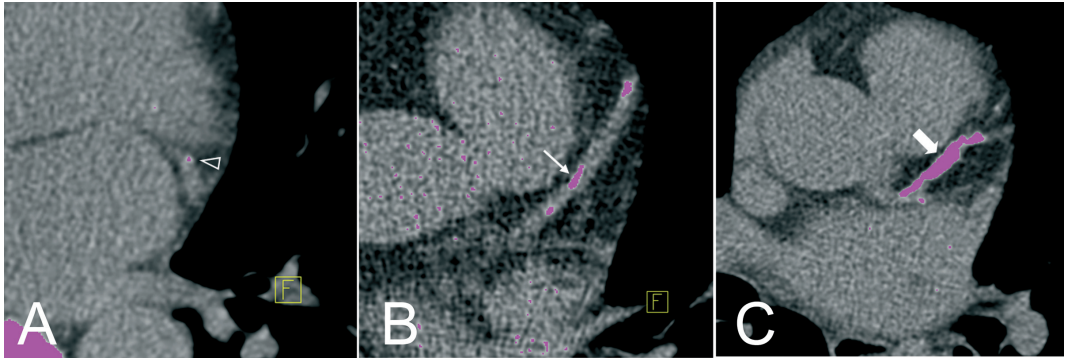
Chapter 11, Figure 1. Measurement of calcium score at the segment level

To classify coronary segments consistently, contrast-enhanced MSCT-CA axial images (A) were available to the observer. Side branches, especially if non-calcified, could have been difficult to detect on non-enhanced images (B, C). Because the quantification software did not allow labelling of the 17 coronary segments individually, the 4 available labels (named as the 4 major coronary vessels) were used interchangeably and applied to coronary segments (D). LM = left main artery; LAD = left anterior descending artery; LCx = left circumflex; IMB = intermediate branch.



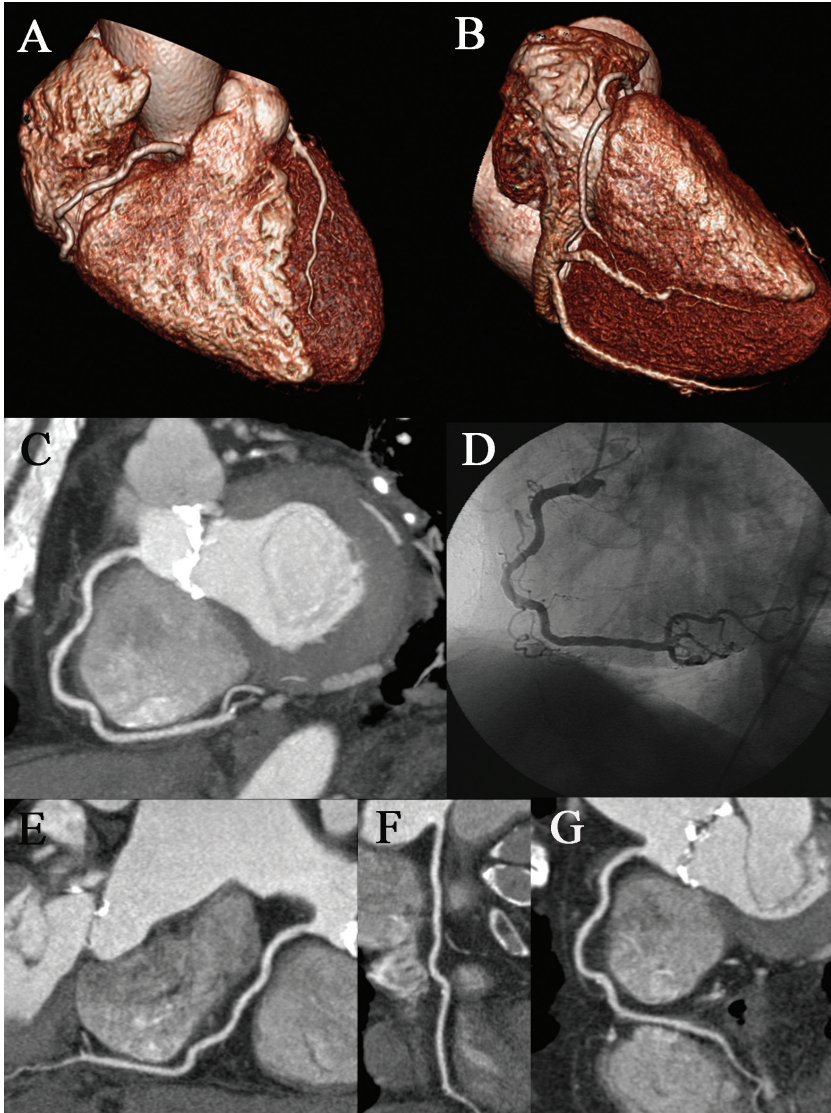
Chapter 11, Figure 2. Method for separation of connected calcifications in a slice

To assign calcifications to the corresponding individual coronary artery segment, there needed to be separation of connected lesions in a slice (A, B). To achieve this, calcifications were edited manually (C) and split (D) using the '3D Edit' function (C, insert and arrow) of the software (syngo Calcium Scoring). LAD = left anterior descending artery; LCx = left circumflex.

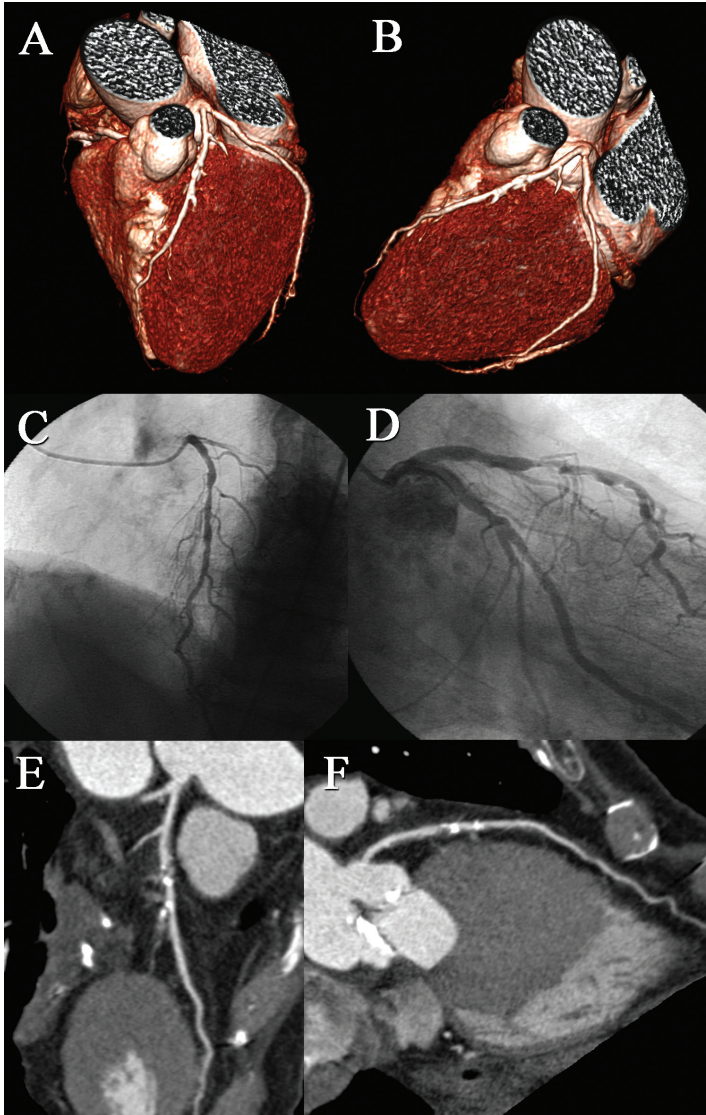


Chapter 11, Figure 3. Calcification morphology

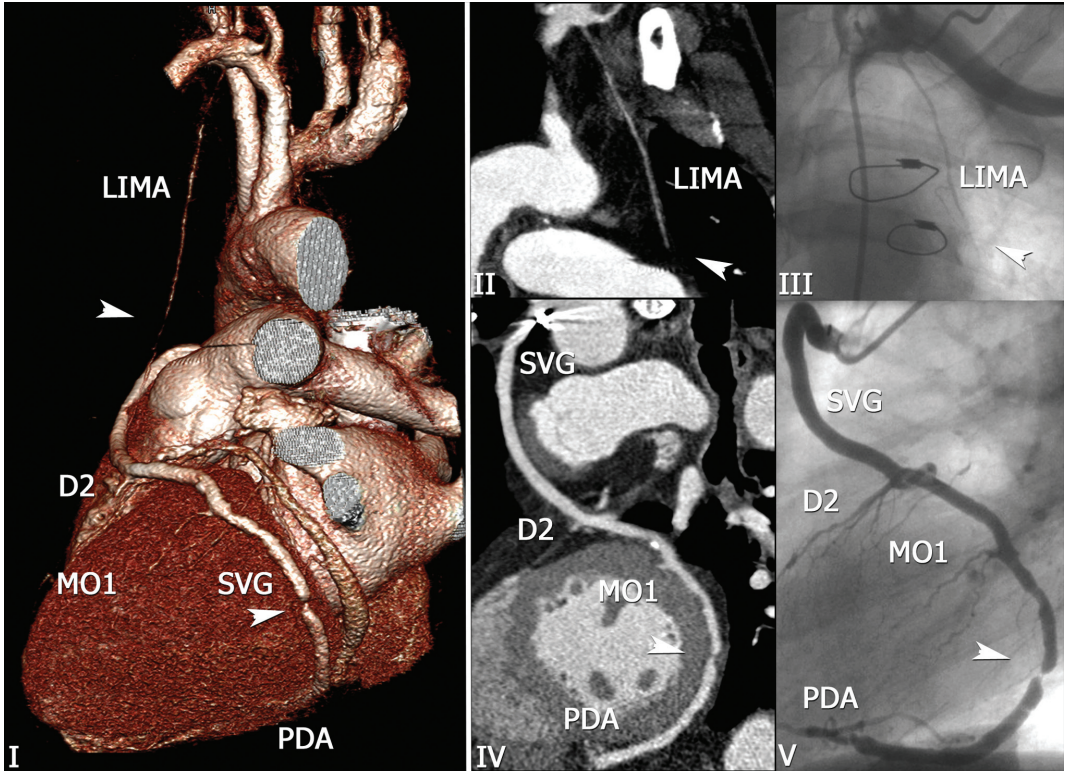
Calcification morphology was classified as spotty (A, arrowhead), wide (B, arrow) and diffuse (C, gross arrow) based on the width and length of the calcification in relation to the coronary segment diameter (Table 1).



Chapter 14, Figure 1. Three different types of post-processing techniques are shown: volume-rendered (VRT) CTCA images (A,B), a maximum intensity projected (MIP)- (C) and three curved multiplanar reconstructed images (cMPR, E,F,G) show a patent right coronary artery which is confirmed by CCA (D). The bright white spots (C, E, G) represent calcifications of the stenotic aortic valve.

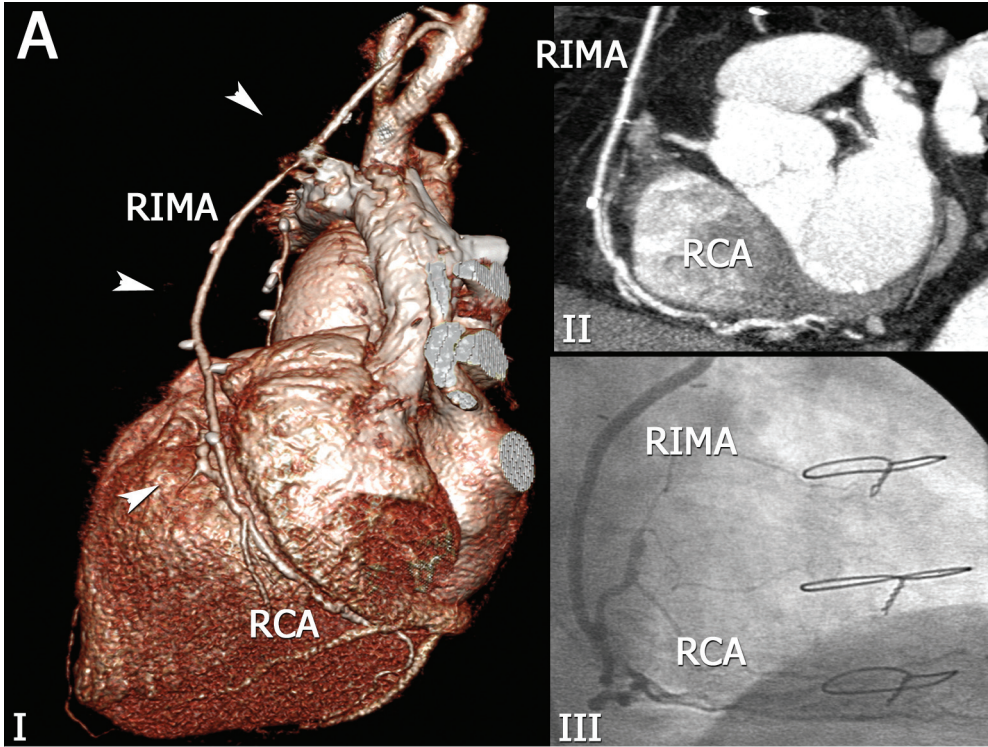


Chapter 14, Figure 2. Volume-rendered (VRT) CTCA image (A,B) reveal the anatomy of the left coronary artery. Two cMPR (E,F) disclose a significant stenosis in the left anterior descending coronary artery which was corroborated by CCA (C,D). Although the VRT images provide an excellent overview of the coronary anatomy they should not be used for the diagnostic assessment of presence of coronary stenoses.



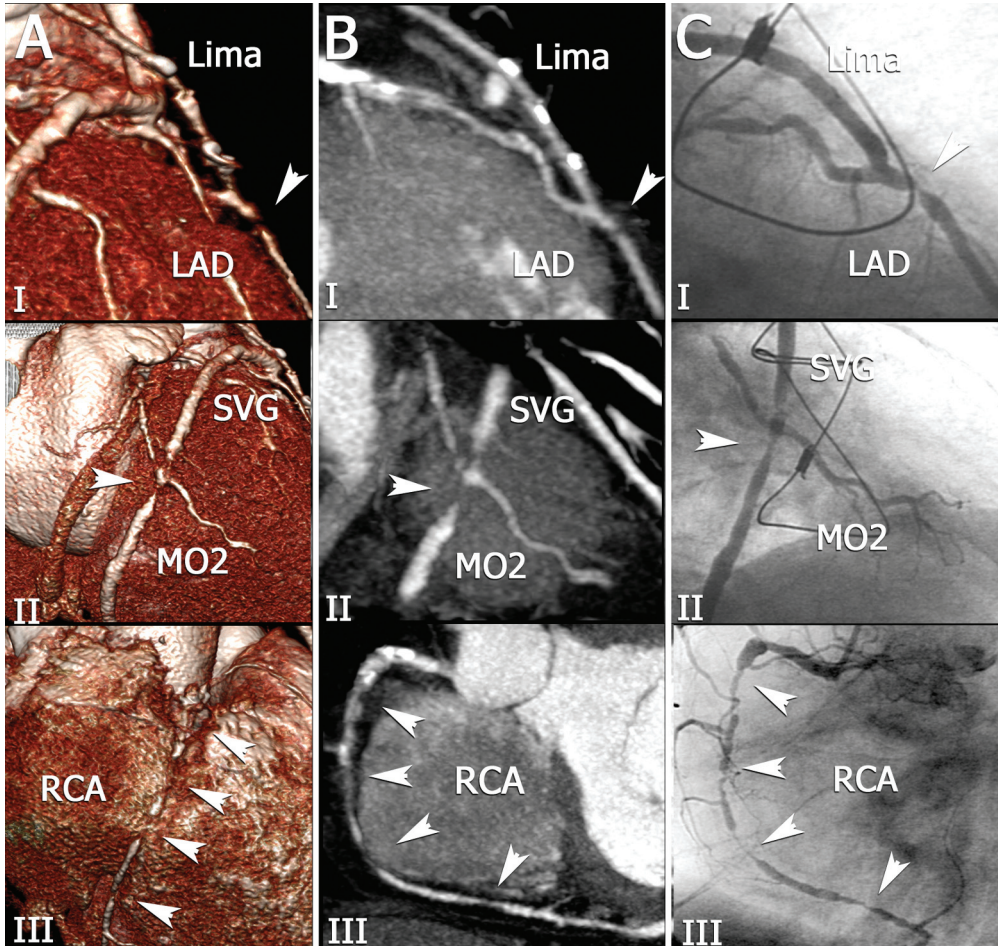
Chapter 15, Figure 1. Arterial and venous graft disease.

Volume-rendered reconstruction (I) and curved multiplanar reformations (II,IV) of a CT scan and corresponding conventional angiography (III, V), which show an occluded left internal mammary artery (LIMA, arrow in I,II,III) and obstructed vein graft (SVG). The venous graft has three coronary anastomoses (and 3 graft segment): second diagonal branch (D2), first marginal branch (MO1), posterior descending artery (PDA), of which the terminal segment is significantly stenosed (arrow I,IV,V).



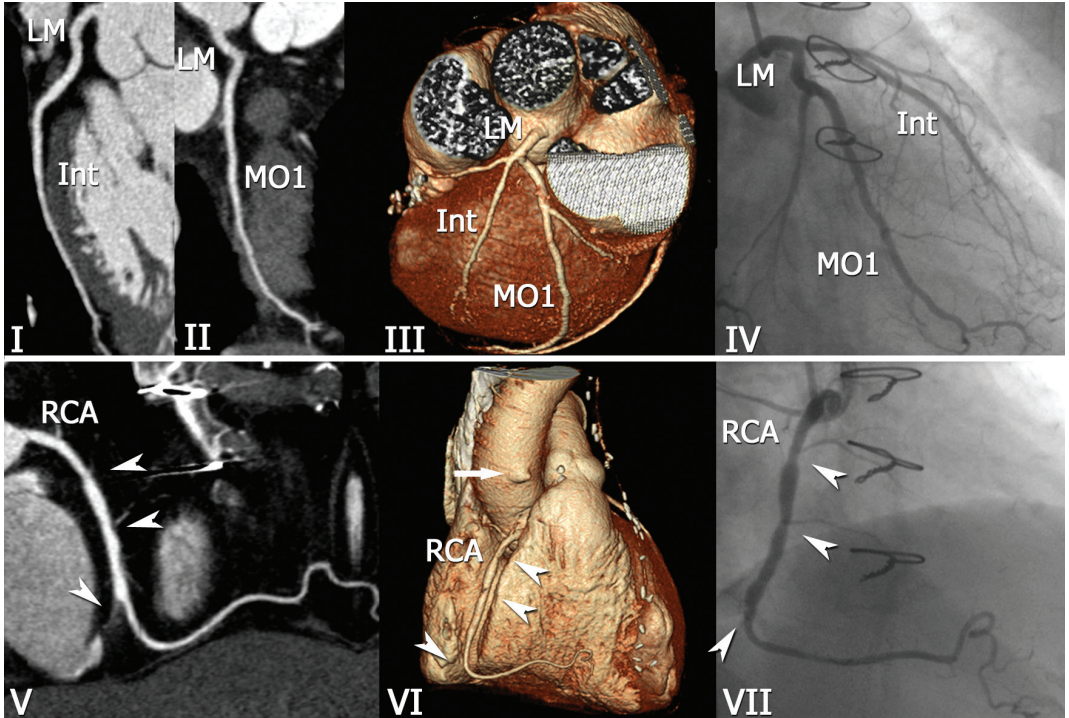
Chapter 15, Figure 2. Patent right internal mammary artery graft.

Panel A. CT (Volume-rendered reconstruction (I), multiplanar reconstruction (II)) and conventional angiogram (III) of a patent right internal mammary artery (RIMA, arrows) connected to the RCA without obstructive disease.



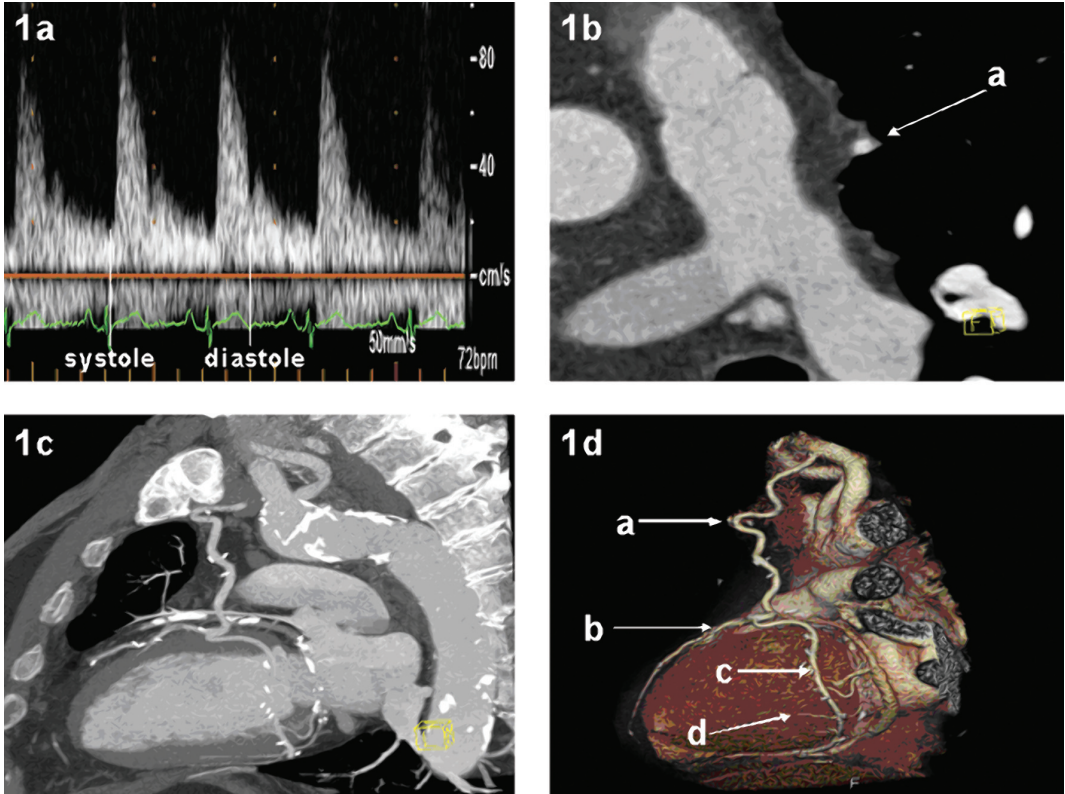
Chapter 15, Figure 3. Bypass graft and coronary run-off disease.

CT (3D volume rendering (A); maximum intensity projection (B)) and conventional angiography (C), of a patent LIMA anastomosed to the LAD. Distal to the anastomosis is a significant lesion (arrow) in the run-off branch (I). A vein graft (SVG) is significantly obstructed (arrow) proximal and distal to the anastomosis with a marginal branch (MO2) (II). The (bypassed) RCA is diffusely diseased with extensive calcification and several sites of significant narrowing (III, arrows).

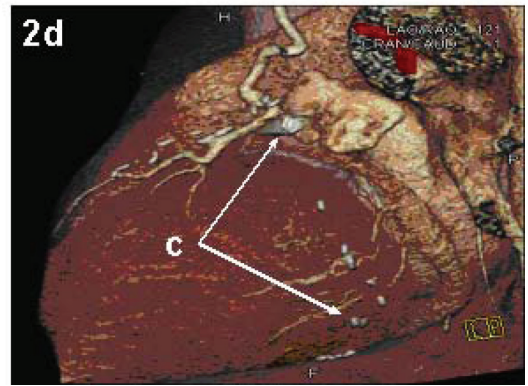
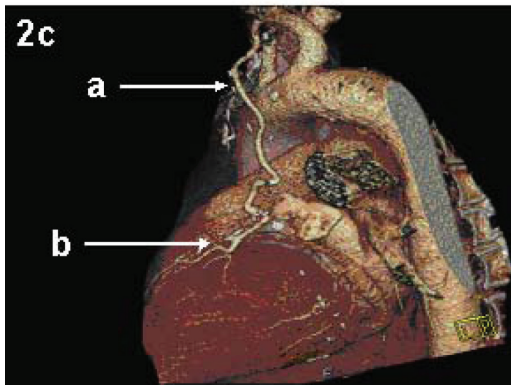
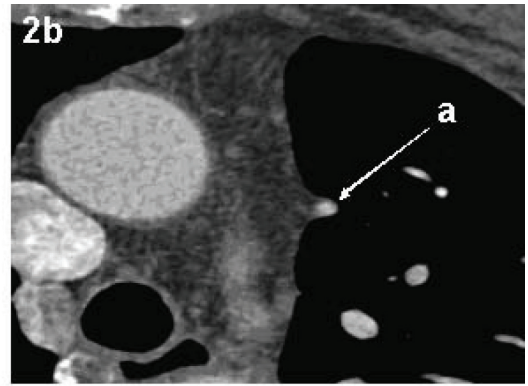
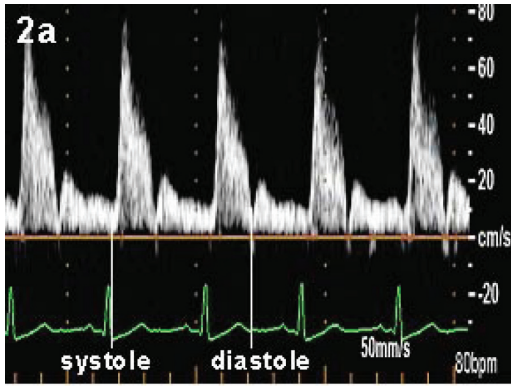


Chapter 15, Figure 4. Non-grafted coronary arteries.

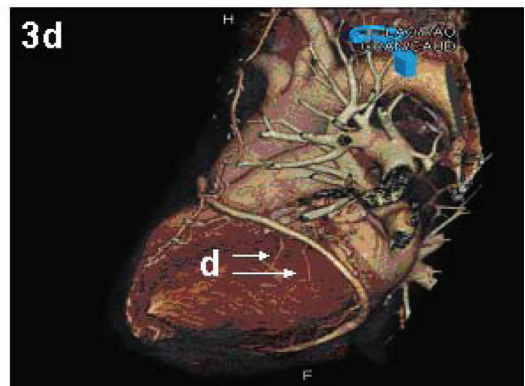
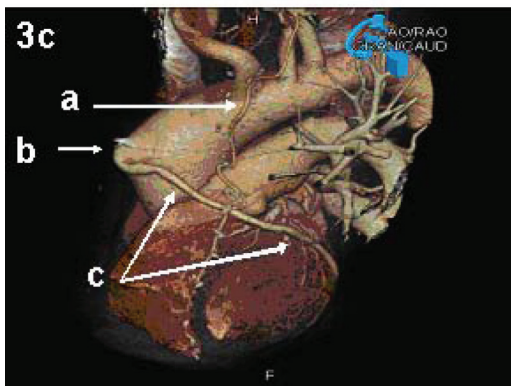
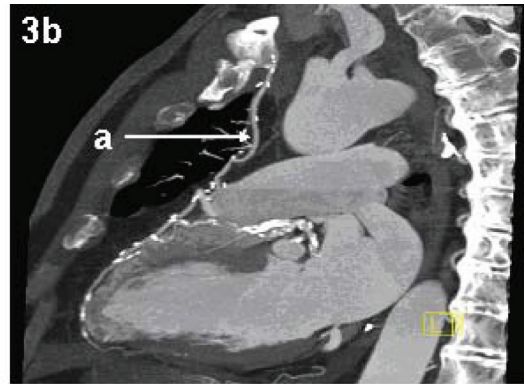
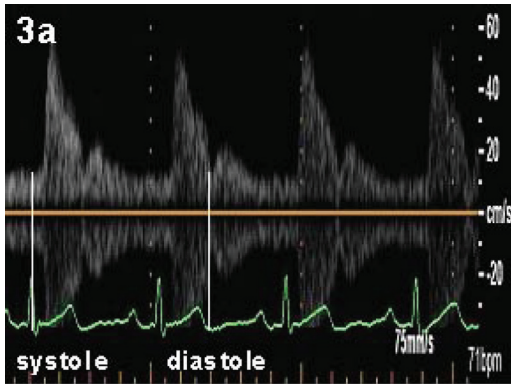
Patient with an occluded vein graft to the distal RCA (arrow, panel VI), and occluded arterial graft to the left anterior descending coronary artery. The proximal and mid-segment of the RCA show plaque without significant narrowing (arrow heads), and the distal RCA is completely occluded. (V-VII). The left main coronary artery (LM), intermediate branch (Int) and first marginal branch (MO1) are all without significant disease (I-III).



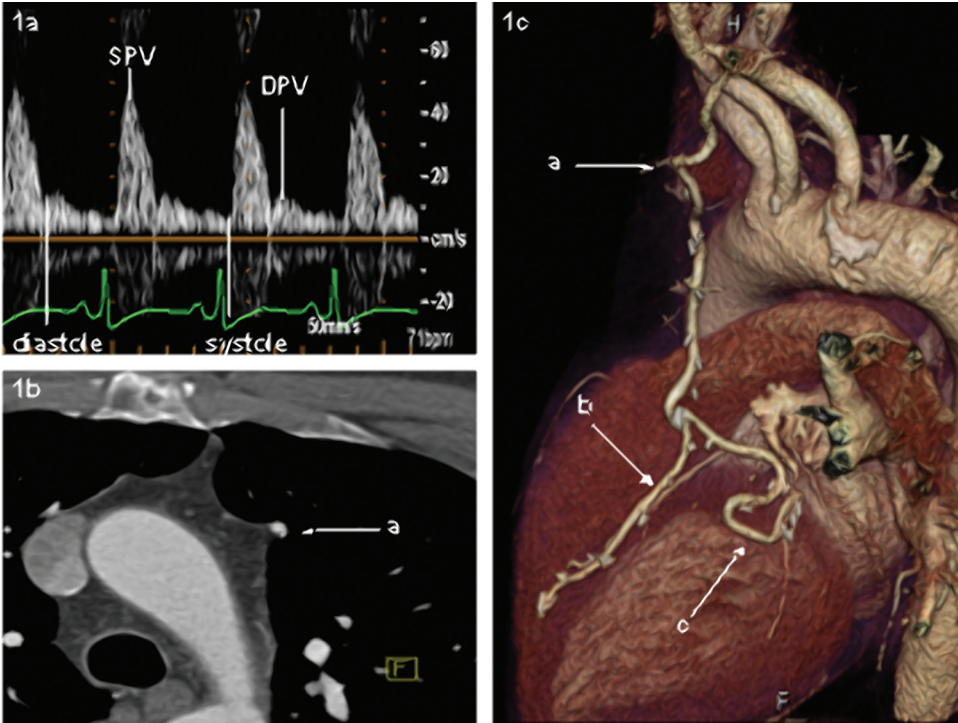
Chapter 16, Figure 1. Late follow-up main stem transthoracic ultrasonography (1a) and DSCT coronary angiography of a patent composite arterial T graft from the transverse (1b), lateral (1c) and anterolateral view (1d). (a) main stem of the T graft; (b) LIMA branch of the T graft; (c) FRIMA branch of the T graft; (d) native obtuse margin branch. DSCT, Dual-source computed tomography; LIMA, left internal mammary artery; FRIMA, free right internal mammary artery.



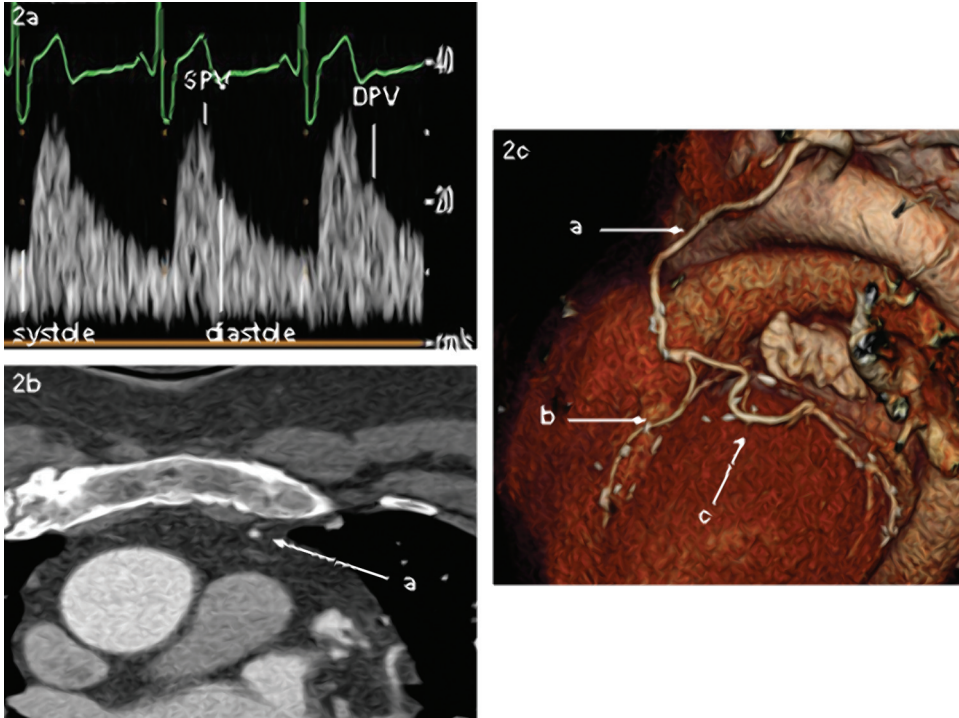
Chapter 16, Figure 2. Late follow-up main stem transthoracic ultrasonography (2a) and DSCT coronary angiography of a composite arterial T graft from the transverse (2b), anterolateral (2c) and lateral view (2d). (a) main stem of the T graft; (b) LIMA branch of the T graft; (c) occluded FRIMA branch of the T graft. Abbreviations as in Figure 1.



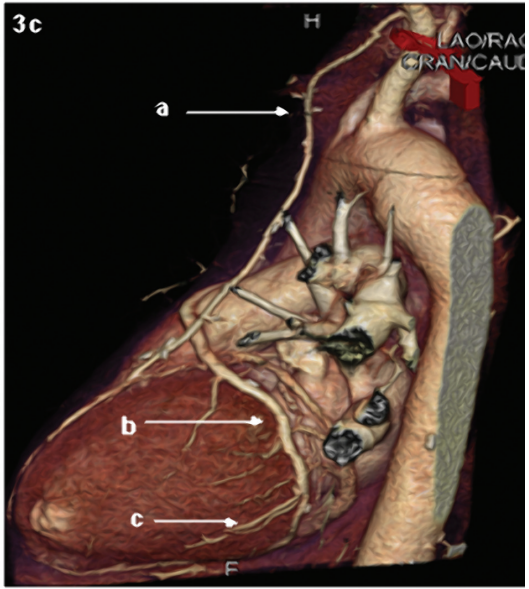
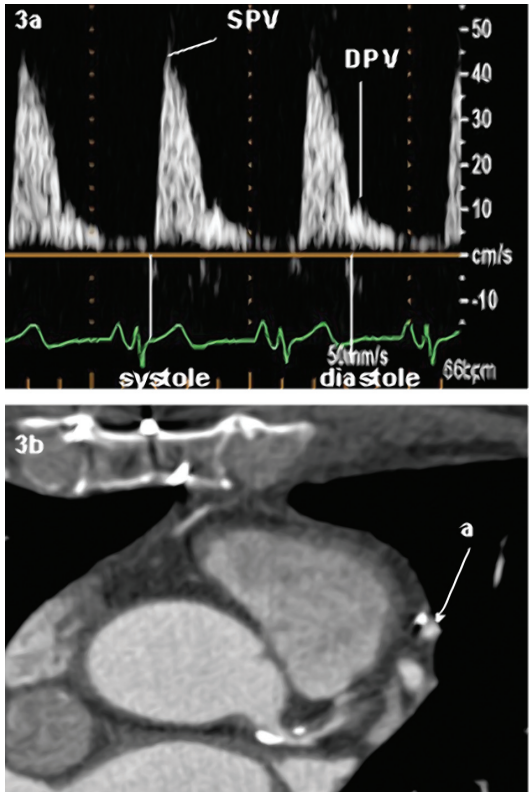
Chapter 16, Figure 3. Late follow-up transthoracic ultrasonography (3a) and DSCT coronary angiography of a patent single LIMA graft to the LAD with an additional patent venous graft from the lateral (3b,3d) and anterolateral (3c) view. (a) LIMA graft; (b) proximal venous graft anastomoses to the aorta; (c) patent venous jump graft to the lateral and inferior wall; (d) native obtuse margin branches. LAD, left anterior descending artery. Abbreviations as in Figure 1.



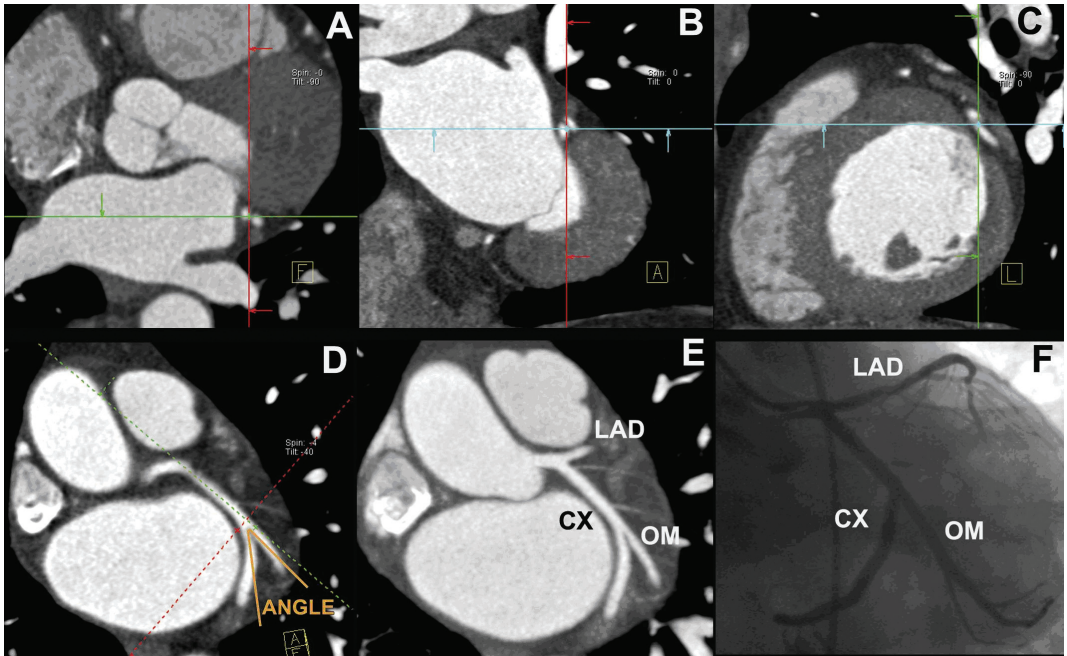
Chapter 17, Figure 1. Late follow-up main stem transthoracic ultrasonography (1a) and DSCT coronary angiography of a patent composite arterial T-graft from the transverse (1b) and anterolateral view (1c). (a) main stem of the T-graft; (b) LIMA branch of the T-graft; (c) too large, not kinking, patent FRIMA branch of the T-graft. DSCT, Dual-source computed tomography; LIMA, left internal mammary artery; FRIMA, free right internal mammary artery; SPV, systolic peak velocity (cm/s); DPV, diastolic peak velocity (cm/s).



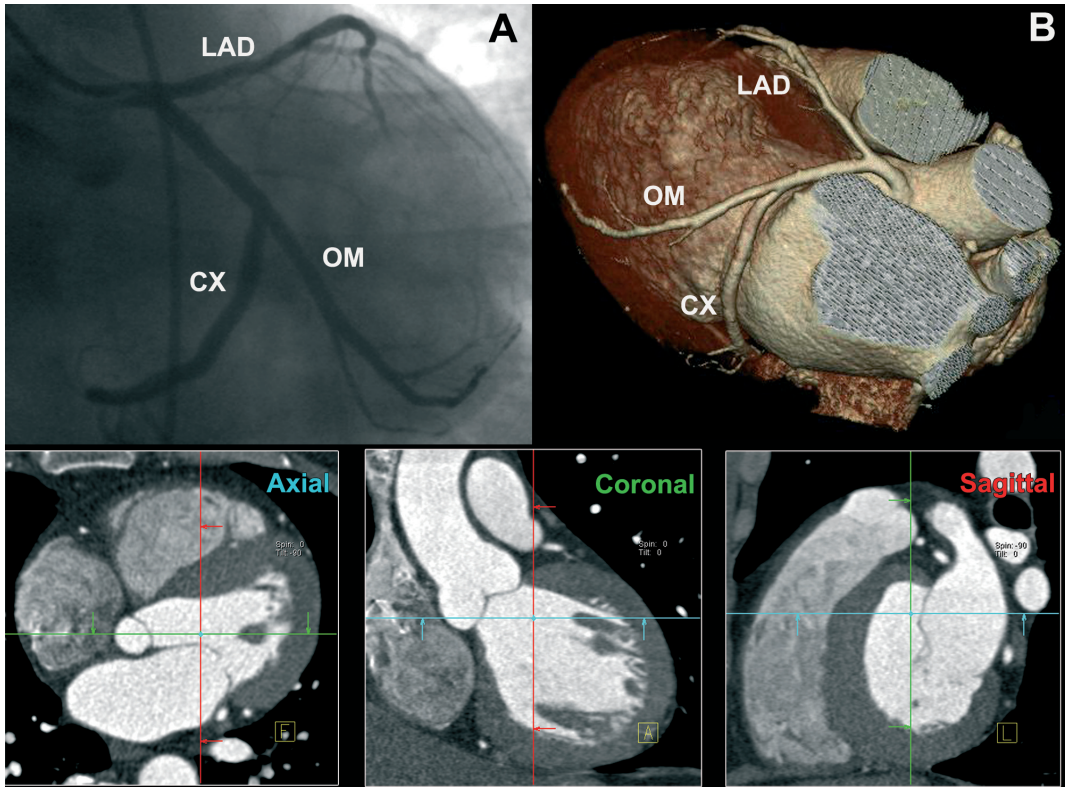
Chapter 17, Figure 2. Late follow-up main stem transthoracic ultrasonography (2a) and DSCT coronary angiography of a composite arterial T-graft from the transverse (2b) and anterolateral view (2c). (a) main stem of the T-graft; (b) string sign LIMA branch of the T-graft; (c) patent FRIMA branch of the T-graft. Abbreviations as in Figure 1.



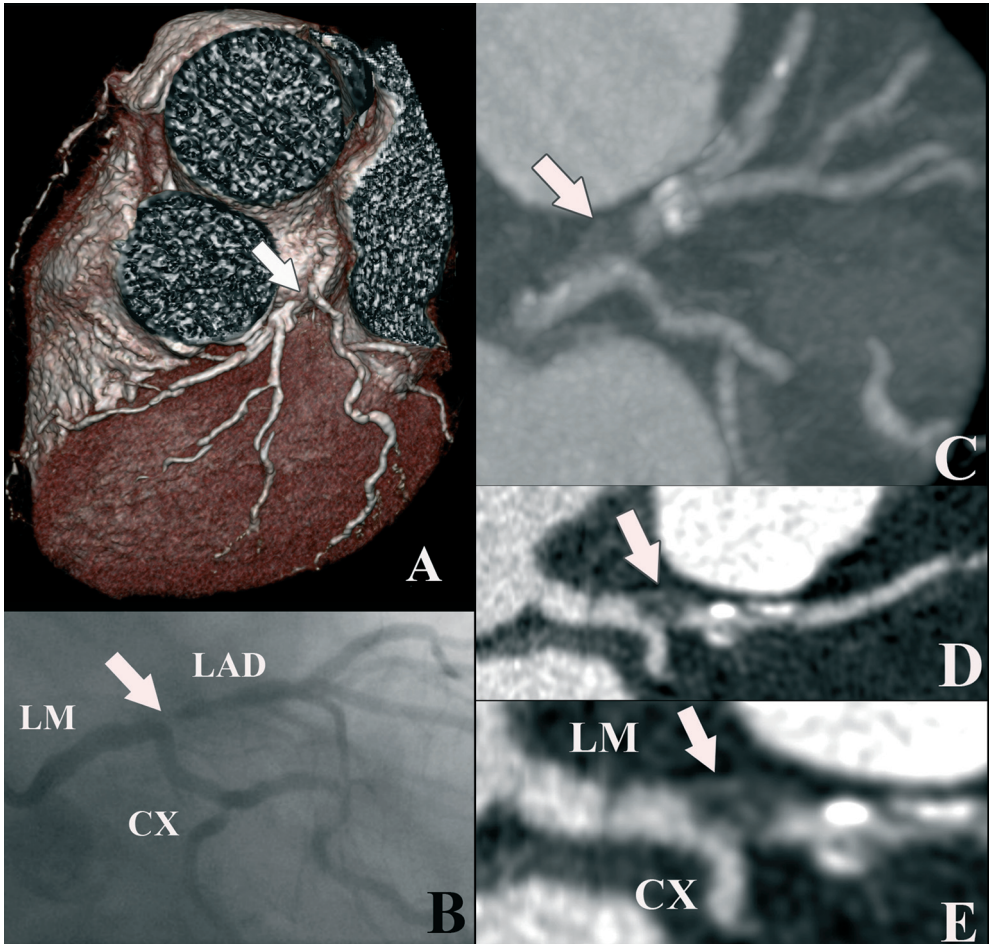
Chapter 17, Figure 3. Late follow-up transthoracic ultrasonography (3a) and DSCT coronary angiography of a patent single LIMA graft to the LAD from the transverse view (3b) with an additional patent venous graft from the lateral view (3c). (a) patent LIMA graft. (b) patent venous jump graft to the lateral and inferior wall. (c) native obtuse margin branches. Abbreviations as in Figure 1.



Chapter 18, Figure 1a. Visualization of the circumflex-obtuse marginal bifurcation by invasive coronary angiography (a) and volume-rendered computed tomography coronary angiography (b). The three-dimensional representation of the heart, as shown in (b), can be obtained by summation of the 'raw' axial computed tomography images that have a defined x - y - z dimension. The conventional planes that are used for visualization of this volume data set are the axial plane (axial), the coronal plane (coronal) and the sagittal plane (sagittal). CX, circumflex coronary artery; LAD, left anterior descending coronary artery; OM, obtuse marginal branch.



Chapter 18, Figure 1b. Scrolling of axial images provides a quick view of the data set to assess crudely the main features of the coronary anatomy. To obtain a precise view of the structure of interest, in this example the circumflex-obtuse marginal bifurcation, the planes of visualization need to be orientated to the geometrical orientation of the coronary structures. As a first step, the three conventional image planes are centered at the level of the branching point (a-c). The three-dimensional nature of the CT data allows to subsequently tilt these image planes in any orientation. The resulting multiplanar reconstruction (d) precisely shows the relationship of the main vessel with the side branch and is used to assess the angle between the initial course of distal portion of the main vessel and side branch (in this example, 31°). Also shown is a maximum intensity projection computed tomography image (e) to demonstrate the anatomical correlation with the angiographic view. We did not use this maximum intensity projection reconstruction to determine bifurcation angles. CX, circumflex coronary artery; LAD, left anterior descending coronary artery; OM, obtuse marginal branch.



Chapter 18, Figure 3. CT coronary angiogram and corresponding conventional angiogram in a patient presenting with unstable angina. The volume-rendered CT image (A) suggests the presence of a significant ostial narrowing (arrow) of the LAD. On ICA (B) the stenosis (arrow) was classified as Medina type 0.1.0. Maximal intensity projected (C) and multiplanar reconstructed (D and E) CT images however showed additional significant involvement of the distal LM (arrow) and thus reclassified the lesion as Medina type 1.1.0. CX: circumflex coronary artery, LAD: left anterior descending coronary artery, LM: left main coronary artery.